



The
University
Of
Sheffield.

Investigation of the Sialidases of Periodontal Pathogens

By:

Andrew Frey

A thesis submitted for the degree of
Doctor of Philosophy

The University of Sheffield
School of Clinical Dentistry
Unit of Oral and Maxillofacial Pathology

31/08/2016

I. Contents

II.	List of Figures	6
III.	List of Tables	10
IV.	Acknowledgements.....	11
V.	Abbreviations	12
VI.	Abstract.....	14
1	Chapter 1: Introduction	16
1.1	Teeth and major oral diseases	16
1.1.1	Periodontitis.....	16
1.1.2	Periodontitis-A Considerable Burden	18
1.2	Periodontitis-Aetiology	19
1.2.1	Bacterial Colonisation of the Periodontium and its Role in Periodontitis	19
1.2.2	The Importance of Inflammation in Periodontitis	23
1.2.3	Other Factors in Periodontitis Onset and Progression	37
1.3	Periodontitis-Systemic influences.....	38
1.3.1	Head and Neck Cancer	38
1.3.2	Heart Disease and Atherosclerosis	39
1.3.3	Rheumatoid Arthritis.....	39
1.4	Treatment of Periodontitis	40
1.5	Virulence Factors of the Periodontal Pathogens	41
1.5.1	<i>Porphyromonas gingivalis</i>	41
1.5.2	<i>Tannerella forsythia</i>	43
1.5.3	<i>Fusobacterium nucleatum</i>	46
1.5.4	Biofilm Formation	48
1.6	The Anti-Virulence Approach.....	51
1.7	Sialic Acid, Sialidases, and Virulence	52
1.7.1	Sialic Acid	52
1.7.2	Sialidases	53
1.7.3	Sialic Acid in the Oral Cavity.....	56
1.7.4	Sialic Acid and the Immune System	56
1.7.5	Sialidases of Periodontal Pathogens	58

1.8	Sialidase Inhibition	63
1.8.1	Viral Sialidase-The Driving Force Behind Inhibitor Development.....	63
1.8.2	Sialidase Inhibitors	63
1.8.3	Sialidase Inhibition-Potential Impact on Virulence.....	64
1.8.4	Sialidase Inhibition-Impact on the Host Immune Response.....	65
1.8.5	Aims and Hypothesis-The Prospect of Sialidase Inhibitors as a Treatment for Periodontitis.....	65
2	Chapter 2: Biochemical Characterisation of Periodontal Pathogen Sialidases.....	68
2.1	Introduction-The Sialidases of <i>P. gingivalis</i> and <i>T. forsythia</i>	68
2.2	Materials and Methods- Biochemical Characterisation of Periodontal Pathogen Sialidases.....	69
2.2.1	Bacterial Strains, Growth Conditions, and Plasmids.....	69
2.2.2	Sialidase Activity of Whole Bacteria.....	71
2.2.3	DNA Extraction.....	72
2.2.4	Polymerase Chain Reaction (PCR).....	72
2.2.5	Restriction Endonuclease Digestion of Plasmid DNA or PCR products.....	73
2.2.6	DNA Ligation	73
2.2.7	Bacterial Transformation	74
2.2.8	Protein Production and Purification by Affinity Chromatography.....	75
2.2.9	BCA Assays	77
2.2.10	Sodium Dodecyl Sulphate-Poly Acrylamide Gel Electrophoresis (SDS-PAGE).....	78
2.2.11	Biochemical Studies of Sialidases and Sialidase Subunits.....	79
2.2.12	Structural Characterisation of NanH -Crystal Trials	82
2.3	Results.....	83
2.3.1	Bioinformatic Analysis of NanH and SiaPG	83
2.3.2	Production of SiaPG-CBM, SiaPG-CT, and NanH-CT.....	102
2.3.3	Production of Periodontal Pathogen Sialidases: NanH and SiaPG.....	116
2.3.4	Expression and Purification of Other Enzymes	127
2.3.5	Sialidase Protein Production-a Summary.....	129
2.3.6	Biochemical Characterisation of Purified Periodontal Pathogen Sialidases.....	131
2.3.7	Inhibition of Periodontal Pathogen Sialidases by Zanamivir	148
2.4	Discussion.....	156
2.4.1	pH, Pathogen Sialidases, and Periodontitis	156
2.4.2	The Importance of Sialic Acid Linkage preference for <i>T. forsythia</i>	159

2.4.3	The Importance of Sialyl Lewis Ligands for <i>T. forsythia</i>	162
2.4.4	<i>T. forsythia</i> NanH- the RIP Motif of the Catalytic Domain is Essential for Catalysis, and the N-terminal CBM is involved in Ligand Binding.....	162
2.4.5	Zanamivir Inhibits Periodontal Pathogen Sialidases.....	163
2.5	Summary.....	164
3	Chapter 3: Investigating the Targeting of Host Sialoglycans by Periodontal Pathogens- the Effects on Growth and Biofilm Formation, and the Impact of Zanamivir.....	168
3.1	Introduction.....	168
3.2	Materials and Methods- Investigating the Targeting of Host Sialoglycans by Periodontal Pathogens- the effects on Growth and Biofilm Formation, and the Impact of Zanamivir.....	171
3.2.1	Enzyme synergy in Sialic Acid Release from Salivary Mucin.....	171
3.2.2	Bacterial Strains and Growth Conditions.....	171
3.2.3	Collection and preparation of Human Saliva.....	172
3.2.4	Culture of Periodontal Pathogens on Defined Media Supplemented with Host Sialic Acid Sources.....	173
3.2.5	Biofilm Assays.....	173
3.3	Results.....	174
3.3.1	Release of Sialic Acid from Mucin glycoproteins by Periodontal Pathogen Sialidases is enhanced by <i>T. forsythia</i> Sialate-O-Acetylerase.....	174
3.3.2	<i>P. gingivalis</i> is Capable of Growth Utilising Host Glycoproteins as Sole Carbon and Nitrogen Sources, and this is Enhanced by NanS.....	178
3.3.3	Biofilm Formation of Periodontal Pathogens on Host Glycoproteins, and the Potential for Zanamivir to Inhibit Periodontal Pathogen Biofilm Formation.....	188
3.4	Discussion.....	200
3.5	Summary.....	206
4	Chapter 4: The Role of Sialidases in Host-Pathogen Interactions, and Disruption by Sialidase Inhibition.....	210
4.1	Introduction.....	210
4.2	Materials and Methods-The Role of Sialidases in Host-Pathogen Interactions, and Disruption by Sialidase Inhibition.....	212
4.2.1	Culture of Human Cell Lines.....	212
4.2.2	Antibiotic Protection Assays.....	212
4.2.3	Cell Viability Assays.....	213
4.2.4	Immuno-Fluorescence Microscopy; Visualisation of Cell-Surface Sialic Acid	214
4.2.5	Immune-Signalling in Oral Epithelial Cells.....	216

4.3	Results.....	221
4.3.1	Zanamivir has no Detrimental Effects on Oral Epithelial Cell or Periodontal Pathogen Viability.....	221
4.3.2	Periodontal Pathogen Sialidases Cleave Sialic Acid from Host Cell Surfaces and this can be Inhibited by Zanamivir.....	226
4.3.3	Zanamivir inhibits Attachment and Invasion of Oral Epithelial Cells by <i>T. forsythia</i> , <i>P. gingivalis</i> , and the sialidase-negative <i>F. nucleatum</i>	242
4.3.4	Zanamivir inhibits Attachment and Invasion of Oral Epithelial Cells During Infection with Multiple Periodontal Pathogens.....	250
4.3.5	<i>T. forsythia</i> Sialidase Influences Pro-Inflammatory Signalling in Epithelial Cells, and this is Affected by Zanamivir.....	260
4.4	Discussion.....	270
4.4.1	Host Cells Are Desialylated by Purified sialidases and Live Periodontal Pathogens.....	270
4.4.2	The Sialidase Inhibitor Zanamivir Inhibits Periodontal Pathogen Association with Host Cells.....	273
4.4.3	The Influence of Periodontal Pathogen Sialidases on Pro-Inflammatory Signalling.....	277
4.5	Summary.....	280
5	Summary and Concluding Discussion.....	282
5.1	Summary of Findings by Chapter.....	282
5.1.1	Chapter 2- Purification and Characterisation of Periodontal Pathogen Sialidases.....	282
5.1.2	Chapter 3- Investigating the Targeting of Host Sialoglycans by Periodontal Pathogens- the effects on Growth and Biofilm Formation, and the Impact of Zanamivir.....	283
5.1.3	Chapter 4-The Role of Sialidases in Host-Pathogen Interactions, and Disruption by Sialidase Inhibition.....	284
5.2	Periodontal Pathogen Sialidase Biochemistry and Future Directions.....	286
5.3	Ripe for Targeting: Bacterial Sialidases and their Associated Pathways are Multifunctional Virulence Factors in Periodontitis.....	286
5.4	Discussing the Potential for a Sialidase Inhibitor-Based Product for Treatment or Prevention of Periodontal Disease.....	293
5.4.1	Sialidase Inhibitors in Products for Periodontitis Treatment-Future Directions.....	293
5.4.2	Formulation of Products Containing Sialidase Inhibitors.....	294
5.4.3	Regulation of Consumer Products.....	295
5.5	In Conclusion.....	299

6	Bibliography	300
7	Appendices.....	321
7.1	Full Sequences of sialidases closely related to NanH from 92.A2	322
7.2	Full Sequences of Sialidases Closely Related to SiaPG from ATCC 33277.....	325
7.3	CBM/NTD Sequences of Sialidases Closely Related to SiaPG from ATCC 33277 .	330
7.4	Prediction of Secretion Sequences Using SignalP	331
7.5	Details of DNA and Protein Sequences Concerning <i>T. forsythia</i> NanH.....	332
7.6	Details of DNA and Protein Sequences Concerning <i>P. gingivalis</i> SiaPG.....	335
7.7	SignalP Predictions of secretion sequence	337
7.8	An Alignment of NanH from <i>T. forsythia</i> strains 43037 and 92.A2, Performed using ESPript	338
7.9	Partial List of EU Requirments to be Submitted before Liscensing of a Product under the “Medicine” Classification	339
7.10	Publications Arising due to Work Performed As Part of This Project	340

II. List of Figures

Figure 1.1.	Cross-sectional representation of a posterior tooth in health and disease.	17
Figure 1.2.	Periodontal bacteria complexes in the subgingival plaque.	22
Figure 1.3.	Summary of TLR activation and key signalling events leading to pro-inflammatory signalling.....	31
Figure 1.4.	The complement cascade featuring complement (C) proteins 1-9.	35
Figure 1.5.	Stages of biofilm formation.	49
Figure 1.6.	Graphic representations of A) Neu5Ac and B) a sialoglycoprotein.	52
Figure 1.7.	Conserved features of sialidases.....	54
Figure 1.8.	Uptake and utilisation of sialic acid in gram negative bacteria.	61
Figure 1.9.	Sialidase inhibitors are structural analogues of sialic acid.....	64
Figure 2.1	The amino acid sequence of NanH highlights distinct domains.	83
Figure 2.2.	Primary amino acid sequence homology in sialidases closely related to NanH from <i>T. forsythia</i>	87
Figure 2.3.	Alignment of <i>T. forsythia</i> sequences and prediction of secondary structural features.....	91
Figure 2.4.	Predicted structure and features of <i>T. forsythia</i> NanH modelled using the crystal structure of a closely related glycoside hydrolase from <i>P. distasonis</i>	93

Figure 2.5. The amino acid sequence of SiaPG appears to only contain a sialidase domain only.....	94
Figure 2.6. Alignment of <i>Porphyromonas</i> sialidases.....	98
Figure 2.7. Predicted structure and features of <i>P. gingivalis</i> SiaPG modelled using the crystal structure of a sialidase from <i>B. thetaiotaomicron</i>	99
Figure 2.8. Alignment of <i>P. gingivalis</i> sialidase N-terminal domains.....	100
Figure 2.9. Linear schematic of NanH and SiaPG.	102
Figure 2.10. Targeting sialidase domains.....	103
Figure 2.11. PCR amplification of A) nanH-CT, B) siaPG-CBM, and C) siaPG-CT from <i>P. gingivalis</i> genomic DNA.	107
Figure 2.12. Confirmation of pET-sialidase subunit constructs.	108
Figure 2.13. Expression test and attempted purification of SiaPG-CBM.....	110
Figure 2.14. SDS-PAGE of cell lysates overexpressing SiaPG-CT and NanH-CT.....	111
Figure 2.15. SDS-PAGE of A) SiaPG-CBM, B) NanH-CT, and C) SiaPG-CT following urea solubilisation and affinity chromatography.....	112
Figure 2.16. SDS-PAGE of A) NanH-CT, and B) SiaPG-CBM following step down dialysis to remove urea.....	113
Figure 2.17. Purified NanH-CT displays no activity.....	114
Figure 2.18 Putative NanH CBM co-crystallised with zanamivir.....	116
Figure 2.19 PCR amplification of A) nanH and B) nanH-CT from <i>T. forsythia</i> genomic DNA..	118
.....	118
Figure 2.20 Comparison of codon utilisation between A) nanH or B) siaPG and <i>E. coli</i>	123
Figure 2.21. nanH and siaPG pJET constructs.	124
Figure 2.22. Confirmation of pET21a -NanH construct.....	125
Figure 2.23. Sialidase expression trials.	126
Figure 2.24. Affinity chromatography purification of NanH and SiaPG.....	127
Figure 2.25. Purification of NanH-YMAP.....	129
Figure 2.26 Visualisation of MUNANA cleavage to rapidly confirm sialidase activity.	131
Figure 2.27. pH optima of A) NanH and B) SiaPG.	133
Figure 2.28. pH Optima of A) <i>T. forsythia</i> and B) <i>P. gingivalis</i>	134
Figure 2.29. Reaction kinetics of MUNANA with A) NanH and B) SiaPG.	136
Figure 2.30. Catalytic efficiency of A) NanH and B) SiaPG.	139
Figure 2.31. 3- and 6- sialyllactose.....	141

Figure 2.32. Kinetics of NanH on α 2-3 and α 2-6 linked sialic acid under physiological conditions.....	142
Figure 2.33. Graphic representation of sialyl lewis A/X.....	144
Figure 2.34. Kinetics of Neu5Ac release from SleA and SLeX by NanH.....	145
Figure 2.35. Structures of the substituted amino acids in NanH and NanH-YMAP.	146
Figure 2.36. NanH-YMAP displays no Sialidase Activity.	147
Figure 2.37. Affinity of 3- and 6-sialyllactose for NanH-YMAP.	147
Figure 2.38. Sialidase activity profiles of periodontal pathogens.....	149
Figure 2.39. Sialidase activity profiles of <i>P. gingivalis</i> and <i>T. forsythia</i> strains.....	150
Figure 2.40. Inhibition of A) <i>T. forsythia</i> and B) <i>P. gingivalis</i> by Zanamivir.	151
Figure 2.41. Inhibition of NanH and SiaPG by Zanamivir.	155
Figure 2.42. NanH-CBM Binds 3- and 6- sialyllactose.	163
Figure 3.1. Purification of NanS.	176
Figure 3.2. Enzyme synergy in sialic acid release from BSM, and inhibition by zanamivir..	177
Figure 3.3. Initial testing of defined media for culture of periodontal pathogens.....	180
Figure 3.4. Optimisation of <i>P. gingivalis</i> culture in defined media; the effect of saliva and serum (FBS).	182
Figure 3.5. Growth of <i>P. gingivalis</i> on serum, in the presence of NanS and zanamivir.....	184
Figure 3.6. The effect of NanS on <i>P. gingivalis</i> Growth on Serum and Saliva.....	187
Figure 3.7. <i>P. gingivalis</i> growth on NAM, Neu5Ac, serum, and saliva, and a comparison of biofilm quantification methods.	191
Figure 3.8. Zanamivir has no Effect on <i>T. forsythia</i> biofilm formation on sialoglycoprotein Sources.....	197
Figure 3.9. Zanamivir inhibits <i>P. gingivalis</i> growth and biofilm formation on sialoglycoproteins.	198
Figure 3.10. Crystal violet staining of <i>P. gingivalis</i> biofilms.....	199
Figure 3.11. Sialic acid utilisation operons in A) <i>T. forsythia</i> and B) <i>F. nucleatum</i>	202
Figure 4.1. Viability testing of H357 OSCC cells exposed to <i>T. forsythia</i> and/or Zanamivir.	223
Figure 4.2. Viability testing of OKF6 oral epithelial cells exposed to zanamivir.	224
Figure 4.3. Viability testing of periodontal pathogens exposed to zanamivir.	226
Figure 4.4. Exposure to periodontal pathogens removes sialic acid from epithelial cell surfaces.....	229
Figure 4.5. Quantification of cell surface sialic acid from oral epithelial cells exposed to A) live pathogens B) the effect of pathogen exposure on cell numbers.....	231

Figure 4.6. Purified sialidases desialylate oral epithelial cell surfaces.	234
Figure 4.7. A) Quantification of cell surface sialic acid on oral epithelial cells exposed to NanH and SiaPG. B) Exposure to sialidases or zanamivir has no effect on cell numbers. ...	235
Figure 4.8. NanH desialylates sialyl-lewis A on epithelial cell surfaces.	239
Figure 4.9. NanH desialylates sialyl-lewis X on epithelial cell surfaces.....	241
Figure 4.10. The effect of zanamivir on attachment and invasion of OSCC epithelial Cells.	245
Figure 4.11. The effect of zanamivir on attachment and invasion of immortalised OKF6 epithelial cells.	249
Figure 4.12. Colony morphology of <i>P. gingivalis</i> , <i>F. nucleatum</i> , and <i>T. forsythia</i> during mixed-species enumeration.....	251
Figure 4.13. The effect of zanamivir on attachment and invasion of epithelial cells co-infected with <i>T. forsythia</i> and <i>F. nucleatum</i>	252
Figure 4.14. The effect of zanamivir on attachment and invasion of epithelial cells co-infected with <i>T. forsythia</i> and <i>P. gingivalis</i>	254
Figure 4.15. The effect of zanamivir on attachment and invasion of epithelial cells co-infected with <i>P. gingivalis</i> and <i>F. nucleatum</i>	256
Figure 4.16. The effect of zanamivir on attachment and invasion of epithelial cells co-infected with <i>T. forsythia</i> , <i>F. nucleatum</i> , and <i>P. gingivalis</i>	258
Figure 4.17. IL-8 Secretion of oral epithelial cells exposed to zanamivir, LPS, and NanH. ...	263
Figure 4.18. Secretion of IL-8 by oral epithelial cells infected with <i>T. forsythia</i> , in the presence and absence of zanamivir.....	265
Figure 4.19. Cytokine secretion by oral epithelial cells infected with <i>T. forsythia</i> , in the presence and absence of zanamivir. A) GCSF B) IL-6 C) IL-8 D) MCP-1 E) MIP1 α F) TNF. ...	269
Figure 5.1. Sialidases and sialic acid-mediated interactions enhance periodontal pathogen proliferation and host inflammatory processes through a number of mechanisms.....	291

III. List of Tables

Table 1.1. Clinical descriptive terms for periodontitis.....	18
Table 2.1. <i>E. coli</i> strains.....	70
Table 2.2. Plasmids for cloning and expression.	70
Table 2.3. Reagents for restriction digest of plasmids and PCR products.	73
Table 2.4. SDS-PAGE buffers.	78
Table 2.5. Reagent volumes required for casting of SDS-PAGE resolving gels.	79
Table 2.6. . Design of primers for siaPG, nanH and domain amplification from genomic DNA.	104
Table 2.7. Plasmids constructed for storage or expression of sialidases and sialidase domains.	130
Table 2.8. The effect of salt on sialidase kinetics under different pH conditions.....	137
Table 2.9. The effect of salt on sialidase kinetics under different pH conditions.....	140
Table 2.10. A Comparison of Bacterial Sialidase Reaction Kinetics (K_m and V_{max}) with MUNANA.....	159
Table 2.11 Sialic acid-linkage preferences of sialidases from bacteria associated with different mucosal sites.....	161
Table 3.1. Periodontal pathogen strains.....	172
Table 3.2. Salivary mucins-a summary of glycosylation features.	175
Table 4.1. Cell treatment conditions for IL-8 cytokine analysis.	217
Table 4.2. ELISA kit buffers.....	219
Table 4.3. Cytokines produced by oral epithelial cells.....	220

IV. Acknowledgements

Well I've had an incredible time during my PhD. A rollercoaster of emotions and experiences for sure, but incredible nonetheless, not to mention a whole wealth of academic-and other-experiences.

I must give my wholehearted thanks to Dr Graham P Stafford, who provided invaluable insight and guidance throughout my project. I have gained immensely from his mentorship, developing as a scientist and academic, and with his support I have been able to push myself beyond what I have ever accomplished before.

I would also like to thank Professor Ian Douglas and Dr Craig Murdoch for their critical analysis of my work and lending me their expert opinions in practical matters-in short, there was no problem too great for my supervisory team here at Sheffield. In addition to support from my supervisors, I must thank the efforts and patience of the Postdoctoral Researchers who I had the pleasure of working with during the past four years-Dr Prachi Stafford, Dr Matthew Hicks, Dr Jennifer Parker, and Dr Chatchawal Phansopa, the biochemical wizard. I would also like to thank the Dental School technical staff-I am particularly grateful to Mr Jason Heath and Mrs Brenka McCabb for their top-class laboratory support during my project.

Needless to say I have made some great friends during my time at the Dental school, particularly in the third floor postgraduate office. A special mention must go to my friends Mark Ofield, Genevieve Melling, Lav Darda, Kathryn Naylor, and Charlotte Green, all of whom provided sometimes much-needed morale and encouragement as well as practical advice.

The team at GlaxoSmithKline in Weybridge must also be thanked, particularly my GSK supervisor Dr Jonathon Pratten. With his help I was able to gain great insight into the world of business and science, and consider my project in terms of its commercial relevance. I would also like to thank his colleagues for their time spent providing much valued input and discussion, particularly Dr David Bradshaw and Mrs Nisha Patel.

My special thanks go out to my amazing partner Lucy Wainwright-for her continuous support at home, encouragement, and always being able to listen and debate with me-and my Mum and Dad, and brothers and sister up North, who have always been very supportive of me and believed in my ambitions.

Finally, I am also grateful for and acknowledge the financial support from the British Biomedical and Biological Sciences Research Council (BBSRC) and GlaxoSmithKline (GSK) under the BBSRC-CASE award that made this project possible.

V. Abbreviations

Abbreviation	Description
Amp	ampicillin
BHI	brain heart infusion
bp	base Pairs
BSM	bovine submaxillary mucin
CAL	clinical attachment loss
DANA	2-deoxy-2,3-dehydro-N-acetylneuraminic acid
dH ₂ O	distilled water
DNA	deoxyribonucleic acid
DTT	Dithithreitol
EDTA	ethylenediaminetetra-acetic acid
FBS	foetal bovine serum
g	gram (in the context of mass)
GCF	gingival crevicular Fluid
Glc	glucose
GlcNac	N-acetylglucosamine
Kbp	kilo base pairs
L	litre
M	molar
ManNac	N-acetylmannosamine
mL	millilitre
mM	millimolar
mRNA	messenger RNA
NAM	N-acetylmuramic acid
Neu5,9Ac	5-N, 9-O-acetylneuraminic acid

Neu5Ac	5-N-acetylneuraminic acid
NeuGc	N-glycolylneuraminic acid
OD	optical density
PAGE	poly acrylamide gel electrophoresis
PBS	phosphate buffer saline
PCR	polymerase chain reaction
RNA	ribonucleic acid
ROS	reactive oxygen species
SDS	sodium dodecyl sulphate
TAE	tris-acetate EDTA
TEMED	tetramethylethylenediamine
TSB	tryptic soy broth
p/n/μg	pico/nano/microgram
μL	Microlitre
UV	Ultraviolet
v/v	concentration, volume by volume
w/v	concentration, weight by volume
g	gravitational Force
SNA	lectin from <i>Sambucus nigra</i>
MAA	Lectin from <i>Maackia amurensis</i>
FITC	fluorescein isothiocyanate
TR	texas red
Th	T-helper
IL	Interleukin
TNF	tumour necrosis factor

VI. Abstract

Periodontitis results in destruction of tooth supporting structures, eventually leading to tooth loss, and it affects ~10% of the world's population. Key to its onset and progression is a complex relationship between the periodontal bacteria and the host inflammatory response. The bacteria most associated with severe periodontitis are the so-called periodontal pathogens of the red complex- *Tannerella forsythia*, *Treponema denticola*, and *Porphyromonas gingivalis*. These organisms all express sialidases, which cleave sialic acid from host glycoproteins, and this is believed to contribute to disease.

Considering this, the aims of this project were to further characterise the sialidases of *T. forsythia* and *P. gingivalis* (NanH and SiaPG), to test their inhibition with commercially available chemotherapeutics, and the effect this has on *in vitro* models of virulence.

NanH and SiaPG were successfully purified by affinity chromatography. The enzymes were shown to possess a high degree of activity over various conditions and on different sialic acid ligands. Importantly, both sialidases could be inhibited using the commercially available chemotherapeutic zanamivir (supplied by GlaxoSmithKline, UK) which laid the groundwork for studies testing inhibition of virulence.

The accessory enzyme NanS was shown to bolster sialic acid release from bovine salivary mucin by both NanH and SiaPG. This was important for nutrient acquisition, since NanS also enhanced the growth of *P. gingivalis* in defined media where serum and saliva were the only nutrient sources. These findings also hinted at the possibility of interspecies cooperation in sialic acid release from host sources. Zanamivir also inhibited biofilm formation of *P. gingivalis* on oral-relevant glycoprotein sources.

Zanamivir was also shown to be capable of inhibiting attachment and invasion of oral epithelial cells by *P. gingivalis*, *T. forsythia*, and the sialidase negative pathogen *Fusobacterium nucleatum*, even when multiple species were present during infection. Finally NanH was shown to part-mediate pro-inflammatory signalling in oral epithelial cells in response to *P. gingivalis* LPS, and zanamivir prevented pro-inflammatory cytokine release in cells infected with *T. forsythia*. This highlighted multiple mechanisms by which sialidase inhibition can prevent host-pathogen interactions.

This study broadens our understanding of the multifarious roles of bacterial sialidases in virulence, and indicates that their inhibition with chemotherapeutics could be a promising strategy for periodontitis therapy.

Chapter 1

Introduction

1 Chapter 1: Introduction

1.1 Teeth and major oral diseases

The major oral infections that affect human teeth and gums are outlined in figure 1.1 and range from classical tooth decay (or caries) to root canal infection and periapical abscess formation. Severe gum inflammation often leads to periodontitis, which will be discussed at length below. In short they are caused chiefly by the build up of large amounts of bacterial (or fungal) colonisers within the various environmental niches of the teeth, namely hard tooth surfaces (bathed in oral secretions), gums (gingiva) and underlying niches exposed once infection sets in. One of these underlying environments is termed the periodontium, or supporting structures of the tooth (periodontal ligament, alveolar bone, gingiva cementum). In disease, this site may be colonised by various micro-organisms, leading to inflammation and the onset of periodontitis (figure. 1.1).

1.1.1 Periodontitis

Simply put, periodontitis describes a condition involving inflammation of the periodontal tissues, which can often lead to their destruction. In periodontitis, gingiva recede, the patient suffers from loss of tooth attachment, and in severe or chronic cases, eventually tooth loss. This is distinct from other non-destructive periodontal diseases such as gingivitis (where the gingivae suffer from inflammation as a result of infection but is completely reversible). Clinically, periodontitis is assessed by use of a probe, which attempts to gauge the depth of the periodontal pocket (in millimetres); ideally from the cemento-enamel junction (an anatomical border where the cementum meets enamel) to the bottom of the periodontal pocket. This measurement is termed "Clinical Attachment Loss" (CAL). Other clinical assessments include the presence of periodontitis at different sites (i.e. more than one tooth), the proximity of multiple affected sites, and the presence of bleeding at a given site. In addition to the clinical presentation, the age of the patient (periodontitis usually affects adults, but occasionally it may affect young people as well), the rate of disease progression, and its response to therapy have led to the development of a classification system to describe periodontitis (this is summarised in table 1.1, for a complete list see Armitage, 1999).

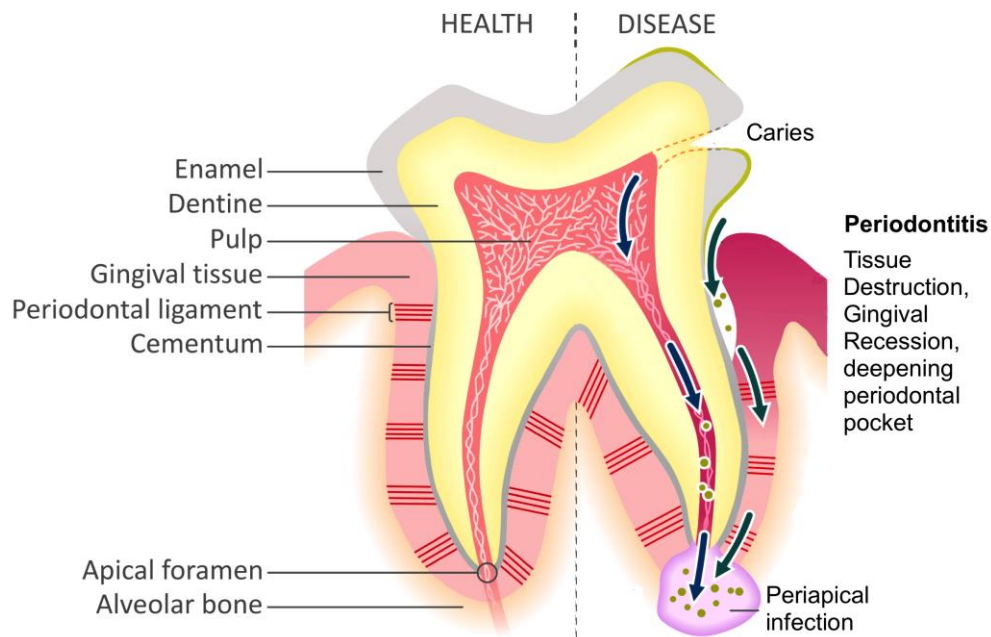


Figure 1.1. Cross-sectional representation of a posterior tooth in health and disease.

Various tissues that comprise the tooth and its supporting periodontium are labelled. In health all structures are intact, including the gingival-tooth junction which forms a tight seal between tooth and gum. The major infections affecting teeth are illustrated, resulting from prolonged plaque biofilm build-up (green material) with caries forming during enamel decay and further penetration through the tooth structures in to the soft tissue and in some cases erupting from the apical foramen to cause periapical infections, which can also be contributed to by migration of subgingival biofilm bacteria in severe periodontal disease (indicated by arrows). Periodontitis is illustrated with the classical gum recession, formation of deep periodontal pockets and a proliferation of subgingival bacteria (green circles). Reproduced from “Advances in Micobial Physiology, Chapter 6: Physiological Adaptations of Key Oral Bacteria” (2014), volume 65, with permssion from Elsevier, license number 4013100857114.

Clinical Category	Sub Category	Distinguishing Features of Subcategory	Notes
Chronic Periodontitis	localised	low number of teeth/sites affected, in the same quadrant	
	generalised	multiple teeth affected, in different quadrants	
Aggressive Periodontitis	localised	low number of teeth/sites affected, in the same quadrant	previously referred to as "juvenile periodontitis"
	generalised	multiple teeth affected, in different quadrants	
Periodontitis As a Manifestation of Systemic Diseases	associated with hematological disorders	includes acquired neutropenia, leukaemia, and other blood disorders	
	associated with genetic disorders	includes a number of inherited conditions	
Necrotizing Periodontal Diseases	necrotizing ulcerative gingivitis	the key difference is that tissue destruction in the latter condition is irreversible	
	necrotizing ulcerative periodontitis		
Periodontal Abscess	gingival, periodontal, or pericoronal abscess		
Periodontitis Associated with Endodontic Lesions			
Developmental or Acquired Deformities and Conditions	localized tooth-related factors that pre-dispose to periodontal disease	may include tooth trauma or abnormality, and dental restorations/appliances	
	mucogingival deformities	includes all manner of soft tissue deformities	
	occlusal trauma-damage to the cusp tips or incisal edge of teeth	may be caused by, or a causative factor of, periodontitis	secondary or primary respectively

Table 1.1. Clinical descriptive terms for periodontitis.

(Based on the summary described in Armitage 1999.)

As well as its importance in assessing disease in a given patient, the ability to quantify periodontitis is valuable for semi-quantitative research, where CAL and the presence of bleeding are frequently used to divide patients/affected sites into different categories, such as those with “mild” “moderate” and “severe” periodontitis (Eke et al. 2012). The other clinical descriptions discussed above may also be included to further delineate periodontitis-patient groups.

1.1.2 Periodontitis-A Considerable Burden

Even though the contribution of periodontitis to other diseases is still under debate (section 1.3), it can be said with certainty that this condition has a high prevalence, with meta-analyses placing global prevalence at ~10-11% (Kassebaum et al. 2014; Marcenes et al. 2013), or 743 million people (Kassebaum et al. 2014). Periodontitis prevalence may also

increase in the future, since its incidence is associated with age, and the mean age of the population is increasing (particularly in developed countries).

Some evidence for an increase in periodontitis incidence over time can be seen in the USA, where the number of periodontitis interventions has ~doubled in two decades (Flemmig & Beikler 2013). Furthermore, in the UK, a recent and highly comprehensive study of oral health -the 2009 Adult Dental Health Survey- showed that although the prevalence of moderate periodontitis had reduced relative to the previous decade, the number of cases of severe periodontitis had increased from 6 to 9% (White et al. 2012).

1.2 Periodontitis-Aetiology

As described above, periodontitis is an inflammatory condition, believed to be initiated by gingivitis, initial inflammation resulting in conditions that favour the growth of certain more virulent bacteria over commensal microflora-for the purposes of this thesis (and in accordance with nomenclature used in other research) this latter group will be referred to as the periodontal pathogens. The change in conditions results in a shift in the periodontal microbiota, termed “dysbiosis” (discussed below, section 1.2.1) and is correlated with periodontitis progression, with pathogens thought to cause inflammation through a number of mechanisms (discussed below, section 1.2.2). However, bacteria are not the only factors involved in causing the inflammation that is ultimately responsible for periodontitis, and in fact much of the destruction is caused by the reaction of the host immune system itself (see below).

1.2.1 Bacterial Colonisation of the Periodontium and its Role in Periodontitis

One of the key aspects of microbial ecology is that bacteria do not exist as static groups of a single species, but as part of a dynamic ecosystem with levels of different species constantly changing as a result of varying conditions. The oral microbiota is no different.

In terms of the oral cavity this diversity was first noticed by the earliest microscopy experiments in the late 1600s by van Leeuwenhoek, and has been used to observe morphologically distinct bacteria in plaque. Progressively improving techniques including electron microscopy provided a comprehensive picture of how different tooth surfaces are colonised (Listgarten 1976). In supragingival plaque, salivary proteins coat the tooth surface, forming the pellicle. The pellicle permits attachment of Gram positive cocci, termed “early colonisers”. Later, firmicutes, including the streptococci can be seen distributed throughout the plaque. These are ‘intermediate colonisers’. At this stage, conditions vary considerably between different positions in the plaque; for example,

adjacent to the tooth the plaque is anaerobic compared to the external surface. This change in conditions is thought to facilitate proliferation of 'late colonisers', including pathogens associated with severe periodontitis.

Sub-gingival plaque formation in the gingival crevice (figure 1.1) eventually initiates periodontal disease. The role of bacteria as aetiological agents in gingivitis is well characterised: for example *Porphyromonas gingivalis* has been shown to be present in a high proportion of gingivitis cases, and in approximately one third of severe cases of periodontal disease (Rôças et al. 2001). In periodontitis, the role of specific organisms is less clear-cut than in other infectious diseases: Symptoms have not been confined to a single organism but rather complexes of organisms, and the same bacterial species may be present in different hosts with or without periodontal disease. This highlights the importance of other factors in the onset and progression of periodontal disease.

However, periodontitis, like gingivitis is marked by a shift in the microbial population, a fact that was noted during the classic studies of Loe and colleagues in the 1960s (Theilade et al. 1966; Loe et al. 1965), but built upon in terms of periodontal disease in the classic studies by Socransky and colleagues in the late 1990s (Ximénez-Fyvie et al. 2000; Socransky et al. 1998) and later built upon by many others. These authors used the then-new technique, DNA hybridization checkerboard analysis to quantify the levels of different bacteria in sub- and supra-gingival plaque of healthy and diseased periodontium from large patient cohorts. Overall bacterial load was increased in disease cases, and the proportion of different species between health and disease was also affected: *Streptococci*, *Veillonella*, and *Capnocytophaga* species were associated with healthy periodontium, while *Campylobacter* and *Fusobacterium* species were associated with disease, and most associated with severe disease were *P. gingivalis*, *Tannerella forsythia* (formerly *Tannerella forsythensis* and *Bacteroides forsythus*) and the spirochaete *Treponema denticola*.

Furthermore, cluster analysis was used to identify these bacteria as members of different consortia associated with periodontal disease progression, giving rise to the concept of colour coded bacterial complexes associated with health and disease (figure 1.2); the proportion of the periodontal microbiota accounted for by the different complexes varies between health and disease, with a higher proportion of what were termed orange and red complex organisms (figure 1.2) associated with more severe disease. The emergence of next-generation sequencing technologies has further validated this association (Liu et al. 2012, Jünemann et al. 2012), and shown the presence of novel non-culturable organisms

belonging to the recently described un-named TM7 and SR1 phyla in addition to the already allocated 'red-complex' bacteria (Dewhirst et al. 2010, Liu et al. 2012). This work also identified potential contributions from several less well studied organisms such as *Filifactor alocis*, which may now describe an expanded 'red-complex' (Schlafer et al. 2010; Griffen et al. 2012) . However, research has yet to establish how crucial these organisms are *in vivo*, despite a proliferation of *in vitro* experiments (Aruni et al. 2014).

Since these early studies describing the microbial complexes involved in periodontitis, the term "dysbiosis" has been coined to describe the complicated shifts in microbiota that are associated with disease in conditions including periodontitis (Darveau 2010; Hajishengallis et al. 2012) and other conditions such as inflammatory gastro-intestinal (GI) diseases (Matsuoka & Kanai 2015). The association of shifts in the microbiota (or dysbiosis) and the resulting inflammation is probably the most widely accepted cause of periodontitis, although other factors (section 1.2.3) do play roles in modulating inflammation and microbiota shifts.

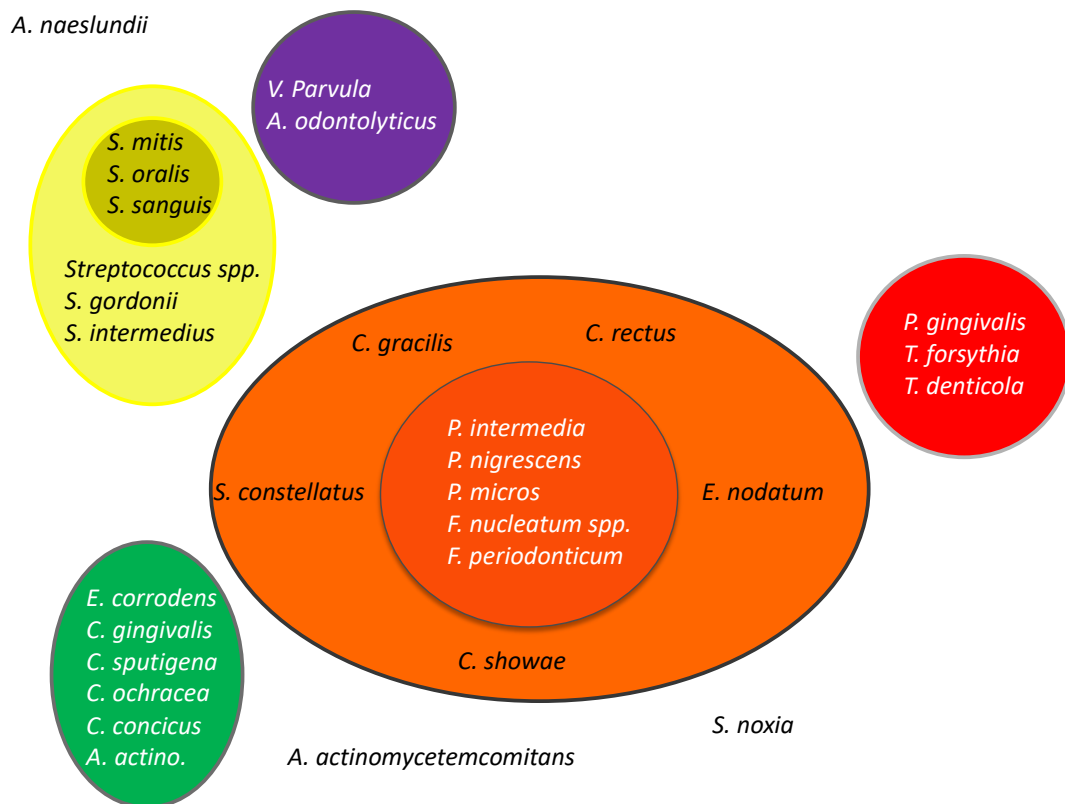


Figure 1.2. Periodontal bacteria complexes in the subgingival plaque.

Purple complex: *Veillonella parvula* and *Actinomyces odontolyticus*. Green complex: *Eikenella corrodens*, *Capnocytophaga gingivalis*, *Capnocytophaga sputigena*, *Capnocytophaga ochracea*, *Campylobacter concisus*, and *Aggratibacter actinomycetemcomitans*. Yellow complex: *Streptococcus mitis*, *Streptococcus oralis*, *Streptococcus sanguis*, *Streptococcus gordonii*, and *Streptococcus intermedius*. Orange complex: *Campylobacter gracilis*, *Campylobacter rectus*, *Campylobacter showae*, *Streptococcus constellatus*, *Eubacterium nodatum*, *Prevotella intermedia*, *Prevotella nigrescens*, *Peptostreptococcus micros*, *Fusobacterium nucleatum*, and *Fusobacterium periodonticum*. Red complex: *Porphyromonas gingivalis*, *Tannerella forsythia*, and *Treponema denticola*. Non-clustered associated bacteria: *Aggratibacter actinomycetemcomitans*, *Selenomonas noxia*, and *Actinomyces naeslundii*. (Adapted from Socransky et al. 1998, with permission from John Wiley and Sons, license number 3990801197733.)

1.2.2 The Importance of Inflammation in Periodontitis

Given that the presence and levels of different bacteria cannot predict the outcome of periodontitis, or explain why different patients respond differently to treatment, the role of the host immune system has been extensively studied. Cellular and humoral effectors are regulated by immune signalling molecules, which are themselves modulated by the presence of bacteria.

1.2.2.1 *Overview of the Response to Periodontal Pathogens and Innate Immunity*

Epithelial cells, fibroblasts, and innate immune cells are all encountered by pathogens on colonisation of the periodontium, and all of these cells are capable of contributing to the inflammatory response. Epithelial cells are the first encountered during colonisation and secrete a number of cytokines, including interleukin-8 (IL-8, also known as CXCL8), which is responsible for increasing blood vessel permeability and GCF flow, neutrophil migration and monocyte adhesion in blood vessels (Hajishengallis & Hajishengallis 2013).

Pathogens may penetrate the oral epithelium, making contact with gingival and periodontal ligament fibroblasts. Similarly to epithelial cells, fibroblasts secrete pro-inflammatory cytokines including IL-6, IL-8, and tumour necrosis factor (TNF), and other cytokines. This fibroblast response has been shown to be important in maintaining inflammation and potentially plays a role in periodontal disease progression, even though this is less well understood than epithelial cell interactions (Morandini et al., 2010; Sun, Shu, Li, & Zhang, 2010).

Many of the responses by the innate immune system are initiated by the interaction of several conserved bacterial surface components such as lipopolysaccharide (LPS) of Gram-negative bacteria, teichoic acids of Gram positives and other repeating structures of various pathogen types such as flagella, pili and surface proteins. In addition, lysed bacteria release genetic material that is also recognised by innate immune components. As a whole these conserved molecules are known as 'pathogen associated molecular patterns' (PAMPs). It is the recognition of these PAMPs by pattern recognition receptors (or PRRs, such as Toll-like receptors, (TLRs, reviewed later in this introduction) that elicits the release of host cytokines by cells that initially encounter pathogens, such as epithelial cells. As a result these signals cause the recruitment of immune cells such as neutrophils and macrophages which in turn then release further pro-inflammatory cytokines including tumour necrosis factor- α (TNF- α), IL-6, and IL-1 (Shaddox et al. 2011; Morandini et al. 2010). It is well established that during periodontitis, levels of these cytokines correlate with both

inflammation but also increased bone resorption (reviewed in Di Benedetto, et al., 2013), though ultimately production of receptor activator of nuclear factor κ B (RANKL) is responsible for the imbalance in osteoblast and osteoclast turnover that causes bone resorption (favoured by the increase in osteoclast number and activity). These signals, produced primarily by PAMP-activated neutrophils cause changes in macrophage phenotype, which themselves also express pro-inflammatory cytokines in the presence of PAMPS (Bodet & Grenier 2010).

In addition to neutrophils and macrophages, dendritic cells (DCs) are another group of innate immune cells with professional phagocytic capacity. These are present in the epithelia of blood vessels and within mucosal surfaces, including the gingiva, and in addition to cytokine production these cells also act to stimulate adaptive immunity as antigen presenting cells: DCs migrate from the epithelia to lymph nodes, where they are effective in stimulating T- cells, including Cytotoxic T-lymphocytes, also called natural killer T-lymphocytes (NKTs). Periodontitis lesions are rich in mature DCs, distinct from DCs in the surrounding gingival tissue (and in non-chronic tissue infections) because DCs typically mature as they migrate to lymph nodes (Tew et al. 2012), a trait also seen in other chronic conditions (such as atherosclerosis). In addition to production of pro-inflammatory cytokines, mature DCs may contribute to inflammation by antigen presentation on the CD1d receptor, which is recognised by NKTs, and some periodontal pathogens appear to activate specific subclasses of NKTs through antigen processing by DCs. For example, *A. actinomycetemcomitans* stimulates type 1 NKTs via antigen presentation by DCs *in vitro*, as does *P. gingivalis* in the presence of exogenous IFN γ , hinting at the importance of DCs in periodontal disease progression.

1.2.2.2 Innate Immune Components and Periodontitis

Neutrophils and macrophages are considered the most important sources of pro-inflammatory cytokines in periodontitis, which contribute to the switching of host cell phenotypes to states more associated with disease. In the case of innate immunity, this means overactivation of neutrophils to produce a number of cytokines and increased migration into the periodontium (section 1.2.2.2.1), and for macrophages it means the majority of the population differentiate to become “M1” macrophages-associated with inflammation, rather than “M2”-associated with healing and inflammatory regulation (section 1.2.2.2.2).

1.2.2.2.1 Neutrophils

Neutrophils are terminally differentiated leukocytes, which differentiate in the bone marrow and enter cardiovascular circulation. IL-17 is the major cytokine associated with activation and recruitment of neutrophils, as it causes up-regulation of granulocyte colony stimulating factor (G-CSF). Circulating neutrophils migrate to endothelial cells of tissues throughout the body, following a chemokine gradient of host secreted factors. At the gingivae, neutrophils migrate into the gingival crevice, coordinated by the presence of localised gradients of CXCL8, ICAM-1, and E-selectin (Hajishengallis & Hajishengallis 2013).

Once at the endothelium of the target tissue (gingivae) neutrophils utilise glycoprotein ligands-for example, the sialoglycan residue sialyl lewis X is important in mediating this interaction (Lowe 2003)-to bind endothelial cell surface E-selectin and initiate “crawling motility”, which leads ultimately to integrin dependent tight adhesion. Tight adhesion is mediated by integrin LFA-1 on neutrophils which binds the ICAM-1 receptor on endothelial cells, and the neutrophil moves via crawling motility to endothelial tight junction-a site suitable for transmigration-movement across the endothelium (Ley et al. 2007). Once they have reached their target tissue-in this case the periodontium-they are activated by stimulation of various receptors. These include TLRs, cytokine receptors, and perhaps most importantly the Fcγ receptor IIa, which binds Fcγ (heavy, conserved antibody chain)-important for recognition of antigens, which may be present on bacterial surfaces. Stimulation of the neutrophil via the Fcγ receptor IIa triggers a phagocytic response by the neutrophils, where bacteria are engulfed in intracellular vesicles-phagosomes, which fuse with lysosomes, forming phagolysosomes-an important mechanism in bacterial clearance. These phagolysosomes contain reactive oxygen species (ROS), and neutrophil serine proteases, including cathepsin G and neutrophil elastase- all of which are bactericidal. In addition these and other antibacterial products can also be released during degranulation, a poorly understood process by which neutrophils release pre-stored vesicular granules that act on extracellular microbes but also possibly contribute to inflammation and tissue damage in many conditions (Lacy 2006). Tissue damage leads to the production of host-cell derived damage associated molecular patterns (DAMPs) these include host DNA, chromatin associated proteins, heat shock proteins and intracellular metabolites such as uric acid (Shi et al. 2003; Kang et al. 2015). An additional, recently discovered function of activated neutrophils is the production of neutrophil extracellular traps (NETs). These consist of chromatin; DNA-and associated proteins such as histones, polysaccharides, and antimicrobials (White et al. 2016), which function by immobilisation and entrapment of

microbes-preventing further invasion of the tissue before killing with degranulation products. NETs were described relatively recently, with their role in periodontitis still under some debate: Studies of patients have found that levels of NETs are increased during periodontitis compared to healthy sites (Vitkov et al. 2009), and it has been suggested that the inability to clear NETs results in increased concentrations of neutrophil pro-inflammatory products, contributing to destructive inflammation. On the other hand, a decrease in the levels of NETs may contribute to disease progression-periodontitis is an age related condition, and age has been associated with decreases in NET production (Hazeldine et al. 2014). However, the contribution of NET production to disease is unclear since aging causes other effects that probably contribute to periodontitis.

Neutrophils have a short lifespan after differentiation, and are cleared after 6-8 hours, through apoptosis and phagocytosis by macrophages with phagocytic clearance playing an important role in downregulation of neutrophil recruitment, due to inhibition of IL-23, which mediates IL-17 production (Stark et al. 2005). Evidence for the importance of neutrophils in periodontitis comes from observations of patients with deficiencies in neutrophil production- known as neutropenia, a condition that arises under a variety of circumstances including autoimmune disease, HIV/AIDS, or as a result of chemo- or radiotherapy treatments and also in a wide range of congenital genetic conditions (Donadieu et al. 2011) such as Fanconi anaemia that are associated with severe periodontal disease (Goswami et al. 2016). Interestingly, one study noted an improvement in oral health with recombinant G-CSF treatment as part of an attempt to restore immunological status (Matarasso et al. 2009).

Excessive neutrophil activation may also contribute to periodontitis, due to their multiple pro-inflammatory mechanisms (ROS, and proteases can damage host cells, and stimulated neutrophils produce pro-inflammatory cytokines). Studies of periodontitis patients have linked disease severity with neutrophil hyper-reactivity, and disease severity has been associated with a single nucleotide polymorphism in the genes encoding Fcγ receptor IIa (Yamamoto et al. 2004), implying that neutrophil sensitivity to stimuli does play a role in periodontal disease. Several neutrophil responses may be involved in periodontitis: Neutrophil elastase (and other proteases) are elevated during periodontitis, and elastase is thought to be predictive (with other biomarkers) for periodontitis progression (Gul et al. 2016).

1.2.2.2.2 Macrophages

Peripheral blood monocytes migrate through the endothelium and differentiate to macrophages, which phagocytose bacteria and produce a variety of cytokines, playing a role in clearance of pathogens and in regulation of inflammation. On activation by bacteria, bacterial products, or cytokines/chemokines, macrophages can display varying phenotypes, a process termed polarisation. Macrophages may polarise into one of two subtypes, M1 or M2, although there is no strict distinction between the two, with macrophages falling on a spectrum from M1 to M2, with some macrophages termed “regulatory macrophages” (Sima & Glogauer 2013). In essence, M1 macrophages are considered pro-inflammatory, secreting IL-6, IL-8, and TNF among other cytokines, while M2 macrophages are considered to be associated with healing, secreting IL-10 and other factors. This is reflected in periodontitis, with several studies indicating that the M1 subpopulation is the dominant subset during periodontitis (Gonzalez et al., 2015; Yu et al., 2016, and others), although a recent study highlighted the potential for M1 macrophages to downregulate osteoclastogenesis *in vitro* (Yamaguchi et al. 2016), suggesting a more complicated picture for the role of macrophage subsets in periodontitis.

1.2.2.2.3 Toll-Like Receptors

Toll like receptors (TLRs) are expressed by multicellular eukaryote hosts, and impact heavily on bacterial infections due to their function in recognising PAMPs, and activating various inflammatory signalling cascades. At least ten TLRs have been characterised in humans, associated with the plasma membrane (TLRs -1, -2, -4, -5, -6, -10) and intracellular endosomes (TLRs -3, -7, -8, -9). All TLRs consist of an extracellular leucine rich repeat (LRR) region involved in ligand binding, a membrane spanning, and a cytosolic TLR/IL-1R (TIR) domain which functions in signal transduction. The TLRs and their intracellular signalling are summarised in figure 1.3.

TLRs -2, -4 and -9 are thought to be those responsible for immune signalling resulting in inflammation during periodontitis, as these TLRs have been shown to be upregulated in patients with aggressive periodontitis, both localised and generalised (Sahingur et al. 2013; Wara-Aswapati et al. 2012; Kikkert et al. 2007). TLR-2 recognises peptidoglycan and bacterial lipoproteins, and has been shown to be up-regulated in periodontal ligament cell lines exposed to *P. gingivalis*, *P. intermedia*, *F. nucleatum*, or *A. actinomycetemcomitans* (Sun et al. 2010). *T. forsythia* has also been shown to induce pro-inflammatory cytokines through TLR-2 activation via Bacteroides surface protein A-discussed later (Kikkert et al. 2007).

TLR-4 recognises bacterial LPS, and while the importance of TLR-2 appears clear cut, the role of TLR-4 for certain periodontal pathogens is less well defined. *P. intermedia*, *F. nucleatum*, or *A. actinomycetemcomitans* but not *P. gingivalis* have been shown to induce production of pro-inflammatory cytokines through TLR-4. Some studies indicate that *P. gingivalis* LPS does not readily activate TLR-4, only doing so in high concentrations (Wara-Aswapati et al. 2012). On the other hand, comparison of pro-inflammatory cytokines in periodontitis-patient blood showed that periodontal therapy results in a decreased sensitivity to *P. gingivalis* LPS (Kikkert et al. 2007). These findings highlight the importance of different species acting synergistically to stimulate multiple TLRs and cause inflammation during periodontitis.

TLR-9 is activated by non-methylated CpG DNA motifs found in bacteria and viruses. TLR-9 has been shown to be upregulated during periodontitis, in tissues affected by periodontitis (Sahingur et al. 2013), and in cell lines challenged with *P. gingivalis*. The up-regulation of TLR-9 is also of interest as herpesviruses have been shown to be associated with periodontitis (Alexandra et al. 2008; Grande et al. 2011). It is therefore entirely possible that bacteria and viruses act synergistically in activation of TLR-9, and when coupled with additional pro-inflammatory signalling of TLRs -2 and -4 this causes more severe disease compared to infection with bacteria alone.

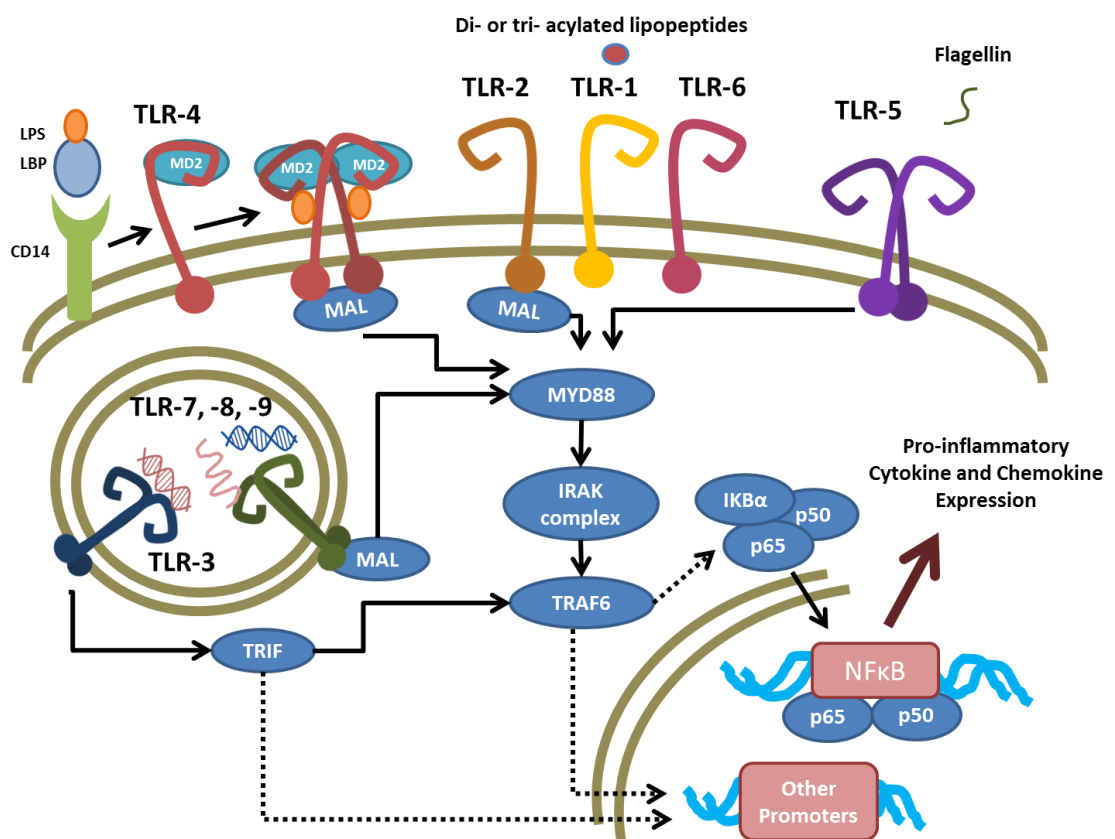


Figure 1.3. Summary of TLR activation and key signalling events leading to pro-inflammatory signalling.

TLR-4 and -5 form homodimers on binding to their ligands; TLR-5 recognises flagellin, while TLR-4 recognises lipid A of LPS through LPS binding protein (LBP), and activation through formation of a complex with myeloid differentiation factor 2 (MD2) and CD14. TLR-2 forms a heterodimer with TLR-1 or -6 on binding either triacetylated or diacetylated lipopeptides, respectively. TLR-1 appears to share ligand specificity with TLR-2, and may have other unique ligands. The ligands for the intracellular TLRs -7 and -8 are single stranded (ss) RNA, TLR-9; unmethylated CpG rich DNA, while TLR-3 recognises double stranded (ds) RNA. All of the intracellular TLRs form homodimers on binding their ligands. All TLRs with the exception of TLR-3 signal through myeloid differentiation factor 88 (MyD88), which requires an interaction between TIR and a MyD88 adaptor-like (MAL) Protein. MyD88 complexes with Il-1 receptor associated kinase (IRAK) proteins, sometimes termed the “myddosome”, and this allows signalling through TNF receptor associated factor (TRAF) 6. Through further signalling molecules, this ultimately results in degradation of inhibitor of NFκB (IκBα), releasing p50 and p65, and formation of the NFκBp65p50 complex, a key promoter of pro-inflammatory gene expression. Some intermediate signalling molecules are not shown, indicated by dotted lines (reviewed in Gay, Symmons, Gangloff, & Bryant, 2014; McClure & Massari, 2014).

Two other pro-inflammatory promoters are also activated downstream of TRAF 6, cAMP-responsive element-binding protein (CREB), and Activator Protein 1 (AP-1). TLR-3 does not act through the myddosome, instead operating through TIR domain-containing adaptor protein inducing IFN β (TRIF), which may activate TRAF6 and associated downstream signalling, but primarily acts to stimulate an antiviral response: TRIF activates a signalling cascade which activates IFN-regulatory factor (IRF) promoters, resulting in expression of interferon (IFN) stimulated response elements (ISREs) 3 and 7, production of type I IFN, and ultimately, stimulation of other antiviral responses such as T-cell activation. All signal transduction pathways are part-regulated by cross-talk during regulation of apoptosis or cell survival.

1.2.2.2.4 Complement

Complement is present in human serum, including GCF and functions directly in innate immunity through bacterial killing or opsonisation, and can stimulate cytokine production and activation of innate or adaptive immune cells. Complement activation occurs via a protein cascade (designated C1-9) and may occur through one of three pathways; classical, lectin binding, or alternative, as summarised in figure 1.4. Ultimately, the pathway results in production of membrane attack complexes (MACs) on pathogen surfaces, causing them to lyse. Complement also marks pathogens for phagocytosis (termed opsonisation). (reviewed in G. Hajishengallis, 2010). Given the involvement of complement in a variety of immune functions, over-stimulation or disruption of regulatory pathways can result in or influence disease progression.

Multiple mechanisms involving complement upregulation have been linked with periodontitis. It was observed that patients with periodontal disease have increased complement cleavage products in their GCF (Schenkein & Genco 1977), and more severe periodontal disease (increased pocket depth) is associated with an increase in cleavage products (Niekrash & Patters, 1986). An experimental human gingivitis model also showed a positive correlation between inflammation (gingival indices and BOP), and increased cleavage products (Patters et al. 1989). In addition, periodontitis therapy reduces the amount of complement cleavage products in the GCF of patients being treated for periodontitis, and decreases levels of C3 gene expression (Niekrash & Patters, 1986). Furthermore, expression of C3 by gingival tissue is also down-regulated following non-surgical periodontal treatment, relative both to before-treatment, and to healthy control patients (Beikler et al. 2008).

This correlation between complement cascade upregulation and periodontal disease hints at a possible role of complement in causation of periodontitis, but is unsurprising given the corresponding increase in bacterial load seen in study participants-i.e. upregulation of the complement system could be a product of periodontal disease rather than a contributing factor. However, it has been shown that C3b and C5a complement factors are required for alveolar bone loss during *P. gingivalis* infection in murine models, and that expression of pro-inflammatory cytokines (TNF, IL-1 β , IL-6, and IL-17) is inhibited by a C5aR antagonist (Liang et al. 2011, Abe et al. 2012). A C5aR antagonist was also shown to reduce expression of pro-inflammatory cytokines and inhibit alveolar bone loss in a murine model of periodontitis. These studies point to the importance of C5a in up-regulation of other inflammatory responses rather than other complement factors in direct cellular killing (i.e. autoimmunity through deposition of complement on host cells). Therefore, complement and C5a activation in particular is important in promoting inflammation, and together with TLR based signalling determines the progression of periodontitis (Hajishengallis & Lambris 2010).

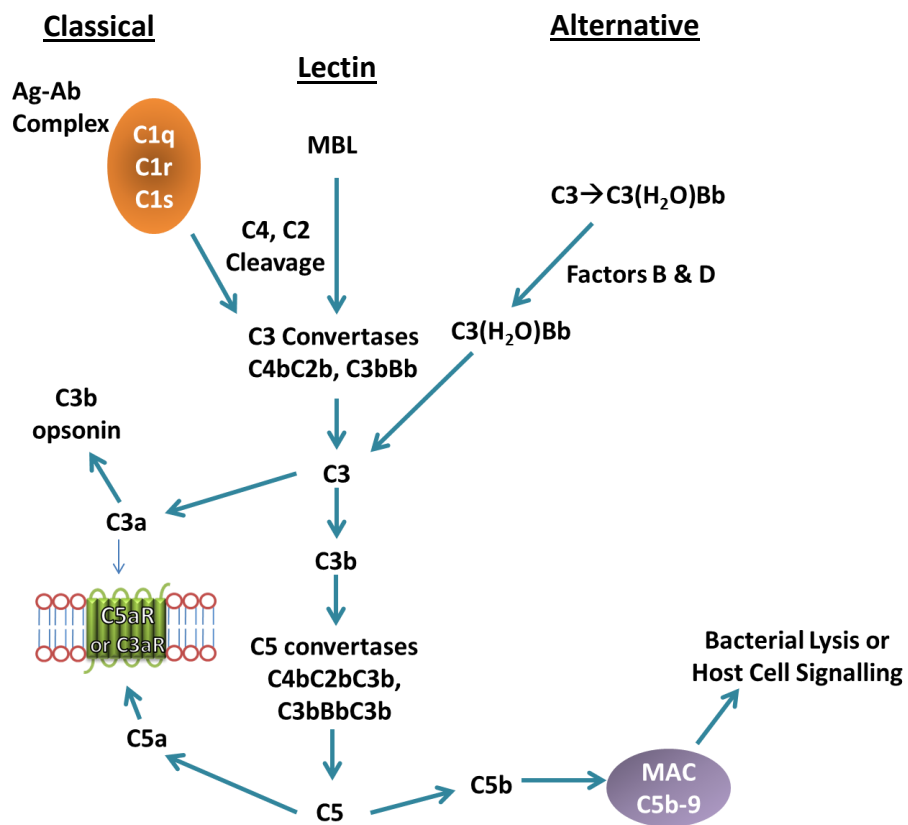


Figure 1.4. The complement cascade featuring complement (C) proteins 1-9.

The classical pathway begins at the antigen-antibody (Ag-Ab) complex, to which the C1q subunit of C1 binds, activating and causing C4 and C2 cleavage. The lectin pathway also causes C4 and C2 cleavage, but is initiated by mannose binding lectin (MBL) which recognises bacterial glycans. C4 and C2 cleavage results in formation of C3 convertases C4bC2b and C3bBb (The C2a and C4a subunits diffuse away). The alternative pathway results from hydrolysis of C3 to C3(H₂O), a C3b analogue. The presence of factors B and D, results in formation C3(H₂O)Bb, another C3 convertase. At this point, all three pathways converge, and the C3 convertases cleave C3 to C3b and C3a. C3b acts during opsonisation through the complement receptors (CRs) 1 and 3 present on phagocytic cells, but may also interact with previous products of the cascade to form C5 convertases; C4bC2bC3b, and C3bBbC3b. C5 is then cleaved into two subunits, with functions for both products. C5a and C3a both regulate the C3a receptor (C3aR) and C5a receptor (C5aR, of which there are two, C5a1 and C5a2) G-protein coupled receptors (GPCRs) on leukocytes, resulting in leukocyte activation and migration-and ultimately upregulation of inflammation. C5a also interacts with C5aR-like (C5aRL) GPCR, which has regulatory roles in complement-mediated activation of leukocytes. C5b begins the terminal pathway, binding to (microbial) cell membranes, and forming a complex with C6-9, which is termed the membrane attack complex (MAC). This results in bacterial lysis, or host signalling at sub lytic concentrations (Reviewed in Hajishengallis & Lambris, 2010; Hajishengallis, 2010).

1.2.2.3 *Adaptive Immune Response*

T- and B- cells differentiate and mature in the lymph nodes, and may migrate to host tissues. Both groups of lymphocytes have been found in periodontitis lesions, implying a role for both during periodontitis. Several studies indicate that B-cells and a humoral immune response do not contribute to clearance of periodontal pathogens and resolution of periodontitis: Mice immunised with the pathogens *P. gingivalis* and *F. nucleatum* express circulating antibodies against these pathogens in their serum, but when infected with both *P. gingivalis* and *F. nucleatum* this does not illicit protection from colonisation and disease (Choi et al. 2001; Gemmell et al. 2002). More recently however, immunization of mice utilizing certain adjuvants or specific *P. gingivalis* proteins to generate specific anti-virulence factor antibodies has shown that given appropriate stimulation, B-cells and antibody production can contribute to periodontal disease resolution (Wilensky et al. 2016; Curtis et al. 1999).

T-cells definitely play a part in periodontitis progression, but the picture is complex. Earlier histological studies of periodontitis lesions seemed to show that T-cells were important in preventing periodontal disease, with the switch from a gingivitis to periodontitis lesion coinciding with decreases and increases of T- and B- cell levels, respectively (Yamazaki et al. 1993). In addition to confirming the association of B-cells with periodontitis, CD8+ T-cells were later shown to be important in suppressing osteoclastogenesis (Choi et al. 2001). However, CD8+ T-cells are not the only T-cell type present during periodontitis. Sub-populations of T-helper (Th, also known as CD4+) cells have also been described, beginning with the Th1 and Th2 subsets, the levels of Th1 being considered most important in periodontitis progression since this subset expresses higher levels of RANKL (reviewed in Hienz, Paliwal, & Ivanovski, 2015). In addition, Th17 and Treg subsets of Th cells have been described, with pro- and anti-inflammatory roles, and over-stimulation of either subset seems to be capable of progressing periodontal disease: *T. forsythia* has been shown to stimulate the proliferation of Th17 cells in mice via its surface-layer (discussed further in section 1.5.2), and this coincides with increased alveolar bone loss (Settem et al. 2013). The final subset of Th cells-Treg- has been shown to infiltrate periodontitis lesions to a greater extent than gingivitis lesions, possibly implying that they are important in mediating the switch to periodontitis (Nakajima et al. 2005). There is also a possibility of crosstalk between the innate and adaptive immune responses through Th cells (the Treg and Th17 subpopulations), and the complement system. Increased activation of the complement

system has been shown to increase Th17 cell proliferation in mice stimulated by mannan (activating the lectin binding pathway), mice deficient in the receptor for C5a (C5aR) do not display increased Th17 cell proliferation (Hashimoto et al. 2010).

1.2.3 Other Factors in Periodontitis Onset and Progression

1.2.3.1 Age

Severe periodontitis usually occurs from ~38-40 years of age, with severity sometimes increasing as the patient ages, but often remaining stable (Kassebaum et al. 2014). Indeed, its presence in children is often referred to as juvenile –or- early onset periodontitis, though these classifications are supposedly redundant, in favour of the term “aggressive periodontitis”, since age-dependent classification has never been validated (Armitage 2013). In any case, aging and accompanying cellular senescence in general is marked by progressive modifications to the immune system as a result of anti-stress responses, which primarily act to control aging. However, the progressive alterations to the immune system results in what has been termed “immunosenescence” or “inflamm-aging”, where extensive immune-modification results in greater susceptibility to infection, neoplasia, and autoimmunity (reviewed in Ebersole et al., 2016). However, biomarkers associated with age/immunosenescence and age-related conditions occur to similar extents in both healthy and non-healthy individuals (Baggio, et al. 1998). Furthermore, not all adults are affected by periodontitis, so other factors must play roles in modulating the microbiota and inflammatory response.

1.2.3.2 Diabetes and Obesity

Periodontitis is associated with diabetes (Eke et al. 2016) and obesity (Gaio et al. 2016), and it has been suggested that there may be a causal or bi-directional relationship between either condition and periodontitis.

The majority of research between periodontitis and diabetes has focused on type 2 diabetes, in which patient genetics, diet, and body mass index (BMI) play central roles resulting in resistance to insulin. Periodontitis has been suggested to cause increased susceptibility to type 2 diabetes by increasing circulating levels of TNF, which acts to cause insulin resistance through a number of mechanisms. The onset of diabetes causes neutrophil dysfunction as well as increased levels of IL-1 and TNF, both of which are considered important in periodontitis progression (reviewed in Gurav, 2012).

Obesity or a high BMI also appears to be a risk factor for periodontitis (Eke et al. 2016; Suvan et al. 2015). *In vivo* rat models showed that obesity alone may be sufficient to induce

periodontitis (Cavagni et al. 2013), or exacerbate periodontitis symptoms (Cavagni et al. 2015), as evidenced by alveolar bone loss in rats that were overweight due to high fat/calorie diets. Suggested mechanisms for this include increased circulating pro-inflammatory cytokines in obese individuals (Vincent & Taylor 2006) and increased oxidative stress in the periodontal pocket/GCF of obese individuals (Atabay et al. 2016).

1.2.3.3 *Smoking*

Smoking is a well-established risk factor in many diseases, and periodontitis is no exception (Eke et al. 2016). Suggested mechanisms linking smoking to periodontitis (reviewed in Johannsen, Susin, & Gustafsson, 2014) include exposure to higher levels of ROS (in cigarette smoke), decreased neutrophil migration, decreased levels of osteoprotegerin (the antagonist of RANKL), and decreased antibody production (smokers display decreased levels of serum Ig, particularly IgG2).

1.3 Periodontitis-Systemic influences

Although periodontitis does not cause mortality directly, it does have a high prevalence and considerable morbidity, and a growing body of evidence hints at its contribution to other conditions (reviewed in Han, Houcken, Loos, Schenkein, & Tezal, 2014). This includes head and neck cancer, atherosclerosis/heart disease, and other morbid conditions such as rheumatoid arthritis.

1.3.1 Head and Neck Cancer

Although the possible correlation between head and neck (and other) cancers with periodontitis is well documented (Moergel et al. 2013; Tezal et al. 2005; Wen et al. 2014), establishing a causal relationship between the two is difficult due to the role of smoking in both conditions. However, it was been shown that in men who self-report as having-never-smoked, the incidence of smoking related cancers (including head and neck cancers) was increased in men with advanced periodontitis (Michaud et al. 2016). While this correlation does not prove causality, mechanisms by which periodontal pathogens might contribute to oral cancer have been described, with cell-based studies highlighting the ability of *P. gingivalis* to increase migration, invasiveness, and cancer/stem cell associated biomarkers in an oral squamous cell carcinoma (OSCC) cell line (Ha et al. 2015). An *in vivo* model also showed that in mice with induced oral carcinomas, infection with *P. gingivalis* and *F. nucleatum* caused increases in tumour growth (size) and invasion, as well as increased expression of certain biomarkers in the oral mucosa that are either associated with oral cancer or cause increased tumourigenesis, such as the proinflammatory cytokine IL-6 (Gallimidi et al. 2015). However, this work is still in its infancy and it will be of interest to

note how this story develops over the coming years. It is notable though that the common oral bacterium *Fusobacterium nucleatum* has been strongly linked with colorectal cancer, via the action of its surface adhesin FadA (Rubinstein et al. 2013). This fact alongside various observations regarding *P. gingivalis* in terms of anti-apoptotic action suggest several mechanisms that might lead one to believe periodontal pathogens may be cancer promoting, if not causing (Whitmore & Lamont 2014; Kuboniwa et al. 2008).

1.3.2 Heart Disease and Atherosclerosis

The association and causative link between periodontitis and heart disease (or more specifically atherosclerosis) is fairly well established, with an ever-growing body of evidence indicating that patients with increased severity of periodontitis are more likely to suffer from atherosclerosis and other cardiovascular disease (CVD) (Demmer & Desvarieux 2006; Beck & Offenbacher 2005; Spahr et al. 2006), or experience additional cardiac problems (Reichert et al. 2016). There is also evidence indicating periodontal bacteria and associated inflammatory responses play a causative role in the development of heart disease: A high proportion of atheromatous plaques extracted from CVD patients have been shown to contain DNA from a variety of periodontal pathogens (Haraszthy et al. 2000), and viable periodontal pathogens have been isolated from atheromatous plaques in patients with chronic periodontitis (Padilla et al. 2006). Several mechanisms by which the periodontal pathogens contribute to atherosclerosis/CVD have been suggested (reviewed in Schenkein & Loos, 2013): Firstly, increased levels of systemic biomarkers/inflammatory mediators relevant or associated with both atherosclerosis/CVD and periodontitis-such as IL-6, C-reactive protein, and low density lipids. Secondly, through induction of self-recognising antibodies, as seen in the case of antibodies against the heat shock protein (HSP) 60 of *P. gingivalis*. Aortic inflammation in response to periodontitis has also been shown *in vivo* using a rat model (Miyajima et al. 2014), where ligature-induced-periodontitis increased pro-inflammatory cytokine expression in circulating monocytes (Tumour Necrosis Factor (TNF) and IL-6), and monocytes also displayed increased adhesion to vascular endothelial cells, which themselves displayed greater intracellular markers of inflammation (VCAM-1 and NFκB).

1.3.3 Rheumatoid Arthritis

Rheumatoid arthritis is perhaps the most well established extra-oral condition linked with periodontitis, with an early observation of their association made by Hippocrates (460-370 BC). More recent, wider-scale studies have confirmed this association (Joseph et al. 2013; Chou et al. 2015). Mouse models have shown that periodontal bacteria can influence the

progression of Rheumatoid Arthritis, with *P. gingivalis* playing a central role in disease (Yamakawa et al. 2016). In humans, associations between the levels of *P. gingivalis*, periodontal disease, and rheumatoid arthritis severity have also been reported (Mikulski et al. 2014; de Smit et al. 2012). A biological mechanism has also been described, which implies that periodontal disease and more specifically *P. gingivalis* is a causative factor of rheumatoid arthritis: *P. gingivalis* possesses genes encoding a peptidyl arginine deaminase (PAD), which citrullinates some of its expressed proteins (Gabarrini et al. 2015). Protein citrullination is usually only performed in higher eukaryotes including humans (indeed, *P. gingivalis* is the first bacteria shown to possess the capacity for protein citrullination). This results in the generation of anti-citrullinated-peptide antibodies, which possess self-recognising properties and are highly associated with rheumatoid arthritis onset (Gabarrini et al. 2015).

1.4 Treatment of Periodontitis

Treatment of periodontitis aims primarily to prevent further attachment loss, primarily by removing the periodontal pathogens responsible for promoting inflammation, and in some cases removing severely inflamed or damaged tissue (which is also beneficial in reducing the periodontal pocket depth). The two approaches used here can be considered surgical and non-surgical. Systemic antibiotics such as azithromycin (Muniz et al. 2013) can be administered as an adjunct to mechanical removal of the subgingival plaque, and this results in improved clinical parameters compared to treatment in their absence (Guerrero et al. 2005), with at least one study suggesting that this is due to the complete removal of red complex organisms by the antibiotic-therapeutic adjunct (Jünemann et al., 2012), although recolonization and re-population by red complex species post-treatment is likely even in the case of antibiotic-treated individuals (Johnson et al. 2008). In any case, despite treatment a proportion of patients poorly-respond to periodontal therapy, and it appears that post-treatment, in these patients the levels of certain periodontal pathogens (including the red-complex pathogens) are higher than in patients who respond to treatment, or in healthy controls (Colombo et al. 2009).

Considering the impact of periodontitis on the quality of life of patients, its apparent involvement in other conditions, and the occasional inability to successfully treat disease, research into the virulence mechanisms of the periodontal pathogens with a view to improving treatment is a worthwhile pursuit.

1.5 Virulence Factors of the Periodontal Pathogens

As discussed above, the Gram negative, anaerobic red complex organisms *T. forsythia*, *P. gingivalis*, and *T. denticola* are the three sub-gingival species most strongly correlated with severity of periodontitis (Socransky et al. 1998), and of these three organisms, *T. forsythia* and *P. gingivalis* are the focus of this thesis. Also associated with periodontitis are species comprising the orange complex, of which the gram negative, anaerobic *Fusobacterium* spp. including *Fusobacterium nucleatum* and its various subspecies are prominent members, so *F. nucleatum* is also focused on in later chapters. These pathogens can be considered distinct from commensals due to their expression of virulence factors, which can be defined as “processes or products of pathogenic organisms which contribute to disease”. While technically all of the processes involved in a pathogen’s lifecycle will contribute to disease by simply allowing survival of the pathogen (for example, carbon metabolism or amino acid synthesis), virulence factors are usually taken to mean those that damage the host directly (for example, a secreted toxin) or indirectly (for example, lipopolysaccharide (LPS) over-stimulating an inflammatory response). Virulence factors may also allow persistence of a microbial pathogen despite an immune response or allow competition with other bacteria in its environment. For example, the ability to persist in the face of a lack of freely available nutrients, or the presence of antibiotics, may permit spread of an organism from the original site of colonisation to other sites within the host. Factors that allow attachment to surfaces (including host cell surfaces) and invasion (also termed internalisation) of host cells can also be considered virulence factors.

1.5.1 *Porphyromonas gingivalis*

Perhaps the most well characterised member of the red complex, *P. gingivalis* has been called the “Keystone Pathogen” (Hajishengallis et al. 2012), being considered the most important organism in causing or maintaining inflammation and resulting dysbiosis responsible for periodontal disease progression. Some of its most important virulence factors are its fimbriae, capsule, and its arginine/lysine proteases-the gingipains.

1.5.1.1 *Fimbriae*

P. gingivalis expresses two different fimbriae on its surface; major and minor (also called long and short), which are composed of protein subunits FimA and Mfal, respectively. Major fimbriae are considered important for initial attachment as they have been shown to bind epithelial cells (Umemoto & Hamada 2003), and in the case of endothelial cells major fimbriae attach via the host cell integrins (Yilmaz et al. 2002). Major fimbriae are also involved in binding to *Streptococcus oralis* and *Streptococcus gordonii*- early/intermediate

colonizers of the gingiva (Park et al. 2005; Maeda et al. 2004) *P. gingivalis* strains possess multiple copies of the *fimA* gene, with variations coding for slightly different proteins. Based on variation of *fimA* genes, the major fimbriae have been classified into 6-types, types I-V and Ib (Amano, Nakagawa, Okahashi, & Hamada, 2004). Strains expressing Type II major fimbriae have been shown to be associated with more severe periodontitis compared to strains expressing the other types, and were found to have greater attachment and invasiveness during infection of host cells. In periodontally healthy patients positive for *P. gingivalis* colonisation, type I fimbriae strains were the most prevalent (Amano et al., 2004), highlighting the relevance of different strains to periodontal infection, and inferring that different fimbriae can influence the outcome of periodontal infection.

The role of minor fimbriae in virulence is less well characterised. However, mutant strains of *P. gingivalis* that did not express minor or major fimbriae have shown complete loss of adherence to oral epithelial cells, while strains expressing only minor fimbriae retained some ability to adhere to epithelial cells. Invasion of host cells was also reduced 8-fold in minor fimbriae deficient strains (Umemoto & Hamada 2003).

1.5.1.2 **Polysaccharide Capsule**

Polysaccharide capsules are a common feature of Gram negative bacteria, and are thought to function by 'covering' other surface antigens which would otherwise make the organism vulnerable to an adaptive immune response, or complement deposition. It has been observed that non-encapsulated strains of *P. gingivalis* are more virulent than encapsulated strains in a mouse abscess model (Singh et al. 2011), but are unable to spread systemically. *P. gingivalis* non-encapsulated strains also induce higher cytokine secretion (IL-6, IL-10, TNF- α , and IFN- γ) in macrophages than wild type strains, and undergo phagocytosis more rapidly (Singh et al. 2011), as well as inducing cytokine transcription more rapidly in human gingival fibroblasts. This highlights the importance of the capsule in *P. gingivalis* immune evasion.

1.5.1.3 **Gingipains-Secreted Proteases of *P. gingivalis***

P. gingivalis expresses serine proteases, two of which cleave at lysine residues-RgpA and RgpB, and one which cleaves at lysine-Kgp. Termed "gingipains", these are considered paramount to *P. gingivalis* pathogenicity, with evidence for their involvement in multiple pathogenic processes coming from studies of gingipain-deficient mutant strains.

The first study of RgpA and RgpB-null mutants showed almost complete abrogation of proteolytic activity in culture supernatants of a strain deficient in both proteases (activity

was also substantially reduced in strains deficient in one of the two arginine-gingipains) (Nakayama et al. 1995). Functional studies of the double Rgp mutant showed decreased haemagglutination and decreased activation of leukocytes relative to the wild type strain, providing evidence for their role in immune-stimulation and attachment to host cells (Nakayama et al. 1995). Further work using Rgp and Kgp deficient mutants and purified gingipains has confirmed their role in host cell attachment, and in immune system interactions such as serum/complement resistance (Grenier et al. 2003), cleavage of CD4 and CD8 proteins from T-cell surfaces (resulting in downregulation of T-cell responses) (Kitamura et al. 2002), and cleavage and inactivation of antibodies (Vincent et al. 2011). Furthermore, gingipains are important for nutrient acquisition by *P. gingivalis*, since it utilises free amino acids for catabolism, and gingipains have been shown to be required for growth in chemically defined media (containing only host proteins as carbon and nitrogen sources), since they degrade host proteins-releasing amino acids and peptides (Grenier et al. 2001). Gingipains also interfere with intracellular signalling pathways in oral epithelial cells during invasion, specifically, by degradation of mTOR (mammalian target of rapamycin, Stafford et al. 2013), which may be the major mechanism by which *P. gingivalis* induces autophagy or changes to the host-cell lifecycle.

The importance of gingipains are also highlighted by *in vivo* studies, where a mouse model of periodontitis (measuring alveolar bone loss in *P. gingivalis* infected mice) showed that infection with RgpA-deficient strains induce significantly less bone loss than the wild type strain (Wilensky et al. 2013).

1.5.2 *Tannerella forsythia*

Early studies of *T. forsythia* (initially named "*Bacteroides forsythus*") were hampered by an inability to culture it in isolation from other organisms. It was later discovered that exogenous N-acetylmuramic acid (NAM, one of the two monomers in peptidoglycan) was required for the growth of *T. forsythia* in monoculture (Wyss 1989). Despite being poorly understood initially, the organism's biology, virulence factors, and how they contribute to disease are beginning to come to light, partly as result of work described in this thesis. Previously characterised virulence factors include the proteinaceous, glycosylated surface layer (S-layer), Bacteroides surface protein (BspA), and proteases including PrtH (also called "forsythia detaching factor" (FDF)) and karilysin.

1.5.2.1 *T. forsythia* surface layer

The S-layer of *T. forsythia* is composed of two glycosylated proteins; TfsA and TfsB. It appears to be a multi-functional virulence factor. Firstly, it has been shown to interact with

the host immune system in a number of ways: It is antigenic, with periodontitis patients possessing elevated anti-S-layer IgG compared to healthy controls (Yoneda et al., 2003). However, this humoral immune response does not result in clearance of *T. forsythia*, possibly due to biofilm formation preventing antibody binding, or the fact that *T. forsythia* does not penetrate deeply into the tissues. The S-layer also functions in serum resistance (Shimotahira et al., 2013), and could therefore be considered important for survival due to the presence of GCF in the periodontal pocket. S-layer deficient mutants have been shown to increase the viability of macrophages resulting in more rapid expression of pro-inflammatory cytokines (IL-1 β and TNF- α) compared to wild type *T. forsythia* (Sekot et al., 2011), indicating a role for the S-layer in delaying, or perhaps redirecting the innate immune response. The importance of S-layer glycosylation in immune modulation by *T. forsythia* has been the focus of recent studies. The gene encoding WecC, responsible for incorporation of a trisaccharide motif into the S-layer glycan of *T. forsythia* was deleted, resulting in increased uptake and phagocytosis by dendritic cells (DCs), followed by antigen presentation and increase in secretion of the Th17-activating cytokines IL-6 and IL-23. Thus, this glycosylation under the control of WecC is key in delaying the immune response. The importance of the S-layer in immune modulation is underlined by *in vivo* studies: Wild type *T. forsythia* was shown to inhibit Th17 T-cell responses, while a mutant with an altered terminal glycan moiety (lacking the pseudaminic acid branch-a sugar related to sialic acid) induced robust Th17 responses and phagocytosis dependent killing, resulting in reduced alveolar bone loss in mice infected with S-layer deficient *T. forsythia* compared to mice infected with the wild type strain (R P Settem et al., 2013).

In addition to immune-modulatory functions, the S-layer is also involved in mechanisms of attachment in the oral cavity: mutant strains lacking one or both Tfs proteins have shown reduced adherence or invasion of oral epithelial cells (Sakakibara et al. 2007). Furthermore, Tfs single or double mutants also show decreased haemagglutination compared to the wild type. Given that bleeding occurs during non-destructive periodontal disease where *T. forsythia* may not be present, or only in low numbers, attachment to red blood cells could be a useful mechanism of adherence allowing *T. forsythia* to colonise, or do so more extensively. Haemagglutination by *T. forsythia* (via the S-layer) appears to be sensitive to sialyllactose (Murakami et al. 2002), highlighting the importance of host glycoconjugates in *T. forsythia* attachment, a particularly important observation in the context of the work described in this thesis. In addition to host cell binding, S-layer deficient *T. forsythia*

mutants show decreased co-aggregation with the early coloniser *S. sanguinis* compared to wild type *T. forsythia* (Shimotahira et al., 2013).

1.5.2.2 ***Bacteroides Surface Protein A***

A second important virulence factor for *T. forsythia* is BspA, also expressed at the surface of *T. forsythia*. Similarly to the S-layer, BspA is considered a multifunctional virulence factor for *T. forsythia*. Roles include attachment and invasion of epithelial cells (Mishima & Sharma 2011), coaggregation with orange and red complex species, and immune system modulation (Myneni et al. 2012). BspA consists of four subunits: The N-terminal, leucine rich repeats (LRRs), Bacterial Ig-like domains, and the C-terminal. In the context of attachment, *T. forsythia* mutants deficient in BspA show a twofold decrease in aggregation with *F. nucleatum* compared to the wild type, but do not show a significant decrease in biofilm formation (Sharma et al. 2005). These findings indicate a central role for BspA in initial colonisation of the periodontium by *T. forsythia* with *F. nucleatum* as a bridging organism. Another study investigated the role of BspA in epithelial cell co-infection with *T. forsythia* and *P. gingivalis*: *T. forsythia* BspA mutants displayed decreased attachment and invasion of oral epithelial cells in both the presence and absence of *P. gingivalis* (or *P. gingivalis* outer membrane vesicles) compared to wild type *T. forsythia* (Inagaki et al. 2006). However, the study did not show decreased co-aggregation of BspA mutants with *P. gingivalis*, in contrast to the co-aggregation studies with *F. nucleatum*. Taken together, these studies point to a mechanism by which *T. forsythia* co-aggregates with *F. nucleatum*, allowing initial colonisation, which is followed by association with epithelial cells through a BspA dependent pathway that acts synergistically with *P. gingivalis*, or *P. gingivalis* outer membrane vesicles (Inagaki et al. 2006).

Similarly to the S-layer, BspA appears to play roles in immune-modulation, and adhesion and maintaining colonisation in the oral cavity: Regarding immunity, BspA has been shown to act through TLR-2 (Hajishengallis et al., 2002), and is antigenic; causing production of specific IgG and IgA in the serum in mice immunized with BspA. Again, the humoral response was not sufficient to clear *T. forsythia*. Furthermore, a mouse model of periodontitis comparing wild type to BspA deficient strains showed that BspA is important in alveolar bone resorption (Sharma, Inagaki, Honma, et al., 2005) presumably due to induction of cytokines through TLR-2 activation, resulting in differentiation of osteoclasts.

1.5.2.3 *Secreted Proteases*

The *T. forsythia* genome encodes several putative proteases, but karilysin and PrtH (also called forsythia detaching factor, FDF) have been the subject of study due to their multiple apparent functions in virulence. The two proteases are distinct; karilysin has been termed metalloprotease-like, while PrtH is considered similar to caspases due to its caspase like fold (incidentally, the *P. gingivalis* gingipains also possess caspase-like folds).

Karilysin has been shown to play roles in immunomodulation, firstly by protecting *T. forsythia* from the antimicrobial effects of human serum. Karilysin was shown to inhibit deposition of complement components activating the classical and alternative pathways (MBL and C4). Even so, *T. forsythia* is recognised by complement (as evidenced by C3 deposition on the *T. forsythia* surface), but karilysin also interferes with the terminal pathway (from complement component C5 onwards) (Jusko et al. 2012). A second metalloprotease from *T. forsythia*, mirolysin, has also been shown to prevent deposition of complement components (in the classical, alternative, and terminal pathways), contributing to complement resistance of *T. forsythia* (Jusko et al. 2015). In addition to its functions in immune-evasion by preventing the action of complement, *T. forsythia* may upregulate inflammation by interacting with macrophages. Karilysin was shown to cleave membrane-associated TNF from macrophages, and as well as increasing levels of soluble TNF, levels of IL-6 (another pro-inflammatory cytokine), were also increased.

Exposure of host cells to *T. forsythia* extracts led to the discovery of a cytopathic “forsythia detaching factor” (FDF), which was later cloned and expressed in *E. coli*, and further characterised, enabling its designation as PrtH (Nakajima et al. 2006). Although the cell-killing activity of PrtH has been characterised, its mode of action and precisely how it contributes to disease remains unclear. However it may show some clinical relevance: A 5-year longitudinal study showed that periodontitis patients with higher levels of PrtH (quantified by real-time PCR) displayed greater attachment loss over a five year period.

1.5.3 *Fusobacterium nucleatum*

F. nucleatum is currently subdivided into five subspecies; *nucleatum*, *polymorphum*, *vincentii*, *fusiforme*, and *necrophorum* (Dzink et al. 1990). *Fusobacterium nucleatum* subsp. *nucleatum* (*F. nucleatum*) and *Fusobacterium nucleatum* subsp. *polymorphum* (*F. polymorphum*) are the most common subspecies isolated from the human oral cavity. The major role of *Fusobacterium* spp. in periodontitis pathogenesis appears to be during association with host cells and other bacteria, where it utilises its adhesins to aid in colonising the plaque, and by doing so it can facilitate other pathogens' attachment.

F. nucleatum has been shown to play a role in adherence of other periodontal pathogens, implicating this species' importance in the progression of periodontal disease. It has been well established that *F. nucleatum* co-aggregates with Gram positive early colonisers (Kolenbrander et al. 1989), and that this is important for its integration into the oral microbial community of the supra-gingival plaque (He et al. 2012). Furthermore, membrane capture approaches (where one bacterial species is immobilised to a surface, then exposed to suspensions containing other bacteria to observe inter-species co-aggregation) and analysis of 16S ribosomal-DNA have been used to highlight the ability of *F. nucleatum* to adhere to a number of different species enriched from saliva, including *Gemella*, *Granulicatella*, *Neisseria*, and *Peptostreptococcus* species, as well as non-culturable unclassified organisms (Wang et al. 2011). Therefore, perhaps its most important virulence factors are those that enable attachment to host and bacterial cells.

It has also been shown that *F. nucleatum* subsp. *nucleatum* and *polymorphum* strains do adhere forming mono-species biofilms *in vitro*, but slowly and to varying degrees. However, in the presence of the early colonisers *V. parvula* and *A. oris*, *F. nucleatum polymorphum* and *nucleatum* rapidly adhered and proliferated (Biyikoğlu et al. 2012), thus the presence of these early colonisers is likely key in allowing adherence of *F. nucleatum*. As well as co-aggregating with early coloniser organisms, *F. nucleatum* also forms synergistic biofilms with *T. forsythia* (Sharma et al. 2005), and together the two act synergistically in causing alveolar bone loss (Settem et al. 2012), highlighting the importance of co-aggregation of *F. nucleatum* with other pathogens during periodontitis. In addition to bacterial co-aggregation, *F. nucleatum* has been shown to attach to host cells via the adhesin FadA (Han et al. 2005), a factor also associated with colon cancer as mentioned above (Rubinstein et al. 2013).

The mechanisms by which inter-species and host cell attachment is achieved were classified into two groups based on inhibition of aggregation by D-galactose or L-arginine: Lactose and related sugars have been shown to prevent aggregation of *F. nucleatum nucleatum* with other periodontal bacteria (Kolenbrander et al. 1989; Kolenbrander & Andersen 1989). However, *F. nucleatum* subsp. *polymorphum* appears to utilise an arginine sensitive mechanism for co-aggregation: Arginine binding proteins from bacterial lysates were purified using immobilised arginine, and mass spectrometry identified candidate proteins potentially responsible for *F. polymorphum* binding to Gram positive early colonisers (Edwards et al. 2007). Construction of mutants deficient in one of these

candidates followed by co-aggregation studies revealed that the outer membrane protein RadD was largely responsible for aggregation with several early-colonising Streptococci (Kaplan et al. 2009). Thus, RadD can be considered key to *F. nucleatum polymorphum* initial attachment.

1.5.4 Biofilm Formation

All three pathogens exist in the sub- and supra- gingival plaque as part of a mixed species biofilm, and this state contributes to disease pathogenesis.

Initial adherence allows further bacterial proliferation at a given site. Be it an environmental or host-associated ecological niche, the presence of different microbial species results in development of a mixed-species community of micro organisms attached to this surface (Nobbs et al. 2011). The bacterial community is enclosed in a matrix composed of bacterial and host products, and environmental substrates (Branda et al. 2005). This type of community is termed a biofilm, and is in stark contrast to the now redundant idea of bacteria existing in isolation with no interactions between different species. Biofilm formation (outlined in figure. 1.5) occurs by initial attachment and bacterial growth resulting in a monolayer, microcolonies form consisting of clusters of multiple species with adaptations for their location in the biofilm, eventually these microcolonies form different structures, as determined by microscopy. For instance, fluorescence microscopy has been used to characterise structures and architecture of polymicrobial biofilms in the context of oral microbiota (Zijngel et al., 2010). Expression of different factors is required at each stage of biofilm formation, so cell signalling including quorum sensing has been extensively studied in a number of bacteria (reviewed in Davey, George, & Toole, 2000). Different positions in the biofilm also present different ecological niches (e.g. anaerobic at colonised surface-aerobic externally, a higher concentration of bacterial metabolites at colonised surface, exposure to flow conditions at external surface, higher pH at colonised surface-neutral externally). Thus, biofilm formation may indirectly facilitate colonisation of organisms that were previously unable to do so.

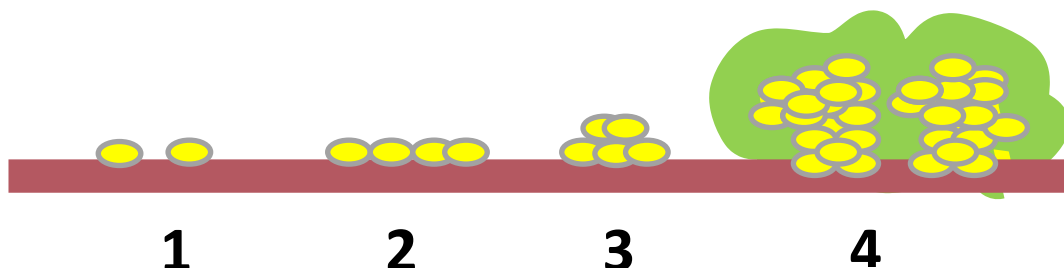


Figure 1.5. Stages of biofilm formation.

1) Initial attachment; bacteria attach to a surface, such as the gingival epithelium. 2) Proliferation; bacteria replicate at the surface 3) Formation of microcolonies; bacteria undergo further proliferation and coaggregation (between organisms of the same or multiple species), such as aggregation of fusobacteria and streptococci. 4) Biofilm formation; organisms form matrix enclosed structures, resulting in increased persistence and survival while attached to the surface.

1.5.4.1 ***Subgingival Plaque-Periodontal Biofilms***

Sub- and supra- gingival plaque can be considered a perfect example of a biofilm (Periasamy & Kolenbrander, 2009; Rosan & Lamont, 2000; Zijngje et al., 2010): Initial colonisers adhere to the acquired pellicle, followed by intermediate colonisers including streptococci. Resulting anaerobic conditions permit colonisation by the periodontal pathogen *F. nucleatum*, which adheres to the streptococci as described above. *F. nucleatum* acts as a bridging organism allowing colonisation of the biofilm by *T. forsythia* and *P. gingivalis*. Bacteria are enclosed in a matrix consisting of bacterial products, host salivary proteins including those composing the pellicle, mucins, and DNA, as well as environmental substrates consumed by the host. The biofilm state confers a variety of advantages on composing bacteria, these are discussed below.

1.5.4.2 ***Inter-species interactions***

Adhesion between species is important in oral biofilm formation. Colonisation by periodontal pathogens relies on mixed species biofilm formation: It has been shown that *P. gingivalis* initially colonises by adhering to receptors on *S. gordonii* (and other streptococci) via its major and minor fimbriae (Park et al. 2005; Lamont et al. 2002; Maeda et al. 2004). The receptor for *P. gingivalis* fimbriae on *S. oralis* has been shown to be Glyceraldehyde-3-

Phosphate (GAPDH) (Maeda et al. 2004). Furthermore, *P. gingivalis* forms poor monospecies biofilms *in vitro* using saliva as a growth substrate, under static and flow conditions, but does form biofilms in the presence of oral streptococci and *F. nucleatum* (Periasamy & Kolenbrander 2009). In addition, *F. nucleatum* has been shown to be important in facilitating colonisation and subsequent biofilm formation of *T. forsythia* (Sharma et al. 2005). These studies point to the importance of co-aggregation by periodontal pathogens in biofilm formation.

1.5.4.3 **Tolerance to Environmental Conditions**

Colonisation is not the only advantage to biofilm formation: *F. nucleatum* has been shown to have increased oxygen tolerance in a biofilm state compared to planktonic cells (Gursoy et al. 2010), and has been shown to increase the oxygen tolerance of *P. gingivalis* in a mixed species biofilm (Diaz et al. 2002). Furthermore, proteomics studies of *T. forsythia* have also shown the upregulation of oxidative stress response genes in biofilm compared to planktonic state, and that biofilms resisted oxidative stress when exposed to hydrogen peroxide (Pham et al. 2010).

1.5.4.4 **Antibiotic Resistance**

Bacteria in a biofilm often display resistance to antibiotics that they are sensitive to in a planktonic state, and this has been shown to be true for periodontal pathogens (Sedlacek & Walker 2007; S.-M. Kim et al. 2011). Suggested mechanisms of increased antibiotic resistance for periodontal biofilms include the inability of antibiotics to diffuse through the extracellular matrix (Gilbert et al. 1997), and that antibiotic resistance genes are upregulated (Kim et al. 2011). 'Persister cells' are another proposed mechanism of antibiotic resistance (reviewed in Wood et al. 2013), though this mechanism has not been described in periodontal pathogen biofilms. This describes a subset of the bacterial population in a biofilm that display decreased metabolism meaning that antibiotics which target dividing cells do not affect them. The implication of biofilms for treatment of periodontitis is that patients who receive a course of antibiotics should only do so in combination with debridement. This mechanical disruption of the biofilm allows antibiotics to inhibit growth of any remaining bacteria before a new biofilm structure can form. This theory is supported by studies of periodontitis patients undergoing biofilm therapy, i.e. improvement in clinical parameters (e.g. periodontal pocket depth) when also treated with systemic antibiotics is more pronounced than in patients who do not receive antibiotics (Guerrero et al. 2005).

1.5.4.5 *Changes in Metabolism*

Differences in metabolism between biofilm and planktonic cells are also evident. Proteomic and transcriptomic studies have highlighted several metabolic pathways with proteins that differ between periodontal pathogens in biofilm and planktonic states. In *T. forsythia*, proteins involved in butyrate production from catabolism of glutamate and succinate were shown to be down regulated in biofilm cells (Pham et al. 2010), a pathway which is also downregulated in *P. gingivalis* biofilms (Lo et al. 2009) hinting at the importance of this pathway during colonisation by periodontal pathogens.

Proteins associated with sialic acid metabolism in *T. forsythia* were also shown to be up regulated in a biofilm state, and *T. forsythia* can substitute its requirement for the bacterial product N-acetylmuramic acid (NAM) for sialic acid, but only in the biofilm state (Roy 2010). Taken together, this highlights the importance of free sialic acid in proliferation of *T. forsythia* in the host, and prevention of sialic acid release from host glycoproteins could be a useful method in preventing *T. forsythia* growth.

1.6 The Anti-Virulence Approach

Some periodontitis patients, and people with infections more generally, are not successfully treated by conventional antibiotics (discussed in section 1.4). While for many infections this may be due to antibiotic resistance, for periodontitis the explanation may revolve around the polymicrobial nature of the condition: Since periodontitis appears to be part-mediated by the periodontal microbiota, and antibiotics will target the entire microbiota rather than pathogenic species specifically, their ability to re-establish a health-associated bacterial population (i.e. pathogens in low abundance, commensals in high abundance) may be somewhat limited.

This inability to treat bacterial infections has led to research and development of the so-called “anti-virulence approach” to target the virulence factors of specific pathogens or groups of pathogens, including those responsible for periodontitis. This has been seen in the case of the gingipains of *P. gingivalis*, with several plant extracts (Lohr et al. 2015), active molecules (isolated from extracts, Kariu et al. 2016), and short peptides (Huq et al. 2013) shown to reduce gingipain activity, with *in vitro* studies showing reductions in *P. gingivalis* biofilm formation (Kariu et al. 2016), and disruption of bacterial nutrient acquisition leading to decreased *P. gingivalis* growth (Huq et al. 2013). Plant extracts that inhibit gingipains have also shown disruption of host-*P. gingivalis* interactions; attachment and invasion of host cells, and cytokine production (Lohr et al. 2015), though this could be

due to interactions between the active ingredients and host cells, rather than targeting the gingipains.

Quorum sensing, which is involved in periodontal pathogen biofilm formation, has also been investigated as an anti-virulence target. The auto-inducer 2 (AI-2) of *F. nucleatum* enhances biofilm formation by *F. nucleatum* and also other periodontal pathogens (*T. forsythia* and *P. gingivalis*), and this increase in biofilm formation is inhibited by the presence of quorum sensing inhibitors (Jang et al. 2013).

As alluded to at the beginning of section 1.5, this project aims to examine the potential to target periodontal pathogen sialidases as anti-virulence approach, since all three red complex species possess sialidases. Furthermore, they and other periodontal pathogens possess mechanisms for metabolising the products of sialidase activity, and the activity of pathogen sialidases could be important for host-pathogen interactions.

1.7 Sialic Acid, Sialidases, and Virulence

1.7.1 Sialic Acid

Sialic acid describes a family of 9-carbon sugars, ubiquitous in nature. These sugars are typically present at the termini of glycan (polysaccharide) chains present on glycolipids or glycoproteins (figure 1.6), which can be cell associated or extracellular/secreted. The glycan chains may be termed sialoglycans, with the term sialoglycoconjugates used to describe a sialoglycan as part of either a glycolipid or glycoprotein.

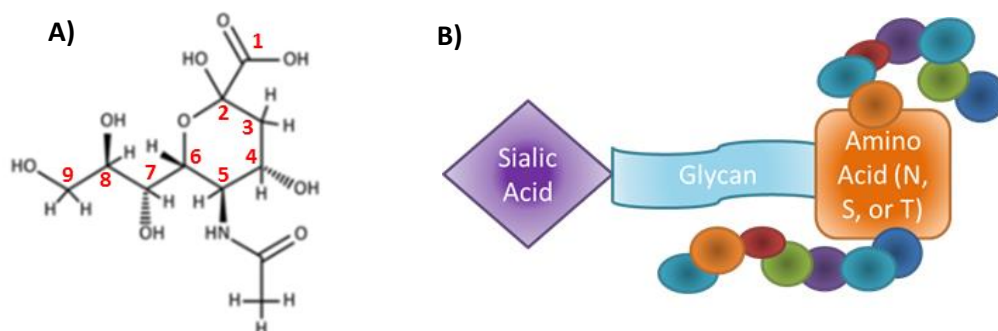


Figure 1.6. Graphic representations of A) Neu5Ac and B) a sialoglycoprotein.

Neu5Ac contains 9 carbons (excluding the acetyl group), numbered C1-9 as indicated.

Sialoglycans present in sialoglycoproteins are linked to the underlying protein via the amino acids asparagine (N-linked glycosylation) or serine or threonine (O-linked glycosylation).

The most common sialic acid in humans and other eukaryotes is N-acetylneuraminic acid (5-N-acetylneuraminic acid, Neu5Ac, figure 1.6) and is the only core sialic acid synthesised by humans, though another structurally and chemically similar mammalian sialic acid (N-glycolylneuraminic acid, Neu5Gc) may be obtained from the diet and incorporated into our glycans. Sialic acid may be further modified by the presence of additional chemical groups, substituting one of the hydroxyl groups at carbons (C) -4, -7, -8, and -9 for O-acetyl, O-methyl, O-sulfate, O-lactyl or phosphate groups. Lactones may also be present as modification of the sialic acids in some human glycans. In addition to the sialic acid itself, the linkage to the underlying glycan chain affects the properties and interactions of the sialoglycan with other molecules. In humans, the sialic acid is linked through the C-2 of sialic acid to C-3 or C-6, or sometimes C-8 of the underlying sugar. Finally, the underlying (branched) glycan chain and glycan class (glycolipid or glycoprotein type) also affect the structure-function of the sialoglycan. This massive potential variety of sialoglycoconjugates has been termed “the sialome” (Cohen & Varki 2010).

1.7.2 Sialidases

Given the ubiquitous expression of sialic acids on eukaryotic cell membranes and secretions, it is unsurprising that humans express their own sialidases to modulate glycoprotein sialylation and thus function. To date, four mammalian sialidases have been characterised, designated Neu1, Neu2, Neu3, and Neu4, with different substrate specificities (Reviewed in Miyagi & Yamaguchi 2012), but do share some conserved features (discussed further in the next paragraph). The sialidases are also largely localised to one specific cellular location, namely lysosomes (Neu1), cytosol (Neu2), plasma membrane (Neu3) and lysosomal or mitochondrial membrane (Neu4), however, the sialidases may mobilise elsewhere in response to certain stimuli, such as exposure to PAMPS causing TLR activation (Amith et al. 2010).

As a consequence of global expression of sialic acid in higher eukaryote tissues and thus the abundance of a potential food source, many pathogens also possess sialidase enzymes, which have been shown to serve a multitude of functions in different pathogens. Despite the vast phylogenetic differences between humans and pathogens, there appear to be some similar features between bacterial and mammalian sialidases: Sequence alignment software can be used to align amino acid sequences that may initially appear to show no homology based on the crystal structure of one of the aligned proteins. Based on the structure of Neu2, mammalian Neu and bacterial Nan sialidases appear to show some conserved sequences with similar topology (Miyagi & Yamaguchi 2012), indicating these

structural features are important for sialidase function. These include the characteristic β -propeller (made up of several (~ 5) “blades” formed by β -sheets), several “Asp-boxes” (conserved sequences with the residues S/T-X-D-X-G-X-X-W/F/Y) positioned between the β -propeller blades (not necessarily between all blades), and a “RIP” domain (the residues arginine-isoleucine-proline, R-I-P) which is highly conserved among bacterial and mammalian sialidases, and thus considered essential for catalytic activity. In addition to the sequence catalytic region, sialidases may possess subunits that appear to serve non-catalytic functions, such as the Carbohydrate Binding Module (CBM) seen in some sialidases (Park et al. 2013) including the *T. forsythia* sialidase (further discussed in section 2.3.1.1, and elsewhere in chapter 2). These features are identified in figure 1.7.

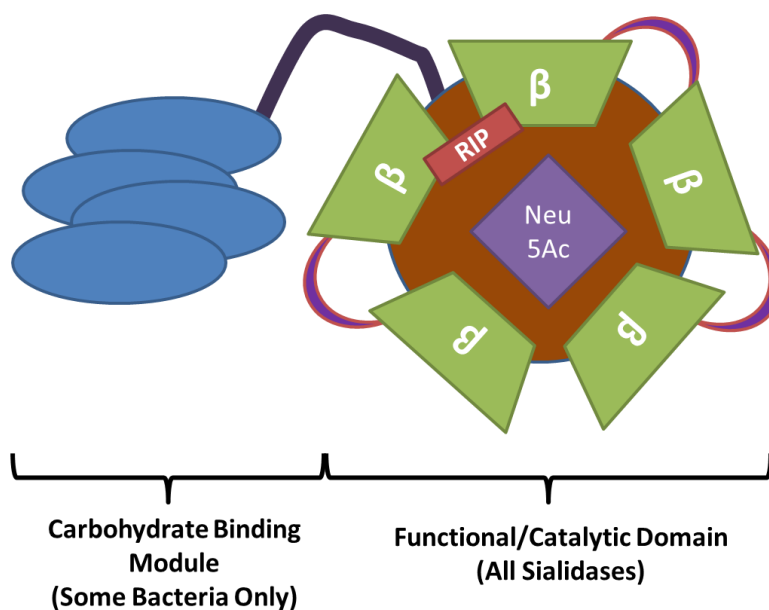


Figure 1.7. Conserved features of sialidases.

β -propeller blades, Asp-boxes and the RIP domain are indicated (green trapezoids, purple crescents, and a red box, respectively). Neu5Ac is shown in the diagram to highlight the position of the β -propeller around the sialic acid binding pocket. Numbers of Asp-boxes and β -propellers vary between different sialidases. A single carbohydrate binding module (CBM) is indicated here, but some bacterial sialidases (such as NanH in *Vibrio cholerae*) possess two, one at both C- and N- terminals of the protein.

Perhaps the most extensively studied sialidase is the Neuraminidase (NA) of influenza (so called since the enzyme was initially shown to release N-acetylneuraminic Acid). Found in the viral lipid envelope, this sialidase is thought to function in virus exit from host cells,

since the viral adhesin Haemagglutinin (HA) binds to host cell-membrane associated sialic acid preventing virus release in the absence of NA. NA may also assist influenza virus in evasion of binding and immobilization by host mucins.

Sialidases are also present in a wide variety of host-associated bacteria, with some possessing multiple sialidases. An example of sialidases as an important virulence factor for a bacterial pathogen can be seen in *Streptococcus pneumoniae*- a commensal of the nasopharynx and opportunistic pathogen, causing meningitis and pneumonia. The sialidases of *S. pneumoniae*, NanA and NanB, have been extensively studied, and have been shown to contribute to the pathogenesis of *S. pneumoniae* through several mechanisms; NanA is important in mediating attachment and invasion of human brain and laryngeal epithelial cells, and in biofilm formation (Brittan et al. 2012; Uchiyama et al. 2009). The role of NanB is less well understood, though it does show different substrate specificity (Gut et al. 2008), and is optimum at a lower pH. Considering that different sialidases may be required for cleavage of different types of sialic acid, or have different specificities due to structural differences in the underlying glycans, it might be the case that *S. pneumoniae* requires multiple sialidases for colonisation of different sites or host species. Certainly, the pathogenicity of *S. pneumoniae* is affected by expression of different sialidases; for example, NanC expressing strains (a third sialidase, not present in all strains of *S. pneumoniae*) have been shown to be more frequently associated with haemolytic uremic syndrome in children with necrotizing pneumonia than strains that do not encode *nanC* (Janapatla et al. 2013).

The virulence of various GI pathogens is also partly reliant on sialidases. Examples of this can be seen in toxigenic *Vibrio cholerae*, which utilises sialidases to unmask GM1 gangliosides-the ligand for its toxin (Galen et al. 1992) or obtain sialic acid as a nutrient (Almagro-Moreno & Boyd 2009). Both of these studies also show decreased virulence and/or colonisation of sialidase-deficient *V. cholerae* in mouse models. Another example of the importance of sialidases for GI pathogens can be seen in *Salmonella* and *Clostridium* infections: Similarly to cholera they use free sialic acid as a nutrient source, and this is important for their proliferation-mutant strains deficient in sialic acid catabolic genes displayed decreased ability to proliferate in mice following antibiotic treatment (Ng, et al. 2013). In this case sialic acid acquisition from host sugars may be heavily dependent on other bacteria present in the microbiota, highlighting the importance of microbial interactions in sialic acid acquisition from a nutritional perspective.

1.7.3 Sialic Acid in the Oral Cavity

Sialic acid-initially named since it was first discovered in saliva, and named for the Greek “σίαλον/sialon,” meaning saliva-is abundant in the oral cavity as part of various sialoglycoconjugates. These can be cell membrane associated or secreted. Cell membrane-associated sialic acids often play roles in receptor structure-function, and in some cases may regulate their activity. This is seen in the case of the TLRs (discussed below).

Mucins are the most abundant proteins in saliva, composing ~26% of salivary protein content (Rayment et al. 2000). These proteins can be described as “bottle brush” in appearance (Lewis & Lewis 2012), with a large number of glycan chains capped with sialic acid extending from a protein backbone. Mucins function to trap and exclude particles by formation of net-like structures, and can also bind lectins and adhesins (host or bacterial), as well as growth factors, antibodies, and cytokines. Furthermore, mucin production is upregulated in response to the presence of PAMPs (reviewed in McGuckin et al. 2011), and during periodontitis (Sánchez et al. 2013) highlighting its role in innate immunity, and hinting that it would be advantageous for bacteria to avoid mucin binding, harness mucin for adhesion purposes, or degrade mucin for use as a growth substrate.

GCF is similar in composition to serum, and in serum the most prevalent glycoproteins (gammaglobulins) are sialylated. Since periodontal pathogens are exposed to GCF (and presumably gammaglobulins), an ability to process sialic acid might prove beneficial in metabolism of glycoproteins for nutrient and energy acquisition. Fetuin is another sialylated glycoprotein present on mucosal surfaces and in serum and saliva. Fetuin functions to dampen inflammatory responses to infection and physical damage (Wang & Sama 2013), and *T. forsythia* has been shown to bind and degrade fetuin for the purposes of attachment (Roy et al. 2011). It is tempting to speculate that fetuin degradation by pathogens plays a role in periodontal disease progression due to fetuin’s role in immune modulation.

1.7.4 Sialic Acid and the Immune System

An important role of sialic acid is to down-regulate immunity: Classical studies have shown sialic acid to be a self-associated molecular pattern (SAMP), acting through a variety of mechanisms to downregulate immune system activity (see below). Furthermore, it has been shown that sialic acid regulates (at least partially) the activation of receptors associated with pro-inflammatory responses. Given the overall immune dampening activity attributed to sialic acid, the effect of sialidases on immune activation has been extensively studied.

1.7.4.1 ***Sialic Acid and Toll Like Receptors***

TLRs are important in pro-inflammatory immune signalling, and are thought to mediate inflammation during periodontitis. TLRs -2, -4, and presumably -9 are heavily glycosylated, a requirement for functionality (Feng et al., 2012; J. Sun et al., 2006), but the importance of sialylation has only become apparent recently. It has been shown that human Neu1 sialidase complexes with TLRs -2 and -4 present on DCs and macrophages (Stamatos et al. 2010; Amith et al. 2010), resulting in pro-inflammatory responses including cytokine signalling and DC maturation. The intracellular (endosomal) TLR-9 is also regulated by the activity of the human sialidase Neu1 (Abdulkhalek & Szewczuk 2013). However, no-one to date has studied the effect of sialidases on TLR stimulation in epithelial cells, which is likely to be important since these are the first cells that periodontal-and-other pathogens come into contact with, and are likely important in initiating immune signalling.

1.7.4.2 ***Sialic Acid and Complement***

The recognition of sialic acid as a Self-Associated Molecular Pattern (SAMP) by complement involves factor H, which binds to sialoglycans present on host cells and prevents complement deposition (Meri & Pangburn 1990). Later studies have shown that the extent of O-acetyl modifications of the sialic acid side chain is what determines factor H binding (reviewed in Varki & Gagneux, 2012). *T. forsythia* possesses a sialate-O-acetyl esterase capable of cleaving an acetyl- modification present on di-acetylated sialic acid (Neu5,9Ac). If *T. forsythia* does remove either the sialic acid or the di-acetylation present on some host sialoglycans on cell membranes, it could result in complement deposition on host cell membranes and subsequent destruction of host cells-further contributing to periodontal disease. Indeed, it has been shown that NanS is capable of converting Neu5,9Ac to Neu5Ac at the cell surface (Phansopa et al. 2015), so this might be a possibility.

1.7.4.3 ***Siglecs***

“Sialic acid-recognizing immunoglobulin-like superfamily lectins” (Siglecs) describe a series of vertebrate cell-surface glycoproteins that function to bind sialic acid, resulting in positive or negative regulation of the immune system. Siglec-1 (sialoadhesin) was first to be characterized; shown to be involved in binding of erythrocytes by macrophages, and that this binding was abolished by a bacterial sialidase (Crocker et al. 1991). Later, a number of different lectins including a B-cell adhesion molecule-CD22, siglec-2 (Sgroi et al. 1993), myelin associated glycoprotein-MAG, siglec-4 and siglec-15 (Angata et al. 2007), and CD33 were shown to be involved in sialic acid dependent cell-cell adhesion. Initially dubbed “sialoadhesins”, the term “siglecs” was eventually accepted (Varki & Angata 2006).

Siglecs are often described as one of two groups; conserved between mammals and even between vertebrates, or evolutionarily divergent-showing variation between species (Varki & Angata 2006). CD33-related (CD33r) siglecs are evolutionarily diverse, and are thought to inhibit inflammation by binding sialic acid residues on their external domains, followed by recruitment of intracellular phosphatases such as SHP-1 and SHP-2. This is thought to inhibit phosphorylation of kinases associated with other surface membrane receptors, and ultimately reduce expression of inflammatory molecules (Paul et al. 2000). On the other hand, some CD33r-siglecs appear to upregulate inflammatory responses. An example of this can be seen in siglec-15, which has been shown to bind adaptor proteins DAP12 and DAP10, which in turn recruit the tyrosine-phosphatase Syk, suggesting siglec-15 can upregulate pro-inflammatory signalling cascades (Angata et al. 2007). Furthermore, siglec-15 has been shown to upregulate the differentiation of osteoclast precursors into osteoclasts (Hiruma et al. 2011), therefore this siglec could be important in mediating bone resorption, and perhaps play an important role in periodontitis.

1.7.5 Sialidases of Periodontal Pathogens

Given the multifarious roles of sialic acid in the immune system and its presence on the surface of host cells and secretions on mucosal surfaces, an ability to express sialidases stands to benefit any organisms attempting to colonise these areas. In addition to sialidases, bacteria may also possess sialic acid utilisation systems, permitting them to metabolise sialic acid for energy, or incorporate sialic acid into other structures. Examples of characterised sialic acid uptake and utilisation pathways are summarised in figure 1.8.

Given that the oral cavity is also a rich source of sialic acids, sialidases and glycosidases more broadly speaking could be of potential value to a coloniser of the periodontium, not least for nutrient acquisition. In any case, the periodontal pathogens of the red complex all possess sialidases. Most research of red complex pathogen sialidases has focussed on its role in virulence of *T. forsythia* and *P. gingivalis* and is discussed below. *T. denticola* has also recently been shown to express a surface exposed sialidase, which functions in protection from complement (Kurniyati et al. 2013).

1.7.5.1 *Tannerella forsythia* Sialidase

T. forsythia was thought to possess two sialidases-SiaHI and NanH. SiaHI was initially characterised by cloning *T. forsythia* open reading frames into *E. coli* and screening the recombinant strains for sialidase activity using a fluorogenic substrate (Ishikura et al. 2003). Recombinant SiaHI appeared to display sialidase activity in this first study, which was qualitative in nature (i.e. the presence of fluorescence resulting from sialidase-fluorogenic

substrate was used for highthroughput screening), but in a later study SiaHI did not appear to display sialidase activity (Thompson et al. 2009). The availability of the *T. forsythia* genome allowed discovery of a sialidase which shared homology with an orthologue from the closely related organism *Bacteroides fragilis* (Thompson et al. 2009). Termed NanH, this sialidase is characterised by several features, including a secretion signal sequence, putative carbohydrate binding moiety (CBM) at its N-terminal, three aspartic acid-boxes and a “RIP” domain considered important for catalytic activity as part of its C-terminal. NanH was found to be in close proximity to other genes thought to be involved in sialic acid uptake and metabolism, and together with NanH these form a sialic acid utilisation operon (Stafford, Roy, Honma, & Sharma, 2012, further discussed in chapter 3, section 3.4).

Sialidase activity is also considered an important virulence factor with functions for *T. forsythia* besides metabolism. For example, NanH deficient *T. forsythia* mutants show reduced attachment to a variety of epithelial cell lines (Honma et al. 2011), suggesting that sialidase is involved in unmasking epitopes present on host glycoconjugates enabling *T. forsythia* attachment. Perhaps in a scenario involving co-infection of oral epithelial cells with *T. forsythia* and other pathogens such as *F. nucleatum* (which shows lactose-dependent adhesion), sialidase activity would also bolster attachment of *Fusobacterium*.

NanH has also been shown to be important in biofilm formation on sialoglyconjugates; for *in vitro* growth, *T. forsythia* requires NAM (*in vivo* this is presumably generated by other autolysed bacteria), though NAM can be substituted for sialic acid, albeit at a higher concentration. It was then observed that the sialidase inhibitor oseltamivir could inhibit *T. forsythia* biofilm growth on a variety of sialoglyconjugates (including mucin, fetuin, and 6-sialyllactose) suggesting that host factors act as source of sialic acid, and that *T. forsythia* sialidase is important for proliferation in its niche within the host (Roy et al. 2011).

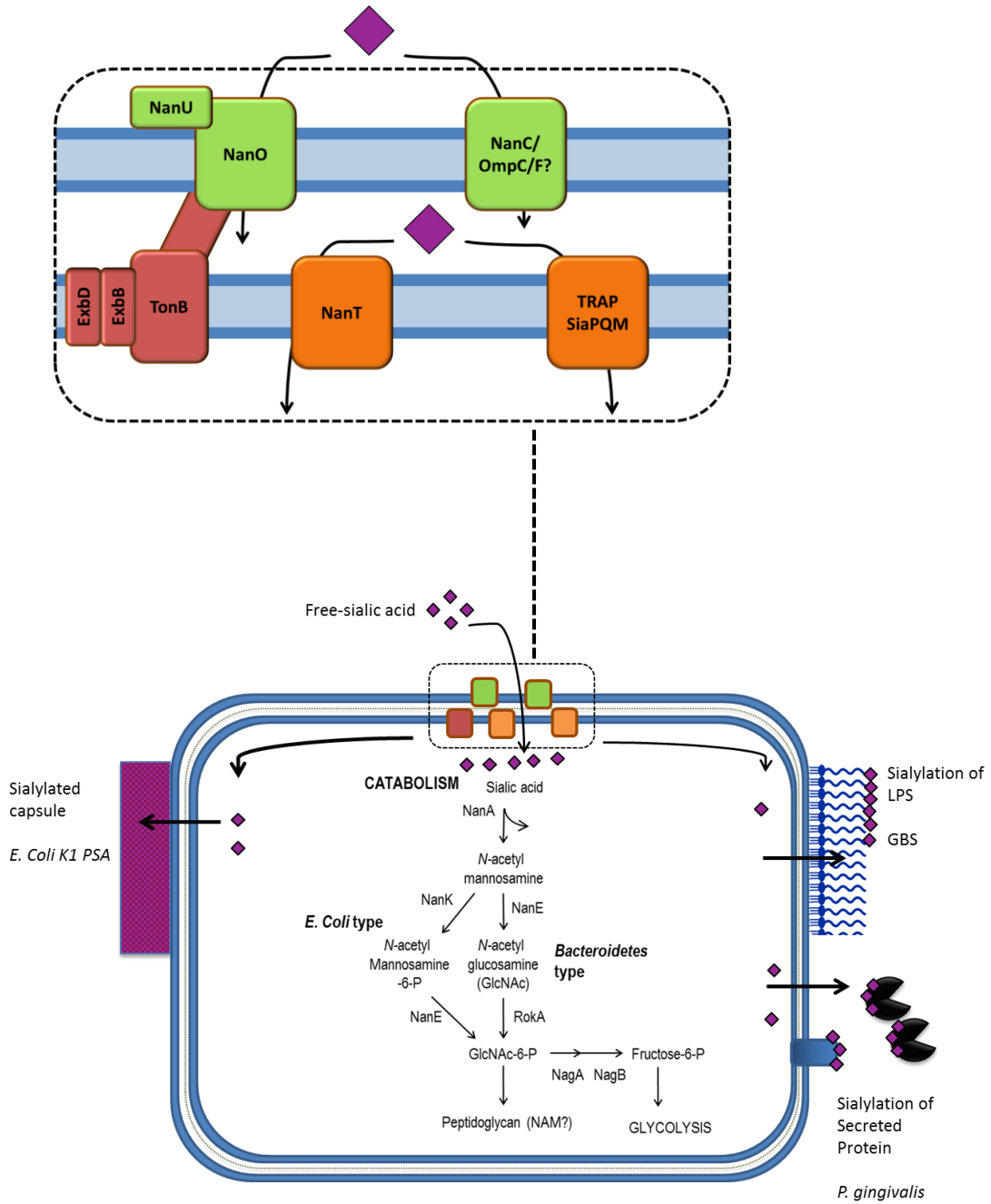


Figure 1.8. Uptake and utilisation of sialic acid in gram negative bacteria.

Sialic acid can be transported across the outer membrane by active processes, as seen in *T. forsythia* (and *Bacteroides*) where sialic acid is sequestered by NanU, and actively transported by NanO, which is energised by the TonB-ExbB-ExbD complex. Bacteria lacking specific transporters presumably use general porins for outer membrane sialic acid transport. Sialic acid can then be transported across the inner membrane via a number of mechanisms, including NanT (as seen in *T. forsythia*) or the SiaPQM Tripartite-ATP independent Transporter (TRAP) complex (as seen in *F. nucleatum*). Sialic acid is then metabolised, starting with an N-acetylneuraminase lysase (NanA), followed by one of two pathways: In *E. coli* this involves (NanK) and (NanE), and in Bacteroidetes this involves (NanE) and (RokK). At this point the two pathways converge, and the end product (N-acetylglucosamine-6-phosphate, GlcNAc-6-P) undergoes conversion to Fructose-6-Phosphate, which undergoes glycolysis. *T. forsythia* is thought to be able to utilise GlcNAc-6-P as a substrate for NAM biosynthesis. As an alternative to metabolism, some bacteria are apparently capable of sialylating their surface structures or secreted proteins. This is seen in some capsular polysaccharides (such as in *E. coli* K1 strains), LPS (Group B streptococci, GBS), or secreted proteins (such as *P. gingivalis* gingipains).

1.7.5.2 *Porphyromonas gingivalis* Sialidase

P. gingivalis possesses sialidase activity, with one sialidase-related gene; PG0352, and two genes annotated as O-sialoglycoproteases; PG0778, and PG1724 (Aruni et al. 2011).

PG0352 is analogous to the NanH sialidase of *T. forsythia*, possessing the characteristic putative CBM, Asp-boxes and FRIP domain, and a similar predicted structure (sections 1.7.2 and 2.3.1). PG0352 deficient mutants have been used to highlight multiple roles for this sialidase in the virulence of *P. gingivalis*, with mutants showing reduced adherence and invasion of oral epithelial cells (Aruni et al. 2011). Interestingly, biofilm formation of *P. gingivalis in vitro* is impaired in PG0352 deficient mutants, though biofilm formation is restored by addition of Neu5Ac (Li et al. 2012). Furthermore, PG0352 deficient mutants display altered morphology and reduced capsule formation compared to the parent strain. Perhaps *P. gingivalis* (or the strain used in this study) incorporates Neu5Ac into its capsule, or requires Neu5Ac as a precursor for synthesis of other capsular sugars. This mutant also displayed decreased resistance to human serum, which is perhaps unsurprising due to the reduction in capsule formation, though the absence of sialidase could also contribute to complement mediated killing. This reduced ability to survive complement, and the deficiencies in biofilm formation, could also be due to altered gingipain activity/structure, since it has been shown that Neu5Ac is a major component of RgpA glycosylation (Rangarajan et al. 2005). Since *P. gingivalis* lacks the genetic ability to synthesize sialic acid (at least by known pathways), sialidase activity is likely key in acquisition of exogenous sialic acid for reprocessing.

In summary, sialidases are expressed by all three red complex species, and sialic acid utilisation pathways are present in other periodontal pathogens (Stafford et al. 2012), as well as other bacteria. Given that pathogen sialidases appear to have multiple contributions to virulence, they represent a strong candidate for inhibition as an anti-virulence approach, with the ultimate aim to apply sialidase inhibition to treatment of periodontitis in patients.

1.8 Sialidase Inhibition

1.8.1 Viral Sialidase-The Driving Force Behind Inhibitor Development

Influenza neuraminidase (NA, N) is one of the two components of the current human flu vaccine (the other being Haemagglutinin, H) but both are prone to point mutations or different virus strains may recombine on co-infection of the same host, resulting in progeny with an alternative combination of H and N antigens. As a result, annual manufacture of vaccines based on the N and H antigens of the most prevalent influenza strains is required.

The need to treat influenza infection lead to the development of sialidase (or neuraminidase) inhibitors. These aim to prevent the effects of aiming to prevent the virus from exiting host cells, thus halting viral proliferation. Sold under the names Tamiflu and Relenza, the sialidase inhibitors oseltamivir and zanamivir are licensed worldwide as a treatment for flu.

1.8.2 Sialidase Inhibitors

Sialidase inhibitors are structural analogues of sialic acid (figure 1.9), and act by competing with native ligands for the sialidase active site. Interestingly, the catalytic intermediate 2-deoxy-2,3-dehydro-N-acetylneuraminic acid (DANA) was shown to be bind viral NA with greater affinity than sialic acid (Meindl et al. 1974), and further derivatives of DANA and Neu5Ac led to the development of different inhibitors.

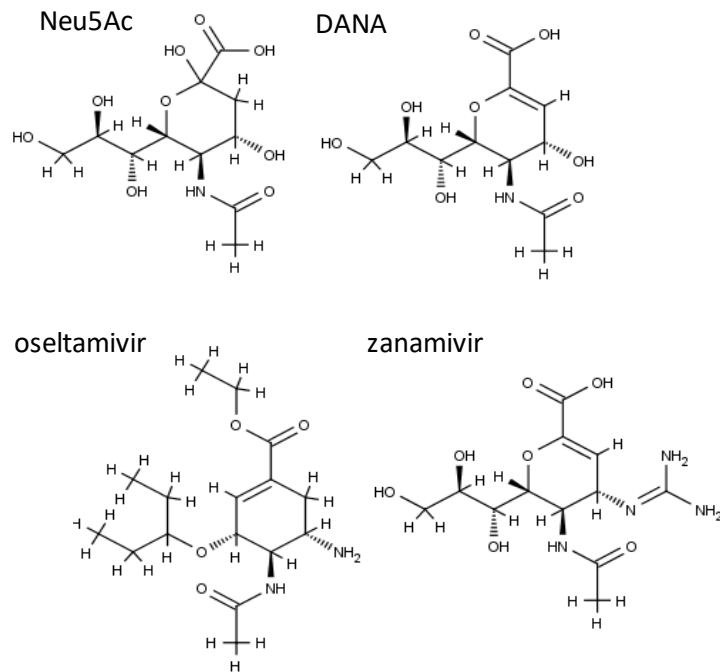


Figure 1.9. Sialidase inhibitors are structural analogues of sialic acid.

Neu5Ac shown with the sialidase inhibitors DANA (2-deoxy-2,3-dehydro-N-acetylneuraminic acid), oseltamivir, and zanamivir. (Credit for Image: Chatchawal Phansopa, Stafford Group, University of Sheffield.)

1.8.3 Sialidase Inhibition-Potential Impact on Virulence

Conventional antibacterial chemotherapy targets ubiquitous bacterial processes.

Unfortunately, this comes with several drawbacks, including disruption of the host normal flora, and selection of antibiotic resistant bacteria. An alternative to conventional antimicrobial chemotherapy is to target virulence factors or pathogenic processes, which avoids issues seen with disruption of normal flora and antibiotic resistance. Given the role of sialidases in biofilm and capsule formation, host cell invasion, adherence, and immune modulation in a number of periodontal pathogens, sialidase inhibitors are a potential anti-virulence drug that could be used to treat periodontitis. Initial supporting evidence comes from studies of sialidase deficient strains of *P. gingivalis*, *T. denticola*, and *T. forsythia*.

T. forsythia has been shown to form biofilms in the presence of a variety of sialoglycoconjugates, including saliva, sialyllactose and mucin, but the sialidase inhibitor oseltamivir inhibits this in a dose dependent manner (Roy et al. 2011), while biofilms cultured in the presence of sialic acid remain unaffected by oseltamivir. In addition,

attachment of *T. forsythia* to epithelial cells is inhibited in the presence of DANA (Honma et al. 2011). Sialidase activity has also been shown to modulate virulence of *T. denticola*, since sialidase deficient mutants display decreased complement sensitivity and ability to cause tissue damage in a murine abscess model, and the sialidase activity of *T. denticola* has been shown to be decreased in the presence of the sialidase inhibitor DANA (Kurniyati et al. 2013). These studies demonstrate the potential of sialidase inhibitors as anti virulence compounds against periodontal pathogens.

1.8.4 Sialidase Inhibition-Impact on the Host Immune Response

Given that a pro-inflammatory response is also responsible for the pathology seen in periodontitis, an ability to regulate this would result in decreased morbidity. TLRs -2 and -4 are activated in response to periodontal pathogens (Sahingur et al. 2013; Wara-Aswapati et al. 2012; Papadopoulos et al. 2012). These TLRs have been shown to be extensively glycosylated, hinting at the potential for sialidases to unmask ligand binding sites (da Silva Correia & Ulevitch 2002). TLR-2 and -4, activated by bacterial lipoprotein and bacterial LPS, respectively, have been shown to form a complex with the human sialidase Neu1 (Amith et al. 2010), and desialylation is required for receptor activation . Furthermore, LPS induced expression of IL-6, IL-12p40, and TNF- α by mature DCs is reduced in the presence of zanamivir or DANA (Stamatos et al. 2010), and macrophages show reduced LPS-activation in the presence of Zanamivir, DANA, and oseltamivir (Amith et al. 2009). While this reduced activity is due to the inhibition of human sialidases, exogenous sialidases were shown to increase TLR -2 and -4 activation (Amith et al. 2010), and the ability to inhibit pro-inflammatory signalling through sialidase-regulated TLR activation is another advantage for sialidase inhibitors as potential therapeutic agents in periodontitis.

1.8.5 Aims and Hypothesis-The Prospect of Sialidase Inhibitors as a Treatment for Periodontitis

Periodontal pathogens of the red complex express sialidases with multiple functions for themselves and other pathogenic organisms. Given the apparent role of sialidases in pathogenic processes, sialidase inhibitors could be potential anti-virulence compounds. Thus, this project aimed to investigate the effect of sialidase inhibitors on host cell association and host-pathogen interactions, as well as in biofilm formation and growth of periodontal pathogens. This study also aimed to further characterise the periodontal pathogen sialidases using biochemical approaches. It was hypothesised that zanamivir or other sialidase inhibitors would inhibit periodontal pathogen sialidase activity, and subsequently inhibit biofilm formation of periodontal pathogens on sialoglycoproteins, as

well as inhibiting host-pathogen interactions including host-bacteria association and immunomodulation.

Chapter 2

Biochemical Characterisation **of Periodontal Pathogen** **Sialidases**

2 Chapter 2: Biochemical Characterisation of Periodontal Pathogen Sialidases

2.1 Introduction-The Sialidases of *P. gingivalis* and *T. forsythia*

The ecological niche in which periodontal pathogens live is rich in glycoproteins and glycolipids. In the supragingival plaque these may be from the surfaces of oral epithelial cells, or salivary mucins and other salivary proteins. The subgingival plaque is also exposed to these glycoprotein sources and others including components of gingival crevicular fluid (GCF, more similar in composition to serum) and immune cells that infiltrate the periodontium, such as neutrophils and macrophages. Glycoproteins and glycolipids themselves are a source of sialic acid which often caps the sugar chains, or glycans (the ends furthest from the protein backbone in glycoproteins, or cell surface in the case of glycolipids), and these can be termed sialoglycans. Host secretions are rich in sialoglycans, for instance, 80% of the oligosaccharide chains in salivary mucins are estimated to be sialylated (Levine et al. 1987), and serum proteins in healthy humans contain ~1% w/w sialic acid (Carter & Martin 1962). Cell surfaces are also rich in sialic acid, with a single erythrocyte plasma membrane thought to possess more than 10 million sialic acid molecules (Varki A, Schauer R. Sialic Acids. In: Varki A, Cummings RD, Esko JD, et al., editors. Essentials of Glycobiology. 2nd edition. Cold Spring Harbor (NY): Cold Spring Harbor Laboratory Press; 2009. Chapter 14. Available at: <http://www.ncbi.nlm.nih.gov/books/NBK1920/>).

Release of sialic acid can provide a carbon source for bacteria or expose underlying glycans which can then be targeted by other enzymes (Stafford et al. 2012). As well as its potential roles in bacterial nutrition, sialic acid has a number of functions for the host, and it has been suggested that sialic acid release can have consequences for disease progression in a number of infections (Feng et al. 2013; Chang et al. 2012; Li et al. 2012).

Given the abundance of sialic acid in the oral cavity it is unsurprising that many pathogens and some commensals possess sialidase enzymes capable of cleaving sialic acid from the sialoglycans. *T. forsythia*, *P. gingivalis*, and *T. denticola* comprise the “red complex,” present in subgingival plaque because of their association with severe periodontitis (Socransky et al. 1998). All three members of the red complex possess sialidases. In *T. forsythia*, a candidate protein dubbed “SiaHI” was initially suggested to be responsible for this (Ishikura et al. 2003), but an overwhelming body of evidence has shown that the sialidase NanH (TF0035), is primarily responsible for sialidase activity in *T. forsythia* (Roy et al. 2011; Honma et al. 2011; Thompson et al. 2009).

Strains of *P. gingivalis* also possesses a sialidase (PG0352), termed “SiaPG” for the purposes of this work. Although SiaPG (PG0352) is currently annotated as a “putative sialidase” in the NCBI protein database (<http://www.ncbi.nlm.nih.gov/protein/AAQ65563.1>), the function of PG0352 has been confirmed through construction and testing of gene-knockout strains (Li et al. 2012; Aruni et al. 2011).

Previous studies have highlighted the importance of sialidases in the virulence of *T. forsythia* and *P. gingivalis* (Li et al. 2012; Aruni et al. 2011; Honma et al. 2011). However, purification and biochemical characterisation of NanH has not been described, besides its initial characterisation in *E.coli* cell lysates (Thompson et al. 2009) and preliminary characterisation by our group (Roy et al. 2011), and to our knowledge only one publication has shown preliminary characterisation of purified SiaPG (Li et al. 2012). Elucidation of ligand specificity and conditions under which these enzymes function would provide information regarding their activity and functions *in vivo*. Furthermore, as described above, a number of studies have highlighted the importance of periodontal pathogen sialidases in biofilm formation, attachment and invasion of host cells, and ultimately disease. Given the multitude of apparent functions for pathogen sialidases, they are a strong candidate for targeting pharmacologically, with a view to preventing these virulence mechanisms. However, before any *in vitro* virulence studies could be performed, it had to be established if the periodontal pathogen sialidases could be inhibited using commercially available sialidase inhibitor compounds.

This chapter describes the ultimately successful attempts to clone and purify functional NanH and SiaPG, along with attempts to clone and purify the NanH-C Terminal (catalytic) Domain (CTD), SiaPG-Carbohydrate Binding Module (SiaPG-CBM) and SiaPG-C Terminal (catalytic) Domain (SiaPG-CTD). Production of active pathogen sialidases allowed determination of their activity on various substrates including host-relevant ligands. Furthermore, the efficacy of the sialidase inhibitor zanamivir, produced as the pharmaceutical preparation Relenza™ by GSK, for inhibition of the periodontal pathogen sialidases was investigated.

2.2 Materials and Methods- Biochemical Characterisation of Periodontal Pathogen Sialidases

2.2.1 Bacterial Strains, Growth Conditions, and Plasmids

E. coli strains were required for cloning and protein expression work. All *E. coli* were cultured on Luria Bertani agar (LB agar) or Lysogeny broth (LB broth) (Thermo Fisher

Scientific). When attempting transformation, or culturing transformed strains, these were cultured on LB agar or LB broth supplemented with 50 µg/ml ampicillin, as the plasmids used confer ampicillin resistance. All cultures were incubated at 37°C, broth cultures were shaken at 200-250 rpm. *E. coli* growth for protein expression studies is described in section 2.2.8.

<i>E. coli</i> Strain	Genotype	Reference
DH5α	<i>fhuA2 Δ(argF-lacZ)U169 phoA glnV44 Φ80 Δ(lacZ)M15 gyrA96 recA1 relA1 endA1 thi-1 hsdR17</i>	New England Biolabs (NEB)
BL21 Origami B (DE3)	F ⁻ <i>ompT hsdS_B(r_B⁻ m_B⁻) gal dcm lacY1 ahpC (DE3) gor522:: Tn10 trxB (Kan^R, Tet^R)</i>	Novagen (MerckMillipore)

Table 2.1. *E. coli* strains.

Details of the *E. coli* BL21 origami B and *E. coli* DH5α strains are currently available at: http://www.merckmillipore.com/GB/en/product/Origami%E2%84%A2-B%28DE3%29-Competent-Cells---Novagen,EMD_BIO-70837

-and-

<https://www.neb.com/products/c2987-neb-5-alpha-competent-e-coli-high-efficiency>

Plasmids for cloning and expression work were either the pET plasmids pET21a, or pET20b, or the pJET plasmid which was commercially available with the blunt ended ligation kit used in this work (see below). The plasmid features are summarised in table 2.2.

Plasmid	Description	Phenotype	Source
pET21a	Suitable as a cloning vector, also for protein expression with N-terminal His+ tag for affinity chromatography	Ampicillin Resistant	Novagen
pET20b	Suitable as a cloning vector, also for protein expression with C-terminal His+ tag for affinity chromatography	Ampicillin Resistant	Novagen
pJET	Cloning vector only. Suitable for blunt ended ligation.	Ampicillin Resistant	Thermo-Fisher Scientific

Table 2.2. Plasmids for cloning and expression.

2.2.2 Sialidase Activity of Whole Bacteria

Bacteria were scraped from agar plates and washed by resuspension in 1ml PBS pH 7.4 (Sigma Aldrich) and centrifuged at 13000 xg for 2 minutes. Supernatant was disposed of and bacteria were resuspended in PBS pH 7.4 before use in a reaction mixture containing PBS pH 7.4 (Sigma Aldrich) and 0.1 mM of 4-methylumbelliferyl N-acetyl- α -D-neuraminic acid sodium salt (MUNANA; carbosynth, UK), at an optical density at 600nm (OD_{600}) of 0.05, and incubated at 37 °C for up to 24 hours in clear flat-bottomed 96 well polystyrene plates (Greiner, UK).

Sialidase activity was quantified by observing the cleavage of MUNANA to yield Neu5Ac and the fluorochrome 4-Methylumbelliferone (4-MU). In early work described here, the periodontal pathogen sialidase activity was quantified immediately using a Polarstar Galaxy plate reader (BMG Labtech) where fluorescence was measured at excitation 355nm, emission 430-10nm. This was advantageous as it allowed reaction mixtures to be quantified over time, but these fluorescence parameters and the Flurostar plate reader itself were not sensitive to small changes in 4-MU release. Therefore, the majority of sialidase activity experiments were performed according to a different protocol; Reaction mixtures were set up, and at any given time point 50 μ l of reaction mixture was removed and quenched by addition of 75 μ l of 100mM sodium carbonate buffer, pH 10.5 (a mixture of sodium carbonate and bicarbonate made according to buffer reference table, currently available at <http://www.sigmaaldrich.com/life-science/core-bioreagents/biological-buffers/learning-center/buffer-reference-center.html>). This quenching step stopped the reaction and equalised the pH (4-MU fluorescence is pH sensitive, optimum at \geq pH 10). Fluorescence was measured with excitation at 350 nm, emission 450 nm, using a Tecan Infinite M200 microplate reader.

The sialidase inhibitor zanamivir (GlaxoSmithKline, UK) was used in assays to test the effect of sialidase inhibition. Zanamivir was dissolved in water at 50mM, and diluted into reaction mixtures at a variety of concentrations, from 0-10mM.

Sialidase activity of different periodontal pathogens was measured as the fluorescence at 450 nm after excitation at 350 nm and expressed as arbitrary units. Sialidase activity of different bacteria in the presence of inhibitor was expressed as the percentage change in fluorescence at a given concentration of inhibitor, compared to fluorescence in the absence

of inhibitor, as determined by the formula:

$$\frac{\text{fluorescence at 0mM zanamivir}}{\text{fluorescence at 0-10mM zanamivir}} \times 100 = \text{Change in Fluorescence (\%)}$$

2.2.3 DNA Extraction

2.2.3.1 Genomic DNA

Periodontal pathogen genomic DNA was extracted from cultures harvested from agar plates, which were washed twice by resuspension in PBS and centrifugation at 13000 g. Extractions were performed using the Wizard Genomic DNA Purification kit (Promega), according to the manufacturer's instructions.

2.2.3.2 Plasmid DNA

Plasmid extraction was performed on 5ml of overnight liquid cultures of *E. coli*, using the ISOLATE II Plasmid Miniprep kit (Biolone), according to manufacturer's instructions.

2.2.4 Polymerase Chain Reaction (PCR)

PCRs performed in this project were attempting to amplify DNA for further cloning work: High-Fidelity PCR was performed using the *Phusion*[®] PCR kit (New England Biolabs), which has proofreading capabilities resulting in a low rate of nucleotide insertion errors during the amplification stage of the PCR reaction. PCRs were performed to obtain a number of different products, each of which required extensive optimisation, including primer design, adjustments of primer concentration, reaction mixture size, and Thermocycling conditions. Therefore, the PCR reaction conditions that were successful for each product are shown in appropriate results section in this chapter (sections 2.3.2 and 2.3.3).

2.2.4.1 Agarose Gel Electrophoresis

Agarose gels were prepared using 1-1.5% agarose (w/v) in 1x TAE (Tris Base, Acetic acid, EDTA), with 5 µg/ml ethidium bromide added to the gel before casting. Agarose gels were run in 1x TAE on a BioRad mini-sub[®]-cell GT system or BioRad sub-cell[®] GT systems (for small and large gels, respectively). DNA was visualised using a UV transilluminator-GBOX (Syngene) with associated imaging software programs GeneSnap or Genesys (Syngene). Various standards were used to assess DNA band sizes, described alongside the agarose gels in the appropriate results section in this chapter (sections 2.3.2 and 2.3.3).

2.2.4.2 Purification of PCR Products

PCR Products (and restriction endonuclease digestion products, below) were excised from agarose gels using a scalpel, and extracted using the QIAquick Gel Extraction kit (QIAGEN).

2.2.5 Restriction Endonuclease Digestion of Plasmid DNA or PCR products

Plasmids and PCR products underwent digestion using *NdeI* and *XhoI* restriction enzymes (or others as appropriate) and reagents were purchased from New England Biolabs.

Reagents are described in table 2.3. Reactions were incubated at 37°C for a total of 3 hours.

Reagent	Volume (μl) Per 60μl Reaction
<i>NdeI</i>	2
<i>XhoI</i>	2
Plasmid/PCR Product (concentration varied)	44.4
Buffer 4 (10x concentration)	6
BSA	0.6
(CIP)	2

Table 2.3. Reagents for restriction digest of plasmids and PCR products.

CIP; calf intestinal alkaline phosphatase, was only added to plasmid digestion reactions, after 2 hours of incubation. A further 1μl of each restriction enzyme was also added after 1 hour of incubation. DNA was purified by use of the same gel extraction method used for agarose gels, treating the gel volume as 100μl, and eluted in dH₂O. The concentrations of digested, purified plasmids and PCR products were checked using a Nanodrop.

Restriction endonuclease digestion reactions underwent agarose gel electrophoresis, and where appropriate, extraction and purification of products from agarose gels was performed using the QIAquick Gel Extraction kit (QIAGEN).

2.2.6 DNA Ligation

Ligation of restriction digested plasmids and PCR products or GeneStrings™ was carried out using Instant Sticky-end Ligase Master Mix (New England Biolabs, NEB) or T4 DNA ligase (NEB). Plasmid vector and PCR products were mixed at a molar ratio of 1:5 (plasmid:PCR product), and for Instant Sticky-end Ligase, an equal volume of Instant Sticky-end Ligase Master Mix was added to the vector-PCR product mix. T4 DNA ligase was added to reactions with volumes adjusted to make 1x enzyme and 1x ligation buffer, in accordance with the manufacturer's instructions. In both cases, the ligation reaction was incubated at

room temperature (approximately 16 °C) overnight. Post-reaction ligation mixture was used directly for transformations.

2.2.7 Bacterial Transformation

E. coli strains were either chemically competent (DH5 α) or electrocompetent (BL21 Origami).

2.2.7.1 Transformation of *E. coli* DH5 α

E. coli DH5 α (NEB) were transformed according to the manufacturer's protocol: One vial of competent cells was thawed on ice for 10 minutes, 3 μ l of ligation reaction mix was added, and gently mixed, before heat shock at 42 °C for 30 seconds. The cells were then incubated on ice for 5 minutes, after which 900 μ l of SOC media was added. The cells were left to recover by incubating at 37 °C, with shaking at 200 rpm. 50 μ l of recovered cell suspension was plated onto LB agar supplemented with 50 μ g/ml ampicillin, and incubated overnight at 37 °C. Colonies were patched by spreading over an area approximately 5 mm in diameter on a fresh LB agar plate (also supplemented with 50 μ g/ml ampicillin) and incubated overnight at 37 °C.

2.2.7.2 Transformation of *E. coli* BL21 Origami

2.2.7.2.1 Preparation of Electrocompetent BL21 Origami

Preparation of electrocompetent *E. coli* largely involves removal of ionic components from the bacterial suspension in order to prevent arcing during electrotransformation.

E. coli were cultured in 25 ml LB broth to an OD₆₀₀ of 0.5-0.7 (mid log phase). Cultures were pelleted by centrifugation at 3500 g for 15 minutes, then resuspended gently in 25 ml ice-cold 10 % glycerol, and incubated on ice for 30 minutes. *E. coli* were pelleted, resuspended, and incubated in ice cold 10 % glycerol twice more; resuspended once in 12.5 ml glycerol, then in 1 ml glycerol. *E. coli* were aliquoted into 50 μ l aliquots and stored at -80 °C until use in electrotransformation.

2.2.7.2.2 Electrotransformation

A Biorad Micropulser system was used according to manufacturer's instructions. Briefly, 10-100 ng of plasmid DNA was gently mixed with a 50 μ l aliquot of electrocompetent *E. coli*. *E. coli*-plasmid mixtures were added to pre-chilled 0.1 cm electroporation cuvettes. The suspension was electroporated using a BioRad micropulser at the EC1 setting (1.8 kV potential difference, 200 Ω , time constants 1.0-4.0 milliseconds). After electroporation, cells in the cuvette were immediately mixed with 1 ml of room temperature LB, and incubated for 1 hour at 37 °C, with shaking at 200 rpm. 50 μ l of recovered cell suspension

was plated onto LB agar supplemented with 50 µg/ml ampicillin, and incubated overnight at 37 °C. Colonies were patched by spreading over an area approximately 5 mm in diameter on a fresh LB agar plate (also supplemented with 50 µg/ml ampicillin and incubated overnight at 37 °C.

2.2.8 Protein Production and Purification by Affinity Chromatography

Expression strains could be induced to produce protein, then lysed, and lysates could undergo affinity chromatography to purify expressed protein. This relies on the production of a 6-Histidine tag (His⁺ tag) conjugated to the protein of interest in the cell lysate. In this project this was achieved using pET plasmid vectors. The His⁺ tagged protein can weakly bind to immobilised nickel (hence the term “affinity chromatography”), while the rest of the cell lysate flows through or is washed off. The His⁺ tagged protein is eluted from the nickel (Ni²⁺) using buffer containing imidazole, which interacts more strongly with nickel than the His⁺ tag.

In addition to His⁺ affinity chromatography, Glutathione-S-Transferase (GST) affinity chromatography was also performed. The principle remains the same, but the protein is tagged with a large (26kDa) GST tag, which binds immobilised reduced glutathione. The protein can be eluted using buffer with reduced glutathione, causing the protein to become disassociated from the reduced glutathione, or the GST-tag cleaved from the protein of interest using thrombin, releasing the protein.

Affinity chromatography only works for purification of proteins in solution. Both readily soluble and initially-insoluble proteins were produced during this project. In the case of the latter, proteins had to undergo an initial urea-solubilisation step prior to affinity chromatography, and afterwards the protein had to undergo re-folding by slowly reducing the concentration of urea present, with the intention that it retains its solubility.

2.2.8.1 Protein Expression

E. coli expression strains were incubated at 37 °C, shaking at 200 rpm overnight in LB broth supplemented with 50 µg/ml ampicillin. This was used to seed 2YT broth supplemented with 50 µg/ml ampicillin, and incubated at 37 °C, shaking at 200 rpm for ~2.5 hours until OD₆₀₀ 0.5-0.7 was reached (mid log phase). At this point, *E. coli* were induced to express proteins by addition of 1 mM IPTG, and were incubated at 25 °C, shaking at 200 rpm for up to 20 hours. *E. coli* were pelleted by centrifugation at 7000 g for 15 minutes, and were frozen at -20 °C for storage until purification, or underwent protein purification immediately.

2.2.8.2 **Purification of Soluble Proteins**

E. coli that had been induced to express readily-soluble protein were thawed, if required, and resuspended in resuspension buffer (50 mM Sodium Phosphate buffer, 0.5 mM NaCl, 20 mM imidazole pH 7.4). *E. coli* were lysed by passing through a French press three times at 1000 bar, and the lysate was centrifuged at 15000 g for 45 minutes. Supernatant underwent affinity chromatography using a 1ml Ni²⁺ column (GEHealthcare, UK) at a flow rate of 1 ml/min, and washed using 10-20 ml wash buffer (50 mM sodium phosphate buffer, 0.5 mM NaCl, 40 mM imidazole pH 7.4) at a flow rate of 2 ml/min. Protein was either manually eluted from the column in 1 ml fractions using elution buffer (50 mM sodium phosphate buffer, 0.5 mM NaCl, 300mM imidazole pH 7.4) at a flow rate of 1 ml/min, or eluted using an AKTA-Prime HPLC and a gradient elution of 50-500 mM imidazole in elution buffer at a flow rate of 1 ml/min over 10-15 1ml fractions. Cell lysates, flow through, wash through, and elutions were tested for the presence of over-expressed protein and purity using SDS-PAGE (see below) pure protein-containing fractions were pooled and dialysed using dialysis buffer, (50 mM sodium phosphate, 200 mM sodium chloride, pH 7.4) for 10-18 hours at 4 °C, and could be stored at 4 °C in the short term (up to a week) or longer-term at -20°C.

2.2.8.3 **Purification of Initially-Insoluble Proteins**

E. coli that had been induced to express initially-insoluble proteins were thawed, if required, and resuspended in resuspension buffer (50mM sodium phosphate buffer, 0.5mM NaCl, 20mM imidazole pH 7.4). *E. coli* were lysed by passing through a French press three times at 1000 bar, and the lysate was centrifuged at 15000 g for 45 minutes.

The insoluble fraction of the cell lysate was suspended in resuspension buffer containing 8 M urea, and incubated for 3 hours at room temperature, on lab rollers. The suspension was centrifuged at 15000 g for 45 minutes, then subjected to affinity chromatography using a 1ml Ni²⁺ column (GEHealthcare, UK) at a flow rate of 1 ml/min, and washed using 10-20 ml wash buffer (8 M urea, 50mM Sodium Phosphate buffer, 0.5 mM NaCl, 40 mM imidazole pH 7.4) at a flow rate of 2 ml/min. Protein was manually eluted from the column in 1 ml fractions using elution buffer (8 M urea, 50 mM sodium phosphate buffer, 0.5 mM NaCl, 300 mM imidazole pH 7.4) at a flow rate of 1 ml/min, cell lysates, flow through, wash through, and elutions were tested for the presence of over-expressed protein and purity using SDS-PAGE (see below). Pure protein-containing fractions were pooled and underwent step-down dialysis to remove urea, and attempt to refold the protein, while maintaining

solubility. Dialysis was performed in five stages using dialysis buffer (50 mM Sodium Phosphate, 200 mM Sodium Chloride, pH 7.4), which contained either 4 M, 1 M, 0.5 M, 0 M, and 0 M urea, respectively. All stages were performed for 2 hours, except for the first 0 M urea stage (the fourth stage), which was performed for ~20 hours (overnight).

2.2.8.4 Protein Purification using GST-Affinity Chromatography

E. coli that had been induced to express readily-soluble GST-tagged proteins were thawed, if required, and resuspended in PBS (100 mM sodium Phosphate Monobasic-Potassium Phosphate Dibasic buffer, with 50 mM NaCl, pH 7.4). *E. coli* were lysed by passing through a French press three times at 1000 bar, and the lysate was centrifuged at 15000 g for 45 minutes. Supernatant underwent affinity chromatography using a 1 ml GSTrap column (GEHealthcare, UK) at a flow rate of 1 ml/min, and washed using 10-20 ml PBS at a flow rate of 2 ml/min. The GST tag was cleaved by injection of 1 ml of 1 mg/ml thrombin (Sigma Aldrich, in PBS) onto the column, followed by incubation at room temperature for 4 hours (or at 4 °C overnight). Protein was eluted from the column using PBS into 1 ml fractions. To remove thrombin, fractions were incubated with 50 µl Benzamidine-agarose beads (Sigma Aldrich) per fraction on lab rollers at 4 °C for 30 minutes. Benzamidine agarose was removed by centrifugation for 5 minutes at 15000 g, and purified protein was placed into fresh Eppendorf tubes.

2.2.8.5 LPS-Decontamination of Purified NanH

Purified NanH for use in experiments aiming to investigate immunomodulation of epithelial cells (chapter 4, sections 4.2.5 and 4.3.5.1) had to be free of residual LPS from the *E. coli* expression strain. Purified NanH underwent treatment with polymixin agarose beads (Sigma Aldrich) at a volume of beads considered appropriate according to the manufacturer's instructions. NanH was incubated with the polymixin-agarose beads for 1 hour at 4 °C, with agitation using lab rollers. Beads were removed by centrifugation at 16000 g for 5 minutes.

2.2.9 BCA Assays

BCA assays were routinely performed to check protein concentrations, using the Pierce BCA assay kit (Thermo-Fisher Scientific), according to manufacturer's instructions. Samples and bovine serum albumin (BSA) standards for production of standard curves were always diluted in the same buffer during each assay.

2.2.10 Sodium Dodecyl Sulphate-Poly Acrylamide Gel Electrophoresis (SDS-PAGE)

2.2.10.1 SDS-PAGE Gel Preparation

Buffers and reagents to make gels were prepared in house with reagents and instructions shown in table 2.4, or bought from commercial suppliers.

Buffer Name	Reagents	Instructions
Upper Tris	6.06 g Tris Base, 0.4 g SDS	Reagents dissolved in dH ₂ O, adjusted to pH 6.8 with HCl, total volume 100 ml.
Lower Tris	18.17 g Tris Base, 0.4 g SDS	Reagents dissolved in dH ₂ O, adjusted to pH 8.8 with NaOH, total volume 100 ml
Running Buffer	12 g Tris Base, 4 g SDS, 57.5 g glycine	Reagents dissolved in 1000 ml dH ₂ O to make a stock solution. Prior to use, 160 ml was added to 840 ml dH ₂ O.
Loading Buffer	40 ml 100 mM Tris-HCl, 10 ml 20% glycerol, 1 g SDS, 0.1 g Bromophenol Blue, 200mM DTT	Reagents mixed to make a stock without DTT. DTT added prior to use.

Table 2.4. SDS-PAGE buffers.

DTT-Dithiothreitol, dH₂O-deionised water. Reagents purchased from Thermo-Fisher Scientific.

Polyacrylamide gels were prepared prior to SDS-PAGE using the reagents as described in table 2.5. The resolving gel was prepared and cast first; reagents were combined in the order shown in the table from top to bottom, with the volumes shown here sufficient for two 1 mm-depth SDS-PAGE gels cast using BioRad-supplied glass plates and gel casting stations. After pouring into the casting station (leaving ~1 cm room for the stacking gel), the gel was levelled using isopropanol (which also prevented air bubbles from disrupting gel formation), which was washed from the gel with water prior to adding the stacking gel, into which a comb was placed to form wells. After the gel was set, it was placed in a BioRad SDS-PAGE tank (mini PROTEAN Tetra System) and the tank filled with running buffer. Loading buffer was added to protein samples and heated at 95 °C for 5 minutes, before loading into the wells of the SDS-PAGE gel, with the inclusion of a molecular weight marker in at least one well (pre-stained EZ run Protein Ladder, ThermoFisher Scientific). Gels were

run at 100-220 V (constant amps) for up to 3 hours until the loading dye was seen to have left the gel or the molecular weight marker was well distributed. The gel was removed from the glass plates and stained using InstantBlue™ (Expedeon) for at least 45 minutes at room temperature with agitation.

Reagent	Resolving Gel		Stacking Gel
	12% Gel	15% Gel	
Lower Tris	2.5 ml	2.5 ml	-
Upper Tris	-	-	2.1 ml
Acrylamide	3 ml	3.75ml	4.725 ml
dH ₂ O	4.3 ml	3.55 ml	0.975 ml
TEMED	5 ul	5 ul	17 ul
APS	350 ul	350 ul	100 ul

Table 2.5. Reagent volumes required for casting of SDS-PAGE resolving gels.

TEMED- Tetramethylethylenediamine, APS-Ammonium Persulphate, dH₂O-deionised water.

2.2.11 Biochemical Studies of Sialidases and Sialidase Subunits

Purification of the sialidases of *P. gingivalis* (SiaPG) and *T. forsythia* (NanH) enabled studies of the enzymes in isolation from their native organisms.

2.2.11.1 pH optima derivation of periodontal pathogen sialidases

The fluorogenic sialic acid substrate MUNANA (described further in section 2.3.6) was used to ascertain the activity of NanH and PGsia under different pH conditions. 2.5 nM NanH or 5 nM SiaPG was incubated in the presence of 0.1mM MUNANA, in a variety of 20 mM buffers; Sodium Citrate-Citric Acid (pH 3-6.4) Sodium Phosphate Monobasic-Dibasic (pH 6.8-8.8), or Sodium Carbonate-Sodium Bicarbonate (pH 9.2-10.5), at room temperature for up to 2 minutes. At 1 and 2 minutes, 50µl of each reaction was quenched in 75µl of 100mM sodium carbonate buffer, pH 10.5. Fluorescence at each time point was measured at excitation at 350 nm, emission 450 nm, using a Tecan Infinite M200 microplate reader. Sialidase activity of whole pathogens was also carried out using reaction conditions described in section 2.2, but PBS was replaced with the buffers described here, and reactions were quenched at 30 second time points. Sialidase activity of whole pathogens or

purified sialidases was expressed as the fluorescence at 450 nm after excitation at 350 nm (arbitrary units).

2.2.11.2 *Reaction kinetics of Periodontal Pathogen Sialidases with MUNANA*

MUNANA was exposed to NanH or SiaPG. Reactions contained 1 or 2.5 nM NanH or SiaPG and a variable concentration of MUNANA, in one of a variety of buffers: Either 50 mM sodium phosphate, 200 mM NaCl, pH 7.4, or 20 mM sodium phosphate buffer, pH 7.2, or 20 mM sodium citrate buffer, pH 5.2, or 20 mM sodium citrate buffer, 20 mM NaCl, pH 5.2. These were incubated at room temperature for up to 3 minutes, with 50 µl of each reaction removed at 1 minute intervals, and the reaction was halted and pH equalised by addition of 75 µl sodium carbonate buffer, pH 10.5. Fluorescence at each time point was measured at excitation at 350 nm, emission 450 nm, using a Tecan Infinite M200 microplate reader, and application of a 4-MU standard curve enabled quantification of the rate of 4-MU release. The initial rate in all conditions tested appeared to occur between the 2 and 3 minute time points, and Initial Rate, or Velocity (V_0 , 4-MU release µmol/min/mg enzyme) was plotted against ligand concentration (µM), and the K_M , V_{max} determined using the following equation:

$$Y = V_{max} \times X / (K_M + X)$$

Where X is the substrate concentration, and Y is the enzyme velocity, V_{max} is the maximum enzyme velocity, and K_M is the Michaelis-Menten constant.

2.2.11.3 *Inhibition of Purified Sialidases*

2.5 nM NanH or 5 nM PGsialase was incubated in the presence of 0.1 mM MUNANA, in 50 mM Sodium Phosphate 200 mM NaCl, pH 7.4 (to mimic host physiological conditions), in the presence of different concentrations of zanamivir. Sialidase inhibition was expressed as the percentage change in fluorescence at a given concentration of inhibitor, compared to fluorescence in the absence of inhibitor, as determined by the formula described in section 2.2. In the case of zanamivir, sialidase inhibition (%) was plotted against log[inhibitor], and the variable slope model was applied to obtain the IC_{50} of zanamivir for SiaPG and NanH, using the equation:

$$Y = 100 / (1 + 10^{(\text{Log}IC_{50} - X) \times \text{Hillslope}})$$

Where Y=Sialidase Activity, relative to no inhibitor condition (%), X= logarithm [inhibitor], and Hillslope refers to the steepness of the curve.

2.2.11.4 ***Quantification of Sialic Acid Release from host-glycans; Thiobarbituric Acid Assay***

Release of sialic acid from the host-relevant ligands 3-sialyllactose, 6-sialyllactose, 3-sialyl lewis A (SLeA), 3-sialyl lewis X (SLeX), and bovine submaxillary mucin (BSM) by NanH and SiaPG was carried out in a number of different assays (described in sections 2.2.10.5, 2.3.6, and 3.2.1, and 3.3.1), and released sialic acid was quantified by the thiobarbituric acid (TBA) assay, using a protocol based on work by Aminoff et al. (Aminoff 1961). After digestion of host ligand by NanH or SiaPG, 50µl of the resulting reaction mix containing free sialic acid was oxidised by addition of 25 µl of 20 mM Sodium Periodate in 60 mM H₂SO₄, and incubated at 37 °C for 30 minutes. Oxidation was halted by addition of 25µl 2% (w/v) sodium arsenite in 250 mM H₂SO₄. Oxidised sialic acid was labelled with a thiol group by addition of 200 µl 100 mM Thiobarbituric Acid pH 9.0 and heating at 95 °C for 7.5 minutes. In some reactions, the resulting chromophore was extracted by vortexing with 500 µl acidified butanol (butanol containing 5 % (v/v) 12 M HCl) and centrifugation at 15000 g for 2 minutes. 100 µl of reaction mix or 100 µl of butanol-extracted chromophore was added to the wells of a clear 96 well plate, and the absorbance at 549 nm was measured using a TECAN plate reader. By performing the TBA assay on a standard curve of known sialic acid (Neu5Ac) concentrations in the above assay, and blank conditions containing ligand but no sialidase, Neu5Ac release (µM) from the above ligands was determined.

2.2.11.5 ***Reaction kinetics of Periodontal Pathogen Sialidases With Host-Relevant Ligands***

The host relevant ligands 3-sialyllactose, 6-sialyllactose, 3-sialyl lewis A (SLeA), and 3-sialyl lewis X (SLeX) were exposed to NanH or SiaPG before undergoing the TBA assay described above (section 2.2.10.4) to determine the release of Neu5Ac over time. Reactions contained 50 nM NanH or SiaPG and a variable concentration of ligand, in 50 mM sodium phosphate, 200 mM NaCl (pH 7.4). These were incubated at 37 °C for up to 15 minutes, and 50 µl of each reaction was removed at different time points and oxidised by addition of 25 µl of 20 mM Sodium Periodate in 60 mM H₂SO₄ (halting sialidase activity and starting the TBA assay). After determination of the initial rate, usually between 0.5-1 or 1-2, minutes for each ligand at all concentrations tested, release of Neu5Ac Initial Rate, or Velocity (V₀, Neu5Ac release µmol/min/mg enzyme) was plotted against ligand concentration (µM), and the K_m, V_{max} determined using the following equation:

$$Y = V_{max} * X / (K_M + X)$$

Where X is the substrate concentration, and Y is the enzyme velocity, V_{max} is the maximum enzyme velocity, and K_M is the Michaelis-Menten constant.

2.2.11.6 *Investigation of Protein-Ligand Binding*

A fluorescence based tryptophan quenching assay was used to quantify binding of proteins to a variety of potential ligands. This relied on the presence of tryptophan residues, which fluoresce at ~330 nm on excitation at 295 nm. Binding of a protein to a given ligand results in conformational changes in the peptide, further exposing the tryptophan residues to excitation (leading to increased fluorescence), or enclosing the tryptophan residues and decreasing excitation (resulting in decreased fluorescence).

Proteins were diluted to 0.1 μ M in 50 mM sodium phosphate, 200 mM sodium chloride, and 195 μ l was dispensed to the wells of a UV clear 96 well plate (Greiner, UK) and 5 μ l of ligand at 20 x concentration. Conditions were incubated at 25 °C for 5 minutes and fluorescence was quantified using a TECAN 200M infinite series plate reader (Tecan, Switzerland). Fluorescence was measured at excitation 295 nm, emission scanned from 315-380 nm, slit apertures were 5 nm each. Changes in protein fluorescence in the presence of a given concentration of ligand were plotted as a percentage change in fluorescence from the protein-only condition, and used to determine the B_{max} and K_d of a given ligand using the following equation:

$$Y = B_{max} / X(K_d + X)$$

Where X is the final concentration of ligand, Y is the percentage change in protein fluorescence in relation to the protein-only fluorescence signal, and B_{max} is the extrapolated maximum specific binding.

2.2.12 **Structural Characterisation of NanH -Crystal Trials**

Structural characterisation of NanH CBM and its binding with ligands requires X-ray crystallography approaches. To this end, high throughput crystal screens were set up using a Hydra liquid dispensing robot (Art Robbins Instruments, USA) to seed 96 well-sitting drop crystallisation plates (Greiner, UK) using the commercially available crystal trial buffer suite; JCSG+ (Qiagen, UK). Each sitting drop well contained a 1 μ l droplet of 1.6 mg/ml NanH CBM. During attempts to co-crystallise with zanamivir, 25 mM zanamivir was incubated on ice for 30 minutes with NanH CBM before spotting on sitting drop plates as described.

2.3 Results

2.3.1 Bioinformatic Analysis of NanH and SiaPG

Establishing the similarity of periodontal pathogen sialidases to those from other bacteria was an important first-step before purification and biochemical characterisation and one that could potentially yield new information on these enzymes. A bioinformatics approach was taken, which also allowed the prediction of sialidase-protein structures based on similarity to other sialidases, and to establish the presence of putative functional domains.

2.3.1.1 *NanH Possesses a Sialidase Domain and Putative Carbohydrate Binding Module (CBM)*

NanH is the major sialidase of *T. forsythia*, a BLAST search was carried out on NanH from *T. forsythia* 92.A2 (<http://blast.ncbi.nlm.nih.gov/Blast.cgi>)- this was the original sequenced strain of *T. forsythia* that was erroneously annotated as ATCC 43037 by the Forsyth Institute, and this revealed two distinct domains as indicated in figure 2.1. These are the “BNR associated N superfamily”- a sequence of ~200 residues (in NanH this is 149 residues without the signal peptide, or 197 with signal peptide). The BNR associated superfamily is a conserved sequence located at the N-terminus among similar proteins. The second domain was part of the “sialidase superfamily”, and this was which was shown to contain the catalytic active site and predicted β -propellers which are a feature associated with the active site of sialidases, discussed later.

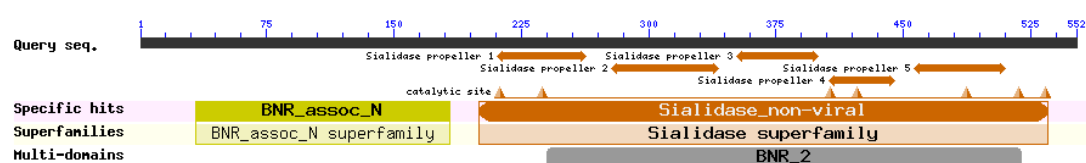


Figure 2.1 The amino acid sequence of NanH highlights distinct domains.

The NanH sequence from *T. forsythia* 92.A2 underwent a BLAST search against non-redundant protein sequences to reveal two distinct domains; the N-terminally located BNR_assoc_N superfamily, and the Sialidase superfamily. The active site and β -propellers which are a characteristic feature of sialidases are also highlighted.

Unsurprisingly, the most homologous sequences found by the BLAST came from *T. forsythia* strains, followed by other *Bacteroidetes*. The majority of alignments with strong homology came from the closely related *Bacteroides* spp., but there were some proteins

from other genera identified, including *Porphyromonas*. (although *P. gingivalis* was not listed). Alignments of a selection of the proteins closely related to NanH were performed using Clustal Omega and ESPript (figure 2.2). These sequences were obtained from four *T. forsythia* strain sequences that are present in the public databases, two *Parabacteroides* species with the greatest homology to NanH, two *Bacteroides* species with the greatest homology to NanH, and one each from *Allistaphanes*, *Porphyromonas*, and *Dysgonomonas* species, which were genera only listed once on the protein BLAST search. The precise sequences and strain details can be seen in appendix 7.1. Key findings from this alignment were that the sialidases have greater homology in the C-terminal sialidase superfamily domain (from residue 198 in the alignment, 197 in *T. forsythia* NanH), and across all the enzymes in this group of bacteria this sequence is quite well conserved; the lowest homology was 58.92% between the sialidases in *B. fragilis* and *Allistipes* spp., and all *T. forsythia* sialidases had >97% homology.

A)

	1	10	20	30	40																																						
Allistipes_spp.M	KKR	TF	WLI	AS	SLR	I	HNPI	D	I	L	L	R	M	N	V	L	P	Q	I	R																					
T.forsythia_K816M	KKR	F	LIV	C	F	A	S	M	Q	I	I	R	A	D	S	V	V	Q	N	PI	D	I	L	L	R	M	N	V	L	P	Q	I	R								
T.forsythia_92_A2M	KKR	F	W	I	C	L	F	A	S	M	Q	M	T	R	A	D	S	V	V	Q	N	PI	D	I	L	L	R	M	N	V	L	P	Q	I	R						
T.forsythia_3313M	KKR	F	L	I	V	C	L	F	A	S	M	Q	M	T	R	A	D	S	V	V	Q	N	PI	D	I	L	L	R	M	N	V	L	P	Q	I	R					
T.forsythia_43037M	KKR	F	W	I	C	L	F	A	S	M	Q	M	T	R	A	D	S	V	V	Q	N	PI	D	I	L	L	R	M	N	V	L	P	Q	I	R						
D.gordoniiM	KK	S	I	F	Y	L	C	L	F	I	A	Q	T	A	F	A	D	S	L	Y	V	R	E	QI	D	I	L	L	R	M	N	V	L	P	Q	I	R				
D.distasonisM	KK	T	F	L	Y	F	C	L	F	I	V	Q	T	A	F	A	D	S	I	Y	V	R	E	QI	D	I	L	L	R	M	N	V	L	P	Q	I	R				
Porphyromonas_sp.31_2	ME	F	T	Y	L	L	I	S	T	Y	K	Q	K	H	E	K	T	F	L	Y	F	C	L	F	I	V	Q	T	A	F	A	D	S	L	Y	V	R	E	Q				
DysgonomonasM	KN	L	F	L	S	F	F	L	L	S	L	T	I	N	S	A	S	D	F	V	K	I	K	A	PI	D	I	L	L	R	M	N	V	L	P	Q	I	R			
B.fragilisM	KK	A	V	I	L	S	L	F	C	L	F	L	C	A	I	F	V	V	Q	A	D	T	I	F	V	R	E	TI	D	I	L	L	R	M	N	V	L	P	Q	I	R
B.thetaiotaomicronM	KR	N	H	I	L	T	L	L	L	G	C	S	I	F	V	R	A	S	D	F	V	F	V	H	Q	TI	D	I	L	L	R	M	N	V	L	P	Q	I	R		

	50	60	70	80	90	100																																																	
Allistipes_spp.	V	D	A	V	Q	C	D	V	L	S	L	T	V	E	F	C	P	D	T	D	T	K	S	M	A	E	L	L	L	F	Y	S	C	E	A	V	R	Q	C	L	H	F	S	D	V	S	T	S	A	H	N	V	M		
T.forsythia_K816	I	D	A	T	K	C	D	V	L	N	R	L	T	I	R	F	C	N	E	D	K	L	S	E	V	K	A	V	R	L	F	Y	A	C	E	A	A	T	C	R	S	R	F	A	D	V	T	V	S	S	H	N	I	R	
T.forsythia_92_A2	I	D	A	T	K	C	D	V	L	N	R	L	T	I	R	F	C	N	E	D	K	L	S	E	V	K	A	V	R	L	F	Y	A	C	E	A	A	T	C	R	S	R	F	A	D	V	T	V	S	S	H	N	I	R	
T.forsythia_3313	I	D	A	T	K	C	D	V	L	N	R	L	T	I	R	F	C	N	E	D	K	L	S	E	V	K	A	V	R	L	F	Y	A	C	E	A	A	T	C	R	S	R	F	A	D	V	T	V	S	S	H	N	I	R	
T.forsythia_43037	I	D	A	T	K	C	D	V	L	N	R	L	T	I	R	F	C	N	E	D	K	L	S	E	V	K	A	V	R	L	F	Y	A	C	E	A	A	T	C	R	S	R	F	A	D	V	T	V	S	S	H	N	I	R	
D.gordonii	I	D	AQ	K	D	V	L	N	K	F	T	L	Q	F	C	N	E	T	N	L	S	D	I	K	A	I	R	L	F	Y	S	C	E	A	P	A	R	E	C	H	F	N	D	V	T	V	S	F	T	P	C			
D.distasonis	I	D	AQ	K	D	V	L	N	E	I	I	Q	I	Q	I	C	D	N	V	L	S	D	I	K	A	I	R	L	F	Y	S	C	E	A	P	S	K	E	C	H	F	N	D	V	T	V	S	S	H	I	P	C		
Porphyromonas_sp.31_2	I	D	AQ	K	D	V	L	N	E	I	I	Q	I	Q	I	C	D	N	V	L	S	D	I	K	A	I	R	L	F	Y	S	C	E	A	P	S	K	E	C	H	F	N	D	V	T	V	S	S	H	I	P	C		
Dysgonomonas	L	D	AA	N	S	K	V	L	N	V	K	V	N	L	D	K	E	V	N	L	S	E	I	K	S	I	E	L	L	Y	S	C	E	C	V	Q	R	E	C	K	T	F	Y	A	D	V	T	V	S	K	D	V	P	C
B.fragilis	L	D	AK	E	S	Q	T	L	N	V	V	L	N	L	D	K	E	C	V	N	L	S	E	I	K	S	I	E	L	L	Y	S	C	E	A	L	Q	D	S	C	K	K	F	A	D	V	T	V	S	S	N	T	P	C
B.thetaiotaomicron	L	D	AK	E	S	R	M	H	E	I	V	L	D	F	G	R	S	V	L	S	D	V	Q	A	V	E	L	L	Y	S	C	E	A	L	Q	D	R	C	K	N	R	F	A	D	V	T	V	S	S	H	R	P	C	

	110	120	130	140	150	160																																																		
Allistipes_spp.	T	H	S	A	N	F	S	Y	S	M	Q	E	V	S	K	I	CR	K	V	V	H	S	R	Q	P	M	V	C	C	N	F	Y	M	V	S	V	C	N	P	D	A	S	L	T	E	L	R	A	R	V	S				
T.forsythia_K816	T	H	S	A	N	F	S	Y	S	F	R	Q	D	E	V	T	T	V	AN	T	L	L	K	T	R	Q	P	M	V	C	C	N	F	Y	M	V	S	V	S	D	R	N	T	S	L	S	K	L	T	P	T	V	T		
T.forsythia_92_A2	T	H	S	A	N	F	S	Y	S	F	R	Q	D	E	V	T	T	V	AN	T	L	L	K	T	R	Q	P	M	V	C	C	N	F	Y	M	V	S	V	S	D	R	N	T	S	L	S	K	L	T	P	T	V	T		
T.forsythia_3313	T	H	S	A	N	F	S	Y	S	F	R	Q	D	E	V	T	T	V	AN	T	L	L	K	T	R	Q	P	M	V	C	C	N	F	Y	M	V	S	V	S	D	R	N	T	S	L	S	K	L	T	P	T	V	T		
T.forsythia_43037	T	H	S	A	N	F	S	Y	S	F	R	Q	D	E	V	T	T	V	AN	T	L	L	K	T	R	Q	P	M	V	C	C	N	F	Y	M	V	S	V	S	D	R	N	T	S	L	S	K	L	T	P	T	V	T		
D.gordonii	T	H	V	A	N	F	S	Y	S	F	K	Q	D	E	V	T	A	P	AN	T	I	L	T	S	K	Q	P	M	V	C	C	N	F	Y	M	V	S	V	S	D	R	N	T	S	L	S	R	V	S	F	T	M	P		
D.distasonis	T	H	E	A	L	S	Y	S	F	R	Q	D	E	V	T	A	P	L	S	R	T	V	EL	T	S	K	Q	P	M	V	C	C	N	F	Y	M	V	S	V	S	D	R	N	T	S	L	L	A	K	V	A	T	T	M	P
Porphyromonas_sp.31_2	T	H	E	A	L	S	Y	S	F	R	Q	D	E	V	T	A	P	L	S	R	T	V	EL	T	S	K	Q	P	M	V	C	C	N	F	Y	M	V	S	V	S	D	R	N	T	S	L	L	A	K	V	A	T	T	M	P
Dysgonomonas	T	H	A	N	S	Y	S	F	K	K	T	E	L	S	T	L	KN	E	I	L	J	A	D	Q	L	F	C	C	N	F	Y	M	V	S	V	S	D	R	N	T	S	L	S	N	V	A	T	I	D						
B.fragilis	T	H	A	N	F	S	Y	S	F	K	K	S	E	V	T	P	CN	Q	V	V	K	G	D	Q	K	L	F	C	C	N	F	Y	M	V	S	V	S	D	R	N	T	S	L	S	K	V	T	A	D	I	A				
B.thetaiotaomicron	T	H	A	I	F	S	Y	S	F	K	C	A	E	V	L	CP	SA	K	V	V	L	K	S	H	Y	K	L	F	C	C	N	F	Y	M	V	S	V	S	D	R	N	T	S	L	F	T	K	I	S	S	E	L		

	170	180	190	200	210	220																																													
Allistipes_spp.	V	V	N	C	K	I	F	Y	A	C	D	SR	D	V	V	R	R	M	C	V	R	A	C	D	H	S	M	A	V	R	I	P	C	L	Y	T	N	S	C	S	L	I	C	V	Y	D	V	R	R	S
T.forsythia_K816	A	V	I	N	D	K	P	A	V	I	AG	E	Q	A	V	R	R	M	C	V	R	A	C	D	D	C	S	A	S	F	R	I	P	C	L	Y	T	N	S	C	T	L	I	C	V	Y	D	V	R	R
T.forsythia_92_A2	A	V	I	N	D	K	P	A	V	I	AG	E	Q	A	V	R	R	M	C	V	R	A	C	D	D	C	S	A	S	F	R	I	P	C	L	Y	T	N	S	C	T	L	I	C	V	Y	D	V	R	R
T.forsythia_3313	A	V	I	N	D	K	P	A	V	I	AG	E	Q	A	V	R	R	M	C	V	R	A	C	D	D	C	S	A	S	F	R	I	P	C	L	Y	T	N	S	C	T	L	I	C	V	Y	D	V	R	R
T.forsythia_43037	A	V	I	N	D	K	P	A	V	I	AG	E	Q	A	V	R	R	M	C	V	R	A	C	D	D	C	S																							

```

350      360      370      380      390      400
Allistipes spp. QCPCHCITMDCCTVFPFQVFDKIRDPACLISSKDCEIWHHEPVARINTTRAQVAEVE
T.forsythia_KS16 QCPCHCITMDCCTVFPFQVFDKIRDPACLISSKDCEIWHHEPVARINTTRAQVAEVE
T.forsythia_92_A2 QCPCHCITMDCCTVFPFQVFDKIRDPACLISSKDCEIWHHEPVARINTTRAQVAEVE
T.forsythia_3313 QCPCHCITMDCCTVFPFQVFDKIRDPACLISSKDCEIWHHEPVARINTTRAQVAEVE
T.forsythia_43037 QCPCHCITMDCCTVFPFQVFDKIRDPACLISSKDCEIWHHEPVARINTTRAQVAEVE
P.gordonii QCPCHCITMDCCTVFPFQVFDKIRDPACLISSKDCEIWHHEPVARINTTRAQVAEVE
P.distasonis QCPCHCITMDCCTVFPFQVFDKIRDPACLISSKDCEIWHHEPVARINTTRAQVAEVE
Porphyromonas_sp.31_2 QCPCHCITMDCCTVFPFQVFDKIRDPACLISSKDCEIWHHEPVARINTTRAQVAEVE
Dysgonomonas QCPCHCITMDCCTVFPFQVFDKIRDPACLISSKDCEIWHHEPVARINTTRAQVAEVE
B.fragilis QCPCHCITMDCCTVFPFQVFDKIRDPACLISSKDCEIWHHEPVARINTTRAQVAEVE
B.thetaiotaomicron QCPCHCITMDCCTVFPFQVFDKIRDPACLISSKDCEIWHHEPVARINTTRAQVAEVE

```

```

410      420      430      440      450      460
Allistipes spp. PCVLMNMRDNRCCSRAVAITNDLCKIWEHPSSRSALQESVCMASLISKVAKDNITCKK
T.forsythia_KS16 PCVLMNMRDNRCCSRAVAITNDLCKIWEHPSSRSALQESVCMASLISKVAKDNITCKK
T.forsythia_92_A2 PCVLMNMRDNRCCSRAVAITNDLCKIWEHPSSRSALQESVCMASLISKVAKDNITCKK
T.forsythia_3313 PCVLMNMRDNRCCSRAVAITNDLCKIWEHPSSRSALQESVCMASLISKVAKDNITCKK
T.forsythia_43037 PCVLMNMRDNRCCSRAVAITNDLCKIWEHPSSRSALQESVCMASLISKVAKDNITCKK
P.gordonii PCVLMNMRDNRCCSRAVAITNDLCKIWEHPSSRSALQESVCMASLISKVAKDNITCKK
P.distasonis PCVLMNMRDNRCCSRAVAITNDLCKIWEHPSSRSALQESVCMASLISKVAKDNITCKK
Porphyromonas_sp.31_2 PCVLMNMRDNRCCSRAVAITNDLCKIWEHPSSRSALQESVCMASLISKVAKDNITCKK
Dysgonomonas PCVLMNMRDNRCCSRAVAITNDLCKIWEHPSSRSALQESVCMASLISKVAKDNITCKK
B.fragilis PCVLMNMRDNRCCSRAVAITNDLCKIWEHPSSRSALQESVCMASLISKVAKDNITCKK
B.thetaiotaomicron PCVLMNMRDNRCCSRAVAITNDLCKIWEHPSSRSALQESVCMASLISKVAKDNITCKK

```

```

470      480      490      500      510      520
Allistipes spp. LLFSPNDNTTDCRHITITIKSLDCCCTWLPY.SLMLDRCDSWCYSCLSMIDRETVCISYE
T.forsythia_KS16 LLFSPNDNTTDCRHITITIKSLDCCCTWLPY.SLMLDRCDSWCYSCLSMIDRETVCISYE
T.forsythia_92_A2 LLFSPNDNTTDCRHITITIKSLDCCCTWLPY.SLMLDRCDSWCYSCLSMIDRETVCISYE
T.forsythia_3313 LLFSPNDNTTDCRHITITIKSLDCCCTWLPY.SLMLDRCDSWCYSCLSMIDRETVCISYE
T.forsythia_43037 LLFSPNDNTTDCRHITITIKSLDCCCTWLPY.SLMLDRCDSWCYSCLSMIDRETVCISYE
P.gordonii LLFSPNDNTTDCRHITITIKSLDCCCTWLPY.SLMLDRCDSWCYSCLSMIDRETVCISYE
P.distasonis LLFSPNDNTTDCRHITITIKSLDCCCTWLPY.SLMLDRCDSWCYSCLSMIDRETVCISYE
Porphyromonas_sp.31_2 LLFSPNDNTTDCRHITITIKSLDCCCTWLPY.SLMLDRCDSWCYSCLSMIDRETVCISYE
Dysgonomonas LLFSPNDNTTDCRHITITIKSLDCCCTWLPY.SLMLDRCDSWCYSCLSMIDRETVCISYE
B.fragilis LLFSPNDNTTDCRHITITIKSLDCCCTWLPY.SLMLDRCDSWCYSCLSMIDRETVCISYE
B.thetaiotaomicron LLFSPNDNTTDCRHITITIKSLDCCCTWLPY.SLMLDRCDSWCYSCLSMIDRETVCISYE

```

```

530
Allistipes spp. SSQABTFQAVKIDLIK.
T.forsythia_KS16 SSQABTFQAVKIDLIK.
T.forsythia_92_A2 SSQABTFQAVKIDLIK.
T.forsythia_3313 SSQABTFQAVKIDLIK.
T.forsythia_43037 SSQABTFQAVKIDLIK.
P.gordonii SSQABTFQAVKIDLIK.
P.distasonis SSQABTFQAVKIDLIK.
Porphyromonas_sp.31_2 SSQABTFQAVKIDLIK.
Dysgonomonas SSQABTFQAVKIDLIK.
B.fragilis SSQABTFQAVKIDLIK.
B.thetaiotaomicron SSQABTFQAVKIDLIK.

```

B)

	1)	2)	3)	4)	5)	6)	7)	8)	9)	10)	11)
1) <i>Allistipes</i> spp.	100	68.66	68.66	68.28	68.66	63.5	65.67	65.36	60.52	58.92	59.48
2) <i>T. forsythia</i> _KS16	68.66	100	97.22	97.77	97.77	74.54	73.93	73.37	63.75	65.61	64.87
3) <i>T. forsythia</i> _92.A2	68.66	97.22	100	97.96	97.96	74.16	73.74	73.18	63.38	65.8	65.61
4) <i>T. forsythia</i> _3313	68.28	97.77	97.96	100	98.14	74.91	74.3	73.74	63.94	66.17	65.43
5) <i>T. forsythia</i> _ATCC 43037	68.66	97.77	97.96	98.14	100	75.09	74.3	73.74	63.57	65.99	65.43
6) <i>P. gordonii</i>	63.5	74.54	74.16	74.91	75.09	100	85.56	85.19	66.17	66.67	65
7) <i>P. distasonis</i>	65.67	73.93	73.74	74.3	74.3	85.56	100	98.71	64.81	67.53	66.98
8) <i>Porphyromonas</i> _Sp.31_2	65.36	73.37	73.18	73.74	73.74	85.19	98.71	100	65	67.16	66.42
9) <i>Dysgonomonas</i>	60.52	63.75	63.38	63.94	63.57	66.17	64.81	65	100	66.73	65.43
10) <i>B. fragilis</i>	58.92	65.61	65.8	66.17	65.99	66.67	67.53	67.16	66.73	100	77.76
11) <i>B. thetaiotaomicron</i>	59.48	64.87	65.61	65.43	65.43	65	66.98	66.42	65.43	77.76	100

Figure 2.2. Primary amino acid sequence homology in sialidases closely related to NanH from *T. forsythia*.

BLAST revealed a number of sequences with homology to *T. forsythia* (strain 92.A2) NanH. All were annotated as “sialidase” in the NCBI database, with the exception of the entry for *Allistipes* spp., which was annotated as “bNR/Asp-box repeat protein”. These sequences were aligned in Clustal Omega, followed by ESPript. A) ESPript Alignment of Sequences similar to *T. forsythia* NanH. B) Percentage Identity Matrix from Clustal Omega, the numbers shown represent % homology between each sialidase.

Protein BLAST searches (BLASTP) and sequence alignments shown above shed some light on the domains of *T. forsythia* NanH, but these alone cannot accurately predict secondary structural features. To do this, Multalin was used to align the *T. forsythia* NanH amino acid sequences with the sequence of a glycoside hydrolase from *Parabacteroides distasonis*- a candidate sialidase-for which the crystal structure has been determined (Protein Data Bank-PDB-ID: 4FJ6). The resulting alignment was analysed using ESPript to predict secondary structural features using the *P. distasonis* candidate sialidase. Percentage equivalence with a threshold global score of 0.7 was used to determine the similarity between aligned amino acid residues and the overall alignment. The resulting alignment shown in figure 2.3 gave an indication of the secondary structural features of *T. forsythia*. Notably, all but one of the secondary structural predictions fell completely within sequences with a high degree of similarity (as determined by the above parameters, framed in blue)-indicating, at least to some degree, that the secondary structural prediction is valid. The alignment appeared to display characteristic features found in sialidases; Asp-boxes and the RIP motif, the latter of which is considered essential for sialidase activity. A total of five Asp-boxes were found in the aligned sialidases (starting at residues 237, 317, 377, 422 and 484). These are short motifs with the amino acid sequence S/T-X-D-X-G-X-X-W/F/Y. Asp-boxes were initially discovered in sialidases, and later in a number of carbohydrate-active enzymes, yet their precise function has yet-to-be elucidated (Copley et al. 2009).

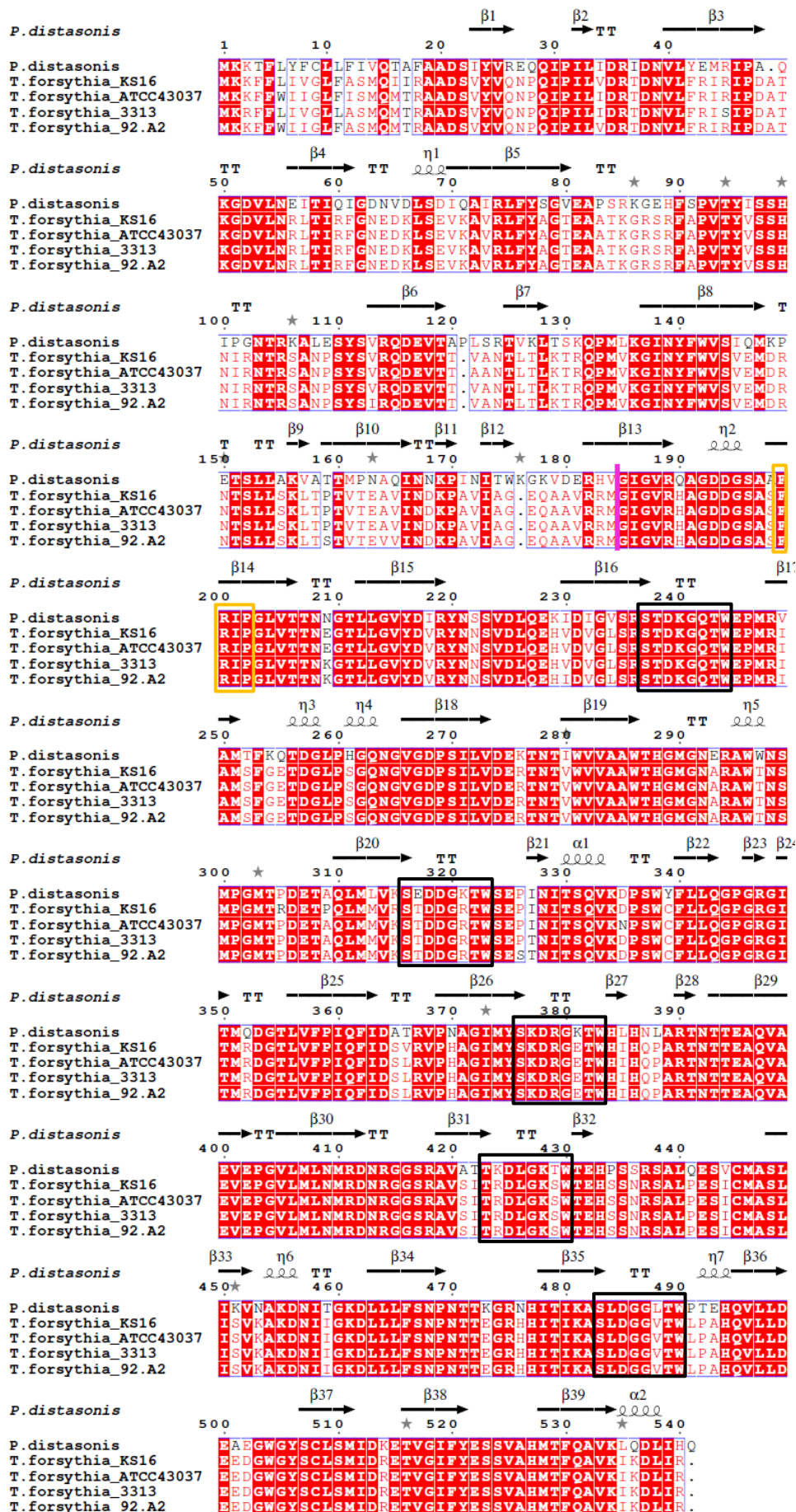


Figure 2.3. Alignment of *T. forsythia* sequences and prediction of secondary structural features.

The crystal structure from *P. distasonis* glycoside hydrolase (PDB ID: 4FJ6) was used as a template to predict structural features of *T. forsythia* NanH, and *P. gingivalis* SiaPG, with alignments between the sialidases performed using Multalin, and secondary structural predictions and other sequence analysis using ESPript. To establish similarity between aligned residues, percentage equivalence with a global score of 0.7 was used. Aligned sequences above the percentage equivalent threshold are framed in blue, and aligned residues above this threshold are shown in red. Strictly conserved residues are shown in white on a red background. Secondary structural features are shown above the alignment: The η symbol refers to a 3_{10} -helix, α -helices, 3_{10} -helices and π -helices are displayed as medium, small, and large squiggles, respectively. β -strands are rendered as arrows, strict β -turns as TT letters and strict α -turns as TTT. Boxes are used to highlight the (F/Y)RIP domain (orange) and Asp-boxes (black). The predicted boundary between the Secretion Signal Sequence and N-terminal (CBM), and C-Terminal Domain (CTD, sialidase domain) are indicated by a pink vertical line at residue 185.

Based on the protein BLAST and alignment results, NanH from *T. forsythia* was predicted to be composed of two domains and a secretion signal sequence. These were dubbed the “C-Terminal Domain (CTD)”, which was identified as the sialidase superfamily by the protein BLAST, and contains the catalytic active site. The function of the N-terminal domain is less obvious, it does not possess a sialidase active site. However, the sequence was well conserved between the *T. forsythia* strains, and appears to share structural features with the *P. distasonis* N-terminal (figure 2.4), as well as being characterised as a conserved feature, the “BNR_assoc_N superfamily” by the BLAST search. Considering this, we hypothesized that this N-terminal could have a putative carbohydrate binding function, similar to the Carbohydrate Binding Modules (CBMs) seen in other organisms. CBMs appear to function in binding of an enzyme to a given carbohydrate ligand (a polysaccharide or glycan), while the active site is then in a better position for catalytic activity, i.e. the CBM assists in ligand-enzyme interactions but does not have any activity.

Although the structure of *T. forsythia* NanH is not currently published, the structure of a glycoside hydrolase—a candidate sialidase from the closely related *Parabacteroides distasonis* was used to predict the structure of *T. forsythia* NanH and highlight the location of discrete domains, in combination with amino acid sequence alignment (Figure 2.4). The *P. distasonis* glycoside hydrolase structure is available on RSCB-Protein Data Bank, <http://www.rcsb.org/pdb/explore/explore.do?structureId=4FJ6>.

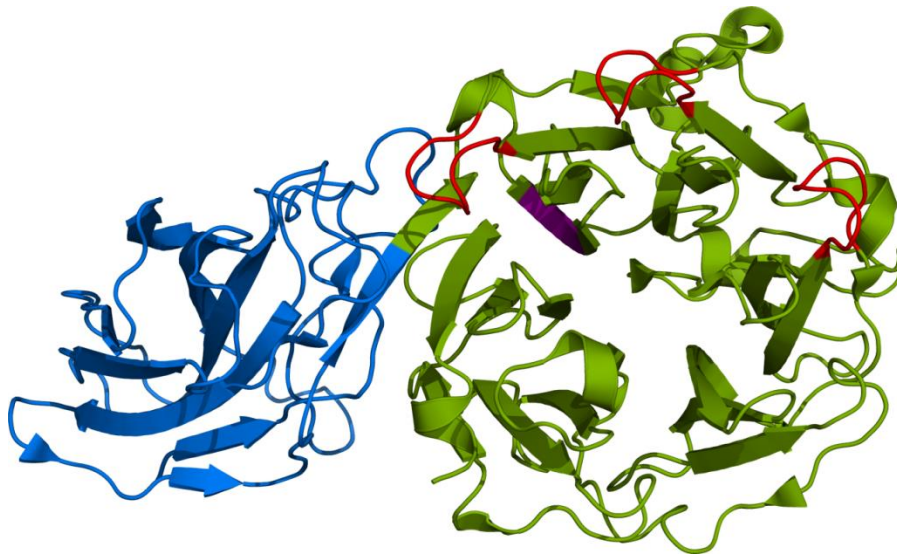


Figure 2.4. Predicted structure and features of *T. forsythia* NanH modelled using the crystal structure of a closely related glycoside hydrolase from *P. distasonis*.

BDI_2946; PDB ID: 4FJ6), with arrows, spirals, and coils representing β -sheets, α -helices and loop regions, respectively. Based on bioinformatic analysis of *T. forsythia* NanH, the domains of BDI_2946 corresponding to the CBM, c-terminal catalytic domain, FRIP motif, and Asp boxes of *T. forsythia* NanH were coloured in blue, green, purple, and red, respectively. The image was rendered in PyMOL (www.pymol.org). Note the position of the Asp-boxes surrounding the active site, and FRIP domain within the catalytic active site.

2.3.1.2 *SiaPG Possesses a Sialidase Domain and a Domain of Unknown Function*

P. gingivalis possesses a gene annotated as encoding a “putative sialidase”-PG0352-in *P. gingivalis* strain W83. Here, and in preliminary characterisation work by Li et al. (Li et al. 2012), PG0352 is dubbed SiaPG. SiaPG from *P. gingivalis* strain ATCC33277 also underwent the protein BLAST, but this time only the sialidase superfamily domain at the C-terminal end was identified, the N-terminal part of the protein was not annotated (figure 2.5).

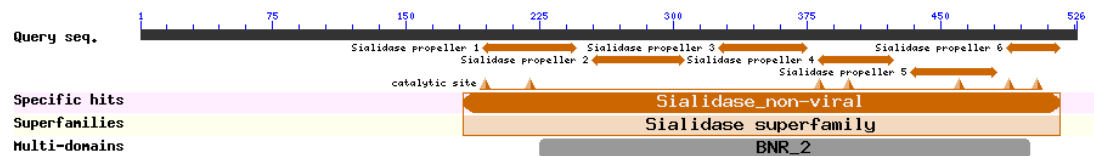


Figure 2.5. The amino acid sequence of SiaPG appears to only contain a sialidase domain.

The SiaPG protein sequence from *T. forsythia* 92.A2 underwent a BLAST search against non-redundant protein sequences to reveal the Sialidase Domain. The active site and β -propellers which are a characteristic feature of sialidases are also highlighted. The BLAST search has also annotated SiaPG sialidase domain as similar to a NanH sialidase.

The C-terminal sialidase superfamily domain was annotated, and this included the catalytic sites and β -propellers which are a common feature in sialidases. The BLAST found that the sialidase domain in PGsia appeared to contain six β -propellers, compared to the five seen in NanH.

Further BLAST searches with just the N-terminal (non-annotated) SiaPG sequence were performed, excluding *Porphyromonas* spp. from the search parameters (inclusion of *Porphyromonas* spp. yielded *Porphyromonas* and some *Bacteroides* sialidases, similar hits to the BLAST search performed with the full SiaPG sequence). Unfortunately this approach failed to highlight any homologous protein sequences for the SiaPG N-terminal (only two protein sequences with low sequence coverage and low homology were found, discussed below), and did not yield any insight into a putative function for this N-terminal portion.

The most homologous sequences found by the BLAST came from sialidases in *P. gingivalis* strains and other *Porphyromonas* spp. Sequences annotated as sialidases, glycosyl hydrolases, or uncharacterized proteins from other members of the *Bacteroidetes* were also identified in the BLAST search, including *Prevotella* spp. and gut-commensal organisms (*Bacteroides* spp. and *Barnesiella viscericola*). The annotated proteins from six of the *P.*

gingivalis strains, and some of the other *Bacteroidetes* were aligned using Clustal Omega and ESPript. Most of the protein sequences from the non-*Porphyromonas* genera were much larger than those from the *Porphyromonas* spp., which rendered their alignments difficult to interpret. The putative sialidase sequences from *Porphyromonas gingivalis* and a related organism, *Porphyromonas gulae* (a coloniser of the periodontium in animals) were aligned (figure 2.6). Sequences possessed a high degree of homology; *P. gulae* and *P. gingivalis* sialidases displayed ~88% homology, while the lowest observed homology between the *P. gingivalis* strains was 96.96%. The alignment also highlighted the presence of the characteristic, highly conserved F/YRIP domain (which is considered essential for sialidase activity), located at residue 193, and four Asp-boxes (a motif with the sequence T/S-X-D-X-G-X-X-W/F/Y, discussed above, section 2.3.1.1), located at residues 231, 293, 363, and 413 in the consensus sequence.

A)

	1	10	20	30	40	50
P.gingivalis_W83	MANN	TLLAKTRR	YVCLV	GFCW	LMAMMHLSG	QEV
P.gingivalis_F0570	MANN	TLLAKTRR	YVCLV	GFCW	LMAMMHLSG	QEV
P.gingivalis_AJW4	MANN	TLLAKTRR	YVCLV	GFCW	LMAMMHLSG	QEV
P.gingivalis_W4087	MANN	TLLAKTRR	SVCLV	VFC	LMAMMHLSG	QEV
P.gingivalis_ATCC_33277	MANN	TLLAKTRR	YVCLV	VFC	LMAMMHLSG	QEV
P.gingivalis_A7A1-28	MANN	TLLAKTRR	SVCLV	VFC	LMAMMHLSG	QEV
P.gulae_COT-052_OH4119	MANN	TLLARTLR	SVCLV	VFC	LVAMLRLTA	QEV
P.gulae_COT-052_OH2179	MLRLTA	QEV

	60	70	80	90	100
P.gingivalis_W83	LVKVAL	SESLPP	CAKQIRI	GFSLPK	ETEEKVTAL
P.gingivalis_F0570	LVKVAL	SESLPP	CAKQIRI	GFSLPK	ETEEKVTAL
P.gingivalis_AJW4	LVKVAL	SESLPP	CAKQIRI	GFSLPK	ETEEKVTAL
P.gingivalis_W4087	LVKVAL	SESLPP	CAKQIRI	GFSLPK	ETEEKVTAL
P.gingivalis_ATCC_33277	LVKVAL	SESLPP	CAKQIRI	GFSLPK	ETEEKVTAL
P.gingivalis_A7A1-28	LVKVAL	SESLPP	CAKQIRI	GFSLPK	ETEEKVTAL
P.gulae_COT-052_OH4119	LVKVI	LSEPLPP	NAKQIRI	SYSFPQ	DTKDKVTAL
P.gulae_COT-052_OH2179	LVKVI	LSEPLPP	NAKQIRI	SYSFPQ	DTKDKVTAL

	110	120	130	140	150
P.gingivalis_W83	KGRVSY	SDFPISKED	RTTALSAD	SVAGRRFF	YLAADIGPV
P.gingivalis_F0570	KGRVSY	SDFPISKED	RTTALSAD	SVAGRRFF	YLAADIGPV
P.gingivalis_AJW4	KGRVSY	SDFPISKED	RTTALSAD	SVAGRRFF	YLAADIGPV
P.gingivalis_W4087	KGRVSY	SDFPISKED	RTTALSAD	SVAGRRFF	YLAADIGPV
P.gingivalis_ATCC_33277	KGRVSY	SDFPISKED	RTTALSAD	SVAGRRFF	YLAADIGPV
P.gingivalis_A7A1-28	KGRVSY	SDFPISKED	RTTALSAD	SVAGRRFF	YLAADIGPV
P.gulae_COT-052_OH4119	KGRVSY	SDFPISKED	CVITLSAD	SVAGRRFF	YLAADIGPV
P.gulae_COT-052_OH2179	KGRVSY	SDFPISKED	CVITLSAD	SVAGRRFF	YLAADIGPV

	160	170	180	190	200
P.gingivalis_W83	ARVEE	VAVDGRPLP	KEI	SPASRR	LYRC
P.gingivalis_F0570	ARVEE	VAVDGRPLP	KEI	SPASRR	LYRC
P.gingivalis_AJW4	ARVEE	VAVDGRPLP	KEI	SPASRR	LYRC
P.gingivalis_W4087	ARVEE	VAVDGRPLP	KEI	SPASRR	LYRC
P.gingivalis_ATCC_33277	ARVEE	VAVDGRPLP	KEI	SPASRR	LYRC
P.gingivalis_A7A1-28	ARVEE	VAVDGRPLP	KEI	SPASRR	LYRC
P.gulae_COT-052_OH4119	ARVEE	VAVDGRPLP	KEI	SPASRR	LYRC
P.gulae_COT-052_OH2179	ARVQ	EAVDGRPLP	KEI	SPASRR	LYRC

	210	220	230	240	250
P.gingivalis_W83	TANGTL	IAMADRRKYN	QTDLPED	IDIVMRR	STDGGK
P.gingivalis_F0570	TANGTL	IAMADRRKYN	QTDLPED	IDIVMRR	STDGGK
P.gingivalis_AJW4	TANGTL	IAMADRRKYN	QTDLPED	IDIVMRR	STDGGK
P.gingivalis_W4087	TANGTL	IAMADRRKYN	QTDLPED	IDIVMRR	STDGGK
P.gingivalis_ATCC_33277	TANGTL	IAMADRRKYN	QTDLPED	IDIVMRR	STDGGK
P.gingivalis_A7A1-28	TANGTL	IAMADRRKYN	QTDLPED	IDIVMRR	STDGGK
P.gulae_COT-052_OH4119	TAKGTL	IAMADRRKYN	QTDLPED	IDIVMRR	STNNGG
P.gulae_COT-052_OH2179	TAKGTL	IAMADRRKYN	QTDLPED	IDIVMRR	STNNGG

	260	270	280	290	300
P.gingivalis_W83	NHGF	GDVALVQT	QAGKLLM	IFVGGVGLW	QSTPDRP
P.gingivalis_F0570	NHGF	GDVALVQT	QAGKLLM	IFVGGVGLW	QSTPDRP
P.gingivalis_AJW4	NHGF	GDVALVQT	QAGKLLM	IFVGGVGLW	QSTPDRP
P.gingivalis_W4087	NHGF	GDVALVQT	QAGKLLM	IFVGGVGLW	QSTPDRP
P.gingivalis_ATCC_33277	NHGF	GDVALVQT	QAGKLLM	IFVGGVGLW	QSTPDRP
P.gingivalis_A7A1-28	NHGF	GDVALVQT	QAGKLLM	IFVGGVGLW	QSTPDRP
P.gulae_COT-052_OH4119	NHGF	GDVALVQT	KARKLLM	IFVGGVGLW	QSTPDRP
P.gulae_COT-052_OH2179	NHGF	GDVALVQT	QAGKLLM	IFVGGVGLW	QSTPDRP

	310	320	330	340	350
P.gingivalis_W83	SPPRDIT	HFI	FGKDCADPGRSRWLASFCASG	QGLVLP	SGRITFVAAIRES
P.gingivalis_F0570	SPPRDIT	HFI	FGKDCADPGRSRWLASFCASG	QGLVLP	SGRITFVAAIRES
P.gingivalis_AJW4	SPPRDIT	HFI	FGKDCADPGRSRWLASFCASG	QGLVLP	SGRITFVAAIRES
P.gingivalis_W4087	SPPRDIT	HFI	FGKDCADPGRSRWLASFCASG	QGLVLP	SGRITFVAAIRES
P.gingivalis_ATCC_33277	SPPRDIT	HFI	FGKDCADPGRSRWLASFCASG	QGLVLP	SGRITFVAAIRES
P.gingivalis_A7A1-28	SPPRDIT	HFI	FGKDCADPGRSRWLASFCASG	QGLVLP	SGRITFVAAIRES
P.gulae_COT-052_OH4119	SPPRDIT	HFI	FGKDCADPGRSRWLASFCASG	QGLVLP	SGRITFVAAIRES
P.gulae_COT-052_OH2179	SPPRDIT	HFI	FGKDCADPGRSRWLASFCASG	QGLVLP	SGRITFVAAIRES

	360	370	380	390	400
P.gingivalis_W83	GQEVV	LNNYVLYSDDEG	DTW	QLSDCAYRRGDEAKLSLMPDGRVLM	SI
P.gingivalis_F0570	GQEVV	LNNYVLYSDDEG	DTW	QLSDCAYRRGDEAKLSLMPDGRVLM	SV
P.gingivalis_AJW4	GQEVV	LNNYVLYSDDEG	DTW	QLSDCAYRRGDEAKLSLMPDGRVLM	SV
P.gingivalis_W4087	GQEVV	LNNYVLYSDDEG	DTW	QLSDCAYRRGDEAKLSLMPDGRVLM	SI
P.gingivalis_ATCC_33277	GQEVV	LNNYVLYSDDEG	DTW	QLSDCAYRRGDEAKLSLMPDGRVLM	SV
P.gingivalis_A7A1-28	GQEVV	LNNYVLYSDDEG	DTW	QLSDCAYRRGDEAKLSLMPDGRVLM	SV
P.gulae_COT-052_OH4119	GQEVV	LNNYVLYSDDEG	DTW	QLSDCAYRRGDEAKLSLMPDGRVLM	SV
P.gulae_COT-052_OH2179	GQEVV	LNNYVLYSDDEG	DTW	QLSDCAYRRGDEAKLSLMPDGRVLM	SV

	410	420	430	440	450
P.gingivalis_W83	GRQES	RQRFFALSSDDGLTWERAKQFE	GIHDPGCNGAMLOVKRNGR	DOVL	
P.gingivalis_F0570	GRQES	RQRFFALSSDDGLTWERAKQFE	GIHDPGCNGAMLOVKRNGR	DOVL	
P.gingivalis_AJW4	GRQES	RQRFFALSSDDGLTWERAKQFE	GIHDPGCNGAMLOVKRNGR	DOVL	
P.gingivalis_W4087	GRQES	RQRFFALSSDDGLTWERAKQFE	GIHDPGCNGAMLOVKRNGR	DOVL	
P.gingivalis_ATCC_33277	GRQES	RQRFFALSSDDGLTWERAKQFE	GIHDPGCNGAMLOVKRNGR	DOVL	
P.gingivalis_A7A1-28	GRQES	RQRFFALSSDDGLTWERAKQFE	GIHDPGCNGAMLOVKRNGR	DOVL	
P.gulae_COT-052_OH4119	GRQES	RQRFFALSSDDGLTWERAKQFE	GIHDPGCNGAMLOVKRNGR	DOVL	
P.gulae_COT-052_OH2179	GRQES	RQRFFALSSDDGLTWERAKQFE	GIHDPGCNGAMLOVKRNGR	DOVL	

	460	470	480	490	500
P.gingivalis_W83	HSLPLGPDGRRD	GAVYLF	DHVS	GRWSAPVVVNSGSSAYS	SDMTLLADGTIG
P.gingivalis_F0570	HSLPLGPDGRRD	GAVYLF	DHVS	GRWSAPVVVNSGSSAYS	SDMTLLADGTIG
P.gingivalis_AJW4	HSLPLGPDGRRD	GAVYLF	DHVS	GRWSAPVVVNSGSSAYS	SDMTLLADGTIG
P.gingivalis_W4087	HSLPLGPDGRRD	GAVYLF	DHVS	GRWSAPVVVNSGSSAYS	SDMTLLADGTIG
P.gingivalis_ATCC_33277	HSLPLGPDGRRD	GAVYLF	DHVS	GRWSAPVVVNSGSSAYS	SDMTLLADGTIG
P.gingivalis_A7A1-28	HSLPLGPDGRRD	GAVYLF	DHVS	GRWSAPVVVNSGSSAYS	SDMTLLADGTIG
P.gulae_COT-052_OH4119	HSLPLGPDGRRD	GAVYLF	DHVS	GRWSAPVVVNSGSSAYS	SDMTLLADGTIG
P.gulae_COT-052_OH2179	HSLPLGPDGRRD	GAVYLF	DHVS	GRWSAPVVVNSGSSAYS	SDMTLLADGTIG

	510	520
P.gingivalis_W83	YFVEE	DEISLVFIRFVLDLDFDVRQ
P.gingivalis_F0570	YFVEE	DEISLVFIRFVLDLDFDARQ
P.gingivalis_AJW4	YFVEE	DEISLVFIRFVLDLDFDARQ
P.gingivalis_W4087	YFVEE	DEISLVFIRFVLDLDFDARQ
P.gingivalis_ATCC_33277	YFVEE	DEISLVFIRFVLDLDFDARQ
P.gingivalis_A7A1-28	YFVEE	DEISLVFIRFVLDLDFDARQ
P.gulae_COT-052_OH4119	YFVEE	DEISLVFIRFVLDLDFDAGL
P.gulae_COT-052_OH2179	YFVEE	DEISLVFIRFVLDLDFDAGQ

B)

	1)	2)	3)	4)	5)	6)	7)	8)
1) <i>P.gingivalis</i> _W83	100	99.05	98.86	97.34	97.15	96.96	88.4	91.63
2) <i>P.gingivalis</i> _F0570	99.05	100	99.43	97.15	96.96	96.77	88.78	91.83
3) <i>P.gingivalis</i> _AJW4	98.86	99.43	100	96.96	96.77	96.58	88.59	91.63
4) <i>P.gingivalis</i> _W4087	97.34	97.15	96.96	100	97.15	97.34	88.97	91.43
5) <i>P.gingivalis</i> _ATCC_33277	97.15	96.96	96.77	97.15	100	99.81	88.4	91.83
6) <i>P.gingivalis</i> _A7A1-28	96.96	96.77	96.58	97.34	99.81	100	88.59	91.83
7) <i>P.gulae</i> _COT-052_OH4119	88.4	88.78	88.59	88.97	88.4	88.59	100	94.42
8) <i>P.gulae</i> _COT-052_OH2179	91.63	91.83	91.63	91.43	91.83	91.83	94.42	100

Figure 2.6. Alignment of *Porphyromonas* sialidases.

BLAST revealed a number of sequences with homology to SiaPG from *P. gingivalis* strain ATCC 33277. Those shown here were annotated as “sialidase” or “Putative Sialidase” in the NCBI database. These sequences were aligned in Clustal Omega, followed by ESPrpt. A) ESPrpt alignment of sequences similar to SiaPG from *P. gingivalis* ATCC 33277. B) Percentage identity matrix from Clustal Omega, the numbers shown represent % homology between each sialidase. The individual input sequences and strain details can be viewed in appendix 7.2. Boxes are used to highlight the (F/Y)RIP domain (orange) and Asp-boxes (black). The predicted boundary between the secretion signal sequence and N-terminal (CBM), and c-terminal domain (CTD, sialidase domain) are indicated by a pink vertical line at residue 188.

The *P. distasonis* glycosyl hydrolase has only 23 % homology to SiaPG, and was deemed unsuitable for rendering a model, so the SiaPG sequence was analysed using the Phyre 2 Database (available at: <http://www.sbg.bio.ic.ac.uk/phyre2/html/page.cgi?id=index>), and imaged using Pymol (figure 2.7). This application uses a PSI-BLAST to align the input sequence (SiaPG in this case) to other proteins, and then compares this list of homologues to crystal structures available in Protein Data Bank (PDB), and then the input sequence (SiaPG in this case) can be modelled. The alignment carried out by Phyre 2 revealed that the most homologous available crystal structure in PDB was sialidase VPI 5482 (BTSA) from *Bacteroides thetaiotaomicron* (PDB ID: 4BBW). This sialidase only shared 26% homology with SiaPG (The *P. distasonis* glycosyl hydrolase used to model *T. forsythia* was the second hit), but Phyre 2 was able to model SiaPG (figure 2.7). The first 126 residues were excluded from the model by Phyre 2 as they were not homologous with the *B. thetaiotaomicron* sialidase, but the following 378 residues (127-521) were modelled with 100% confidence. As expected the C-terminal domain forms a predicted six-component beta-sheet domain,

whereas the N-terminus is likely to form a novel domain that is hard to predict using these methods.

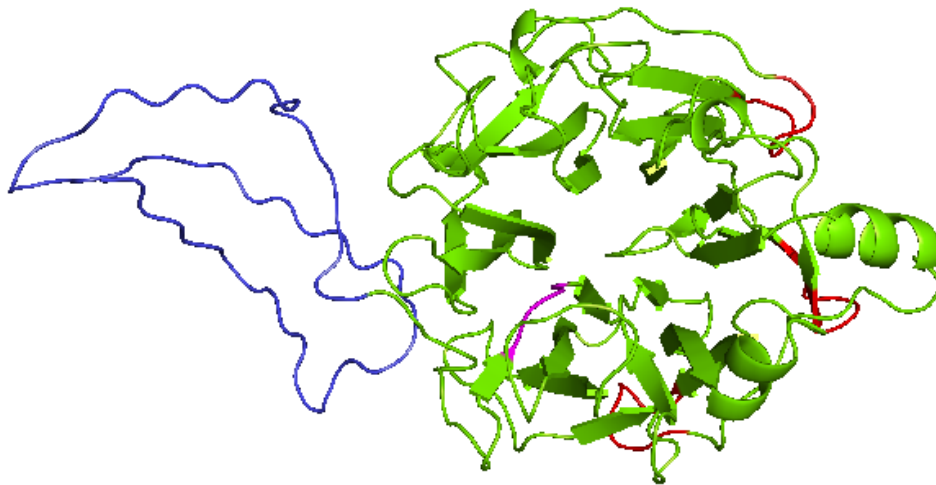
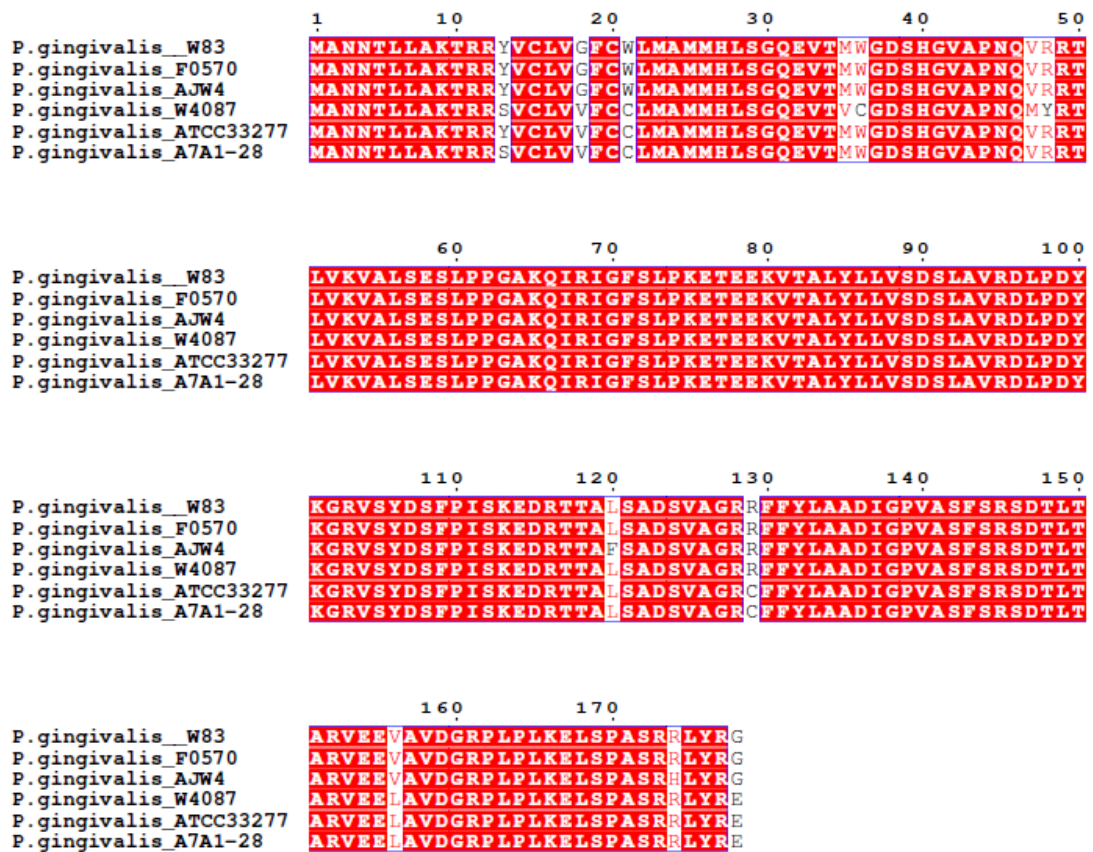


Figure 2.7. Predicted structure and features of *P. gingivalis* SiaPG modelled using the crystal structure of a sialidase from *B. thetaiotaomicron*.

(VPI_5482; PDB ID: 4BBW). The image was rendered in PyMOL (www.pymol.org). Arrows, spirals, and coils represent β -sheets, α -helices and loop regions, respectively. Based on bioinformatic analysis of SiaPG, the domains of VPI_5482 corresponding to part of the N-terminal Domain, C-terminal catalytic domain, YRIP motif, and Asp boxes of SiaPG were coloured in blue, green, purple, and red, respectively. Orientated so that the arrangement of β -propellers is visible in the sialidase domain. Note the position of the Asp-boxes surrounding the active site, and FRIP domain within the catalytic active site.

2.3.1.2.1 Attempted Functional Prediction of the SiaPG-N-terminal Domain

The SiaPG N-terminal domain (SiaPG-NTD) function remained difficult to ascertain through bioinformatics analysis-this domain contains ~178 residues (including the secretion signal sequence), but in the above model the first 127 residues of SiaPG were excluded. The N-terminal domain was highly conserved between the *Porphyromonas* spp. (figure 2.7), and in *P. gingivalis* strains the homology was very high, the lowest homology between strains was 93.82% (figure 2.8).



	1)	2)	3)	4)	5)	6)
1) <i>P.gingivalis</i> _W83	100	100	98.88	94.94	97.19	96.63
2) <i>P.gingivalis</i> _F0570	100	100	98.88	94.94	97.19	96.63
3) <i>P.gingivalis</i> _AJW4	98.88	98.88	100	93.82	96.07	95.51
4) <i>P.gingivalis</i> _W4087	94.94	94.94	93.82	100	96.63	97.19
5) <i>P.gingivalis</i> _ATCC_33277	97.19	97.19	96.07	96.63	100	99.44
6) <i>P.gingivalis</i> _A7A1-28	96.63	96.63	95.51	97.19	99.44	100

Figure 2.8. Alignment of *P. gingivalis* sialidase N-terminal domains.

The first 198 residues of SiaPG in six *P. gingivalis* strains were aligned in Clustal Omega, followed by ESPrpt. A) ESPrpt alignment of sequences similar to SiaPG from *P. gingivalis* ATCC 33277. B) Percentage identity matrix from Clustal Omega, the numbers shown represent % homology between each SiaPG N-terminal domain. The individual input sequences and strain details can be viewed in appendix 7.3.

Since BLAST alone had not indicated the function of the SiaPG-NTD (discussed in this section, above) Phyre 2 was used in an attempt to predict the structure function of the SiaPG-NTD. Unfortunately there were no crystal structures available with a high coverage or homology for the SiaPG-NTD. The best alignment was a C-terminal domain of inner

membrane protein from *Salmonella enterica* (PDB identified this as a membrane protein), but this only covered 16% of the SiaPG-NTD with 40% identity, so this was not considered an appropriate model.

Ultimately, although bioinformatics failed to ascertain a function for SiaPG-NTD, the fact that it is highly conserved between *P. gingivalis* (and other *Porphyromonas* spp.) suggests it has an important function in *P. gingivalis* (and other *Porphyromonas* spp.). The partial similarity with an inner membrane protein (discussed in the previous paragraph) might suggest that this domain anchors the SiaPG to the surface of *P. gingivalis*. However, other functions for this domain could not be ruled out, so for the purposes of this project (and for ease of discussion in the context of *T. forsythia* NanH), it was tentatively dubbed the “SiaPG-CBM”.

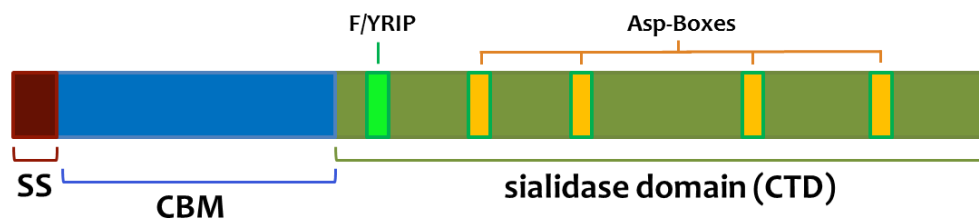
2.3.1.3 **Summary of the Bioinformatics Analysis of SiaPG and NanH**

The purified whole sialidases could yield insights into their target ligands within the pathogens' hosts, and studying the sialidases in isolation from pathogens could provide insight into their precise roles in virulence, and might highlight potential biochemical applications. Purification and study of the sialidase domains is perhaps an even more intriguing prospect, but this requires elucidation of the domain boundaries in NanH and SiaPG. To this end, the protein domains were modelled and predicted before the first stage of sialidase cloning.

Both sialidases were analysed using the NCBI protein BLAST, and aligned to proteins from different strains/species. This appeared to yield two distinct domains for NanH; a sialidase domain with catalytic activity (containing five characteristic β -propellers and the highly conserved RIP domain), and a N-terminal domain which was hypothesized to be a carbohydrate binding module (CBM). NanH from *T. forsythia* was modelled onto a closely related enzyme from *P. distasonis*, revealing the predicted structures of the NanH-CBM, and NanH-C-Terminal Domain (NanH-CTD).

The BLAST and sequence alignments for SiaPG highlighted the sialidase domain at the C-terminal domain (with six characteristic β -propellers and the highly conserved RIP domain), but the N-terminal domain (NTD) function was not immediately obvious. Modelling of SiaPG based on a related sialidase structure from *B. thetaiotaomicron* was beneficial, providing a structural model for the whole catalytic domain, but did not highlight a function for the NTD. However, this was highly conserved between *P. gingivalis* strains, and was considered likely to have a function, so it was termed “SiaPG-CBM”.

Both sialidases were of a similar size (521 and 546 residues for SiaPG and NanH, respectively). They did not share sequence homology; aligning their sequences in Clustal Omega showed they only had 23 % identity. However, both sialidases could be divided into two domains (and a secretion signal sequence); the C-terminal domain (CTD) with sialidase activity, and an N-terminal domain or carbohydrate binding module (CBM). The distinct domains were visible in the case of both sialidase's predicted structures. Both sialidases possessed four-five Asp-boxes in their CTDs, and the RIP motif was located upstream of the Asp-boxes in both sequences. Both sialidases were submitted to SignalP to predict the location of the secretion signal sequence (<http://www.cbs.dtu.dk/services/SignalP/>) (appendix 7.4). The features and domains of both enzymes are summarised in Figure 2.9.



Sialidase	Gene/Protein Size	Domains	Domain Location (Residue Numbers)	(F/Y)RIP domain (Residues and residue numbers)	Asp-Box (Location-Residue Numbers)
NanH	57.4 kDa	NanH-SS	1-20	FRIP, 210-213	237-244, 316-323, 376-383, 422-429, 483-490
		NanH-CBM	21-165		
		NanH-CTD	166-552		
SiaPG	54.8 kDa	SiaPG-SS	1-31	YRIP, 192-195	231-238, 292-299, 362-269, 411-418
		PGsia-CBM	32-188		
		PGsia-CTD	189-525		

Figure 2.9. Linear schematic of NanH and SiaPG.

Both periodontal pathogen sialidases were divided into two domains and the Secretion Signal (SS), the Carbohydrate Binding Module (CBM) and the C-Terminal domain, (CTD) which possesses the RIP domain and Asp-Boxes characteristic of sialidases. The domains and their positions in each enzyme are summarised in the table below the linear schematic.

2.3.2 Production of SiaPG-CBM, SiaPG-CT, and NanH-CT

NanH and SiaPG are both encoded by genes approximately 1500bp in size. The analysis described in section 2.3.1 delineated SiaPG and NanH into the secretion signal sequence two domains and; the CBM, and the CTD. The nucleotide sequences encoding these are ~80 bp, ~500 bp, and ~1000 bp in size, respectively. To elucidate the function of each domain in isolation, attempts were made to express and purify the individual domains of NanH and

SiaPG. The first stage in this was performed by attempting to use a polymerase chain reaction (PCR) approach to produce DNA fragments encoding the sialidase domains, by using PCR primers designed to target the domain-encoding sequences in the genomic DNA of *T. forsythia* and *P. gingivalis*. Ultimately this meant three PCR products could be produced for each sialidase, two encoding the individual domains, and one encoding the whole sialidase (figure 2.10). The signal sequence was excluded during primer design, with the intention of producing fully mature proteins in the cytoplasm of the expression strain.

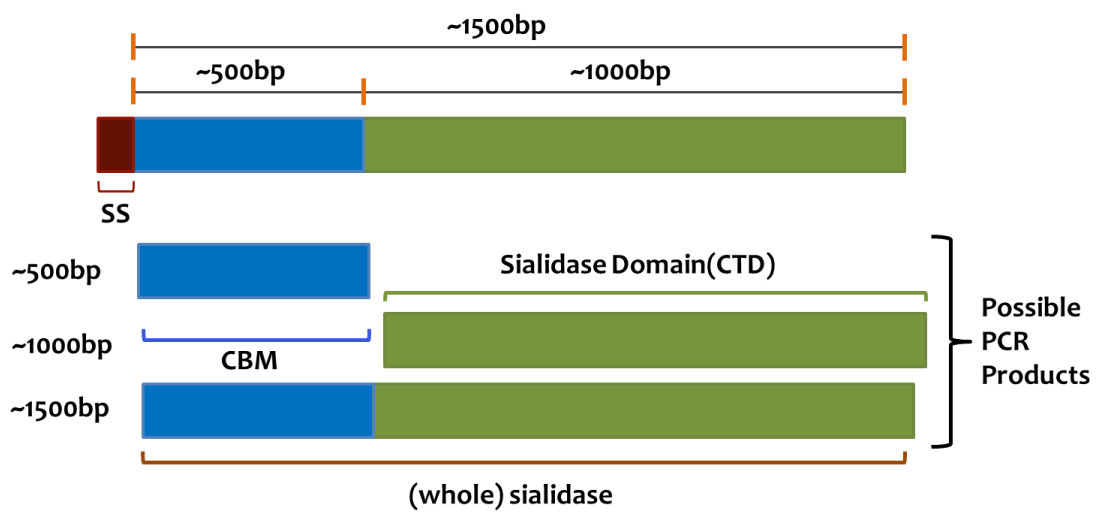


Figure 2.10. Targeting sialidase domains.

Both *P. gingivalis* and *T. forsythia* possess sialidase-encoding genes that could be delineated into the CBM- and CTD-encoding regions, as well as the sequence encoding the whole protein. Primers were designed to produce PCR products encoding the different domains and a whole sialidase-encoding product. These were of the size indicated by the scale bars. Primer binding sites are indicated by orange lines on the scale bars.

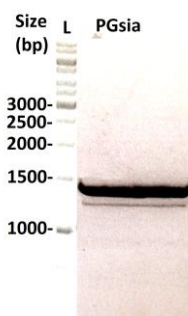
A variety of primers were designed to amplify *siaPG* and *nanH* domains from genomic DNA extracted from *P. gingivalis* and *T. forsythia*. These are outlined in table 2.6.

Designation	Primer Name	Primer Sequence (5'-3')	Targets
A	TF0035N-NdeI-Fwd	AATAC <u>CATATG</u> _GCGGACAGTGTTTTAC	nanH,
B	TF0035C-XhoI-Rev	AATA <u>CTCGAG</u> _TCGTATCAGGTCTTT	nanH, nanH-CT
C	TF0035C-NdeI-Fwd	AATAC <u>CATATG</u> _ATCGGGGTGCGTCAT	nanH-CT
D	TF0035N-NdeI-Fwd(2)	AATAC <u>CATATG</u> _GCGGACAGTGTTTACGTAC	nanH,
E	TF0035C-XhoI-Rev(2)	AATA <u>CTCGAG</u> _TCGTATCAGGTCTTTGAT	nanH, nanH-CT
F	TF0035C-NdeI-Fwd(2)	AATAC <u>CATATG</u> _ATCGGGGTGCGTCATGCG	nanH-CT
G	TF0035C-NdeI-Fwd(3)	AATAC <u>CATATG</u> _GCGGACAGTGTTTACGTAC	nanH-CT
H	PG0352N-NdeI-Fwd	AATAC <u>CATATG</u> _GAAGTCACTATGTGGGGGG	SiaPG, SiaPG-CBM
I	PG0352N-XhoI-Rev	AATA <u>CTCGAG</u> _TTGCCGGACATCGAAGAGATC	SiaPG-CBM
J	PG0352C-NdeI-Fwd	AATAC <u>CATATG</u> _TATAGGGGGTATGAGGCC	SiaPG, SiaPG-CT
K	TF0035C-XhoI-Rev	AATA <u>CTCGAG</u> _CAGACGACGGGAGGCAG	SiaPG, SiaPG-CT

Table 2.6. Design of primers for siaPG, nanH and domain amplification from genomic DNA.

For ease of description, the primers are designated letters A-K. Primer name indicates the product produced: PG0352-siaPG, TF0035-nanH, the letters “C” or “N” indicates the primer position on the sialidase gene; C-C-terminal, N-N-terminal or CBM. The restriction enzyme used is also indicated in the primer name (*XhoI* or *NdeI*). Primers include a sequence for restriction digest at their 5' ends, separated from the sialidase-gene specific sequence by an underscore. Combinations of different primers were designed to produce whole sialidase (without secretion signal sequence), sialidase-CT, or sialidase-CBM. Restriction sites are underlined in the primer sequence.

After genomic DNA extraction from *T. forsythia* and *P. gingivalis*, various PCR conditions were tested in a series of experiments to amplify the PCR products discussed above. PCRs used primers attempting to yield *nanH-CT* (combinations of primers B, C, E, F, and G), *siaPG-CBM* (primers H and I), and *siaPG-CT* (primers J and K). Experiments focused on changing annealing temperatures and primer concentrations in an attempt to obtain PCR products. After multiple PCR failures, PCR was performed on *nanH* already present in a pET plasmid construct, and PCR products thought to represent *nanH-CT*, *siaPG-CBM*, and *siaPG-CT* were produced (figure 2.11). The NanH-CBM had been produced separately (Chatchawal Phansopa., Stafford Research Group, University of Sheffield, manuscript in preparation).



Reagent	5x Kit Buffer	100-1000ng/ μ l genomic DNA	10 μ M Primer H or J	10 μ M Primer K	2mM dNTPs	Polymerase	Deionised Water	DMSO/deionised water
Volume (μ l)	4	0.5	1	1	0.2	0.2	11	0.6

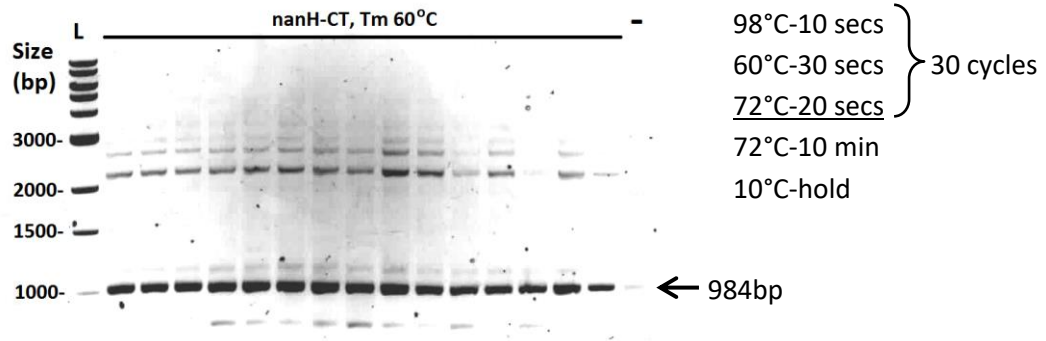
2.3.2.1 Cloning of PCR Products Encoding Sialidase Domains

The PCR products were excised from their agarose gels, and purified using commercially available kits. Purified PCR products were digested with *Nde*I and *Xho*I restriction enzymes, and the reaction mixes were purified a second time. These digested PCR products corresponding to *siaPG-CT*, *siaPG-CBM*, and *nanH-CT*, were purified using a commercially available kit, before further processing, with the aim of producing pET- plasmid constructs:

pET plasmids were chosen as vectors due to their inclusion of these restriction sites in appropriate locations, and the presence of a 6-histidine (His^+) tag at the 3' end (C-terminal in the expressed protein) for affinity chromatography purification of the expressed protein (section 2.3.2.2). Undigested pET plasmids were digested using *Nde*I and *Xho*I restriction enzymes, with calf alkaline phosphatase present. The digested reaction mix then underwent agarose gel electrophoresis, and the bands corresponding to digested pET plasmid were extracted using commercially available kits.

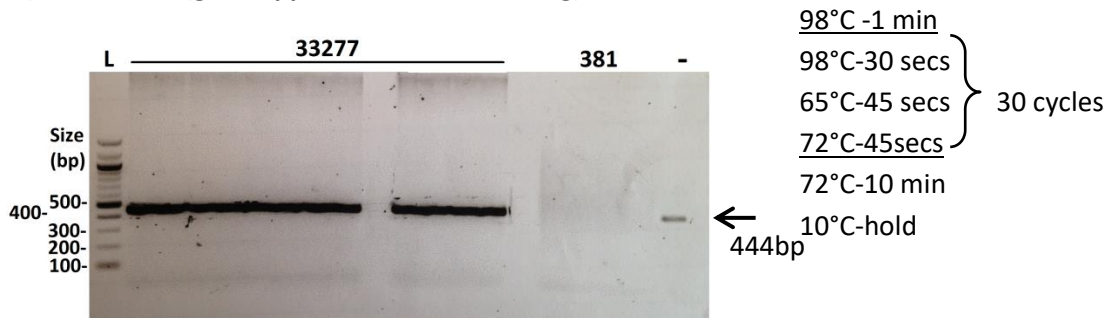
Digested PCR products underwent ligation with digested pET-20b plasmids, followed by transformation using heat shock into commercially available *E. coli* DH5 α . Resulting bacterial colonies underwent colony PCR followed by restriction digest to confirm the presence of an insert at the expected size (figure 2.12). The resulting plasmid constructs were transformed into *E. coli* Origami B (EC origami), for expression. Transformed *E. coli* DH5 α were cultured and pET20b-constructs extracted. All constructs were sequenced using an in house sequencing service to confirm insertion of the coding sequence, and that no mutations had occurred during the cloning process.

A) *nanH-CT* (gel cropped for ease of viewing)



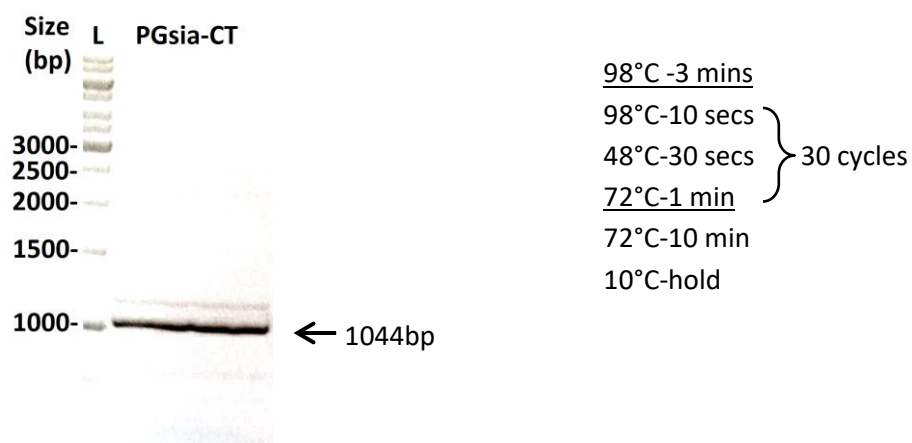
Reagent	5x Kit Buffer	100-1000ng/ul Plasmid DNA	Primer E	Primer F	dNTPs	Polymerase	Deionised Water	DMSO
Volume (µl)	4	0.2	1	1	0.2	0.2	12.8	0.6

B) *siaPG-CBM* (gel cropped for ease of viewing)



Reagent	5x Kit Buffer	100-1000ng/µl Genomic DNA	10µM Primer H	10µM Primer I	2mM dNTPs	Polymerase	Deionised Water
Volume (µl)	10	2.5	2.5	2.5	0.5	0.5	31.5

C) siaPG-CT (gel cropped for ease of viewing)

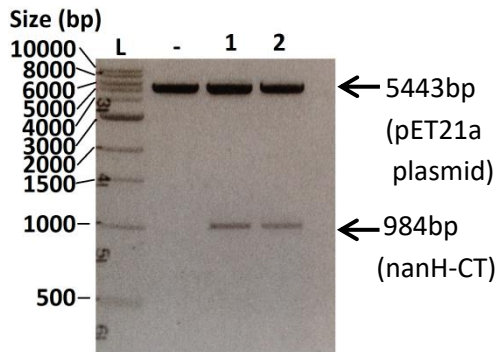


Reagent	5x Kit Buffer	100-1000ng/ μ l genomic DNA	10 μ M Primer H or J	10 μ M Primer K	2mM dNTPs	Polymerase	Deionised Water	DMSO/deionised water
Volume (μ l)	4	0.5	1	1	0.2	0.2	11	0.6

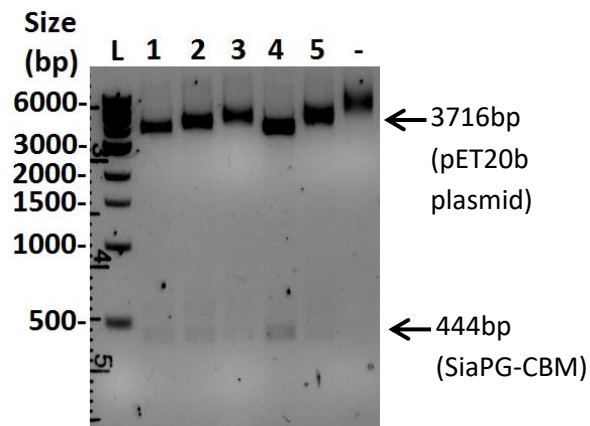
Figure 2.11. PCR amplification of A) nanH-CT, B) siaPG-CBM, and C) siaPG-CT from *P. gingivalis* genomic DNA.

1.5% (w/v) Agarose gel, DNA-absent negative controls indicated by “-”. Expected PCR products and their sizes are indicated by arrows. Reaction mixtures, thermocycling conditions, primer pairs, and primer annealing temperatures (T_m) are indicated, adjacent to the agarose gel images. Gel B) *siaPG-CT* contains reactions performed on genomic DNA from two strains of *P. gingivalis*; ATCC 33277, and 381, only the PCR on genomic DNA from ATCC 33277 resulted in products.

A) pET21a-NanH-CT



B) pET20b-siaPG-CBM



C) pET20b-siaPG-CBM

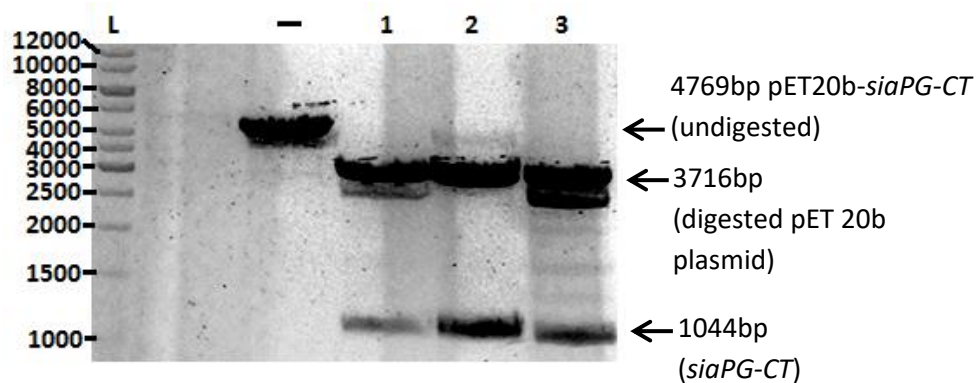


Figure 2.12. Confirmation of pET-sialidase subunit constructs.

1.5 % (w/v) agarose gel. Restriction digestion products and their expected sizes are indicated by arrows. A) pET21a-nanH-CTD B) pET20b-siaPG-CBM C) pET20b-siaPG-CTD

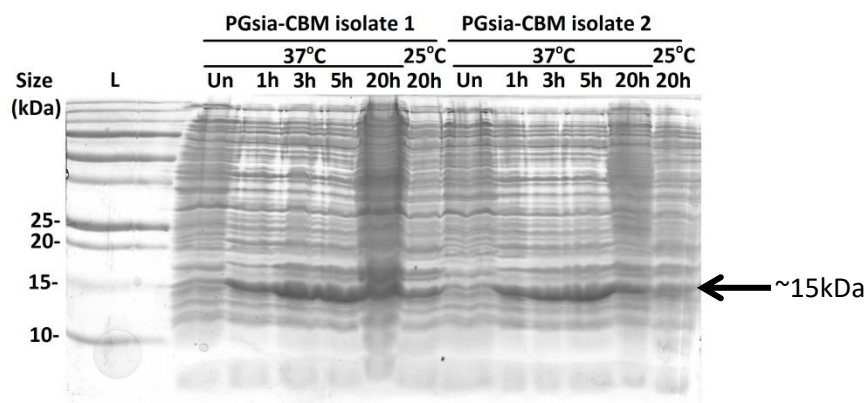
2.3.2.2 **Expression and Purification of Sialidase Subunits**

To test expression of sialidase domains, cultures of transformed EC Origami B were grown to OD₆₀₀ 0.5 and induced with 1 mM IPTG, and harvested at different time points. All harvested bacterial cultures were diluted to OD₆₀₀ 1.0, 1 ml of this suspension was pelleted, and resuspended in 100 µl of SDS loading buffer. 10-30 µl of this bacterial suspension underwent SDS-PAGE (the volume of bacterial suspension was constant during each individual experiment).

2.3.2.2.1 Expression and Initial Attempts to Purify PGsia-CBM

SiaPG-CBM appeared to be successfully expressed, with bands at ~15 kDa visible in SDS-PAGE of *E. coli* (expression strain) cell lysates, at the size expected for the SiaPG-CBM (~15 kDa, figure 2.13. A). Affinity chromatography on the soluble fraction of the cell lysates was carried out. Unfortunately, a band corresponding to the SiaPG-CBM was present in the insoluble fraction of the cell lysate, not the eluted fractions (figure 2.13 B).

A) Expression test of SiaPG-CBM; whole cell lysates



B) Affinity Chromatography of SiaPG-CBM; soluble fraction

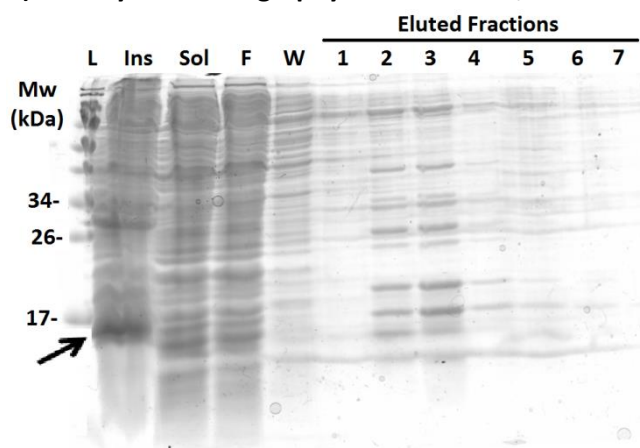


Figure 2.13. Expression test and attempted purification of SiaPG-CBM.

SDS-PAGE gel, 12 % (v/v) polyacrylamide gel. L=Mw Ladder (kDa, size approximation based on manufacturer's guide) A) SiaPG-CBM from two expressions strain clones, induced and harvested at different time points as indicated, h=hours, Un=un-induced. The arrow indicates the band corresponding to SiaPG-CBM B) Attempted purification of SiaPG-CBM on soluble fraction of expression strain lysates. Ins=Insoluble Fraction of cell lysate, Sol=soluble fraction of cell lysate F=Flow Through, W=Wash Through, 1-7= Eluted fractions. The arrow indicates the possible SiaPG-CBM in the insoluble fraction of the cell lysate.

2.3.2.2.2 Expression and Solubility Testing of SiaPG-CT and NanH-CT

After observing the apparent insolubility of SiaPG-CBM, NanH-CTD and SiaPG-CTD underwent expression testing and solubility testing. EC origami containing the pET20b-*nanH-CTD* and pET20b-*siaPG-CTD* were induced to express NanH-CTD and SiaPG-CTD, and cell lysates of induced cultures were separated into insoluble and soluble fractions. The NanH-CT (~37 kDa) appeared to be highly overexpressed and insoluble, while the SiaPG-CT

was less overexpressed, a band corresponding to SiaPG-CTD was present at the appropriate size in the insoluble fraction (~35 kDa) (figure 2.14).

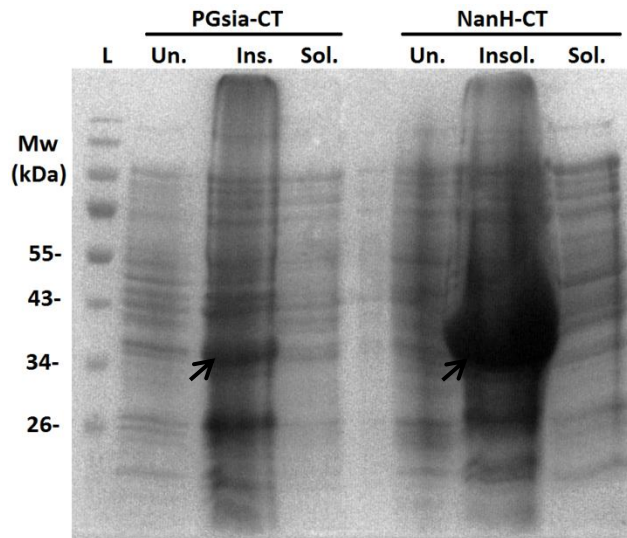


Figure 2.14. SDS-PAGE of cell lysates overexpressing SiaPG-CT and NanH-CT.

12% (v/v) polyacrylamide gel. L=Mw Ladder (kDa, size approximation based on manufacturer's guide), Un= non-induced fraction of cell lysate Ins=insoluble fraction of cell lysate, Sol=soluble fraction of cell lysate. Arrows indicate the bands suspected to correspond to SiaPG-CT (~37 kDa) and NanH-CT (~40 kDa).

2.3.2.2.3 Solubilisation and Re-Purification of Sialidase Domains

In an attempt to solubilise the overexpressed proteins, the insoluble fraction of the cell lysates were incubated in buffer containing 8M Urea, agitated by vortex then by lab-rollers, at room temperature for 3 hours. The resulting mixture was centrifuged to remove still-insoluble proteins and cell debris, and urea-solubilised fractions could then undergo affinity chromatography followed by SDS-PAGE to confirm their presence or absence in the cell lysate-soluble fraction, urea-insoluble, urea-solubilised, flow through, wash through, and elution stages of purification. SiaPG-CBM and NanH-CT appeared to be successfully purified in this way (figure 2.15 A and B), but the band corresponding to SiaPG-CT appeared to be present in the flow through and still-insoluble fractions during purifications, not the eluted fractions (figure 2.15 C).

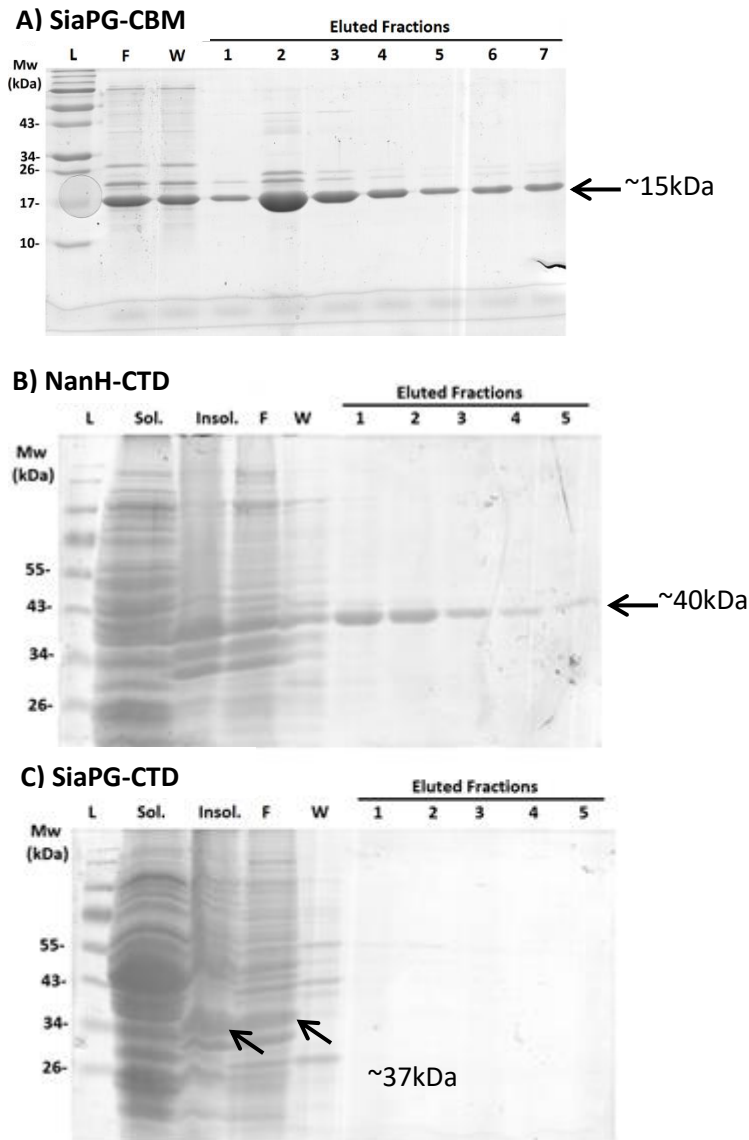


Figure 2.15. SDS-PAGE of A) SiaPG-CBM, B) NanH-CT, and C) SiaPG-CT following urea solubilisation and affinity chromatography.

A) 15% (v/v) polyacrylamide gel, B) & C) 12% (v/v) polyacrylamide gel. L=Mw Ladder (kDa, size approximation based on manufacturer's guide), Insol=Still-Insoluble Fraction of cell lysate, Sol=soluble fraction of cell lysate F=Flow Through, W=Wash Through, 1-7= Eluted fractions.

Fractions containing purified NanH-CT or SiaPG-CBM were pooled and dialysed in decreasing concentrations of urea, a process termed step-down dialysis. The resulting dialysed solution was centrifuged to separate out precipitant before SDS-PAGE. While a significant proportion of the urea-solubilised proteins (NanH-CT or SiaPG-CBM) appeared to

have precipitated once all the urea had been removed by dialysis, some protein remained soluble in the dialysed solutions i.e. NanH-CT and SiaPG-CBM appeared to have been purified and were soluble (figure 2.16).

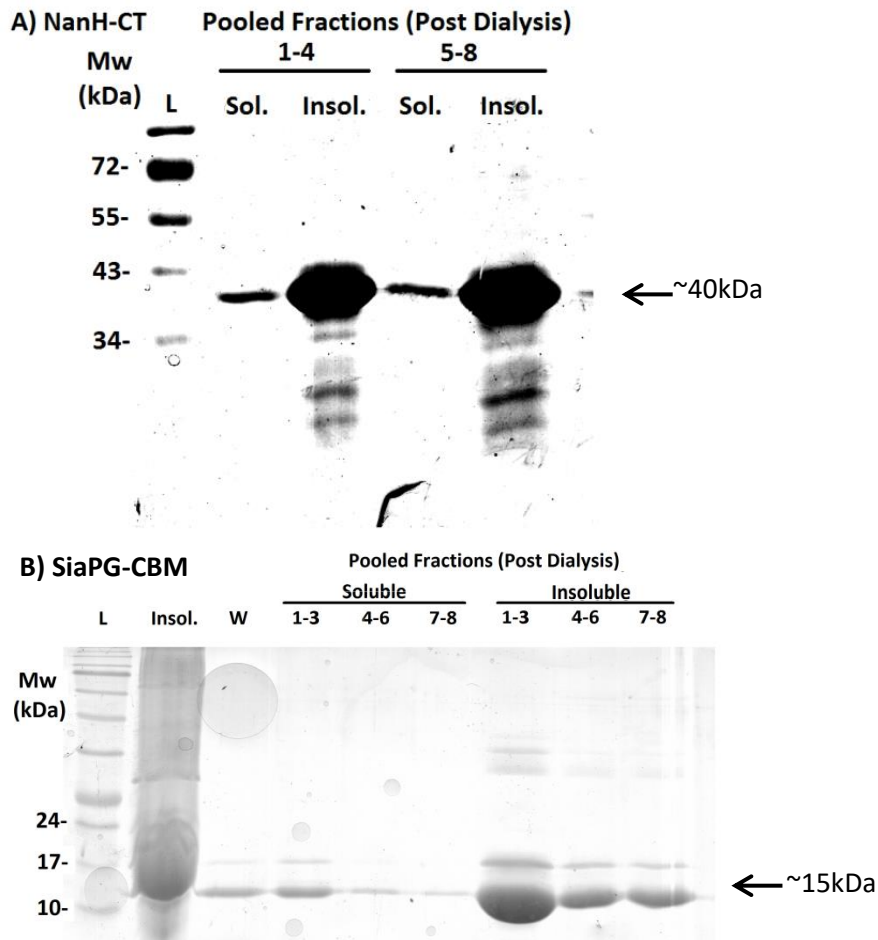


Figure 2.16. SDS-PAGE of A) NanH-CT, and B) SiaPG-CBM following step down dialysis to remove urea.

A) 12% (v/v) polyacrylamide gel, B) 15% (v/v) polyacrylamide gel. L=Mw Ladder (kDa, size approximation based on manufacturer's guide), Sol=soluble fraction of dialysed elution fractions after affinity chromatography, Insol= insoluble fraction of dialysed elution fractions after affinity chromatography. Numbers above lanes indicate which eluted fractions from affinity chromatography were pooled for dialysis.

Ultimately, NanH-CTD, and SiaPG-CBM were purified, and after step dialysis appeared to remain in an apparently soluble form, but the NanH-CTD was later shown to be inactive (lacking sialidase activity, section 2.3.2.2.4), possibly due to incorrect re-folding during urea resolubilisation and step-down dialysis, resulting in a structure unlike the native NanH-CTD.

It was intended to test the ability of SiaPG-CBM to bind different sialic-acid ligands, but unfortunately the timeframe of this project did not permit further optimisation of sialidase domain expression, and the low protein yields and low stability after step down dialysis made ligand binding studies impractical.

2.3.2.2.4 Attempted Characterisation of NanH-CT domain

NanH is predicted to possess two functional domains, the carbohydrate binding module (CBM), and C-terminal (CT) domain, the latter of which contains the enzyme active site. Studying the two domains in isolation might yield useful insights into the function of the CBM and its importance in enzyme-host ligand interactions, and could highlight the potential for inhibitors that target the CBM instead of the enzyme active site. The NanH-CT domain might display altered ligand-specificity, with potential applications for biotechnology.

NanH-CT, which contains the NanH active site, appeared to be successfully purified. It was anticipated that NanH-CT would possess sialidase activity. The fluorescence based MUNANA assay described in was applied to test the sialidase activity of NanH-CT.

Unfortunately, both visualisation of activity with UV light and image capture, and the use of a plate reader to try and detect low levels of 4-MU fluorescence showed that the NanH-CT purified here possessed no sialidase activity. The NanH-CT also had no activity when tested in the thiobarbituric acid assay with 3-sialyllactose as a substrate (Figure 2.17).

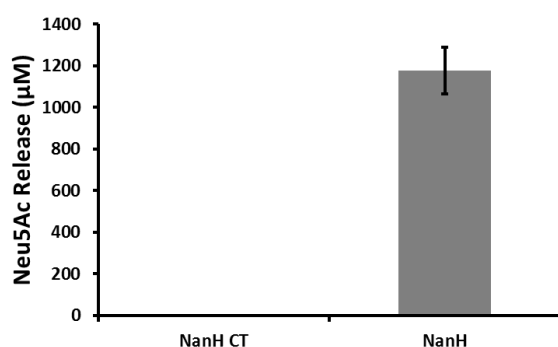


Figure 2.17. Purified NanH-CT displays no activity.

3-SL was exposed to NanH and NanH-CT for 15 minutes, followed by a TBA assay. Data shown represent the mean of three experimental repeats. Error bars=SD.

This lack of sialidase activity might infer that the protein was incorrectly folded during translation by the *E. coli* expression system. Given that whole NanH is codon optimised for expression in *E. coli*, and was readily soluble after lysis of the *E. coli* expression system, but the NanH-CT was not codon optimised (nanH-CT was obtained using PCR amplification of *T. forsythia* genomic DNA), and was insoluble after lysis of the expression system, this might be the case. It could also be the case that the NanH-CT is less stable or does not fold correctly without the presence of the NanH-CBM at the N-terminal of the protein. On the other hand, it was possible to obtain a low yield of soluble NanH-CT using urea solubilisation followed by stepdown dialysis, and it might be the case that NanH requires the CBM for ligand binding, so even soluble, stable NanH-CT would not possess sialidase activity, these are still open questions.

Fluorescence spectroscopy (which relies on similar principles to the tryptophan quenching experiments discussed in section 2.3.6.5) could provide information on tertiary and quaternary structure, but this approach would rely on comparison of the resulting spectrum to closely related proteins, and since these subunits are unique (generated as part of this project) this approach was not possible. Nuclear magnetic resonance spectroscopy (NMR) could have been used to provide a limited amount of structural information, assuming the proteins would remain stable in water for a short amount of time, but given the low protein yields following step-down dialysis and the time consuming nature of NMR and subsequent analysis, this was not feasible as part of this project.

2.3.2.3 Structural Characterisation of NanH-CBM from *T. forsythia*

As mentioned previously, the NanH-CBM had been produced during previous work and shown to bind a variety of sialic acid containing ligands (Chatchawal Phansopa, Stafford Research Group, University of Sheffield, manuscript in preparation). Part of this work highlighted the ability of the NanH-CBM to bind sialic acid-ligands, which I have also confirmed in tryptophan quenching experiments (not shown). It was also desirable to obtain the structure of ligands in complex with the NanH-CBM. To this end, attempts were made to crystallise the CBM of *T. forsythia* NanH, and co-crystallisation with a variety of ligands are ongoing. The use of robotics allowed set up of large scale crystallisation trials using commercially available crystallisation buffers. Two conditions yielded putative crystals of NanH CBM co-crystallised with zanamivir, these are shown in figure 2.18. The shape and size of the crystals suggested that they could be protein crystals, so these conditions were considered to be promising candidates for further optimisation. However,

the crystals shown here did not undergo any X-ray diffraction, so the possibility that they are not protein crystals could not be ruled out.

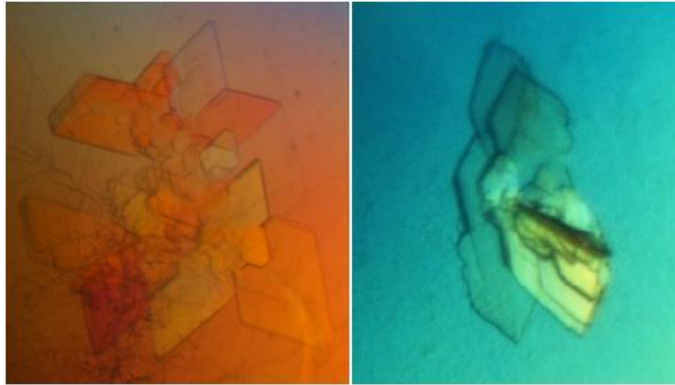


Figure 2.18 Putative NanH CBM co-crystallised with zanamivir.

Images captured under light microscopy using a polarised lens, 25x magnification + camera zoom function. Left pane- Crystal trial conditions: 1.6 mg/ml NanH CBM, 25mM zanamivir, 0.2M Magnesium Chloride, 0.1M Tris pH 8.5. 50% (w/v), 3.4 M 1,6-Hexanediol. Right pane- Crystal trial conditions: 1.6 mg/ml NanH CBM, 25 mM zanamivir, 1.6 M Sodium citrate pH 6.5.

Although obtaining these crystals-which may represent NanH-CBM in complex with zanamivir-was an exciting development, unfortunately, elucidating the crystal structure of NanH-CBM in complex with zanamivir was not possible in the timeframe of this project.

2.3.3 Production of Periodontal Pathogen Sialidases: NanH and SiaPG

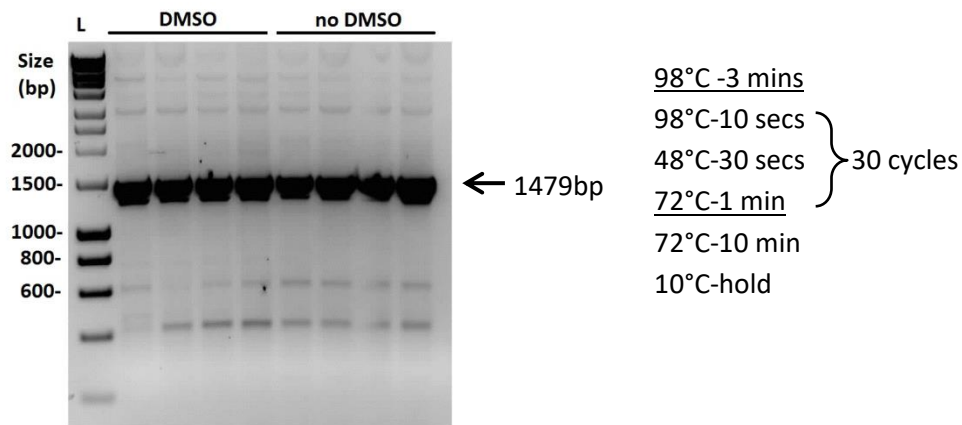
Investigating whole periodontal pathogen sialidases in isolation from the organisms that utilise them was a key focus of this project. This required production of sialidase-encoding DNA fragments, and expression and purification of pathogen sialidases.

2.3.3.1 PCR Approach to Production and Amplification of NanH and SiaPG

Initial attempts to produce whole *siaPG* and *nanH* from genomic DNA from *P. gingivalis* and *T. forsythia* used various PCR conditions in a series of experiments using combinations of primers attempting to yield *nanH* (primers A, B, D, and E), and *siaPG* (primers H and K). Experiments focused on changing annealing temperatures and primer concentrations in an attempt to obtain PCR products. After multiple PCR failures for *nanH* amplification from *T. forsythia* genomic DNA, PCR was performed on *nanH* already present in a pET plasmid construct, and PCR products thought to represent *nanH* and *siaPG* were produced (figure 2.19). It later transpired that there had been a mistake during the submission of the genome of *T. forsythia* strain 43037 (considered the type strain for *T. forsythia*) to the NCBI

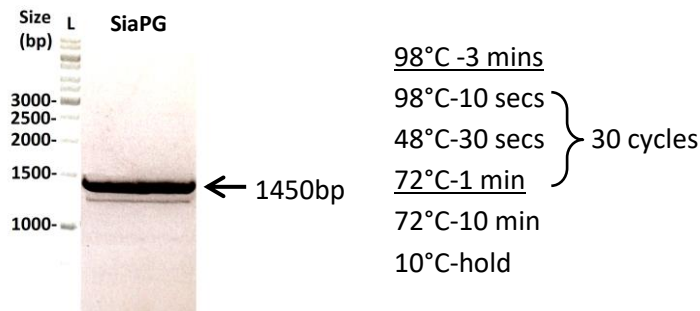
and oralgen genomic databases, instead, the genome of *T. forsythia* strain 92.A2 had been submitted and labelled as *T. forsythia* strain 43037 by the team at the Forsyth Institute in Boston (see Friedrich et al. 2015). Since PCR primers had been designed based on these databases, using what was actually the *T. forsythia* 92.A2 genome, it is perhaps unsurprising that PCRs using *T. forsythia* 43037 genomic DNA templates failed so often.

A) *nanH*



Reagent	5x Kit Buffer	100-1000ng/ μ l Plasmid DNA	Primer A	Primer B	2mM dNTPs	Polymerase	Deionised Water	DMSO/deionised water
Volume (μ l)	4	0.5	1	1	0.2	0.2	11	0.6

B) *SiaPG* (Gel Cropped for ease of viewing)



Reagent	5x Kit Buffer	100-1000ng/ μ l genomic DNA	10 μ M Primer H or J	10 μ M Primer K	2mM dNTPs	Polymerase	Deionised Water	DMSO/deionised water
Volume (μ l)	4	0.5	1	1	0.2	0.2	11	0.6

Figure 2.19 PCR amplification of A) *nanH* and B) *nanH*-CT from *T. forsythia* genomic DNA..

1.5% (w/v) Agarose gel, DNA-absent negative controls indicated by “-“. Expected PCR products and their sizes are indicated by arrows. Reaction mixtures, thermocycling conditions, primer pairs, and primer annealing temperatures (T_m) are indicated, adjacent to the agarose gel images.

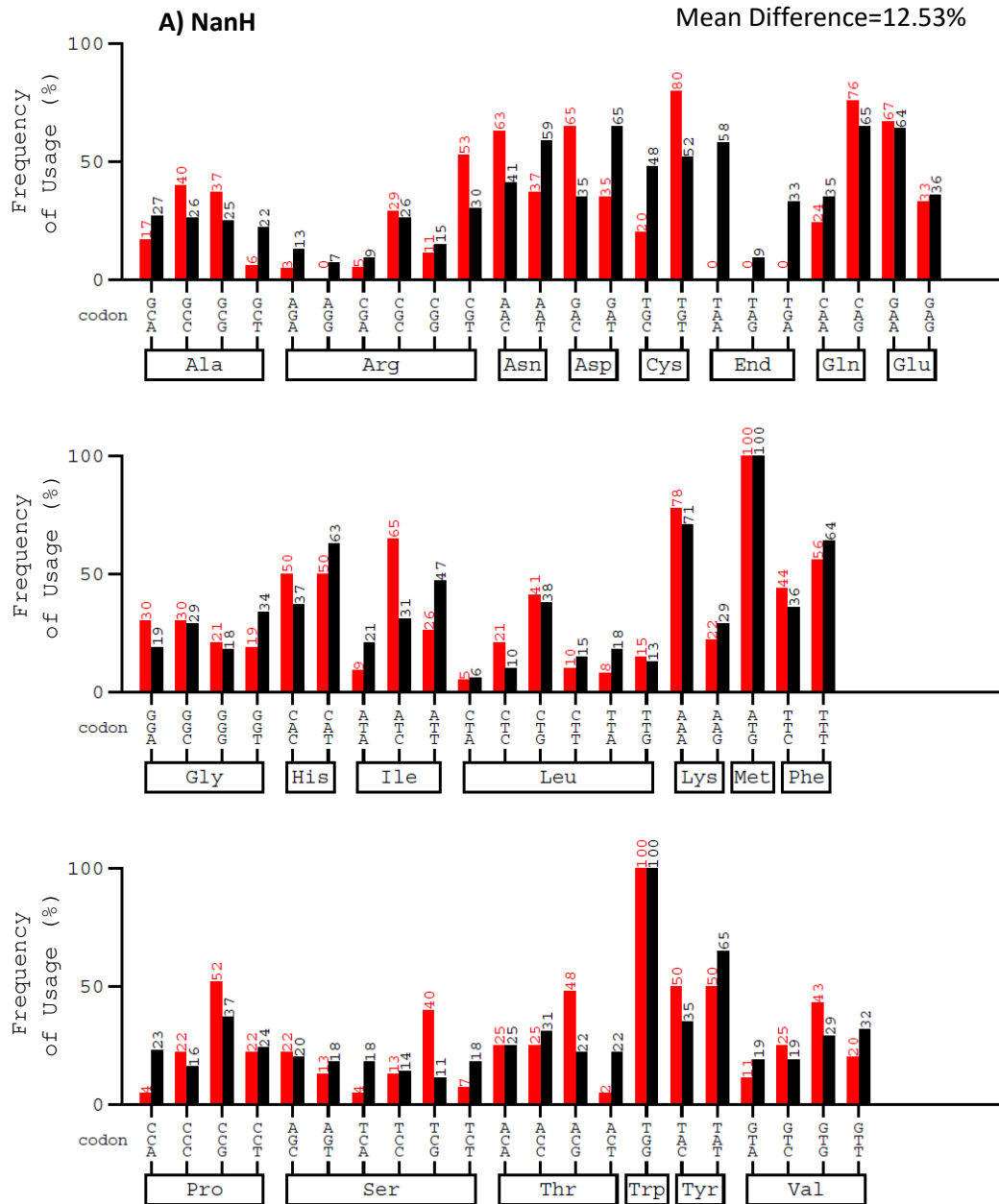
Although the PCR to produce *nanH* and *siaPG* from genomic DNA was successful, PCRs were difficult to reproduce and ligation into pET-plasmids and transformation of *E. coli* storage vectors was never optimised. This, and the insolubility of the sialidase domains produced by native genomic DNA sequences (section 2.3.2.2) alongside the discovery by others in our laboratory that even full-length NanH produced from a PCR product cloning was insoluble prompted an alternative method of sialidase gene production-namely gene synthesis with codon optimisation of *siaPG* and *nanH*.

2.3.3.2 **Gene Synthesis Approach to Production and Amplification of *siaPG* and *nanH***

Gene synthesis is an increasingly popular alternative to more traditional methods of cloning with the aim of protein expression, partly due to its relative inexpense (1 kb can now be produced for £200). This is also attractive since many of the synthesis companies offer an optional codon optimisation step, where the target gene's codons are changed to encode the same amino acids of the original gene, but match the preferentially-used codons in a given organism, according to proprietary algorithms. To assess whether or not codon optimisation would be beneficial, the native *nanH* and *siaPG* codons were compared to the codon preference in *E. coli*, using the Graphical Codon Usage Analyser (GCUA), freely available at <http://gcua.schoedl.de/index.html>. *T. forsythia nanH* was shown to possess a mean difference of 12.53%, between *nanH* frequency of codon usage and frequency of *E. coli* codon usage, while for *siaPG* codon usage compared to *E. coli* codon usage, this mean difference was 13.27% (figure 2.20). While the mean difference between *siaPG* or *nanH* and *E. coli* codon usage may not seem high, some codons differed in frequency of usage by ~30%, as seen for isoleucine (Ile, I) and asparagine (Asp, N). The difference in codon usage of these residues is noteworthy, since they are critical to the function of the sialidase catalytic domain (in the F/Y-R-I-P motif) and Asp-boxes, respectively.

Ultimately, for this project, *siaPG* and *nanH* were synthesised and codon optimised for expression in *E. coli*. Both sialidase sequences were designed without the secretion signal sequence, and included restriction sites for *NdeI* and *XhoI* at 5' and 3' sites, respectively. The resulting codon optimised sialidase-encoding nucleotides can be viewed in appendices 7.5 and 7.6. Synthesised DNA strands were obtained from GeneArt as linear fragments (GeneStrings) and ligated into pJET plasmids (ThermoFisher Scientific) via blunt-ended ligation, with a commercially available kit, followed by transformation into commercially available *E. coli* DH5 α . Successful construction of pJET-*nanH* and pJET-*siaPG* (pJET-

sialidases) was confirmed by restriction digestion of plasmids extracted from the transformed *E. coli*, followed by agarose gel electrophoresis (figure 2.21).



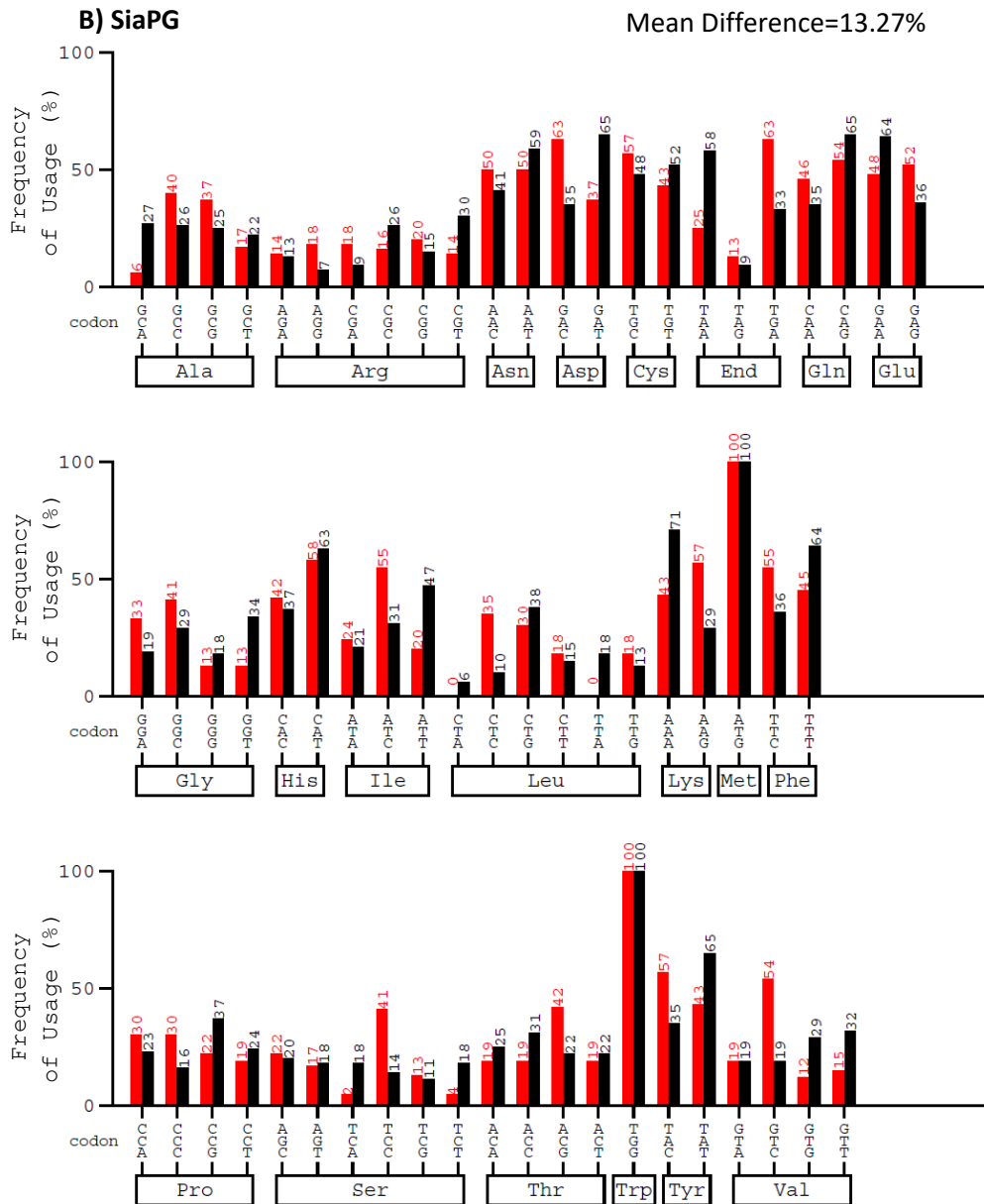


Figure 2.20 Comparison of codon utilisation between A) *nanH* or B) *siaPG* and *E. coli*.

Nucleotide sequences encoding *nanH* and *siaPG* were compared against the *E. coli* genome to assess the frequency each codon is used with, using the GCUA (<http://gcu.schoedl.de/index.html>). Red= frequency (%) of a given codon used in *nanH* or *siaPG*, black= frequency (%) of a given codon used in *E. coli*.

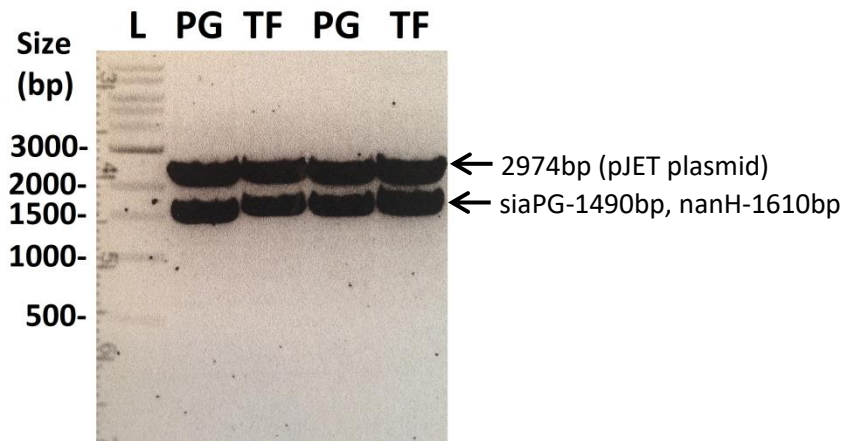


Figure 2.21. *nanH* and *siaPG* pJET constructs.

1.5% (w/v) agarose gel, restriction digestion products and their expected sizes are indicated by arrows. PG=pJET-*siaPG*, TF=pJET-*nanH*.

The bands corresponding to *siaPG* or *nanH* were extracted from the agarose gel with a commercially available kit, before further processing, with the aim of producing pET-plasmid constructs: Undigested pET-21a plasmids were digested using *NdeI* and *XhoI* restriction enzymes, with calf alkaline phosphatase present. The digested reaction mix then underwent agarose gel electrophoresis, and the bands corresponding to digested pET plasmid (~5.4 kbp for pET21a and ~3.5 kbp for pET20b) were extracted using commercially available kits.

Digested codon optimised-genes encoding *nanH* and *siaPG* underwent ligation with digested pET21a, followed by electro-transformation using heat shock into commercially available *E. coli* DH5 α . Resulting bacterial colonies underwent colony PCR followed by restriction digest to confirm the presence of an insert at the expected size (figure 2.22).

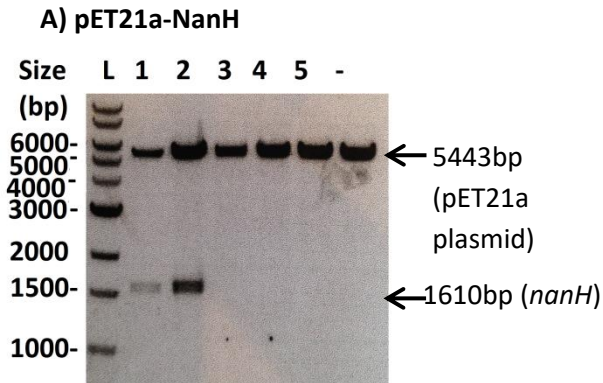


Figure 2.22. Confirmation of pET21a -NanH construct.

1.5% (w/v) agarose gel. Restriction digestion products and their expected sizes are indicated by arrows. A) pET21a-*nanH* B) pET1-*siaPG*

Transformed *E. coli* DH5 α were cultured and pET21a-constructs extracted. All constructs were sequenced to confirm insertion of the sialidase-encoding sequence, and that no mutations had occurred during the cloning process. The pET21a-*nanH* and pET21a-*siaPG* constructs were transformed into EC origami B), for expression.

2.3.3.3 *Expression and Purification of Periodontal Pathogen Sialidases*

Expression of NanH and SiaPG in EC origami B was tested in a similar fashion to the sialidase domains: cultures of transformed EC Origami B were grown to OD₆₀₀ 0.5 and induced with 1 mM IPTG, and harvested at different time points. All harvested bacterial cultures were diluted to OD₆₀₀ 1.0, 1 ml of this suspension was pelleted, and resuspended in 100 μ l of SDS loading buffer. 10-30 μ l of this bacterial suspension underwent SDS-PAGE, the volume of bacterial suspension was constant during each individual experiment (Figure 2.23).

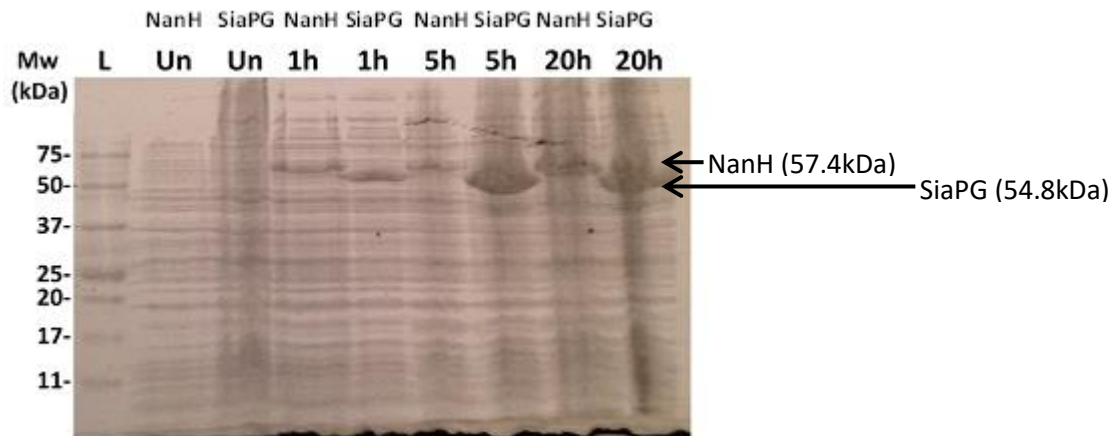


Figure 2.23. Sialidase expression trials.

SDS-PAGE using 15 % (v/v) SDS-PAGE gels showing cell lysates of *E. coli* overexpressing A) NanH and SiaPG. Cultures were grown at 37 °C to OD₆₀₀ 0.5, then induced with IPTG and cultures were incubated at different times and temperatures as indicated, and collected at different time points. Expected protein sizes and bands thought to represent proteins of interest are indicated by arrows. L=Mw weight marker (size approximation based on manufacturer's guide). Un; un-induced expression strains (strains prior to induction with IPTG), h; hours.

After expression trials, larger scale cultures of pET-sialidase EC Origami were cultured, and these underwent purification. This included lysis by French pressure cell, centrifugation to remove insoluble proteins and cell debris, and affinity chromatography using nickel columns to isolate the His⁺ tagged proteins.

Soluble and insoluble fractions of the cell lysate, flow through and wash through from the nickel columns, and eluted fractions were collected, and underwent SDS-PAGE to determine the presence of NanH or SiaPG at any of these stages. NanH and SiaPG were found to be present in the soluble fraction of the cell lysate, and were successfully eluted as pure protein in the elution fractions (figure 2.24). Only soluble proteins are likely to be functional in biochemical tests and other *in vitro* work, so the fact that both sialidases were readily soluble and apparently stable in a low salt buffer (50 mM sodium phosphate, 200 mM NaCl) was a major advantage. Unlike the insoluble sialidase-domains (section 2.3.2.2), the yield of protein from the sialidase producing cultures was quite high; a litre of EC Origami induced to produce NanH or SiaPG could yield up to 15 ml of ~2-5 mg/ml of either protein, and during some purification batches NanH or SiaPG would be present in the wash

or flow through stages during affinity chromatography, possibly due to exceeding the binding capacity of the Nickel column, or re-use of the column resulting in loss of Nickel.

This large quantity of purified SiaPG and NanH made it possible to carry out biochemical tests and other *in vitro* studies of the two periodontal pathogen sialidases, described in this chapter and others.

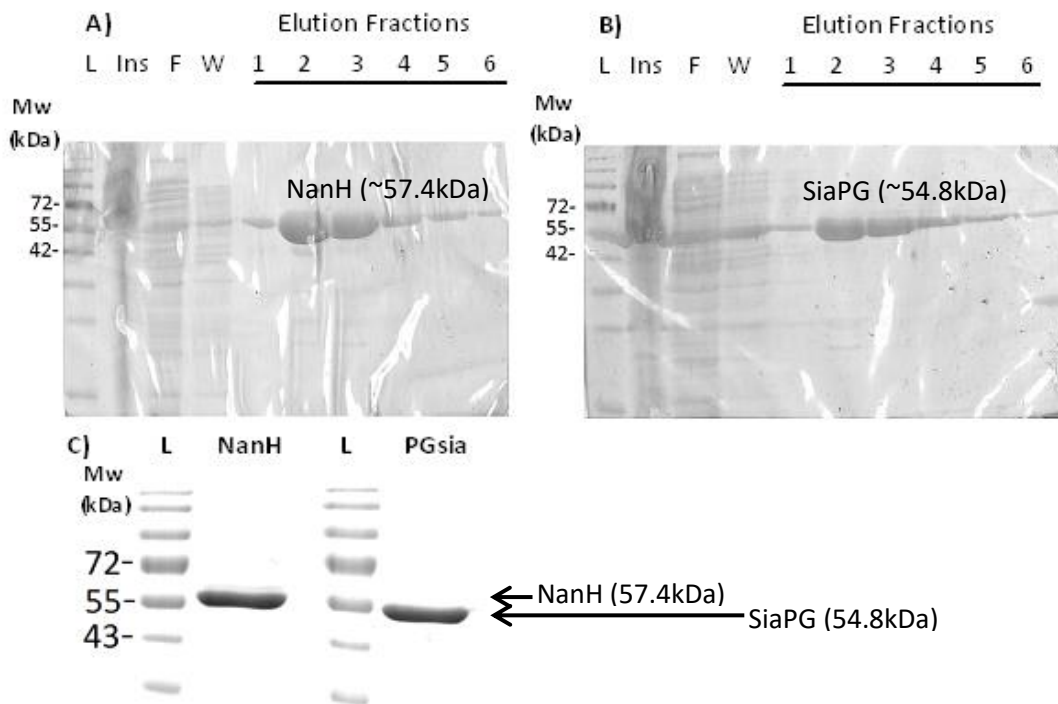


Figure 2.24. Affinity chromatography purification of NanH and SiaPG.

A) NanH, B) SiaPG, C) NanH and SiaPG post-dialysis. 12% (v/v) polyacrylamide gels. L=Mw Ladder (kDa, size approximation based on manufacturer's guide), Ins=Insoluble Fraction, F=Flow Through, W=Wash Through, 1-6= Eluted fractions. Note: C) is NanH and SiaPG from two separate SDS-PAGE gels, imaged using the same parameters and shown side by side.

2.3.4 Expression and Purification of Other Enzymes

Although the focus of this project was on the sialidases NanH and SiaPG, other proteins were expressed and purified, creating more avenues for biochemical and other *in vitro* studies related to SiaPG and NanH. These proteins were the Sialate-*O*-Acetyltransferase from *T. forsythia* (NanS) (section 3.3.1.1), and an active site mutant of NanH (below), where the conserved FRIP motif had been mutated to YMAP, with the aim of producing an inactive

sialidase with the same structure and ligand binding capacity as native NanH and to probe the importance of the FRIP motif on biochemical activity of NanH.

2.3.4.1 ***Purification of a NanH-Active Site Mutant Sialidase***

The active site of NanH contains a FRIP motif in the catalytic β -propeller which is highly conserved between sialidases, the motif is almost always F/YRIP, although isoleucine is sometimes substituted for leucine (S. Kim et al. 2011). It was hypothesized that mutation of this conserved region would abrogate NanH sialidase activity, while probably retaining its native configuration. An inactive sialidase could be useful for future studies, since it would not have any catalytic activity, but might still retain its capacity to bind ligands: An inactive sialidase mutant could be used to accurately study the cellular targets of the native sialidase. In the future, an inactive sialidase might represent a sialidase inhibitor itself, if it was capable of outcompeting the native enzyme for its ligand.

Although it might have been possible to choose any combination of amino acids with the result of abrogation of activity, in an attempt to preserve a tertiary structure most similar to the native protein, specific residues were chosen to replace three of four present in the FRIP motif, the resultant mutated motif being YMAP. The amino acid substitutions are further discussed in section 2.3.6.5.

Previous work had changed the sequence of the codon optimised *nanH* through a PCR-based approach, mutating the resulting protein motif from FRIP \rightarrow YMAP (Jennifer Parker, Stafford Research Group, University of Sheffield, unpublished). Importantly, this quick change PCR had been carried out on the codon optimised NanH, i.e. encoding a mutated version of the active NanH described here (section 2.3.3).

This protein was termed NanH-YMAP. The plasmid encoding NanH-YMAP had been transformed into EC origami for expression. NanH-YMAP was successfully purified using the same protocol as NanH (figure 2.25). Protein yield after purification of NanH-YMAP was typically lower than for NanH, 1 litre of EC origami culture could yield 10ml of \sim 1-2 mg/ml protein, though this was sufficient for the scope of this project. Testing of the activity of this mutant and its functionality in ligand binding is outlined in section 2.3.6.5.

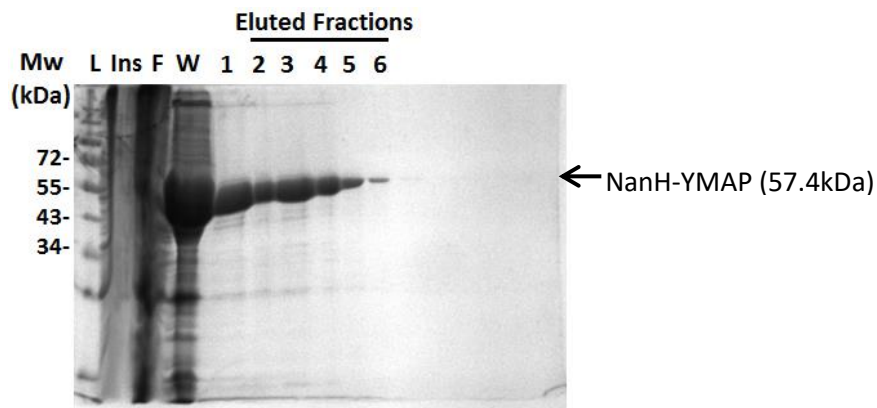


Figure 2.25. Purification of NanH-YMAP.

SDS-PAGE using 12% (v/v) polyacrylamide gel. L=Mw Ladder (kDa, size approximation based on manufacturer's guide), Ins=Insoluble Fraction, F=Flow Through, W=Wash Through, 1-6= Eluted fractions.

2.3.5 Sialidase Protein Production-a Summary

Bioinformatic approaches highlighted the presence of two domains in both sialidases-NanH and SiaPG, from *T. forsythia* and *P. gingivalis*, respectively-which were dubbed the carbohydrate binding module (CBM) and the C-terminal domain (CTD), the former thought to play a role in ligand binding (in *T. forsythia* at least), and the latter being responsible for sialidase activity. Before studies of the sialidases and their domains, production of NanH, SiaPG, and their domains NanH-CTD, PGsia-CBM, and PGsia-CTD was attempted. This involved production of a number of plasmid constructs, summarised in table 2.7.

These plasmid constructs were transformed into *E. coli* BL21 Origami for expression. Ultimately, the sialidase subunits were only purified producing a low yield, but the whole sialidases NanH and SiaPG were successfully purified with high yields, ideal for further studies. It is important to note that these were codon optimised for expression by *E. coli*, rather than the native *T. forsythia* or *P. gingivalis* sialidase genes. This could explain the high yield of soluble protein during expression by *E. coli*, compared to the mostly insoluble sialidase domain sequences which were obtained by PCR using *T. forsythia* or *P. gingivalis* genomic DNA as a template. Furthermore the codon optimised *T. forsythia nanH* was designed based on the *nanH* gene from *T. forsythia* strain 92.A2-an accident due to the incorrect submission of 92.A2 genome in place of the *T. forsythia* 43037 genome on the NCBI and oralgen databases. However, considering that the two NanH protein sequences share 98% homology with each other-11 amino acid substitutions out of 539 residues, and

none of these occur within Asp-Boxes or the FRIP domain, it is likely that the two sialidases possess almost identical activity. An alignment of the two sialidases can be viewed in appendix 7.8

Name of Construct	Details of Construct	Transformed into <i>E. coli</i> Strain(s)
pJET-NanH	pJET plasmid containing codon optimised, gene synthesised nanH	DH5 α
pJET-siaPG	pJET plasmid containing codon optimised, gene synthesised siaPG	DH5 α
pET21a-NanH	pET21a plasmid containing codon optimised, gene synthesised nanH	DH5 α , EC Origami
pET21a-siaPG	pET21a plasmid containing codon optimised, gene synthesised siaPG	DH5 α , EC Origami
pET20b-NanH-CT	pET20b plasmid containing native nanH-CT	DH5 α , EC Origami
pET20b-siaPG-CBM	pET20b plasmid containing native siaPG-CBM	DH5 α , EC Origami
pET20b-siaPG-CT	pET20b plasmid containing native siaPG-CT	DH5 α , EC Origami

Table 2.7. Plasmids constructed for storage or expression of sialidases and sialidase domains. .

pJET plasmids were used as secondary storage vectors and to ensure continued amplification of codon optimised nanH and siaPG, while pET plasmids were used for storage and ultimately for protein expression. “Native” and “codon optimised, gene synthesised” refers to the source of the inserted sequence present in the plasmid, either a PCR construct from pathogen DNA, or synthetically produced and optimised for expression in *E. coli*.

2.3.6 Biochemical Characterisation of Purified Periodontal Pathogen Sialidases

Elucidating the conditions and under which NanH and SiaPG can function is an important first step in characterising the activity of these enzymes. The initial studies of purified NanH and SiaPG shown here were performed using the model sialic acid-substrate MUNANA, which allows quantification of sialidase activity through detection of 4-MU release from MUNANA (Neu5Ac is also produced when MUNANA is cleaved). Although this ligand is not present in the pathogens' hosts, it is a widely used substrate for high throughput testing of sialidases (Cabezas et al. 1989; Han et al. 2000; Tailford et al. 2015).

A simple MUNANA-based activity test to confirm activity of purified NanH and SiaPG was frequently used to confirm that a given batch of protein, or diluted protein, possessed sialidase activity before use in further studies (figure 2.26). MUNANA based assays were also used to quantify sialidase activity under variable pH conditions.

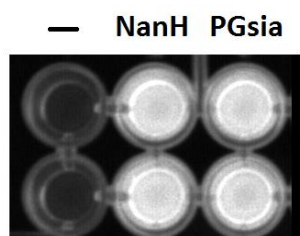


Figure 2.26 Visualisation of MUNANA cleavage to rapidly confirm sialidase activity.

MUNANA was exposed to no enzyme (-), or NanH, or SiaPG as indicated. In the case of sialidase activity resulting in release of 4-MU, fluorescence under UV light can be seen.

Further work utilised thiol- labelling of free (non-conjugated) sialic acid to study sialidase cleavage of Neu5Ac from 3- and 6-sialyllactose (3- and 6-SL) to determine any preference or specificity for two types of sialic acid linkages- i.e using the thiobarbiturate based assay for sialic acid. The activity of NanH on the host relevant ligands 3-sialyl lewis A and 3-sialyl lewis X (SleA and SleX) using the thiol- labelling method is also reported and discussed below. Furthermore, the MUNANA based assay was used to elucidate the efficacy of zanamivir for the purified sialidases and live pathogens, providing a backdrop for *in vitro* studies on the effect of sialidase inhibitors on periodontal pathogen virulence.

2.3.6.1 *Periodontal Pathogen Sialidases Display Broad pH Optima*

Understanding the pH under which sialidases function is important for further biochemical and other *in vitro* experiments, and may yield information on where and when the sialidase

act during infection; for instance, different sites within the host are likely to possess different pH conditions, and in the case of periodontitis, the periodontium may show variable pH as periodontal disease progresses (Bickel & Cimasoni 1985; Eggert et al. 1991; Galgut 2001).

MUNANA was exposed to SiaPG and NanH under different pH conditions, and the sialidase activity quantified by release of 4-MU (and Neu5Ac), resulting in an increased fluorescence. Optimum 4-MU fluorescence occurs on excitation at ~345-380nm, with fluorescence emission at ~445-454 nm. However, 4-MU fluorescence is also pH dependent, with optimal fluorescence under these wavelengths occurring at pH 10.5 (Mead et al. 1955).

It is possible to measure the fluorescence of 4-MU at lower pH in a given experiment, provided all conditions are under the same pH, although this will result in decreased sensitivity as the fluorescence of 4-MU is decreased. An alternative is to use a lower excitation wavelength of 331 nm, and record fluorescence emission at 368nm-this almost completely abrogates the effect of pH on fluorescence of 4-MU under the higher wavelength measurements, although this also decreases assay sensitivity (Strachan et al. 1961).

To negate the impact of pH on fluorescence while retaining assay sensitivity, a quenching/equilibrating step was performed; an excess amount of pH 10.5 buffer was added to stop the reaction (the enzymes lose their activity at high pH) and equilibrate the reaction to above pH 10.

Both sialidases appeared to display optimum activity under moderately acidic conditions: SiaPG at pH 5.6, and NanH at ~pH 5.2 (figure 2.27). Notably, activity is present across a wide pH range; activity of NanH is above 50 % between pH4-6.8, only dropping below 10 % above pH 8.4, or below pH 4.4. Similarly for SiaPG, activity remains above 50 % between pH4.4-6.4, only dropping below 10 % above pH 8.0, or below pH 4.4.

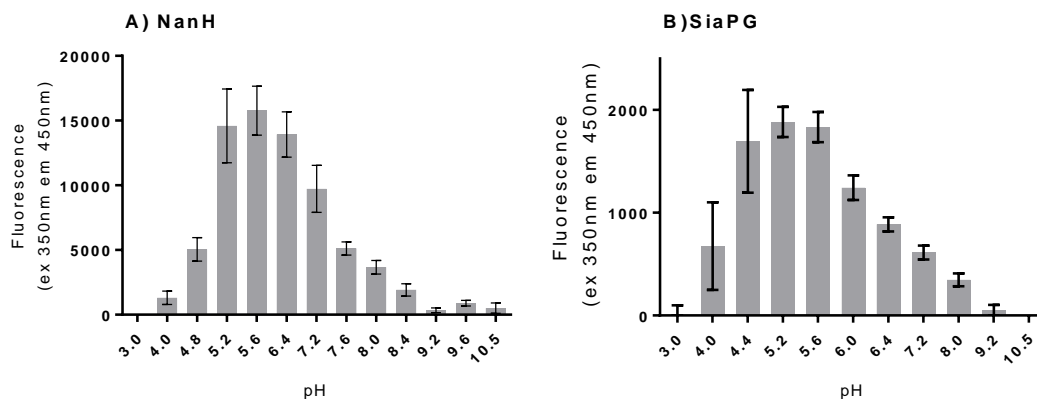


Figure 2.27. pH optima of A) NanH and B) SiaPG.

MUNANA was exposed to NanH or SiaPG for 1 minute under a variety of pH conditions. Reactions were performed in clear microtitre plates for 1 minute, before being quenched with an excess of pH 10.5 buffer to ensure fluorescence reading of 4-MU was obtained at the same pH for each condition, and to stop the reaction. Data shown represent the mean of two experiments, where each condition was repeated three times per experiment. Error bars=SEM.

MUNANA was also exposed to live pathogens-*T. forsythia* and *P. gingivalis* whole cells- under different pH conditions in an assay similar to the one described above, and sialidase activity quantified. It was important to establish the sialidase activity of whole pathogens under similar conditions to their purified enzymes, both for practical purposes and to confirm the activity of the whole, live pathogens could take place under the same broad-pH conditions as the purified enzymes. In contrast to the purified sialidases, *P. gingivalis* and *T. forsythia* whole cell sialidase activity was optimum under nearly neutral conditions (figure 2.28), with *T. forsythia* highest at pH 6.8, and *P. gingivalis* also at pH 6.8. In addition, the live pathogens appear to display higher relative sialidase activity over a broader pH range than their purified sialidases. This might be expected, since cell membranes, surrounding proteins and glycans can stabilise cell-associated proteins, it follows that cell-associated sialidases might display increased pH-stability compared to proteins free in solution (i.e. the purified sialidases). An alternative explanation is that the live pathogens might continue to secrete sialidases into the reaction, replacing any that have become unstable and inactive over time. The data from these experiments are from reactions stopped after

longer time points, the *T. forsythia* reaction was quenched/pH equalised after 30 minutes. Live *P. gingivalis* displayed lower sialidase activity, reactions were quenched/pH equalised after 4 hours. Unfortunately this longer time point produced larger error between experimental repeats, though the trend remained the same between experiments. Using a greater concentration of *P. gingivalis* to counter this was also problematic, perhaps because the absorbance of the resulting bacterial suspension interfered with fluorescence.

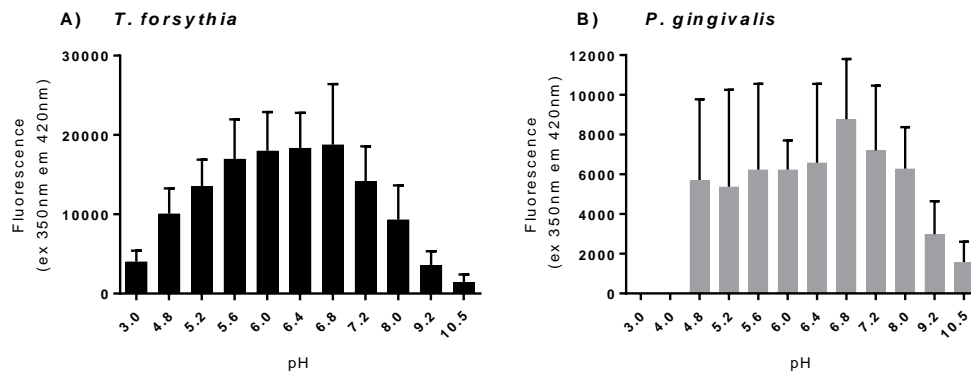


Figure 2.28. pH Optima of A) *T. forsythia* and B) *P. gingivalis*.

MUNANA was exposed to *T. forsythia* or *P. gingivalis* for 30 minutes and 3 hours, respectively, under a variety of pH conditions. Reactions were performed in clear microtitre plates for 1 minute, before being quenched with an excess of pH 10.5 buffer to ensure fluorescence reading of 4-MU was obtained at the same pH for each condition, and to stop the reaction. Data represent the mean of two experimental repeats, where each condition was repeated three times per experiment. Error bars=SD.

Bacterial, viral, and eukaryotic sialidases often display acidic-neutral pH optima (Kurniyati et al. 2013; Cabezas et al. 1989; Park et al. 2013; Manzoni et al. 2007), so it is perhaps unsurprising that both SiaPG and NanH also follow this trend.

2.3.6.2 Reaction Kinetics of Pathogen Sialidases and MUNANA

The model sialic acid-ligand MUNANA is widely used for high throughput testing of sialidase activity, and characterisation of the reaction kinetics of NanH and SiaPG with MUNANA would allow comparison of these with previously characterised sialidases from other pathogens, and to assess the efficacy of sialidase inhibitors.

Given the pH variations in the pathogens' ecological niche, i.e. the conditions the sialidases would encounter in the host it was necessary to evaluate sialidase activity at different pH

conditions. There were also practical implications for this, as *in vitro* work discussed in later chapters was performed under neutral conditions (which are also the normal conditions in the host).

Reaction kinetics for NanH and SiaPG were obtained by quantifying 4-MU release from a variable concentration of MUNANA by the two sialidases, and applying a standard curve of known 4-MU concentrations. Initial rate of 4-MU release ($\mu\text{mol}/\text{min}/\text{mg}$ sialidase) by NanH and SiaPG under the different pH conditions was plotted against MUNANA (the enzyme substrate) concentration to obtain a Michaelis-Menten plot, and subsequently the ligand-enzyme affinity (K_M) and maximum reaction rate (V_{max}) (figure 2.29).

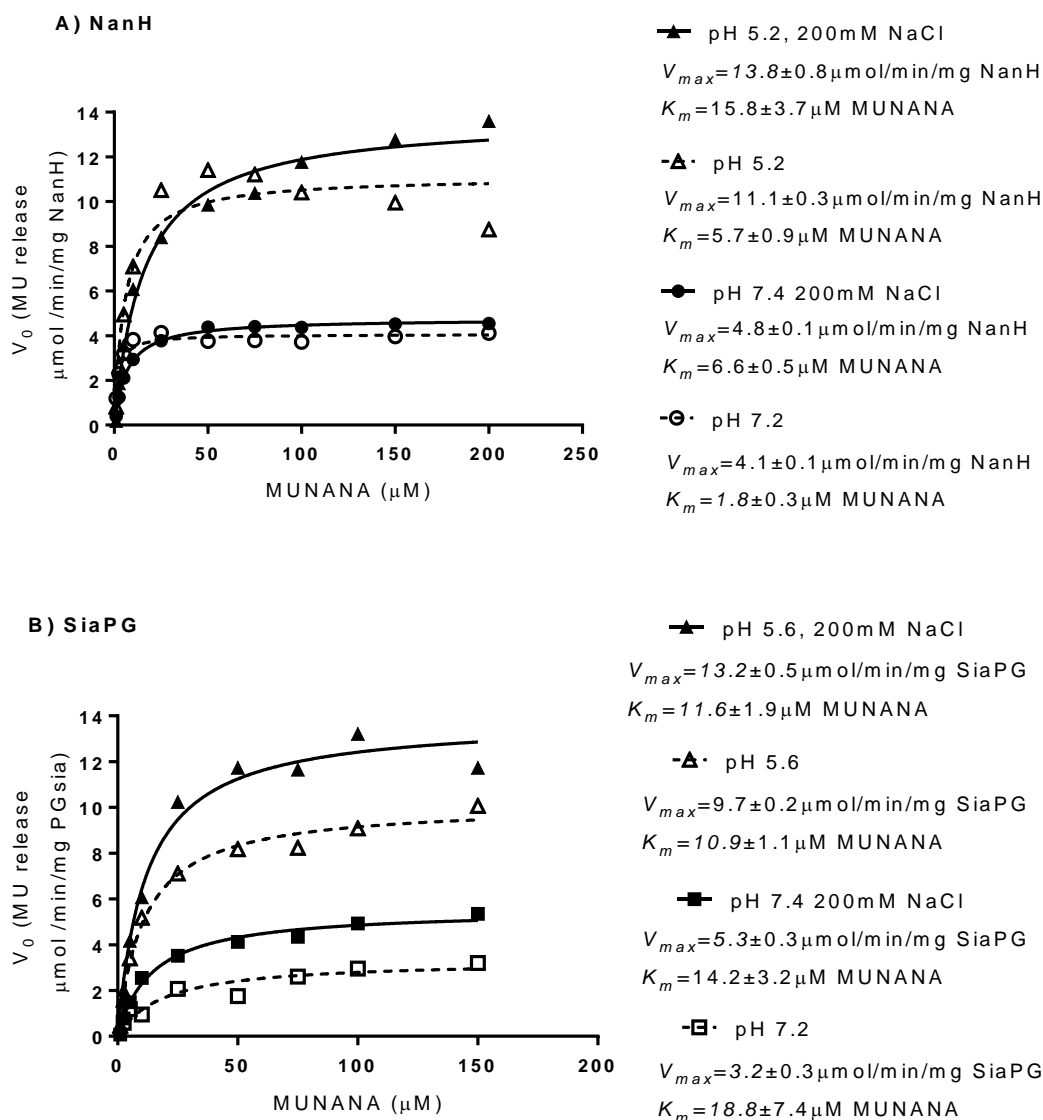


Figure 2.29. Reaction kinetics of MUNANA with A) NanH and B) SiaPG

Variable concentrations of MUNANA were exposed to NanH or SiaPG, under different pH and salinity conditions. Reactions were quenched by addition of pH 10.5 buffer at 1, 2, and 3 minutes, and the rate of 4-MU release (V_0) determined by application of a 4-MU standard curve. This was plotted against [MUNANA] to obtain the Michaelis-Menten plots. The V_{max} , K_M and associated error (SD) of MUNANA cleavage by NanH and SiaPG are displayed.

The V_{max} of NanH and SiaPG are both higher at their acidic (optimum) pH conditions compared to neutral conditions: At pH 5.2 NanH V_{max} was $11.1 \mu\text{mol}/\text{mg}/\text{min NanH}$, compared to $11.1 \mu\text{mol}/\text{mg}/\text{min NanH}$ at pH 7.2. For SiaPG, at pH 5.6 V_{max} was 9.7

$\mu\text{mol}/\text{mg}/\text{min}$ SiaPG, compared to $3.2 \mu\text{mol}/\text{mg}/\text{min}$ SiaPG at pH 7.2. After this first finding, a buffer with physiological pH 7.4, and with higher salinity (200mM NaCl)-used in work described here in other chapters as it more closely mimics physiological conditions-was also tested. It was expected that this physiological buffer would display very similar kinetics to the pH 7.2 buffer (with a small difference in pH of 0.2 between the two conditions), but in the NanH condition both K_M and V_{max} were increased relative to the pH 7.2 (no salt) condition (table 2.8). SiaPG also displayed an increase in V_{max} (table 2.8). The pH 5.2 and 5.6 conditions were repeated for NanH and SiaPG, with the higher salinity (200mM NaCl) to observe if the reaction kinetics were also shifted at this pH. Again, for NanH, both the K_M and V_{max} were increased relative to the pH 5.2 (no salt) condition (table 2.8), and SiaPG displayed an increased V_{max} in the presence of NaCl. In the case of NanH, the presence of 200mM NaCl shifted the V_{max} by a factor of ~ 1.2 in both acidic and neutral conditions, while K_M was shifted by similar factors of 2.8 and 3.7 at acidic or neutral pH, respectively. For SiaPG, the presence of 200mM NaCl shifted the V_{max} by a factors of 1.1 and 0.8 in acidic and neutral conditions, respectively, while K_M was shifted by similar factors of 1.3 and 3.7 at acidic or neutral pH, respectively. Interestingly, the reaction between NanH and MUNANA in the pH 5.2, no salt condition appears to display product or substrate inhibition (indicated by the decrease in reaction rate when $[\text{MUNANA}] > 100\mu\text{M}$), but in the presence of 200mM NaCl, substrate/product inhibition is not visible (figure 2.29 A).

Enzyme	pH Conditions	V_{max} ($\mu\text{mol}/\text{min}/\text{mg}$ Sialidase)		Salt-induced Fold change in V_{max}	K_m (μM MUNANA)		Salt-induced Fold Change in K_m
		No Salt	200mM NaCl		No Salt	200mM NaCl	
NanH	Acidic-Enzyme Optimum	11.1 \pm 0.3	13.8 \pm 0.8	1.2	5.7 \pm 0.9	15.8 \pm 3.7	2.8
	Neutral-Host pH	4.1 \pm 0.1	4.8 \pm 0.1	1.2	1.8 \pm 0.3	6.6 \pm 0.5	3.7
SiaPG	Acidic-Enzyme Optimum	9.7 \pm 0.2	13.2 \pm 0.5	1.3	10.9 \pm 1.1	11.6 \pm 1.9	1.1
	Neutral-Host pH	3.2 \pm 0.3	5.3 \pm 0.3	1.7	18.8 \pm 7.4	14.2 \pm 3.2	0.8

Table 2.8. The effect of salt on sialidase kinetics under different pH conditions.

V_{max} and K_m data shown in Figure 2.29 were tabled to allow easy comparison of the change in K_m and V_{max} between different pH conditions in the presence and absence of NaCl. The salt-induced fold change was obtained by dividing the V_{max} or K_m of the 200mM NaCl condition from the no-salt condition for both pH conditions. Error=SD.

The apparent increase in maximum reaction speed (increased V_{max}), but decreased affinity (increased K_M) necessitated an alternative plot; in this case the rate of MU release against concentration of sialidase active sites (MU release /min –at a given concentration of enzyme active sites, as opposed to $\mu\text{M}/\text{min}/\text{mg}$ enzyme seen in the above plots). This establishes the K_{cat} , which can be divided by K_M to obtain catalytic efficiency under acidic (enzyme optimum) and neutral (host-environment) pH conditions (figure 2.30). A separate curve to obtain K_{cat} was required as the reaction velocity (V_0) used in calculating K_{cat} uses different units to that of V_{max} .

Interestingly, salt appeared to decrease the catalytic efficiency of NanH; K_{cat}/K_m changed by a factor of 0.5 and 0.3 for acidic and neutral conditions, respectively. Conversely, for SiaPG the catalytic efficiency was increased in the presence of salt, i.e. K_{cat}/K_m changed by a factor of 1.3 and 1.5 for acidic and neutral conditions, respectively (table 2.9).

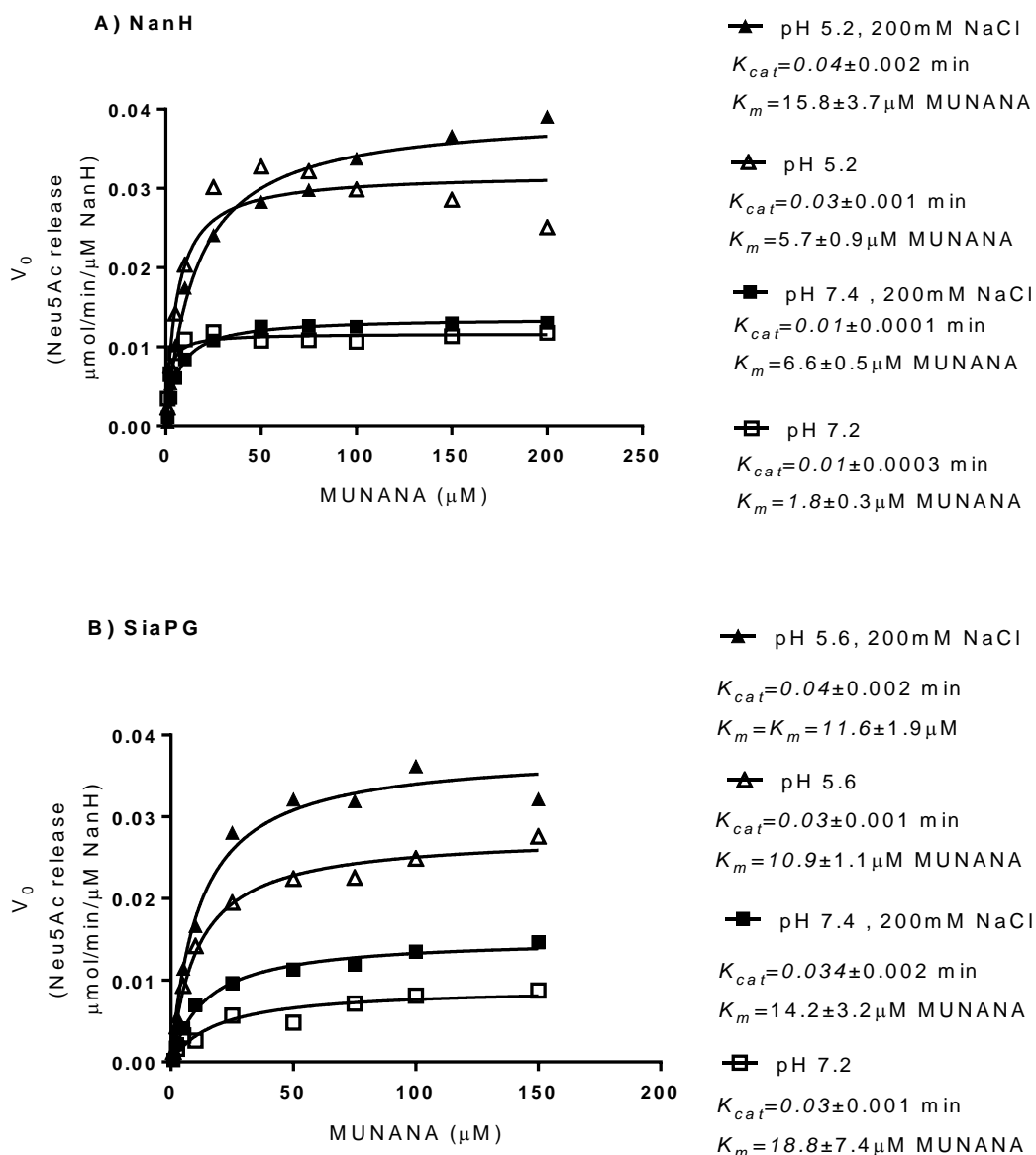


Figure 2.30. Catalytic efficiency of A) NanH and B) SiaPG.

Variable concentrations of MUNANA were exposed to NanH or SiaPG, under different pH and salinity conditions. Reactions were quenched by addition of pH 10.5 buffer at 1, 2, and 3 minutes, and the rate of 4-MU release determined by application of a 4-MU standard curve. This was plotted against [MUNANA] to obtain the Michaelis-Menten plots. The K_{cat} , K_m and associated error (SD) of MUNANA cleavage by NanH and SiaPG are displayed.

		K_{cat} (min)		K_m (μ M MUNANA)		K_{cat}/K_m (min ⁻¹ μ M ⁻¹)		Salt-induced Fold Change in K_{cat}/K_m
		No Salt	200mM NaCl	No Salt	200mM NaCl	No Salt	200mM NaCl	
NanH	Acidic-Enzyme Optimum	0.03±0.001	0.04±0.002	5.7±0.9	15.8±3.7	0.005263	0.00253	0.5
	Neutral-Host pH	0.011±0.0003	0.013±0.0001	1.8±0.3	6.6±0.5	0.006111	0.00197	0.3
SiaPG	Acidic-Enzyme Optimum	0.03±0.001	0.04±0.002	10.9±1.1	11.6±1.9	0.002752	0.00345	1.3
	Neutral-Host pH	0.03±0.001	0.034±0.002	18.8±7.4	14.2±3.2	0.001596	0.00239	1.5

Table 2.9. The effect of salt on sialidase kinetics under different pH conditions.

K_{cat} and K_m data shown in figure 2.30 were tabled to allow easy comparison of the change in K_m and K_{cat} between different pH conditions in the presence and absence of NaCl. The salt-induced fold change was obtained by dividing the K_{cat}/K_m of the 200mM NaCl condition from the no-salt condition for both pH conditions. Error=SD.

2.3.6.3 Preference of NanH for Different Sialic Acid Linkages

In humans, sialic acid is typically found at the terminating end of N- or O-glycans, linked to the underlying sugar-usually a galactose (Gal) or N-Acetyl Galactosamine (GalNAc)-via its second carbon, and either the third, sixth, and sometimes eighth carbon in the underlying sugar (reviewed in (Cohen & Varki 2010) and (Varki & Gagneux 2012)). This is termed α 2-3, α 2-6, or α 2-8 linked sialic acid. Bacteria, such as *E. coli* K12, may possess polymeric sialic acid within glycans, linked through the second carbon and eighth carbon on the sialic acid (poly α 2-8 linked sialic acid). Some human cells also possess poly α 2-8 Neu5Ac, but in the periodontium the most commonly encountered sialic acids are α 2-3 and α 2-6 linked sialic acid, and therefore the ability of periodontal pathogen sialidases to act on these was examined.

In a series of experiments, the sialoconjugates α 2-3, and α 2-6 sialyllactose (3- and 6-SL, depicted in figure 2.31) were exposed to NanH to release sialic acid. These short glycans are commonly used in studies assessing linkage specificity of sialidases (Tailford et al. 2015; Thompson et al. 2009; Li & McClane 2013), but unlike the MUNANA based assay, which quantifies sialidase activity by measuring the release and fluorescence of 4-MU, the products of sialic acid release from sialyllactose are not readily quantifiable using fluorometric methods.

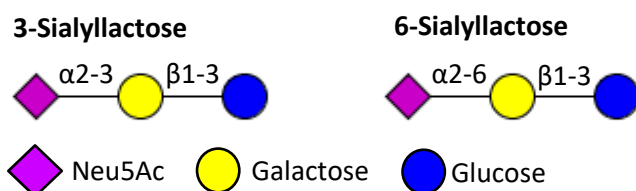


Figure 2.31. 3- and 6- sialyllactose.

Trisaccharides of glucose-galactose-Neu5Ac used to probe sialidase specificity, due to the only difference being the linkage between Neu5Ac and Galactose. Image rendered in Glyco Workbench (Ceroni et al. 2008).

Quantification of free sialic acid required adaptation of the Thiobarbituric Acid (TBA) assay described by Aminoff (Aminoff 1961). This assay results in labelling of free sialic acid in a given sample with a thiol group, allowing sialic acid to be arbitrarily quantified by spectrophotometry: A standard curve of known sialic acid concentrations can also undergo the TBA assay and spectrophotometry, and applied to obtain the actual concentration of sialic acid in the sample. In this work, a high throughput version of the TBA assay was optimised-the key difference being smaller reaction volumes, and absence of a chromophore solubilisation/enhancement step at the end of the assay, which was included in other TBA assays shown in section 3.3.1.

Variable concentrations of 3- and 6-SL were exposed to NanH, in a 50mM sodium phosphate, 200mM NaCl, pH 7.4 buffer to imitate physiological conditions in the host. Reactions were halted at given time points by oxidation with sodium periodate-the first step of the TBA assay, which was immediately carried out to completion. The TBA assay was always performed with a Neu5Ac standard curve alongside the sialidase treated ligands.

Digestion of variable concentrations of the sialyllactose ligands enabled plotting of the Michaelis-Menten curve, and subsequently to obtain the ligand-enzyme affinity (K_M) and maximum reaction rate (V_{max}) of NanH for 3- and 6-SL (Figure 2.32 A). A separate curve to obtain K_{cat} was also plotted (Figure 2.32 B), as the initial velocity (V_0) used in calculating K_{cat} uses different units to that of V_{max} .

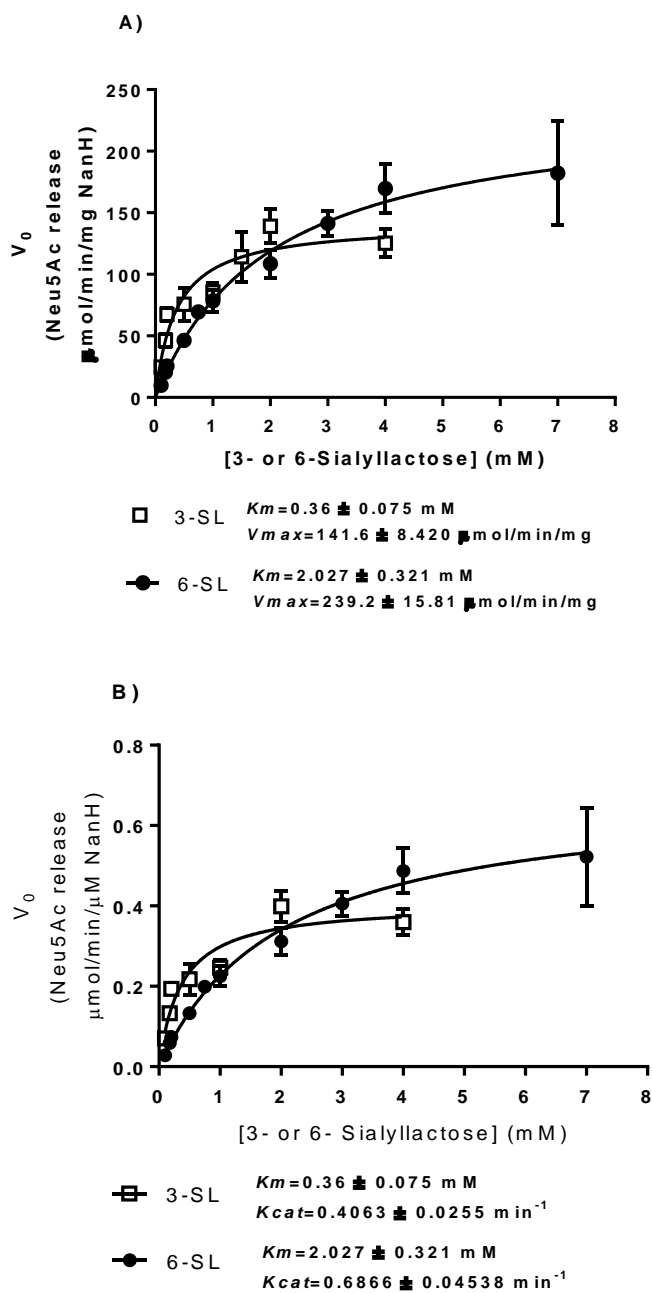


Figure 2.32. Kinetics of NanH on α 2-3 and α 2-6 linked sialic acid under physiological conditions.

Variable concentrations of 3- and 6-SL were digested with NanH, reactions were stopped at different time points and immediately subjected to the TBA assay. Application of a standard curve enabled determination of the rate of Neu5Ac release. The reaction was performed in buffer intended to mimic physiological conditions; 50mM Sodium Phosphate, 200mM NaCl, pH 7.4. A) K_M and V_{max} of NanH for 3- and 6-SL B) K_M and K_{cat} of NanH for 3- and 6-SL. The K_M , K_{cat} and K_{cat}/K_M of NanH for 3- and 6-SL are displayed beneath the plots. Data shown represent the mean of three experimental repeats. Error bars=SD.

NanH displayed a much higher affinity for 3-SL than 6-SL; with a K_M of 0.36 and 2.027mM, respectively-a fivefold difference. However the maximum reaction rate was lower for 3-SL than 6-SL; with a V_{max} of 141.6 and 239.2 μ mol/min/mg, respectively. The K_{cat} of NanH for 3-SL and 6-SL was obtained and the catalytic efficiency determined. NanH was shown to be a much more efficient catalyst for 3-SL ($K_{cat} / K_M = 1.122 \text{ min}^{-1}\text{mM}^{-1}$) than 6-SL ($K_{cat} / K_M = 0.339\text{min}^{-1}\text{mM}^{-1}$).

2.3.6.4 ***Activity of NanH on the Sialic acid Ligands Sialyl Lewis A and Sialyl Lewis X***

Sialyl lewis A (SLeA) and sialyl lewis X (SLeX) are important sialic acid-containing human antigens. These short glycans are isomers, consisting of the same sugar chains, differing in only the fucose-N-acetylglucosamine linkage, which is $\alpha 4$ in the case of SLeA and $\alpha 3$ in the case of SLeX, and the terminal galactose-N-acetylglucosamine linkage which is $\beta 3$ in the case of SLeA and $\beta 4$ in the case of SLeX (Figure 2.33). SLeA/X are involved in a number of cancers including oral cancer (Renkonen et al. 1999), they play roles in neutrophil tissue migration (Lowe 2003), and are involved in bacterial attachment to host cells. SLeA/X may also be expressed on salivary glycoproteins such as salivary mucins, which are glycoproteins that comprise 16-26% of salivary total protein content. In the context of the periodontium, SLeX is highly expressed on neutrophils, where it has been extensively studied for its role in binding endothelial selectins enabling tissue migration (discussed further in chapter 5) and endothelial cells can also express SLeX. SLeA is an isomer of SLeX, is also expressed on a variety of cells, and is also capable of binding selectins (Melorose et al. 1991). Given the apparent multi-functionality of SLeA/X for the host, the ability to cleave sialic acid from one or both of these could influence a number of processes and contribute to virulence. The kinetics of NanH activity on SLeA and SLeX were obtained by exposure of SLeA and SLeX to NanH, followed by a TBA assay (experiments were similar to the kinetics studies of NanH desialylation of 3- and 6- SL in section 2.3.6.4).

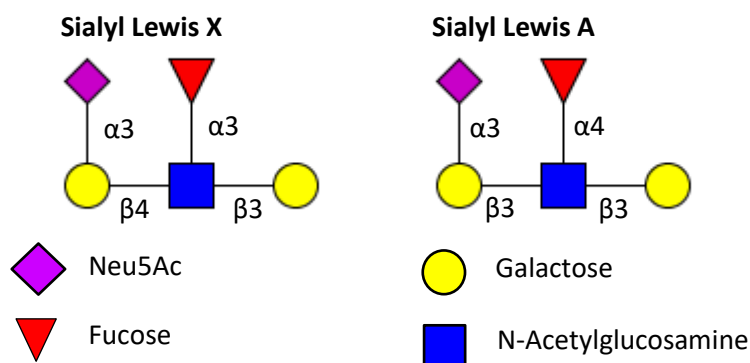


Figure 2.33. Graphic representation of sialyl lewis A/X.

Sialyl lewis A and X are isomers of the same polysaccharide sequence. Image rendered in Glyco Workbench (Ceroni et al. 2008).

NanH displayed greater efficacy in cleavage of SleA than SleX: The maximum rate of reaction was apparently not too dissimilar; V_{max} for NanH SleA desialylation was 41.45 $\mu\text{mol}/\text{min}/\text{mg}$ NanH, compared to 35.15 $\mu\text{mol}/\text{min}/\text{mg}$ NanH for SleX desialylation. However, the affinity of NanH for SleA was tenfold greater; the K_M of NanH for the two sialyl lewis ligands was 0.20mM SleA, compared to 2.05mM SleX (figure 2.34). Discussing the efficacy of NanH in desialylation of SleA/X in the context of other enzymes is difficult, since to our knowledge there have been no studies (besides work presented here) which establish Michaelis-Menten kinetics of any sialidases with either SleA or SleX. However, apparently not all sialidases possess greater catalytic efficiency for SleA, with all human sialidases (Neu1-4) showing greater efficacy in desialylation of SleX than SleA (Shiozaki et al. 2011).

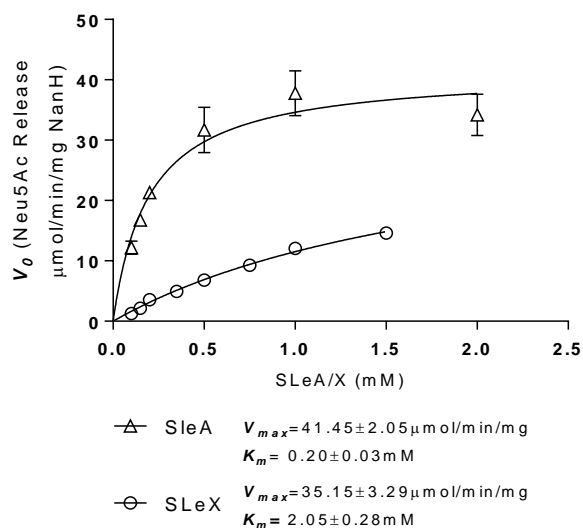


Figure 2.34. Kinetics of Neu5Ac release from SleA and SLeX by NanH

Variable concentrations of SLeA/X were digested with NanH, reactions were stopped at different time points and immediately subjected to the TBA assay. Application of a standard curve enabled determination of the rate of Neu5Ac release. The K_m and V_{max} of NanH for SleA and SLeX are displayed beneath the plots. Data shown represent the mean of three experimental repeats. Error bars=SD.

2.3.6.5 *Sialidase Active Site Mutation Abrogates Sialidase Activity, but not Ligand-Binding Capacity*

The NanH active site contains a highly conserved FRIP motif, thought to be important for catalytic activity. This was mutated in previous work to YMAP in an attempt to abrogate activity (Jennifer Parker, Stafford Research Group, The University of Sheffield). F→Y is actually a conservative mutation, likely to preserve function since this residue is used in other sialidases (e.g. SiaPG). R→M was chosen since the amino acids are similar in mass ($M_w=156$ and 131 , respectively). Perhaps lysine (K) could have been substituted for R instead of substitution with M, but retaining the positive charge by mutating R→K might not have resulted in loss of sialidase activity. I→A mutations were chosen since they are both hydrophobic amino acids, and it was considered possible that use of leucine (L) instead of alanine for the substitution would not result in loss of sialidase activity. For reference, the structures of the native amino acids alongside the residues chosen for substitution are shown in figure 2.35.

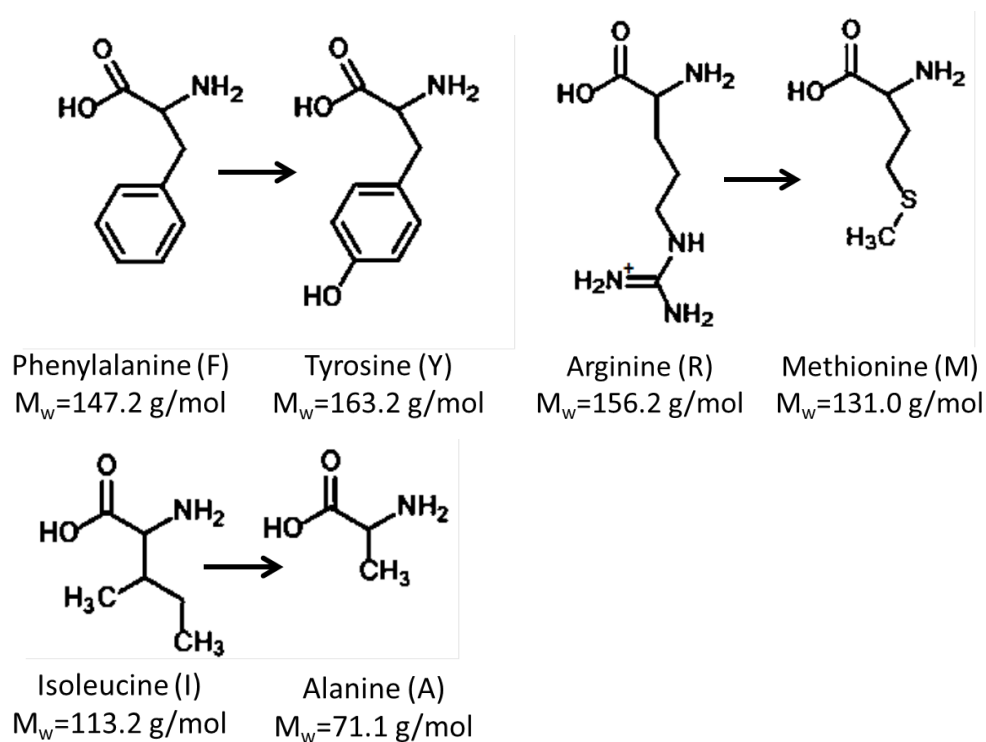


Figure 2.35. Structures of the substituted amino acids in NanH and NanH-YMAP.

The FRIP motif was mutated to YMAP, the native and substituted amino acids are shown adjacent to each other. Arrows = substituted amino acid. Molar mass (M_w) is also shown.

In addition to showing that this motif is required for catalytic activity, an inactivated sialidase is potentially a useful for probing sialidase-host ligand interactions if the sialidase is still capable of ligand binding following inactivation, since the ligand will not be turned over, the inactive sialidase could perhaps be used in a variety of ligand binding studies. The mutation of FRIP \rightarrow YMAP was performed with this in mind, it was hoped that the replaced residues would not disrupt the protein structure, and that NanH-YMAP would retain its capacity to bind host ligands, or to see if ligand affinity is altered by a (small) modification of the active site.

The NanH active site mutant (NanH-YMAP) was successfully purified and was shown to be inactive (figure 2.36).

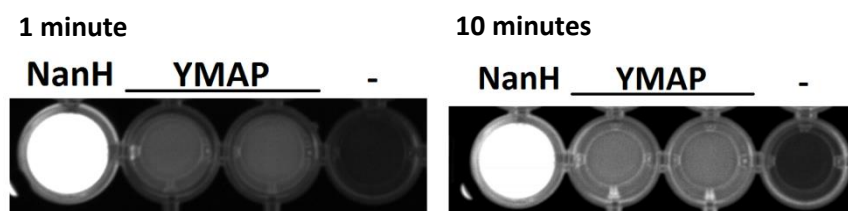


Figure 2.36. NanH-YMAP displays no Sialidase Activity.

NanH or NanH-YMAP were exposed to MUNANA for 1 minute or 10 minutes before imaging under UV-light. The low-level fluorescence of YMAP in these images is likely due to UV-light fluorescence of protein. Negative control was MUNANA without enzyme.

NanH-YMAP underwent ligand-enzyme interaction studies with 3- and 6-SL. These assays relied on the intrinsic fluorescence of tryptophan to assess conformational change of the enzyme on binding the two ligands. NanH-YMAP was shown to be capable of binding both 3- and 6- sialyllactose (figure 2.37).

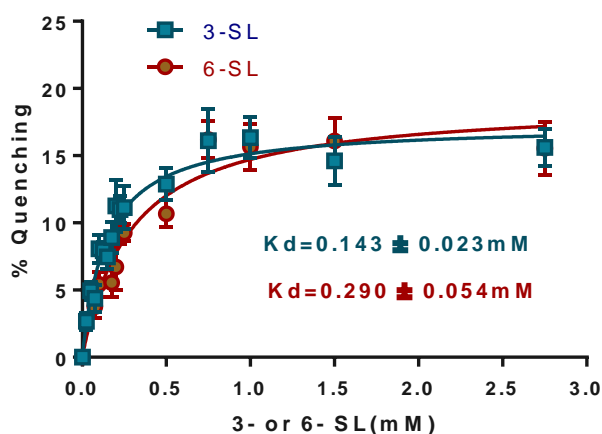


Figure 2.37. Affinity of 3- and 6-Sialyllactose for NanH-YMAP.

NanH-YMAP was exposed to variable concentrations of 3- and 6-SL, and the resulting change in protein fluorescence (%) used to ascertain the affinity (K_D) of the two ligands for NanH-YMAP. Data represent the mean of three experimental repeats, error bars=SEM. Statistical difference between the two data sets was assessed using an extra sum of squares F-test ($p=0.002$).

The affinity (K_D) of NanH-YMAP for 3- and 6-SL were determined here as 0.143 mM and 0.290 mM, respectively. An extra sum of squares F-test was used to assess whether or not a single curve could be adequately fitted to both data sets, but this revealed that the datasets were significantly different from each other ($p=0.002$). This result follows the

trend shown in the studies of active, whole NanH, reflected by the K_M values (figure 2.32) i.e. that NanH-YMAP shows higher affinity for 3-SL than 6-SL. The data imply that NanH-YMAP is capable of binding sialic acid-ligands without catalysing sialic acid release, with similar ligand preferences to active (wild type, non-mutant) NanH and that the conserved FRIP site is indeed key for catalytic activity in NanH. Future work using NanH-YMAP could yield insights into which host sialoglycans are preferentially targeted by NanH.

2.3.6.6 Summary-Biochemical Characterisation of Purified Periodontal Pathogen Sialidases

The key results shown in this section were that both sialidases from *T. forsythia* (NanH) and *P. gingivalis* (SiaPG) display broad pH optima, which is likely to be an adaptation to their ecological niche, where pH is variable. NanH was shown to be capable of cleaving both 3- and 6- linked sialic acid, although it is a more efficient catalyst for 3- linked sialic acid. Furthermore, NanH was capable of desialating the important host sialoglycans SLeA and SLeX, though NanH displayed a tenfold greater affinity for SLeA than SLeX. In addition, the importance of the FRIP residues to NanH sialidase function was also established. Overall, it was implied that the enzymes are broad-specificity sialidases, capable of functioning under a variety of conditions likely to be found in the oral cavity.

2.3.7 Inhibition of Periodontal Pathogen Sialidases by Zanamivir

A key aim of this project is to ascertain the potential of sialidase inhibitors to abrogate or inhibit virulence processes mediated by pathogen sialidases. The main focus of the project is on the inhibitor zanamivir, chosen partly because it is licensed worldwide for the treatment of influenza and might more-easily transition to other therapeutic areas than novel or unlicensed inhibitors. Therefore, ascertaining the ability of zanamivir to inhibit periodontal pathogen sialidase activity, and that of the purified sialidases, was of paramount importance.

2.3.7.1 *T. forsythia* and *P. gingivalis* Possess Sialidase Activity, Which is Inhibited by Zanamivir

Before studying the effects of zanamivir on inhibition of whole pathogens, the sialidase activity of the periodontal pathogens used in this work had to be assessed. A variety of strains underwent characterisation of sialidase activity. The various wild type strains of *T. forsythia* and *P. gingivalis* possessed sialidase activity, while *F. nucleatum* strains did not (figure 2.38).

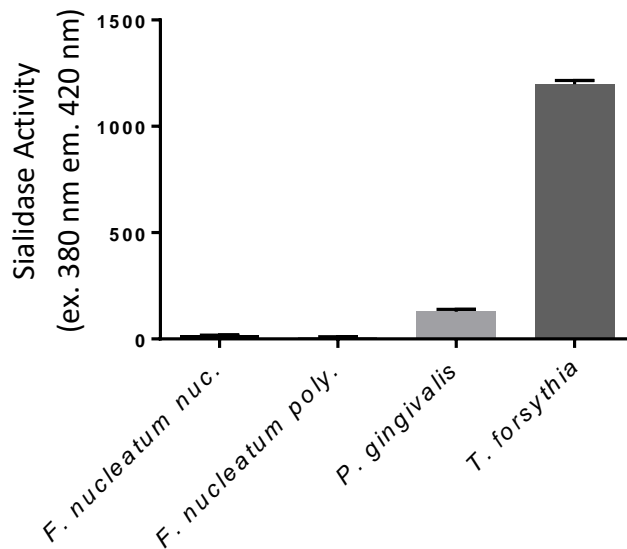


Figure 2.38. Sialidase activity profiles of periodontal pathogens.

Pathogens were resuspended in Phosphate Buffer Saline and Exposed to MUNANA. The fluorescence of the reactions (excitation 380nm emission 420nm) was measured after 30 minutes. Nuc= subspecies *nucleatum*, poly= subspecies *polymorphum*. Data shown represent the mean of three experimental repeats. Error bars=SD.

The absence of sialidase activity in *F. nucleatum* strains was expected, as *F. nucleatum* (*polymorphum* and *nucleatum*) do not possess any predicted sialidase genes in its published genome sequence, though *F. nucleatum* does possess a sialic acid utilisation operon (Stafford et al. 2012). *P. gingivalis* possessed some sialidase activity, and *T. forsythia* possessed the most. Further testing of other strains of *P. gingivalis* strain ATCC33277 and strain 381 (for which we had a sialidase deficient mutant courtesy of Prof A Sharma, SUNY, Buffalo, USA) and *T. forsythia* 43037 and 92A.2 revealed sialidase activity to be a conserved feature, and the sialidases NanH and SiaPG were shown to be the sialidases responsible for sialidase activity by testing the sialidase mutant strains *T. forsythia* $\Delta nanH$ and *P. gingivalis* $\Delta siaPG$, where sialidase activity was completely abrogated compared to their parent strains (figure 2.39).

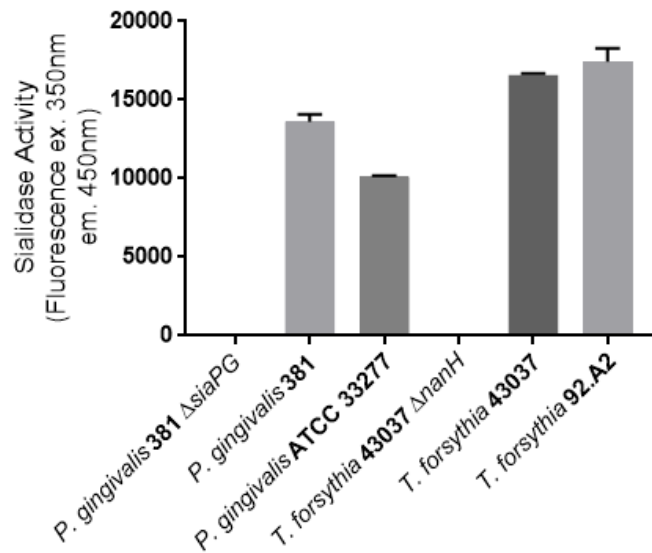


Figure 2.39. Sialidase activity profiles of *P. gingivalis* and *T. forsythia* strains.

Bacteria were resuspended in PBS and Exposed to MUNANA. The fluorescence of the reactions (excitation 350nm emission 450nm) was measured after 30 minutes for *T. forsythia*, and 4 hours for *P. gingivalis*. Reactions were stopped at each time point by addition of an excess of pH 10.5 Sodium Carbonate Buffer. Data shown represent the mean of three experimental repeats. Error bars=SD.

Whole *P. gingivalis* and *T. forsythia* underwent the MUNANA based assay to determine sialidase activity in the presence of variable concentrations of zanamivir. Both pathogens displayed decreased sialidase activity as zanamivir concentration was increased (figure 2.40). The decrease in activity was far more drastic for *P. gingivalis*, with a decrease in activity of ~70% in the presence of 10 mM zanamivir, compared to *T. forsythia* which only showed a decrease of ~25%.

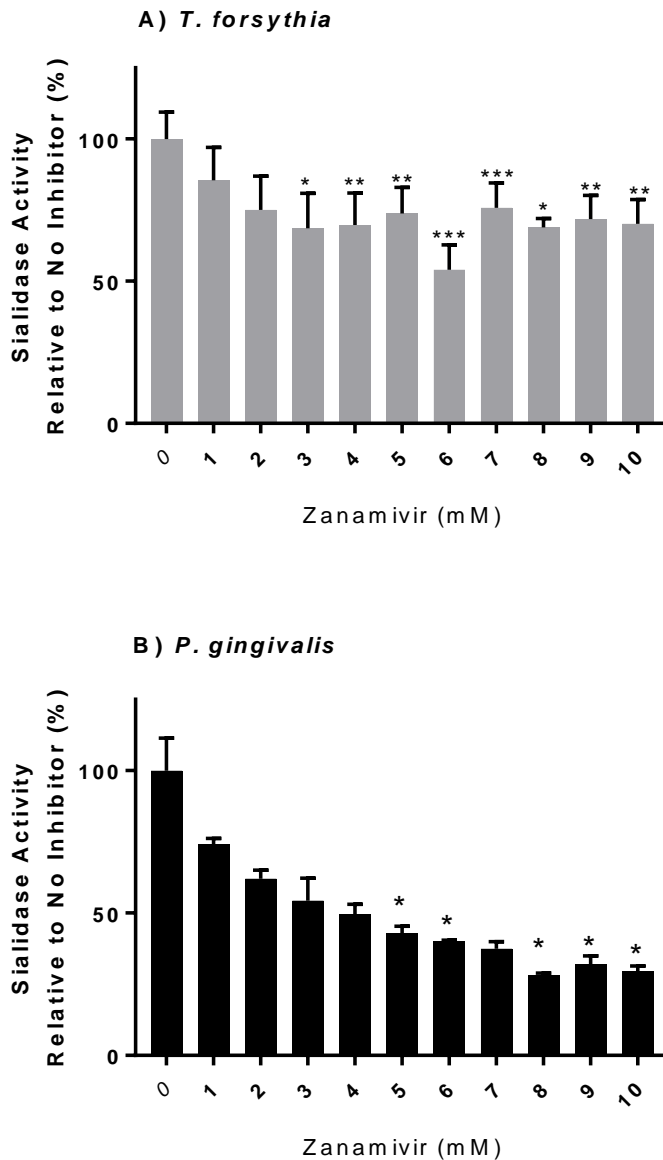
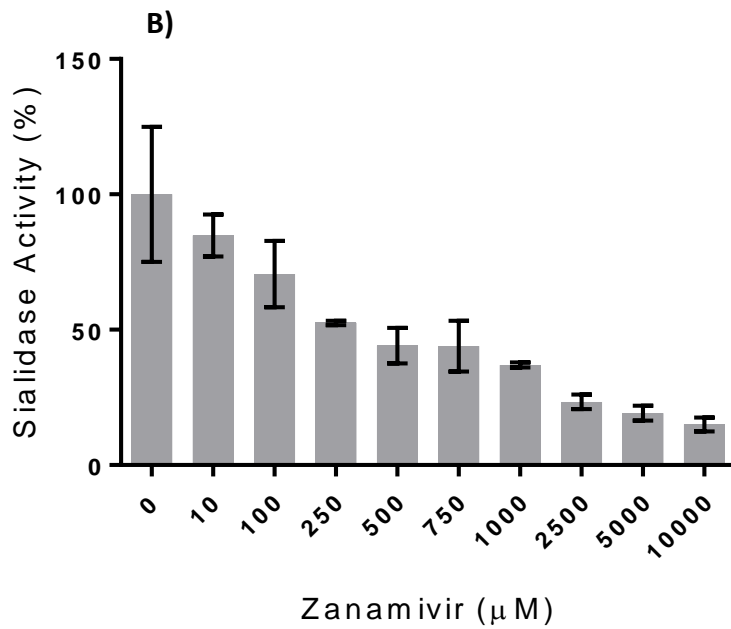
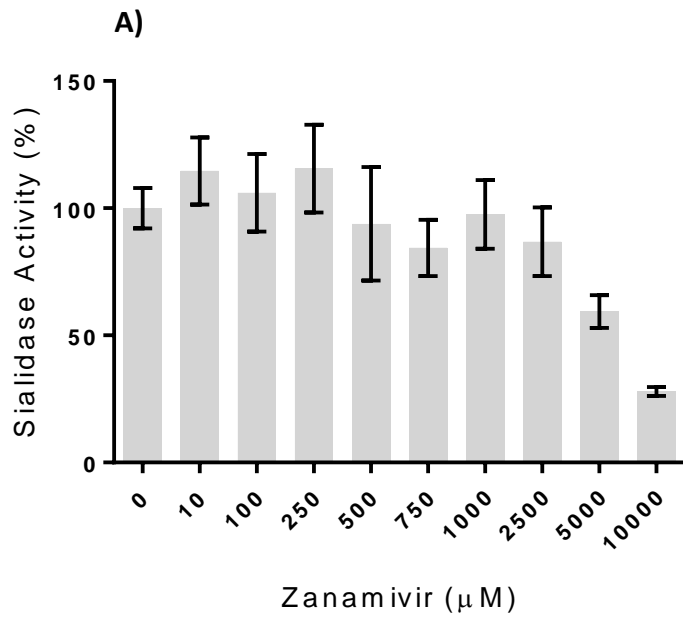


Figure 2.40. Inhibition of A) *T. forsythia* and B) *P. gingivalis* by Zanamivir.

MUNANA was exposed to *T. forsythia* or *P. gingivalis* in the presence of zanamivir for 1 hour and 4 hours, respectively, and sialidase activity expressed as the difference in 4-MU fluorescence relative to conditions with no inhibitor. Experiments were repeated twice, each condition performed in triplicate per experiment. Data shown represent the mean of one representative experiment. Error bars=SD. Significant reductions in sialidase activity between the no inhibitor condition and the conditions containing zanamivir at different concentrations were determined by one-way ANOVA with repeated measures, with Dunnet's correction for multiple comparisons (* $p < 0.05$, ** $p < 0.01$, *** $p < 0.001$).

2.3.7.2 *Efficacy of Zanamivir for Pathogen Sialidases*

The Inhibitory Constant (IC₅₀) of a given inhibitor for an enzyme represents the concentration at which the inhibitor has abrogated half of the enzyme's activity on a given ligand, and represents the efficacy of the inhibitor. The efficacy of zanamivir for inhibition of MUNANA desialylation by NanH and SiaPG was obtained. Both NanH and SiaPG were inhibited by zanamivir, although zanamivir was far more efficacious during inhibition of SiaPG than inhibition of NanH (figure 2.41): The IC₅₀ of zanamivir was found to be 369µM for SiaPG and 6.16mM (6156µM) for NanH. These IC₅₀ values are comparable to those seen for zanamivir inhibiting sialidases from other human-dwelling bacteria, such as in the case of *V. cholerae* (0.1 mM), *S. pneumoniae* (5 mM), *Arthrobacter ureafaciens* (5 mM) (Nishikawa et al. 2012), and *Ruminococcus gnavus* (11.89mM) (Tailford et al. 2015). Knowledge of the IC₅₀ of zanamivir for SiaPG and NanH had implications for work described in later chapters, investigating the impact of zanamivir on virulence processes mediated by the pathogen sialidases.



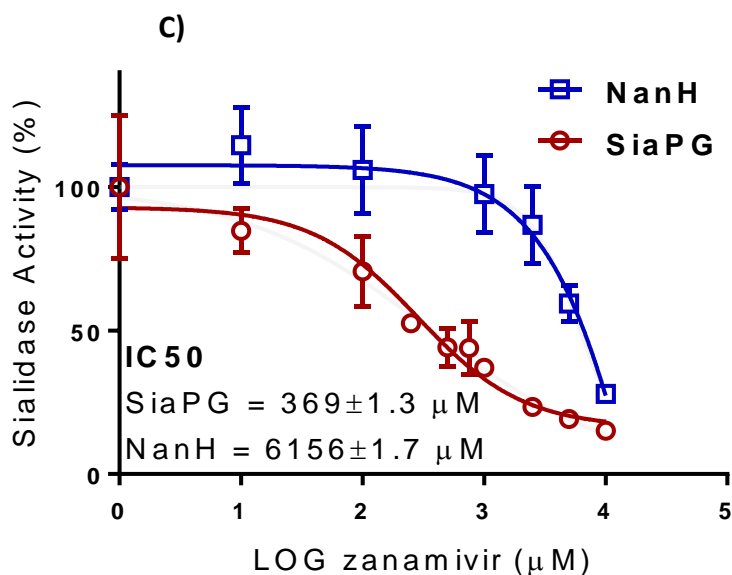


Figure 2.41. Inhibition of NanH and SiaPG by Zanamivir.

A) Inhibition of NanH and B) Inhibition of SiaPG by zanamivir, expressed as a percentage of sialidase activity relative to a condition with no inhibitor. C) Plot of the LOG [zanamivir] against % of sialidase activity relative to no inhibitor allows determination of the IC₅₀ of zanamivir for inhibition of MUNANA cleavage by NanH and SiaPG. Data represent the mean of three experimental repeats, where each condition was repeated three times. Error bars=SEM.

2.4 Discussion

Bioinformatics work delineated the sialidases of *T. forsythia* (NanH) and *P. gingivalis* (SiaPG) into the CBM and CTD domains; the CBMs were proposed to assist in ligand binding, and the CTD were suggested to have catalytic activity, respectively. Therefore, attempts were made to clone, express and purify both the whole sialidases-NanH and SiaPG-and their CBM and CTD domains separately from each other. The cloning process using genomic DNA from *T. forsythia* to amplify sialidase-encoding DNA was plagued with difficulties. This may have been due to the incorrect annotation of the *T. forsythia* 92.A2 genome as *T. forsythia* 43037 in the NCBI and oralgen databases (i.e. the primers for PCR amplification of sialidase were designed to target the *T. forsythia* 92.A2 genomic DNA, but *T. forsythia* 43037 genomic DNA was present in PCR reactions). Ultimately, a codon optimisation approach where the *nanH* sequence was altered to contain the preferred codons of *E. coli*, meant that NanH from strain 92.A2 was successfully expressed in *E. coli*, which was successfully purified. Importantly, the amino acid sequences of NanH from *T. forsythia* 43037 and 92.A2 have ~98% homology, and the substituted amino acids occur away from key regions of the enzyme (The FRIP motif and Asp Boxes), meaning it is unlikely there would be any differences in ligand specificity in NanH from both strains. *siaPG* was successfully amplified by PCR from genomic DNA, but a codon optimisation approach was also taken, and SiaPG was successfully expressed and purified.

After purification of the sialidases, some of the most important objectives of this part of the project could be addressed: Characterisation of NanH and SiaPG-under what conditions do they function? Do the sialidases show a preference for different sialic acid linkages? Do the sialidases preferentially target specific host sialoglycans, such as sialyl Lewis A and X? And perhaps most importantly, are the pathogen sialidases inhibitable using commercially available compounds?

2.4.1 pH, Pathogen Sialidases, and Periodontitis

Supragingival oral biofilms are well studied, and are known to result in acidic pH due to sugar fermentation by various bacterial species. Particularly well described is the contribution of *Streptococcus mutans* and various *Lactobacilli* –which produce lactic acid, damaging enamel, and ultimately leading to caries (tooth decay). pH in the supragingival environment is usually physiological (approximately neutral), but has been shown to vary widely in short spaces of time, as highlighted by pH measurements of plaque after food consumption (Edgar 1982). *In vitro* studies of individual organisms (Takahashi & Yamada 1999) and mixed species oral biofilms (Vroom et al. 1999; Edlund et al. 2013) have also

highlighted the potential for variable pH in these biofilms. The data shown here indicate a broad range of activity under variable pH conditions for the sialidases of *T. forsythia* and *P. gingivalis*, and given that *T. forsythia* and *P. gingivalis* do colonise the supragingival biofilm, this might explain why their sialidases are capable of activity over the broad pH range shown here.

However, the subgingival biofilm is the most important ecological niche for *T. forsythia* and *P. gingivalis*. It is isolated from salivary flow, and is therefore likely to be less prone to rapid changes in pH. The pH of the periodontium during disease progression has been the focus of some debate. Early patient studies have indicated a link between increasing periodontal inflammation and pH of the GCF, i.e. a basic pH was associated with periodontitis progression (Bickel & Cimasoni 1985). However, others have failed to find this association, and cite the use of metallic electrodes during the previous studies as a factor affecting the pH of the GCF being measured (Eggert et al. 1991), or that there are wide variations in pH even within a single periodontal pocket (Galgut 2001). *In vitro* studies of mixed periodontal biofilms have also shown pH gradients within their biofilms (Vroom et al. 1999). Taking all this into account, it is likely that the ability to function under a wide variety of pH conditions would enable periodontal pathogens to more effectively colonise and survive in the supra- and sub-gingival biofilms. Therefore, the broad pH optimum of the periodontal pathogen sialidases may enable them to function under these variable pH conditions, and contribute to the proliferation and survival of *T. forsythia* and, perhaps to a lesser extent, *P. gingivalis*, since sialidases may enhance protein degradation, assisting with nutrient acquisition (discussed further in the next chapter).

Reaction kinetics of MUNANA cleavage by NanH and SiaPG were performed, to observe the effect of pH on reaction kinetics. NanH and SiaPG were more efficient catalysts under mildly acidic conditions compared to neutral conditions, unsurprising given their apparent pH optima (5.2 and 5.6, respectively). A kinetics experiment was also performed where salt (200 mM NaCl) was included in the neutral pH condition with the intention of mimicking physiological conditions, which would be used in experiments involving host-relevant sialic acid ligands, and later studies of human cells. Interestingly, the presence of salt shifted the enzyme-MUNANA affinity (K_M) and maximum reaction rate (V_{max}) for both NanH and SiaPG. Addition of salt to acidic conditions also shifted these parameters. In the case of NanH at either pH condition, affinity was decreased but maximum reaction rate increased. Overall though, NanH was a more efficient catalyst in the absence of salt. SiaPG displayed

decreased affinity and maximum rate of reaction in the presence of salt, under acidic and neutral conditions. Furthermore, in the case of NanH under acidic conditions, product-or-substrate inhibition does not appear to occur in the presence of salt, but it does in its absence, which could be beneficial if there is a high concentration of sialoglycans at a specific location, such as at the cell surface, or in certain glycoproteins such as salivary mucin. It should also be noted that regardless of the NaCl dependent changes in activity, the enzymes show high affinity (K_M in the low μM range in either presence or absence of salt) and rapid reaction rate (high V_{max}).

The finding that the presence of NaCl can affect enzyme catalysis is not entirely surprising. Salt ions can interact directly with proteins through their charged amino acid side chains-potentially affecting enzyme stability (and ability to change conformation on ligand binding). Furthermore, if salt ions interact with charged side chains at the enzyme active site or binding pocket, this might inhibit catalysis, and this is termed “electrostatic shielding”. This type of salt inhibition has been shown to affect enzymes that interact with charged or polarised ligands, while this inhibitory effect of salt is minimal for enzymes with non-polar ligands, the salt ions only affecting protein structural stability by interaction with charged amino acids away from the ligand binding site (Warren & Cheatum 1966).

Discussion of the periodontal pathogen sialidases relative to those from other organisms is difficult, though many studies do use MUNANA as a substrate. Discussion is further complicated due to the use of different units for reporting maximum reaction rates (V_{max}) in different studies. Comparisons of ligand affinity are easier to discuss, and can be compared directly. Sialidases from a variety of organisms, including the ones shown in this study, and their kinetic parameters- K_M and V_{max} -with respect to MUNANA are shown in table 2.10. The table highlights that NanH and SiaPG, produced and analysed as part of this project actually have a very high affinity (low K_M) for the model ligand MUNANA, relative to the other (non-periodontal pathogen) sialidases characterised by others, indicating that NanH and SiaPG are highly active compared to other sialidases (see references in table 2.10). The same is true of the sialidase from the third red complex pathogen, *T. denticola*, which has been reported to have the highest affinity (lowest K_M) for MUNANA of all enzymes presented in the table.

Organism	Sialidase Designation	K_m	V_{max}	Source
<i>Tannerella forsythia</i>	NanH	15.6 μ M	13.8 μ mol/min/mg enzyme	This study
		33 μ M	Enzyme not purified-Vmax not comparable	(Thompson et al. 2009)
<i>Porphyromonas gingivalis</i>	SiaPG	11.6 μ M	13.2 μ mol/min/mg enzyme	This study
<i>Treponema denticola</i>	TDE0471	0.019 μ M	0.6nmol/min/nM enzyme	(Kurniyati et al. 2013)
<i>Bacteroides thetaiotaomicron</i>	VPI-5482	110 μ M	Not reported	(Park et al. 2013)
<i>Salmonella typhimurium</i>	NanH	250 μ M	Enzyme not purified-Vmax not comparable	(Hoyer et al. 1991)
		370 μ M	Not reported	(Minami et al. 2013)
<i>Ruminococcus gnavus</i>	NanH	590 μ M	1.37 μ M/min (enzyme concentration not reported)	(Tailford et al. 2015)

Table 2.10. A Comparison of Bacterial Sialidase Reaction Kinetics (K_m and V_{max}) with MUNANA.

2.4.2 The Importance of Sialic Acid Linkage preference for *T. forsythia*

The oral cavity is rich in sialoglycans, and this presents many possible benefits for pathogens capable of harnessing the sialic acid, the underlying glycoprotein, or otherwise manipulating host processes that are regulated by sialic acid. Therefore, discovering the sialoglycans preferentially targeted by pathogen sialidases is an important milestone in understanding, and possibly treating, periodontal pathogen virulence.

Periodontal pathogens might encounter sialoglycans from saliva, serum and GCF, or those on cell surfaces. Previous studies have looked at sialic acid linkages in these sources as means to diagnose or prognose oral cancer. Briefly, these found that α 2-6 linkages are more prevalent in human saliva than α 2-3 linkages (Vajaria et al. 2014), but α 2-3 linkages are more prevalent in oral tissues and serum (Shah et al. 2008). The studies also found the prevalence of both types of linkage, or the activity of α 2-3 and α 2-6 sialyltransferases (enzymes that sialate the glycans), were greater in oral cancer patients compared to healthy controls.

T. forsythia's ecological niche is in close proximity to the tissue, both in the supragingival biofilm where it colonises the most anaerobic location (i.e. closest to the host tissue) and in the periodontal pocket. *T. forsythia* is thought to be exposed to low salivary flow in this location (compared to the supragingival environment), but a large amount of GCF, which is similar in composition to serum. The data shown here indicate that NanH has a preference for α 2-3 linkages, and this appears to fit the narrative that these linkages are more prevalent in the described ecological niche of *T. forsythia*: i.e. *T. forsythia* is more likely to encounter α 2-3 linked sialic acids than α 2-6 linked sialic acids, and it follows that its sialidase-NanH-is adapted accordingly. This apparent linkage preference is in agreement with the preliminary work on NanH by Thompson et al., who showed that NanH released more sialic acid from α 2-3 than α 2-6 linked sialic acids over time (Thompson et al. 2009). Many bacterial sialidases do appear to be capable of targeting both types of sialic acid linkage, but often display greater efficacy in cleavage of one of the two linkages, as indicated in table 2.11.

Organism	Sialidase	Linkages Targeted	Linkage Preference	Reference
<i>Streptococcus pneumoniae</i>	NanA	α 2-3, α 2-6	α 2-6	(Gut et al. 2008)
	NanB	α 2-3	α 2-3	(Gut et al. 2008)
	NanC	α 2-3	α 2-3	(Xu et al. 2011)
<i>Pseudomonas aeruginosa</i>	PAO1 neuraminidase	α 2-3, α 2-6	unknown	(Cacalano et al. 1992)
<i>Pasturella multocida</i>	NanB	α 2-3, α 2-6	α 2-6	(Mizan et al. 2000)
	NanH	α 2-3, α 2-6	α 2-3	(Mizan et al. 2000)
<i>Clostridium perfringens</i>	NanI	α 2-3, α 2-6	α 2-3	(Li & McClane 2013)
	NanJ	α 2-3, α 2-6	α 2-6	(Li & McClane 2013)
	NanH	α 2-3, α 2-6	α 2-3	(Li & McClane 2013)
<i>Salmonella typhimurium</i>	NanH	α 2-3, α 2-6	α 2-3	(Hoyer et al. 1991)
<i>Corynebacterium diphtheriae</i>	NanH	α 2-3, α 2-6	α 2-6	(Kim et al. 2010)
<i>Bacteroides thetaiotaomicron</i>	VPI-5482	α 2-3, α 2-6	α 2-6	(Park et al. 2013)
<i>Vibrio cholerae</i>	NanH	α 2-3, α 2-6	α 2-3	(Eneva et al. 2015)
<i>Porphyromonas gingivalis</i>	SiaPG	α 2-3, α 2-6	unknown	(Li et al. 2012)
<i>Treponema denticola</i>	TDE0471	α 2-3, α 2-6	unknown	(Kurniyati et al. 2013a)
<i>Tannerella forsythia</i>	NanH	α 2-3, α 2-6	α 2-3	This study, (Thompson et al. 2009)
<i>Actinomyces viscosus</i>	NanH	α 2-3, α 2-6	α 2-3	(Yeung & Fernandez 1991)
<i>Streptococcus oralis</i>	NanA	α 2-3, α 2-6	α 2-3	(Byers et al. 2000)
<i>Streptococcus mitis</i> *	NanA*	Unknown*	Unknown	(Johnston et al. 2010)

Table 2.11 Sialic acid-linkage preferences of sialidases from bacteria associated with different mucosal sites.

Blue=Respiratory Tract, Green=GI tract, Pink=Oral Cavity. *P. multocida* is a respiratory pathogen of cattle, and can cause wound infections in humans. *Not all *S. mitis* isolates possess sialidase activity, and the ability to target both sialic acid linkages is unknown, but presumably both α 2-3 and α 2-6 linkages can be targeted, as inferred by its homology with NanA from other streptococci.

It is interesting to note that although the gut and respiratory tract bacteria seem to possess a mixture of sialidases with a higher efficacy for either α 2-3 or α 2-6 linked sialic acid, so far no oral bacteria sialidases have shown this, instead they display higher efficacy for α 2-3 linked sialic acid. In fact this seems to generally be the case for most bacterial sialidases of

human-dwelling organisms, and could reflect biochemical/biophysical properties that inherently make this linkage more labile to enzymatic cleavage.

2.4.3 The Importance of Sialyl Lewis Ligands for *T. forsythia*

The secreted salivary mucins are an important source of SLeA/X, and many different cell types are capable of expressing SLeA and SLeX on their surfaces, including endothelial and epithelial cells, and leukocytes. Given the ubiquitous presence of SLeA/X in the oral cavity or peridontium, it follows that *T. forsythia* sialidase would be capable of cleaving sialic acid from these ligands.

NanH appears to display almost tenfold greater efficacy for SLeA than SLeX, despite the only difference between the two ligands being the fucose-GalNAc linkage. As well as its possible presence on mucin (though SLeX is perhaps the more prevalent isoform), SLeA is present on oral/laryngeal epithelial cells (where its expression is upregulated in head and neck cancers (Renkonen et al. 1999; Wiest et al. 2010)), and erythrocytes. Therefore, the preference of NanH for SLeA might reflect its ecological niche of the periodontal pocket or gingival crevice, where it is most likely to encounter SLeA due to infiltration of blood cells and inflammatory exudate. Targeting of cellular sialyl lewis is discussed further in chapter 5.

2.4.4 *T. forsythia* NanH- the RIP Motif of the Catalytic Domain is Essential for Catalysis, and the N-terminal CBM is involved in Ligand Binding

Bioinformatics highlighted two domains of *T. forsythia* NanH, the CTD with catalytic activity, containing the Asp Boxes and highly conserved RIP motif-and the carbohydrate binding module or CBM which was considered likely to have ligand binding properties. The NanH FRIP motif was mutated to YMAP, expressed (the resulting enzyme was named NanH-YMAP), and was shown not to possess catalytic activity. Despite this, NanH-YMAP retained the ability to bind 3- and 6-SL with high (K_d in the micro molar range) affinity. Since NanH appears to retain binding capacity in the absence of substrate turnover it might be useful for structural or other enzyme-ligand studies, where the absence of substrate turnover would allow studies of the enzyme in complex with its ligand. This might include pull down assays with host-cell or secreted glycoprotein sources (such as saliva) to establish preferential targets of NanH in the host. However, at least one study of RIP motif mutation in a bacterial sialidase (NanH from *C. perfringens*) has also been performed previously (Chien et al. 1996), where arginine was mutated to isoleucine. In this case the enzyme activity on 3-SL was reduced tenfold, but it did result in changes to the whole enzyme

structure (indicated by decreased antibody-binding during western blotting). If the FRIP→YMAP mutation in this work did result in significant conformational change to NanH (particularly the NanH CTD) and abrogation of ligand binding capacity it might be the case that the ligand binding is due to the NanH CBM.

The NanH CBM was shown to have ligand binding properties (and no catalytic activity) in work occurring alongside this project (Stafford Research Group, University of Sheffield): The CBM was successfully expressed and purified, then tested in tryptophan quenching experiments in a manner similar to the NanH-YMAP ligand binding assays shown in section 2.3.6.5. This showed that the CBM was capable of binding both 3- and 6-SL (figure 2.42) with high affinity ($K_D = 528$ and $334 \mu\text{M}$, respectively), confirming that this domain was a novel CBM. This represents a potentially new subfamily of CBMs, distinct from that of the *Vibrio cholerae* sialidase, which is the founding member of the CBM40 subfamily.

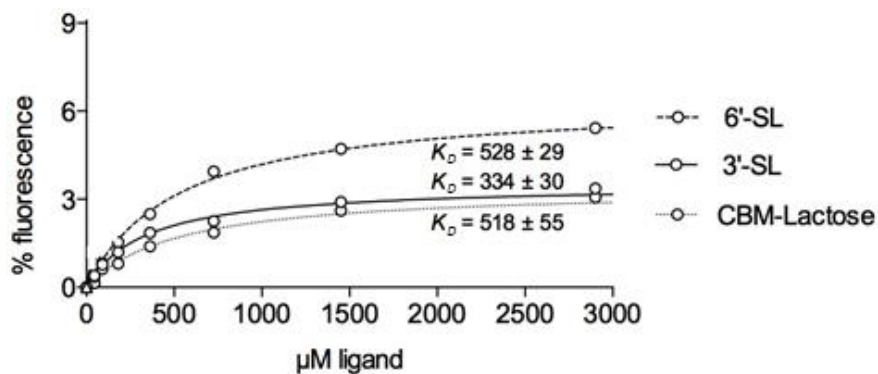


Figure 2.42. NanH-CBM Binds 3- and 6- sialyllactose. .

NanH-CBM was exposed to variable concentrations of 3- and 6-SL, and the resulting change in protein fluorescence (%) used to ascertain the affinity (K_D) of the two ligands for NanH-YMAP. Data represent the mean of three repeats, error bars=SEM. (Data collected, processed, and plotted by Chatchawal Phansopa, Stafford Research Group, University of Sheffield).

2.4.5 Zanamivir Inhibits Periodontal Pathogen Sialidases

Zanamivir was shown to possess a greater inhibitory efficacy (a lower IC₅₀) for SiaPG than NanH. The discrepancy in IC₅₀ between the two sialidases is in line with the finding for the whole pathogen sialidase inhibition assay-that zanamivir is more effective at inhibiting *P. gingivalis* than *T. forsythia* sialidase activity. Nonetheless, both *T. forsythia* and *P. gingivalis*

sialidase activity appeared to be significantly inhibited by zanamivir. This finding was crucial for the rest of this project, which aims to evaluate the potential for sialidase inhibitors (using zanamivir as a case study) in preventing periodontal pathogen virulence.

Assuming periodontal pathogen virulence is inhibited by zanamivir (or other inhibitors), the ultimate aim would be to create formulations to apply sialidase inhibitors to treat or prevent periodontitis. While zanamivir appears to be reasonably efficacious in its inhibition of *P. gingivalis* sialidase activity (IC₅₀ ~300µM), the relatively high (~6mM) IC₅₀ of zanamivir for NanH is mirrored in studies of other bacterial sialidases, which report a high IC₅₀ of zanamivir for a purified bacterial sialidase, or that live pathogen sialidase activity is more readily abrogated by other inhibitors (Tailford et al. 2015; Nishikawa et al. 2012). This might have consequences for developing zanamivir (or another inhibitor with millimolar efficacy) as a therapeutic; an efficacy in the millimolar range may not justify taking an antimicrobial agent forward for further development. On the other hand, given that a therapeutic for periodontitis would probably be a topical treatment applied to the site of infection, rather than a systemic treatment, a therapeutic designed to obtain localised millimolar concentrations of an active ingredient could be possible.

Chlorhexidine (Molar mass 506.47 g/mol) is one example of a frequently used active ingredient for control of oral biofilms or oral bacteria. Perhaps its most frequent use is in over-the-counter mouthwashes, where it can be present at 0.2%, or ~4mM (Corsodyl Mouthwash, GlaxoSmithKline). In dental gels, which are also over-the-counter, the concentration of chlorhexidine is higher; at 1 % or ~20 mM (Corsodyl dental gel, GlaxosmithKline). Chlorhexidine has also been used in dental gels in clinical settings at 2% (~40mM), as an adjunct to apical periodontitis therapy to disinfect the root canal (Wang et al. 2007). Considering that at least some active ingredients, such as chlorhexidine, are present at millimolar concentrations in both clinical and consumer products designed to treat or prevent gingivitis/periodontitis, it is not unreasonable to suggest that zanamivir, or other sialidase inhibitors, could be included at these concentrations in formulations designed to treat or prevent periodontitis.

2.5 Summary

The sialidases from *T. forsythia*-NanH, and *P. gingivalis*-SiaPG were codon optimised for expression by *E. coli*. Purification of these sialidases was successful, and they underwent biochemical characterisation: This highlighted their pH optima, which has practical implications but also highlights their ability to function under a wide range of conditions; a

useful ability in the oral environment. Secondly, NanH was shown to be a broad host-range sialidase but act preferentially on α 2-3 linked sialic acid, possibly providing insights into its functions *in vivo*. The highly conserved NanH FRIP motif was also shown to be essential to enzyme function, but its mutation to YMAP did not prevent NanH binding to sialic acid-ligands. Furthermore, both SiaPG and NanH were inhibited by zanamivir, though zanamivir displayed much greater efficacy for SiaPG (IC₅₀=235 μ M) than for NanH (IC₅₀=6309 μ M).

The biochemistry of periodontal pathogen sialidases provides useful insights into their ligand preferences and the potential to inhibit these interactions. However, more experiments were required to ascertain the contribution of pathogen sialidases to disease. With this in mind the next two chapters of this thesis focus on how the sialidases contribute to pathogen growth and biofilm formation on host sialoglycoproteins, and how sialidases contribute to host-pathogen interactions. The effect of the sialidase inhibitor zanamivir on pathogen growth and biofilm formation, and host-pathogen interactions is also examined.

Chapter 3

Investigating the Targeting of
Host Sialoglycans by
Periodontal Pathogens- the
Effects on Growth and Biofilm
Formation, and the Impact of
Zanamivir

3 Chapter 3: Investigating the Targeting of Host Sialoglycans by Periodontal Pathogens- the Effects on Growth and Biofilm Formation, and the Impact of Zanamivir

3.1 Introduction

In the host, secretions and all cell surfaces are rich in glycoproteins and glycolipids, glycoproteins possess one or more polysaccharide chains (glycans), which are covalently attached to serine or threonine residues (O-linked glycans, O-glycosylation), or asparagine (N-linked glycans, N-glycosylation). Glycolipids are fatty acids present in cell membranes with glycans extending away from the cell. As described elsewhere in this thesis, Sialic acids often cap these glycans, the most common of which in humans is Neu5Ac (5-N-acetyl neuraminic acid). However, Neu5Ac can have additional chemical modifications, such as possession of additional chemical groups at its 9th carbon: O-acetylation, -methylation, -sulphylation and others (Cohen & Varki 2010). Sialic acid affects structure-function of glycoproteins; one of the most important properties is its negative charge, leading to high hydrophilicity and interactions with other molecules. In the context of the oral cavity and the periodontium, two secretory fluids represent rich sources of sialoglycans: Gingival Crevicular Fluid (GCF) is similar to serum in composition, and is therefore rich in glycoproteins such as fetuin, immune components (such as complement, IgA antibodies, and cytokines), and numerous others, all of which can be sialic acid capped. In periodontal disease, bleeding may also occur, introducing further serum/blood plasma glycans into the periodontium. Saliva is another secretion present orally and an important source of mucins, which are secretory glycoproteins. Salivary mucins are predominantly composed of mucins MUC7, MUC5B, and to a lesser extent MUC4 and other salivary proteins.

Given the prevalence of sialic acid in the oral cavity and periodontium, it is unsurprising that periodontal pathogens and human dwelling bacteria more broadly have adapted to interact with sialic acid and sialoglycoproteins.

The previous chapter highlighted the ability of sialidases from *T. forsythia* and *P. gingivalis* to cleave sialic acid from a variety of sources; the two most common sialic acid linkages in humans were cleaved (α 2-3 and α 2-6 linked sialic acid), and the host-relevant sialyl-lewis A and X sialoglycans were also desialyated by pathogen sialidases in in vitro biochemical assays. Free sialic acid is a particularly important nutrient for *T. forsythia* and potentially other oral organisms (e.g. *F. nucleatum nucleatum*). *T. forsythia* usually requires an

exogenous source of N-acetylmuramic acid (NAM) for growth because it lacks two gene homologues required for intermediate stages of NAM synthesis; UDP-N-acetylglucosamine-enolpyruvate transferase and UDP-enolpyruvate reductase (Wyss 1989; Sharma 2011). However, *T. forsythia* growing in a biofilm is capable of bypassing this NAM requirement in the presence of Neu5Ac (Roy et al. 2010), highlighting the importance of sialic acid for *T. forsythia*.

The importance of sialic acid release for the other red complex periodontal pathogens *P. gingivalis* and *T. denticola* is less clear. Both of these organisms possess sialidase enzymes, but lack the uptake and catabolic genes seen in other periodontal pathogens. It may be the case that sialic acid removal is a means to “soften up” glycoproteins for further digestion by proteases. It has been shown that salivary mucins treated with sialidases are more rapidly degraded by proteolytic activity than intact mucins (Takehara et al. 2013). *P. gingivalis* possesses the gingipains-arginine and lysine proteases (RgpA, RgpB, and Kgp) and these are considered key virulence factors of *P. gingivalis* (Curtis et al. 1999). Gingipains are considered important for nutrient acquisition by *P. gingivalis*. Furthermore, their inhibition can reduce the growth of *P. gingivalis* in culture and during biofilm formation (Eick et al. 2003; Kariu et al. 2016), implying that inhibiting the gingipains decreases amino acid/peptide release, and *P. gingivalis* growth is slowed as it cannot rapidly acquire amino acid nutrients. Since sialic acid acts to protect glycoproteins from proteolytic degradation—a factor important for growth in this pathogen, then sialidase activity could be an important virulence factor with a role in nutrient acquisition for *P. gingivalis*. *T. denticola* also possesses a serine protease, “dentilisin” (Ishihara et al. 1996), which is considered an important virulence factor, and since *T. denticola* also catabolises free peptides or amino acids for nutritional purposes (Hook et al. 1971), the expression of sialidase may be important in their release from sialoglycoproteins for nutritional purposes in *T. denticola*.

As mentioned above, host glycoproteins represent a nutrient source for periodontal pathogens, and they can also present epitopes for pathogen adhesion. Both of these factors could contribute to biofilm formation by a given pathogen, and since a high proportion of glycoproteins are sialylated, sialidases are considered to be important contributors to biofilm formation. The gut pathogen *V. cholerae* is one example where sialidase acquisition and utilisation is clearly involved in growth, since it possesses appropriate genes, annotated as *nan-nag* (Jermyn & Boyd 2002), and can grow using sialic acid as a sole carbon source. Some of the Nan proteins downstream of NanH in the sialic

acid acquisition and catabolism pathway were essential for this-mutants deficient in *nanA* (neuraminase lyase) or *nanE* (N-acetylmannosamine-6P epimerase) were unable to grow on sialic acid alone (Almagro-Moreno & Boyd 2009).

Perhaps the best studied in terms of biofilm formation are the commensal but frequently opportunistic pathogens of the nasopharynx *Streptococcus pneumoniae* and *Pseudomonas aeruginosa*. *S. pneumoniae* expresses three sialidases, NanA, NanB, and NanC, of which NanA is considered the most important for virulence (Brittan et al. 2012). Mutant strains deficient in NanA show reduced ability to adhere to airway epithelial cells, and reduced biofilm formation in microtitre plates compared to their parent strains (Parker et al. 2009). NanA deficiency also abrogated the ability of *S. pneumoniae* to colonise the nasopharynx in a mouse model (Brittan et al. 2012). *P. aeruginosa* also possesses a sialidase-PA2794 (dubbed “pseudaminidase” in the NCBI protein database)-and mutant strains deficient in PA2794 display reduced biofilm formation, as well as a decreased ability to colonise the nasopharynx in a mouse model (Soong et al. 2006). Both of these organisms appear to use their sialidases to facilitate attachment to desialylated GM1 ganglioside, a glycan of four sugars; galactose-N-Acetylglucosamine-Galactose-Glucose (Gal β 1,2GalNAc β 1,4Gal β 1,4Glc) attached to the cell membrane via ceramide (a fatty acid). Interestingly, particularly with regards to the aims of this project, sialidase inhibitors were also able to reduce biofilm formation of the wild type (sialidase-expressing) strains of *S. pneumoniae* and *P. aeruginosa* (Brittan et al. 2012; Soong et al. 2006). However, these biofilm studies were not performed on glycoprotein-coated surfaces, so the importance of sialidases in attachment and biofilm formation of these respiratory pathogens to glycoproteins is not entirely clear.

Regarding periodontal pathogens, *P. gingivalis* and *T. forsythia* sialidases have been shown to be important for biofilm formation: A sialidase deficient *P. gingivalis* mutant strain was found to display abrogated biofilm formation relative to its parent strain (Li et al. 2012), although the capsule of the strain (W83) used in the study was also disrupted when its sialidase was knocked out, which could also account for the changes in biofilm formation. Furthermore, biofilm formation was only characterised on plastic surfaces, so the role of sialidases in biofilm formation of *P. gingivalis* on host glycoproteins from this work is also unclear.

Given the above, pathogen sialidases can be said to be an important virulence factor, boosting periodontal pathogen growth through nutrient acquisition pathways, aiding in colonisation by increasing attachment to surface-associated glycans, and aiding biofilm

formation. The previous chapter showed the ability of zanamivir to inhibit *P. gingivalis* and, to a lesser extent, *T. forsythia* sialidase activity. Therefore, the work described in this chapter aimed to study the growth and biofilm formation of periodontal pathogens on sialoglycoproteins, and if growth and biofilm formation could be inhibited by zanamivir. This also involved testing the ability of the sialidases to cleave sialic acid from bovine submaxillary mucin (BSM)-a common model of human salivary mucins, and salivary mucin represents a glycoprotein source rich in sialic acid that periodontal pathogens would be exposed to. Furthermore, an accessory enzyme-NanS- which is co-expressed with NanH as part of the *nan* operon of *T. forsythia* (described below), was tested for its impact on the activity of these sialidases on mucin.

3.2 Materials and Methods- Investigating the Targeting of Host Sialoglycans by Periodontal Pathogens- the Effects on Growth and Biofilm Formation, and the Impact of Zanamivir

3.2.1 Enzyme synergy in Sialic Acid Release from Salivary Mucin

Bovine submaxillary mucin (6 μ M) was incubated for 30 minutes at 37 °C in the presence of NanS, NanH, PGsia, NanS + NanH, and NanS + PGsia. Reactions with NanH + NanS or SiaPG + NanS were performed in the presence or absence of 0.5 mM zanamivir. All reactions were carried out in 50 mM sodium phosphate buffer, 200 mM NaCl, and all enzymes were included at 100 nM. In reactions containing two enzymes, both were included at 100 nM per enzyme. After incubation, reactions immediately underwent the TBA assay as described in section 2.2.10.4.

3.2.2 Bacterial Strains and Growth Conditions

Strains of the periodontal pathogens *Fusobacterium nucleatum*, *Tannerella forsythia*, and *Porphyromonas gingivalis* used in this work are summarised in table 3.1. All periodontal pathogens were cultured at 37°C under anaerobic conditions (10% CO₂, 10% H₂, 80% N₂) in a Don-Whitley mini-macs anaerobic cabinet. *P. gingivalis* and *F. nucleatum* strains were cultured on Fastidious Anaerobe Agar (Lab M, Lancashire, UK) supplemented with 5% (v/v) oxalated horse blood (Thermo Fisher Scientific, UK), for 2-3 days before harvesting for use in experiments or cultured on fresh media. *T. forsythia* strains were cultured on Fastidious Anaerobe Agar (Lab M, UK) supplemented with 5 % (v/v) Oxalated Horse Blood (Thermo Fisher Scientific), 10 μ g/ml N-acetylneuraminic acid (NAM) (Sigma Aldrich, UK), and 25 μ g/ml Gentamicin (Sigma-Aldrich) for 3-7 days before harvesting for use in experiments or culture on fresh media. In addition, a strain of *T. forsythia* deficient in the gene encoding

NanH (*T. forsythia* $\Delta nanH$) was intermittently subcultured in the presence of 10 $\mu\text{g/ml}$ erythromycin to ensure maintenance of the antibiotic resistance cassette marker responsible for sialidase inactivation.

Species	Strain	Notes
<i>Tannerella forsythia</i>	ATCC 43037	<i>T. forsythia</i> type strain, supplied by William Wade, QMUL, UK
	92.A2	Genome sequenced strain- supplied by Floyd Dewhirst, Forsyth Institute, Boston, MA, USA
	TFM0035($\Delta nanH$)	Derived from <i>T. forsythia</i> ATCC 43037, gift from Prof A Sharma, University at Buffalo, USA
<i>Porphyromonas gingivalis</i>	ATCC 33277	Sheffield strain collection
	381	Supplied by A Sharma, University at Buffalo, USA
<i>Fusobacterium nucleatum</i>	NCTC 25586	<i>F. nucleatum</i> subspecies <i>nucleatum</i> , supplied by William Wade, QMUL, UK
	NCTC 10953	<i>F. nucleatum</i> subspecies <i>polymorphum</i> , from ATCC (directly purchased)

Table 3.1. Periodontal pathogen strains.

The mutant strain *T. forsythia* $\Delta nanH$ was a gift from Professor Ashu Sharma (University of Buffalo, New York, USA). Note that the genome of the *T. forsythia* strain 92.A2 had been previously submitted to NCBI and Oralgen databases annotated as that of *T. forsythia* ATCC 43037-an error only rectified in 2015. This had repercussions for work described in chapter 2, which involved attempts to amplify genomic DNA of *T. forsythia* ATCC 43037.

3.2.3 Collection and preparation of Human Saliva

Human saliva was collected from healthy adult volunteers who had not consumed food or drink for 1 hour prior to collection. Saliva was pooled (4-5 volunteers per pool, each contributing 5-10ml of saliva), centrifuged at 3500xg for 30 minutes, and sterile filtered using 0.45 μm sterile filters. Sterile saliva was stored at -20°C until ready for use. Ethical approval to collect adult human saliva from healthy people was held by the University of Sheffield, School of Clinical Dentistry, ethics permission number 31.

3.2.4 Culture of Periodontal Pathogens on Defined Media Supplemented with Host Sialic Acid Sources

A carbon and nitrogen deficient media (defined media) was formulated based on previous studies (Milner et al. 1996; Oda et al. 2007), containing the following compounds: 10 mM monosodium phosphate, 10mM potassium chloride, 2mM citric acid, 1.25 mM magnesium chloride, 0.1mM iron (III) chloride, 20 μ M calcium chloride, 0.1 μ M sodium molybdate, 25 μ M zinc chloride, 50 μ M manganese chloride, 5 μ M copper (II) chloride, 10 μ M cobalt (II) chloride, and 5 μ M boric acid. After formulation, media was sterile filtered using 0.45 μ m filters. Defined media was supplemented with 5 μ g/ml hemin, 50 μ g/ml gentamicin, 1 μ g/ml menadione (vitamin K), various sialoglycoproteins: Including either 6 μ M bovine submaxillary mucin (BSM), 1, 5 or 10 % (v/v) pooled human saliva, or 1, 5, or 10 % (v/v) foetal bovine serum (FBS). FBS and saliva were also used as co-supplements. Conditions were also supplemented with 10 mM zanamivir. In some experiments, hemin and menadione were omitted. After supplementation, media was sterile filtered using 0.45 μ m filters. Media was equilibrated overnight at 37°C, anaerobically. Bacteria were harvested from agar plates and resuspended in defined media, centrifuged at 10000 g for 2 minutes and resuspended in defined media, twice, to wash the bacteria. Bacteria were resuspended to an OD₆₀₀ of 2.5 in defined media, before dilution to OD₆₀₀ 0.05 in 1-5 ml defined media with various supplement conditions as above. Cultures were incubated at 37 °C anaerobically for up to 7 days. At various time points (usually 24 hour intervals), 100 μ l samples of cultures were transferred to transparent, flat 96 well plates (Greiner) and their (absorbance) OD₆₀₀ was measured using a TECAN M200 infinite plate reader.

3.2.5 Biofilm Assays

T. forsythia, *F. nucleatum*, and *P. gingivalis* were cultured in the wells of a 96-well tissue culture plate (poly-lysine coated, Greiner): Bacteria were resuspended to an OD₆₀₀ of 0.05 in Tryptic Soy Broth (TSB; Sigma-Aldrich) supplemented with 2 % (w/v) yeast extract, 1 μ g/ml vitamin K, 5 μ g/ml hemin, 50 μ g/ml gentamicin, and either no additional supplements, 0.17 mM NAM, or 6 mM N-acetylneuraminic acid. In conditions testing host glycoproteins, 100 μ l of 6 μ M bovine submaxillary mucin (BSM), 100 % (v/v) pooled human saliva as collected above, or fetal bovine serum (FBS) was added to plate wells and left to coat the wells by incubation at 4 °C overnight. In conditions testing the effect of sialidase inhibition, the supplemented TSB was further supplemented with 10 mM zanamivir. All media was equilibrated overnight in anaerobic conditions at 37 °C. Cultures were incubated for 5 days at 37 °C under anaerobic conditions (10% CO₂, 10% H₂, 80% N₂) in an anaerobic cabinet. To quantify planktonic or total growth, all conditions underwent OD₆₀₀

measurement using a Tecan Infinite M200 Plate Reader. Conditions were set up in triplicate during each assay.

Crystal violet staining was tested as a means of quantifying biofilm formation, and was used to visualise biofilm formation: 100 µl of 0.1 % crystal violet solution was added to each well and incubated at room temperature for 30 minutes. After incubation, crystal violet was removed and wells were gently washed 3-4 times with PBS pH 7.4, before visualisation using light microscopy or extraction with 100 µl 80:20 Ethanol: Acetone. Direct counting techniques were also used for biofilm quantification: Biofilms were gently washed twice using 100 µl PBS to remove planktonic cells, and biofilms were vigorously resuspended in PBS and serially diluted where appropriate. Bacteria were enumerated by counting using a Helber chamber (Hawksley) under phase contrast microscopy, 400 x magnification.

3.3 Results

3.3.1 Release of Sialic Acid from Mucin glycoproteins by Periodontal Pathogen Sialidases is enhanced by *T. forsythia* Sialate-O-Acetyltransferase

Secretory mucins are a group of glycoproteins likely to be encountered by periodontal pathogens as they represent a major component of salivary-mucins account for approximately 16-26 % of the total salivary protein content (Zalewska et al. 2000; Rayment et al. 2000). Furthermore, their concentration in saliva is correlated with severity of periodontal disease, and mucins have been called a non-immunological response to periodontitis (Sánchez et al. 2013). Mucins have been grouped into the high and low molecular weight MG1 and MG2 mucins, which are products of the MUC5b (and to a lesser extent MUC4) and MUC7 genes, respectively. Mucins, including these salivary mucins are heavily glycosylated (table 3.1) and of their O-glycosylated sugar chains, which make up 40-80% of their mass (Levine et al. 1987; Zalewska et al. 2000), a high proportion are sialylated (Zalewska et al. 2000). Sialic acids possess a number of functions in mucin including contributing to an overall negative charge and structure-function (Zalewska et al. 2000). As well as its contribution to mucin structure function, sialic acids have been shown to protect mucin from proteolytic degradation (Takehara et al. 2013).

Mucin	Gene	Domain				
		Protein Domains	Features	Glycosylation	Sialylation	Review
MG1	MUC5b (MUC4 to a lesser extent)	N-terminal Region (1321 Residues)	Cys- rich	GalNAc- Thr/Ser	118 Sialic Acid- containing units	(Zalewska et al. 2000; Levine et al. 1987)
		Tandem Repeat Region (3750 residues)	29-residue Ser/Thr-rich tandem repeats, short Cys- rich regions			
		C-Terminal Region (879 Residues)	Cys- rich			
MG2	MUC7	N-terminal Region (144 Residues)	"Histatin-like" - Histidine Rich	Primarily GalNAc- Thr/Ser, also GlcNAc-Asn	67 sialic acid- containing units	(Zalewska et al. 2000; Levine et al. 1987)
		Tandem Repeat Region (115-138 residues)	23-Residue Ser/Thr-rich Tandem Repeats			
		C-Terminal Region (75 Residues)	No Cys-			

Table 3.2. Salivary mucins-a summary of glycosylation features.

MG1 is the high Mw salivary mucin, MG2 is the low Mw salivary mucin. Glycosylation refers to the sugar-amino acid linkage between the numerous branched glycans present on the mucin. "sialic acid-containing units" refers to the number of oligosaccharide chains with Neu5Ac at their non-reducing ends (furthest from the protein backbone of the mucin).

In humans, the native sialic acid Neu5Ac may be further modified by additional chemical groups (Cohen & Varki 2010). A common modification in humans is the presence of an additional O-acetyl group at Carbon 9 (C-9) to become Neu5,9Ac (5,N-acetyl-9,O-acetylneuraminic acid). As part of a sialoglycan, Neu5,9Ac has been shown to resist the activity of bacterial sialidases that would cleave the mono-acetylated Neu5Ac (Corfield 1992). Recent work including data generated as part of this project has shown that *T. forsythia* produces a sialate-O-acetyl esterase (NanS) that catalyses removal of the additional acetylation, converting Neu5,9Ac to Neu5Ac (Phansopa et al. 2015, includes work performed as part of this project-appendix 7.10). Before investigating how NanS impacted sialic acid cleavage from salivary mucin by the periodontal pathogen sialidases, NanS had to be purified.

3.3.1.1 Purification of the Sialate-O-Acetyltransferase, NanS, from *T. forsythia*

T. forsythia possesses a *nan* operon (Roy et al. 2010), dedicated to harvesting and uptake of sialic acid. One of the *nan* genes encodes a sialate-O-acetyltransferase, NanS. This enzyme is capable of removing the second (O-)acetyl- group from Neu5,9Ac-a prevalent human sialic acid-which is otherwise resistant to NanH de-sialylation of sialoglycans (Phansopa et al. 2015). NanS was successfully purified using a method developed by Dr Chatchawal Phansopa in our laboratory (Figure 3.1) by Glutathione-S-Transferase (GST) affinity chromatography followed by thrombin cleavage of the fusion protein, as described previously (Phansopa et al. 2015). Protein yield after purification of 1 litre of expression strain-culture was typically 10ml of ~1mg/ml of this 76.3 kDa protein, this was sufficient for the scope of this project. Activity of NanS was confirmed using p-nitrophenol acetate (pNP-Ac), which was incubated with NanS, which de-acetylated pNP-Ac, producing pNP; a yellow chromophore which could be visualised (Phansopa et al. 2015).

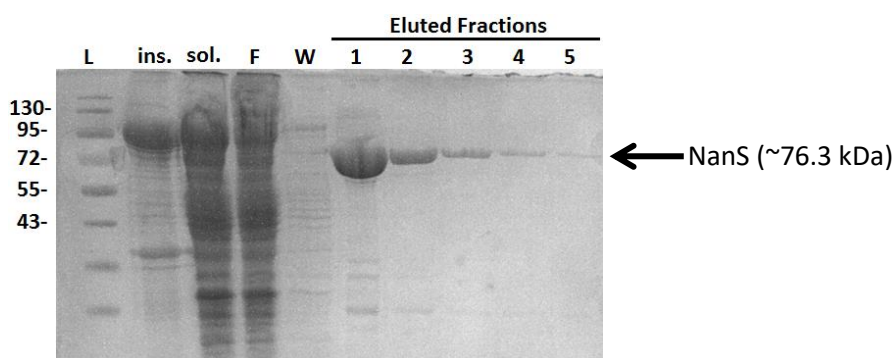


Figure 3.1. Purification of NanS.

SDS-PAGE using 12% (v/v) polyacrylamide gel. L=Mw Ladder (kDa, size approximation based on manufacturer's guide), Ins. =Insoluble Fraction of cell lysate, sol=soluble fraction of cell lysate, F=Flow Through, W=Wash Through, 1-5= Eluted fractions. This purification was performed as part of this project-i.e. by Andrew Frey.

3.3.1.2 *NanS Boosts The Activity of SiaPG and NanH to Release Sialic Acid From Mucin*

Mucins have been shown to contain high levels of di-acetylated Neu5,9Ac, which is often resistant to the activity of bacterial sialidases, and NanS was shown to be a sialate-O-acetyltransferase, which acts to remove the second acetylation, forming Neu5Ac, which was then susceptible to sialidase activity (Phansopa et al. 2015, appendix 7.10).

The impact of NanS and zanamivir on sialic acid release from mucin by the periodontal pathogen sialidases NanH and SiaPG was assessed, and the ability of zanamivir to inhibit cleavage of sialic acid from this host-relevant sialoglycan was also tested. Experiments utilised bovine submaxillary mucin (BSM), since it is relatively cheap, commonly used in studies involving salivary mucins and is a rich and often used source of (diacetylated) sialic acid (Varki & Diaz 1983). BSM was digested for half an hour with various enzyme and zanamivir combinations before undergoing the TBA assay to quantify sialic acid release, with significant differences assessed using repeated measures one-way ANOVA, with Bonferroni correction for multiple comparisons (figure 3.2).

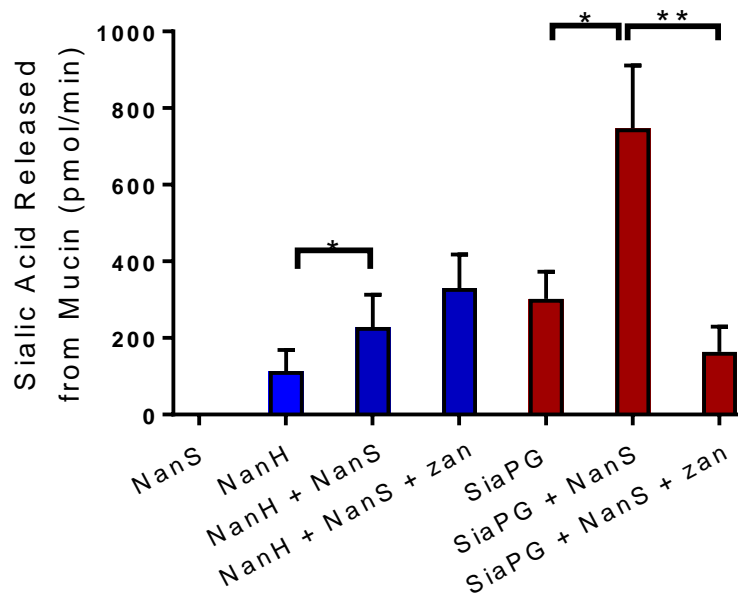


Figure 3.2. Enzyme synergy in sialic acid release from BSM, and inhibition by zanamivir.

BSM was incubated with either NanS, NanH, or SiaPG alone, or NanS+NanH or NanS+SiaPG, in the presence or absence of 0.5mM zanamivir, before undergoing the TBA assay to assess sialic acid release. Data based on the mean of three experiments, each condition was tested in triplicate during each experiment. Error Bars=SEM. Significance determined by one-way ANOVA with repeated measures, with Bonferroni correction for multiple comparisons (* $p < 0.05$, ** $p < 0.01$).

As expected, NanS alone did not release any sialic acid from salivary mucin, but it did double sialic acid release by NanH (from 113 to 228 pmol/min, $p = 0.033$) and the relative increase in sialic release in the presence of NanS was even greater for SiaPG (from 302

pmol/min to 746 pmol/min). It was also noteworthy that SiaPG released more sialic acid than NanH, although these changes were not deemed statistically significant (302 and 113 pmol/min, respectively in the absence of NanS, $p=0.136$, or 746 and 228 pmol/min, respectively in the presence of NanS, $p=0.091$). 0.5 mM zanamivir could significantly inhibit the sialic acid release from mucin treated with SiaPG and NanS, reducing sialic acid release to a level lower than SiaPG alone (SiaPG; 302 pmol/min, SiaPG + NanS; 746 pmol/min, SiaPG + NanS + Zan; 164 pmol/min). NanH sialidase activity was not inhibited at this concentration of zanamivir. The finding that SiaPG, but not NanH, was significantly inhibited by 0.5 mM zanamivir is in accordance with the NanH and SiaPG inhibitory curves used to obtain the IC₅₀ (shown in section 2.4.5), which revealed that zanamivir had an IC₅₀ of 0.36 mM for SiaPG (lower than 0.5mM used in this assay), but zanamivir had an IC₅₀ of 6.15 mM for NanH (greater than the 0.5mM used in this assay). Concentrations of zanamivir higher than 0.5 mM were found to produce high levels of precipitate and interfere with the production of the chromophore during the TBA assay, rendering free-sialic acid quantification impossible or difficult, so only sialidase inhibition by 0.5mM zanamivir was tested during this experiment. This might be overcome in future experiments using High Performance Liquid Chromatography (HPLC) based approaches to assess sialic acid cleavage from mucin, or indeed other substrates.

NanS was incapable of sialic acid release by itself, but it improved sialic acid release from salivary mucin by both NanH and SiaPG sialidases, more-than doubling sialic acid release by both sialidases. SiaPG was capable of releasing more sialic acid than NanH, both in the presence and absence of NanS. However, commenting on how the release of sialic acid from salivary mucin contributes to periodontal pathogen proliferation cannot be ascertained from this experiment alone. It could be the case that NanS-improved sialic acid release assists in nutrient acquisition by periodontal pathogens (discussed below), and this increases their ability to proliferate. To investigate this, experiments involving the growth of periodontal pathogens in the presence of salivary mucin, whole saliva, and serum were performed.

3.3.2 *P. gingivalis* is Capable of Growth Utilising Host Glycoproteins as Sole Carbon and Nitrogen Sources, and this is Enhanced by NanS

Sialic acid has been shown to protect salivary proteins from degradation (Takehara et al. 2013). It was suspected that sialic acid release from host glycoproteins would enable more rapid proteolysis for nutrient acquisition by *P. gingivalis* (and perhaps other periodontal pathogens), meaning sialidases could contribute to increased growth of *P. gingivalis*, and

that sialidase inhibition (using zanamivir) could limit growth of *P. gingivalis*. Furthermore, given that NanS was capable of enhancing the release of sialic acid from heavily di/tri acetylated sialic acid glycoproteins of by the *P. gingivalis* sialidase, NanS might enhance *P. gingivalis* growth on host glycoproteins.

This idea was tested using a culture based approach, using media supplemented with host glycoproteins. However, using conventional growth media (brain heart infusion or tryptic soy based media) could interfere with the experiment, since these are rich in sialoglycans from sources besides the ones desired for testing, and these media contain other nutrients that might compensate for the effects of experimental conditions, masking any meaningful result. Therefore, optimisation of a chemically defined media capable of growing *P. gingivalis* was performed.

3.3.2.1 **Optimisation of Chemically Defined Media**

This defined media was based on formulations in previous studies (Milner et al. 1996; Oda et al. 2007), followed by studies of the effect of NanS and zanamivir on *P. gingivalis* growth on host glycoproteins as sole carbon and nitrogen sources. It consisted of a number of metal salts (10 mM monosodium phosphate, 10 mM potassium chloride, 2mM citric acid, 1.25 mM magnesium chloride, 0.1 mM Iron (III) chloride, 20µM calcium chloride, 0.1 µM sodium molybdate, 25 µM zinc chloride, 50 µM manganese chloride, 5 µM copper (II) chloride, 10 µM cobalt (II) chloride, and 5 µM boric acid), which are considered to be an important basal media capable of supporting the growth of a variety of micro organisms (Milner et al. 1996). During initial optimisation this was supplemented with either 10 % (v/v) fetal bovine serum (FBS), 10 % (v/v) pooled human saliva, or 6 µM bovine submaxillary mucin (BSM) as sole carbon and nitrogen sources (Figure 3.3). Gentamicin (50 µg/ml) was always present in the media (to suppress contamination, but all organisms were resistant at levels up to 500 µg/ml), and the effect of hemin on *P. gingivalis* cultures was also tested during growth (figure 3.4). *P. gingivalis*, *T. forsythia* and *F. nucleatum* were tested for their ability to grow in this defined media (figure 3.3).

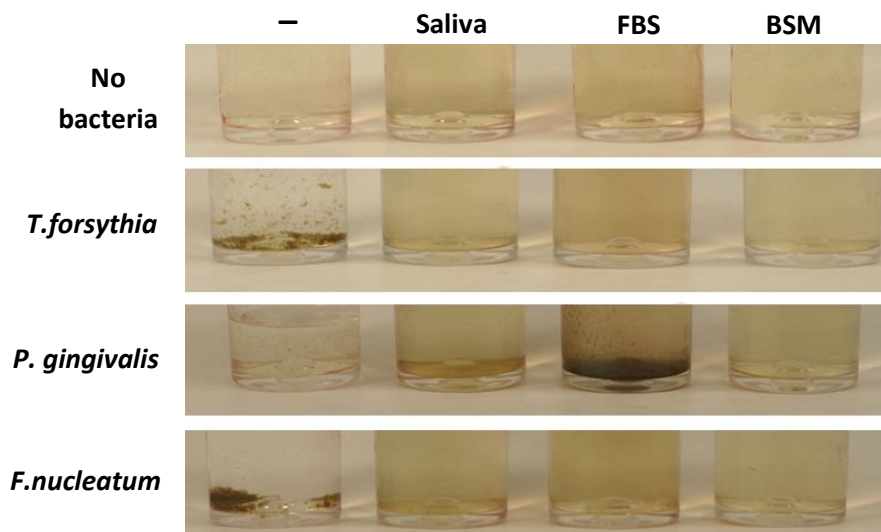


Figure 3.3. Initial testing of defined media for culture of periodontal pathogens.

Defined media cultures of *T. forsythia*, *P. gingivalis*, and *F. nucleatum* were grown anaerobically for 5 days, with different host-glycoprotein substrates as indicated, Saliva=pooled human saliva, SerumFBS=fetal bovine serum, BSM=bovine submaxillary mucin, — = no-glycoprotein supplement/negative control.

P. gingivalis was the species most capable of growth in this defined media, as indicated by visible growth (aggregates or possibly biofilm) localised at the bottom of culture containers. Growth was not observed in the no-bacteria control for any glycoprotein, and allowed a qualitative estimation of turbidity which indicates bacterial growth. *P. gingivalis* growth (as indicated by visible differences between cultures containing either *P. gingivalis* or no-bacteria) appeared to be dependent on the type of glycoprotein supplement, with mucin resulting in no visible (or very little) growth, followed by saliva, and the most prolific *P. gingivalis* growth was seen in serum-supplemented media. *T. forsythia* and *F. nucleatum* may have been capable of limited growth in all three conditions, as indicated by the slight turbidity of the three suspensions compared to the negative control, and this appears to be particularly localised at the bottom of the cultures. There also appears to be some formation of aggregates in conditions containing bacteria but no glycoprotein source, possibly due to sequestration of hemin by bacteria.

P. gingivalis was most capable of growth in this defined media, so growth of *P. gingivalis* was taken forward for a further optimisation step; testing the effect of dual supplementation of the defined media with saliva and FBS. This experiment was also

performed in the absence of hemin, since the dark pigmentation of *P. gingivalis* seen in the above culture might mask differences in absorbance between culture conditions, and it was previously shown that defined media-cultures of *P. gingivalis* could grow in the absence of hemin, without black pigmentation occurring (Oda et al. 2009), this was shown to be the case here (figure 3.4). Cultures were grown for 5 days and Optical Density at 600nm (OD₆₀₀) readings were taken every 24 hours to assess growth. *P. gingivalis* cultures were unable to grow in 1 or 5 % (v/v) serum (at least in the absence of exogenous hemin), and it appeared that saliva was capable of boosting the growth of *P. gingivalis* in the presence of 10 % (v/v) FBS (heat-inactivated) in a dose dependent manner; at 72 hours (the timepoint with the highest optical density for all conditions) cultures with 10% FBS and 0, 1, or 5% (v/v) saliva had OD₆₀₀ values of 0.33, 0.37, and 0.45, respectively. However, each condition was only repeated once, so this cannot be definitively reported based on this experiment.

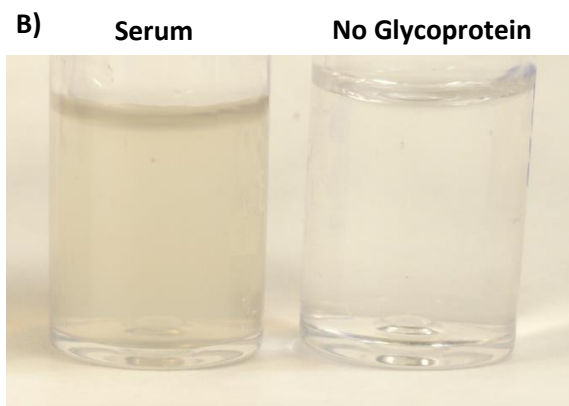
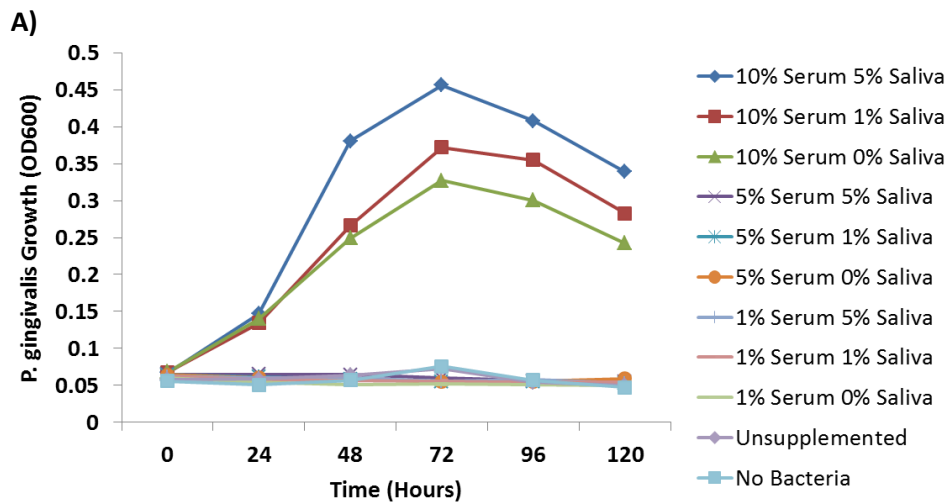


Figure 3.4. Optimisation of *P. gingivalis* culture in defined media; the effect of saliva and serum (FBS)

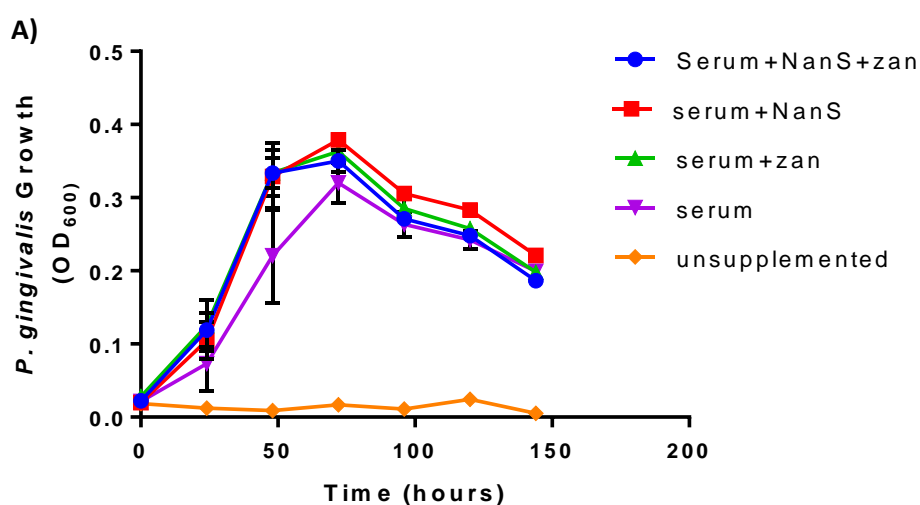
Defined media was supplemented with different quantities of FBS and human saliva as indicated (% values are v/v), and used to grow *P. gingivalis* for 5 days, with growth measurements taken every 24 hours. A) Growth Curve of *P. gingivalis* in Defined Media. Unsupplemented=media Containing no additional supplements, No bacteria=Saliva and serum only without *P. gingivalis* inoculation. Data shown represent the readings taken from a single repeat of each condition. B) Comparison of *P. gingivalis* cultures grown in defined media without hemin, in the presence or absence of 10 % v/v serum.

The defined media optimisation experiments highlighted the ability of *P. gingivalis* to grow in the presence of 10 % FBS as a nutrient source (figures 3.4 and 3.5). Human saliva appeared to enhance growth, as seen by the increased density of cultures, with 5 % saliva increasing the OD₆₀₀ of cultures by a factor of ~1.5 at 72 hours, relative to the 0 % saliva, 10 % FBS condition. It was then possible to carry out further experiments testing the effect of

NanS and zanamivir on the ability of *P. gingivalis* to utilise these host glycoproteins for growth.

Initial experiments were performed to test the effects of both NanS and zanamivir on the growth of *P. gingivalis* in defined media supplemented with FBS (figure 3.5). In NanS-containing conditions, supplemented media was exposed to NanS for 12 hours prior to addition of *P. gingivalis*, the intention being to negate the effects of any degradation of NanS after exposure to *P. gingivalis* proteases. *P. gingivalis* was then inoculated into the supplemented, defined media and incubated for 6 days at 37°C, anaerobically. Growth was recorded every 24 hours by measuring the optical density of the cultures at 600nm (figure 3.5). Statistical differences between conditions at each time point were assessed by one-way ANOVA with repeated measures, with Tukey's correction for multiple comparisons.

It is important to note that the presence of NanS as a source of amino acids itself should have little impact on *P. gingivalis* growth in this experiment-FBS has been shown to contain approximately 3900 µg/ml total protein content (Zheng et al. 2006), and was present at 10 % in cultures, meaning cultures contained 390 µg/ml of protein from FBS. NanS was present at 50 nM, or 0.382 µg/ml, meaning that in conditions containing NanS, the increase in protein content would be negligible compared to the level of FBS protein.



B)

Condition	Time (hours)					
	24	48	72	96	120	144
serum vs. unsupplemented	0.6006	0.2315	0.0213	0.0565	0.0194	0.006
serum+zan vs. unsupplemented	0.2598	0.0287	<0.0001	0.0416	<0.0001	0.0046
serum+NanS vs. unsupplemented	0.2065	0.0616	<0.0001	0.019	0.0003	<0.0001
Serum+NanS+zan vs. unsupplemented	0.1208	0.0115	0.0091	0.0065	0.0064	0.0065
serum+zan vs. serum	0.8833	0.5221	0.5494	0.9914	0.9306	>0.9999
serum+NanS vs. serum+zan	0.8906	0.9979	0.4595	0.7474	0.3355	0.2563
serum+NanS vs. serum	0.8812	0.4364	0.3407	0.5426	0.2034	0.361
Serum+NanS+zan vs. serum	0.2976	0.384	0.9333	>0.9999	0.9861	0.8899
Serum+NanS+zan vs. serum+NanS	0.9829	>0.9999	0.6171	0.6594	0.0858	0.1513
Serum+NanS+zan vs. serum+zan	>0.9999	>0.9999	0.9512	0.9949	0.9084	0.5382

Figure 3.5. Growth of *P. gingivalis* on serum, in the presence of NanS and zanamivir.

Conditions containing NanS were pre-treated with 50nM NanS for 12 hours prior to inoculation with *P. gingivalis*, and zanamivir conditions supplemented with 10mM zanamivir. A) Growth curve of *P. gingivalis* in defined conditions. Serum=10% FBS. Zanamivir=10mM zanamivir. NanS=50nM NanS. Data represent the mean of three experiments, where each condition was repeated once per experiment. Error Bars= SEM. B) Descriptive statistics of *P. gingivalis* growth in defined conditions. Significant differences between all of the conditions were assessed by one-way ANOVA with repeated measures, with Tukey's correction for multiple comparisons, at each time point. The unsupplemented condition was almost always significantly different from the other conditions at all time points from 48 hours onwards, where the adjusted p-value=<0.05, shaded in blue.

The lag, exponential, stationary and death phases of these cultures of *P. gingivalis* can be seen (figure 3.5 A). In all conditions, the boundary between each phase occurs (roughly) at the 24, 48-72, and 96-148 hour time points, although the onset of the lag and exponential phases may be delayed in the serum only condition, compared to the other conditions. Conditions containing NanS had greater optical density compared to conditions without NanS at each time point i.e. NanS appeared to increase the total growth of *P. gingivalis* in both the presence and absence of zanamivir, but the increase in growth was not statistically significant, at any time point. However, the experiments above were performed with just one repeat per condition, per experiment; perhaps more experimental repeats per condition would yield data with decreased error and greater significance.

The effect of zanamivir on *P. gingivalis* growth in this series of experiments was less clear: Conditions containing serum without NanS actually displayed more *P. gingivalis* growth in the presence of zanamivir at all time points. However, conditions containing serum and NanS displayed lower *P. gingivalis* growth in the presence of zanamivir. Regardless, there were almost no statistically significant effects of zanamivir on the cultures, with the exception of the unsupplemented condition (figure 3.5 B), where the unsupplemented cultures displayed significantly lower levels of *P. gingivalis*. This experiment using serum as a nutrient source for *P. gingivalis* did not definitively answer whether or not *P. gingivalis* growth on serum (FBS) and saliva is enhanced by NanS. Perhaps if conditions had undergone more repeats during each experiment, or if they had been altered further (through increasing serum, or the inclusion of hemin) a significant trend would become apparent.

3.3.2.2 ***NanS Enhances P. gingivalis* Growth in the Presence of Human Saliva**

In addition to the importance of serum as a nutrient source, the data in section 3.2.1 show increased sialic acid release from salivary mucin by *P. gingivalis* sialidase (SiaPG) in the presence of NanS. Therefore, another set of defined media experiments was performed to study the effects of both saliva (which contains high levels of mucins) and NanS on *P. gingivalis* growth (serum was also present in all conditions, figure 3.6). Statistical significance was determined by repeated measures 2-way ANOVA at each time point, which also enabled assessment of a possible interaction between the presence of both NanS and saliva on *P. gingivalis* growth.

In accordance with the previous saliva-containing experiment (Section 3.2.2.1, figure 3.5), *P. gingivalis* growth was enhanced by the presence of saliva. However, the increased

growth in the presence of saliva was only statistically significant in the condition that contained NanS, The addition of NanS in the presence of serum alone caused no significant increase in *P. gingivalis* growth (figure 3.6). The differences in growth were greatest at the 96 hour time point, when the serum, serum + NanS, serum + saliva, and serum + saliva + NanS conditions had optical densities of 0.084, 0.897, 0.124, and 0.1784, respectively (Serum + Saliva + NanS condtion was significantly different from both of the condtions without saliva, $p < 0.05$, but not from the condition containing saliva without NanS).

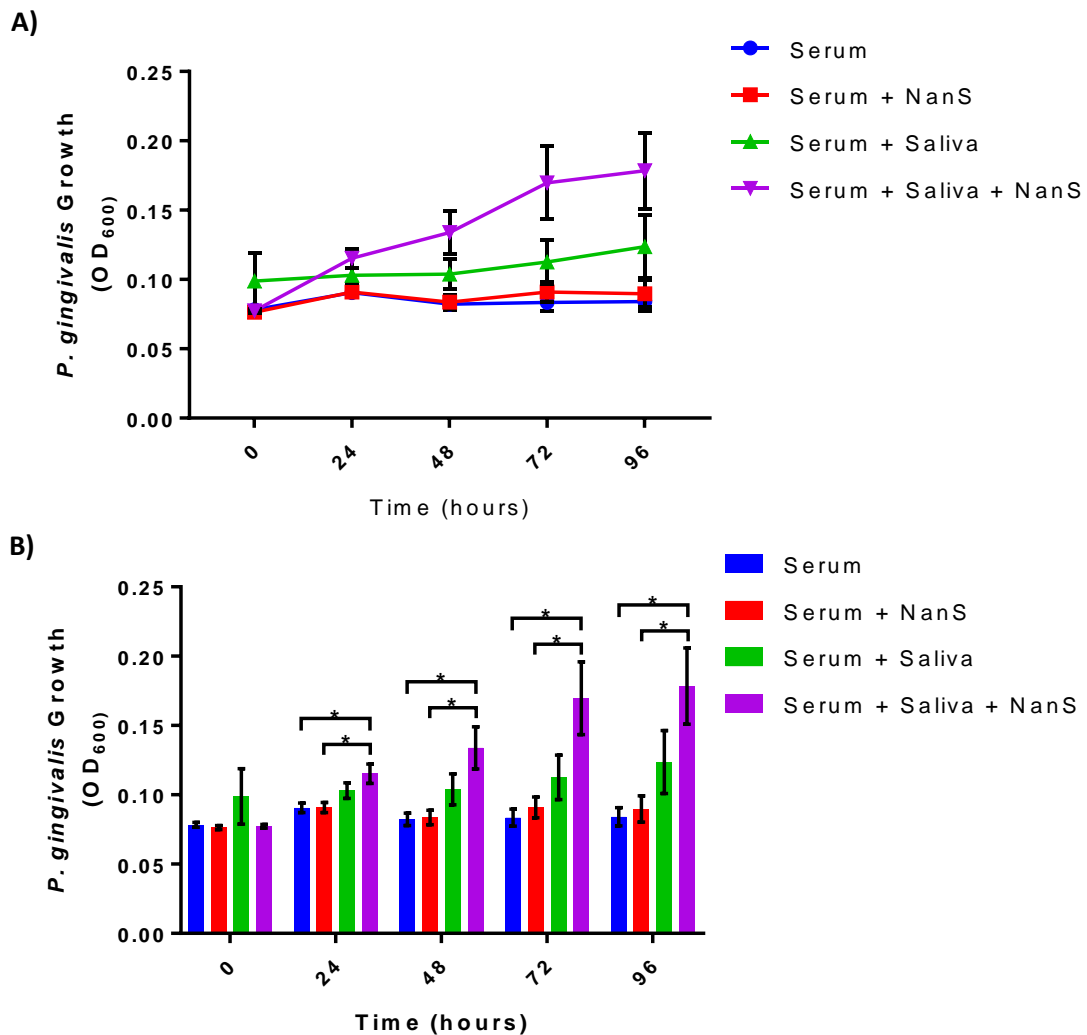


Figure 3.6. The effect of NanS on *P. gingivalis* growth on serum and saliva.

Conditions containing NanS were pre-treated with 50nM NanS for 12 hours prior to inoculation with *P. gingivalis*. Serum=10% FBS, Saliva=5% Pooled Human Saliva, NanS=50nM NanS. Data represent the mean of three experiments, where each condition was repeated three times per experiment. A) Growth curve of *P. gingivalis* in the presence of combinations of Serum, Saliva, and NanS. Error Bars=SEM. B) *P. gingivalis* growth over time, displayed to highlight differences between conditions. Error bars=SEM. Significant differences caused by the presence of NanS and/or saliva were established by two-way ANOVA with repeated measures, and Tukey's correction for multiple comparisons (multivariate analysis), at each time point. NanS was found to have a significant effect on *P. gingivalis* growth from the 24 hour condition onwards ($p < 0.05$). Significant differences at each time point, revealed by the multivariate analysis with Tukey's correction for multiple comparisons, are indicated (* $p < 0.05$).

Ultimately, these experiments show that *P. gingivalis* can utilise host glycoproteins as sole carbon and nitrogen sources, specifically serum and saliva. These are particularly relevant since *P. gingivalis* is exposed to GCF (similar in composition to serum) and saliva during periodontal colonisation and subsequent periodontal disease. Furthermore, the *T. forsythia* sialate-O-acetyltransferase, NanS, seems to be capable of enhancing the growth of *P. gingivalis* in the presence of these nutrient sources, particularly saliva. This could be due to the increased rate of sialic acid release by SiaPG from salivary mucins (figure 3.3) and perhaps other salivary proteins, resulting in increased proteolysis and free amino acids which can be readily utilised by *P. gingivalis*. In addition, zanamivir appeared to inhibit the release of sialic acid from mucin (figure 3.3) and is an exciting finding in the context of the oral microbiota. In addition, the potential of the sialidase inhibitor zanamivir to prevent *P. gingivalis* growth on serum and saliva as a sole carbon and nitrogen source could also be evaluated. That said, the effect of zanamivir on *P. gingivalis* cultures with serum (FBS) as a sole nutrient source was minimal, possibly due to lower levels of glycoprotein sialylation compared to saliva, decreasing the importance of sialidases to cultures with only FBS as a nutrient source- however in the case of saliva these data may differ. Ideally, more experiments with different culture conditions (such as the presence of hemin, or different concentrations of saliva, or cultures with mixtures of mucin and serum) could be performed to test if this is truly the case.

It was also hoped that *T. forsythia* could also be cultured using a form of the defined media, perhaps with additional supplements such as NAM, or Neu5Ac, and attempting to quantify biofilm formation if there is no observable planktonic growth. Unfortunately, optimisation of *T. forsythia* growth in a defined media was not possible during the timeframe of this project, despite several attempts. It might be more feasible to co-culture *T. forsythia* with *P. gingivalis* in these minimal media experiments, which would also serve the purpose of testing interspecies co-operation in nutrient acquisition from host glycoproteins.

3.3.3 Biofilm Formation of Periodontal Pathogens on Host Glycoproteins, and the Potential for Zanamivir to Inhibit Periodontal Pathogen Biofilm Formation

Although the ability to utilise host glycoproteins as sole carbon sources for growth is a useful ability for pathogens, their ability to form biofilms is considered key during periodontal disease. Indeed, treatment focuses on mechanical removal of the subgingival biofilm and any calcified plaque, followed by oral hygiene measures to maintain low levels of plaque. Even so, some patients are either unable to comply, or do not comply with oral

hygiene measures, and in some patients periodontitis continues to progress despite initial removal of the sub-gingival biofilm. Given this, inhibition of periodontal pathogen biofilm formation could be extremely beneficial for treatment or prevention of periodontitis.

Gene-knockout studies of periodontal pathogens have highlighted the importance of sialidases in biofilm formation by *P. gingivalis* and *T. forsythia* (Roy et al. 2011; Li et al. 2012). Since host surfaces are coated in glycoproteins, the decrease in biofilm formation seen in these sialidase-deficient strains may be due to the function of pathogen sialidases in nutrient acquisition, or by exposure of underlying glycans for pathogen attachment. Given this, sialidase inhibitors might be applied to prevent biofilm formation by periodontal pathogens, with the ultimate aim being the application of sialidase inhibitors as therapeutics or preventatives for periodontitis, since biofilm formation is important for disease progression. In fact the sialidase inhibitor oseltamivir was successful in *in vitro* experiments testing this question for *T. forsythia* (Roy et al. 2011), but zanamivir has not been tested to date, and neither has the effect of sialidase inhibitors on *P. gingivalis* biofilm formation.

3.3.3.1 ***Establishing Growth Conditions for P. gingivalis Biofilms on Glycoprotein Coated Surfaces***

Conditions selected for optimisation of biofilm formation contained either Neu5Ac (human sialic acid), NAM (N-Acetylmuramic acid; peptidoglycan monomeric unit, normally required for *T. forsythia* mono-culture), or the glycoprotein sources foetal bovine serum (FBS), bovine submaxillary mucin (BSM), or pooled human saliva.

Tryptic Soy Broth (TSB) supplemented with 2% Yeast Extract, 1mg/ml hemin, 1mg/ml menadione, and 50µg/ml gentamicin was used for all cultures. Bacteria were taken from agar plates, washed twice in TSB, and seeded into 96-well tissue culture (poly-lysine coated) plates at OD₆₀₀ 0.05. Cultures were further supplemented by NAM or Neu5Ac, which were included in bacterial media during biofilm culture, or by glycoproteins, which had been pre-coated onto the biofilm assay plate by adding mucin, serum, or saliva to the plate and incubating at 4 °C for 18 hours. After inoculation of media, biofilm plates were incubated for 5 days at 37 °C anaerobically. Total bacterial growth (planktonic and biofilm growth) was quantified by measuring the OD₆₀₀ of cultures. After removing the planktonic culture and gently washing the biofilm twice with PBS, two approaches were tested to assess biofilm formation; crystal violet staining, and bacterial counting using a Helber chamber with phase contrast microscopy. A condition containing no bacteria, but either NAM, Neu5Ac, or the glycoprotein coatings was used as a control for microbial

contamination of media or supplements, and underwent absorbance testing (for total growth) and crystal violet staining (for biofilm formation), these also acted as blank controls; the absorbance values of these “no bacteria” conditions were subtracted from the other conditions. Significant differences between the unsupplemented condition and the other conditions were assessed by one-way ANOVA with Dunnet’s correction for multiple comparisons.

The resulting experiments showed that *P. gingivalis* was capable of varying degrees of growth and biofilm formation in media supplemented with NAM or Neu5Ac, and on glycoprotein pre-coated surfaces, and that bacterial counting using a Helber Chamber and microscopy was a more accurate method for biofilm quantification than crystal violet staining (figure 3.7). NAM and Neu5Ac were selected since these are utilised by *T. forsythia* during biofilm formation, and it was initially hoped that mixed species biofilm assays could be performed, and a comparison of mixed-culture and mono-culture growth on NAM and Neu5Ac would be required. Unfortunately it was not possible to perform mixed-species experiments within the timeframe of this project.

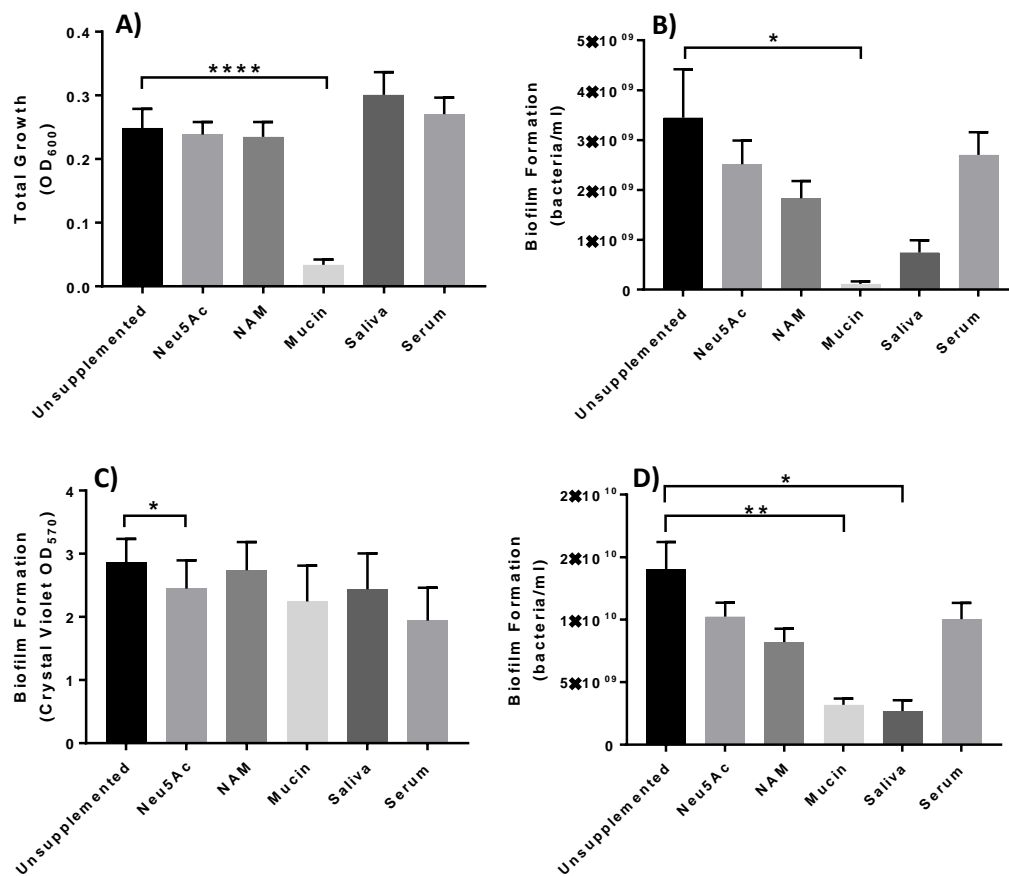


Figure 3.7. *P. gingivalis* growth on NAM, Neu5Ac, serum, and saliva, and a comparison of biofilm quantification methods.

Bacteria were cultured for 5 days at 37 °C, anaerobically, in the presence of NAM or Neu5Ac, or on surfaces coated with the glycoproteins mucin, saliva, or serum. A) Total Growth; OD₆₀₀ of the culture was used to quantify bacteria in both biofilm and planktonic states. B) Biofilm formation; quantified by crystal violet staining. C) Biofilm formation, quantified by resuspension of biofilms and counting the number of bacteria under phase contrast microscopy. D) Biofilm formation normalised to total growth (biofilm formation (Bacteria/ml) x Total Growth (OD₆₀₀)). Error bars =SEM. Statistical differences determined by repeated measures one-way ANOVA, with Dunnett correction for multiple comparisons *p>0.05, **p>0.01.

P. gingivalis was capable of similar levels of total growth (biofilm and planktonic) in all conditions tested, except for in the mucin-coated conditions, where total growth on mucin coated wells was decreased compared to those of the non-supplemented condition (OD_{600} 0.03 in mucin coated conditions, compared to OD_{600} 0.25 in unsupplemented conditions, almost an eightfold difference, $p=0.0001$). Experiments using pre-coated surfaces-with serum and/or saliva appeared to slightly enhance total growth, but the changes were not significant.

The two methods of quantifying biofilm formation seem to show different results (figure 3.7 B and C): The crystal violet staining method implied that none of the conditions resulted in any changes in biofilm formation. The actual bacterial count (obtained through microscopy) showed that *P. gingivalis* biofilm formation on mucin, and to a lesser extent saliva, was significantly lower than the unsupplemented condition (unsupplemented, saliva-coated, and mucin-coated conditions had biofilms of 3.45×10^9 , 7.46×10^8 , and 1.16×10^8 bacteria/ml, but only the mucin coated condition was significantly different from the unsupplemented condition, $p=0.027$). NAM, Neu5Ac, and serum-coated conditions appeared to show some decreased biofilm formation compared to the unsupplemented condition, but these changes were not statistically significant. These results were also reflected in the normalised data (adjusted for total growth), where only *P. gingivalis* biofilm formation on mucin, and to a lesser extent saliva, was significantly lower than the unsupplemented condition (unsupplemented, saliva-coated, and mucin-coated conditions had normalised biofilms of 1.4×10^{10} , 2.7×10^9 , and 3.2×10^{10} bacteria/ml, $p=0.0186$ and 0.0046 , respectively).

Ultimately, it was decided to use the direct counting (by resuspension of biofilms and microscopy) of bacteria during assessment of biofilm formation: Crystal violet staining tended to show larger variation between experimental repeats (compared to counting). Additionally, in the case of at least one of the conditions (*P. gingivalis* cultured on mucin-coated plates) the moderate level of crystal violet staining indicating a level of biofilm formation similar to other conditions did not correspond with the low level of total growth seen in the measurement (OD_{600}) of the planktonic and biofilm culture. There was also a concern that crystal violet could partially stain the glycoprotein coated surfaces, which would lead to an erroneous finding that biofilms had formed. Also, the crystal violet staining procedure required multiple washes to remove excess crystal violet after staining, which was often observed to result in partial detachment and loss of the biofilm from the

surface of the wells. Biofilm detachment was still something of a problem during the wash steps preceding the counting method, but detachment due to wash steps was more severe in using the crystal violet method. Expressing biofilm formation (biofilm count) relative to the total bacterial growth (OD₆₀₀ of cultures prior to crystal violet staining) proved to be somewhat useful, providing confirmation that decreases in biofilm formation (rather than simply reflecting any decrease in total growth) was occurring. This method of normalising biofilm formation to total growth as a means to ensure quantification of reduced biofilm formation, rather than simply reduced overall-growth, has been utilised previously by others (Honma et al. 2007; Frank et al. 2007; Chen et al. 2002). Therefore, in this work, biofilm formation (following resuspension of biofilms and microscopic counting) and biofilm formation relative to total bacterial growth is displayed.

3.3.3.2 ***The Ability of Zanamivir to Inhibit P. gingivalis and T. forsythia Glycoprotein-Dependent Biofilm Formation.***

The results above (4.2.3.2) showed that it was possible to grow *P. gingivalis* biofilms on host glycoprotein-coated surfaces, while this was already established for *T. forsythia* (Roy et al. 2011; Roy et al. 2010). The next step was to establish whether or not biofilm formation on these surfaces could be inhibited by zanamivir. The rationale being that mucin, serum, and saliva are rich in sialic acid, and sialic acid is a potential nutrient itself, but also caps other sugars in the underlying glycan chains which bacteria could metabolise or adhere to, which would be exposed by action of pathogen sialidases. So it might be the case that a sialidase inhibitor such as zanamivir could prevent or inhibit pathogen adhesion to or metabolism of host glycoproteins, resulting in decreased biofilm formation. Indeed, *T. forsythia* biofilm formation on sialoglycoproteins is inhibited by the sialidase inhibitor oseltamivir (Roy et al. 2010; Roy et al. 2011), so it was hoped this effect could be replicated with zanamivir, for both *P. gingivalis* and *T. forsythia*.

T. forsythia and *P. gingivalis* were cultured in media supplemented with NAM or Neu5Ac, or in the presence of surfaces coated with mucin (BSM), saliva (pooled human saliva), or serum (FCS). Cultures were also performed in the presence or absence of 10 mM zanamivir to test the effect of sialidase inhibition on biofilm formation. After inoculation at OD₆₀₀ 0.05, and incubation for 5 days at 37 °C anaerobically, the total growth of cultures (bacteria in planktonic and biofilm states) was assessed by measuring the OD₆₀₀ of cultures, and biofilm formation was assessed by bacterial counting using a Helber chamber and microscopy. Since only the effect of zanamivir on growth in the presence of a given nutrient

was under investigation, individual T-tests were used to assess statistical significance in each nutrient condition in the presence and absence of zanamivir.

T. forsythia (figure 3.8) total growth in the glycoprotein-coated conditions appeared to be slightly elevated in the presence of zanamivir, and in the mucin- and serum-coated conditions the increase was shown to be significant by T-test (OD₆₀₀ of 0.044 against 0.061 in mucin, and OD₆₀₀ of 0.056 against 0.076 in serum). In the Neu5Ac supplemented condition, there was almost no change; a slight, non-significant decrease in total growth was observed.

In terms of biofilm formation, zanamivir produced no significant changes in any of the conditions. The only possible difference (which was determined to be non-significant by T-test) was a ~1.5 fold increase in biofilm formation in the saliva-coated condition in the presence of zanamivir (from 1.52x10⁷ bacteria/ml to 2.39x10⁷ bacteria/ml). In the Neu5Ac supplemented condition, there was almost no change; similarly to the total growth, a slight non-significant decrease in total growth was observed which was also shown in biofilm imaging. The inability of zanamivir to reduce biofilm formation appears to correlate with the information shown in chapter 2 (section 2.3.7), where zanamivir was shown to have low efficacy for sialidase inhibition of live *T. forsythia*.

Representative images showing the crystal violet staining and subsequent quantification of the *T. forsythia* biofilms appears to correlate with the bacterial counting method of biofilm quantification -i.e. Biofilms contained only low numbers of organisms, and that Neu5Ac had the greatest amount of biofilm formation.

Regarding *P. gingivalis*, figure 3.9 A shows that the total growth (biofilm and planktonic growth) of *P. gingivalis* in the mucin-coated condition was significantly reduced in the presence of zanamivir-from OD₆₀₀ 0.21 to 0.11 (p<0.05, i.e. zanamivir reduced total growth of *P. gingivalis* in mucin-coated conditions by approximately half). The other glycoprotein-coated conditions (saliva and serum) also showed very small, non-significant reductions in total growth in the presence of zanamivir (saliva; OD₆₀₀ 0.35 and 0.33 in the absence and presence of zanamivir, serum; OD₆₀₀ 0.37 and 0.35 in the absence and presence of zanamivir). *P. gingivalis* grown in Neu5Ac-supplemented media showed almost identical total growth in the presence and absence of zanamivir.

Figure 3.9 B shows that the biofilm formation of *P. gingivalis* appeared to be reduced in all conditions in response to zanamivir: In the case of mucin- and saliva-coated conditions, the

reduction was approximately one third (mucin; from 2.32×10^9 to 1.69×10^9 bacteria/ml, saliva; from 2.78×10^9 to 1.88×10^9 bacteria/ml). However, only in the case of saliva was the reduction found to be significant due to variation between repeats. *P. gingivalis* grown in serum-coated conditions showed a smaller reduction in biofilm formation, with zanamivir reducing biofilm formation by approximately one sixth (from 3.57×10^9 to 3.01×10^9 bacteria/ml), but the reduction was not found to be significant. For the Neu5Ac-supplemented condition, biofilm formation was reduced by approximately one quarter in the presence of zanamivir (from 4.22×10^9 to 3.25×10^9 bacteria/ml). Normalisation of the biofilm data relative to total growth resulted in almost the same trend (that zanamivir reduced biofilm formation), but the effect on saliva appeared to be negated by normalisation, while the effect of zanamivir in reducing biofilm formation of *P. gingivalis* on mucin became a significant reduction (from 7.65×10^9 to 5.22×10^9 bacteria/ml).

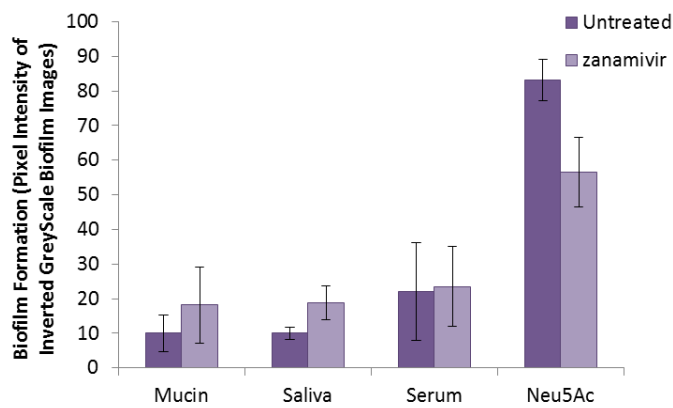
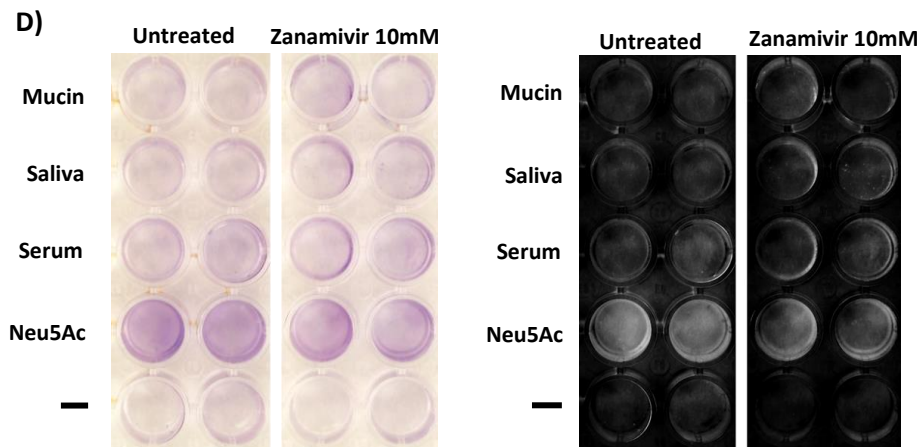
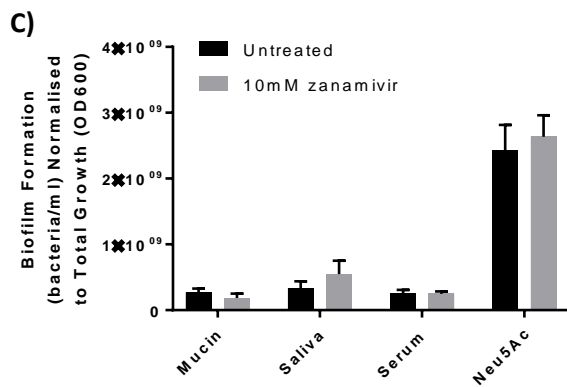
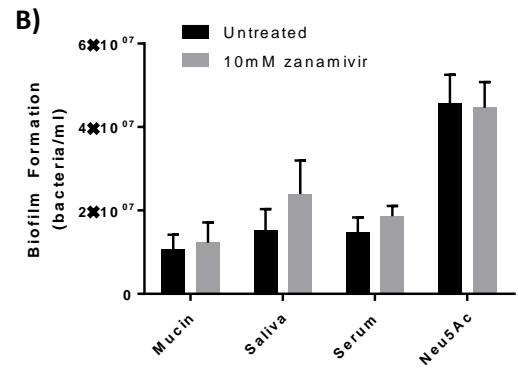
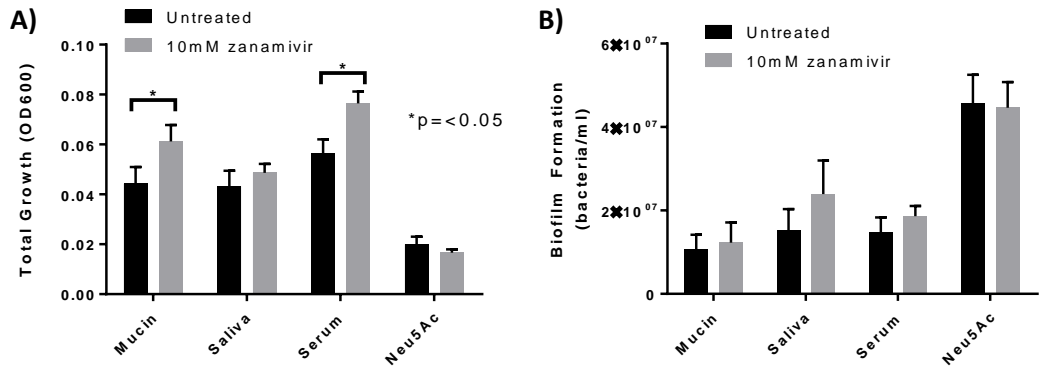


Figure 3.8. Zanamivir has no effect on *T. forsythia* biofilm formation on sialoglycoprotein sources.

Bacteria were cultured for 5 days at 37 °C anaerobically, in the presence of Neu5Ac, or on surfaces coated with the glycoproteins mucin, saliva, or serum. All conditions were performed in the presence or absence of zanamivir A) Total growth, OD₆₀₀ of the culture was used to quantify bacteria in both biofilm and planktonic states. B) Biofilm formation, quantified by resuspension of biofilms and counting the number of bacteria under microscopy. C) Normalisation of Biofilm Formation to Total Growth. All data shown represent the mean of three biological repeats, where conditions were tested three times per experiment. Error bars =SEM. Significance determined by T-test, *p=>0.05. D) Crystal violet stained *T. forsythia* biofilms in the presence or absence of zanamivir. The negative control (-) contains no bacteria or glycoprotein coating, but underwent the crystal violet staining procedure before imaging, which was converted to greyscale and colours inverted to allow quantification of biofilm formation using image processing software (ImageJ). Data shown represent the mean of the two conditions in the image shown. Error bars =SD.

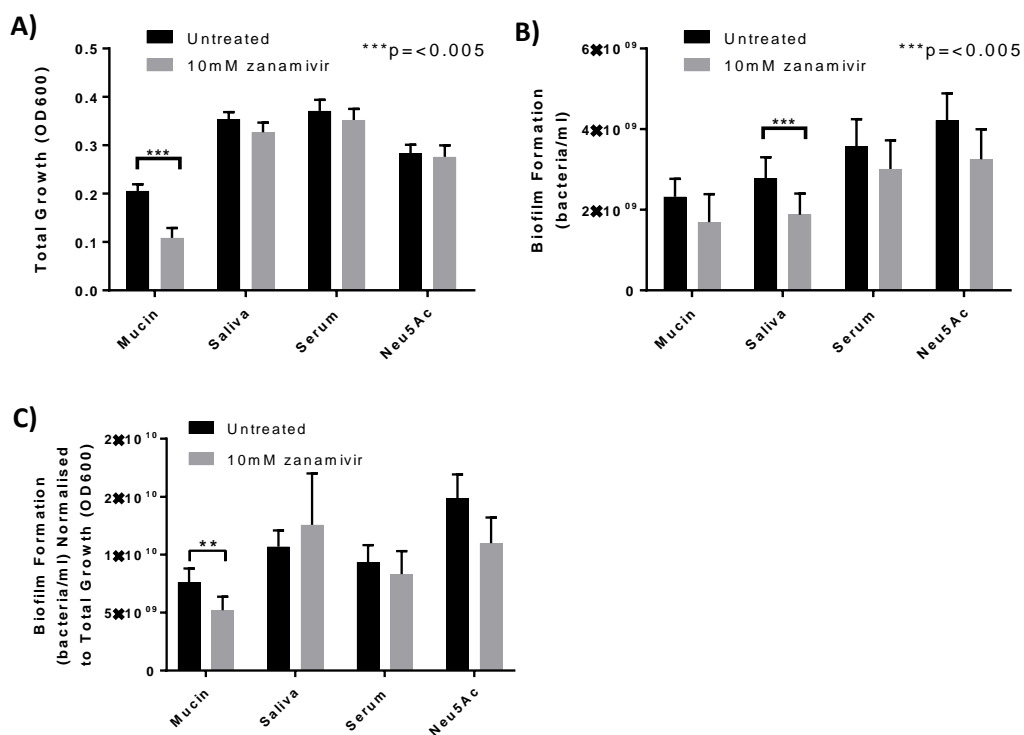


Figure 3.9. Zanamivir inhibits *P. gingivalis* growth and biofilm formation on sialoglycoproteins.

Bacteria were cultured for 5 days at 37 °C anaerobically, in the presence of Neu5Ac, or on surfaces coated with the glycoproteins mucin, saliva, or serum. All conditions were performed in the presence or absence of zanamivir. A) Total growth; OD₆₀₀ of the culture was used to quantify bacteria in both biofilm and planktonic states. B) Biofilm formation, quantified by resuspension of biofilms and counting the number of bacteria under microscopy. All data shown represent the mean of three biological repeats, where conditions were tested three times per experiment. Error bars =SEM. Significance determined by T-test, **p=>0.01, ***p=>0.005.

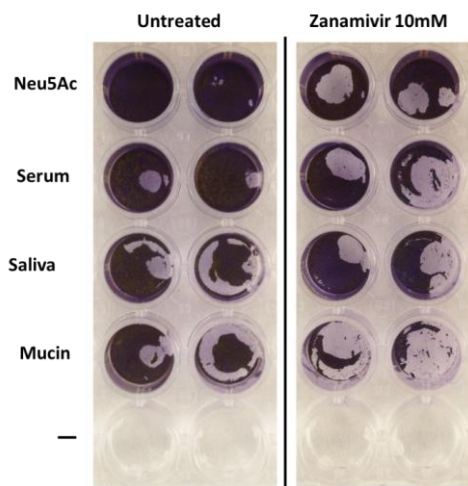


Figure 3.10. Crystal violet staining of *P. gingivalis* biofilms.

P. gingivalis biofilms were cultured on Neu5Ac, serum, saliva, or mucin in the presence or absence of zanamivir, before undergoing the crystal violet staining procedure. The negative control (-) contains no bacteria or glycoprotein coating, but underwent the crystal violet staining procedure.

The crystal violet-stained images of the *P. gingivalis* biofilms in figure 3.10 appeared to confirm the data shown in figure 3.9; that zanamivir reduced the biofilm formation of *P. gingivalis* in all conditions. However, it was not considered appropriate to quantify biofilm formation with image processing, which was done in the case of *T. forsythia*, since aggregates of the *P. gingivalis* biofilm appeared to have become detached and removed during the wash steps involved in crystal violet staining, which would interfere with the results. Qualitatively speaking, biofilms show much more dense purple staining, indicating thick biofilms with high numbers of *P. gingivalis*, compared to those seen for *T. forsythia* (figure 3.8 D). *P. gingivalis* biofilms cultured in the presence of zanamivir appeared to become more readily detached than in the absence of zanamivir, most drastically in the mucin-coated condition. This perhaps indicates that sialidase activity acts to improve *P. gingivalis* attachment to host glycans rather than assisting in nutrient acquisition for *P. gingivalis*, at least in culture conditions used here. Future work might test this in adhesion assays, where *P. gingivalis* would be incubated on surfaces coated with host glycoproteins for a short period of time (~3 hours), followed by bacterial enumeration. Inhibition of attachment would provide some support for the use of sialidase inhibitors as periodontitis therapeutic, since a decrease in the ability of *P. gingivalis* to attach to surfaces could be beneficial to periodontal disease treatment. Furthermore, perhaps after a two day culture

(as seen more frequently during *in vivo* biofilm studies of *P. gingivalis*) the differences in biofilm formation in the presence and absence of zanamivir would be greater. Five-day incubations were used in this work because *T. forsythia* requires that period of time to reach levels suitable for biofilm assessment, so using the same culture time for both species might have allowed a more direct comparison of biofilm formation, and it was the intention to perform mixed-species biofilm cultures-which is more representative of the situation *in vivo*.

In summary, *T. forsythia* was shown to be capable of forming biofilms on mucins, serum, and saliva coated surfaces, though Neu5Ac or NAM supplements appeared to promote biofilm formation more so than glycoprotein-coated surfaces (mucin, saliva, or serum), but this might be expected given the need to release the sugars from glycans with glycoprotein sources over freely included sugars. Furthermore, zanamivir had no effect on *T. forsythia* biofilm formation on host glycoprotein coated surfaces or biofilm formation in the presence of Neu5Ac.

P. gingivalis was also shown to be capable of forming biofilms on mucin, serum, or saliva coated surfaces (and in the presence of Neu5Ac or NAM). The number of bacteria in the *P. gingivalis* biofilms was much greater than that of *T. forsythia*. Interestingly, salivary mucin appeared to inhibit *P. gingivalis* biofilm formation and planktonic growth. Furthermore, unlike the *T. forsythia* condition, *P. gingivalis* appeared to reduce biofilm formation on all glycoprotein coated surfaces and biofilm formation in the presence of Neu5Ac (though only significantly in the case of saliva and possibly mucin coated surfaces).

As well as optimising experimental conditions for *P. gingivalis* it would be interesting to test the effect of NanS on *P. gingivalis* biofilm formation, which could have several effects: NanS may boost biofilm formation on host substrates due to its influence on nutrient acquisition, which was seen in the defined media experiments. NanS may also decrease the inhibitory effects of mucin (BSM) seen in these assays, since it was shown to enhance sialic acid release from mucin, and cleavage of sialic acid increases the rate of mucin proteolysis (Takehara et al. 2013).

3.4 Discussion

Since sialoglycoproteins represent an important source of nutrients for periodontal pathogens, and sialic acid that caps their glycans represents a barrier to further metabolism, periodontal pathogen sialidases may be an important virulence factor aiding in nutrient acquisition from the host. Sialidases may also contribute to bacterial attachment

to underlying glycans or proteins, an important factor in colonisation and biofilm formation. Investigating these sialidase-mediated processes, and the ability to inhibit them using zanamivir was the initial motivation for work described in this chapter.

For some of the periodontal pathogens, sialic acid itself appears to be a potential nutrient: *T. forsythia* possesses a dedicated sialic acid utilisation (*nan*) operon, of which *nanH* is one of nine genes (figure 3.11 A) thought to be involved in sialic acid release (*nanH*, *nanS*), uptake (*nanO*, *nanU*, *nanT*), and initial stages of catabolism (*nanA*, *nanE*, *nahA*, *nanM*) (Stafford et al. 2012). The release of sialic acid has been shown to be particularly important as a nutrient for *T. forsythia*, since it is able to substitute its requirement for exogenous N-acetylmuramic acid (NAM) for sialic acid (Neu5Ac) when growing in a biofilm (Roy et al. 2010; Pham et al. 2010).

Interestingly, some periodontal pathogens appear to possess partial analogues of the *nan* operon, such as *F. nucleatum subsp. nucleatum*, where genes for sialic acid uptake (*siaP*, *siaQ*, *SiaM*) and catabolism (*nanA*, *nanK*, *nanE*), but no genes encoding enzymes for sialic acid release are present (figure 3.11 B). In the case of these periodontal pathogens that do not possess sialidases it is assumed that *in vivo* they rely on sialidases from other bacteria in the sub-gingival biofilm to release sialic acid, which they can then uptake and metabolise.

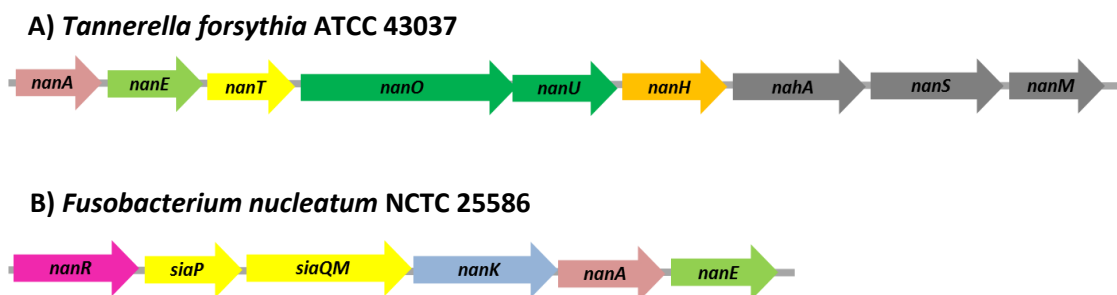


Figure 3.11. Sialic Acid Utilisation Operons in A) *T. forsythia* and B) *F. nucleatum*

nanA (peach)- neuraminidase, *nanR* (pink)-transcriptional regulator, *nanE* (light green), N-acetylmannosamine-6P epimerase, *nanK* (blue), ManNAc kinase, *nanT* and *siaPQM* (yellow)-the (inner) membrane transporters, respectively; major facilitator superfamily permease, Neu5Ac TRAP (tripartite ATP-independent periplasmic) transporter, *nanOU* (dark green)-TonB-dependent sialic acid outer membrane transport system, *nanS*, *nahA*, *nanM* (grey)-the accessory genes, respectively; sialate 9-O-acetylerase, beta hexosaminidase, sialic acid mutarotase. Adapted from Stafford et al. 2012, permitted under the Creative Commons Attribution-NonCommercial 4.0 Unported license (CCNC), or the Creative Commons Attribution license 4.0 (CCBY).

There are also periodontal pathogens that possess sialidases but no other *nan* homologues, such as *P. gingivalis*. However, the *P. gingivalis* sialidase may play a role in nutrient acquisition: *P. gingivalis* relies on free amino acids, in particular, serine, threonine, arginine, asparagine, aspartic acid and glutamic acid are rapidly consumed in culture (Dashper et al. 2001). *P. gingivalis* is also able to utilise amino acids in the form of short peptides. This requirement for amino acids is met due to the action of *P. gingivalis*-secreted proteases, or gingipains, the most important of which are the lysine and arginine gingipains Kgp and Rgp (Grenier et al. 2003). Sialic acid has been shown to protect the salivary mucins MUC5b and MUC7 from proteolysis (Takehara et al. 2013). Therefore, it might be the case that *P. gingivalis* sialidase aids the gingipains in proteolytic cleavage of salivary components (and possibly other secreted and host-cell associated glycoproteins). Furthermore, since bacterial sialidases can upregulate inflammation (discussed in chapter 5), and in the context of periodontal disease inflammation leads to increased GCF flow and bleeding, sialidase activity could increase amino acid sources available to *P. gingivalis*.

In addition to its glycoprotein-protective functions, sialic acid itself can be chemically modified, resulting in protection from the effect of sialidase; Neu5Ac (5-N-Acetylneuraminic Acid) on human glycans can be further modified to possess an additional Acetyl group at its 9th carbon, at which point it is called Neu5,9Ac (9-O-Acetyl, 5-N-Acetylneuraminic Acid). This di-acetylated sialic acid has shown the ability to resist cleavage from its underlying glycan chain by several sialidases, which do have activity on mono-acetylated Neu5Ac-glycans (Corfield 1992). The data presented here show that *P. gingivalis* SiaPG is better able to de-sialylate mucin than *T. forsythia* NanH, but its activity is doubled by the presence of the *T. forsythia* NanS. (A BLAST search confirmed that *P. gingivalis* does not encode any homologues of NanS.) This might shed some light on the situation *in vivo*, when the pathogens form part of a community that interacts with the host and with each other within biofilms. In this case, the above data suggest the periodontal pathogens *T. forsythia* and *P. gingivalis* act in tandem to release sialic from mucin: NanS from *T. forsythia* converts Neu5,9Ac to Neu5Ac, and SiaPG (and to a lesser extent, NanH) is then able to extensively desialylate mucin, which has been shown to enhance mucin degradation (Takehara et al. 2013). The degradation of mucin could have several benefits for *T. forsythia* and *P. gingivalis*, so this dual-enzyme synergy might contribute directly to periodontal disease, but it might be countered by sialidase inhibition- which was not directly tested here given the difficulty in establishing this defined media. Given the potential of mucin as a nutrient source for pathogens, and that evasion of mucin prevents entrapment of pathogens, the ability to degrade mucin represents a potential boon for pathogen proliferation. Since sialic acid is a major component of mucin protecting it from degradation, and may itself represent a nutrient source, the ability to desialylate mucin represents an important virulence mechanism for pathogens.

Given this enzymatic synergy observed, it was essential to test whether the sialate esterase activity might boost growth of *P. gingivalis* on diacetylated sialic acid glycoprotein sources. Although amino acids or carbohydrates released from host glycoproteins could bolster periodontal pathogen growth, this is difficult to study using monoculture-based approaches due to the presence of other nutrients in the growth media. In this work, *P. gingivalis* alone appeared to be capable of growth in defined media containing only serum glycoproteins as carbon sources, even in iron limited conditions (where no exogenous hemin was added to culture). Furthermore, *P. gingivalis* growth was bolstered by the presence of human saliva, implying that saliva does provide additional nutrients for *P. gingivalis*. The heavily glycosylated salivary mucins compose a significant proportion of the salivary

glycoproteome, so these could be an important nutrient source for *P. gingivalis*, and are thought to be rich in diacetylated sialic acid (Phansopa et al. 2015; Varki & Diaz 1983), which could hinder the ability of *P. gingivalis* sialidase to act on sialylated mucins. In turn, failure to remove sialic acid could render mucins less susceptible to proteolysis by the gingipains, denying *P. gingivalis* a source of amino acids for metabolism, or at least slowing amino acid/peptide release. Since *T. forsythia* NanS can remove the second acetyl group, it might make salivary mucins more susceptible to proteolysis-thus boosting the growth of *P. gingivalis*. Indeed, this was shown to be the case in this chapter: NanS increased the growth of *P. gingivalis* with serum and saliva as sole carbon and nitrogen sources, and perhaps *in vivo* NanS also aids *P. gingivalis* in nutrient acquisition at the periodontium. Further evidence for increased proteolysis of host sialoglycoproteins due to NanS de-acetylation could be obtained by treating saliva, serum or mucin with gingipains or *P. gingivalis* culture supernatant, in the presence or absence of NanS, followed by SDS-PAGE and staining for (glyco)protein.

Further work using defined media could use mixed species cultures of *P. gingivalis* and *T. forsythia* (and *F. nucleatum*) to find if the pathogens support each other during nutrient acquisition from host sialoglycans and subsequent growth. In addition to the possibility of testing the importance of sialidase for single species (*T. forsythia* or *P. gingivalis*) or mixed species pathogen cultures using *T. forsythia* or *P. gingivalis* mutants deficient in NanH or SiaPG, our lab group has also recently generated a *T. forsythia* mutant strain deficient in NanS, so the contribution of NanS to *T. forsythia* or mixed-periodontal pathogen nutrient acquisition from host sialoglycoproteins could also be examined. In addition to these more conventional growth studies, these effects of sialidase or NanS deficiency could be tested in biofilm assays using defined media instead of TSB. This might also result in more pronounced differences in biofilm formation in the presence of zanamivir, since the sole nutrient source in these assays would be the sialoglycoproteins.

P. gingivalis biofilm formation on surfaces coated with serum, saliva, and mucin was shown to be decreased in the presence of zanamivir. Although the decrease in biofilm formation was only up to ~one third (in the cases of biofilm formation on mucin and saliva), relative to the absence of zanamivir, the assay did take place over five days-a shorter incubation time might have yielded a more striking difference between zanamivir and no-zanamivir conditions. In any case, zanamivir did decrease *P. gingivalis* biofilm formation significantly on human saliva, and to varying degrees on mucin, serum and slightly in Neu5Ac

supplemented media. Furthermore, total (planktonic and biofilm) growth of *P. gingivalis* was only significantly inhibited by zanamivir in mucin-coated conditions (though it was slightly inhibited in the other conditions). Considering this, it could be the case that the *P. gingivalis* sialidase is important for attachment to host glycoproteins, and this aids in biofilm formation, while the importance of sialidases for *P. gingivalis* nutrient acquisition was less important. However, this experiment did take place in Tryptic Soy Broth (TSB) with 2% Yeast Extract, conditions which are rich in amino acids for *P. gingivalis* to metabolise, possibly rendering the glycoprotein coated surfaces less important from a nutritional perspective; i.e. in less nutrient rich conditions, the host glycoproteins might have been an important source of nutrients, and the presence of zanamivir might have made a more striking difference to *P. gingivalis* biofilm formation.

It was also observed that mucin decreased both the biofilm formation and total growth of *P. gingivalis* compared to the other conditions, and that the presence of zanamivir resulted in further decreases in biofilm formation. Salivary mucins have been shown to display growth- or- biofilm inhibitory activity against oral bacteria, particularly against streptococci (Frenkel & Ribbeck 2015; Wei et al. 2006). Against *P. gingivalis*, peptides derived from the N-terminal of MUC7 have been shown to inhibit growth, although this does require high peptide concentrations (the MIC reported in the study is $>100\mu\text{M}$) (Wei et al. 2006). In this assay, $6\mu\text{M}$ mucin was sufficient to inhibit *P. gingivalis* biofilm formation and planktonic growth, and zanamivir further decreased biofilm formation. The difference might be due to the strains used: In the above study (Wei et al. 2006), the encapsulated strains W50 and 381 were used, but in the biofilm assays described here the non-encapsulated ATCC 33277 was used; perhaps the absence of a capsule renders *P. gingivalis* more susceptible to the inhibitory effects of salivary mucin, and *P. gingivalis* growth is further inhibited by the presence of zanamivir, possibly because mucin glycoproteins are less susceptible to proteolysis if they retain their sialic acid, meaning the mucin-derived peptides retain their inhibitory properties. Therefore, the biofilm experiments described here could be repeated with encapsulated strains and with clinical isolates (obtained from patients attending the University of Sheffield Dental Hospital).

Regarding *T. forsythia*, Neu5Ac has been shown to substitute the requirement for exogenous NAM in *T. forsythia* biofilm formation, and a sialidase deficient *T. forsythia* mutant strain has been shown to display reduced biofilm formation on host glycoproteins relative to its parent strain. Furthermore, inhibition of biofilm formation on host

glycoproteins in wild type *T. forsythia* is also seen in the presence of the sialidase inhibitor oseltamivir (Roy et al. 2010; Roy et al. 2011). Given this, it was hoped that zanamivir could also inhibit biofilm formation. Unfortunately, the above results indicated that zanamivir does not significantly inhibit biofilm formation under the current experimental conditions. This might be expected given the results shown in chapter 2 (section 2.3.7), which appear to indicate that zanamivir is not an efficacious inhibitor of *T. forsythia* sialidase activity-10mM zanamivir only inhibits *T. forsythia* sialidase activity on the model sialic acid ligand MUNANA by 25%, whereas for *P. gingivalis* this figure was ~80%.

3.5 Summary

Sialic acid, its underlying glycan chain, and the proteinaceous components of human sialoglycoproteins represent potential nutrient sources for bacteria, and the ecological niche in which periodontal pathogens exist is an environment rich in sialoglycoproteins. From a nutritional perspective, release of sialic acid could directly benefit pathogens with appropriate uptake and catabolic pathways, as in the case of *T. forsythia* and *F. nucleatum*, or render proteins more susceptible to proteolytic digestion in organisms lacking these pathways, as in the case of *P. gingivalis*. In addition, sialyl groups on host glycoproteins might represent a barrier to pathogens attempting to attach to underlying glycans, and their desialylation could boost pathogen attachment. Therefore, sialidases could play important roles in periodontal pathogen nutrition and attachment to host surfaces, both of which could contribute to biofilm formation, with consequences for periodontal disease. Furthermore, *T. forsythia* secretes an accessory enzyme, NanS, which removes a second, protective acetyl- group from sialic acids present on oral glycoproteins and this may boost sialic acid release by sialidases from other periodontal pathogens.

Experiments presented in this chapter showed that *T. forsythia* NanS doubled sialic acid release from salivary mucin (which is rich in diacetylated sialic acid) by the *T. forsythia* and *P. gingivalis* sialidases NanH and SiaPG, with SiaPG & NanS displaying the greatest amount of sialic acid release, and this sialic acid release was inhibited by zanamivir. This perhaps suggests interspecies co-operation in sialic acid release from oral host-glycoproteins. This prompted further work investigating the impact of NanS on *P. gingivalis* growth on host sialoglycoproteins as sole carbon and nitrogen sources: *P. gingivalis* was capable of growing on serum alone, and growth was increased in the presence of human saliva. Growth of *P. gingivalis* on saliva and serum, but not serum alone, was increased in the presence of *T. forsythia* NanS, providing support for the theory that sialic acid release from saliva (which contains glycoproteins rich in diacetylated sialic acid) is important for *P. gingivalis*

nutritional purposes, possibly by rendering glycoproteins more susceptible to proteolytic cleavage, releasing amino acids or peptides which can be catabolised by *P. gingivalis*.

Finally, the ability of *T. forsythia* and *P. gingivalis* to form biofilms on surfaces coated with host glycoproteins, and the potential to inhibit them with zanamivir was investigated. Only *P. gingivalis* biofilm formation was significantly inhibited by zanamivir, and the lack of inhibition for total growth (planktonic and biofilm growth) of *P. gingivalis* might suggest that biofilm formation was inhibited because *P. gingivalis* was unable to attach to the glycoprotein coated surfaces in the presence of zanamivir, rather than zanamivir causing inhibiting nutrient acquisition. Future biofilm studies might test the formation of *P. gingivalis* biofilms on host glycoproteins in defined media, or quantify the impact of sialidase inhibition on mixed-species biofilms.

As well as mediating bacterial growth and biofilm formation, it was considered likely that periodontal pathogen sialidases play roles pathogen interactions with host cells, including attachment and invasion of host cells by bacteria, and modulation of the host innate immune response. The latter is particularly important for periodontitis since host inflammation is responsible for the tissue destruction seen in periodontal disease. With this in mind, work described in the next chapter aimed to investigate the role of *T. forsythia* and *P. gingivalis* sialidases in host-pathogen interactions, and the potential for sialidase inhibitors to disrupt these interactions.

Chapter 4

The Role of Sialidases in Host- Pathogen Interactions, and Disruption by Sialidase Inhibition

4 Chapter 4: The Role of Sialidases in Host-Pathogen Interactions, and Disruption by Sialidase Inhibition

4.1 Introduction

Pathogen sialidases have been implicated in a variety of host-pathogen interactions by studies of sialidase-gene knockout bacteria: One of the most well studied pathogens in this regard is the nasopharyngeal commensal and pathogen *Streptococcus pneumoniae*, which possess three sialidases; NanA, B, and C. *S. pneumoniae* mutants deficient in NanA or NanB show decreased attachment to host cells *in vitro* (Brittan et al. 2012). Mouse models of respiratory tract infection also highlight the importance of sialidases during infection with *S. pneumoniae*; NanA and B mutants lack the ability to colonise the lungs and nasopharynx in a respiratory infection model, and are unable to cause sepsis if intravenously administered (Manco et al. 2006).

Sialidase is also important for virulence of the gut pathogen *Vibrio cholerae*, with the most virulent serotypes (the toxigenic O1 and at least one strain of O139) possessing a sialidase (NanH) and sialic acid utilisation genes (Jermyn & Boyd 2002). NanH (and sialic acid utilisation) is a multifunctional virulence factor for *V. cholera*: It has been shown to act in synergy with the cholera toxin during virulence, unmasking the cholera toxin receptor, the GM1 ganglioside on intestinal epithelial cells (Venerando et al. 1982; Galen et al. 1992). Most importantly, *V. cholerae* mutant strains deficient in *nanH* show decreased virulence in mouse models of cholera (Galen et al. 1992). *V. cholerae* also possesses sialic acid utilisation genes (*nan-nag* genes) (Jermyn & Boyd 2002). This is likely to confer a growth advantage *in vivo*, and indeed *V. cholera* is able to grow using sialic acid as a sole carbon source (*in vivo* this is presumably obtained by release from host sialoglycans by NanH), and *nanH*-deficient mutants possess a decreased ability to colonise the mouse intestine (Almagro-Moreno & Boyd 2009), although this may also be due to decreased attachment of *V. cholerae* rather than decreased growth.

Periodontal pathogens have also been subjected to sialidase knockout. *T. forsythia nanH* sialidase mutants ($\Delta nanH$) displayed decreased attachment to oral epithelial cells compared to wild type *T. forsythia* (Honma et al. 2011). Different strains of *P. gingivalis* have also been made deficient in SiaPG (PG0352, $\Delta siaPG$) (Li et al. 2012; Aruni et al. 2011), although the exact implications for virulence are less clear because the sialidase mutants display defects in capsule formation, although $\Delta siaPG$ strains do show decreased association with oral epithelial cells (Aruni et al. 2011; Li et al. 2012). The virulence of

Δ siaPG mutants in a mouse abscess model is also decreased relative to the parent strain, where subcutaneous injections of wild type *P. gingivalis* (strain W83) resulted in the formation of abscesses and ultimately lethal infection (the mice died within 6 days), and both abscess formation and lethality were not seen in mutant *P. gingivalis* W83 Δ siaPG (Li et al. 2012). Finally, sialidase deficient mutants of *Treponema denticola* have also been studied, and these display reduced complement evasion and decreased virulence in a mouse abscess model, where sialidase deficient *T. denticola* induced smaller lesions relative to their parent strain (Kurniyati et al. 2013).

Given the apparent importance of sialidase expression for periodontal pathogen-host interactions, and subsequent virulence, abrogation of sialidase activity using sialidase inhibitors might have anti-virulence effects. This chapter discusses the ability of purified SiaPG and NanH to desialylate host cells, and the influence of zanamivir in disruption of host-pathogen interactions of *T. forsythia*, *P. gingivalis*, and the sialidase negative bacterium *Fusobacterium nucleatum*. Specifically, the ability of zanamivir to disrupt attachment and invasion of periodontal pathogens to oral epithelial cells, and the influence of pathogen sialidases and zanamivir on oral epithelial cell pro-inflammatory responses were investigated. Despite the seemingly-limited ability of zanamivir to inhibit *T. forsythia* sialidase activity, and no effect of *T. forsythia* biofilm formation, zanamivir was capable of inhibiting SiaPG and NanH to a lesser extent extent, as well as having some inhibitory effect on *P. gingivalis* biofilm formation. Furthermore, zanamivir is a well characterised active ingredient licensed globally for use in human medicines with a wealth of pharmacology and toxicology profiling-meaning that it might transition more easily into a novel periodontitis therapeutic than a completely new active ingredient.

4.2 Materials and Methods-The Role of Sialidases in Host-Pathogen Interactions, and Disruption by Sialidase Inhibition

4.2.1 Culture of Human Cell Lines

Immortalized human oral keratinocytes (OKF6/Tert2) (Dickson et al. 2000) were kindly provided by Dr J. Rheinwald (Harvard Medical School, Cambridge, MA) and were grown in keratinocyte-serum free media supplemented with defined growth supplements (DKSFM, Fisher Scientific, Loughborough, UK). Cells were grown to 70–90% confluence and media was changed every 2–4 days. The Oral Squamous Cell Carcinoma (OSCC) cell line H357 (Thomas et al. 2001; Sugiyama et al. 1993)-a generous gift from Professor S. Prime, University of Bristol, UK-was grown in Dulbecco's Modified Eagle Medium (DMEM) supplemented with 10% (v/v) foetal bovine serum (FBS), 2mM L-glutamine, and 100units/ml Penicillin-Streptomycin (Sigma Aldrich). Cells were incubated at 37°C, 5% CO₂ when not undergoing media changes or passaging.

4.2.2 Antibiotic Protection Assays

OKF6 or H357 cells were cultured as described, and resuspended at a density of either 1.2×10^5 - 2×10^5 cells ml⁻¹ in DKSFM or DMEM, and seeded into the wells of a 24-well tissue culture plate (Greiner, UK), 1 ml of suspension per well. Each experiment required a control condition (no sialidase inhibitors) and a sialidase inhibition condition (media for assay supplemented with 10 mM zanamivir), both repeated in triplicate, and in duplicate on two plates; one plate for "total associated" bacteria, and one for "invaded" bacteria. To allow adherence to the plates, cells were incubated as above for approximately 18 hours if seeded at 2×10^5 , or 48 hours if seeded at 1.2×10^5 cells/ml. After incubation, media was removed and the cells in one well were detached by trypsinisation and counted by haemocytometry, to determine the number of cells per well.

The remaining cells were incubated for 1 hour in DKSFM or DMEM supplemented with 2% BSA, then washed twice with PBS pH 7.4 (Sigma Aldrich). Bacteria for use in the antibiotic protection assay were resuspended in DKSFM, and quantified using a Helber chamber (Hawksley) under phase contrast microscopy, 400 x magnification. Bacterial suspensions were diluted to a ratio of 1:100 host cells: bacteria in DKSFM or DMEM, either unsupplemented (for negative controls) or supplemented with 10mM zanamivir (for testing the effect of sialidase inhibition). Additionally, bacterial suspension (conditions with and without zanamivir) were added to empty wells of the "invasion" plate. These bacteria form the bacterial "viability" control.

These suspensions were incubated with the host cells at 37 °C, 5 % CO₂ for 1.5 hours, or in empty wells containing no host cells. After incubation, the wells were washed twice with PBS, and DKSFM or DMEM supplemented with 200 µg/ml metronidazole (and for the sialidase inhibition condition, with 10 mM zanamivir) was added to wells of the designated “invasion” plate, then incubated at 37 °C, 5 % CO₂ for 1 hour. Media from wells containing bacteria and host cells for “total associated” and “invaded” conditions was removed, and cells were washed twice with PBS before lysis using 200 µl of deionised water (dH₂O) and scraping with a pipette tip for one minute. The “viability” control bacteria were resuspended by pipette mixing.

Bacteria obtained from the suspension of the “viability” wells, and cell lysates of the “total associated” and “invasion” wells then underwent four tenfold serial dilutions, and the undiluted suspensions and serial dilutions were plated onto agar by Miles-Misra methodology; each serial dilution and bacterial suspension was given three 10µl spots onto agar appropriate for the organism, and incubated under the previously described conditions. Incubation times for bacteria were 1.5-2 times longer than those listed above.

After incubation and colony counting, the following formula was used to determine the number of bacteria/ml in each well of the “total associated” “invasion” or “viability” plates:

$$\text{number of colonies} \times \text{dilution factor} \times 20 = \text{number of bacteria/ml}$$

After ascertaining the mean number of viable bacteria/ml from the “viability” controls for no sialidase inhibitor and 10mM zanamivir conditions, it was possible to calculate the percentage of viable bacteria that were associated with and had invaded the OKF6 cells using the following formula, and by subtracting percentage invaded from the percentage associated, the number of attached bacteria was obtained:

$$\frac{\text{Number of bacteria/ml}}{\text{mean viable number of bacteria}} \times 100 = \% \text{ Viable bacteria}$$

4.2.3 Cell Viability Assays

4.2.3.1 MTT Assays

MTT assays were only used to test the effect of zanamivir on cellular metabolism in OKF6 cells. 100µl of OKF6 cells in DKSFM were seeded at a density of 2x10⁵ cells/ml into the wells of a 96 well tissue culture plate (Greiner), and incubated for 24 hours at 37°C, 5% CO₂. Cells were then washed twice with PBS, and media supplemented with 1000 µg/ml MTT, and 0, 2.5, 5, 7.5, or 10 mM zanamivir was added. Cells were incubated for 2.5 hours at 37 °C, 5 %

CO₂. MTT-supplemented DKSFM was removed, and cells were washed twice using PBS. Next, formazan crystals (formed by metabolism of MTT by viable OKF6 cells) were solubilised using acidified isopropanol (Isopropanol supplemented with 0.125 % HCl). Levels of formazan were quantified by measuring absorbance at 540 nm with a reference at 630 nm using a Tecan Infinite M200 plate reader.

4.2.3.2 ***LDH Assays***

LDH assays rely on detection of lactate dehydrogenase, released from lysed or porous cells into culture supernatant. Quantification of LDH in supernatants from H357 cells (during cytokine secretion experiments, section 4.2.5) and OKF6 cells (during zanamivir cytotoxicity testing) in various experiments was performed using the cytotox 96 LDH assay kit (Promega), according to manufacturer's instructions. Briefly, the assay detects the presence of LDH in culture supernatant by formation of a red formazan salt by components of a proprietary assay buffer and LDH, by mixing 50 µl of assay buffer with 50 µl of culture supernatant, incubating at 37 °C for 30 minutes, and quenching the reaction with a 25 µl of a proprietary stop solution. Reaction optical density is then measured at OD₄₉₀ to quantify LDH. A negative control consisting of media alone was used in all assays.

In the case of H357 cells in cytokine secretion experiments, cell culture supernatants were harvested at different time points, having been exposed to a number of conditions (see section 4.3.5 for conditions and time points). 50 µl of culture supernatant immediately underwent the LDH assay prior to storage at -20 °C. In the case of OKF6 cells, an experiment was designed to replicate the exposure to zanamivir seen in the antibiotic protection assay. A 96-well tissue culture plate (Greiner) was seeded with 25000 OKF6 cells/well in 100 µl of DK-SFM and incubated overnight at 37 °C, 5 % CO₂. Supernatant was removed, cells washed twice with PBS, and replaced with 100µl of either DKSFM or DKSFM with 10 mM zanamivir, and incubated for 2.5 hours at 37 °C, 5 % CO₂. 50 µl of this culture supernatant immediately underwent the LDH assay.

4.2.4 **Immuno-Fluorescence Microscopy; Visualisation of Cell-Surface Sialic Acid**

4.2.4.1 ***Lectin Staining for Host Cell Surface Sialic Acid***

H357 cells were passaged as described (section 4.2.1) and seeded at a density of 1.5x10⁵ cells/ml in DMEM into the wells of a 24-well tissue culture plate which contained sterile glass coverslips (BDH). These were incubated at 37 °C anaerobically for 18 hours before undergoing sialic acid staining (or enzyme treatment before staining).

Cells underwent sialic acid staining using lectins from *Sambucus nigra* (SNA), *Maackia amurensis* (MAA), or *Cancer antennarius* agglutinin (CAA) (Vector Labs). These lectins are specific for α 2-6, α 2-3 linked Neu5Ac, and diacetylated sialic acids (including Neu5,9Ac), respectively. After treatment, cells were washed twice with 500 μ l PBS followed by application of lectins: 4 μ g/ml SNA- fluorescein isothiocyanate conjugate (SNA-FITC, Vector labs) or 8 μ g/ml biotinylated-MAA (Vector labs), for 30 minutes at 37 °C, 5 % CO₂. Cells were washed twice with 500 μ l PBS and in conditions containing Biotinylated lectin, underwent a second incubation with 2 μ g/ml Texas Red-Streptavidin, for 30 minutes at 37 °C. Lectin stained cells were washed three times with 500 μ l PBS and fixed with 500 μ l 2 % (w/v) Paraformaldehyde for 15 minutes at 37 °C. Coverslips with fixed cells were removed from wells and mounted onto glass slides with ProLong Gold Antifade Mountant (containing DAPI, ThermoFisher Scientific). Mounted cells were incubated for at least 18 hours and visualised within one week.

4.2.4.2 ***Antibody Staining for Host Cell Surface Sialyl Lewis A and X***

H357 cells were passaged as described (section 4.2.1) and seeded at a density of either 1.5x10⁵ cells/ml in DKSFM or DMEM into the wells of a 24-well tissue culture plate which contained sterile glass coverslips (BDH). These were incubated at 37 °C anaerobically for 18 hours before undergoing staining for sialyl lewis A (SLeA) or sialyl lewis X (SLeX) (or enzyme treatment before staining).

Cell monolayers were washed twice with PBS. Murine Anti-SLeA IgG1 (Invitrogen), or murine Anti-SLeA IgM (Sigma-Aldrich) was diluted 1 in 500 in PBS, and incubated with washed epithelial cell monolayers for 30 minutes, at 37 °C. In isotype control conditions, non-specific rabbit IgG1 (Invitrogen) or murine IgM (Sigma-Aldrich) was diluted 1 in 500 in PBS, and incubated with cell monolayers in place of anti-SLeA/X antibodies.

Anti-SLeA/X Antibodies were removed, and cells were washed three times in PBS. A secondary antibody-Goat anti-Mouse IgG1-FITC conjugated-was diluted 1 in 500 in PBS and applied to the cells, and incubated for 30 minutes at 37 °C. Stained cells were washed three times with PBS, and fixed using 2 % (w/v) paraformaldehyde for 15 minutes at 37 °C. The use of FITC conjugated secondary antibodies enabled visualisation of Sialyl Lewis A/X with fluorescence microscopy.

Coverslips with fixed cells were removed from wells and mounted onto glass slides with ProLong Gold Antifade Mountant (containing DAPI, ThermoFisher Scientific). Mounted cells were incubated for at least 18 hours and visualised within one week.

4.2.4.3 *Enzymatic Treatment of Host Cell Surfaces*

Prior to the staining described above, H357 cell monolayers were treated with the purified periodontal pathogen sialidases NanH and SiaPG. Sialidases were diluted to 100 nM in PBS, added to the oral epithelial cell monolayers, and incubated at 37 °C for 2 hours. Enzymes were removed and monolayers washed twice before undergoing lectin or antibody staining. For sialidase inhibition conditions, 10 mM zanamivir was included during enzyme treatment of oral epithelial cells.

4.2.4.4 *Fluorescence Microscopy, Image Processing, and Sialic Acid Quantification*

Slides were visualised using an Axiovert 200M fluorescence microscope (Zeiss) and associated Axiovert software (Zeiss). Slides were imaged at 100 x, 400 x, or 1000 x magnification. To allow comparison of sialic acid staining, images of different conditions in the same experiment were captured using the same parameters for fluorescence intensity and weighting, and exposure time for a given fluorescence colour channel.

All images were processed using Fiji-imageJ, Software (Schindelin et al. 2012 freely available at <https://fiji.sc/>). Fluorescence background subtraction was performed for all images using the same parameters for each fluorescence colour channel in a given experiment.

For surface staining quantification, three fields of view were imaged at 400 x magnification, processed as described, and the mean pixel brightness of each image was obtained. Cell nuclei were manually counted to obtain the number of cells in each image, and the level of staining expressed as Mean Fluorescence Intensity (MFI) per cell.

4.2.5 *Immune-Signalling in Oral Epithelial Cells*

4.2.5.1 *Cell Treatments and Harvesting of Conditioned Media*

H357 cells were cultured as described, resuspended at a density of 2×10^5 cells/ml in DMEM (10 % serum, 2 mM L-glutamine), and seeded into the wells of a 6-well tissue culture plate (Greiner, UK), 2ml of suspension per well. Cells were incubated for 18-24 hours at 37 °C, 5 % CO₂, and exposed to a variety of different conditions (table 4.3), each condition was performed in duplicate during each experiment. Prior to treatment, one well underwent trypsinisation and haemocytometry to obtain the number of cells per well at the start of the experiment. In conditions with live bacteria, cells were seeded at a given multiplicity of infection (MOI). Treated cells were incubated for 4 or 24 hours at 37 °C, 5 % CO₂. Supernatants were collected, and cells were either detached from wells by trypsinisation

and counted by haemocytometry as described, or were lysed using lysis buffer; RIPA buffer, Sigma, with DNase (Sigma-Aldrich), and Protease Inhibitor Cocktail (Roche), with cell lysates stored at -20°C. Collected supernatants immediately underwent an LDH assay (section 4.2.3.1), before storage at -20 °C before ELISA.

Condition	Concentration or Seeding Density	Serum	Commercial ELISA kit
Untreated	-	0.1% or 10%	BD Biosciences & BioLegend
Zanamivir	10mM	0.1% or 10%	BD Biosciences & BioLegend
<i>T. forsythia</i>	1:50 -or- 1:100 -or- 1:200	0.1% or 10%	BD Biosciences & BioLegend
<i>P. gingivalis</i>	1:50 -or- 1:100 -or- 1:201	10%	BD Biosciences & BioLegend
<i>T. forsythia</i> , zanamivir	1:100, 10mM	0.1 or 10%	BD Biosciences & BioLegend
<i>P. gingivalis</i> , zanamivir	1:100, 10mM	10%	BD Biosciences & BioLegend
<i>T. forsythia</i> ΔNanH	1:100,	0.1 or 10%	BD Biosciences & BioLegend
<i>T. forsythia</i> ΔNanH, zanamivir	1:100, 10mM	0.1 or 10%	BD Biosciences & BioLegend
LPS	1, 10, or 100 ng/ul	10%	BioLegend
NanH	50nM	10%	BioLegend
LPS, NanH	10ug/ml, 50nM	10%	BioLegend
LPS, NanH, zanamivir	10ug/ml, 50nM,	10%	BioLegend

Table 4.1. Cell treatment conditions for IL-8 cytokine analysis.

Cells in 6-well tissue culture plates were treated with the above conditions, 2 ml of each treatment condition per well, and processed as described. Some conditions were tested at different concentrations, and different serum concentrations were tested in some conditions as indicated. LPS: Lipopolysaccharide extracted from *P. gingivalis*, NanH: purified NanH treated with polymixin agarose. Seeding density: Multiplicity of infection (MOI), the ratio of host: bacterial cells.

4.2.5.2 *P. gingivalis* Lipopolysaccharide Extraction

P. gingivalis ATCC33277 LPS was extracted using a commercially available LPS extraction kit (IntronBio). Briefly, *P. gingivalis* was cultured in liquid media as described, to an OD₆₀₀ of 3-5. Culture was transferred to microfuge tubes and centrifuged at 13000 g to pellet bacteria. Supernatant was removed, lysis buffer added and mixed thoroughly by vortex. 200 µl chloroform was added, mixed, and incubated at room temperature for 5 minutes. Reactions were centrifuged at 13000 g for 20 minutes, and the upper fraction of the reaction (easily distinguished due to its appearance (clear and colourless compared to the

dark and turbid lower fraction) was transferred to a pre-weighed microfuge tube. 800 µl of purification buffer was added, and the reaction incubated at -20 °C for 10 minutes before centrifugation at 13000 g for 20 minutes. Supernatant was removed, and 1 ml 70 % ethanol added and mixed by inversion. The reaction was centrifuged at 13000 g for 3 minutes and the supernatant removed, the pellet was air dried for 5 minutes and dried using an Eppendorf SpeedVac leaving purified LPS. LPS was dissolved in Tris HCl, pH 8.0 and incubated at 95 °C for 5 minutes.

4.2.5.3 ***Quantification of the Pro-Inflammatory Cytokine IL-8 by ELISA***

Cell supernatants were thawed and processed using commercially available CXCL8 ELISA kits (Biolegend or BD Biosciences).

Buffers for both kits are described in table 4.4. Capture antibody was diluted in capture buffer according to kit-specific recommendations and incubated in 96-well Nunc Maxisorp ELISA plates (Sigma-Aldrich) overnight at 4 °C. Wells were aspirated and washed three times with 300 µl wash buffer, and blotted with absorbent paper to remove residual buffer. 200 µl blocking buffer was added to wells and incubated for two hours at room temperature (~20 °C), and washed as above. A standard curve of CXCL8 concentrations were prepared by dilution of CXCL8 in assay diluent, and cell supernatants were diluted 3-4 fold in assay diluent, added to wells, and incubated for 2 hours at room temperature. Wells were washed five times as above, and 100 µl of working detector (or detection antibody alone in the case of the biolegend kit) was added to the wells. Plates were sealed and incubated for 1 hour at room temperature, and washed seven (or five) times as described. The Biolegend kit required an extra step at this point, where working detector was added to wells and washed seven times. Substrate solution was added to each well. Reactions were incubated for 30 minutes at room temperature in the dark, and 50 µl of stop solution was added. The absorbance at 450 nm and 570 nm was obtained using a TECAN M200 plate reader, the absorbance at 570 nm subtracted from absorbance at 450 nm, and the CXCL8 standard curve was applied to quantify CXCL8 (pg/ml) for cell supernatant. This could be standardised to cell counts (haemocytometry) or cell lysate protein content (obtained using BCA) to provide CXCL8 pg/ml/cell, or CXCL8 relative to cellular protein (% w/w), although results shown here are not standardised, in accordance with the bulk of the literature.

Kit	Buffer Name	Composition
BioLegend	Capture Buffer	Proprietary kit buffer + capture antibody 1:200 (antibody:buffer)
BioLegend	Wash Buffer	PBS+0.05% (v/v) Tween-20
BioLegend	Blocking Buffer	Proprietary kit buffer, diluted five fold with PBS
BioLegend	Assay Diluent	Proprietary kit buffer, diluted five fold with PBS
BioLegend	Working Detector	HRP-avidin
BioLegend	Substrate Solution	Proprietary kit buffer
BioLegend	PBS	137 uM NaCl, 8.2uM Na ₂ HPO ₄ , 1.5uM KH ₂ PO ₄ , 2.7uM KCl, pH 7.0
BDbiosciences	Capture Buffer	85mM sodium carbonate, 15mM sodium bicarbonate, pH 9.5
BDbiosciences	Wash Buffer	PBS+0.05% (v/v) Tween-20
BDbiosciences	Blocking Buffer	PBS+10% FBS
BDbiosciences	Assay Diluent	PBS+10% FBS
BDbiosciences	Working Detector	Detection Antibody+Streptavidin-Horseradish Peroxidase
BDbiosciences	Substrate Solution	Tetramethylbenzidine
BDbiosciences	PBS	137 uM NaCl, 8.2uM Na ₂ HPO ₄ , 1.5uM KH ₂ PO ₄ , 2.7uM KCl

Table 4.2. ELISA kit buffers.

PBS-Phosphate Buffered Saline, HRP-Avidin-Horseradish Peroxidase-streptavidin conjugate, capture antibody-biotinylated anti CXCL8 antibody, FBS-foetal bovine serum.

4.2.5.4 *Multiplex Cytokine Bead Array*

The University of Sheffield offers an in house service for detection of multiple cytokines in cell culture supernatants. This makes use of a Bead-based array supplied by BDbiosciences, the “BD Cytometric Bead Array (CBA)”. Briefly, antibodies against the protein of interest are immobilised onto fluorescent beads, which is incubated with a given sample. A fluorescent antibody against the protein of interest is then applied, and the bead’s fluorescence increases relative to the concentration of the protein of interest. Reactions containing known concentrations of the protein of interest are also performed, to produce a standard curve of known protein concentration. This is applied to quantify the protein of interest. In this project, this involved detection of cytokines that were suspected to be secreted by oral epithelial cells and might be influenced during infection with *T. forsythia*, and treatment with 10mM zanamivir. The cytokines quantified were Granulocyte Colony Stimulating Factor (GCSF), Interleukin -6, -8 (IL-6, IL-8), Monocyte Chemoattractant Protein (MCP-1), Macrophage Inflammatory Protein (MIP1 α), and Tumour Necrosis Factor (TNF), further details are shown in table 5.3.

Name	Abbreviation	Also Known As	Functional Notes	Reference (Relevance to Oral Epithelium or Periodontitis)
Granulocyte Colony Stimulating Factor	GCSF	Colony Stimulating Factor 3 (CSF 3)	Stimulates activity and replication of Granulocytes of Neutrophil lineage. Particularly mature neutrophils.	(Sugiyama et al. 2002; Shaddox et al. 2011; Ramage et al. 2016)
Interleukin-6	IL-6	Interferon- β -2 (IFN- β 2)B cell stimulating factor (BSF-2), hepatocyte stimulating factor (HSF), others.	Many functions in stimulation of innate and adaptive immunity, hence its numerous aliases.	(Shaddox et al. 2011; Morandini et al. 2010b; Ara et al. 2009; Ramage et al. 2016)
Interleukin-8	IL-8	Chemokine (C-X-C motif) Ligand 8, Neutrophil Attractant Factor	Chemoattractant for Leukocytes, primarily neutrophils. Other pro-inflammatory effects on other cell types in high concentrations.	(Shaddox et al. 2011; Sugiyama et al. 2002; Ramage et al. 2016)
Monocyte Chemoattractant Protein-1	MCP-1	Chemokine (C-C motif) Ligand 2 (CCL2)	Chemoattractant for monocytes.	(Shaddox et al. 2011; Pradeep et al. 2009)
Macrophage Inflammatory Protein 1α	MIP1 α	Chemokine (C-C motif) Ligand 3 (CCL3)	Chemoattractant of granulocytes and innate immune cells including T-lymphocytes.	(Morandini et al. 2010b; Shaddox et al. 2011)
Tumour Necrosis Factor	TNF	TNF α , TNF superfamily member 2	Activates pro-inflammatory responses in all cell types through NF κ B and JNK (MAPK) pathways.	(Shaddox et al. 2011; Ramage et al. 2016; Davanian et al. 2012)

Table 4.3. Cytokines produced by oral epithelial cells.

The cytokines outlined were considered likely to be produced by oral epithelial cells, important in periodontitis, and could be assayed for using the CBA produced by BD Biosciences.

The above cytokines were detected using a Cytometric Bead Array (CBA) Human Inflammatory Cytokines Kit (BD Biosciences, USA), following the manufacturer's instructions for quantification of cytokines from cell culture supernatant (full instructions available at http://www.bdbiosciences.com/external_files/Doc_Recon_2.0/pm/others/23-11112.pdf). Acquisition was performed with a BD FACSarray flow cytometer (BD Biosciences, Belgium), and initial data processing was performed using FCAP Array™ V3.0 software. Cytokine bead arrays were performed as part of a service offered by the Flow Cytometry Core Facility in the School of Medicine and Biomedical Sciences, University of Sheffield. Further data processing and application of cytokine standard curves was performed using Graphpad Prism V 7.0 software.

4.3 Results

4.3.1 Zanamivir has no Detrimental Effects on Oral Epithelial Cell or Periodontal Pathogen Viability

Experiments described in this and the previous chapter involved exposure to zanamivir in an attempt to inhibit the sialidase activity of pathogens or purified sialidases, and observe the effect of pathogen sialidase inhibition in models of disease processes. The apparent ability of zanamivir to inhibit host-pathogen association, or to inhibit cytokine secretion could be explained by a detrimental effect of zanamivir on host cell viability or metabolism: i.e. If the host cells were killed by zanamivir (and subsequently lysed), the number of bacteria able to attach and invade during the antibiotic protection assays would appear reduced, or fewer cytokines would be produced since cell numbers are lower. These results could also occur due to bacterial killing, since dead pathogens might be less likely to illicit an immune response, or would not form colonies on agar plates during the antibiotic protection assay. Bacterial killing could also explain some of the detrimental effects of zanamivir on *P. gingivalis* biofilm formation and growth in sialoglycan-supplemented minimal media seen in the previous chapter (sections 3.3.2).

Considering the above, it was important to assess the effects of zanamivir on the viability of oral epithelial cells bacteria.

4.3.1.1 Zanamivir has no Effect on Oral Epithelial Cell Viability

Data obtained during experiments described in section 4.3.5, as well as some additional experiments showed that zanamivir did not influence epithelial cell-line viability: Firstly, during the cytokine secretion experiments (section 4.3.5) culture supernatant was harvested and underwent an assay to detect the usually-cytosolic enzyme lactate dehydrogenase (LDH), a commonly used indicator of cell lysis. This assay relies on the production of a red formazan salt by LDH, which can be quantified by spectrophotometry. No significant differences in LDH levels were observed in culture supernatants from any of the conditions, as determined by one-way ANOVA with Tukey's correction for multiple comparisons (figure 4.1 A), with untreated, zanamivir, *T. forsythia*, and *T. forsythia* + zanamivir conditions presenting no significant changes in LDH levels compared to the untreated condition. Furthermore, cells were counted to allow normalisation of cytokine secretion to the number of cells in each condition, and cell counting could also be used to determine viability and metabolic activity (inferred by cell growth over the 24 hours of treatment). Counting showed that there were no significant changes in cell numbers between each condition, when expressed as a total count of cells after 24 hours of

treatment or as the fold change of cells relative to the number of cells at the start of the experiment i.e. cell growth (figure 4.1 B), with untreated, zanamivir, *T. forsythia*, and *T. forsythia* + zanamivir conditions containing ~464000, ~485000, ~430000, and ~469000 cells, respectively.

The effect of zanamivir on OKF6 cells was tested in cytokine-quantification experiments, so these were tested in a separate set of experiments, where cells were cultured in tissue culture plates, and exposed to different concentrations of zanamivir for 2.5 hours (the duration of the antibiotic protection assay). Culture supernatants underwent either an LDH assay to detect cell lysis/permeability, or an MTT assay (3-(4,5-dimethylthiazol-2-yl)-2,5-diphenyltetrazolium bromide) to test viability (figure 4.2). The latter assay relies on production of a purple formazan salt from MTT by metabolically active cells (specifically via the activity of oxidoreductases on MTT, and these enzymes require NAD(P)H), and the level of formazan can be quantified by spectrophotometry. The assays showed that zanamivir does not affect LDH release into culture supernatant, or formazan formation from MTT, in OKF6 cells exposed to zanamivir under conditions used in the antibiotic protection assay (significance determined by repeated measures one-way ANOVA, with all conditions compared to the untreated cells, with Tukey's correction for multiple comparisons).

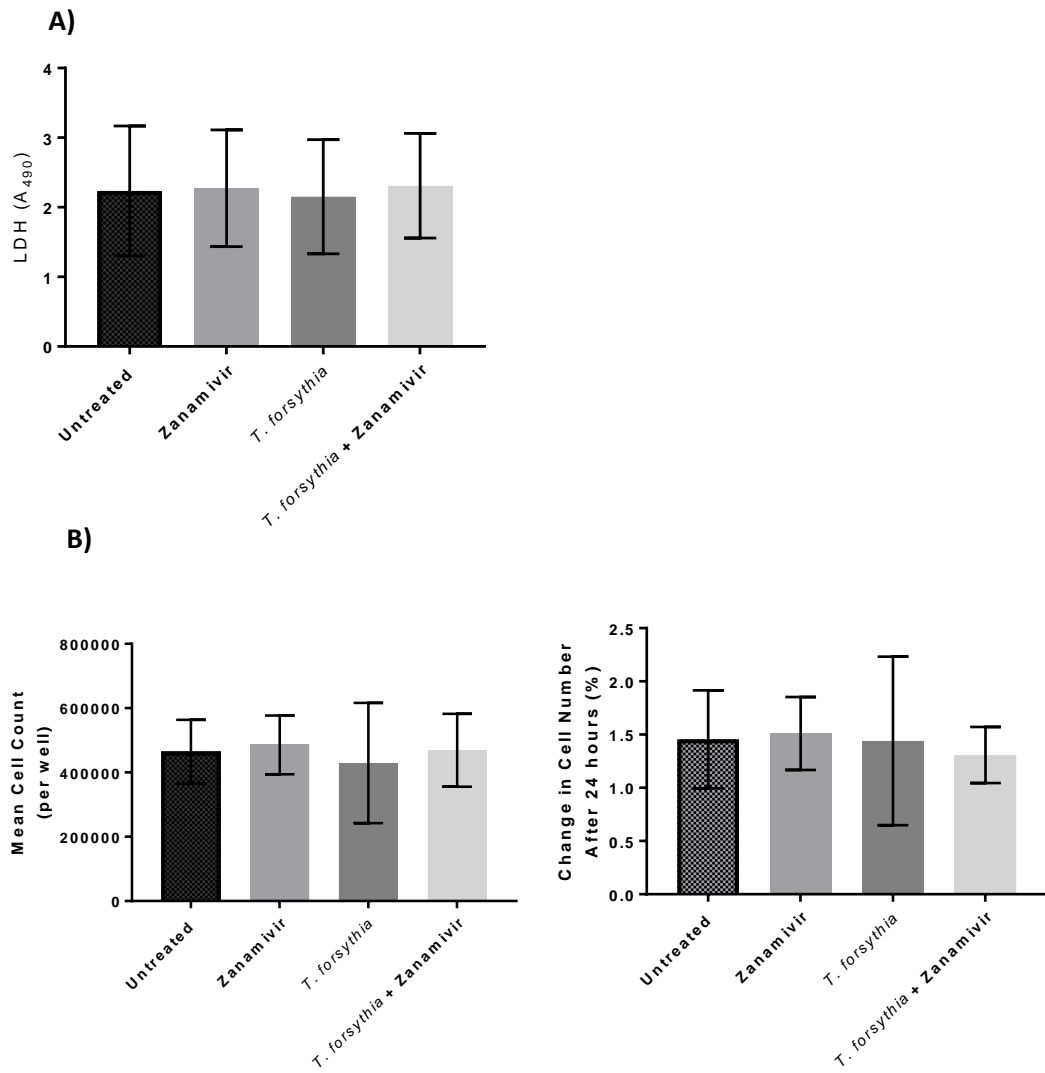


Figure 4.1. Viability testing of H357 OSCC cells exposed to *T. forsythia* and/or zanamivir.

The oral epithelial cell line H357 was exposed to *T. forsythia* in the presence and absence of 10mM zanamivir for 24 hours, followed by A) an LDH assay on culture supernatant, quantified as the absorbance following detection of formazan formed during the LDH assay, and B) cell counting, where data is described as cell numbers, or as the fold change in number of cells between 0 and 24 hours. Data shown represent the mean of three experiments, where each condition was repeated twice per experiment. Error bars=SD. No significant differences were found (where $p < 0.05$), as determined by one way ANOVA, with repeated measures and Tukey's correction for multiple comparisons.

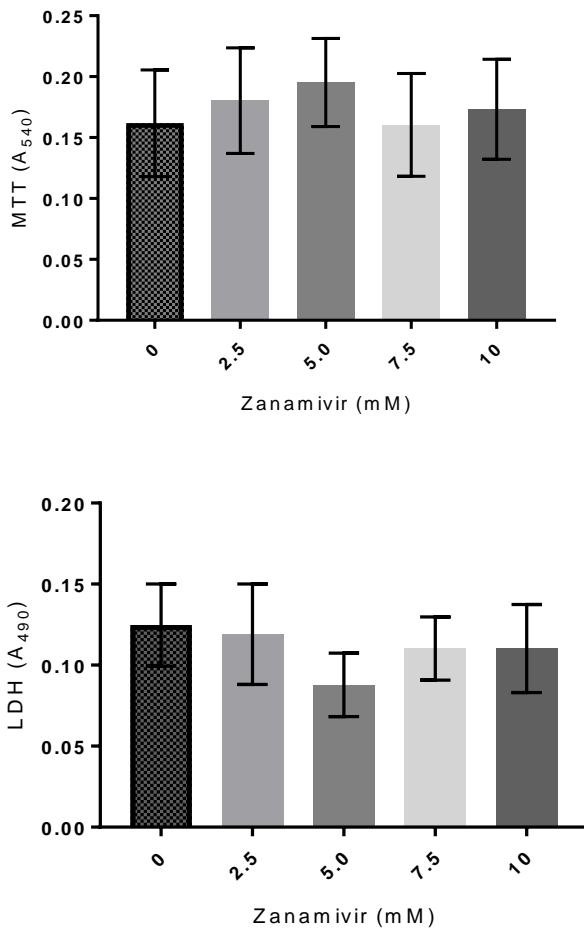


Figure 4.2. Viability testing of OKF6 oral epithelial cells exposed to zanamivir.

The oral epithelial cell line OKF6 was exposed to *T. forsythia* in the presence and absence of 10 mM zanamivir for 2.5 hours, followed by A) an MTT assay on cells or B) an LDH assay on culture supernatant, with the absorbance at 490 and 540 nm for LDH and MTT, respectively, used to relatively quantify levels of MTT and LDH. Data shown represent the mean of two experiments, where each condition was repeated three times per experiment. Error bars=SEM. No significant differences were found (where $p < 0.05$), as determined by one way ANOVA, with repeated measures and Tukey's correction for multiple comparisons.

4.3.1.2 *Zanamivir is not Directly Detrimental to Periodontal Pathogen Viability*

Data obtained during experiments described in sections 4.3.3-4 showed that periodontal pathogen viability was not affected by zanamivir: During antibiotic protection assays, as well as enumerating the number of bacteria that had attached or invaded host cells, a viability condition was also enumerated, for the purposes of the experiment this allowed the level of bacteria-host cell association to be expressed as the percentage of viable

bacteria that had attached to or invaded host cells. It also served as evidence for any effect of zanamivir on bacterial viability: *T. forsythia*, *P. gingivalis*, and *F. nucleatum* were enumerated following the single species antibiotic protection assays described in section 4.3.3, with the “viability” condition containing the suspension used to infect host cells, consisting of live bacteria which had been incubated for 2.5 hours in the presence or absence of 10 mM zanamivir (figure 4.3). The effect of zanamivir on each individual species was of interest, and required independent assessment, therefore, T-tests for each species comparing zanamivir-treated to untreated were performed to assess statistical significance. T-test was deemed the most appropriate statistical test to use in this instance, as the viability of each species is independent from the others, so three separate T-tests were performed to compare the viability of each species in the presence and absence of zanamivir. Zanamivir had almost no effect on the viability of all *T. forsythia*, *P. gingivalis*, and *F. nucleatum* with fold-changes in the number of viable bacteria of 1.12 ($p=0.141$), 1.13 ($p=0.024$), and 0.92 ($p=0.509$) in the presence of zanamivir (relative to the untreated condition), respectively. *P. gingivalis* did apparently display a significant increase in viability in the presence of zanamivir, but even if zanamivir does increase its viability by ~ 1.1 fold while the number of host-cell associating organisms remains the same, this would not account for the large decrease seen in the percentage of viable *P. gingivalis* associating with oral epithelial cells in the presence of zanamivir (figure 4.10).

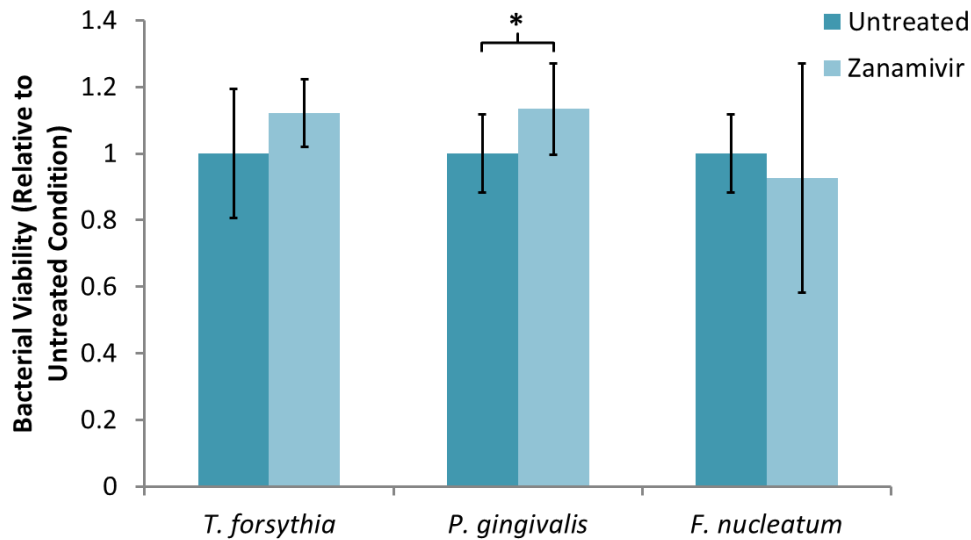


Figure 4.3. Viability testing of periodontal pathogens exposed to zanamivir.

T. forsythia, *P. gingivalis*, and *F. nucleatum* were incubated in the presence and absence of 10mM zanamivir for 2.5 hours, followed by enumeration of viable organisms by agar plate counts, and data were expressed as the change in cell numbers relative to the untreated condition. Data shown represent the mean of three experiments, where each condition was repeated three times per experiment. Error bars=SD. Significance determined by T-test (* $p < 0.05$).

Ultimately, these data show that under assay conditions the sialidase inhibitor zanamivir does not have any effect on oral epithelial cell viability, and no directly-detrimental effect on periodontal pathogen viability (i.e. although zanamivir does not kill pathogens directly, it may deprive them of nutrient sources, which would not be determined by these experiments). The absence of bacterial killing-while still interfering with virulence processes such as host cell association and cytokine induction-does in fact strengthen the case for the use of zanamivir as a therapeutic: Unlike conventional antimicrobials which target all bacteria in the microbiota, targeting processes that are beneficial to pathogens (and not as important for commensals) might reduce the proportion of pathogenic organisms in the microbiota, aiding in resolution of periodontal disease.

4.3.2 Periodontal Pathogen Sialidases Cleave Sialic Acid from Host Cell Surfaces and this can be Inhibited by Zanamivir

As shown in chapter 3, the sialidase inhibitor zanamivir can inhibit sialidase activity in *P. gingivalis* and to a lesser extent *T. forsythia*, and that this trend is also seen with their purified recombinant sialidases (section 2.3.7). Taken together with evidence that

periodontal pathogen-host cell interactions appear to be at least partially mediated by pathogen sialidases, this chapter aims to investigate if the sialidase inhibitor zanamivir can influence the interactions of *T. forsythia* and *P. gingivalis* with host cells. Considering this, it was first necessary to examine if the periodontal pathogen sialidases have the ability to cleave sialic acid from oral epithelial cells.

4.3.2.1 ***Cleavage of α 2-3 and α 2-6 linked sialic acid by Periodontal Pathogen Sialidases***

Oral epithelial cells (oral squamous cell carcinoma, OSCC, cell line H357) were cultured on glass coverslips to ~70% confluence in a monolayer. Cells were exposed to *T. forsythia* and *P. gingivalis*, or treated with their purified sialidases (NanH and SiaPG), in the presence and absence of zanamivir, as described below. Treated cells were stained with lectins from *Maackia amurensis* (MAA) and *Sambucus nigra* (SNA), which are specific for α 2-3 and α 2-6 linked sialic acid, respectively. To allow visualisation, lectins were either purchased as Fluorescein Isothiocyanate (FITC) conjugated versions, or as biotinylated lectins, which enabled labelling with Texas Red (TR)-Streptavidin (which binds to the biotin moiety of the lectin). Cells were then fixed with paraformaldehyde, before the coverslips were mounted onto glass microscope slides with a light-resistant antifade mount that contained a nuclear stain (DAPI, within ProLong Antifade-Gold), and visualised using immunofluorescence microscopy.

T. forsythia and *P. gingivalis* were washed twice and resuspended in PBS at OD₆₀₀ 0.5, applied to H357 monolayers, and incubated for 2 hours at 37°C to test the ability of live pathogens to desialylate epithelial cell membranes, in the presence or absence of zanamivir to test its potential to inhibit cleavage of cell surface sialic acids by the pathogens. A high concentration (10 mM) was chosen to ensure sialidase inhibition, since a lower concentration may not inhibit live *T. forsythia* effectively. The relatively high IC₅₀ (~6.3 mM) of zanamivir for purified NanH activity on MUNANA also suggests that the use of a high concentration of zanamivir (10 mM) in these assays would be required in order to obtain some measure of *T. forsythia* sialidase inhibition. After treatment with live *P. gingivalis* or *T. forsythia* in the presence or absence of zanamivir, cells then underwent lectin staining as described, followed by paraformaldehyde fixation, and they were mounted and visualised as described above (figure 4.4). After visualisation and image processing, the level of α 2-3 and α 2-6 linked sialic acid was quantified as the mean fluorescence intensity (MFI) per image (figure 4.5 A). A more appropriate way to express staining would be as the MFI/cell, but the *P. gingivalis* condition displayed a significantly

lower cell count (figure 4.5 B) compared to the untreated control, which could skew the result if expressed as MFI/Cell. In any case, both MFI/Cell and MFI are presented. Significant differences between each condition and the untreated control were tested using one way ANOVA, with Dunnet's correction for multiple comparisons.

Exposure of oral epithelial cells to *T. forsythia* resulted in a twofold reduction in α 2-6 linked sialic acid relative to the untreated control, however this was not considered statistically significant under the one way ANOVA described above (MFIs of 147 and 75, respectively, $p=0.14$, using T-test in this comparison yields a p -value of 0.02) and this reduction was not inhibited in the presence of zanamivir (MFI of 87). α 2-3 linked cell surface sialic acid was apparently not reduced by the presence *T. forsythia*, relative to the control (MFIs of 256 and 302, respectively, $p=0.67$). This was surprising, since data shown in section 2.3.6.3 highlights the higher catalytic efficiency *T. forsythia* NanH for α 2-3 linked sialic acid rather than α 2-6 linked sialic acid (K_{cat} / K_M of $1.122 \text{ min}^{-1}\text{mM}^{-1}$ and $0.339\text{min}^{-1}\text{mM}^{-1}$, respectively). However, linkage type is not the only factor in sialidase-ligand interactions-the underlying glycan can also play a role, as seen in the case of the ligands sialyl lewis A and X (section 2.3.6.4), which both contain α 2-3 linked sialic acid, but displayed great differences in their affinity for NanH. Another explanation could be that since this experiment was conducted with staining on live, unfixed cells that host surface sialic acid cycling is more rapid for α 2-3 linked sialic acid (i.e. host cells may have higher 3-sialyltransferase activity to replenish surface sialic acids). In addition these experiments were conducted on live unfixed bacteria and since *T. forsythia* is more sensitive to oxygen than *P. gingivalis* (Graham Stafford, unpublished observation) this could explain why *T. forsythia* appeared to have only a small effect on surface sialic acid, while the *P. gingivalis* effect was more pronounced.

Discussing the significant reduction in α 2-3 and α 2-6 linked staining caused by *P. gingivalis* is more difficult, partly due to the significant reduction in cell numbers seen in *P. gingivalis*-containing conditions (the mean number of cells/field of view in untreated, *P. gingivalis*, and *P. gingivalis* + zanamivir conditions were 25, 7, and 4, respectively). The reduction in levels of surface sialic acid could also be due to the action of *P. gingivalis* gingipains, which could cleave sialoglycoproteins from the surface of the cell: While this would not affect sialic acid directly, loss of the sialoglycoprotein from the cell surface would result in an apparent reduction of surface sialic acid.

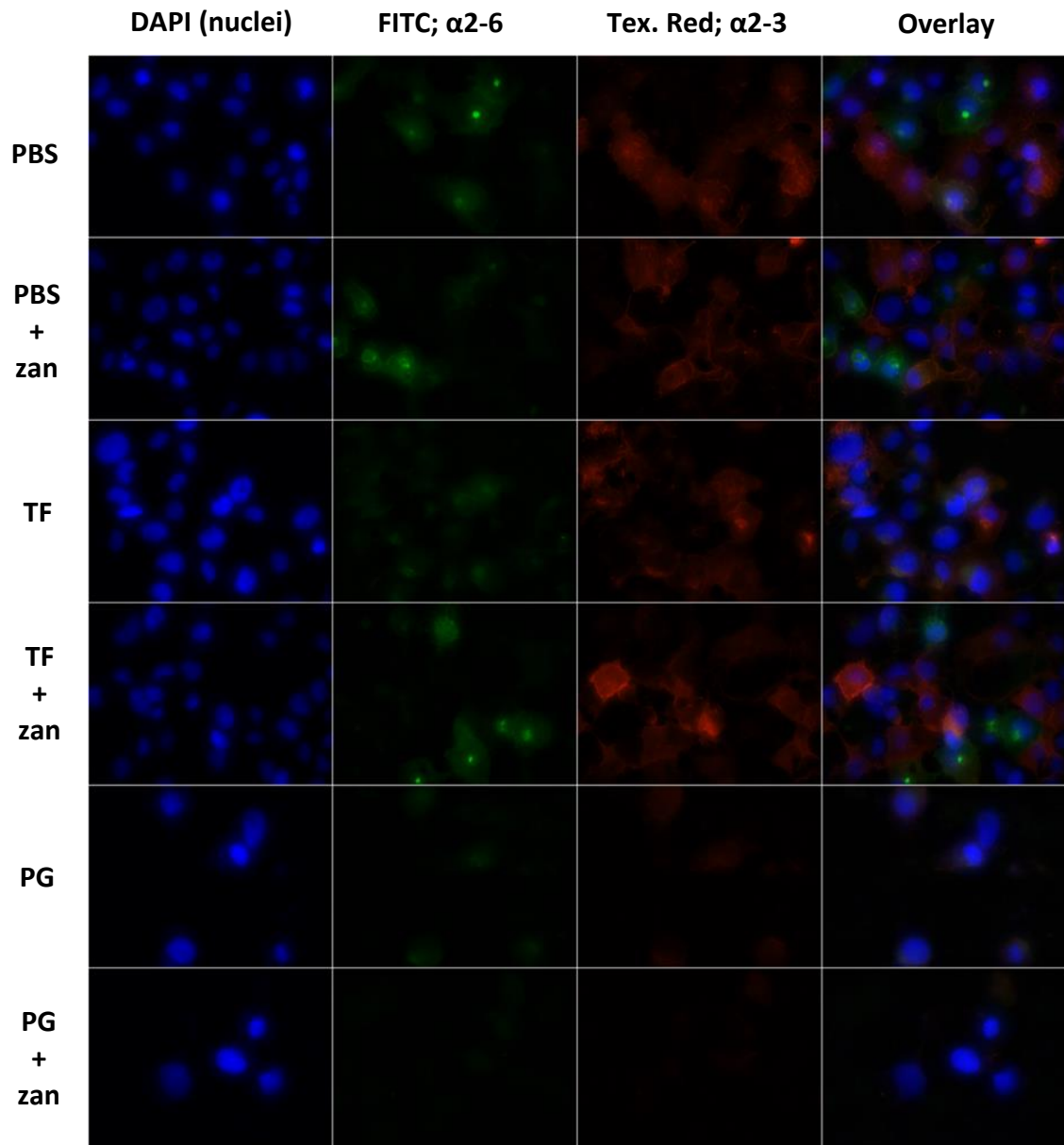


Figure 4.4. Exposure to periodontal pathogens removes sialic acid from epithelial cell surfaces.

Cells were stained with lectins for α 2-3 (red) and α 2-6 (green) linked sialic acid. Prior to staining, cells were exposed to *T. forsythia* and *P. gingivalis* suspended in PBS, in the presence or absence of 10mM zanamivir, as indicated. All images were visualised using the same microscopy and image processing parameters (fluorescence intensity, exposure time and background subtraction). Images were captured in three fields of view, images shown are representative of each condition.

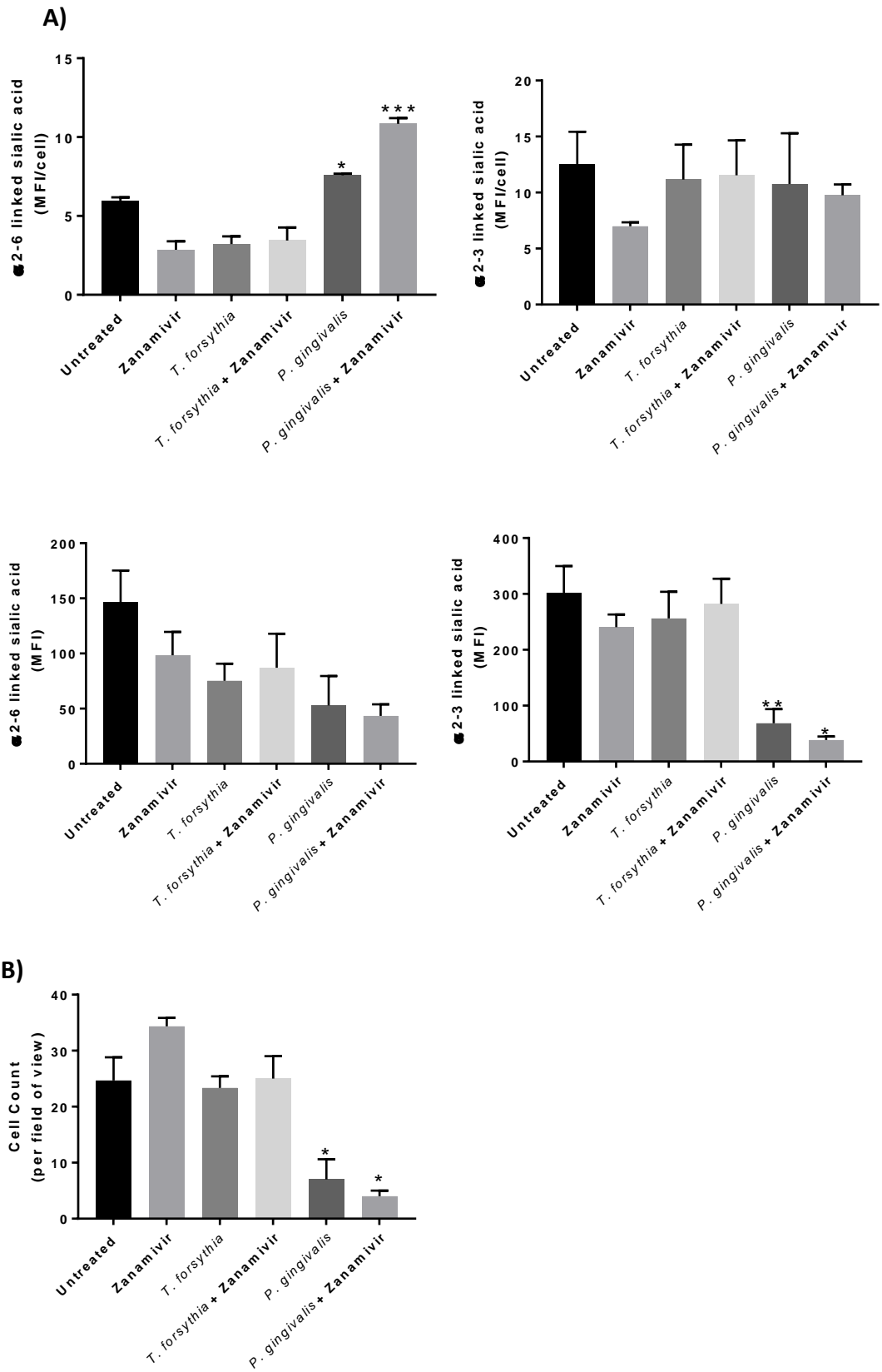


Figure 4.5. Quantification of cell surface sialic acid from oral epithelial cells exposed to A) live pathogens B) the effect of pathogen exposure on cell numbers.

A) Cells were stained with lectins for α 2-3 and α 2-6 linked sialic acid. Prior to staining, cells were exposed to *T. forsythia* and *P. gingivalis* suspended in PBS, in the presence or absence of 10mM zanamivir, as indicated. All images were visualised using the same microscopy and image processing parameters (fluorescence intensity, exposure time and background subtraction). After processing, images could undergo A) staining quantification, to obtain the mean fluorescence intensity (MFI) per field of view, and this could be standardised to cell count (MFI/Cell). B) Cells were counted and expressed as-the number of cells per field of view. Data show the mean of three fields of view per condition, from one experiment. Error Bars =SD, significant deviation from the untreated condition only was determined by repeated measures one way ANOVA with Dunnet's correction for multiple comparisons (* $p < 0.05$, ** $p < 0.01$, *** $p < 0.001$).

Exposure to pathogens resulted in loss of α 2-3 and α 2-6 linked sialic acid from host cells, and this could be due to the action of pathogen sialidases, or from pathogen proteases removing the sialoglycoproteins. It is also possible that this happens due to host-cell mediated processes, such as the mobilisation of human sialidases to the membrane, seen during host cell responses to pathogens (Amith et al. 2009; Stamatou et al. 2010), or perhaps desialylation is caused by apoptotic processes (Meesmann et al. 2010). Certainly, in these experiments *P. gingivalis* reduced the numbers of cells present at the end of the assay, and this was evident during image capture and subsequent cell-number quantification (Figure 4.5 B).

Since these data were difficult to interpret due to the variation in cell numbers, the apparent possible interference by *P. gingivalis*, and the possible response of host cells to live periodontal pathogens, assays with the purified pathogen sialidases were performed. NanH and SiaPG were diluted in PBS at a concentration of 100 nM, applied to H357 monolayers, and incubated for 2 hours at 37 °C. Cells then underwent lectin staining, imaging, and processing as described above (figure 4.6). Purified enzymes did not cause significant changes to cell numbers, as determined by repeated measures one-way ANOVA, with Dunnett's correction for multiple comparisons.

NanH caused reductions in α 2-3 and α 2-6 linked sialic acid from oral epithelial cell surfaces (Figures 5.6), however these were not deemed statistically significant by the one-way ANOVA described here. In the untreated and NanH conditions, α 2-3 linked sialic acid staining (MFI/Cell) was 3.6 and 0.9, respectively ($p=0.07$), and α 2-6 linked sialic acid staining (MFI/Cell) was 2.6 and 0.9, respectively ($p=0.09$). The presence of zanamivir did not prevent the decreases in cell surface sialic acid of either linkage type. Qualitatively, images appeared to confirm this assessment—that NanH desialylated both types of linkage, and was not inhibited by zanamivir (figure 4.6).

Quantitatively, SiaPG reduced staining to a lesser extent, though reductions were not considered significant by one-way ANOVA. Zanamivir slightly, though not significantly, inhibited loss of α 2-3 linked sialic acid caused by SiaPG (figure 4.7). Qualitatively however, the change in surface sialic acid appeared to be more drastic, particularly for α 2-6 linked sialic acid. This may be due to the presence of nuclear staining in the green channel (DAPI can emit green fluorescence), as evidenced by the green present in the SiaPG-FITC panel in

figure 4.6, but not seen in the overlay. Adjustments to parameters during image acquisition or processing might have removed the apparent nuclear staining, but would have rendered SiaPG incomparable to the other conditions. Flow cytometry would have been an alternative approach to assessing sialic acid staining following treatment with enzymes, and this was attempted during this project, but proved difficult to optimise.

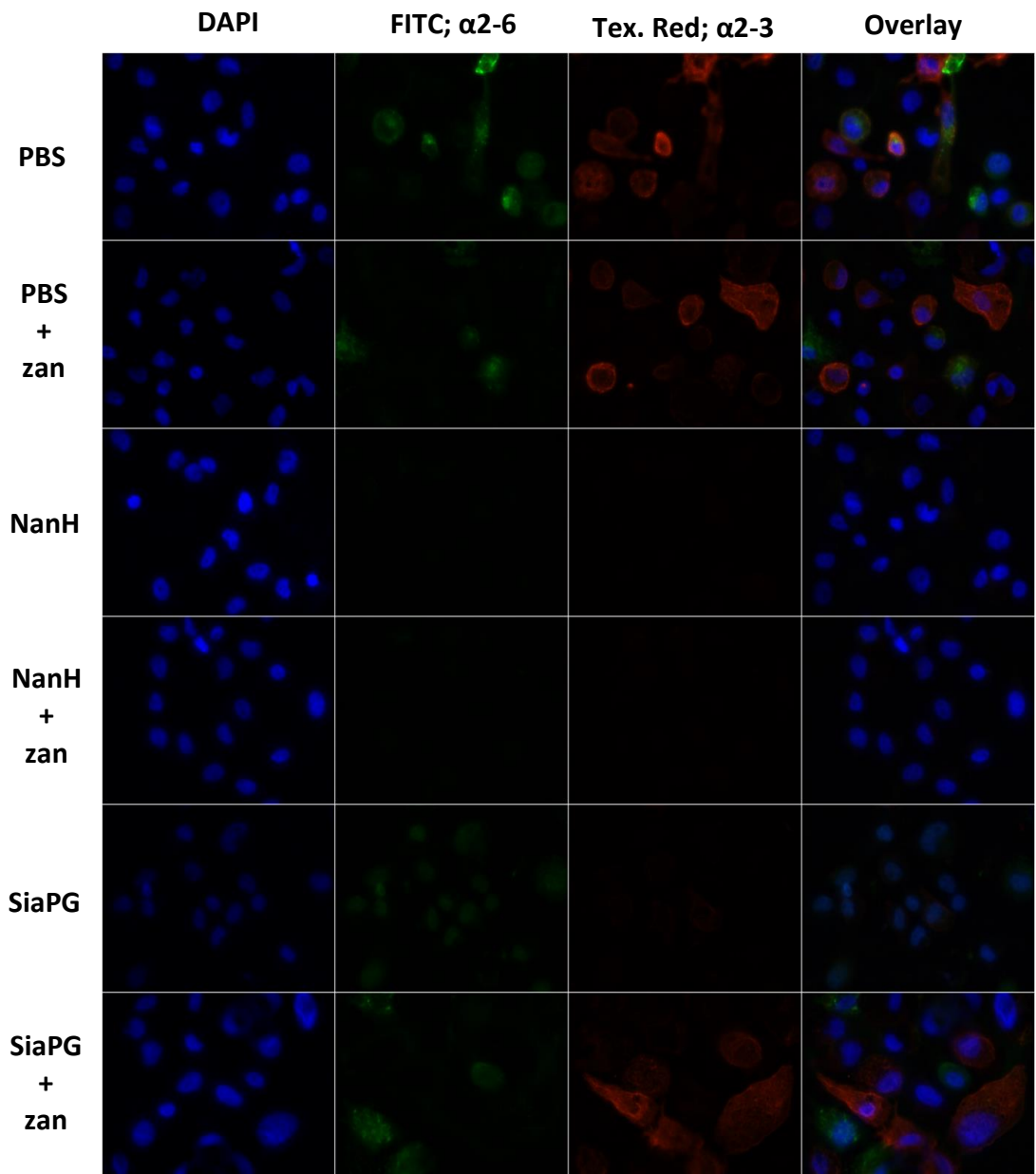


Figure 4.6. Purified sialidases desialylate oral epithelial cell surfaces.

Cells were stained with lectins for α 2-3 and α 2-6 linked sialic acid in red and green, respectively. Prior to staining, cells were treated with NanH and SiaPG in PBS, in the presence or absence of 10mM zanamivir, as indicated. All images were visualised using the same microscopy and image processing parameters (fluorescence intensity, exposure time and background subtraction). Images were captured in three fields of view, and this was repeated in three separate experiments. Images shown are representative of each condition.

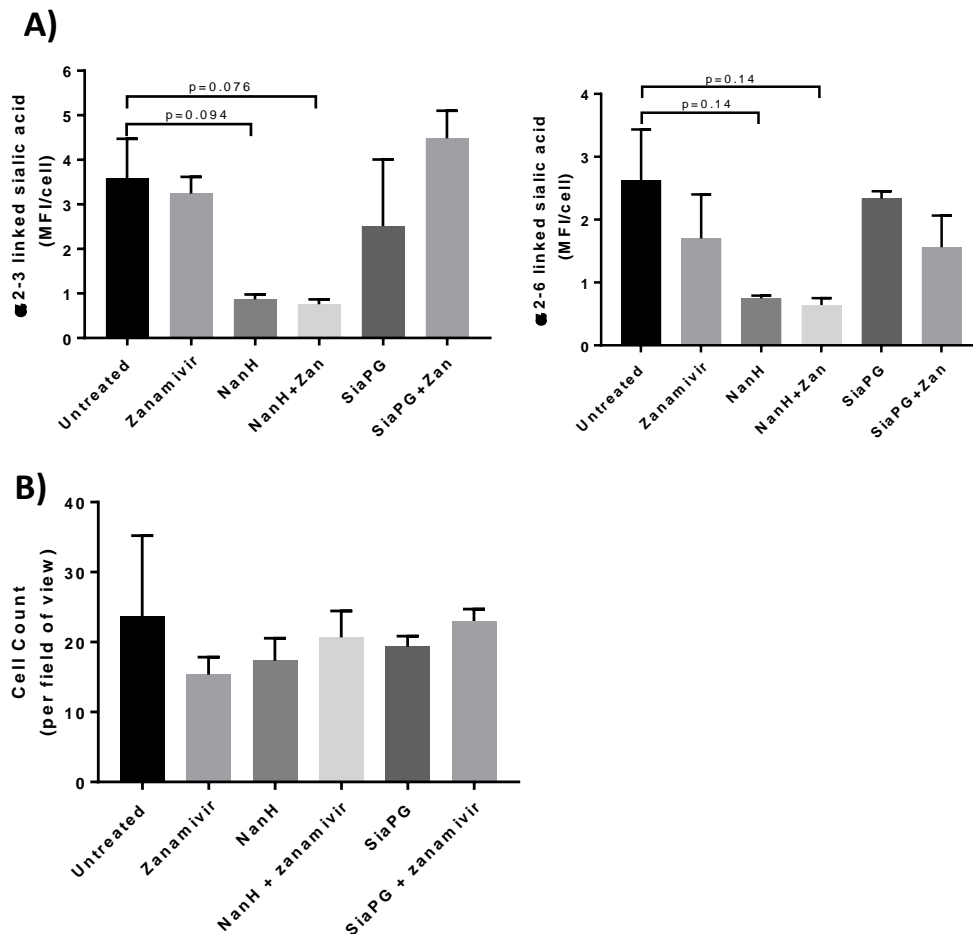


Figure 4.7. A) Quantification of cell surface sialic acid on oral epithelial cells exposed to NanH and SiaPG. B) Exposure to sialidases or zanamivir has no effect on cell numbers.

Cells were stained with lectins for α 2-3 and α 2-6 linked sialic acid. Prior to staining, cells were exposed to PBS-diluted NanH, SiaPG, or PBS alone, in the presence or absence of 10 mM zanamivir, as indicated. All images were visualised using the same microscopy and image processing parameters (fluorescence intensity, exposure time and background subtraction. Images were captured in three fields of view, and after processing could undergo A) Quantification of the effect of NanH and SiaPG on α 2-3 and α 2-6 linked sialic acid, expressed as MFI/cell. Error Bars =SD, Significance determined by repeated measures one-way ANOVA, with Dunnet's correction for multiple comparisons (where $p < 0.15$, the p-value is indicated). B) Cells were counted to obtain the number of cells per field of view and the effect of zanamivir in enzyme treated and untreated conditions was compared, error bars=SEM, significant deviation from the untreated condition only was determined by repeated measures one way ANOVA with Dunnet's correction for multiple comparisons (none discovered).

4.3.2.2 *NanH acts on cell surface Sialyl-Lewis A and X*

Here, in chapter 3, the *T. forsythia* sialidase NanH was shown to release sialic acid from SLeA and SLeX, with greater affinity for SLeA (K_m of 0.2 and 2.0, respectively). This experiment was in the context of soluble SLeA/X, non-glycoprotein conjugated. To investigate the ability of NanH to cleave sialic acid from cell surface membrane associated SLeA/X, the (OSCC) cell line H357 was cultured on glass coverslips, treated under a number of conditions (described below), followed by staining with FITC-conjugated anti-SLeA or anti-SLeX antibodies. This enabled visualisation of cell surface SLeA/SLeX using fluorescence microscopy, and staining was quantified by image processing software using the level of green fluorescence in a given image, expressed as mean fluorescence intensity (MFI). MFI was normalised to the number of cells in a given image (MFI/cell), and by imaging three fields of view per condition in three separate experiments, the levels of SLeA/X staining between the conditions could be compared. Significant differences between the conditions were determined using repeated measures one-way ANOVA with Tukey's correction for multiple comparisons.

Prior to staining, cells were incubated with or without NanH to determine whether or not it could target cell surface SLeA/X. Conditions were also tested in the presence or absence of zanamivir to determine the potential to inhibit cell surface SLeA/X desialylation by NanH.

NanH was shown to be capable of cleaving sialic acid from both SLeA and SLeX on oral epithelial cells, and zanamivir was partially capable of inhibiting SLeA desialylation (figure 4.8-9). Staining quantification showed that NanH decreased the levels of epithelial cell membrane SLeA and SLeX by approximately two thirds; from 3.5 to 1.2 MFI/Cell in the case of SLeA, and 3.26 to 1.03 MFI/Cell in the case of SLeX ($p < 0.01$ in both cases). Zanamivir was only capable of slightly inhibiting sialic acid release from cell surface SLeA/X by NanH under experimental conditions, from 1.2 to 1.5 MFI/Cell in the case of SLeA, and from 1.0 to 1.1 MFI/cell in the case of SLeX, and in both cases this inhibition was not statistically significant compared to the NanH only condition.

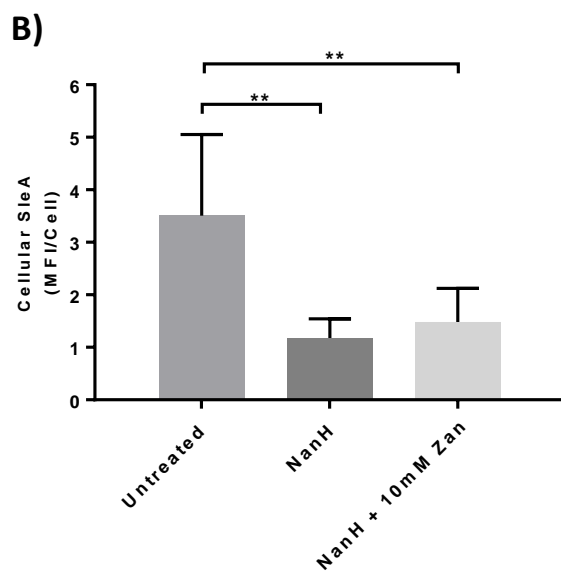
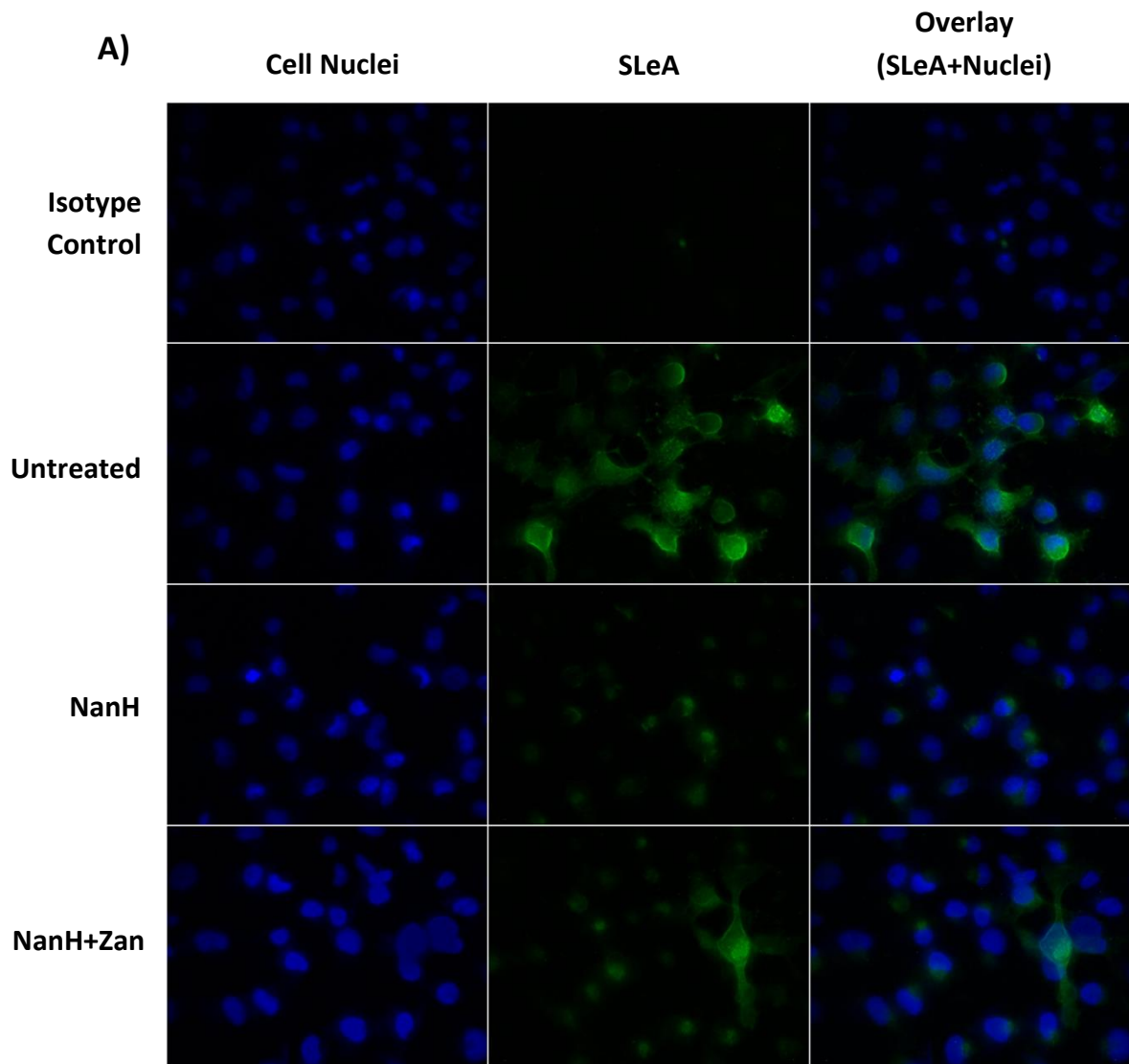


Figure 4.8. NanH desialyates sialyl-lewis A on epithelial cell surfaces.

A) Fluorescence Microscopy. Cells were stained with rabbit anti-SLeA antibodies, followed by secondary staining with FITC-conjugated goat anti rabbit antibodies. Stained cells were mounted onto microscope slides with a DAPI stain to visualise nuclei. Prior to staining, cells were treated with NanH in PBS, in the presence or absence of 10 mM zanamivir (zan), as indicated. All images were visualised using the same microscopy and image processing parameters (fluorescence intensity, exposure time and background subtraction). Images were captured in three fields of view, in three separate experiments. Images shown are representative of each condition. Isotype control=non-specific primary antibody raised in rabbit. B) Quantification of SLeA staining. The mean level of FITC fluorescence in the green channel of each image corresponds to the level of SLeA staining, or Mean Fluorescence Intensity (MFI). MFI was normalised to the number of cells in a given image (MFI/Cell). The MFI/cell of the isotype control condition was subtracted from the MFI/cell in each condition and plotted. Data shown represent the mean from three fields of view, repeated in three separate experiments. Error Bars=SD. Significance determined by repeated measures one-way ANOVA with Tukey's correction for multiple comparisons (** $p < 0.01$).

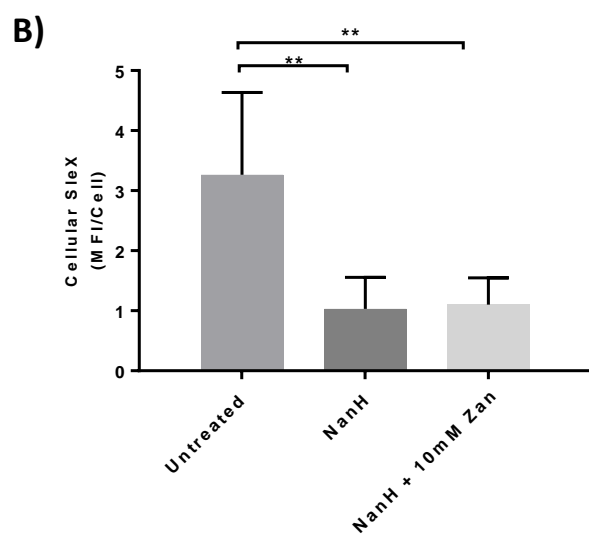
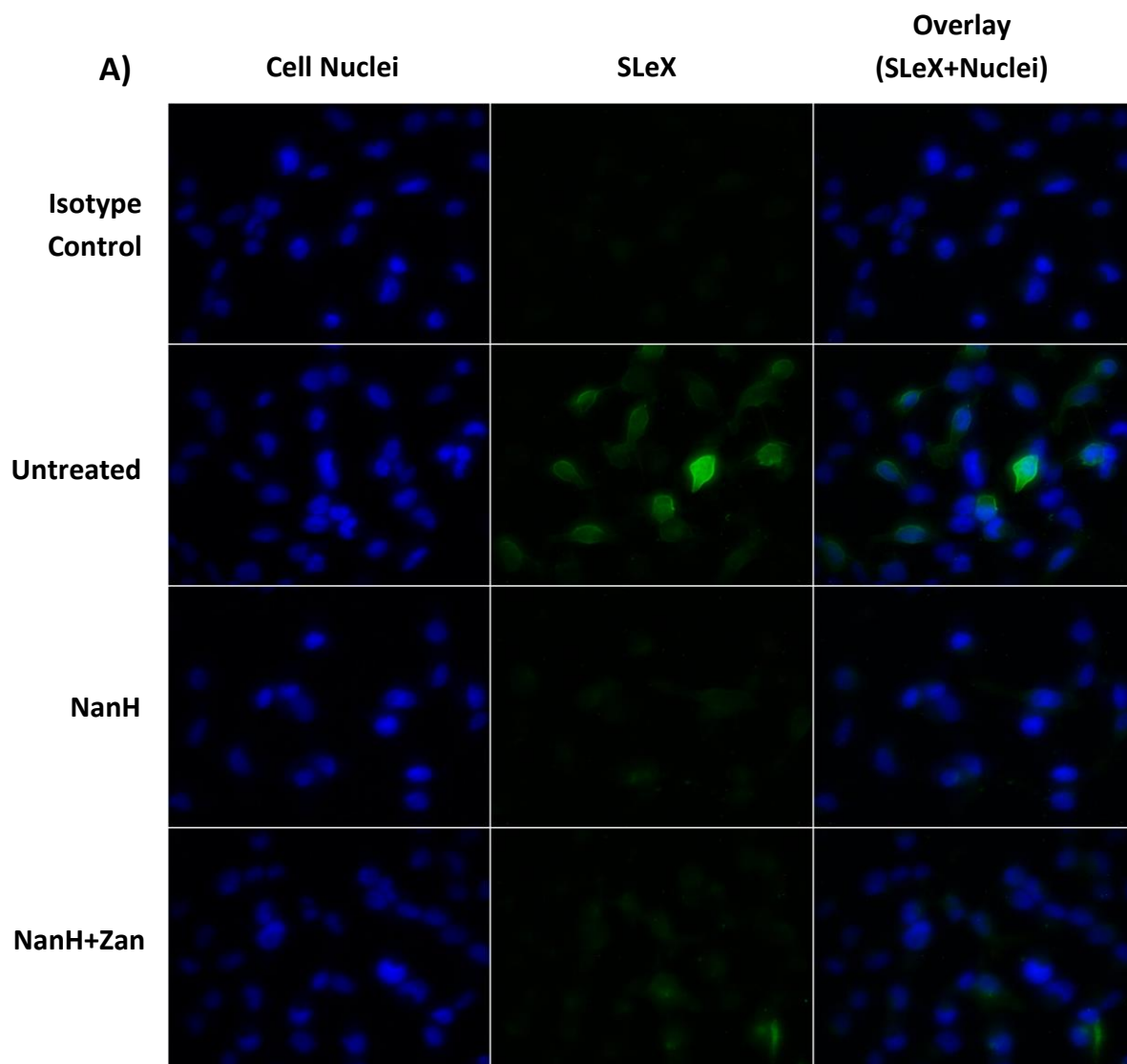


Figure 4.9. NanH desialylates sialyl-lewis X on epithelial cell surfaces.

A) Fluorescence Microscopy. Cells were primary-stained with murine anti-SLeX antibodies, followed by secondary staining with FITC-conjugated goat anti mouse antibodies. Stained cells were mounted onto microscope slides with a DAPI stain to visualise nuclei. Prior to staining, cells were treated with NanH in PBS, in the presence or absence of 10mM zanamivir (zan), as indicated. All images were visualised using the same microscopy and image processing parameters (fluorescence intensity, exposure time and background subtraction). Images were captured in three fields of view, in three separate experiments. Images shown are representative of each condition. Isotype control=non-specific primary antibody raised in rabbit. B) Quantification of SLeX staining. The mean level of FITC fluorescence in the green channel of each image corresponds to the level of SLeX staining, or Mean Fluorescence Intensity (MFI). MFI was normalised to the number of cells in a given image (MFI/Cell). The MFI/cell of the isotype control condition was subtracted from the MFI/cell in each condition and plotted. Data shown represent the mean from three fields of view, repeated in three separate experiments. Error Bars=SD. Significance determined by repeated measures one-way ANOVA with Tukey's correction for multiple comparisons (** $p < 0.01$).

4.3.3 Zanamivir inhibits Attachment and Invasion of Oral Epithelial Cells by *T. forsythia*, *P. gingivalis*, and the sialidase-negative *F. nucleatum*

Bacterial attachment and invasion was tested in a series of antibiotic protection assays: Cell lines (described below) were cultured as a monolayer, and infected in the presence or absence of zanamivir with *P. gingivalis*, *T. forsythia*, or *F. nucleatum*, which was included as a control pathogen to see if zanamivir had any effect on attachment and invasion of host cells by sialidase-negative organisms and since it is an important bridging organism in periodontal sub-gingival biofilms and is also known to synergise with *T. forsythia* and *P. gingivalis* in cell-interactions assays (Metzger et al. 2009; A. Sharma et al. 2005). All infections were carried out at a multiplicity of infection (MOI) of 1:100 host cells: bacteria. After infection, cells were incubated at 37 °C, 5 % CO₂, for 1.5 hours, then washed to remove non-cell-associated bacteria. Infected cells were lysed, and lysates spotted onto agar. This enabled enumeration of the total number of bacteria associated with host cells (bacteria that had attached to external surface of, or invaded host cells). A second infected host cell monolayer undergoes an additional step, where infected cells are treated with metronidazole prior to lysis; this kills bacteria attached to their external surface, leaving only bacteria which have invaded host cells, which are enumerated after plating of cell lysates onto agar. Subtraction of the invaded bacteria from the total number of associated bacteria provides the number of bacteria attached to the host cells. Bacterial suspension used to initially infect the host cells is retained and the number of bacteria in this suspension that survive the duration of the assay is used to obtain the number of host cell-associated bacteria between experiments (where different MOIs are used). The percentage of viable bacteria that associate with host cells was determined. Significant differences in attachment, invasion, and total association were assessed by a series of paired T-tests. This test was considered appropriate since the only objective was to compare the effect of zanamivir on bacterial attachment, invasion, and total association, independently of each other. Testing for statistically significant differences in bacterial attachment, invasion, and total association for each species was not the objective of this study.

The OSCC cell line H357 was used in the antibiotic protection assay, since it is a well characterised, frequently used model for oral epithelium-bacteria interactions (Suwannakul et al. 2010; Al-Taweel et al. 2016), and for practical purposes since it proliferates rapidly. H357 cells were infected with either *T. forsythia*, *P. gingivalis*, or *F. nucleatum* subsp. *nucleatum* (MOI 1:100), in the presence or absence of zanamivir. For all three pathogens,

zanamivir significantly reduced one or more aspects of host cell association (figure 4.10). The percentage of viable *T. forsythia* attachment, invasion, and total association with H357 cells were all significantly reduced in the presence of zanamivir; attachment from 4.6 to 1.2 %, invasion from 3.4 to 1.6 %, and total association from 8.0 to 2.8 % (with p-values of <0.0001, <0.01, and <0.00001, respectively, according to paired T-test), i.e. a 3-4-fold reduction. The percentage of viable *P. gingivalis* also showed significantly reduced invasion in the presence of zanamivir; from 4.5 to 1.8% (p= <0.01), i.e. over 2-fold reduction. The total associated *P. gingivalis* was also decreased in the presence of zanamivir, although the change was not significant. For the sialidase negative *F. nucleatum*, invasion was slightly, though not significantly inhibited by zanamivir, but the attached and total associated number of bacteria was significantly reduced by zanamivir, from 21.8 to 7.2 % (p=<0.05) and 36.6 to 18.2 % (p=<0.05), respectively.

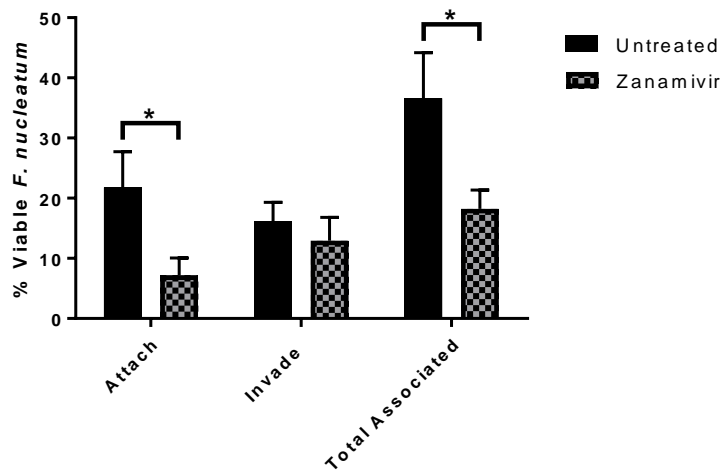
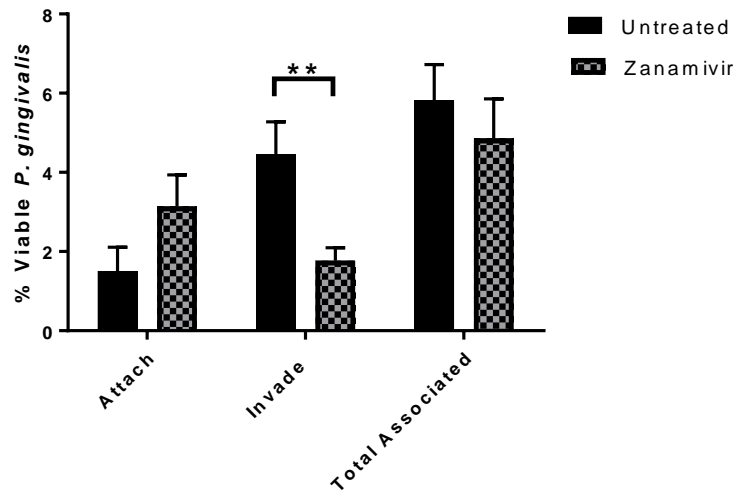
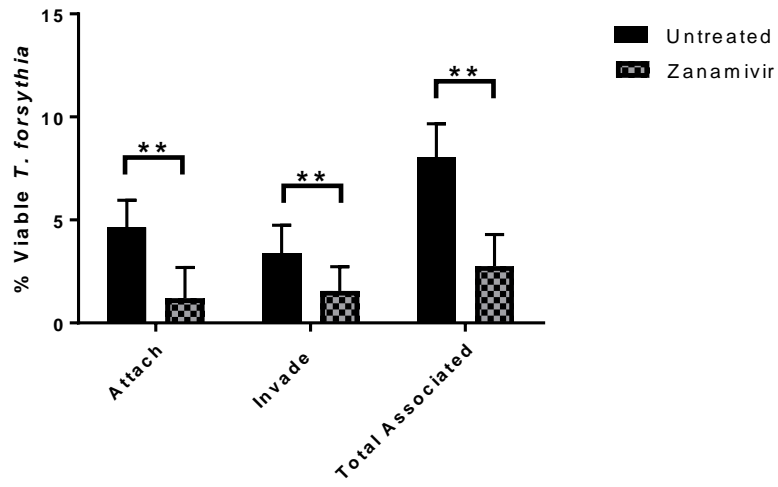


Figure 4.10. The Effect of Zanamivir on Attachment and Invasion of OSCC Epithelial Cells.

Antibiotic protection assays were performed in the presence or absence of zanamivir with either *T. forsythia*, *P. gingivalis*, or *F. nucleatum*. Bacterial attachment, invasion, and total association with host cells was normalised to the number of bacteria that were used to infect each condition that had survived the duration of the assay (the percentage of viable bacteria). Zanamivir=10mM zanamivir present during host cell exposure to bacteria. Data represent the mean from three independent experimental repeats, and each condition was repeated in triplicate during each experiment. Error bars=SEM, Significance determined by paired T-test, * $p < 0.05$, ** $p < 0.01$.

Antibiotic protection assays were also performed using the same procedures as described above but using the immortalised oral keratinocyte cell line, OKF6 (Dickson et al. 2000). Since these cells are considered more closely related to oral epithelial cells in the host, assays done using these cells might be considered a better model for host-pathogen interactions. Again, for all three pathogens, zanamivir reduced one or more aspects of host cell association for *T. forsythia* and *P. gingivalis* (figure 4.11).

The percentage of viable *T. forsythia* attachment, invasion, and total association with OKF6 cells were all significantly reduced in the presence of zanamivir; attachment from 3.2 to 1.0 %, invasion from 2.5 to 0.3 %, and total association from 5.8 to 1.4 % (p-values were <0.05, <0.01, and <0.05, respectively). The percentage of viable *P. gingivalis* also showed significant reductions in attachment, invasion, and total association; attachment from 0.9 to 0.1%, invasion from 0.7 to 0.1%, and total association from 1.7 to 0.2% (p-values were <0.05, <0.05, and <0.01, respectively). For the sialidase negative *F. nucleatum*, attachment was not affected by zanamivir, but the number of invaded and total associated number of bacteria were significantly reduced by zanamivir; invasion from 4.6 to 1.3 %, (3-fold reduction, $p < 0.001$) and total association 5.6 to 2.6 % (2-fold reduction, $p < 0.01$). Interestingly, in this cell line, most of the *F. nucleatum* that were associated with host cells appeared to have invaded the host cells, rather than simply remaining attached to the external surface, and this trend was consistent in all experimental repeats.

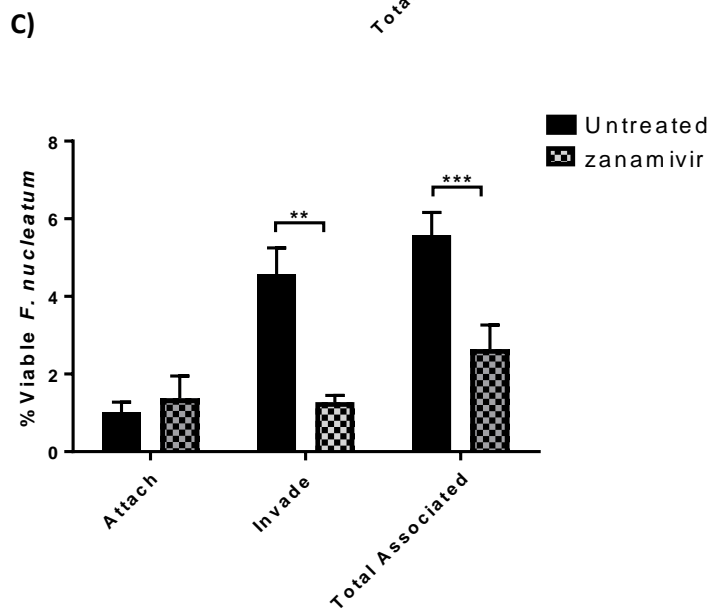
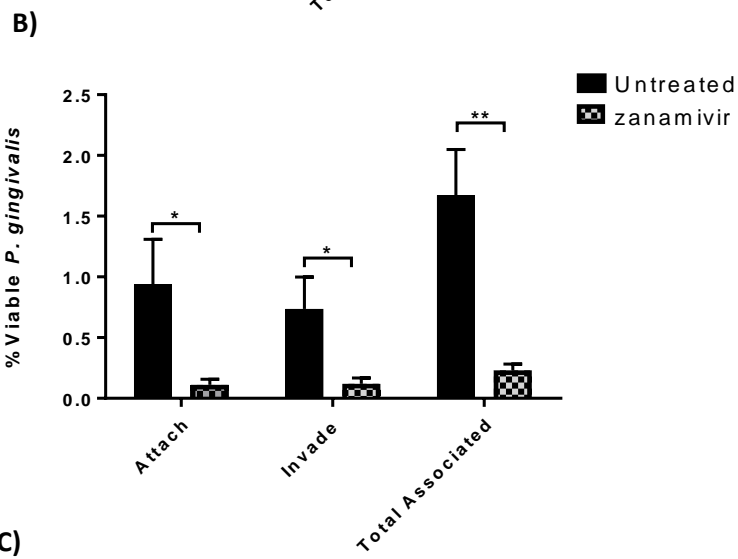
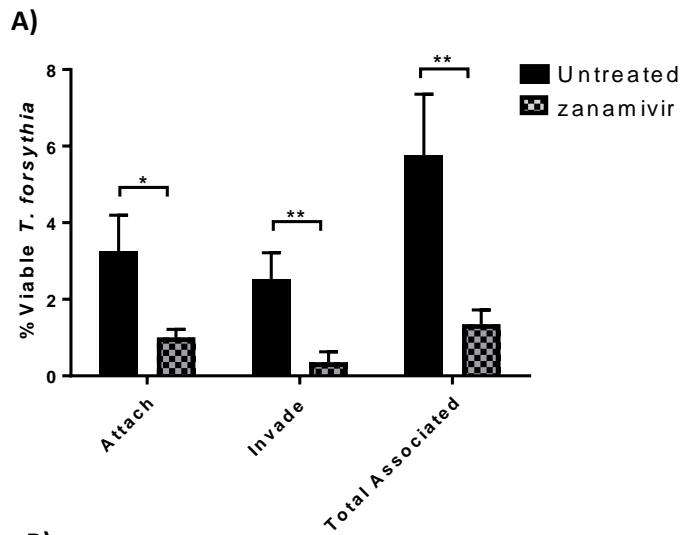


Figure 4.11. The effect of zanamivir on attachment and invasion of immortalised OKF6 epithelial cells.

Antibiotic protection assays were performed in the presence or absence of zanamivir with either A) *T. forsythia*, B) *P. gingivalis*, or C) *F. nucleatum*. Bacterial attachment, invasion, and total association with host cells was normalised to the number of bacteria that were used to infect each condition that had survived the duration of the assay (the percentage of viable bacteria). Zanamivir=10mM zanamivir present during host cell exposure to bacteria. Data represent the mean from three experimental repeats, and each condition was repeated in triplicate during each experiment. Error bars=SEM, Significance determined by T-test, * $p < 0.05$, ** $p < 0.01$.

Zanamivir was consistently capable of reducing bacterial association with host cells; significant reductions in the total number of associated bacteria (the sum of attached and invaded bacteria) were seen for all three periodontal pathogens. *T. forsythia* was the most drastically affected by zanamivir, with association reduced by a factor of approximately threefold and fivefold in H357 and OKF6 cell lines, respectively. This was surprising given the apparently limited inhibition of *T. forsythia* by zanamivir (section 2.3.7.1) but maybe only a small reduction in activity is enough to abrogate interactions at a host-pathogen interface. There are many potential reasons for these differences, but it is of note that zanamivir does affect interactions with both OSCC (H357) and immortalised (OKF6) oral epithelial cell lines in these assays.

4.3.4 Zanamivir inhibits Attachment and Invasion of Oral Epithelial Cells During Infection with Multiple Periodontal Pathogens

In addition to single species antibiotic protection assays, experiments were also performed where multiple periodontal pathogens were used to infect cells; this is more representative of the situation *in vivo*, where host cells encounter multiple species at once. This is particularly relevant during host cell association, since periodontal pathogens have been shown to act in synergy during attachment and invasion (Saito et al. 2012; Inagaki et al. 2006; Kirschbaum et al. 2010).

Antibiotic protection assays were carried out in the manner described above, using H357 oral epithelial cells. MOI was maintained at 1:100 host cells: bacteria, so for infections using two species, the ratio was 1:50:50 (host cells: species 1: species 2), and for infections with all three species, the ratio was 1:33:33:33 (host cells: species 1: species 2: species 3). *T. forsythia*, *P. gingivalis*, and *F. nucleatum* were used in a variety of combinations to infect epithelial cell monolayers. In addition to quantifying the numbers of all bacteria-not distinguishing between species during an assay-the levels of each individual species in a given assay could be enumerated by colony counting on agar plates, since the colony morphologies of *T. forsythia*, *F. nucleatum*, and *P. gingivalis* are distinct from each other (figure 4.12). All possible combinations were tested in this way, with data described below.

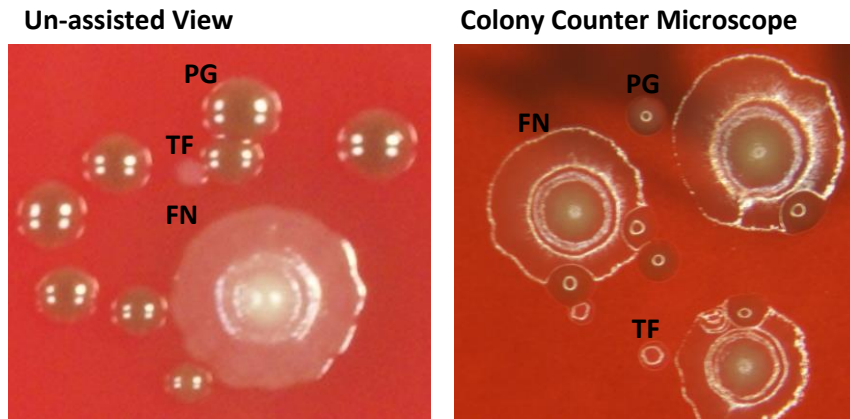


Figure 4.12. Colony morphology of *P. gingivalis*, *F. nucleatum*, and *T. forsythia* during mixed-species enumeration.

Images of mixed-species agar cultures to highlight differences in colony morphology. One colony representative of each species is labelled on the images. *P. gingivalis* (PG) forms opaque black pigmented colonies, *T. forsythia* (TF) forms translucent grey colonies, and *F. nucleatum* (FN) forms large beige colonies, translucent at the edges with a raised, opaque centre.

4.3.4.1 *T. forsythia* and *F. nucleatum* Co-Infection

Host cells were infected, in the presence or absence of zanamivir. The attachment, invasion, and total association of both species were reduced in the presence of zanamivir, though due to variation between repeats this reduction was not always significant.

T. forsythia had a significant reduction in bacterial invasion, from 3.8 to 1.5 % ($p < 0.05$), and a near-significant reduction in total association, from 9.3 to 4.5% ($p = 0.053$). *T. forsythia* attachment was also reduced, though not significantly, from 5.5 to 2.9% ($p = 0.17$). In the case of *F. nucleatum*, invasion was significantly reduced, in the presence zanamivir, from 11.4 to 2.2 % ($p < 0.05$), while attachment and total association were both reduced, neither were shown to be significant, from 24.7 to 12.4 % ($p = 0.094$), and 11.4 to 2.2 % ($p = 0.053$), respectively (figure 4.13 A and B).

Quantification of the total number of bacteria (both *T. forsythia* and *F. nucleatum*) shows that zanamivir significantly reduced both invasion and total association of bacteria with host cells, from 7.4 to 1.8 %, and 19.6 to 7.6 % ($p < 0.01$ and $p < 0.05$), respectively (figure 4.13 C).

Overall, these data indicate that Zanamivir has an effect on co-infection levels of *T. forsythia* and *F. nucleatum* in a co-infection situation.

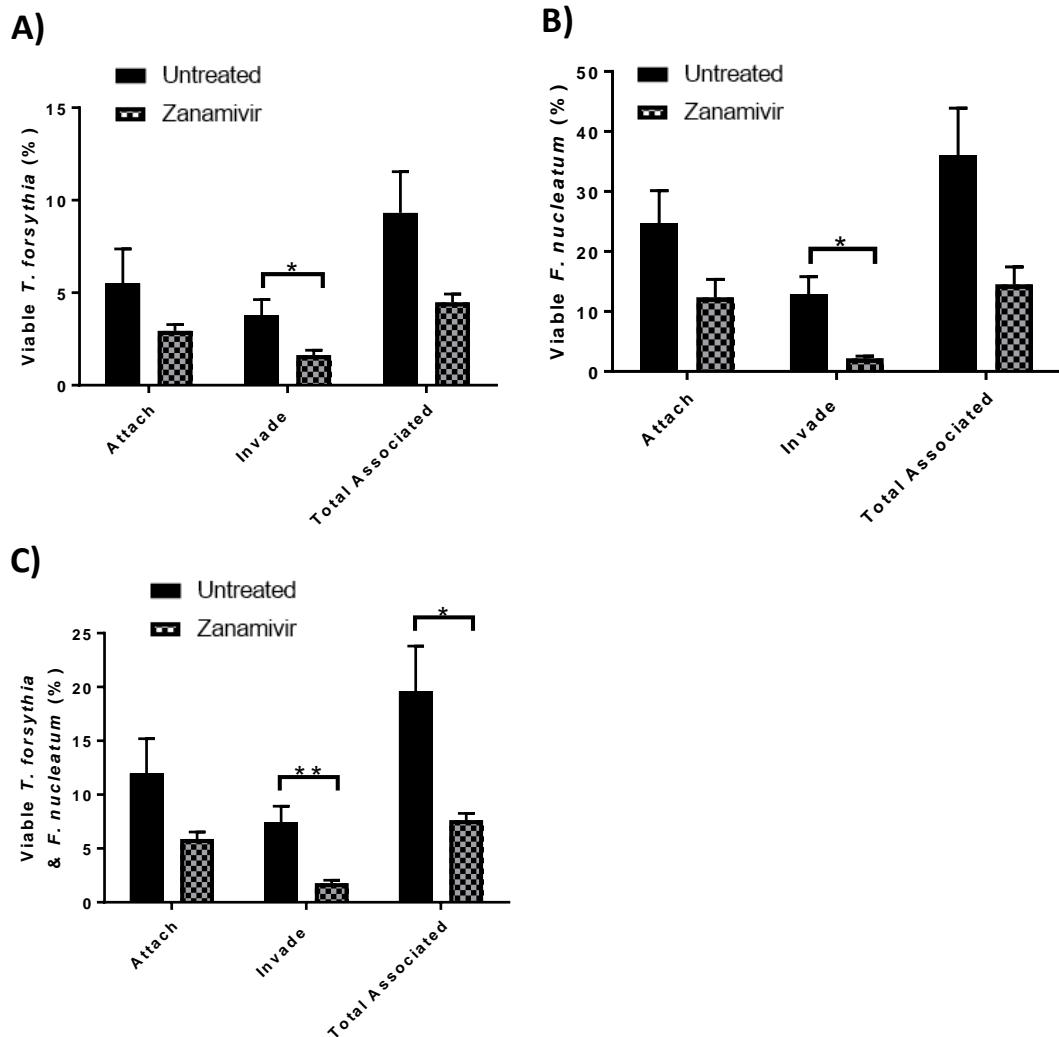


Figure 4.13. The effect of zanamivir on attachment and invasion of epithelial cells co-infected with *T. forsythia* and *F. nucleatum*.

Antibiotic protection assays were performed in the presence or absence of zanamivir with *T. forsythia* and *F. nucleatum*. A) Level of *T. forsythia*-host cell association, B) Level of *F. nucleatum*-host cell association, or C) Level of both *T. forsythia* and *F. nucleatum*-host cell association. Bacterial attachment, invasion, and total association with host cells was normalised to the number of bacteria that were used to infect each condition that had survived the duration of the assay (the percentage of viable bacteria). Zanamivir=10mM zanamivir present during host cell exposure to bacteria. Data represent the mean from three experimental repeats, and each condition was repeated in triplicate during each experiment. Error bars=SEM, Significance determined by paired T-test, * $p < 0.05$, ** $p < 0.01$.

4.3.4.2 *T. forsythia* and *P. gingivalis* co-infection

Host cells were infected, in the presence or absence of zanamivir. The attachment and total association of both species appeared to be reduced in the presence of zanamivir, however, due to variation between experimental repeats, almost no significant differences were found: *T. forsythia* displayed reductions in bacterial attachment, invasion, and total association in the presence of zanamivir (Figure 4.14 A), from 11.6 to 2.0 %, 2.9 to 1.4 %, and 14.5 to 3.6 %, respectively, though only invasion was deemed significant by T-test (with p-values of 0.14, 0.03, and 0.10, respectively). *P. gingivalis* attachment and total association were also reduced by zanamivir, although the decrease was not statistically significant in either case (where $p=0.05$), from 12.7 to 0.25 % ($p=0.068$), and from 14.6 to 2.5 % ($p=0.064$), respectively (figure 4.14 B).

Quantification of both *P. gingivalis* and *T. forsythia* together showed that attachment, total association, and perhaps invasion were reduced in the presence of zanamivir, although again the variation between experiments meant that none of the reductions were statistically significant (figure 4.14 C). Attachment was reduced from 12.1 to 0.8 % ($p=0.076$), invasion from 2.7 to 53% ($p=0.25$), and total association from 14.4 to 2.5 % ($p=0.062$).

Overall, these data indicate that zanamavir has an effect on co-infection levels of *T. forsythia* and *P.gingivalis* in a co-infection situation, although this is perhaps not as striking as in the case of *T. forsythia* and *F. nucleatum*. Given more time, experiments could be repeated, perhaps reducing experimental variation.

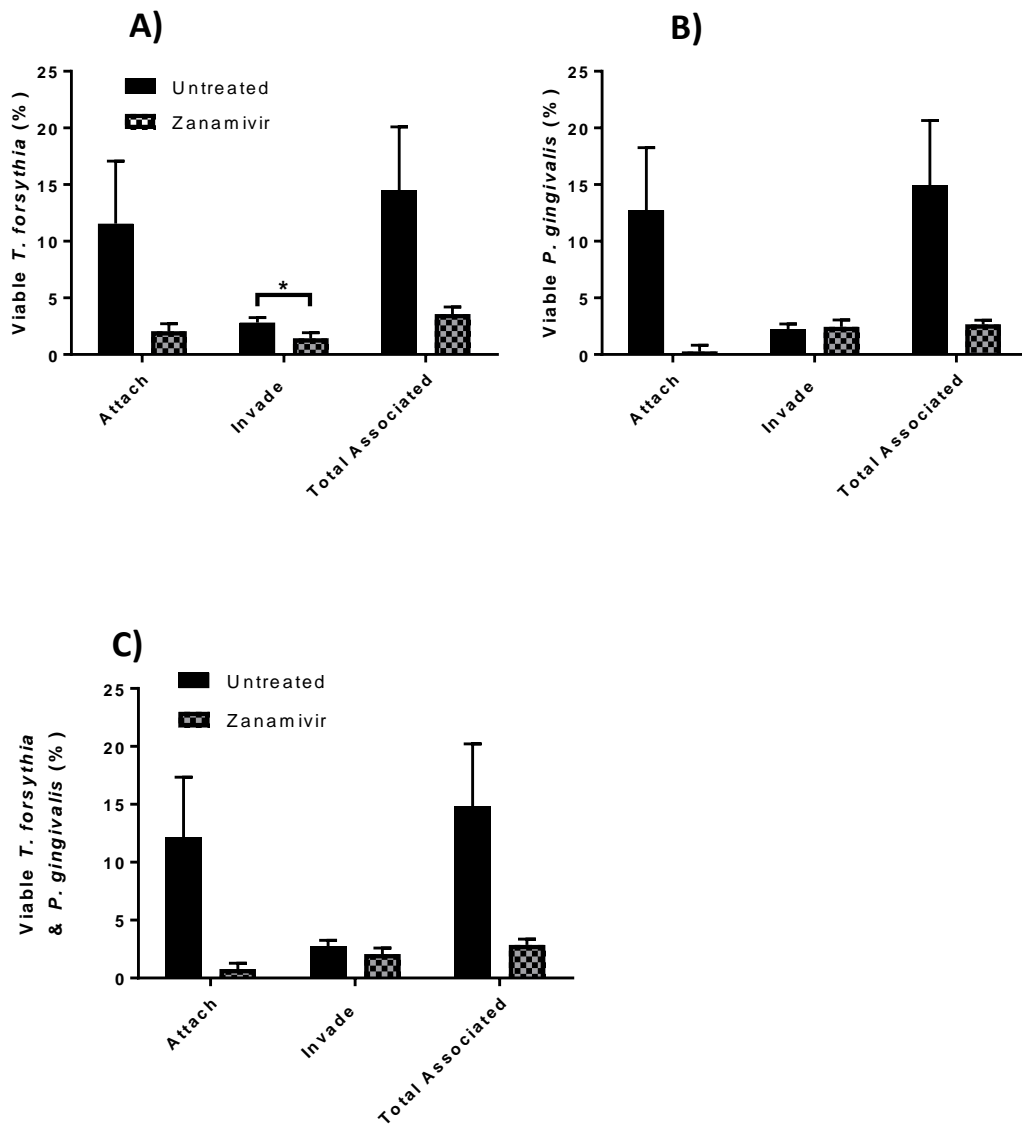


Figure 4.14. The effect of zanamivir on attachment and invasion of epithelial cells co-infected with *T. forsythia* and *P. gingivalis*.

Antibiotic protection assays were performed in the presence or absence of zanamivir with *T. forsythia* and *P. gingivalis* A) Level of *T. forsythia*-host cell association, B) Level of *P. gingivalis*-host cell association, or C) Level of both *T. forsythia* and *P. gingivalis*-host cell association. Bacterial attachment, invasion, and total association with host cells was normalised to the number of bacteria that were used to infect each condition that had survived the duration of the assay (the percentage of viable bacteria). Zanamivir=10mM zanamivir present during host cell exposure to bacteria. Data represent the mean from three experimental repeats, and each condition was repeated in triplicate during each experiment. Error bars=SEM. Significance determined by paired T-test, *p<0.05.

4.3.4.3 *P. gingivalis* and *F. nucleatum* co-infection

Host cells were infected in the presence or absence of zanamivir. The attachment, invasion, and total association *P. gingivalis* was reduced in the presence of zanamivir to varying extents (Figure 4.15 A): *P. gingivalis* bacterial attachment, invasion, and total association were significantly reduced by zanamivir, from 3.9 to 1.15 % ($p < 0.05$), 1.7 to 0.5 % ($p < 0.01$), and 5.5 to 1.7 % ($p < 0.05$). In the case of *F. nucleatum*, invasion and total association appeared to be reduced in the presence of zanamivir, although the decreases were not statistically significant (figure 4.15 B), from 4.0 to 1.6 % ($p = 0.23$), and 7.9 to 6.0 ($p = 0.12$), respectively.

Quantification of the total number of bacteria (both *P. gingivalis* and *F. nucleatum*) shows that zanamivir significantly reduced attachment, invasion, and total association of bacteria with host cells, from 1.9 to 0.8 % ($p < 0.05$), 4.0 to 1.56 % ($p < 0.05$), and 5.9 to 2.4 % ($p < 0.01$), respectively (figure 4.15 C).

Overall, these data indicate that zanamivir has an effect on levels of *P. gingivalis* and *F. nucleatum* in a co-infection situation.

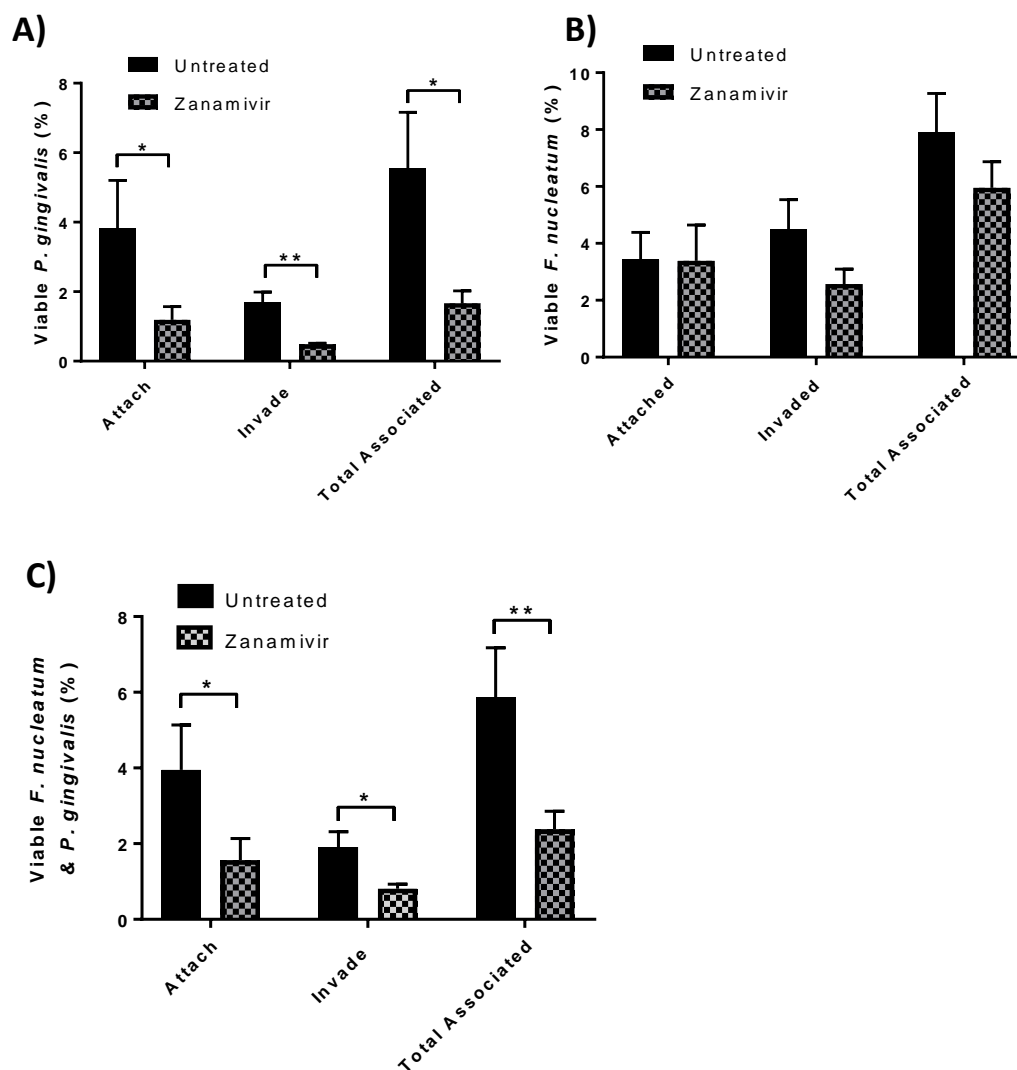


Figure 4.15. The Effect of Zanamivir on Attachment and Invasion of Epithelial Cells Co-infected with *P. gingivalis* and *F. nucleatum*.

Antibiotic protection assays were performed in the presence or absence of zanamivir with *T. forsythia* and *F. nucleatum*. A) Level of *T. forsythia*-host cell association, B) Level of *F. nucleatum*-host cell association, or C) Level of both *P. gingivalis* and *F. nucleatum*-host cell association. Bacterial attachment, invasion, and total association with host cells was normalised to the number of bacteria that were used to infect each condition that had survived the duration of the assay (the percentage of viable bacteria). Zanamivir=10mM zanamivir present during host cell exposure to bacteria. Data represent the mean from three experimental repeats, and each condition was repeated in triplicate during each experiment. Error bars=SEM, Significance determined by paired T-test, * $p < 0.05$, ** $p < 0.01$.

4.3.4.4 *T. forsythia*, *F. nucleatum*, and *P. gingivalis* co-infections

Finally, host cells were infected with all three organisms, in the presence or absence of zanamivir. Enumeration of the individual species revealed that the invasion and total association of all three was reduced in the presence of zanamivir, to varying extents. In the case of *T. forsythia*, these reductions were not significant, though invasion showed the greatest change (figure 4.13 A), from 28.6 to 17.7% in the presence of zanamivir ($p=0.18$). *F. nucleatum* invasion and total association was significantly reduced by zanamivir, from 27.1 to 7.1% and 46.1 to 24.1%, respectively (Figure 4.13 B). In the case of *P. gingivalis*, zanamivir caused a significant reduction in invasion, from 6.5 to 3.0% (Figure 4.13 C).

Quantification of the total number of bacteria (*T. forsythia*, *F. nucleatum*, and *P. gingivalis* enumerated together rather than individually) showed that zanamivir significantly reduced attachment, invasion, and total association of bacteria with host cells, from 17.7 to 7.7%, 9.6 to 7.15%, and 26.14 to 14.6%, respectively (Figure 4.13 D).

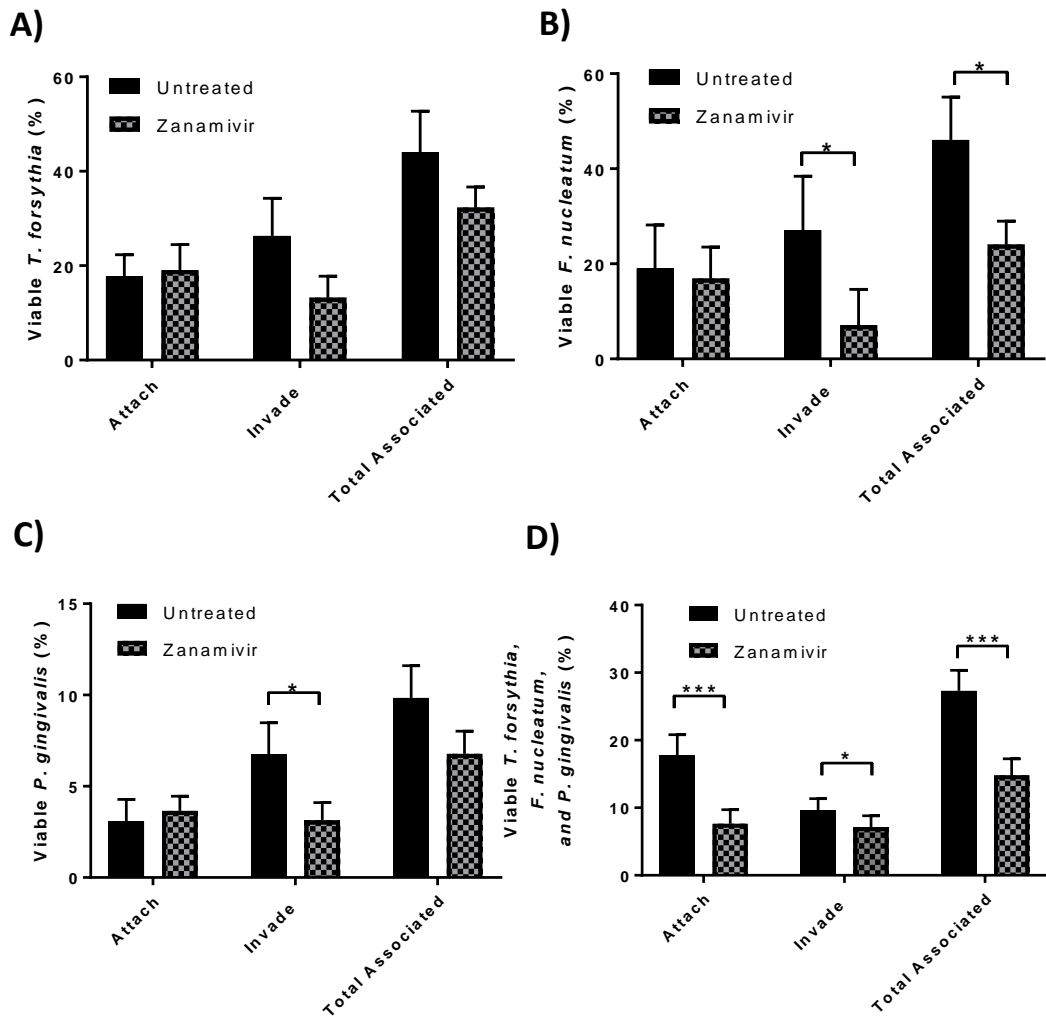


Figure 4.16. The effect of zanamivir on attachment and invasion of epithelial cells co-infected with *T. forsythia*, *F. nucleatum*, and *P. gingivalis*.

Antibiotic protection assays were performed in the presence or absence of zanamivir with *T. forsythia*, *F. nucleatum*, and *P. gingivalis*. A) *T. forsythia*-host cell association, B) *F. nucleatum*-host cell association, C) *P. gingivalis*-host cell association D) *T. forsythia*, *F. nucleatum*, and *P. gingivalis*-host cell association. Bacterial attachment, invasion, and total association with host cells was normalised to the number of bacteria that were used to infect each condition that had survived the duration of the assay (the percentage of viable bacteria). Zanamivir=10mM zanamivir present during host cell exposure to bacteria. Data represent the mean from three experimental repeats, and each condition was repeated in triplicate during each experiment. Error bars=SEM, Significance determined by paired T-test, * $p < 0.05$, ** $p < 0.01$. *** $p < 0.001$.

Taken as a whole, these data show that zanamivir interfered with bacteria-host cell interactions during single-species antibiotic protection assays, where host cells were infected with either *T. forsythia*, *P. gingivalis*, or *F. nucleatum*. Zanamivir reduced bacterial attachment, invasion, and the total association (sum of attached and invaded bacteria) to varying degrees for each pathogenic species. The most drastically affected by zanamivir was *T. forsythia*, which displayed significant reductions in attachment, invasion, and total association in the presence of zanamivir, in both OSCC (H357) and normal-immortalised (OKF6) oral epithelial cell lines. Zanamivir also inhibited *P. gingivalis* association with host cells, with significant differences seen in invasion or total association in OSCC and normalised oral epithelial cell lines, respectively. The most surprising result was that zanamivir inhibited host cell association by the sialidase negative *F. nucleatum*.

Within the mixed species antibiotic protection assays cells were co-infected with combinations of two or three of the periodontal pathogens (*T. forsythia*, *F. nucleatum*, or *P. gingivalis*). It is clear from these that the experiments assessing dual-infections revealed a role for sialidase and zanamivir in reducing co-infection levels, with the most-striking data obtained for the *T.forsythia/F. nucleatum* combination.

However, the triple-infection situation was more difficult to reproduce in separate experiments, at least in terms of enumerating individual species within these assays, and it would be pertinent to consider increasing n-numbers for this experimental set. On the other hand, the combined totals of the two or three species present in each experiment were more consistent: This is evident in the dataset summarising the mixed species experiments, where significant differences between untreated and zanamivir-treated conditions are seen more frequently in the combined totals of the two or three species present in a given experiment, rather than enumeration of individual species. This implies that zanamivir is able to prevent some aspects of host-pathogen association, even in a three-species infection model-which was the most difficult to reproduce in terms of the association levels of individual species.

When enumerating individual levels of the pathogens in the three-species infection experiment, zanamivir was capable of significantly reducing host-bacteria association, but only the total association of *F. nucleatum* was significantly inhibited (according to T-test, where $p=0.05$). However, quantifying levels of all three species together showed that zanamivir significantly reduced attachment and total association of host cells by the three species; attachment was reduced by ~66 %, and total association by ~50 %. Overall

indicating that sialidase inhibition did influence the host-cell interactions of this mini-community experiment.

Although host cell association is important for bacterial colonisation and persistence, ultimately it is the host immune response to pathogens that causes the tissue destruction seen during periodontitis. Therefore, another set of experiments was performed to study the effect of periodontal pathogen sialidases in pro-inflammatory signalling by oral epithelial cells. The ability of the sialidase inhibitor zanamivir to inhibit sialidase mediated-pro-inflammatory signalling was also tested.

4.3.5 *T. forsythia* Sialidase Influences Pro-Inflammatory Signalling in Epithelial Cells, and this is Affected by Zanamivir

A key aspect of disease progression in periodontitis is overstimulation of innate immunity, resulting in destructive inflammation that damages host tissue. Oral epithelial (and endothelial) cells can express some pro-inflammatory signalling molecules in response to pathogens or pathogen components, or as a result of cell damage. Periodontal pathogen sialidases may mediate these processes in a number of ways, possibly directly through desialylation of host cell surfaces leading to complement deposition and cell death, or indirectly by influencing the attachment and invasion of pathogens to host cells.

An important pathway leading to stimulation of the innate immune response is mediated by the Toll Like Receptors (TLRs), with TLRs -2, -4, and -9 (Kikkert et al. 2007; Wara-Aswapati et al. 2012) considered to be important during responses to periodontal pathogens, although there is still some debate regarding which TLRs are most important for recognising specific pathogens, and the relevance of each TLR to periodontitis. TLRs -2 and -4 are present on the plasma membrane, where they recognise extracellular bacterial components, specifically lipoproteins and lipopolysaccharide, respectively. Specifically, the *T. forsythia* BspA protein is also capable of stimulating TLR-2 (Myneni et al. 2012). TLR-9 is an intracellular receptor, present on lysosomal membranes where they recognise bacterial DNA. TLRs -2, -4, and -9 are regulated by the activity of human sialidases Neu1 and/or Neu3, which are mobilised to the plasma membrane (or in the latter case lysosomal membranes) and desialate the TLRs, which are then able to induce gene expression changes through the MyD88 signalling pathway, including production of pro-inflammatory cytokines (Amith et al. 2010; Stamatou et al. 2010; Abdulkhalek & Szewczuk 2013). Given that human sialidases are required for TLR activation, it is possible that pathogen sialidases could mimic this function, causing an increase in TLR activation, resulting in an upregulation

of pro-inflammatory responses. Indeed, it has been shown that recombinant sialidase from *Trypanosoma cruzi* or *S. pneumoniae* is capable of upregulating TLRs -2 and -4 in macrophages and transfected Human Embryonic Kidney (HEK) cells, and that sialidase TLR activation leading to pro-inflammatory signalling could be inhibited using the sialidase inhibitor oseltamivir (Amith et al. 2010). Intracellular TLR-9 signalling is also inhibited by oseltamivir (Abdulkhalek & Szewczuk 2013).

Given that these TLRs are important during periodontitis, are regulated by sialidase, and that sialidase inhibitors can prevent activation of TLR-2 and -4, resulting in decreased pro-inflammatory signalling, investigation of the sialidase inhibitor zanamivir in preventing inflammatory signalling in oral epithelial cells was an exciting prospect. These experiments focused on stimulating the OSCC cell line H357 with the TLR-4 ligand LPS, or live pathogens in the presence and absence of zanamivir, then determining expression of the pro-inflammatory cytokine Interleukin-8 (IL-8, also called CXCL8) by epithelial cells.

4.3.5.1 ***The IL-8 Response of Oral Epithelial Cells to P. gingivalis LPS may be Upregulated by the T. forsythia Sialidase NanH, and this is Inhibitable by Zanamivir***

Although the over-abundance and/or over-activation of neutrophils is considered key in mediation of periodontal inflammation (Hajishengallis & Hajishengallis 2013), epithelial cells can also be stimulated by bacteria to produce proinflammatory cytokines, which act to recruit immune cells. Indeed, the initial production of cytokines that mediates neutrophil recruitment to the gingival tissue probably originates from epithelial and endothelial cells exposed to pathogens or bacterial components.

Bacterial LPS is the ligand for TLR-4 activation, which stimulates production of IL-8 via the Myd88-NFKB signalling pathway. TLR-4 can be expressed in epithelial cells, and its activation is known to be important during immune stimulation by periodontal pathogens. Furthermore, TLR-4 has been shown to require human sialidase for activation, and it was considered likely that periodontal pathogen sialidases would cause increased TLR-4 activation, and that sialidase inhibition would decrease TLR-4 activation and subsequent IL-8 secretion in response to LPS. The OSCC epithelial cell line H357 was chosen for cytokine studies due to its rapid proliferation and ease of culture, and previous work described in this chapter showing some degree of involvement of sialidases in host-pathogen interactions had been performed using this cell line. Cells were exposed to LPS purified from *P. gingivalis* ATCC 33277 for 24 hours, in the presence or absence of NanH and/or zanamivir LPS from *P. gingivalis* was chosen due to its relevance to oral disease. NanH had

undergone LPS decontamination (potential contamination from the *E.coli* expression strain) using polymixin-agarose beads to remove LPS remaining after purification. The secretion of IL-8 into epithelial cell culture media was measured by ELISA, and significant differences determined by one way ANOVA. A high level of day-to-day variation in cytokine secretion was observed between experimental repeats, so ANOVA was performed with no correction for multiple comparisons in order to obtain greater statistical power (Figure 4.14 A), and with Tukey's correction for multiple comparisons to establish the most significant differences (Figure 4.14 B). The p-values discussed in the text below describe the ANOVA without a correction for multiple comparisons

Interestingly, IL-8 secretion by oral epithelial cells was reduced slightly in the presence of zanamivir, from 218 pg/ml in the untreated condition to 185 pg/ml ($p=0.02$). Surprisingly, LPS exposure caused no changes in IL-8 secretion by H357 cells (212 pg/ml). More expectedly, NanH treatment alone also caused no change in IL-8 secretion levels (231 pg/ml) compared to the untreated condition. In contrast, when NanH and LPS were incubated with the same cells simultaneously, an increase in the average levels of secreted IL-8 was observed-270 pg/ml, although this change was not deemed significant by ANOVA ($p=0.2$). However, in the presence of zanamivir, IL-8 secretion by oral epithelial cells in response to LPS & NanH was significantly reduced compared to LPS+NanH, from 270 pg/ml to 164.7 pg/ml ($p=0.007$), which was also significantly lower level than IL-8 secretion in the untreated condition ($p=0.02$).

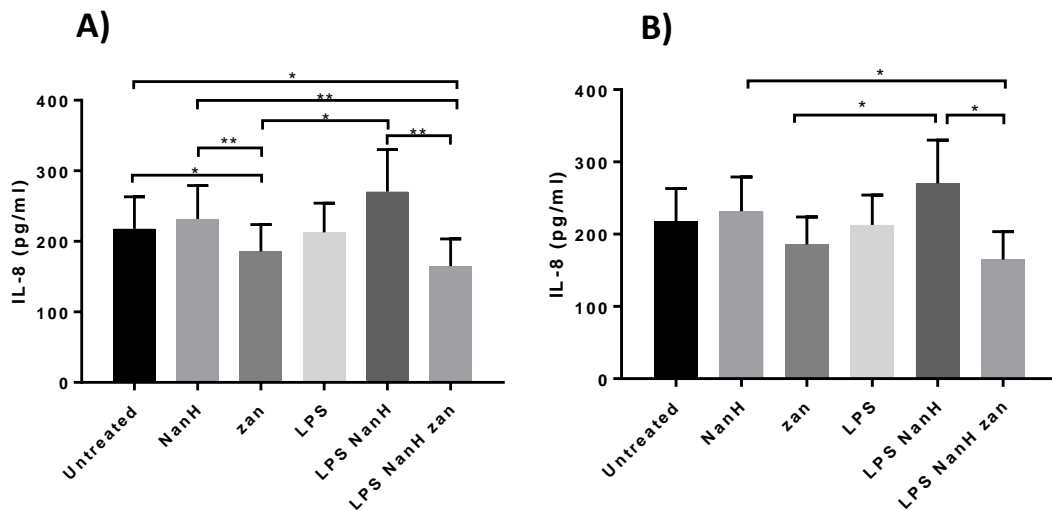


Figure 4.17. IL-8 secretion of oral epithelial cells exposed to zanamivir, LPS, and NanH.

Oral epithelial cells were cultured as monolayers in 6-well tissue culture plates, and exposed to combinations of 50nM NanH (NanH), 10mM zanamivir (zan), and/or 10 μ g *P. gingivalis* LPS (LPS) for 24 hours, before harvesting of cell culture supernatants for IL-8 ELISA to obtain IL-8 secreted by cells in each condition (pg/ml). Data shown represent the mean of four experimental repeats, where each condition was repeated twice per experiment. Error bars =SEM. Significance determined by one way ANOVA A) without and B) with Tukey's correction for multiple comparisons *p<0.05, **p<0.01.

Ultimately, while cells exposed to LPS alone did not display any increased IL-8 secretion, in the presence of NanH plus LPS the IL-8 secretion displayed an increase relative to the LPS only condition, although variation between repeats did mean that with Tukey's correction for multiple comparisons this difference appeared to be non-significant. However, this trend appears to be confirmed since in the presence of zanamivir, IL-8 secretion was reduced in cells exposed to LPS and NanH, to levels lower-than IL-8 secretion in the untreated condition. These results lend support to the idea that periodontal pathogen sialidases upregulate pro-inflammatory signalling in epithelial cells in response to bacterial LPS, possibly by pathways involving TLRs. It also highlights the ability of zanamivir to reduce inflammatory signalling even in the absence of stimulation with bacterial components (at least in this cell line).

4.3.5.2 ***IL-8 Secretion by Oral Epithelial Cells Infected with *T. forsythia* is Reduced in the Presence of Zanamivir.***

Although LPS stimulation of TLR-4 (or other TLRs) is one pathway which may be important during upregulation of inflammatory signalling in periodontitis, live periodontal pathogens are believed to stimulate epithelial cell inflammatory responses in a number of different mechanisms and represent a better model of infection than a single ligand. Therefore, the OSCC oral epithelial cell line H357 was infected with live *T. forsythia* (at a MOI of 1: 100 bacteria: host cells) for 24 hours, in the presence and absence of zanamivir to test the effect of sialidase inhibition on IL-8 secretion as a measurement of pro-inflammatory signalling in response to periodontal pathogen infection. The secretion of IL-8 into epithelial cell culture media was measured again by ELISA. Given the results of the previous experiment, the ability of both zanamivir and *T. forsythia* to influence IL-8 secretion was tested. Therefore, repeated measures 2-way ANOVA with Tukey's correction for multiple comparisons was utilised to test for significant differences between uninfected and *T. forsythia* infected cells, in the presence and absence of zanamivir (Figure 4.15).

Similarly to the LPS experiments described in the previous section, IL-8 secretion was detectable in the untreated condition at 1270 pg/ml. Zanamivir caused no change in IL-8 secretion (1183 pg/ml). *T. forsythia* caused an increase in IL-8 secretion to 1739 pg/ml, however, under this statistical test the increase was apparently not significant ($p=0.10$). In the presence of zanamivir the IL-8 secretion caused by *T. forsythia* infection was reduced to almost the same level as the untreated condition-1269 pg/ml, although this reduction was also apparently not significant ($p=0.10$).

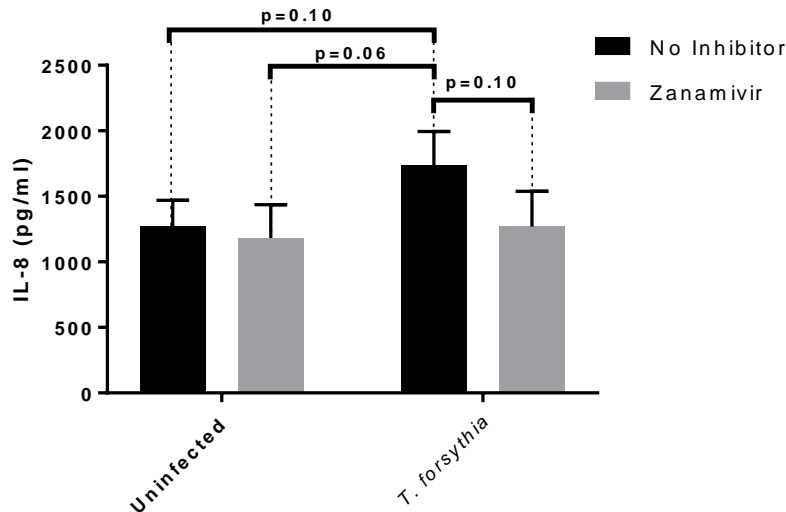


Figure 4.18. Secretion of IL-8 by oral epithelial cells infected with *T. forsythia*, in the presence and absence of zanamivir.

Oral epithelial cells were cultured as monolayers in 6-well tissue culture plates, and exposed to *T. forsythia*, 10mM zanamivir, *T. forsythia* and 10mM zanamivir for 24 hours, before harvesting of cell culture supernatants for IL-8 ELISA. Across all conditions, both *T. forsythia* and zanamivir significantly influenced IL-8 secretion ($p < 0.05$ and < 0.01 , respectively, determined using 2-way ANOVA with repeated measures). Data shown represents IL-8 secretion (pg/ml) in each condition, from the mean of three experimental repeats, where each condition was repeated twice per experiment. Error bars = SEM. Significance between conditions was determined by 2-way ANOVA with repeated measures, with Tukey's correction for multiple comparisons. P-values of 0.1 or less are indicated.

Although the differences in IL-8 secretion between the untreated, and *T. forsythia* and *T. forsythia* + zanamivir conditions could be considered non-significant (with P-values between 0.06 and 0.1), the levels of IL-8 in the *T. forsythia* + zanamivir condition returned to a level almost exactly that of the untreated control. Furthermore, the 2-way ANOVA established that both zanamivir and *T. forsythia* caused significant changes to IL-8 secretion, even if there were no significant differences between conditions. Therefore, it could be the case that zanamivir influences cytokine responses in response to bacterial challenge with *T. forsythia*. These data would be even more convincing if performed with a sialidase negative *T. forsythia* strain, but time did not allow this during my project.

4.3.5.3 ***Broad Cytokine Production induced by T. forsythia Infection of Oral Epithelial Cells is Altered by the Presence of Zanamivir***

IL-8 is only one of a multitude of pro-inflammatory cytokines that could be produced by oral epithelial cells in response to periodontal pathogens. Therefore, a panel of pro-inflammatory cytokines was selected for multiplex analysis using a cytokine bead array (CBA), based on previous studies of inflammatory signalling in oral epithelial cells (table 4.5.). The cytokines were also selected for operational reasons; the manufacturer of the CBA, BD biosciences, only produces kits for a limited number of cytokines.

The same cell culture supernatants from section 4.3.5.3 were analysed using the CBA. H357 Cells had been incubated for 24 hours in the presence of either zanamivir, *T. forsythia*, *T. forsythia* & zanamivir, or left untreated as a control, and the cell culture supernatant removed from cells and stored at -20°C prior to the IL-8 ELISA described in the previous section, then stored again at -20°C until undergoing cytokine quantification using the CBA described here. Secretion (pg/ml) of six pro-inflammatory cytokines (table 4.5) under the described conditions are shown in figure 4.16. Repeated measures 2-way ANOVA with Tukey's correction for multiple comparisons was utilised to test for significant differences between uninfected and *T. forsythia* infected cells, in the presence and absence of zanamivir

Interestingly, cells treated with zanamivir alone showed reduced levels of all six cytokines relative to the untreated condition. This was only deemed significant for IL-8 and MIP1 α , which were reduced from 616 and 1.7 pg/ml to 458 and 0.94 pg/ml ($p=0.02$ and 0.02), respectively.

Cells treated with *T. forsythia* displayed increased levels of five out of the six cytokines, with significant increases in IL-8 and MCP-1 secretion, from 616 and 153.4 pg/ml, to 808 and 232 pg/ml ($p=0.01$ and 0.03), respectively. The presence of zanamivir abrogated these effects; cells treated with *T. forsythia* and zanamivir displayed similar levels of cytokine secretion to the untreated condition, and there were no significant differences in cytokines between untreated and *T. forsythia* + zanamivir-treated conditions (with the exception of MIP1 α , see below). There were also a significant differences in IL-8 secretion in the *T. forsythia* and *T. forsythia* + zanamivir conditions, where zanamivir reduced secretion from 808 pg/ml to 580 pg/ml ($p=0.003$).

The exception to the trend that *T. forsythia* increases cytokine secretion, and zanamivir prevents the change in cytokine secretion was MIP1 α , which was decreased from 1.712 to

0.94 pg/ml ($p=0.025$), and this was further reduced in *T. forsythia* + zanamivir-treated conditions, to 0.45 pg/ml ($p=0.0023$, compared to the untreated condition).

Overall, despite the variability in the data in these experiments, there is a clear trend that *T. forsythia*/LPS challenge alters the cytokine response of oral epithelial cells. These data, though interesting, do however come with the caveat that further repeats are needed to improve statistical power, alongside the need to introduce some element of a dose-response of either immune ligand and introduction of sialidase negative mutant bacteria or sialidase negative enzymes to dissect any role for bacterial sialidase over zanamavir dependent effects on host sialidases.

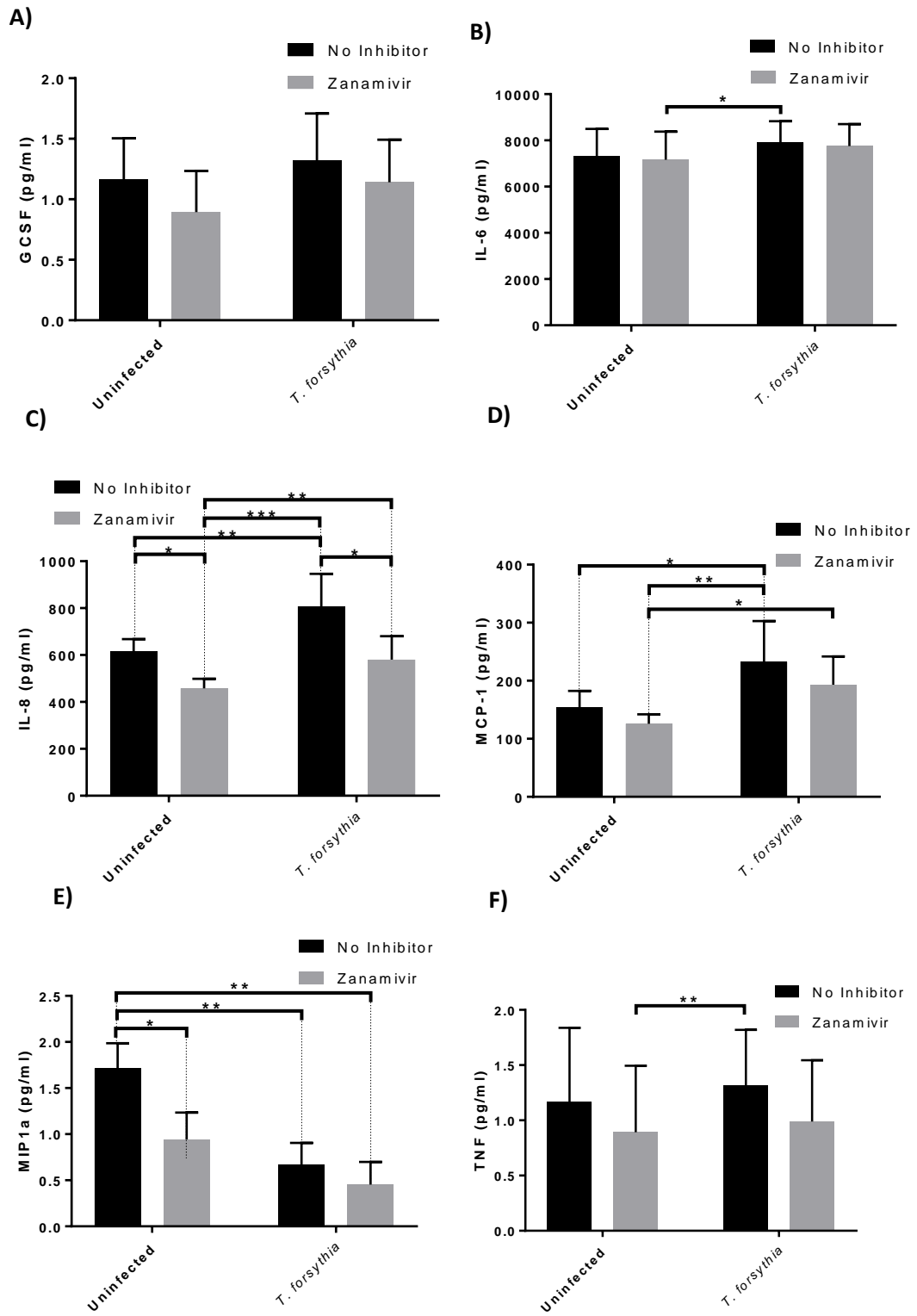


Figure 4.19. Cytokine secretion by oral epithelial cells infected with *T. forsythia*, in the presence and absence of zanamivir. A) GCSF B) IL-6 C) IL-8 D) MCP-1 E) MIP1 α F) TNF.

Oral epithelial cells were cultured as monolayers in 6-well tissue culture plates, and exposed to *T. forsythia* (TF), 10mM zanamivir (zan), or *T. forsythia* and zanamivir (TF+Zan) for 24 hours, before harvesting of cell culture supernatants for CBA multiplex analysis for multiple cytokines. Across all treatment conditions, zanamivir was found to significantly influence secretion of IL-8, MIP1 α , and TNF, determined by 2-way ANOVA with repeated measures ($p < 0.01$, < 0.05 , and < 0.01 , respectively), while *T. forsythia* infection was found to significantly influence secretion of only MIP1 α ($p < 0.05$). Data shown represent the mean of three experimental repeats, where each condition was repeated twice per experiment. Error bars =SEM. Significance determined by 2-way ANOVA with repeated measures, with Tukey's correction for multiple comparisons * $p < 0.05$, ** $p < 0.01$, *** $p < 0.005$.

4.4 Discussion

4.4.1 Host Cells Are Desialylated by Purified sialidases and Live Periodontal Pathogens

The previous results chapters highlighted the ability of *T. forsythia* and *P. gingivalis* sialidases to act on both α 2-3 and α 2-6 linked sialic acid-containing oligosaccharide substrates (3- and 6-sialyllactose), and the sialidases could act on BSM; a host relevant, secreted glycoprotein. However, it was a key part of this thesis to examine their ability to act on these and other glycans in their natural glycoprotein-conjugated cellular context.

It was therefore reassuring that *T. forsythia* was able to desialylate host sialyl-glycans in the context of live human cells, although in this case only the SNA-lectin reactive antigens (containing alpha-6- linked sialic acid ligands) was significantly reduced with the MAA-linked staining indicating a reduction by eye which was not borne out during quantification. One would have expected this to be more of a striking reduction given the enzymatic data but also since a similar experiment, with another oral cell line by Honma et al., (Honma et al. 2011), who also incubated human cells with *T. forsythia*, and observed a reduction in SNA and MAA staining but was performed on cells where fixing was performed before staining, which was not the case in my experiments—a step that may have enhanced this observation.

In the case of *P. gingivalis* it seemed that the human cells suffered damage and death, possibly via the action of gingipains. This made interpreting these data very difficult. Oral epithelial cell numbers appeared to be greatly reduced, compared to the un-infected and *T. forsythia*-infected conditions, as seen in the fluorescence microscopy images in figure 4.4. Indeed, the fields of view shown in figure 4.4 were chosen since other fields of view had fewer epithelial cells. This reduction in oral epithelial cells is likely due to the high concentration of live *P. gingivalis* (cells were exposed to OD₆₀₀ 0.5 bacteria, for both *T. forsythia* and *P. gingivalis*), and subsequent host cell death. The reduction in sialic acid staining of epithelial cell surfaces could also be due to the action of gingipains, which may cleave whole sialoglycoproteins from the cell surface (rather than just the sialic acid). Unfortunately, a lower concentration of bacteria might not possess enough sialidase activity to visibly reduce cell surface desialylation, so further experiments with lower concentrations of bacteria were not performed but may be worthwhile. An alternative possibility for future work would be to test desialylation by *P. gingivalis* gingipain mutants.

As a result of the difficulties in using whole bacteria, experiments were performed with purified sialidases to examine their action on sialyl-glycan ligands in their natural human context. Therefore, unsurprisingly, treatment of oral epithelial cells with purified NanH or SiaPG was capable of desialylating host cell surfaces, reducing both alpha-3- and 6- linked sialic acid (in accordance with the data in section 2.3.6.3) showing that NanH could cleave sialic acid from 3- and 6- sialyllactose). Zanamivir appeared to inhibit this activity (qualitatively) in the case of SiaPG but not NanH-possibly an unsurprising result given that zanamivir appears to be a more efficacious inhibitor of SiaPG than NanH.

In addition to general staining for surface sialic acid, the sialoglycans sialyl lewis A and sialyl lewis X (SLeA and SLeX) were also stained with a view to testing the effect of NanH on these. SLeA and SLeX are short glycan structures present at the termini of various secreted and membrane associated glycoproteins. They are structural isomers, consisting of an N-acetylglucosamine (GlcNAc) and galactose backbone, with Neu5Ac (sialic acid) linked to the galactose via an α 2-3 linkage, and fucose to the GlcNAc, through either an α 3 or α 4 linkage, giving rise to the two isomers-SLeX and SLeA (SLeX/A), respectively. SLeX/A are present in secreted glycoproteins such as mucins, but are also associated with cell surface membranes. SLeX is most highly expressed on leukocytes (and erythrocytes), where it functions as a ligand for E-selectin present on endothelial cells, enabling neutrophil attachment and crawling motility on the endothelial surface (reviewed in Bevilacqua & Nelson 1989). SLeA/X are also expressed on many cell types; endothelial cells for one, but also epithelial cells at mucosal surfaces, including the oral cavity. SLeA/X have been the focus of study due to changes in their levels of expression during various cancers including oral cancer (Renkonen et al. 1999). More recently, the involvement of host cell surface SLeA/X (and that of their selectin receptors) in pathogen association with host cells has come under scrutiny (Komatsu et al. 2012; Magalhaes et al. 2015; Colomb et al. 2013). Therefore it was considered important to study the effect of the purified sialidases on cell-surface SLeA and SLeX. Unfortunately, the timeframe of the project did not permit testing with SiaPG as well as NanH.

SLeX is the most well studied for its role in neutrophil migration-where it is expressed on the surface of neutrophils and binds E-selectin present on endothelial cells, enabling crawling motility and migration across the endothelium into the target tissue (Lowe 2003). SLeA is also capable of binding selectins (Melorose et al. 1991). It was shown in chapter 2 (section 2.3.6.4) that NanH appears to display almost tenfold greater efficacy for SLeA than

SLeX during *in vitro* assay using isolated Sialyl-Lewis oligosaccharides, despite the only difference between the two ligands being the type of fucose-GalNAc and Glc-GalNAc linkages. As well as its presence on mucin (where SLeX is perhaps the more prevalent isoform), SLeA is present on oral/laryngeal epithelial cells, where its expression is upregulated in head and neck cancers and erythrocytes (Renkonen et al. 1999; Wiest et al. 2010).

In the experiments described in this chapter, NanH was capable of desialylating both SLeA and SLeX present on oral epithelial cell surfaces. The exposure to NanH took place over two hours, with a high concentration of NanH, which could explain why no variation in desialylation is apparent between cell surface SLeA and SLeX; i.e sialic acid was cleaved from both to similar extents, as indicated by similar decreases in the level of surface staining for SLeA/X, despite the apparent ~tenfold greater affinity of NanH for free (non-membrane/glycoprotein associated) SLeA compared to free SLeX. The finding that zanamivir did not prevent host desialylation of SLeA/X (SLeA desialylation was only partially inhibited) by NanH was not surprising, given that zanamivir does not appear to display high efficacy for NanH, and any inhibition might have been overcome by the high concentration of enzyme used in these experiments. Another variable to consider is the rate of SLeA/X turnover by oral epithelial cells, and if there is any SLeA/X cleavage, any inhibition by zanamivir might be more evident in a cell line with a higher SLeA/X turnover rate.

How cell surface desialylation, or more specifically cell surface SLeA/X desialylation of oral epithelial cell surfaces (or other cell types) contributes to the pathogenicity of *T. forsythia* (or possibly other periodontal pathogens) is not entirely clear. A number of pathogens have been shown to use SLeA/X antigens, or their selectin receptors for attachment to cell surfaces. In these cases SLeA/X is retained at the cell surface where it acts as a receptor for pathogen attachment, as seen in cells infected with the gastric pathogen *Helicobacter pylori* (Magalhaes et al. 2015), or the respiratory pathogen *P. aeruginosa* (Colomb et al. 2013), and in both of these cases the increase in cell-surface SLeA/X expression was mediated by TNF. However, desialylation of SLeA/X has not been shown to be a feature during host-cell attachment by *H. pylori* or *P. aeruginosa*. However, this might be the case for *T. forsythia*, since sialidase deficient *T. forsythia* (a *nanH* knockout mutant) deficient in sialidase activity displays decreased attachment to oral epithelial cells (Honma et al. 2011).

Even if desialylation of cell surface SLeA/X does not enhance *T. forsythia* attachment to host-cells, decreases in cell surface Neu5Ac may increase inflammation, since Neu5Ac is an

important host recognition molecule, involved in preventing complement deposition on cell surfaces, and SLeA/X are ligands for Siglecs; self-recognition receptors present on innate and adaptive immune cells (but not epithelial layers), which bind sialoglycans present on surfaces of other cell types and dampen signalling pathways which regulate the pro-inflammatory responses of the Siglec-expressing immune cell (Varki & Angata 2006).

4.4.2 The Sialidase Inhibitor Zanamivir Inhibits Periodontal Pathogen Association with Host Cells

It was previously shown that mutant strains of *P. gingivalis* and *T. forsythia* have decreased association (attachment and invasion) with host cells compared to their parent strains (Li et al. 2012; Honma et al. 2011), so the experiments described in this chapter aimed to observe whether or not a reduction in host-bacteria association could also be achieved using the sialidase inhibitor zanamivir. This is the first step in assessing whether zanamivir (and sialidase inhibitors more broadly) might be a useful active compound in reducing levels of these bacteria or their effects in patients.

At first, individual periodontal pathogen species- *T. forsythia*, *P. gingivalis* and *F. nucleatum*-were used to infect oral epithelial cells (both the OSCC cell line H357 and normalised cell line OKF6) in the presence and absence of zanamivir. The trend for all three pathogens was that attachment and invasion was reduced in the presence of zanamivir, with the greatest decreases occurring in attachment and invasion of *T. forsythia*.

The finding that *T. forsythia* and *P. gingivalis* displayed decreased attachment and invasion in the presence of zanamivir was partially expected, given that their sialidases have been shown to be important for attachment and invasion (Li et al. 2012; Honma et al. 2011), and since this chapter shows inhibition of purified *P. gingivalis* sialidase. However, in the case of *T. forsythia* this was not entirely expected given its complete inability to inhibit removal of sialic acid containing ligands from the surface of human cells by either whole cells (this chapter) or enzymes and given that it inhibited whole cell and *T.forsythia* NanH enzyme activity with the model ligand MUNANA only to a limited degree in *in vitro* biochemical assays (section 2.3.7).

Nevertheless, In the presence of zanamavir a significant inhibition of host-cell interaction was observed. There are several explanations for why this may be the case. Firstly, in the case of the human cell experiments the bacterial-cell associated enzymes were presented with native human cell associated complex glycans where both the efficacy of the enzyme might be reduced but also where even a small abrogation of activity causes a larger effect

on human cell interactions. Another explanation is that Zanamavir is also known to act upon host sialidases, in particular Neu1 and 3 which are known to contribute to human cell responses to bacteria (Stamatos et al. 2010; Hata et al. 2008), but zanamivir may also influence bacterial internalisation- as evidenced by these data. Another possibility is that the presence of live *T. forsythia* (but not purified NanH) caused increased mobilisation –or- activation of human Neu1 and/or Neu3 sialidase at the host cell membrane, which might be the case since increased Neu1 activity is seen in cells exposed to bacterial TLR ligands (Amith et al. 2009), which live *T. forsythia* bacteria clearly represent. The other issue to consider is that currently we have no information on the larger glycan context of which glycans are most important for sialidase interactions, or which precisely which glycoproteins mediate pathogen association, and it may be that zanamavir has an influence on both of these in terms of invasion/TLR activation. The other implication here is that *in vivo* even small reductions in activity might be relevant in terms of infection, and hence raise the possibility that these molecules could have clinical benefits.

In addition, the effect of zanamavir on *P. gingivalis* is intriguing given the known association of *P. gingivalis* with integrins during its cellular internalisation process (Yilmaz et al. 2002). In particular the fimbriae of *P. gingivalis* is known to interact with integrin- β 1 (Yilmaz et al. 2002), whose activation status is known to be affected by sialylation levels (Lee et al. 2012), suggesting a potential, but unproven explanation for this observation.

The finding that *F. nucleatum* displayed reduced association in the presence of zanamivir was also somewhat surprising, since *F. nucleatum* does not possess sialidase activity. It could be the case that sialic acid ligands or their receptors partially mediate *F. nucleatum* adhesion to host cells, and a sialic acid analogue like zanamivir could interfere with attachment and subsequent invasion of host cells. The adhesin FadA is highly conserved among oral fusobacteria, and considered important for association with oral epithelial cells (Han et al. 2005), despite the fact that FadA has been shown to bind E-selectin, which is present on endothelial cells (Fardini et al. 2011) but not epithelial cells. However, the native ligand for E-selectin is a sialoglycan (sialyl lewis A/X), so perhaps a sialic acid analogue could interfere with FadA-host cell surface interactions. If this is the case, then this would explain why zanamivir inhibited *F. nucleatum*-host cell association as shown here. The issue with this theory is that epithelial cells are not considered to express selectins, but FadA has been shown to be important for oral epithelial cell association (Han et al. 2005), so perhaps FadA adheres to an alternative sialoglycan receptor on oral

epithelial cells, and this adhesion could be disrupted by using a sialic acid analogue, such as zanamivir.

Although attachment and invasion of epithelial cells by individual pathogen species was reduced by the presence of zanamivir, this is not representative of the situation *in vivo*, where cells are exposed to numerous bacterial species at once. This is important for periodontal pathogens, which appear to act synergistically during host cell infection *in vitro*, enhancing their ability to attach to and invade host cells (Saito et al. 2012; Inagaki et al. 2006; Kirschbaum et al. 2010).

In antibiotic protection assays shown here, mixtures of two or three of the periodontal pathogen species *F. nucleatum*, *T. forsythia*, and *P. gingivalis* were used to infect oral epithelial cells. Generally speaking, the levels of host cell association by pathogens in all multi-species assays were equal to or higher than when individual pathogen species were used to infect cells by themselves. Furthermore, while experimental variation sometimes caused difficulties in establishing significant effects of zanamivir on attachment and invasion of individual species in the assays, the levels of attachment, invasion, and/or total association of all bacterial species in most mixed species assays were significantly reduced in the presence of zanamivir.

The data on co-infections of *T. forsythia* and *F. nucleatum* were particularly intriguing given data in the literature showing that co-cultured *F. nucleatum* and *T. forsythia* interact with each other, having been shown to co-operate during biofilm formation (Sharma et al. 2005). In addition, in a murine infection model of periodontitis they act synergistically and elicit greater alveolar bone loss in co-infections than in mice infected with just one organism (Settem et al. 2012). Rather than simply inhibiting both pathogens in isolation (as seen in the single species assays) the zanamivir-inhibition of invasion could be due to disruption of interactions between *T. forsythia* and *F. nucleatum* which boost their host cell association in the absence of zanamivir. Although *T. forsythia* BspA is primarily responsible for co-aggregation of *T. forsythia* and *F. nucleatum*, BspA is not solely responsible for interactions during biofilm formation, since a BspA deficient mutant strain does not show decreased biofilm formation during co-culture with *F. nucleatum* (a Sharma et al. 2005), perhaps other interactions which are zanamivir-inhibitable are involved in the virulence of *T. forsythia* and *F. nucleatum*.

Several experiments could be performed to expand on these findings. Future work with oral bacteria species might aim to study the effect of sialidase inhibition on host cell association by commensal organisms, with the hope that sialidase inhibitors would more drastically reduce pathogen association with host cells than host cell association by commensal organisms. Assessment of host cell association with more complex bacterial communities could be performed using real time PCR to quantify attachment and invasion of multiple species. More immediate future work might also focus on *T. denticola*, the third red complex pathogen, which also possesses a sialidase-in this case an alternative means of enumeration (such as real time PCR) would be required since it cannot be cultured on agar. present. It would be useful to repeat some of these experiments to obtain the effect of zanamivir concentration on attachment and invasion (dose-response), to see if the same effect could be achieved with a lower concentration of zanamivir. Further studies using sialidase deficient mutant strains of *P. gingivalis* and *T. forsythia* could also be performed to test if zanamivir is acting through inhibition of the pathogen sialidase or another mechanism. Conversely experiments where the influence of host sialidases is suppressed (e.g. NEU1 or NEU3) would allow a dissection of the role of different human sialidases in host-pathogen association. Pathogen infection could also be studied in 3D-models of oral mucosa (Pinnock et al. 2014) could also be performed in the presence and absence of zanamivir, which are more representative of *in vivo* oral mucosa infections. Finally, a zebrafish model of *P. gingivalis* infection has recently been developed at the University of Sheffield School of Clinical Dentistry (manuscript in preparation), and this would probably be a relatively straightforward model to test the effect of sialidase inhibition on *P. gingivalis* infection *in vivo*.

Ultimately, zanamivir reduced both attachment and invasion of oral epithelial cells by periodontal pathogens, and this provides support for its potential application to periodontitis therapy: Attachment is important for bacterial colonisation, and subsequent host cell invasion also aids in bacterial persistence at a site because once internalised the bacteria avoid immune system components, are presented with a possible nutrient supply, and can possibly evade antimicrobial therapy. Attachment and invasion of bacteria to host cells can also stimulate the immune system. Sialidase inhibition might also represent a therapeutic for other bacterial infections where host cell association mediated by sialidases is important during pathogenesis, such as during pulmonary infection with *S. pneumoniae*, or gastrointestinal *Vibrio cholerae* and *Clostridium* infections.

4.4.3 The Influence of Periodontal Pathogen Sialidases on Pro-Inflammatory Signalling

Arguably, the most important factor in periodontal disease progression is the host immune system, which causes tissue destruction in a number of ways. This includes increased complement deposition on host cell surfaces (Schoengraf et al. 2013), or cell damage due to autophagy and Reactive Oxygen Species (Bullon et al. 2012). In the case of alveolar bone loss, the production of cytokines leads to differentiation of osteoclasts-of the cytokines, receptor activator of nuclear factor kappa B ligand (RANKL) is ultimately responsible for osteoclast differentiation (Sima & Glogauer 2013), which cause bone resorption.

Central to over-stimulation of the inflammatory response is the production of pro-inflammatory cytokines. Although immune cells, primarily neutrophils and macrophages, are probably considered the most important source of pro-inflammatory cytokines, oral epithelial cells are also capable of pro-inflammatory cytokine production, and are the host cells first (and perhaps most frequently) encountered by periodontal pathogens in the subgingival plaque.

TLRs -2, -4, and -9 are receptors with bacterial component ligands, and are considered to be important during up-regulation of inflammatory cytokine production in periodontitis, and all three of these have been shown to be regulated by the human sialidase Neu1 (Abdulkhalek & Szewczuk 2013; Amith et al. 2009; Amith et al. 2010). Furthermore, exogenous sialidase has been shown to upregulate the NFκB signalling pathway, downstream of TLR- activation and would ultimately enable cytokine production. Therefore, it was thought that periodontal pathogen sialidases might upregulate pro-inflammatory responses to periodontal bacteria, and this might be inhibited by zanamivir.

Firstly, the role of TLR-4 activation in pro-inflammatory cytokine production was studied by exposing epithelial cells to LPS from *P. gingivalis* (the TLR-2/4 ligand), in the presence and absence of the *T. forsythia* sialidase NanH, and/or zanamivir, and monitoring IL-8 secretion into culture supernatant. In these experiments, NanH appeared to upregulate IL-8 secretion in response to LPS, an effect which was abrogated by zanamivir. This did appear to confirm that pathogen sialidases could upregulate TLR activation and subsequent inflammatory cytokine production. However, experimental variation meant that the change in IL-8 secretion induced by NanH and LPS was slightly outside the threshold for significance determined by T-test, compared to LPS alone ($p=0.055$). Given more time to perform experiments, perhaps with protocol adjustments such as reduced ligand/effector-

incubation times, these results could be confirmed. In addition, at least one study has shown that *P. gingivalis* LPS activates TLR-2 (it may act primarily through TLR-2) (Ara et al. 2009), so perhaps these LPS-based experiments should be repeated using LPS from *E. coli*, which activates only TLR-4.

The ability of zanamivir to inhibit cytokine production by oral epithelial cells in response to live *T. forsythia* was also studied. ELISA experiments indicated that IL-8 production by oral epithelial cells was increased in the presence of *T. forsythia*, and this effect was abrogated by zanamivir. The CBA multiplex assays were also used to test for the production of multiple pro-inflammatory cytokines in these cultures; GCSF, IL-6, IL-8, MCP-1, MIP1 α , and TNF. Results from this assay displayed more variation between repeats than the IL-8 ELISA data, but did appear to show similar trends for all six cytokines (except MIP1 α): Relative to the untreated control, cells exposed to zanamivir alone displayed slightly decreased cytokine production, while cells infected with *T. forsythia* displayed approximately 1.5 fold greater cytokine production, and zanamivir abrogated this *T. forsythia*-induced increase.

However, MIP1 α production appeared to be decreased by similar levels in cells exposed to either zanamivir or *T. forsythia*, and was further reduced in cells exposed to both. This was unexpected, since it is also a pro-inflammatory cytokine which has been shown to be upregulated in various cells/tissues in response to periodontal pathogens (Morandini et al. 2010a; Shaddox et al. 2013), and yet in this experiment it was downregulated by *T. forsythia*. This is difficult to explain. However, it might be the case that the level of expression of MIP1 α was quite low-approaching the minimum detection thresholds for the CBA. (MIP1 α expression was <1.5 pg/ml in the untreated condition). Therefore other methods to quantify expression of MIP1 α might be more appropriate (such as real time PCR or Western Blotting. If MIP1 α expression is proven to be reduced in cells treated with zanamivir and/or *T. forsythia*, one possible explanation might be due to inhibition of TLR-4 activation by zanamivir: An *in vivo* murine model of wound healing showed that mice deficient in TLR-4, or incapable of TLR-4 activation, had three-fold lower levels of MIP1 α in wound fluids (Brancato et al. 2013). Importantly, in this study no bacteria were introduced into the wound, and the absence of LPS or bacteria in the wound was confirmed. This effect of decreased MIP1 α production by interference or complete abrogation of TLR-4 does provide some explanation for why cells in the zanamivir or *T. forsythia* and zanamivir conditions produced lower levels of MIP1 α - since in work presented in section 4.3.5.1 (figure 4.14), cells treated with zanamivir may display decreased TLR-4 activation (as

indicated by decreased IL-8 production in the presence of zanamivir) in response to LPS and NanH (and relative to the untreated control). However, results shown here do not account for the decreased MIP1 α production by epithelial cells exposed to *T. forsythia*, unless MIP1 α production is also regulated through another mechanism that *T. forsythia* can disrupt.

In summary, the precise effects of periodontal-pathogen (or other bacterial components) and periodontal pathogen sialidases on cytokine production in epithelial cells (and other cell types) requires further experiments to confirm the effects of sialidases on cytokine secretion shown here. Use of *E. coli*, *Salmonella* LPS, or BspA from *T. forsythia* might be a more appropriate TLR-4 ligand than LPS from *P. gingivalis*. Future work might also include analysis of other cytokines or pro-inflammatory pathway activation affected by NanH in combination with LPS or other PAMPs such as bacterial flagella. (Other mechanisms that might be studied include caspase activation, or the formation of NF κ Bp65, which regulates several pro-inflammatory responses.) Sialylation of specific surface proteins, such as TLRs following exposure to PAMPs and/or sialidases could also be probed using lectin-based western blotting (with the lectins SNA, MMA, and Wheat Germ Agglutinin, WGA-binds N-acetylglucosamine and Sialic Acid) to assess terminal sialoglycans in TLR4 and other associated sialoglycoproteins (such as MD2 and CD14). The role of specific signalling pathways such as the NF κ B signalling pathway might also be studied using gene-knockdown approaches. Gene knockdown could also be used to assess the importance of host sialidase (e.g. NEU1 or 3) and sialyltransferases in periodontal pathogen- host cell immune interactions.

Evidence that zanamivir does reduce pro-inflammatory cytokines in response to *T. forsythia* is more robust, since IL-8 ELISA confirmed a significant reduction in oral epithelial cells exposed to *T. forsythia*, and during exposure to LPS and NanH. Furthermore, the levels of five out of the six pro-inflammatory cytokines tested were increased in the presence of *T. forsythia*, with significant increases in IL-8 and MCP-1, which were abrogated in the presence of the sialidase inhibitor zanamivir. This latter finding provides support for the use of zanamivir (or other sialidase inhibitors) in periodontitis therapy, since upregulation of inflammation is important for disease progression. As well as characterising the impact of inhibitors on infection of other cell types, future work here might involve mixed species infections, which are more representative of the situation during disease.

4.5 Summary

Fluorescence microscopy revealed that the live periodontal pathogens *T. forsythia* and possibly *P. gingivalis*, as well as their purified sialidases NanH and SiaPG could desialylate host cell membranes, and in the case of purified SiaPG this was inhibited by zanamivir. The sialyl lewis A and X glycans present on host cell surfaces were also desialylated by NanH. An *in vitro* model of *T. forsythia*, *P. gingivalis*, and *F. nucleatum* association with host cells also highlighted the potential of zanamivir to prevent attachment and invasion of oral epithelial cells by periodontal pathogens. Although bacterial colonisation and persistence is important during periodontal disease, ultimately the host inflammatory response causes the tissue destruction seen in periodontitis. Therefore, the effect of sialidase inhibition on cytokine production by oral epithelial cells in response to live *T. forsythia*, or LPS, was examined. Zanamivir appears to decrease the production of multiple cytokines in response to *T. forsythia* to levels seen in untreated cells, most significantly for the important pro-inflammatory cytokine IL-8.

Ultimately, the work described in this chapter showed the inhibitory effects of zanamivir on several pathogenic processes with relevance to three periodontal pathogens, without any observable effect on host cell or pathogen viability. This provides evidence supporting the application of sialidase inhibitors as “anti-virulence” therapeutics in treatment of periodontitis, and the issues this raises from commercial and regulatory standpoints are raised in the concluding chapter.

Chapter 5

Summary and Concluding Discussion

5 Summary and Concluding Discussion

The ultimate aims of this project were to further characterise periodontal pathogen sialidases and their role in virulence, with a view to the testing the potential application of sialidase inhibitors in the treatment of periodontitis. Previous chapters contain the results of experiments designed with this aim in mind, with detailed discussion. Therefore, this chapter is intended to summarise the findings, and discuss how sialidases and their inhibitors might undergo further study. In addition, their potential commercial application in the context of oral healthcare is discussed.

5.1 Summary of Findings by Chapter

5.1.1 Chapter 2- Purification and Characterisation of Periodontal Pathogen Sialidases

- The sialidases of *T. forsythia* and *P. gingivalis* (NanH and SiaPG, respectively) underwent bioinformatics analysis. For NanH this revealed the presence of two functional domains (and the secretion signal sequence); the catalytic C-terminal domain (CTD) and an N-terminal carbohydrate binding module (CBM). For SiaPG, only the catalytic CTD was revealed by bioinformatics approaches, but the N-terminal domain was annotated as a CBM for the purposes of this project.
- The genes encoding the CBM and CTD of SiaPG and the CTD of NanH were amplified by PCR and transformed into *E. coli* expression strains with the aim of establishing the functionality of each domain in isolation. Unfortunately expression of soluble, functional protein was not possible for these sialidase subunits.
- After initial difficulty using conventional PCR approaches, the genes encoding the periodontal pathogen sialidases NanH and SiaPG underwent gene synthesis with codons altered for optimum expression by *E. coli*. Following expression in *E. coli*, soluble, active NanH and SiaPG was successfully purified by affinity chromatography.
- A NanH-active site mutant where the highly conserved FRIP motif (located in the sialic acid binding pocket) was mutated to YMAP was also successfully purified and shown to be inactive. This inactive sialidase still retained binding capacity with sialic acid ligands, and could be useful for future studies of sialidase- host ligand interactions.
- NanH and SiaPG were characterised: The pH optimum of both enzymes was determined to be mildly acidic. The kinetics of enzyme activity on the fluorogenic

substrate MUNANA (a commonly used model sialic acid-containing ligand) were determined under enzyme-optimum and physiological-mimicking conditions. In either case, the sialidases were highly efficacious in cleavage of MUNANA, displaying higher affinity and greater maximum reaction rates for MUNANA than most other bacterial sialidases characterised elsewhere.

- The reaction kinetics of NanH on 3- and 6- sialyllactose under physiological-mimicking conditions were determined, highlighting the ability of NanH to cleave both α 2-3 and α 2-6 sialic acid linkages, but with a much greater catalytic efficiency for α -2-3 linkages. This might hint at the function or targets of NanH *in vivo*.
- NanH was capable of activity on the host relevant sialoglycans sialyl lewis A (SLeA) and sialyl lewis X (SLeX), and although maximum rate of sialic acid release was calculated as similar for both ligands, NanH affinity for SLeA was tenfold greater than SLeX.
- The sialidase inhibitor zanamivir was capable of inhibiting the sialidase activity of *P. gingivalis* and *T. forsythia*, as well as the purified periodontal pathogen sialidases. However the efficacy was much higher (by roughly twentyfold) for SiaPG than NanH, with IC₅₀ of \sim 300 μ M and \sim 6mM, respectively. This has implications for studies of sialidase inhibition on pathogen virulence.

5.1.2 Chapter 3- Investigating the Targeting of Host Sialoglycans by Periodontal Pathogens- the Effects on Growth and Biofilm Formation, and the Impact of Zanamivir

- The sialate 9-O-Acetylcylase, NanS, from *T. forsythia* was purified. This enzyme catalyses the hydrolysis of an acetyl chemical group from the 9th carbon of diacetylated sialic acid. Diacetylated sialic acid on sialoglycans is protected from the activity of many bacterial sialidases. NanS was shown to double sialic acid release from bovine submaxillary mucin (BSM) by both NanH and SiaPG. In the absence of NanS, SiaPG was capable of greater sialic acid release from mucin than NanH. In addition, zanamivir inhibited sialic acid release from mucin by SiaPG, but not NanH. This highlighted the likely importance of inter-species cooperation in sialic acid metabolism in the oral environment and the potential of zanamivir to inhibit sialic acid release from a host-relevant sialoglycoprotein.
- *P. gingivalis* was cultured in defined media using sialoglycans as sole nutrient sources. FBS, pooled human saliva (saliva), and BSM were tested, but only FBS

proved capable of enabling *P. gingivalis* growth. However, saliva was capable of enhancing *P. gingivalis* growth in FBS, and when NanS from *T. forsythia* was added, *P. gingivalis* growth was enhanced further. This sheds some light on bacterial-community interactions in sialic release and its role in nutrient acquisition and subsequent pathogen proliferation.

- Biofilm formation was quantitatively assessed. *T. forsythia* and *P. gingivalis* were capable of biofilm formation on sialoglycoproteins; BSM, FBS, and saliva, as well as in media containing free sialic acid (Neu5Ac) and N-acetylmuramic acid (NAM). In these experiments, zanamivir did not appear to affect *T. forsythia* biofilm formation, but this was difficult to confirm since biofilm formation was lower than that seen in other studies.
- *P. gingivalis* biofilm formation and overall growth seemed to be inhibited by BSM, and this effect was compounded in the presence of zanamivir. Zanamivir also inhibited biofilm formation in the other sialoglycoprotein conditions (and there were also slight decreases in overall growth), with significant effects for saliva and mucin. Crystal violet staining of the *P. gingivalis* biofilms may infer that sialidase inhibition/zanamivir had inhibited *P. gingivalis* adherence to the sialoglycoprotein-coated surface, rather than growth of the organism.

5.1.3 Chapter 4-The Role of Sialidases in Host-Pathogen Interactions, and Disruption by Sialidase Inhibition

- *T. forsythia* and *P. gingivalis* may have been capable of cleaving α 2-3 and α 2-6 linked sialic acid from the surfaces of oral epithelial cells as determined by lectin-staining of sialic acid and fluorescence microscopy. In the case of *T. forsythia*, loss of epithelial cell surface sialic acid may be partially inhibited by zanamivir. *P. gingivalis* also appeared to reduce cell surface sialic acid, and this was not inhibited by zanamivir, but this may have been due to the loss of whole sialoglycoproteins from the cell surface caused by the action of *P. gingivalis* gingipains, or by processes involved in cell death.
- Lectin staining and fluorescence microscopy also showed that NanH and SiaPG enzymes were capable of cleaving both α 2-3 and α 2-6 linked sialic acid from the oral epithelial cell surface. In the case of SiaPG, sialic acid release from oral epithelial cell surfaces was qualitatively inhibited by zanamivir.
- Visualisation and quantification of the sialoglycans SLeA and SLeX on epithelial cell membranes was also achieved by immunofluorescence microscopy, and NanH was

capable of desialylating both SLeA and SLeX on the epithelial cell surfaces.

Zanamivir was capable of partially inhibiting desialation of SLeA. The ability of NanH to cleave sialic acid from these specific glycans may shed further light on the targets and function of NanH *in vivo*.

- Antibiotic protection assays were used to assess the ability of *P. gingivalis*, *T. forsythia*, and *F. nucleatum* to attach to and invade oral epithelial cells. In assays where cells were infected with one of the above species, zanamivir was shown to significantly inhibit attachment, invasion, and total association in almost all cases, and the reduction was most significant for *T. forsythia*.
- Multi-species antibiotic protection assays using all possible combinations of the above pathogens (*P. gingivalis*, *T. forsythia*, and *F. nucleatum*) to infect oral epithelial cells in the presence and absence of zanamivir were carried out. Zanamivir was shown to be capable of inhibiting attachment and invasion of host cells to varying degrees in all cases, including in assays where all three pathogens were used to infect host cells.
- Experiments were designed to test the impact of sialidases and their inhibition on pro-inflammatory signalling in oral epithelial cells. The first experiments aimed to test the effect of NanH sialidase on TLR activation (specifically the TLRs -2 and -4, known to at least partially rely on human sialidase for activity). Cells were treated with combinations of zanamivir, *P. gingivalis* LPS (known to activate TLR -2 and possibly -4), and NanH, followed by harvesting of culture supernatant and IL-8 ELISA. While LPS or NanH in isolation had no effect on IL-8 secretion, cells treated with LPS and NanH at the same time did show greater secretion of IL-8 than the untreated condition, and zanamivir abrogated this effect.
- The effect of zanamivir on pro-inflammatory signalling by oral epithelial cells infected with live *T. forsythia* was also assessed. *T. forsythia* was shown to upregulate secretion of the pro-inflammatory cytokines GCSF, IL-6, IL-8, and MCP-1, though only significantly in the case of IL-8 and MCP-1. Zanamivir was shown to abrogate or limit the increased secretion of IL-8 and MCP-1 (a trend also shared in the other non-significantly increased cytokines) in response to *T. forsythia* cytokine secretion.
- Crucially, zanamivir was shown to have no effect on oral epithelial cell viability or metabolism, in both an immortalised epithelial cell line (OKF6) and an OSCC epithelial cell line (H357). Toxicity is an important consideration in development of

therapeutics, so this was an important finding. Bacterial viability was also unaffected by zanamivir, which is an important requirement for an anti-virulence compound.

5.2 Periodontal Pathogen Sialidase Biochemistry and Future Directions

In chapter 3 the sialidases of *T. forsythia* (NanH) and *P. gingivalis* (siaPG) were purified. NanH underwent more extensive biochemical characterisation, and given just a little bit more time, the same would have been done for SiaPG. NanH was shown to target the sialoglycan SLeA in preference to SLeX. A next step would be to determine precisely which sialoglycans are targeted by *T. forsythia* in a cellular (or secretory) glycoprotein context. This might utilise a glycomics based approach and mass spectrometry to observe desialylation of specific glycoproteins on cell surfaces (or in secretions such as salivary proteins).

Further characterisation of the NanH CTD and CBM domains (and SiaPG) would also be beneficial: The CBM of NanH has been confirmed to have the capacity to bind sialoglycans, but displays no activity. It is likely that it bolsters the catalytic capacity of the CTD by binding to sialic acid ligand and orientating the ligand in a position appropriate for the active site to function, thus increasing enzyme-ligand affinity. Unfortunately this has not been confirmed in the case of NanH, since the CTD was not purified in isolation. Since human sialidases do not possess CBMs, the potential to inhibit the CBM (possibly even with an irreversible inhibitor, providing it was specific for the bacterial sialidase CBM and not human lectins) is an extremely exciting prospect, since it would specifically target the bacterial sialidase-albeit independently of the active site.

5.3 Ripe for Targeting: Bacterial Sialidases and their Associated Pathways are Multifunctional Virulence Factors in Periodontitis

Work described in this thesis builds on previous work highlighting the importance of sialidases for the pathogenesis of periodontal pathogens, and crucially here for the first time, the potential to inhibit their virulence mechanisms with pharmaceutically available sialidase inhibitors. Key to the idea that sialidase inhibitors could treat periodontitis is their potential to shift the dysbiotic microbiota back to a more commensal (or health)-dominated bacterial community (reviewed in figure 5.1). The potential clinical importance of sialidase inhibitors as an adjunct to periodontitis therapy is underlined by a recent study of periodontitis patients showing increased sialidase activity in sites affected by

periodontitis, and that after treatment sites with more severe disease (deep bleeding as opposed to non-bleeding) retained higher sialidase activity (Gul et al. 2016).

Periodontal pathogens possess mechanisms involved in release, uptake, and utilisation of sialic acid: *T. forsythia* makes use of the products of its *nan* operon to release sialic acid (NanS, NanH), followed by uptake (NanO, NanU, NanT), and catabolism (NanA, NanE), and this utilisation pathway is directly relevant for *T. forsythia* proliferation since this enables it to form biofilms on host sialoglycoproteins, and Neu5Ac can substitute *T. forsythia*'s requirement for exogenous NAM (Roy et al. 2010; Pham et al. 2010).

P. gingivalis lacks any homologues for the synthesis of Neu5Ac, and yet Neu5Ac represents an important component of its gingipain RgpA (Rangarajan et al. 2005). SiaPG or other sialidases expressed by the microbiota would probably provide ample free sialic acid for uptake by *P. gingivalis*: While the precise mechanisms of sialic acid uptake in *P. gingivalis* are unknown thus far, this demand could be met by a general porin, and free sialic acid may be sequestered by the *P. gingivalis* secreted protein RagB, which has been shown to bear structural similarity to the sialic acid sequestration protein NanU in *T. forsythia* (Goulas et al. 2015). While it is unclear if *P. gingivalis* can metabolise sialic acid, desialylation of host sialoglycoproteins likely makes them more amenable to the activity of gingipains, since desialylation of salivary mucin makes it more amenable to proteolysis (Takehara et al. 2013), thus, sialidases may enhance *P. gingivalis* nutrient uptake. Furthermore, the activity of enzymes produced by other members of the microbiota could enhance the growth of *P. gingivalis*, as was shown in Chapter 4 of this thesis, where *T. forsythia* NanS enhanced *P. gingivalis* growth on serum (FBS) and human saliva, implying that in vivo this may also help other members of the microbial community, including *P. gingivalis*. In fact the lab now has a *T. forsythia nanS* mutant (G.Stafford, personal communication), which it would be exciting to test in growth experiments and in community experiments to assess the role of this gene in microbial communities.

While *F. nucleatum* does not possess sialidases, it does possess other components of the *nan* operon enabling uptake (unknown outer membrane transporter/porin, and inner membrane transporter system SiaPQM) and catabolism (NanA, NanE, NanK), implying that sialic acid represents a nutrient source for *F. nucleatum*. Furthermore, many *F. nucleatum* strains have been shown to sialylate their outer membrane proteins (Yoneda et al. 2014), which is likely to play roles in immune evasion: Thus, sialic acid utilisation has a direct impact on metabolism and surface phenotype of *F. nucleatum*-which will affect

proliferation- and it must rely on release of sialic acid by other members of the microbiota. It is also of note that the original *T. forsythia* isolation method involved the cross-streaking of *F. nucleatum* with *T. forsythia* (Tanner et al. 1986), which has always been assumed to be due to the cross-feeding of N-acetylmuramic acid, but could equally be sialic acid given these recent reports.

Finally, *T. denticola* also possesses a sialidase (TDE0471), although characterisation and its roles in virulence are only just beginning to come to light (Kurniyati et al. 2013). TDE0471 is expressed on the outer membrane of *T. denticola*, and was shown to prevent complement deposition on its surface. This is likely due to desialylation of complement proteins, which may either inactivate them or increase the activity of the *T. denticola* protease dentilisin, which is also important for complement resistance (McDowell et al. 2009). Furthermore, TDE0471 appears to be important for nutrient acquisition, with *T. denticola* mutants deficient in the sialidase unable to grow with serum as a nutrient source (Kurniyati et al. 2013).

In addition to direct effects on pathogen proliferation, the sialidases are also important for interactions at the mucosal surface and subsequent inflammation: Previous work has highlighted the importance of the sialidases of *P. gingivalis* and *T. forsythia* in host cell attachment and invasion (Honma et al. 2011; Li et al. 2012). In this project, the sialidase inhibitor zanamivir was also capable of inhibiting host cell association by these pathogens and the sialidase negative *F. nucleatum*, even during mixed species infections.

As well as association, pathogen sialidases can modulate or enhance pro-inflammatory signalling (Amith et al. 2009; Amith et al. 2010), and therefore they are likely to be important for onset and progression of periodontal disease. In this project, zanamivir was capable of reducing the pro-inflammatory signalling response to live *T. forsythia*, and the enhanced response to *P. gingivalis* LPS in the presence of NanH. Importantly, the experiments shown in this thesis describing the contribution of pathogen sialidases to pro-inflammatory signalling, and the potential to inhibit this, was performed on oral epithelial cells (previous work focuses on macrophages) and highlights the potential to limit destructive inflammation by dampening signals initiating from oral epithelial cells. Together with the host cell association data (chapter 5) and the capacity of inhibitors to prevent pathogen biofilm formation (shown here in chapter 4 and elsewhere (Roy et al. 2011)), this provides strong support for further investigation of sialidase inhibitors as novel therapeutics.

Ultimately, experiments here did show the ability to inhibit multiple periodontal pathogen virulence processes (host cell association, immunomodulation, and biofilm formation), and shed light on the role of NanS (Phansopa et al. 2015). Further work should focus on the precise targets of sialidase inhibitors, and the ability of different inhibitors to target the periodontal pathogen sialidases. Work elsewhere has highlighted greater efficacy of other sialic acid analogues) and other apparently non-analogous compounds) for bacterial sialidases (Hoon et al. 2014; Walther et al. 2015; Tailford et al. 2015), in some cases with accompanying decreases during *in vitro* models of virulence. Since some of these are used or considered suitable for antiviral therapies, there could be a greater likelihood of their application to periodontitis therapy.

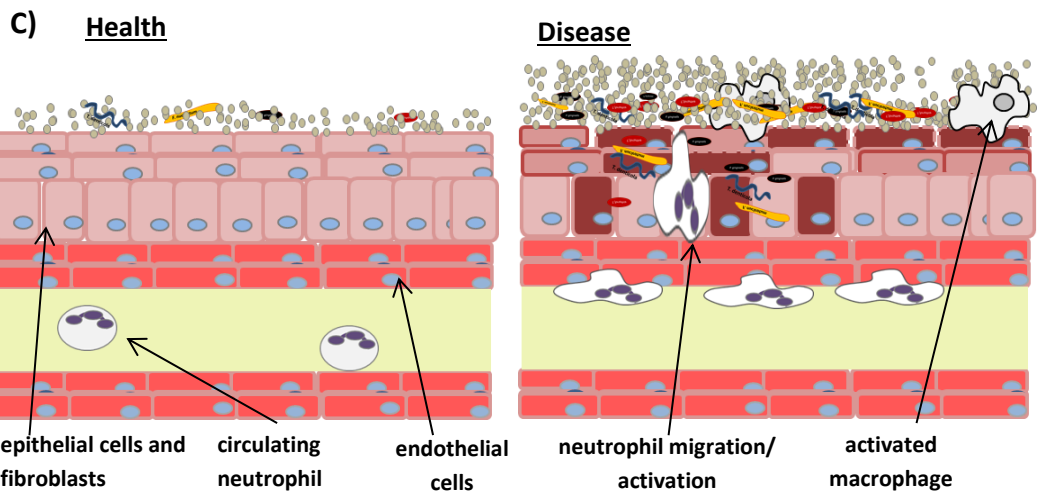
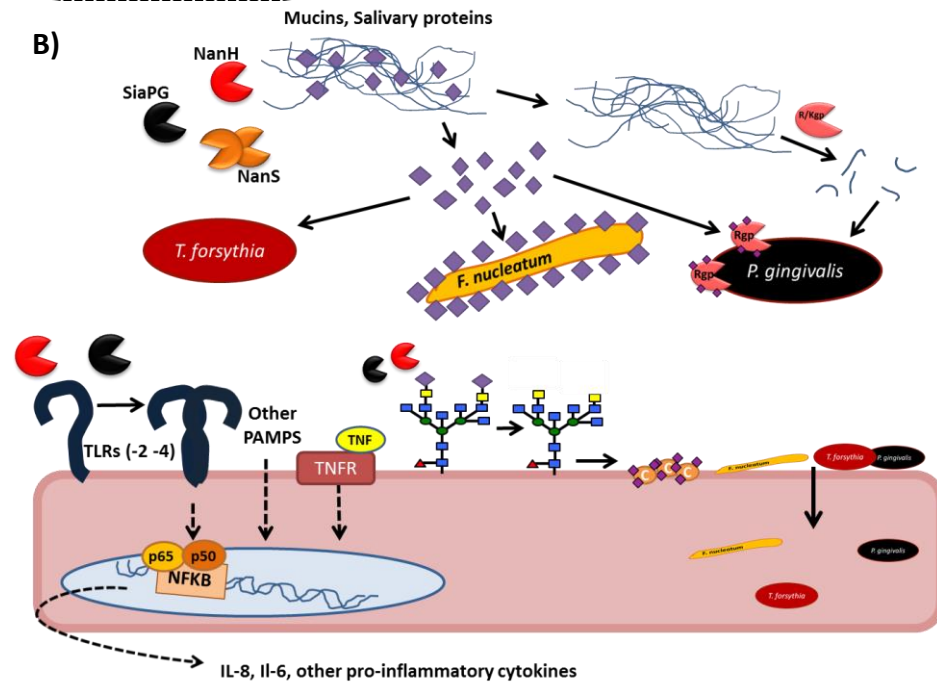
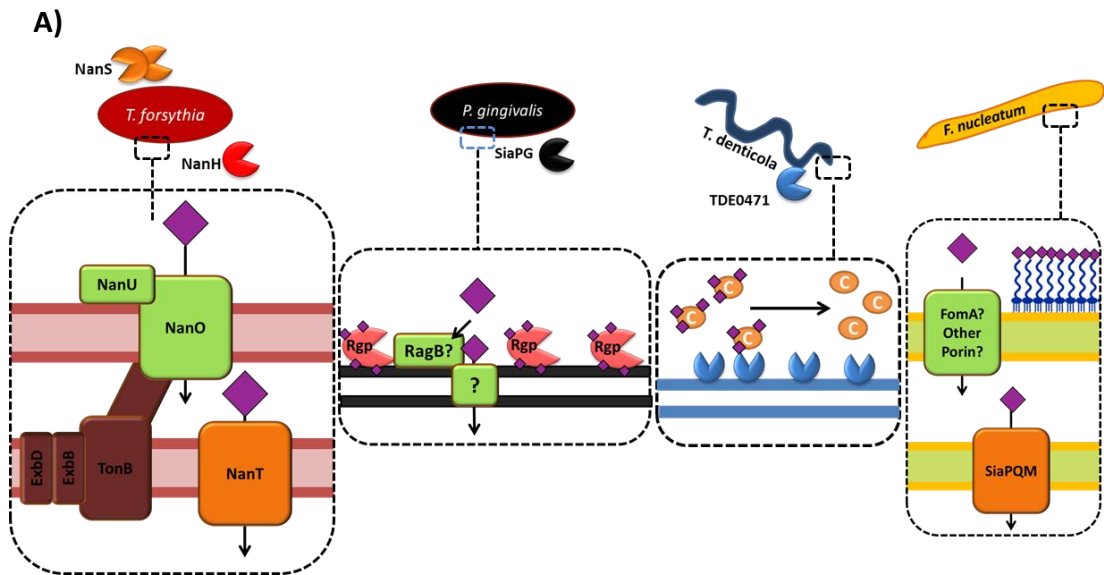


Figure 5.1. Sialidases and sialic acid-mediated interactions enhance periodontal pathogen proliferation and host inflammatory processes through a number of mechanisms.

A) Periodontal pathogens uptake sialic acid through a number of mechanisms, all of which require sialidase activity first to enable sialic acid release (which may be bolstered by accessory enzymes such as NanS). B) Pathogen sialidases at the oral mucosal surface. In addition to increasing nutrient availability (sialic acid or enhanced proteolysis of host sialoglycoproteins), sialidases can interact with sialoglycans on host cell surfaces. This includes immune-stimulatory receptors such as TLRs -2 and -4, which signal through the NF κ B pathway to produce pro-inflammatory cytokines such as IL-6 and IL-8. Desialylation of host cell surfaces may also lead to increased complement deposition, and may expose glycoprotein epitopes that can be recognised by pathogens for attachment, so sialidases can increase attachment and invasion of host cells by pathogens. C) Dysbiosis and destructive inflammation at the periodontal mucosal surface. The processes discussed in B) and C) cause pathogen (and to a lesser extent commensal) proliferation due to increased nutrient availability, and increased ability to attach and persist at the mucosal surface. Increased pathogen proliferation and pro-inflammatory signalling leads to differentiation, recruitment, and activation of immune cells including neutrophils and macrophages, which do not successfully clear pathogens. Ultimately sialidase inhibitors have the potential to disrupt these virulence mechanisms, not only at the sialidase level but possibly at other sialic acid utilisation proteins, since the inhibitors are structural analogues of sialic acid and could also show affinity for enzymes and transporters besides sialidase.

Overall, my work continues to highlight the importance of glycans in interactions of oral bacteria with the host, an understudied area historically. While my focus has been sialic acid and sialidases, other glycans and glycosidases may also play key roles, for example the *T.forsythia nanH* is in an operon with a beta-hexosaminidase that almost certainly acts to cleave underlying galactose or glucose moieties during infections. In addition, I was involved in work with a team from Vienna (University of Natural Lifesciences-Universität für Bodenkultur-BOKU) examining the role of a fucosidase with unusual properties in *T.forsythia* (Megson et al. 2015). It may well prove that the role of glycans is crucial in the oral environment and the fact that periodontal pathogens seem to dedicate a proportion of resource in that direction indicate this might be true. It is certainly the case that periodontal pathogens and other oral bacteria seem to dedicate a significant proportion of their genomes (much like gut bacteria) to genes that potentially have a role in glycan foraging, meaning that this idea of making the most of your niche is extremely pertinent (Martens et al. 2008; Stafford et al. 2012).

While my work has focussed on interactions with glycoproteins, glycoprotein coated surfaces and human cell surfaces, I have also discussed the possible role it has in interbacterial interactions in the section above. However, one other common type of organism present in the oral cavity in particular are fungi. The most prominent of these is arguably *Candida albicans*. Of note there is evidence that *C. albicans* contains N-glycans on its surface that are capped with sialic acid (2,6-linked and lectin reactive) (Soares et al. 2000), this raises the interesting possibility that sialic acid and by extension sialidases may be involved in cross-kingdom inter-pathogen interactions, and represents yet more areas of study.

While my work has focussed on oral micro-organisms and their sialidases, there is a plethora of micro-organisms that contain sialidases, many of which are human pathogens of import, e.g. *S. pneumoniae*, *Vibrio cholera*, *Salmonella typhimurium*, *Gardnerella vaginalis* among others (see chapter 1). Therefore the findings of this thesis, and future work, may have much wider implications on the mechanisms of how bacterial pathogens interact with the host glycome and its implications on immunity and infection. Of particular note are infections at mucosal layers, such as the respiratory or genital tracts, but there are also growing data that sialic acid metabolism is a key trait of gut-dwelling organisms such as *B.thetaimicron*, *Ruminococcus gnavus* and other *Bacteroides* spp. (Martens et al. 2008; Phansopa et al. 2014; Tailford et al. 2015), and has even been shown

to be key during pathogen proliferation, including during *V. cholerae*, *Salmonella*, and Clostridium infections (Almagro-Moreno & Boyd 2009; Ng, J. a Ferreyra, et al. 2013). It is therefore clear that the implications of work shown here and elsewhere that focus on the oral cavity may have larger implications in human microbiology.

5.4 Discussing the Potential for a Sialidase Inhibitor-Based Product for Treatment or Prevention of Periodontal Disease

Given that zanamivir appears to show efficacy in preventing virulence of periodontal pathogens, it could be possible to develop sialidase inhibitors as novel therapeutics for treatment of periodontitis, where the sialidase inhibitor becomes an active ingredient in a given product, or “active” that treats or prevents periodontitis. The simplicity of this statement hides the multitude of options and challenges during product development, which include handling the regulatory issues, efficacy testing, patient or consumer trials and focus groups, and claims that can be made about a given product. An additional layer of complexity is in navigating these issues at a global level. All of these factors feedback to each other during development of a given product.

Perhaps the most fundamental question in product development of sialidase inhibitors is; are they sold to directly to consumers as an over-the-counter treatment or preventative of periodontitis, or are they sold for clinical use, available for use by dental or medical professionals only? I explored some of these issues during a short placement at GSK (Weybridge, UK), so this short section shall attempt to discuss these issues and the potential for sialidase inhibitor-product development in oral healthcare settings.

5.4.1 Sialidase Inhibitors in Products for Periodontitis Treatment-Future Directions

This study does provide evidence for the potential of zanamivir (and perhaps other sialidase inhibitors) as novel active ingredients for products that treat periodontitis. Previous chapters have discussed possible further *in vitro* work that might be performed to continue to characterise the functions of pathogen sialidases and the potential for sialidase inhibition in preventing virulence. A further possibility might be to test the potential of zanamivir or other sialidase inhibitors to prevent virulence or pathogen proliferation and the onset or progression of periodontitis.

This might be achieved through mouse models of periodontitis, where periodontitis is induced through infection with periodontal pathogens, either through spiking of drinking water, or introduction of pathogens with alveolar gavage. (Examples of mouse models of

periodontitis can be seen in Yamaguchi et al. 2016; Settem et al. 2012.) Mice would then be treated with sialidase inhibitors and any differences in gingival recession and alveolar bone loss observed. The pharmacology of the inhibitor would have to be taken into account during design of such experiments: The inhibitor would probably have to be present systemically in order to reach the periodontal pocket, since applying oral patches, chips, or gels to mice might be problematic. While this does not present an issue for inhibitors such as oseltamivir (oral administration) the inhibitor zanamivir might have to be administered differently to achieve systemic concentrations at which it is effective against pathogens.

A less direct approach might be taken to study the ability of sialidase inhibitors to reduce periodontal pathogen levels in the oral cavity or at the periodontium in humans: The sialidase inhibitor oseltamivir is administered orally, and reaches 0.34 µg/ml systemically during conventional anti-flu therapy (Widmer et al. 2010), and clinical trials using intravenous (systemic) zanamivir are also performed (Fritz et al. 1999; Marty et al. 2013), where zanamivir can reach up to ~50 µg/ml (~17 µM) in serum (Marty et al. 2013). Presumably the GCF and saliva of patients undergoing these anti-flu therapies also contains the sialidase inhibitors, thus exposing the periodontal microbiota to zanamivir or oseltamivir. In addition to confirming the presence of inhibitors in the GCF and/or saliva, it would theoretically be possible to compare the periodontal microbiota of patients before or at an early stage of treatment with their microbiota post-treatment, and assess the relative levels of periodontal pathogens before and after treatment. In such studies it probably would not be appropriate to take detailed clinical assessments of periodontal health, since clinical assessments or periodontitis are usually made a few months apart. Any observed impact of sialidase inhibitors on periodontal pathogen abundance in these patients would provide a stronger case for developing sialidase inhibitors for periodontitis therapy.

5.4.2 Formulation of Products Containing Sialidase Inhibitors

Commonly used formulations of consumer products for oral hygiene or treatment products include pastes, mouthwashes, and (less commonly) gels, which can be applied to the teeth, oral cavity and oral mucosa, and these retain their position for a short amount of time. (minutes, gels persist longer than toothpaste and mouthwash). In the case of toothpaste and mouthwash, the concentration of active ingredients in saliva is mostly lost within the first 30-60 minutes after toothbrushing, though some is retained in the oral tissues and is gradually released into saliva over the course of several hours (Duckworth 2013).

More specialised formulations used (or under development for use) in the clinic or for patient-specific therapy include these and other formulations, such as oral patches and chips. Patches are placed on the oral mucosa, retained in position, and release the active ingredient over a longer time scale (minutes-hours), and chips, which are similar devices that can be positioned in the periodontal pocket, where they release the active ingredient over a longer time period (days-weeks (Soskolne et al. 1998)). Periodontal chips have been developed that incorporate and release the antibacterial agent chlorhexidine, and when used as an adjunct to periodontitis therapy (scaling and root planing) their use can result in improvements in clinical parameters and inhibition of pathogen recolonisation compared to patients who do not receive the adjunct (John et al. 2015).

Currently characterised sialidase inhibitors are competitive, i.e. they compete with other ligands in binding to the sialidase. This implies that a continuous concentration of inhibitor needs to be maintained at the periodontal pocket or gingival crevice-where periodontal pathogens colonise and cause disease, in order to continuously inhibit the virulence of periodontal pathogens. This is in contrast to more conventional active ingredients that affect bacteria, such as chlorhexidine, which require only a short timescale to display bactericidal effects.

Given this, a conventional oral healthcare formulation-mouthwash or toothpaste-is unlikely to be useful as this would result in intermittent, short term exposure of pathogens to the inhibitor. Gels and patches applied to the periodontium are a possible formulation, as they remain in position for a longer time period. These could potentially be sold as consumer products, or be available on prescription, but importantly these formulations do not require a clinician to apply the therapeutic. Chips, placed in the periodontal pocket, are another possible formulation. Since these are retained and would release the sialidase inhibitor over the longest time period, these could also be useful for administration of sialidase inhibitors. However, such a product would be limited to clinical use only, due to the requirement for a clinician or trained professional in placing the chip.

Considering the above, sialidase inhibitors could be developed as gels, patches, or chips. The latter two could possibly be sold directly to consumers, but a chip formulation would be a specialist product for use in the clinic only.

5.4.3 Regulation of Consumer Products

Oral healthcare consumer products for sale in the European Union (EU) can be considered to belong to one of three regulatory categories: Cosmetics, medical devices, or medicines.

These have different levels of safety and efficacy testing associated with them, and the classification of a product also affects the types of claims that can be made about what the product does. The United States of America (USA) have different regulatory requirements compared to the EU, with considerations concerning novel active ingredients (discussed below). However, the categories a product containing a sialidase inhibitor might fall under remain the almost the same; cosmetics, medical devices, or drugs (“drugs” being analogous to the EU “medicines” category).

5.4.3.1 *Cosmetics*

Governed by EU directive 76/768/EEC*, a cosmetic product “shall mean any substance... intended to be placed in contact with the various external parts of the human body (epidermis, hair system, nails, lips and external genital organs) or with the teeth and the mucous membranes of the oral cavity with a view exclusively or mainly to cleaning them, perfuming them, changing their appearance and/or correcting body odours and/or protecting them or keeping them in good condition” (EU directive 76/768/EEC, Article 1, page 5). Oral cosmetic products can tread a fine line between this classification and medical device or medicine classifications, as cleaning of the oral cavity and disruption of plaque is required for oral health, but active ingredients with these properties might also be considered a treatment for a given condition.

In an oral health context, toothpastes and mouthwashes often fall into the cosmetics category. However, the presence of certain active ingredients in these formulations, such as chlorhexidine, or high concentrations of other active ingredients, such as fluoride, might result in the product classified as a medical device or medicine, since the nature of the active ingredient is no longer considered to be simply maintaining appearance or odour, and instead could be considered a treatment or preventative of disease.

The nature of the cosmetics category limits the types of claims that can be made about the benefits of a product to maintenance of appearance/odour. This is why the claims made regarding daily, cosmetic toothpastes are limited to using words such as “cleaning”, “freshness”, or “whitening activity” to describe their activity. Given that sialidase inhibitors inhibit virulence of pathogens, it is unlikely that a product containing them as an active would fall into the cosmetics category. Furthermore, the potential benefits of sialidase inhibitors are not limited to cosmetic applications-they prevent virulence- and from a commercial standpoint this might represent a unique selling point, and these claims about

*Currently available at:

<http://eur-ex.europa.eu/LexUriServ/LexUriServ.do?uri=CONSLEG:1976L0768:20100301:en:PDF>

the product could only be made if the sialidase inhibitor-product is classified as a medical device or medicine.

5.4.3.2 **Medical Devices**

Governed by EU directive 3/42/EEC*, medical device “means any instrument, apparatus, appliance, software, material or other article... to be used specifically for diagnostic and/or therapeutic purposes... and which does not achieve its principal intended action in or on the human body by pharmacological, immunological or metabolic means, but which may be assisted in its function by such means.” (EU directive 3/42/EEC, Article 1, pages 5-6).

In terms of oral healthcare consumer products, toothpastes and mouthwashes may fall under this classification if they have a perceived therapeutic or preventative benefit. An example of medical devices in this context is the Corsodyl® (Trademark GlaxoSmithKline, UK) range of daily toothpastes. These have undergone clinical trials to prove that they do have therapeutic and/or preventative benefits: Corsodyl® toothpaste has been shown to “reduce levels of plaque”, “stop bleeding gums”, and appears to “maintain healthy gingiva” (<https://www.gsk-dentalprofessionals.co.uk/our-brands/corsodyl-toothpaste/corsodyl-daily-toothpaste/>). Since these are considered to be mechanical effects, Corsodyl® daily is defined as a medical device.

Sialidase inhibitor-products may fall under the classification of medical devices if they are deemed to have similar modes of action, i.e. mechanical rather than pharmacological. It could be argued that since sialidase inhibitors inhibit virulence by preventing bacterial attachment, biofilm formation, and host-bacteria interactions without killing bacteria directly, that they do have a mechanical mode of action. Indeed, a clinical trial of a sialidase inhibitor-product might have similar findings to the ones stated above for Corsodyl® daily products.

Medical devices are further subdivided into invasive (placed inside the body) and non-invasive devices (placed externally or on the oral mucosa). The duration of device placement is also taken into account, including transient (<60 minutes), short term (<30 days), and long term (>30 days) (EU directive 3/42/EEC, Annex IX, pages 51-54). The precise type of medical device that a sialidase inhibitor-product falls under would be governed largely by its formulation and directions for application: A gel based formulation might be classified as non-invasive, transient or short term. An oral mucosa-patch might be non-invasive transient or short term, while a chip-based formulation might be classified as invasive since it would be placed inside the periodontal pocket. On the other hand, the EU

*Currently available at:

directive governing medical devices states specifically that devices may be considered non-invasive if they are placed above the pharynx ((EU directive 3/42/EEC, Annex IX, page 54, section 2.1).

It might be the case that sialidase inhibitors are deemed to have a primarily pharmacological mode of action, in which case they would be governed by rules concerned with medicinal products. The EU directive governing medical devices appears to recognise the difficulty in distinguishing between these two classifications when it states that “medicinal products [are] covered by Directive 2001/83/EC. In deciding whether a product falls under that Directive or this Directive, particular account shall be taken of the principal mode of action of the product.” (EU directive 3/42/EEC, Article 1, page 8).

5.4.3.3 **Medicines, or Medicinal Products**

Governed by EU Directive 2001/83/EC*, medicinal products include “Any substance or combination of substances presented as having properties for treating or preventing disease in human beings... Any substance or combination of substances which may be used in or administered to human beings with a view to restoring, correcting, or modifying physiological functions by exerting a pharmacological, immunological, or metabolic action” (EU Directive 2001/83/EC, article 1, page 13).

Certainly, it might be considered likely that a sialidase inhibitor-active ingredient could fall under this regulation, especially if (like zanamivir) it inhibits human sialidases. However, if the inhibitor is mainly considered to act through mechanical, non-invasive means, such as reducing levels of plaque or stopping bleeding gums with an oral gel or mouthwash, then such a product might fall under the medical device category. If zanamivir were to be applied to a product, it would probably be classified as a medicine since it is already licensed as a medicine for treatment of flu, and also inhibits human sialidases (Hata et al. 2008) as well as those of the periodontal pathogens.

Candidate-products applying for regulation as a medicine have the most stringent requirements -appendix 7.9 contains some of these, the rest can be viewed in EU Directive 2001/83/EC*, “Title III, Placing on the Market, Chapter I” -making them the most difficult to apply for. This chapter of EU Directive 2001/83/EC does make reference to the possibility of foregoing the submission of clinical trials data to the regulatory authority (which would make the regulatory process slightly easier) if the new product is suitably similar to a reference product that has been on the market for at least eight years. Zanamivir has been sold in the anti-flu drug Relenza for that period of time. Unfortunately for a theoretical

*Currently available at:

<http://eur-lex.europa.eu/legal-content/EN/TXT/PDF/?uri=CELEX:01993L0042-20071011&from=EN>

zanamivir-containing product for treatment of periodontitis, there is a requirement for the reference product to be “of the same pharmaceutical form as the reference product”, so this provision is of little use in terms of more rapidly-progressing a theoretical zanamivir-based product to market.

5.5 In Conclusion

Ultimately, the results of this project expand our knowledge of the molecular microbiology of periodontal pathogens and the pathogenicity of *T. forsythia* and *P. gingivalis*.

Furthermore, the results advocate the potential for sialidase inhibitors as anti-virulence therapeutics for treatment of periodontal disease. Though more research with alternative inhibitors is probably required, and ultimately this project raised more questions than it answered.

However, the discovery of a potential immunomodulatory role for the pathogen sialidases and further characterisation of these enzymes paves the way for further developments in this exciting area of research, and with tenacity this is likely to yield promising results which can be applied to the discovery of new therapeutics. Or in other words- “Do you know what happens to lads who ask too many questions? ...Damned if I know. Probably they get answers, and serve 'em right.” –Terry Pratchett, *Mort* (1987).

6 Bibliography

- Abdulkhalek, S. & Szewczuk, M.R., 2013. Neu1 sialidase and matrix metalloproteinase-9 cross-talk regulates nucleic acid-induced endosomal TOLL-like receptor-7 and -9 activation, cellular signaling and pro-inflammatory responses. *Cellular Signalling*, 25(11), pp.2093–20105.
- Abe, T. et al., 2012. Local complement-targeted intervention in periodontitis: proof-of-concept using a C5a receptor (CD88) antagonist. *Journal of Immunology*, 189(11), pp.5442–8
- Alexandra, S. et al., 2008. NOTE / NOTE Occurrence of herpes simplex virus 1 and three periodontal bacteria in patients with chronic periodontitis and necrotic pulp. *Canadian Journal of Microbiology*, 330, pp.326–330.
- Almagro-Moreno, S. & Boyd, E.F., 2009. Sialic acid catabolism confers a competitive advantage to pathogenic *Vibrio cholerae* in the mouse intestine. *Infection and Immunity*, 77(9), pp.3807–3816.
- Al-Taweel, F.B., Douglas, C.W.I. & Whawell, S.A., 2016. The periodontal pathogen *Porphyromonas gingivalis* preferentially interacts with oral epithelial cells in S phase of the cell cycle. *Infection and Immunity*, (April).
- Aminoff, D., 1961. Methods for the quantitative estimation of N-acetylneuraminic acid and their application to hydrolysates of sialomucoids. *The Biochemical Journal*, 81, pp.384–92.
- Amith, S.R. et al., 2009. Dependence of pathogen molecule-induced toll-like receptor activation and cell function on Neu1 sialidase. *Glycoconjugate Journal*, 26(9), pp.1197–212.
- Amith, S.R. et al., 2010. Neu1 desialylation of sialyl alpha-2,3-linked beta-galactosyl residues of TOLL-like receptor 4 is essential for receptor activation and cellular signaling. *Cellular Signalling*, 22(2), pp.314–24.
- Angata, T. et al., 2007. Siglec-15: an immune system Siglec conserved throughout vertebrate evolution. *Glycobiology*, 17(8), pp.838–46.
- Ara, T. et al., 2009. Human gingival fibroblasts are critical in sustaining inflammation in periodontal disease. *Journal of Periodontal Research*, 44(1), pp.21–7.
- Armitage, G.C., 1999. Development of a Classification System for Periodontal Diseases and Conditions. *Annals of Periodontology*, 4, pp.1–6.
- Armitage, G.C., 2013. Learned and unlearned concepts in periodontal diagnostics: a 50-year perspective. *Periodontology 2000*, 62(1), pp.20–36.
- Aruni, W. et al., 2011. Sialidase and sialoglycoproteases can modulate virulence in *Porphyromonas gingivalis*. *Infection and Immunity*, 79(7), pp.2779–91.
- Aruni, W., Chioma, O. & Fletcher, H.M., 2014. *Filifactor alocis*: The Newly Discovered Kid on the Block with Special Talents. *Journal of Dental Research*, 93(8), pp.725–732.
- Atabay, V.E. et al., 2016. Obesity and oxidative stress in patients with different periodontal status: A case-control study. *Journal of Periodontal Research* (online).

- Baggio, G. et al., 1998. Lipoprotein(a) and lipoprotein profile in healthy centenarians: a reappraisal of vascular risk factors. *FASEB journal : official publication of the Federation of American Societies for Experimental Biology*, 12(6), pp.433–437.
- Beck, J.D. & Offenbacher, S., 2005. Systemic effects of periodontitis: epidemiology of periodontal disease and cardiovascular disease. *Journal of Periodontology*, 76, pp.2089–2100.
- Beikler, T. et al., 2008. Gene expression in periodontal tissues following treatment. *BMC Medical Genomics*, 1, p.30.
- Di Benedetto, A. et al., 2013. Periodontal disease: linking the primary inflammation to bone loss. *Clinical & Developmental Immunology*, 2013 (online).
- Bevilacqua, M.P. & Nelson, R.M., 1989. Selectins. *Journal of Clinical Investigation*, 91, pp.379–387.
- Bickel, M. & Cimasoni, G., 1985. The pH of human crevicular fluid measured by a new microanalytical technique. *Journal of Periodontal Research*, 20(1), pp.35–40.
- Biyikoğlu, B., Ricker, A. & Diaz, P.I., 2012. Strain-specific colonization patterns and serum modulation of multi-species oral biofilm development. *Anaerobe*, 18(4), pp.459–70.
- Bodet, C. & Grenier, D., 2010. Synergistic effects of lipopolysaccharides from periodontopathic bacteria on pro-inflammatory cytokine production in an ex vivo whole blood model. *Molecular Oral Microbiology*, 25(2), pp.102–11.
- Brancato, S.K. et al., 2013. Toll-like receptor 4 signaling regulates the acute local inflammatory response to injury and the fibrosis/neovascularization of sterile wounds. *Wound Repair and Regeneration*, 21(4), pp.624–633.
- Branda, S.S. et al., 2005. Biofilms: The matrix revisited. *Trends in Microbiology*, 13(1), pp.20–26.
- Brittan, J.L. et al., 2012. Pneumococcal neuraminidase A: an essential upper airway colonization factor for *Streptococcus pneumoniae*. *Molecular Oral Microbiology*, 27(4), pp.270–83.
- Bullon, P. et al., 2012. Autophagy in periodontitis patients and gingival fibroblasts: unraveling the link between chronic diseases and inflammation. *BMC Medicine*, 10(1), p.122.
- Byers, H.L. et al., 2000. Isolation and characterisation of sialidase from a strain of *Streptococcus oralis*. *Journal of Medical Microbiology*, 49(3), pp.235–244.
- Cabezas, J. a et al., 1989. Kinetic studies on the sialidase of three influenza B and three influenza A virus strains. *Glycoconjugate journal*, 6(2), pp.219–27.
- Cacalano, G. et al., 1992. Production of the *Pseudomonas aeruginosa* neuraminidase is increased under hyperosmolar conditions and is regulated by genes involved in alginate expression. *Journal of Clinical Investigation*, 89(6), pp.1866–1874.
- Carter, A. & Martin, N.H., 1962. Serum sialic acid levels in health and disease. *Journal of Clinical Pathology*, 15(1), pp.69–72.
- Cavagni, J. et al., 2015. Obesity and Hyperlipidemia Modulate Alveolar Bone Loss in Wistar

- Rats. *Journal of Periodontology*, (February), pp.1–15.
- Cavagni, J. et al., 2013. Obesity may increase the occurrence of spontaneous periodontal disease in Wistar rats. *Archives of Oral Biology*, 58(8), pp.1034–1039.
- Ceroni, A. et al., 2008. GlycoWorkbench: A tool for the computer-assisted annotation of mass spectra of glycans. *Journal of Proteome Research*, 7(4), pp.1650–1659.
- Chang, Y.-C. et al., 2012. Leukocyte Inflammatory Responses Provoked by Pneumococcal Sialidase. *mBio*, 3(1), pp.1–10.
- Chen, W., Palmer, R.J. & Kuramitsu, H.K., 2002. Role of Polyphosphate Kinase in Biofilm Formation by *Porphyromonas gingivalis*. *Infection and Immunity*, 70(8), pp.4708–4715.
- Chien, C.-H., Shann, Y.-J. & Sheu, S.-Y., 1996. Site-directed mutation of the catalytic and conserved amino acids of the neuraminidase gene, nanH, of *Clostridium perfringens* ATCC 10543. *Enzyme and Microbial Technology*, 19(4), pp.267–276.
- Choi, Y. et al., 2001. Osteoclastogenesis is enhanced by activated B cells but suppressed by activated CD8(+) T cells. *European Journal of Immunology*, 31(7), pp.2179–88.
- Choi J, Borrello MA, Smith E, Cutler CW, Sojar H, Z.M., 2001. Prior exposure of mice to *Fusobacterium nucleatum* modulates host response to *Porphyromonas gingivalis*. *Oral Microbiology and Immunology*, p.; 16: 338–344.
- Chou, Y.-Y. et al., 2015. Rheumatoid Arthritis Risk Associated with Periodontitis Exposure: A Nationwide, Population-Based Cohort Study. *PLoS one*, 10(10), (online)
- Cohen, M. & Varki, A., 2010. The sialome--far more than the sum of its parts. *Omics : a Journal of Integrative Biology*, 14(4), pp.455–64.
- Colomb, F. et al., 2013. TNF induces the expression of the sialyltransferase ST3Gal IV in human bronchial mucosa via MSK1/2 protein kinases and increases FliD/sialyl-Lewisx mediated adhesion of *Pseudomonas aeruginosa*. *The Biochemical Journal*, 457, pp.79–87.
- Colombo, A.P. et al., 2009. Comparisons of subgingival microbial profiles of refractory periodontitis, severe periodontitis, and periodontal health using the human oral microbe identification microarray. *Journal of Periodontology.*, 80(9), pp.1132–1421.
- Copley, R., Russell, R. & Ponting, C., 2009. Sialidase-like Asp-boxes: Sequence similar structures within different protein folds. *Protein Science*, (1998), pp.285–292.
- Corfield, T., 1992. Bacterial Sialidases - Roles in Pathogenicity and Nutrition. *Glycobiology*, 2(6), pp.509–521.
- Crocker, P.R. et al., 1991. Purification and properties of sialoadhesin, a sialic acid-binding receptor of murine tissue macrophages. *The EMBO journal*, 10(7), pp.1661–9.
- Curtis, M. et al., 1999. Molecular Genetics and Nomenclature of proteases of *Porphyromonas gingivalis*. *Journal of Periodontal Research*, 34, pp.464–472.
- Curtis, M.A. et al., 1999. Variable carbohydrate modifications to the catalytic chains of the RgpA and RgpB proteases of *Porphyromonas gingivalis* W50. *Infection and Immunity*, 67(8), pp.3816–3823.

- Darveau, R.P., 2010. Periodontitis: a polymicrobial disruption of host homeostasis. *Nature reviews Microbiology*, 8(7), pp.481–90.
- Dashper, S.G. et al., 2001. Sodium ion-driven serine/threonine transport in *Porphyromonas gingivalis*. *Journal of Bacteriology*, 183(14), pp.4142–4148.
- Davanian, H. et al., 2012. Gene expression profiles in paired gingival biopsies from periodontitis-affected and healthy tissues revealed by massively parallel sequencing. *PLoS one*, 7(9) (online)
- Davey, M.E., George, A.O. & Toole, G.A.O., 2000. Microbial Biofilms : from Ecology to Molecular Genetic. *Microbiology and Molecular Biology Reviews*, 64(4), 1092-2172
- Demmer, R. & Desvarieux, M., 2006. Periodontal infections and cardiovascular disease-The heart of the matter. *The Journal of the American Dental Association*, 137(October), pp.14–20.
- Dewhirst, F.E. et al., 2010. The human oral microbiome. *Journal of Bacteriology*, 192(19), pp.5002–17.
- Diaz, P.I., Zilm, P.S. & Rogers, a H., 2002. *Fusobacterium nucleatum* supports the growth of *Porphyromonas gingivalis* in oxygenated and carbon-dioxide-depleted environments. *Microbiology*, 148(Pt 2), pp.467–72.
- Dickson, M. a et al., 2000. Human keratinocytes that express hTERT and also bypass a p16(INK4a)-enforced mechanism that limits life span become immortal yet retain normal growth and differentiation characteristics. *Molecular and Cellular Biology*, 20(4), pp.1436–47.
- Donadieu, J. et al., 2011. Congenital neutropenia: diagnosis, molecular bases and patient management. *Orphanet Journal of Rare Diseases*, 6, p.26.
- Duckworth, R.M., 2013. Pharmacokinetics in the oral cavity: Fluoride and other active ingredients. *Monographs in Oral Science*, 23, pp.125–139.
- Dzink, J., Sheenan, M. & Socransky, S., 1990. Proposal of Three Subspecies of *Fusobacterium nucleatum* Knorr 1922: *Fusobacterium nucleatum* subsp. *nucleatum* subsp. nov. , comb. nov. ; *Fusobacterium nucleatum* subsp. *polymorphum* subsp. nov. , norm. rev. , comb. nov.; and *Fusobacterium nucleatum* subsp. *vincentii* subsp. nov., nom. rev., comb. nov. *International Journal of Systemic Bacteriology*, 40(1), pp.74–78.
- Ebersole, J. et al., 2016. Aging , inflammation, immunity and periodontal disease. *Periodontology 2000*, 72, pp.54–75.
- Edgar, W.M., 1982. Duration of Response and Stimulus Sequence in the Interpretation of Plaque pH Data. *Journal of Dental Research*, 61(10), pp.1126–1129.
- Edlund, A. et al., 2013. An in vitro biofilm model system maintaining a highly reproducible species and metabolic diversity approaching that of the human oral microbiome. *Microbiome*, 1(1), p.25.
- Edwards, M., Grossman, T.J. & Rudney, J.D., 2007. Association of a high-molecular weight arginine-binding protein of *Fusobacterium nucleatum* ATCC 10953 with adhesion to secretory immunoglobulin A and coaggregation with *Streptococcus cristatus*. *Oral Microbiology and Immunology*, 22(4), pp.217–24.

- Eggert, F.M. et al., 1991. The pH of gingival crevices and periodontal pockets in children, teenagers and adults. *Archives of Oral Biology*, 36(3), pp.233–238.
- Eick, S. et al., 2003. Inhibitors of benzamidine type influence the virulence properties of *Porphyromonas gingivalis* strains. *Acta Biochimica Polonica*, 50(3), pp.725–734.
- Eke, P.I. et al., 2016. Risk Indicators for Periodontitis in US Adults: National Health and Nutrition Examination Survey (NHANES) 2009 – 2012. *Journal of Periodontology*, 0(0), pp.1–18.
- Eke, P.I. et al., 2012. Update of the Case Definitions for Population-Based Surveillance of Periodontitis. *Journal of Periodontology*, 83(12), pp.1–8.
- Eneva, R.T. et al., 2015. High Production of Neuraminidase by a *Vibrio cholerae* Non-O1 Strain—the First Possible Alternative to Toxigenic Producers. *Applied Biochemistry and Biotechnology*, 176(2), pp.412–427.
- Fardini, Y. et al., 2011. *Fusobacterium nucleatum* adhesin FadA binds vascular-endothelial cadherin and alters endothelial integrity. *Molecular microbiology*, 82(6), pp.1468–1480.
- Feng, C. et al., 2013. Neuraminidase reprograms lung tissue and potentiates lipopolysaccharide-induced acute lung injury in mice. *Journal of Immunology*, 191(9), pp.4828–37.
- Feng, C. et al., 2012. Sialyl residues modulate LPS-mediated signaling through the Toll-like receptor 4 complex. *PLoS one*, 7(4), (online)
- Flemmig, T.F. & Beikler, T., 2013. Economics of periodontal care: market trends, competitive forces and incentives. *Periodontology 2000*, 62(1), pp.287–304.
- Frank, K.L. et al., 2007. In vitro effects of antimicrobial agents on planktonic and biofilm forms of *Staphylococcus lugdunensis* clinical isolates. *Antimicrobial Agents and Chemotherapy*, 51(3), pp.888–895.
- Frenkel, E.S. & Ribbeck, K., 2015. Salivary mucins protect surfaces from colonization by cariogenic bacteria. *Applied and Environmental Microbiology*, 81(1), pp.332–338.
- Fritz, R.S. et al., 1999. Nasal cytokine and chemokine responses in experimental influenza A virus infection: results of a placebo-controlled trial of intravenous zanamivir treatment. *The Journal of Infectious Diseases*, 180(3), pp.586–93.
- Gabarrini, G. et al., 2015. The peptidylarginine deiminase gene is a conserved feature of *Porphyromonas gingivalis*. *Scientific Reports*, 5 (online).
- Gaio, E.J. et al., 2016. Effect of obesity on periodontal attachment loss progression: a 5-years population-based prospective study. *Journal of clinical periodontology*, 43, pp.557–565.
- Galen, J.E. et al., 1992. Role of *Vibrio cholerae* Neuraminidase in the Function of Cholera Toxin. *Infection and immunity*, 60(2), pp.406–415.
- Galgut, P., 2001. The relevance of pH to gingivitis and periodontitis. *Journal of the International Academy of Periodontology*, (3), pp.61–67.
- Gallimidi, A.B. et al., 2015. Periodontal pathogens *Porphyromonas gingivalis* and

- Fusobacterium nucleatum* promote tumor progression in an oral-specific chemical carcinogenesis model. *Oncotarget*, 8(6), pp.22613–226123.
- Gay, N.J. et al., 2014. Assembly and localization of Toll-like receptor signalling complexes. *Nature Reviews Immunology*, 14(8), pp.546–558.
- Gemmell, E. et al., 2002. Effect of *Fusobacterium nucleatum* on the T and B cell responses to *Porphyromonas gingivalis* in a mouse model. *Clinical and Experimental Immunology*, 128(2), pp.238–44.
- Gilbert, P., Das, J. & Foley, I., 1997. Biofilm Susceptibility to Antimicrobials. *Advances in Dental Research*, 11(1), pp.160–167.
- Gonzalez, O.A. et al., 2015. Differential Gene Expression Profiles Reflecting Macrophage Polarization in Aging and Periodontitis Gingival Tissues. *Immunological Investigations*, 44(7), pp.643–664.
- Goswami, M., Bhushan, U. & Goswami, M., 2016. Dental perspective of rare disease of fanconi anemia: Case report with review. *Clinical Medicine Insights: Case Reports*, 9, pp.25–30.
- Goulas, T. et al., 2015. Structure of RagB, a major immunodominant outer-membrane surface receptor antigen of *Porphyromonas gingivalis*. *Molecular Oral Microbiology*, pp.1–14.
- Grande, S.R. et al., 2011. Relationship between herpesviruses and periodontopathogens in patients with HIV and periodontitis. *Journal of Periodontology*, 82(10), pp.1442–52.
- Grenier, D. et al., 2003. Effect of inactivation of the Arg- and/or Lys-gingipain gene on selected virulence and physiological properties of *Porphyromonas gingivalis*. *Infection and Immunity*, 71(8), pp.4742–4748.
- Grenier, D. et al., 2001. Role of Gingipains in Growth of *Porphyromonas gingivalis* in the Presence of Human Serum Albumin, *Infection and Immunity* 69(8), pp.5166–5172.
- Griffen, A.L. et al., 2012. Distinct and complex bacterial profiles in human periodontitis and health revealed by 16S pyrosequencing. *The ISME journal*, 6(6), pp.1176–85.
- Guerrero, A. et al., 2005. Adjunctive benefits of systemic amoxicillin and metronidazole in non-surgical treatment of generalized aggressive periodontitis: a randomized placebo-controlled clinical trial. *Journal of Clinical Periodontology*, 32(10), pp.1096–107.
- Gul, S. et al., 2016. A Pilot Study of Active Enzyme Levels in Gingival Crevicular Fluid of Patients with Chronic Periodontal Disease. *Journal of Clinical Periodontology*, 43, pp.629–636.
- Gurav, A.N., 2012. Periodontitis and insulin resistance: Casual or causal relationship? *Diabetes and Metabolism Journal*, 36(6), pp.404–411.
- Gursoy, U.K. et al., 2010. Biofilm formation enhances the oxygen tolerance and invasiveness of *Fusobacterium nucleatum* in an oral mucosa culture model. *Journal of Periodontology*, 81(7), pp.1084–91.
- Gut, H., King, S.J. & Walsh, M. a, 2008. Structural and functional studies of *Streptococcus pneumoniae* neuraminidase B: An intramolecular trans-sialidase. *FEBS letters*, 582(23–

24), pp.3348–52.

- Ha, N.H. et al., 2015. Prolonged and repetitive exposure to *Porphyromonas gingivalis* increases aggressiveness of oral cancer cells by promoting acquisition of cancer stem cell properties. *Tumor Biology*, 36(12), pp.9947–9960.
- Hajishengallis, E. & Hajishengallis, G., 2013. Neutrophil homeostasis and periodontal health in children and adults. *Journal of Dental Research*, 93(3), pp.231–7.
- Hajishengallis, G., 2010. Complement and periodontitis. *Biochemical Pharmacology*, 80(12), pp.1992–2001..
- Hajishengallis, G., Darveau, R.P. & Curtis, M. a, 2012. The keystone-pathogen hypothesis. *Nature Reviews. Microbiology*, 10(10), pp.717–25.
- Hajishengallis, G. & Lambris, J.D., 2010. Crosstalk pathways between Toll-like receptors and the complement system. *Trends in immunology*, 31(4), pp.154–63.
- Han, X. et al., 2013. *Porphyromonas gingivalis* Infection-Associated Periodontal Bone Resorption Is Dependent on Receptor Activator of NF- κ B Ligand. *Infection and Immunity*, 81(5), pp.1502–9.
- Han, Y.W. et al., 2005. Identification and Characterization of a Novel Adhesin Unique to Oral Fusobacteria. *Journal of Bacteriology*, 187(15), pp.5330–5340.
- Han, Y.W. et al., 2000. Interactions between periodontal bacteria and human oral epithelial cells: *Fusobacterium nucleatum* adheres to and invades epithelial cells. *Infection and Immunity*, 68(6), pp.3140–6.
- Han, Y.W. et al., 2014. Periodontal disease, atherosclerosis, adverse pregnancy outcomes, and head-and-neck cancer. *Advances in Dental Research*, 26(1), pp.47–55.
- Haraszthy, V.I. et al., 2000. Identification of periodontal pathogens in atheromatous plaques. *Journal of Periodontology*, 71(10), pp.1554–60.
- Hashimoto, M. et al., 2010. Complement drives Th17 cell differentiation and triggers autoimmune arthritis. *The Journal of Experimental Medicine*, 207(6), pp.1135–1143.
- Hata, K. et al., 2008. Limited inhibitory effects of oseltamivir and zanamivir on human sialidases. *Antimicrobial Agents and Chemotherapy*, 52(10), pp.3484–3491.
- Hazeldine, J. et al., 2014. Impaired neutrophil extracellular trap formation: A novel defect in the innate immune system of aged individuals. *Aging Cell*, 13(4), pp.690–698.
- He, X. et al., 2012. Adherence to streptococci facilitates *Fusobacterium nucleatum* integration into an oral microbial community. *Microbial Ecology*, 63(3), pp.532–42.
- Hespell, R. & Canale-Parola E., 1971. Amino acid and glucose fermentation by *Treponema denticola*. *Archives of Microbiology.*, 78, pp.234–251.
- Hienz, S.A., Paliwal, S. & Ivanovski, S., 2015. Mechanisms of bone resorption in periodontitis. *Journal of Immunology Research*, 2015.
- Hiruma, Y., Hirai, T. & Tsuda, E., 2011. Siglec-15, a member of the sialic acid-binding lectin, is a novel regulator for osteoclast differentiation. *Biochemical and Biophysical Research Communications*, 409(3), pp.424–9.

- Honma, K. et al., 2007. Role of a *Tannerella forsythia* exopolysaccharide synthesis operon in biofilm development. *Microbial Pathogenesis*, 42(4), pp.156–66.
- Honma, K., Mishima, E. & Sharma, A., 2011. Role of NanH sialidase in epithelial cell attachment. *Infection and Immunity*, 79(1), pp.393–401.
- Hoon, J. et al., 2014. Bioorganic & Medicinal Chemistry Neuraminidase inhibitory activities of quaternary isoquinoline alkaloids from *Corydalis turtschaninovii* rhizome. *Bioorganic & Medicinal Chemistry*, 22(21), pp.6047–6052.
- Hoyer, L.L. et al., 1991. Purification and properties of cloned *Salmonella typhimurium* LT2 sialidase with virus-typical kinetic preference for sialyl alpha 2-3 linkages. *Journal of biochemistry*, 110(3), pp.462–7.
- Huq, N.L. et al., 2013. Propeptide-Mediated Inhibition of Cognate Gingipain Proteinases. *PLoS ONE*, 8(6). (online)
- Inagaki, S. et al., 2006. *Porphyromonas gingivalis* vesicles enhance attachment, and the leucine-rich repeat BspA protein is required for invasion of epithelial cells by “*Tannerella forsythia*”. *Infection and immunity*, 74(9), pp.5023–8.
- Ishihara, K. et al., 1996. Characterization of the *Treponema denticola* prtP gene encoding a prolyl-phenylalanine-specific protease (dentilisin). *Infect Immun*, 64(12), pp.5178–5186.
- Ishikura, H. et al., 2003. Cloning of the *Tannerella forsythensis* (*Bacteroides forsythus*) siaHI gene and purification of the sialidase enzyme. *Journal of Medical Microbiology*, 52(12), pp.1101–1107.
- Janapatla, R.-P. et al., 2013. Necrotizing pneumonia caused by nanC-carrying serotypes is associated with pneumococcal haemolytic uraemic syndrome in children. *Clinical microbiology and infection : the official publication of the European Society of Clinical Microbiology and Infectious Diseases*, 19(5), pp.480–6..
- Jang, Y.-J. et al., 2013. Autoinducer 2 of *Fusobacterium nucleatum* as a target molecule to inhibit biofilm formation of periodontopathogens. *Archives of oral biology*, 58(1), pp.17–27.
- Jermyn, W.S. & Boyd, E.F., 2002. Characterization of a novel *Vibrio* pathogenicity island (VPI-2) encoding neuraminidase (nanH) among toxigenic *Vibrio cholerae* isolates. *Microbiology*, 148(11), pp.3681–3693.
- Johannsen, A., Susin, C. & Gustafsson, A., 2014. Smoking and inflammation: Evidence for a synergistic role in chronic disease. *Periodontology 2000*, 64(1), pp.111–126.
- John, P. et al., 2015. Adjunctive Effects of a Piscean Collagen-Based Controlled-Release Chlorhexidine Chip in the Treatment of Chronic Periodontitis: A Clinical and Microbiological Study. *Journal of Clinical and Diagnostic Research*, 9(5), p.ZC70-ZC74.
- Johnson, J.D. et al., 2008. Persistence of Extracrevicular Bacterial Reservoirs After Treatment of Aggressive Periodontitis. *Journal of periodontology*, 79(12), pp.2305–2312.
- Johnston, C. et al., 2010. Detection of large numbers of pneumococcal virulence genes in streptococci of the mitis group. *Journal of Clinical Microbiology*, 48(8), pp.2762–2769.

- Joseph, R. et al., 2013. Association between chronic periodontitis and rheumatoid arthritis: A hospital-based case-control study. *Rheumatology International*, 33(1), pp.103–109.
- Jünemann, S. et al., 2012a. Bacterial community shift in treated periodontitis patients revealed by ion torrent 16S rRNA gene amplicon sequencing. *PloS one*, 7(8), (online)
- Jusko, M. et al., 2012. A metalloproteinase karilysin present in the majority of *Tannerella forsythia* isolates inhibits all pathways of the complement system. *Journal of Immunology*, 188(5), pp.2338–49.
- Kang, J.W. et al., 2015. DAMPs activating innate immune responses in sepsis. *Ageing Research Reviews*, 24, pp.54–65.
- Kaplan, C.W. et al., 2009. The *Fusobacterium nucleatum* outer membrane protein RadD is an arginine-inhibitable adhesin required for inter-species adherence and the structured architecture of multispecies biofilm. *Molecular Microbiology*, 71(1), pp.35–47.
- Kariu, T. et al., 2016. Inhibition of gingipains and *Porphyromonas gingivalis* growth and biofilm formation by prenyl flavonoids. *Journal of Periodontal Research*, (5).
- Kassebaum, N.J. et al., 2014. Global Burden of Severe Tooth Loss: A Systematic Review and Meta-analysis. *Journal of Dental Research*, 93, p.20–28.
- Kikkert, R. et al., 2007. Activation of toll-like receptors 2 and 4 by gram-negative periodontal bacteria. *Oral Microbiology and Immunology*, 22(3), pp.145–51.
- Kim, S. et al., 2011. Features and applications of bacterial sialidases. *Applied Microbiology and Biotechnology*, 91(1), pp.1–15.
- Kim, S. et al., 2010. Identification and functional characterization of the NanH extracellular sialidase from *Corynebacterium diphtheriae*. *Journal of Biochemistry*, 147(4), pp.523–533.
- Kim, S.-M., Kim, H.C. & Lee, S.-W.S., 2011. Characterization of antibiotic resistance determinants in oral biofilms. *Journal of Microbiology (Seoul, Korea)*, 49(4), pp.595–602.
- Kirschbaum, M. et al., 2010. Mixture of periodontopathogenic bacteria influences interaction with KB cells. *Anaerobe*, 16(4), pp.461–8.
- Kitamura, Y. et al., 2002. Gingipains in the culture supernatant of *Porphyromonas gingivalis* cleave CD4 and CD8 on human T cells. *Journal of Periodontal Research*, 37(6), pp.464–8.
- Kolenbrander, P.E. & Andersen, R.N., 1989. Inhibition of coaggregation between *Fusobacterium nucleatum* and *Porphyromonas (Bacteroides) gingivalis* by lactose and related sugars. *Infection and Immunity*, 57(10), pp.3204–9.
- Kolenbrander, P.E., Andersen, R.N. & Moore, L. V, 1989. Coaggregation of *Fusobacterium nucleatum*, *Selenomonas flueggei*, *Selenomonas infelix*, *Selenomonas noxia*, and *Selenomonas sputigena* with strains from 11 genera of oral bacteria. *Infection and Immunity*, 57(10), pp.3194–203.
- Komatsu, T. et al., 2012. E-selectin mediates *Porphyromonas gingivalis* adherence to

- human endothelial cells. *Infection and Immunity*, 80(7), pp.2570–6.
- Kuboniwa, M. et al., 2008. *P. gingivalis* accelerates gingival epithelial cell progression through the cell cycle. *Microbes and Infection*, 10(2), pp.122–128.
- Kurniyati, K. et al., 2013. A surface-exposed neuraminidase affects complement resistance and virulence of the oral spirochaete *Treponema denticola*. *Molecular Microbiology*, 89(5), pp.842–56.
- Lacy, P., 2006. Mechanisms of degranulation in neutrophils. *Allergy, asthma, and clinical immunology : official journal of the Canadian Society of Allergy and Clinical Immunology*, 2(3), pp.98–108.
- Lamont, R.J. et al., 2002. Role of the *Streptococcus gordonii* SspB protein in the development of *Porphyromonas gingivalis* biofilms on streptococcal substrates. *Microbiology (Reading, England)*, 148(Pt 6), pp.1627–36.
- Lee, M. et al., 2012. Cleavage of ST6Gal I by Radiation-Induced BACE1 Inhibits Golgi-Anchored ST6Gal I-Mediated Sialylation of Integrin β 1 and Migration in Colon Cancer Cells. *Radiation Oncology*, 7(1), p.47.
- Levine, M.J. et al., 1987. Structural aspects of salivary glycoproteins. *Journal of Dental Research*, 66(2), pp.436–441.
- Lewis, A.L. & Lewis, W.G., 2012. Host sialoglycans and bacterial sialidases: a mucosal perspective. *Cellular microbiology*, 14(8), pp.1174–82.
- Ley, K. et al., 2007. Getting to the site of inflammation: the leukocyte adhesion cascade updated. *Nature reviews. Immunology*, 7(9), pp.678–89.
- Li, C. et al., 2012. Abrogation of neuraminidase reduces biofilm formation, capsule biosynthesis, and virulence of *Porphyromonas gingivalis*. *Infection and Immunity*, 80(1), pp.3–13.
- Li, J. & McClane, B. a, 2013. The Sialidases of *Clostridium perfringens* Type D Strain CN3718 Vary in Their Properties and Sensitivity to Inhibitors. *Applied and Environmental Microbiology*, 80(5), pp.1701–1709.
- Liang, S. et al., 2011. The C5a receptor impairs IL-12-dependent clearance of *Porphyromonas gingivalis* and is required for induction of periodontal bone loss. *Journal of Immunology*, 186(2), pp.869–77.
- Listgarten, M. a, 1976. Structure of surface coatings on teeth. A review. *Journal of periodontology*, 47(3), pp.139–47.
- Liu, B. et al., 2012. Deep sequencing of the oral microbiome reveals signatures of periodontal disease. *PLoS one*, 7(6), p.e37919.
- Lo, A.W. et al., 2009. Comparative transcriptomic analysis of *Porphyromonas gingivalis* biofilm and planktonic cells. *BMC Microbiology*, 9, p.18.
- Loe, H., Theilade, E. & Borglum Jensen, S., 1965. Experimental Gingivitis in Man. *Journal of Periodontology*, 36, pp.177–187.
- Lohr, G., Beikler, T. & Hensel, A., 2015. Inhibition of in vitro adhesion and virulence of *Porphyromonas gingivalis* by aqueous extract and polysaccharides from

- Rhododendron ferrugineum* L. A new way for prophylaxis of periodontitis? *Fitoterapia*, 107, pp.105–113.
- Lowe, J.B., 2003. Glycan-dependent leukocyte adhesion and recruitment in inflammation. *Current Opinion in Cell Biology*, 15, pp.531–538.
- Maeda, K. et al., 2004. Characterization of Binding of *Streptococcus oralis* Glyceraldehyde-3-Phosphate Dehydrogenase to *Porphyromonas gingivalis* Major Fimbriae. *Infection and Immunity*, 72(9), pp.5475–5477.
- Magalhaes, A. et al., 2015. Helicobacter pylori chronic infection and mucosal inflammation switches the human gastric glycosylation pathways. *Biochimica et Biophysica Acta - Molecular Basis of Disease*, 1852(9), pp.1928–1939.
- Manco, S. et al., 2006. Pneumococcal neuraminidases A and B both have essential roles during infection of the respiratory tract and sepsis. *Infection and Immunity*, 74(7), pp.4014–4020.
- Manzoni, M. et al., 2007. Molecular cloning and biochemical characterization of sialidases from zebrafish (*Danio rerio*). *The Biochemical Journal*, 408(3), pp.395–406.
- Marcenes, W. et al., 2013. Global burden of oral conditions in 1990-2010: a systematic analysis. *Journal of Dental Research*, 92(7), pp.592–7.
- Martens, E.C., Chiang, H.C. & Gordon, J.I., 2008. Mucosal Glycan Foraging Enhances Fitness and Transmission of a Saccharolytic Human Gut Bacterial Symbiont. *Cell Host and Microbe*, 4(5), pp.447–457.
- Marty, F.M. et al., 2013. Safety and pharmacokinetics of intravenous zanamivir treatment in hospitalized adults with influenza: an open-label, multicenter, single-arm, phase II study. *The Journal of Infectious Diseases*, 209(4), pp.542–50.
- Matarasso, S. et al., 2009. The effect of recombinant granulocyte colony-stimulating factor on oral and periodontal manifestations in a patient with cyclic neutropenia: a case report. *International Journal of Dentistry*, 2009, p.654239.
- Matsuoka, K. & Kanai, T., 2015. The gut microbiota and inflammatory bowel disease. *Seminars in Immunopathology*, 37(1), pp.47–55.
- McClure, R. & Massari, P., 2014. TLR-Dependent Human Mucosal Epithelial Cell Responses to Microbial Pathogens. *Frontiers in Immunology*, 5(August), pp.1–13.
- McDowell, J. V. et al., 2009. Analysis of a unique interaction between the complement regulatory protein factor H and the periodontal pathogen *Treponema denticola*. *Infection and Immunity*, 77(4), pp.1417–1425.
- McGuckin, M. a et al., 2011. Mucin dynamics and enteric pathogens. *Nature reviews. Microbiology*, 9(4), pp.265–78.
- Mead, J., Smith, J.N. & Williams, R., 1955. The Biosynthesis of the Glucuronides of Umbelliferone and 4-Methylumbelliferone and Their use in Fluorimetric Determination of B-Glucuronidase. *Studies in Detoxication*, 6(1), pp.569–574.
- Meesmann, H.M. et al., 2010. Decrease of sialic acid residues as an eat-me signal on the surface of apoptotic lymphocytes. *Journal of Cell Science*, 123(Pt 19), pp.3347–3356.

- Megson, Z. a et al., 2015. Characterization of an alpha-l-fucosidase from the periodontal pathogen *Tannerella forsythia*. *Virulence*, 6(3), pp.282–292.
- Meindl, P. et al., 1974. Inhibition of Neuraminidase Activity by Derivatives Acid. *Virology*, 463, pp.457–463.
- Melrose, J., Perroy, R. & Careas, S., 1991. Adhesion of Human Cancer Cells to Vascular Endothelium Mediated by Carbohydrate Antigen SLeA. *Biochemical and Biophysical Research Communications*, 179(2), pp.713–719.
- Meri, S. & Pangburn, M.K., 1990. Discrimination between activators and nonactivators of the alternative pathway of complement: regulation via a sialic acid/polyanion binding site on factor H. *Proceedings of the National Academy of Sciences of the United States of America*, 87(10), pp.3982–6.
- Metzger, Z. et al., 2009. Enhanced attachment of *Porphyromonas gingivalis* to human fibroblasts mediated by *Fusobacterium nucleatum*. *Journal of endodontics*, 35(1), pp.82–5.
- Michaud, D.S. et al., 2016. Periodontal disease and risk of all cancers among male never smokers: an updated analysis of the Health Professionals Follow-up Study. *Annals of oncology : official journal of the European Society for Medical Oncology / ESMO*, 27(5), pp.941–947.
- Mikuls, T.R. et al., 2014. Periodontitis and *Porphyromonas gingivalis* in Patients with Rheumatoid Arthritis. *Arthritis Rheumatology*, 66(5), pp.1090–1100.
- Milner, P., Batten, J.E. & Curtis, M. a, 1996. Development of a simple chemically defined medium for *Porphyromonas gingivalis*: requirement for alpha-ketoglutarate. *FEMS microbiology letters*, 140(2–3), pp.125–130.
- Minami, A. et al., 2013. Catalytic preference of Salmonella typhimurium LT2 sialidase for N-acetylneuraminic acid residues over N-glycolylneuraminic acid residues. *FEBS Open Bio*, 3, pp.231–236.
- Mishima, E. & Sharma, A., 2011. *Tannerella forsythia* invasion in oral epithelial cells requires phosphoinositide 3-kinase activation and clathrin-mediated endocytosis. *Microbiology*, 157(Pt 8), pp.2382–91.
- Miyagi, T. & Yamaguchi, K., 2012. Mammalian sialidases: physiological and pathological roles in cellular functions. *Glycobiology*, 22(7), pp.880–96.
- Miyajima, S. et al., 2014. Periodontitis-activated monocytes/macrophages cause aortic inflammation. *Scientific reports*, 4, p.5171.
- Mizan, S. et al., 2000. Cloning and characterization of sialidases with 2-6' and 2-3' sialyl lactose specificity from *Pasteurella multocida*. *Journal of Bacteriology*, 182(24), pp.6874–6883.
- Moergel, M. et al., 2013. Chronic periodontitis and its possible association with oral squamous cell carcinoma - a retrospective case control study. *Head & face medicine*, 9, p.39.
- Morandini, A.C.F. et al., 2010. Differential production of macrophage inflammatory protein-1 alpha, stromal-derived factor-1, and IL-6 by human cultured periodontal ligament

- and gingival fibroblasts challenged with lipopolysaccharide from *P. gingivalis*. *Journal of Periodontology*, 81(2), pp.310–7.
- Muniz, F.W.M.G. et al., 2013. Azithromycin: A new concept in adjuvant treatment of periodontitis. *European Journal of Pharmacology*, 705(1–3), pp.135–139.
- Murakami, Y. et al., 2002. *Bacteroides forsythus* hemagglutinin is inhibited by N-acetylneuraminylactose. *Oral Microbiology and Immunology*, 17, pp.125–128.
- Myneni, S.R. et al., 2012. Identification of a unique TLR2-interacting peptide motif in a microbial leucine-rich repeat protein. *Biochemical and Biophysical Research Communications*, 423(3), pp.577–582.
- Nakajima, T. et al., 2006. Isolation and identification of a cytopathic activity in *Tannerella forsythia*. *Biochemical and Biophysical Research Communications*, 351(1), pp.133–139.
- Nakajima, T. et al., 2005. Regulatory T-cells Infiltrate Periodontal Disease Tissues. *Journal of Dental Research*, 84(7), pp.639–643.
- Nakayama, K. et al., 1995. Construction and characterization of arginin-specific cysteine proteinase (Arg-gingipain)-deficient mutants of *Porphyromonas gingivalis*. *Journal of Biological Chemistry*, 270(40), pp.23619–23626.
- Ng, K.M., Ferreyra, J. a, et al., 2013. Microbiota-liberated host sugars facilitate post-antibiotic expansion of enteric pathogens. *Nature*, 502(7469), pp.96–9.
- Niekrash, C.E. & Patters, M.R., 1986a. Assessment of complement cleavage in gingival fluid in humans with and without periodontal disease. *Journal of periodontal research*, 21(3), pp.233–42.
- Niekrash, C.E. & Patters, M.R., 1986b. Assessment of complement cleavage in gingival fluid in humans with and without periodontal disease. *Journal of Periodontal Research*, 21(3), pp.233–42.
- Nishikawa, T. et al., 2012. Bacterial neuraminidase rescues influenza virus replication from inhibition by a neuraminidase inhibitor. *PloS one*, 7(9), p.e45371.
- Nobbs, a H., Jenkinson, H.F. & Jakubovics, N.S., 2011. Stick to your gums: mechanisms of oral microbial adherence. *Journal of dental research*, 90(11), pp.1271–8.
- Oda, H. et al., 2007. Effect of gamma-immunoglobulin on the asaccharolytic growth of *Porphyromonas gingivalis*. *Journal of Periodontal Research*, 42(5), pp.438–42.
- Oda, H. et al., 2009. Participation of the secreted dipeptidyl and tripeptidyl aminopeptidases in asaccharolytic growth of *Porphyromonas gingivalis*. *Journal of Periodontal Research*, 44(3), pp.362–367.
- Padilla, C. et al., 2006. Periodontal pathogens in atheromatous plaques isolated from patients with chronic periodontitis. *Journal of Periodontal Research*, 41(4), pp.350–353.
- Papadopoulos, G. et al., 2012. Macrophage-Specific TLR2 Signaling Mediates Pathogen-Induced TNF-Dependent Inflammatory Oral Bone Loss. *The Journal of Immunology*, 190, (online)
- Park, K.-H. et al., 2013. Structural and biochemical characterization of the broad substrate

- specificity of *Bacteroides thetaiotaomicron* commensal sialidase. *Biochimica et Biophysica Acta*, 1834(8), pp.1510–9.
- Park, Y. et al., 2005. Short Fimbriae of *Porphyromonas gingivalis* and Their Role in Coadhesion with *Streptococcus gordonii*. *Infection and Immunity*, 73(7), pp.3983–3989.
- Parker, D. et al., 2009. The NanA neuraminidase of *Streptococcus pneumoniae* is involved in biofilm formation. *Infection and Immunity*, 77(9), pp.3722–3730.
- Patters, M., Niekrash, C. & Lang, N., 1989. Assessment of complement cleavage in gingival fluid during experimental gingivitis in man. *Journal of Clinical Periodontology*, 16(1), pp.33–37.
- Paul, S.P. et al., 2000. Myeloid specific human CD33 is an inhibitory receptor with differential ITIM function in recruiting the phosphatases SHP-1 and SHP-2. *Blood*, 96(2), pp.483–90.
- Periasamy, S. & Kolenbrander, P.E., 2009. Mutualistic biofilm communities develop with *Porphyromonas gingivalis* and initial, early, and late colonizers of enamel. *Journal of Bacteriology*, 191(22), pp.6804–11.
- Pham, T.K. et al., 2010. A quantitative proteomic analysis of biofilm adaptation by the periodontal pathogen *Tannerella forsythia*. *Proteomics*, 10(17), pp.3130–41.
- Phansopa, C. et al., 2015. Characterization of a sialate-O-acetyltransferase (NanS) from the oral pathogen *Tannerella forsythia* that enhances sialic acid release by NanH, its cognate sialidase. *The Biochemical Journal*, 472(2), pp.157–167.
- Phansopa, C. et al., 2014. Structural and functional characterization of NanU, a novel high-affinity sialic acid-inducible binding protein of oral and gut-dwelling Bacteroidetes species. *The Biochemical Journal*, 458(3), pp.499–511.
- Pinnock, A. et al., 2014. Characterisation and optimisation of organotypic oral mucosal models to study *Porphyromonas gingivalis* invasion. *Microbes and Infection*, 16(4), pp.310–319.
- Pradeep, a R. et al., 2009. Correlation of gingival crevicular fluid interleukin-18 and monocyte chemoattractant protein-1 levels in periodontal health and disease. *Journal of Periodontology*, 80(9), pp.1454–61.
- Ramage, G. et al., 2016. The epithelial cell response to health and disease associated oral biofilm models. *Journal of Periodontal Research*. (online)
- Rangarajan, M. et al., 2005. Expression of Arg-gingipain RgpB is required for correct glycosylation and stability of monomeric Arg-gingipain RgpA from *Porphyromonas gingivalis* W50. *Infection and Immunity*, 73(8), pp.4864–4878.
- Rayment, S. a et al., 2000. Immunoquantification of human salivary mucins MG1 and MG2 in stimulated whole saliva: factors influencing mucin levels. *Journal of dental research*, 79(10), pp.1765–1772.
- Reichert, S. et al., 2016. Periodontal conditions and incidence of new cardiovascular events among patients with coronary vascular disease. *Journal of Clinical Periodontology*.

- Renkonen, J. et al., 1999. Sialyl-Lewis x/a -decorated selectin ligands in head and neck tumours. *Journal of Cancer Research and Clinical Oncology*, 125, pp.569–576.
- Rôças, I.N. et al., 2001. “Red complex” (*Bacteroides forsythus*, *Porphyromonas gingivalis*, and *Treponema denticola*) in endodontic infections: a molecular approach. *Oral surgery, oral medicine, oral pathology, oral radiology, and endodontics*, 91(4), pp.468–71.
- Rosan, B. & Lamont, R.J., 2000. Dental plaque formation. *Microbes and infection / Institut Pasteur*, 2(13), pp.1599–607.
- Roy, S., 2010. *PhD Thesis: Biofilm Formation and Sialic Acid Utilisation by Tannerella forsythia*, University of Sheffield.
- Roy, S. et al., 2011. Role of sialidase in glycoprotein utilization by *Tannerella forsythia*. *Microbiology*, 157(Pt 11), pp.3195–202.
- Roy, S., Douglas, C.W.I. & Stafford, G.P., 2010. A novel sialic acid utilization and uptake system in the periodontal pathogen *Tannerella forsythia*. *Journal of Bacteriology*, 192(9), pp.2285–93.
- Rubinstein, M.R. et al., 2013. *Fusobacterium nucleatum* Promotes Colorectal Carcinogenesis by Modulating E-Cadherin/B-Catenin Signaling via its FadA Adhesin. *Cell Host and Microbe*, 14(2), pp.195–206.
- Sahingur, S.E. et al., 2013. Increased Nucleic Acid Receptor Expression in Chronic Periodontitis. *Journal of Periodontology*, pp.7–21.
- Saito, A. et al., 2012. *Porphyromonas gingivalis* entry into gingival epithelial cells modulated by *Fusobacterium nucleatum* is dependent on lipid rafts. *Microbial Pathogenesis*, 53(5–6), pp.234–42.
- Sakakibara, J. et al., 2007. Loss of adherence ability to human gingival epithelial cells in S-layer protein-deficient mutants of *Tannerella forsythensis*. *Microbiology*, 153(Pt 3), pp.866–76.
- Sánchez, G. a et al., 2013. Relationship between salivary mucin or amylase and the periodontal status. *Oral Diseases*, 19(6), pp.585–91.
- Schenkein, H.A. & Genco, R.J., 1977. Gingival Fluid and Serum in Periodontal Diseases. *Journal of Periodontology*, 48(12), pp.778–784.
- Schenkein, H.A. & Loos, B.G., 2013. Inflammatory mechanisms linking periodontal diseases to cardiovascular diseases. *Journal of Clinical Periodontology*, 40(SUPPL. 14).
- Schindelin, J. et al., 2012. Fiji: an open-source platform for biological-image analysis. *Nature Methods*, 9(7), pp.676–82.
- Schlafer, S. et al., 2010. Filifactor alocis--involvement in periodontal biofilms. *BMC Microbiol*, 10, p.66.
- Schoengraf, P. et al., 2013. Does complement play a role in bone development and regeneration? *Immunobiology*, 218(1), pp.1–9.
- Sedlacek, M.J. & Walker, C., 2007. Antibiotic resistance in an in vitro subgingival biofilm model. *Oral Microbiology and Immunology*, 22(5), pp.333–9.

- Settem, R.P. et al., 2013. A bacterial glycan core linked to surface (S)-layer proteins modulates host immunity through Th17 suppression. *Mucosal Immunology*, 6(2), pp.415–26.
- Settem, R.P. et al., 2012a. *Fusobacterium nucleatum* and *Tannerella forsythia* induce synergistic alveolar bone loss in a mouse periodontitis model. *Infection and Immunity*, 80(7), pp.2436–43.
- Sgroi, D. et al., 1993. CD22, a B cell-specific immunoglobulin superfamily member, is a sialic acid-binding lectin. *The Journal of Biological Chemistry*, 268(10), pp.7011–8.
- Shaddox, L.M. et al., 2011. Local inflammatory markers and systemic endotoxin in aggressive periodontitis. *Journal of Dental Research*, 90(9), pp.1140–4.
- Shaddox, L.M. et al., 2013. LPS-induced inflammatory response after therapy of aggressive periodontitis. *Journal of Dental Research*, 92(8), pp.702–8.
- Shah, M.H. et al., 2008. Tissue and serum α 2-3- and α 2-6-linkage specific sialylation changes in oral carcinogenesis. *Glycoconjugate Journal*, 25(3), pp.279–290.
- Sharma, A., 2011. Virulence mechanisms of *Tannerella forsythia*. *Periodontology 2000*, 54(1), pp.106–116.
- Sharma, a et al., 2005. Synergy between *Tannerella forsythia* and *Fusobacterium nucleatum* in biofilm formation. *Oral Microbiology and Immunology*, 20(1), pp.39–42.
- Sharma, a. et al., 2005. *Tannerella forsythia*-induced Alveolar Bone Loss in Mice Involves Leucine-rich-repeat BspA Protein. *Journal of Dental Research*, 84(5), pp.462–467.
- Shi, Y., Evans, J.E. & Rock, K.L., 2003. Molecular identification of a danger signal that alerts the immune system to dying cells. *Nature*, 425(6957), pp.516–521.
- Shimotahira, N. et al., 2013. The Surface Layer of *Tannerella forsythia* Contributes to Serum Resistance and Oral Bacterial Coaggregation. *Infection and Immunity*, 81(4), pp.1198–206.
- Shiozaki, K. et al., 2011. Regulation of sialyl lewis antigen expression in colon cancer cells by sialidase NEU4. *Journal of Biological Chemistry*, 286(24), pp.21052–21061.
- da Silva Correia, J. & Ulevitch, R.J., 2002. MD-2 and TLR4 N-linked glycosylations are important for a functional lipopolysaccharide receptor. *The Journal of Biological Chemistry*, 277(3), pp.1845–54.
- Sima, C. & Glogauer, M., 2013. Macrophage subsets and osteoimmunology: Tuning of the immunological recognition and effector systems that maintain alveolar bone. *Periodontology 2000*, 63(1), pp.80–101.
- Singh, A. et al., 2011. The capsule of *Porphyromonas gingivalis* leads to a reduction in the host inflammatory response, evasion of phagocytosis, and increase in virulence. *Infection and Immunity*, 79(11), pp.4533–42.
- de Smit, M. et al., 2012. Periodontitis in established rheumatoid arthritis patients: a cross-sectional clinical, microbiological and serological study. *Arthritis Research & Therapy*, 14(5), p.R222.
- Soares, R.M.A. et al., 2000. Identification of sialic acids on the cell surface of *Candida*

- albicans*. *Biochimica et Biophysica Acta*, 1474(2), pp.262–268.
- Socransky, S.S. et al., 1998. Microbial complexes in subgingival plaque. *Journal of Clinical Periodontology*, 25(2), pp.134–44.
- Soong, G. et al., 2006. Bacterial neuraminidase facilitates mucosal infection by participating in biofilm production. *Journal of Clinical Investigation*, 116(8), pp.2297–2305.
- Soskolne, W.A. et al., 1998. An in vivo study of the chlorhexidine release profile of the PerioChip in the gingival crevicular fluid, plasma and urine. *Journal of Clinical Periodontology*, 25(12), pp.1017–1021.
- Spahr, A. et al., 2006. Periodontal Infections and Coronary Heart Disease-Role of Periodontal Bacteria and Importance of Total Pathogen Burden in the Coronary Event and Periodontal Disease (CORODONT) Study. *Archives of Internal Medicine*, 166, pp.554–559.
- Stafford, G. et al., 2012. Sialic acid, periodontal pathogens and *Tannerella forsythia*: stick around and enjoy the feast! *Molecular Oral Microbiology*, 27(1), pp.11–22.
- Stafford, P. et al., 2013. Gingipain-dependent degradation of mammalian target of rapamycin pathway proteins by the periodontal pathogen *Porphyromonas gingivalis* during invasion. *Molecular Oral Microbiology*, 28(5), pp.366–378.
- Stamatos, N.M. et al., 2010. LPS-induced cytokine production in human dendritic cells is regulated by sialidase activity. *Journal of leukocyte biology*, 88(6), pp.1227–39.
- Stark, M.A. et al., 2005. Phagocytosis of apoptotic neutrophils regulates granulopoiesis via IL-23 and IL-17. *Immunity*, 22(3), pp.285–294.
- Strachan, R., Wood, J. & Hirschmann, R., 1961. Synthesis and Properties of 4-Methyl-2-oxo-1,2-benzopyran-7-yl B-D-Galactoside (Galactoside of 4-Methylumbelliferone). *Journal of Organic Chemistry*, 27, pp.1074–1075.
- Sugiyama, A. et al., 2002. Activation of human gingival epithelial cells by cell-surface components of black-pigmented bacteria: Augmentation of production of interleukin-8, granulocyte colony-stimulating factor and granulocyte-macrophage colony-stimulating factor and expression of. *Journal of Medical Microbiology*, 51(1), pp.27–33.
- Sugiyama, M. et al., 1993. Comparison of integrin expression and terminal differentiation capacity in cell lines derived from oral squamous cell carcinomas. *Carcinogenesis*, 14(10), pp.2171–2176.
- Sun, J. et al., 2006. Structural and functional analyses of the human Toll-like receptor 3. Role of glycosylation. *The Journal of Biological Chemistry*, 281(16), pp.11144–51.
- Sun, Y. et al., 2010. Gram-negative periodontal bacteria induce the activation of Toll-like receptors 2 and 4, and cytokine production in human periodontal ligament cells. *Journal of Periodontology*, 81(10), pp.1488–96.
- Suvan, J.E. et al., 2015. Association between overweight/obesity and increased risk of periodontitis. *Journal of Clinical Periodontology*, 42(8), pp.733–739.
- Suwannakul, S. et al., 2010. Identification of bistable populations of *Porphyromonas*

- gingivalis* that differ in epithelial cell invasion. *Microbiology*, 156(10), pp.3052–3064.
- Tailford, L.E. et al., 2015. Discovery of intramolecular trans-sialidases in human gut microbiota suggests novel mechanisms of mucosal adaptation. *Nature Communications*, 6(May), p.7624.
- Takahashi, N. & Yamada, T., 1999. Effects of pH on the glucose and lactate metabolisms by the washed cells of *Actinomyces naeslundii* under anaerobic and aerobic conditions. *Oral Microbiology and Immunology*, 14(1), pp.60–65.
- Takehara, S. et al., 2013. Degradation of MUC7 and MUC5B in human saliva. *PLoS one*, 8(7), p.e69059.
- Tanner, A.C.R. et al., 1986. *Bacteroides forsythus* sp. nov., a Slow-Growing Fusiform Bacteroides sp. from the Human Oral Cavity. *International Journal of Systemic Bacteriology*, 36(2), pp.213–221.
- Tew, J.G. et al., 2012. Dendritic cells, antibodies reactive with oxLDL, and inflammation. *Journal of Dental Research*, 91(1), pp.8–16.
- Tezal, M., Grossi, S.G. & Genco, R.J., 2005. Is periodontitis associated with oral neoplasms? *The Journal of Periodontology*, 76(3), pp.406–410.
- Theilade, E. et al., 1966. Experimental Gingivitis in Man II. A Longitudinal Clinical and Bacteriological Investigation. *Journal of Periodontal Research*, 1, pp.1–13.
- Thomas, G.J. et al., 2001. Expression of the avB6 integrin promotes migration and invasion in squamous carcinoma cells. *Journal of Investigative Dermatology*, 117(1), pp.67–73.
- Thompson, H. et al., 2009. An orthologue of *Bacteroides fragilis* NanH is the principal sialidase in *Tannerella forsythia*. *Journal of Bacteriology*, 191(11), pp.3623–8.
- Uchiyama, S. et al., 2009. The surface-anchored NanA protein promotes pneumococcal brain endothelial cell invasion. *The Journal of Experimental Medicine*, 206(9), pp.1845–52.
- Umemoto, T. & Hamada, N., 2003. Characterization of biologically active cell surface components of a periodontal pathogen. The roles of major and minor fimbriae of *Porphyromonas gingivalis*. *Journal of Periodontology*, 74(1), pp.119–22.
- Vajaria, B.N. et al., 2014. Salivary Glyco-sialylation changes monitors oral carcinogenesis. *Glycoconjugate Journal*, 31(9), pp.649–659.
- Varki, A. & Angata, T., 2006. Siglecs--the major subfamily of I-type lectins. *Glycobiology*, 16(1), p.1R–27R.
- Varki, A. & Diaz, S., 1983. A neuraminidase from *Streptococcus sanguis* that can release O-acetylated sialic Acids. *The Journal of Biological Chemistry*, 258, pp.12465–12471.
- Varki, A. & Gagneux, P., 2012. Multifarious roles of sialic acids in immunity. *Annals of the New York Academy of Sciences*, 1253, pp.16–36.
- Venerando, B. et al., 1982. Kinetics of *Vibrio cholerae* sialidase action on gangliosidic substrates at different supramolecular-organizational levels. *Biochemical Journal*, 203(3), p.735.

- Vincent, H.K. & Taylor, A.G., 2006. Biomarkers and potential mechanisms of obesity-induced oxidant stress in humans. *International Journal of Obesity (2005)*, 30(3), pp.400–418.
- Vincents, B. et al., 2011. Cleavage of IgG1 and IgG3 by gingipain K from *Porphyromonas gingivalis* may compromise host defense in progressive periodontitis. *FASEB journal : official publication of the Federation of American Societies for Experimental Biology*, 25(10), pp.3741–50.
- Vitkov, L. et al., 2009. Extracellular neutrophil traps in periodontitis. *Journal of Periodontal Research*, 44(5), pp.664–672.
- Vroom, J.M. et al., 1999. Depth Penetration and Detection of pH Gradients in Biofilms by Two-Photon Excitation Microscopy. *Applied and Environmental Microbiology*, 65(8), pp.3502–3511.
- Walther, E. et al., 2015. Antipneumococcal activity of neuraminidase inhibiting artocarpin. *International Journal of Medical Microbiology*, 305(3), pp.289–297.
- Wang, C.S. et al., 2007. Clinical Efficiency of 2% Chlorhexidine Gel in Reducing Intracanal Bacteria. *Journal of Endodontics*, 33(11), pp.1283–1289.
- Wang, H. & Sama, A.E., 2013. Anti-inflammatory role of Fetuin-A in Injury and Infection. *Current Opinions in Molecular Medicine*, 12(5), pp.625–633.
- Wang, R. et al., 2011. Analysis of interspecies adherence of oral bacteria using a membrane binding assay coupled with polymerase chain reaction-denaturing gradient gel electrophoresis profiling. *International Journal of Oral Science*, 3(2), pp.90–7.
- Wara-Aswapati, N. et al., 2012. Induction of Toll-Like Receptor Expression by *Porphyromonas gingivalis*. *Journal of Periodontology*, 84(7).
- Warren, J.C. & Cheatum, S.G., 1966. Effect of neutral salts on enzyme activity and structure. *Biochemistry*, 5, pp.1702–1707.
- Wei, G.X., Campagna, A.N. & Bobek, L. a., 2006. Effect of MUC7 peptides on the growth of bacteria and on *Streptococcus mutans* biofilm. *Journal of Antimicrobial Chemotherapy*, 57(6), pp.1100–1109.
- Wen, B.W. et al., 2014. Cancer risk among gingivitis and periodontitis patients: A nationwide cohort study. *QJM: An International Journal of Medicine*, 107(4), pp.283–290.
- White, D. a et al., 2012. Adult Dental Health Survey 2009: common oral health conditions and their impact on the population. *British Dental Journal*, 213(11), pp.567–72.
- White, P.C. et al., 2016. Neutrophil Extracellular Traps in Periodontitis: A Web of Intrigue. *Journal of Dental Research*, 95(1), pp.26–34.
- Whitmore, S.E. & Lamont, R.J., 2014. Oral Bacteria and Cancer. *PLoS Pathogens*, 10(3), pp.1–3.
- Widmer, N. et al., 2010. Oseltamivir in Seasonal, Avian H5N1 and Pandemic 2009 A/H1N1 Influenza- Pharmacokinetic and Pharmacodynamic Characteristics. , 49(11), pp.741–

765.

- Wiest, I. et al., 2010. Expression of the carbohydrate tumor marker Sialyl Lewis A (Ca19-9) in squamous cell carcinoma of the larynx. *Anticancer Research*, 30(5), pp.1849–1853.
- Wilensky, A. et al., 2013. The role of RgpA in the pathogenicity of *Porphyromonas gingivalis* in the murine periodontitis model. *Journal of Clinical Periodontology*, 40(10), pp.924–32.
- Wilensky, A. et al., 2016. Vaccination with recombinant RgpA peptide protects against *Porphyromonas gingivalis* -induced bone loss. *Journal of Periodontal Research*, (5).
- Wood, T.K., Knabel, S.J. & Kwan, B.W., 2013. Bacterial Persister Cell Formation and Dormancy. *Applied and environmental microbiology*, (September), pp.1–16.
- Wyss, C., 1989. Dependence of proliferation of *Bacteroides forsythus* on exogenous N-acetylmuramic acid. *Infection and Immunity*, 57(6), pp.1757–1759.
- Ximénez-Fyvie, L. a, Haffajee, a D. & Socransky, S.S., 2000. Comparison of the microbiota of supra- and subgingival plaque in health and periodontitis. *Journal of Clinical Periodontology*, 27(9), pp.648–57.
- Xu, G. et al., 2011. Three streptococcus pneumoniae sialidases: Three different products. *Journal of the American Chemical Society*, 133(6), pp.1718–1721.
- Yamaguchi, T. et al., 2016. Proinflammatory M1 macrophages inhibit RANKL-induced osteoclastogenesis. *Infection and Immunity*, (July), p.IAI.00461-16.
- Yamakawa, M. et al., 2016. *Porphyromonas gingivalis* infection exacerbates the onset of rheumatoid arthritis in SKG mice. *Clinical & Experimental Immunology*, pp.1–13.
- Yamamoto, K. et al., 2004. Association of Fcγ receptor IIa genotype with chronic periodontitis in Caucasians. *The Journal of Periodontology*, 75(4), pp.517–522.
- Yamazaki, K. et al., 1993. Immunohistological analysis of memory T lymphocytes and activated B lymphocytes in tissues with periodontal disease. *Journal of Periodontal Research*, 28(5), pp.324–334.
- Yeung, M.K. & Fernandez, S.R., 1991. Isolation of a neuraminidase gene from *Actinomyces viscosus* T14V. *Applied and Environmental Microbiology*, 57(11), pp.3062–3069.
- Yilmaz, O., Watanabe, K. & Lamont, R.J., 2002. Involvement of integrins in fimbriae-mediated binding and invasion by *Porphyromonas gingivalis*. *Cellular microbiology*, 4(5), pp.305–14.
- Yoneda, S. et al., 2014. Ubiquitous Sialometabolism Present among Oral Fusobacteria. *PLoS one*, 9(6), (online)
- Yu, T. et al., 2016. Enhanced Activity of the Macrophage M1/M2 Phenotypes and Phenotypic Switch to M1 in Periodontal Infection. *Journal of Periodontology*, 87(9), pp.1–21.
- Zalewska, A. et al., 2000. Structure and biosynthesis of human salivary mucins. *Acta Biochimica Polonica*, 47(4), pp.1067–1079.
- Zheng, X. et al., 2006. Proteomic analysis for the assessment of different lots of fetal bovine

serum as a raw material for cell culture. Part IV. Application of proteomics to the manufacture of biological drugs. *Biotechnology Progress*, 22(5), pp.1294–1300.

Zijnga, V. et al., 2010. Oral biofilm architecture on natural teeth. *PloS one*, 5(2), p.e9321.

7. Appendices

7.1 Full Sequences of sialidases closely related to NanH from 92.A2

> Sialidase *T.forsythia* 92.A2 NCBI Reference Sequence: WP_014225510.1

MKKFFWIIGLFASMQMTRAADSVYVQNPQIPILVDRTDNVLFIRIPDATKGDVLRNLTIRFGNEDKLSE
VKAVRLFYAGTEAATKGRSRFAPVTYVSSHNIRNTRSANPSYSIRQDEVTTVANTLTLKTRQPMVKGINY
FWVSVEMDRNTSLLSKLTSTVTEVVINDKPAVIAGEQAARRRMGIGVRHAGDDGSASFRIPGLVTTNK
GTLLGVYDVRYNNSVDLQEHIDVGLSRSTDKGQTWEPMRIAMSFGETDGLPSGQNGVGDPSILVDERT
NTVWVVAAWTHGMGNARAWTNSMPGMTPEETAQLMMVKSTDDGRTWSESTNITSQVKDPSWC
FLLQGPGRGITMRDGLTVFPIQFIDSLRVPHAGIMYSKDRGETWHIHQPARTNTTEAQAEEVEPGVLM
LNMRDNRGGSRAVSITRDLGKSWTEHSSNRSALPESICMASLISVKAKDNIIGKDLLFSNPNTTEGRHHI
TIKASLDGGVTWLP AHQVLLDEEDGWGYSCLSMIDRETVGIFYESSVAHMTFQAVKIKDLIR

> Sialidase *T.forsythia* 3313 NCBI Reference Sequence: WP_060828620.1

MKRFFLIVGLLASMQMTRAADSVYVQNPQIPILIDRTDNVLFIRISIPDATKGDVLRNLTIRFGNEDKLSEV
KAVRLFYAGTEAATKGRSRFAPVTYVSSHNIRNTRSANPSYSVRQDEVTTVANTLTLKTRQPMVKGINYF
WVSVEMDRNTSLLSKLTPTVTEAVINDKPAVIAGEQAARRRMGIGVRHAGDDGSASFRIPGLVTTNKG
TLLGVYDVRYNNSVDLQEHVDVGLSRSTDKGQTWEPMRIAMSFGETDGLPSGQNGVGDPSILVDERT
NTVWVVAAWTHGMGNARAWTNSMPGMTPEETAQLMMVKSTDDGRTWSEPTNITSQVKDPSWC
FLLQGPGRGITMRDGLTVFPIQFIDSLRVPHAGIMYSKDRGETWHIHQPARTNTTEAQAEEVEPGVLM
LNMRDNRGGSRAVSITRDLGKSWTEHSSNRSALPESICMASLISVKAKDNIIGKDLLFSNPNTTEGRHHI
TIKASLDGGVTWLP AHQVLLDEEDGWGYSCLSMIDRETVGIFYESSVAHMTFQAVKIKDLIR

> Sialidase *T.forsythia* 43037 NCBI Reference Sequence: WP_046826229.1

MKKFFWIIGLFISMQMTRAADSVYVQNPQIPILIDRTDNVLFIRIPDATKGDVLRNLTIRFGNEDKLSEV
KAVRLFYAGTEAATKGRSRFAPVTYVSSHNIRNTRSANPSYSVRQDEVTTAANTLTLKTRQPMVKGINYF
WVSVEMDRNTSLLSKLTPTVTEAVINDKPAVIAGEQAARRRMGIGVRHAGDDGSASFRIPGLVTTNEG
TLLGVYDVRYNNSVDLQEHVDVGLSRSTDKGQTWEPMRIAMSFGETDGLPSGQNGVGDPSILVDERT
NTVWVVAAWTHGMGNARAWTNSMPGMTPEETAQLMMVKSTDDGRTWSEPINITSQVKNPSWC
FLLQGPGRGITMRDGLTVFPIQFIDSLRVPHAGIMYSKDRGETWHIHQPARTNTTEAQAEEVEPGVLM
LNMRDNRGGSRAVSITRDLGKSWTEHSSNRSALPESICMASLISVKAKDNIIGKDLLFSNPNTTEGRHHI
TIKASLDGGVTWLP AHQVLLDEEDGWGYSCLSMIDRETVGIFYESSVAHMTFQAVKIKDLIR

> Sialidase *T.forsythia* KS16 NCBI Reference Sequence: WP_060831273.1

MKKFFLIVGLFASMQIIRAADSVYVQNPQIPILVDRTDNVLFIRIPDATKGDVLRNLTIRFGNEDKLSEVK
AVRLFYAGTEAATKGRSRFAPVTYVSSHNIRNTRSANPSYSVRQDEVTTVANTLTLKTRQPMVKGINYF
WVSVEMDRNTSLLSKLTPTVTEAVINDKPAVIAGEQAARRRMGIGVRHAGDDGSASFRIPGLVTTNEG
TLLGVYDVRYNNSVDLQEHVDVGLSRSTDKGQTWEPMRIAMSFGETDGLPSGQNGVGDPSILVDERT
NTVWVVAAWTHGMGNARAWTNSMPGMTREDETPQLMMVVRSTDDGRTWSEPINITSQVKDPSWC
LLQGPGRGITMRDGLTVFPIQFIDSVRVPHAGIMYSKDRGETWHIHQPARTNTTEAQAEEVEPGVLM
NMRDNRGGSRAVSITRDLGKSWTEHSSNRSALPESICMASLISVKAKDNIIGKDLLFSNPNTTEGRHHI
TIKASLDGGVTWLP AHQVLLDEEDGWGYSCLSMIDRETVGIFYESSVAHMTFQAVKIKDLIR

>Sialidase *Parabacteroides gordonii* NCBI Reference Sequence:
WP_028730084.1

MKKSIFYLCLLFIAQTAFAADS LYVREQQIPILIDRTDNV LLEMRI PAQKGDV LNKFTLQFGNETNLS DIKAI
RLFYSGTEAPAREGTHFNPVTYVTSFTPGKTRVANPSSYSVKQDEVTAPANTITLTSKQPMVKGP NYFWV
SIEMKPETSLLSRVSFTMPEAVINNKPAAIAWKGKAEAPRRVGVGVRQAGDDGSAAFRIPGMVTTNN
GTLGVDYDIRYNSSVDLQEMVDIGVSRSTDKGQTWEPMQVAMTFGETGGLPHAQNGVGDPSILVDEK
TNTIWVAAWTHGMGNRAWWNSMPGMTPDETAQLVLVKS EDDGKTWSEPINITSQVKDPSWYFL
LQGPGRGITMQDGLTVFPIQFIDATRIPNAGVMYSKDRGKTWHIHLNARTNTTEAQVAEVEPGVLMML
NMRDNRGGSRAVATTKDLGKTWTEHPSSRSALPEPVC MASLIKVDADDNITGKLLLLFSNPNTTKGRN
HITIKASLDGGLTWPAEHQVLLDEAEGWGYTCLSMIDKETV GIFYESSVAHMTFQAIKISDLIKE

>sialidase *Parabacteroides distasonis* ATCC 8503 NCBI Reference Sequence:
WP_011967072.1

MKKTFLYFCLLFIVQTAFAADSIYVREQQIPILIDRIDNVLYEMRI PAQKGDV LNEITI QIGDNVDLS DIQAI
RLFYSGVEAPSRKGEHFSPTVYISSHIPGNTRKALESYSVRQDEVTAPLSRTVKLTSKQPM LKGIN YFWVSI
QMKPETSLLAKVATTMPNAQINNKPINITWKGVDERHVGIGVRQAGDDGSAAFRIPGLVTTNNGTLL
GVYDIRYNSSVDLQEKIDIGVSRSTDKGQTWEPMRVAMTFKQTDGLPHGQNGVGDPSILVDEKTNTI
WVVAAWTHGMGNERAWWNSMPGMTPDETAQLMLVKS EDDGKTWSEPINITSQVKDPSWYFLLQ
GPGRGITMQDGLTVFPIQFIDATRVNAGIMYSKDRGKTWHLHLNARTNTTEAQVAEVEPGVLMMLN
MRDNRGGSRAVATTKDLGKTWTEHPSSRSALQESVCMASLIKVNAKDNITGKDLLLFSNPNTTKGRNH
ITIKASLDGGLTWPEHQVLLDEAEGWGYSCLSMIDKETV GIFYESSVAHMTFQAVKLQDLIHQ

>*Allistipes* spp. bNR/Asp-box repeat protein [*Alistipes* sp.
CAG:435]

MMKRTFWLIALSLLSLTASDSLRIHNPQIPILLDRMDNVLFQIRVPDAVQGDVLESLTVEFGPDTDIKS
MAELRLFYSGTEAVRRQGLRFSPVEYISAHNWVWNTSRANPSSYSVMQEQVSKIGRKVVLHSRQPMVGGI
NYWVSVRMNPDASLLTELRAVSEVVVNGKKIPVACDSRDVRRMGYVRHAGDDHSMAYRIPGL
VTTNSGLIGVYDVRWNSSVDLQERIDIGVSRSTDKGQTWEPMRIAMSFADVDGLPSGQNGVGDPAV
LVDEKTGTI WVMAAWTHGMGNRAWWTNSMPGMEPMETPQLMLARSDDDGRWSEPINITKQVK
DPSWCFLQGPGRGITMRDGLVFAIQFIDKDRMPHAGIIFSKDHGETWHIHNPARSNTTEAQVAEVE
PGVLMMLNMRDNRGGARAVMTTRDLGRTWNEHVSHRTTLREPVC MASLI AVPAEKNVLGKDLLLFSN
PDTTDGRRDITIKASLDGGVTWPYLLLLDEGDSWGYSCLTMIDSQTVGILYESSVAHITFQVVKLDIVR

>Sialidase *Porphyromonas* sp. 31_2 Genbank: KEJ85713.1

MEFTYLLISTYKQKHHEKTFLYFCLLFIVQTAFAADS LYVREQQIPILIDRIDNVLYEMRI PAQKGDV LNEITI
QIGDNVDLS DIQAIRLFYSGVEAPSRKGEHFSPTVYISSHIPGNTRKALESYSVRQDEVTPLSRTVKLTSK
QPMLKGIN YFWVSIQMKPETSLLAKVATTMPNAQINNKPIDITWKGVDERHVGIGVRQAGDDGSA A
FRIPGLVTTNNGTLLGVYDIRYNSSVDLQEKIDIGVSRSTDKGQTWEPMRVAMTFKQTDGLPHGQNGV
GDPSILVDEKTNTIWVVAAWTHGMGNERAWWNSMPGMTPDETAQLMLVKS EDDGKTWSEPINITS
QVKDPSWYFLLQGPGRGITMQDGLTVFPIQFIDATRVNAGIMYSKDRGKTWHLHLNARTNTTEAQV
AEVEPGVLMMLNMRDNRGGSRAVATTKDLGKTWTEHPSSRSALQESVCMASLIKVNAKDNITGKDLLL

SNPNTTKGRNHITIKASLDGGGLTPTEHQVLLDEAEGWGYSCLSMIDKETVGIFYESSVAHMTFQAIKL
QDIIHQ

>Sialidase *B. fragilis* str. 3976T8 WP_032598086.1

MKKAVILFSLFCFLCAIPVVQAADTIFVRETRIPILIERQDNVLFYLRDLDAKESQTLNDVVLNLGEGVNLSEI
QSIKLYYGGTEALQDSGKKRFAPVGYISSNTPGKTLAANPSYSIKKSEVTNPGNQVVLKGDQKLFPGINYP
WISLQMKPGTSLTSKVTADIASITLDGKKALLDVSENGIEHRMGVGVVRHAGDDNSAAFRIPLVTTNK
GTLGVDVRYNSSVDLQEHVDVGLSRSTDGGKTWEKMRLPLAFGEFGGLPAGQNGVGDPSILVDTKT
NNVWVVAAWTHGMGNQRAWWSSHPGMDMNHTAQLVLAKSTDDGKTWSAPINITEQVKDPSWY
FLLQGPGRGITMSDGLVFPQTQFIDSTRVNPAGIMYSKDGKKNWKMHNARTNTTEAQVAEVEPGVL
MLNMRDNRGGSRVAITKDLGKTWTEHESSRKALPESVCMASLISVKAKDNVLGKDLLIFSNTTKG
RYNTTIKISLDGGVTWSPEHQLLLDEGDNWGYSCLSMIDKETIGILYESSVAHMTFQAVKLDIIK

>Sialidase *B. thetaiotaomicron* str. 2789STDY5834899 GenBank: CUP73670.1

MKRNHYLFTLILLGCSIFVKASDTVHVHQTQIPILIERQDNVLFYFRDLDAKESRMMDEIVLDFGRSVNLS
DVQAVKLYYGGTEALQDRGKNRFAPVDYISSHRPGNTLAAIPSYSIKCAEVLQPSAKVVLKSHYKLFPGIN
FFWISLQMKPETSFLT KISSELSVKIDGKEAICEERSPKDIIHRMAVGVRHAGDDGSASFRIPLVTSNK
GTLGVDVRYNSSVDLQEYVDVGLSRSTDGGKTWEKMRLPLSFGYDGLPAAQNGVGDPSILVDTQT
NTIWWVAAWTHGMGNQRAWWSSHPGMDLYQTAQLVMAKSTDDGKTWSKPINITKQVKDPSWYF
LLQGPGRGITMSDGLVFPQTQFIDSTRVNPAGIMYSKDRGKTWKMHNMARTNTTEAQVVEIEPGVLM
LNMRDNRGGSRVAITKDLGKTWTEHPSSRKALQEPVCMASLIHVEAKDNVLDKDILLFSNPNTTRGR
NHITIKASLDGGLTWLPEHQMLLDEGEGWGYSCLTMIDRETIGILYESSAAHMTFQAVKLDLIR

>Sialidase *Dysgonomonas* sp. HGC4 NCBI Reference Sequence:

WP_050709261.1MKNFLSFFLLSLTINSASDTVKIKAPQIPILTDRQDNVLFYIRLDAANSKVLNNVKV
NLDKEVNLNEIKSIKLYYSGTECVQREGKTFYAPVQYISKDVPNGNTFAANSYSVKKTELSTLKNEITLTAD
QPLFPGINYPFWVSIEMKPNASLLSNVQANITDVILDNKSIIAFDKERSVSRKLGIGVRHAGDDKAAAYRI
PGLATSNKGTMLGVYDVRYNNSADLQEYVHVGLSRSDKGGQTWEPMRIIMDFDEYGGLPKAQNGVG
DPAILVDKTTGTIWWVAAWTHGMGNRAWFNSQQGMGIDQTAQLVMVKSDDDGKTWSKPINVT
QLKDPSWYFLLQGPNGITMQDGTIVFASQFIDSERIPNAGIISKDHGKTWQTHNYARTNTTEAQVV
EIEPGVLMNMRDNRGGSRVAITKDMGKTWTEHPSSRSALQEPVCMASIIKVAKDNVLKDKDILLFS
NPNTTKERKDIKASLDGGNTWLPEQQILLDEDYSWGYSCLSMIDKETVGIFYESSVAHMTFQAIKLSDI
IKK

7.2 Full Sequences of Sialidases Closely Related to SiaPG from ATCC 33277

> sialidase *Porphyromonas gingivalis*_ATCC33277 NCBI Reference

Sequence: WP_012458403.1

```
MANNTLLAKTRRYVCLVVFCCLMAMMHLGQEVMTWGD SHGVAPNQVRRRTLKVALSESLPPGAKQIR
IGFSLPKETE EKVTALYLLVSDSLAVRDLDPDYKGRVSYDSFPI SKEDRTTALSADSVAGRCFFYLAAD
IGPVASF SRSDTLTARVEELAVDGRPLPLKELSPASRRLYREYEALFVPGDGGSRNYRIP SILKTANG
TLIAMADRRKYNQTDLPEDIDIVMRRSTDGGKSWSDPRIIVQGEGRNHGFGDVALVQTQAGKLLMIFV
GGVGLWQSTPDRPQRTYI SESRDEGLTWSPPRDITHFIFGKDCADPGRSRWLASF CASGQGLVLP SGR
VMFVAAIRESGQ EYVLNNYVLYSDDEGGTWQLSDCAYHRGDEAKLSLMPDGRVLM SVRNQGRQESRQR
FFALSSDDGLTWERAKQFEGIHDPGCNGAMLQV KRNGRNQMLHSLPLGPDGRRD GAVYLFDHVSGRWS
APVVVNSGSSAYS DMTLLADGTIGYFVEEDEISLVFIRFVLDLDFDARQ
```

> sialidase *Porphyromonas gingivalis*_A7A1-28 NCBI Reference

Sequence: WP_058019243.1

```
MANNTLLAKTRRSVCLVVFCCLMAMMHLGQEVMTWGD SHGVAPNQVRRRTLKVALSESLPPGAKQIR
IGFSLPKETE EKVTALYLLVSDSLAVRDLDPDYKGRVSYDSFPI SKEDRTTALSADSVAGRCFFYLAAD
IGPVASF SRSDTLTARVEELAVDGRPLPLKELSPASRRLYREYEALFVPGDGGSRNYRIP SILKTANG
TLIAMADRRKYNQTDLPEDIDIVMRRSTDGGKSWSDPRIIVQGEGRNHGFGDVALVQTQAGKLLMIFV
GGVGLWQSTPDRPQRTYI SESRDEGLTWSPPRDITHFIFGKDCADPGRSRWLASF CASGQGLVLP SGR
VMFVAAIRESGQ EYVLNNYVLYSDDEGGTWQLSDCAYHRGDEAKLSLMPDGRVLM SVRNQGRQESRQR
FFALSSDDGLTWERAKQFEGIHDPGCNGAMLQV KRNGRNQMLHSLPLGPDGRRD GAVYLFDHVSGRWS
APVVVNSGSSAYS DMTLLADGTIGYFVEEDEISLVFIRFVLDLDFDARQ
```

> sialidase *Porphyromonas gingivalis*_W4087 NCBI Reference

Sequence: WP_043894535.1

```
MANNTLLAKTRRSVCLVVFCCLMAMMHLGQEVTVCGD SHGVAPNQMYRTLKVALSESLPPGAKQIR
IGFSLPKETE EKVTALYLLVSDSLAVRDLDPDYKGRVSYDSFPI SKEDRTTALSADSVAGRRFFYLAAD
IGPVASF SRSDTLTARVEELAVDGRPLPLKELSPASRRLYREYEALFVPGDGGSRNYRIPAILKTANG
TLIAMADRRKYNQTDLPEDIDIVMRRSTDGGKSWSDPRIIVQGEGRNHGFGDVALVQTQAGKLLMIFV
GGVGLWQSTPDRPQRTYI SESRDEGLTWSPPRDITHFIFGKDCADPGRSRWLASF CASGQGLVLP SGR
IMFVAAIRESGQ EYVLNNYVLYSDDEGDTWQLSDCAYRRGDEAKLSLMPDGRVLM SIRNQGRQESRQR
FFALSSDDGLTWERAKQFEGIHDPGCNGAMLQV KRNGRDQVLHSLPLGPDGRRD GAVYLFDHVSGRWS
APVVVNSGSSAYS DMTLLADGTIGYFVEEDEISLVFIWFVLDLDFDARQ
```

> sialidase, Putative *Porphyromonas gingivalis*_W83 Genbank:

AAQ65563.1

```
MANNTLLAKTRRYVCLVGF CWMAMMHLGQEVMTWGD SHGVAPNQVRRRTLKVALSESLPP
GAKQIRIGFSLPKETE EKVTALYLLVSDSLAVRDLDPDYKGRVSYDSFPI SKEDRTTALSADS
VAGRRFFYLAADIGPVASF SRSDTLTARVEEVAVDGRPLPLKELSPASRRLYRGYEALFVPG
DGGSRNYRIPAILKTANGTLIAMADRRKYNQTDLPEDIDIVMRRSTDGGKSWSDPRIIVQGE
GRNHGFGDVALVQTQAGKLLMIFVGGVGLWQSTPDRPQRTYI SESRDEGLTWSPPRDITHFIF
FGKDCADPGRSRWLASF CASGQGLVLP SGRITFVAAIRESGQ EYVLNNYVLYSDDEGDTWQL
SDCAYRRGDEAKLSLMPDGRVLM SIRNQGRQESRQRFFALSSDDGLTWERAKQFEGIHDPGC
NGAMLQV KRNGRDQVLHSLPLGPDGRRD GAVYLFDHVSGRWSAPVVVNSGSSAYS DMTLLAD
GTIGYFVEEGDEISLVFIRFVLDLDFDVRQ
```

> "Hypothetical Protein" *Porphyromonas gingivalis*_F0570 NCBI Reference Sequence:

WP_021665936.1MANNTLLAKTRRYVCLVGF CWMAMMHLGQEVMTWGD SHGVAPNQVR

RTLVKVALSESLPPGAKQIRIGFSLPKETEETKVTALYLLVSDSLAVRDLDPDYKGRVSYDSFP
ISKEDRTTALSADSVAGRRFFFYLAADIGPVASFSDTLTARVEEVAVDGRPLPLKELSPAS
RRLYRGYEALFVPGDGGSRNYRIPAILKTANGTLIAMADRRKYNQTDLPEDIDIVMRRSTDG
GKSWSDPRIIVQGEGRNHGFGDVALVQTQAGKLLMIFVGGVGLWQSTPDRPQRTYISESRDE
GLTWSPPRDITHFIFGKDCADPGRSRWLASFASGQGLVLPGRITFVAAIRESGQEYVLNN
YVLYSDDEGDTWHLSDCAYRRGDEAKLSLMPDGRVLMVSRNQGRQESRQRFALSSDDGLTW
ERAKQFEGIHDPGCNGAMLQVKRNGRDQVLHSLPLGPDGRRDGAVYLFHDHTSGRWSAPVVVN
SGSSAYSDMTLLADGRIGYFVEEGDEISLVFIRFVLDDLFDARQ

> "Hypothetical Protein" *Porphyromonas gingivalis*_AJW4 NCBI
Reference Sequence:

WP_053444411.1MANNTLLAKTRRYVCLVGFCLMAMMHLGQEVMTWGD SHGVAPNQVR
RTLVKVALSESLPPGAKQIRIGFSLPKETEETKVTALYLLVSDSLAVRDLDPDYKGRVSYDSFP
ISKEDRTTAFSADSVAGRRFFFYLAADIGPVASFSDTLTARVEEVAVDGRPLPLKELSPAS
RHLYRGYEALFVPGDGGSRNYRIPAILKTANGTLIAMADRRKYNQTDLPEDIDIVMRRSTDG
GKSWSDPRIIVQGEGRNHGFGDVALVQTQAGKLLMIFVGGVGLWQSTPDRPQRTYISESRDE
GLTWSPPRDITHFIFGKDCADPGRSRWLASFASGQGLVLPGRITFVAAIRESGQEYVLNN
YVLYSDDEGDTWHLSDCAYRRGDEAKLSLMPDGRVLMVSRNQGRQESRQRFALSSDDGLTW
ERAKQFEGIHDPGCNGAMLQVKRNGRDQVLHSLPLGPDGRRDGAVYLFHDHTSGRWSAPVVVN
SGSSAYSDMTLLADGTIGYFVEEGDEISLVFIRFVLDDLFDARQ

> Sialidase *Porphyromonas gulae*_COT-052 OH4119 GenBank:
KGN74638.1

MANNTLLARTLRSVCLVVFCCLVAMLRLTAQEVAVWGDKHXGVPDQAHRTLKIVLSEPLPP
NAKQIRISYSFPQDTKDKVTALYLLVSDSLAVRDLDPDYKGRVSYDSFPISKEDCVITLSADS
VAGRRFFFYLAADIGPVASFSDTLTARVEEVAVDGRPLPFKEVSPASRRLYRGYEALFVPG
DGGSRNYRIPAILKTAKGTLIAMADRRKYNQTDLPEDIDIVMRRSTNGGRSWSDPRIIVQGE
GRNHGFGDVALVQTKARKLLMIFVGGVGLWQSTPDRPQRTYVSESRDEGLTWSPPRDITRFI
FGKDCADPGRSRWLASFASGKGLLLPSGRIMFVAAIRESGQEYVLKNYVLYSDDEGSTWHL
SDCAYRRGDEAKLSLMPDGRVLMVSRNQGRQEEERQRFALSSDDGLTWERAKQFESIHPGC
NGAMLQKWNQRDQMLHSLPLGPDGRRDGAVYLFHDHASVRWSTPVVVNSGSSAYSDMTLLAD
GTIGYFVEEDDEISLVFIRFALDDLFDAGL

>sialidase *Porphyromonas gulae* COT-052 OH2179 NCBI Reference
Sequence: WP_039431766.1

MLRLTAQEVAVWGDKHXGVPDQAHRTLKIALSEPLPPNAKQIRIRYSFPQDTKDKVTALYL
LVSDSLAVRDLDPDYKGRVSYDSFPISKEDCVITLSADSVAGRRFFFYLAADIGPVASFSDT
LTARVQEVAVDGRPLPLKELSPASRRLYRGYEALFVPGDDGSRNYRIPAILKTAKGTLIAMA
DRRKYNQTDLPEDIDIVMRRSTNGGRSWSDPRIIVQGEGRNHGFGDVALVQTQAGKLLMIFV
GGVGLWQSTPDRPQRTYISESRDEGLTWSPPRDITHFIFGKDCADPGRSRWLASFASGQGL
VLPGRITFVAAIRESGQEYVLNNYVLYSDDEGGTQWQLSDCAYHRGDEAKLSLMPDGRVLM
VRNQGRQESRQRFALSSDDGLTWERAKQFEGIHDPGCNGAMLQVRSRGNQMLHSLPLGPD
GRRDGAVYLFHDHTSGRWSTPVVVNSGSSAYSDMTLLADGTIGYFVEEDDEISLVFIRFALDD
LFDAGQ

>glycosyl hydrolase, partial [Bacteroidetes bacterium OLB8]
GenBank: KXX20028.1

AGPVLSEVHLNFKGTSHLKDITQCRIYNTGNVNAFNPKPSGNLLATARIRRSELTLKTREN

LLPGDNHLWLTVDVSPKAVEGNKIDVALKSIRVDDRNYPVNGNPEGSREILLKRVLVLPAG
DYGSKNYRIPAIITADDHSLVILTDKRKDNSIDLPEIDIIAQRSTDGGKRWSEPVTVAKGE
GRYKGYGDACITRTLSGKLVALYVGGPGLWNSTSEKPOGHYMSVSDDNKSWSDPVDITGQL
YGINCPDSVRRHWQSSFFGSGRGLTLRDGRIMAVIAVRESKENHKLNNYVVYSDDEGTTWHV
SQKAIDGGDEAKVVELNDGTILLSSRTAGNRLWAKSTDRGVTWGPKNWHEIWGNACDADI
RYTSTRDGYDKDRILHTLPNAKNRTNVMWLSYDEGTTWVPRKTICKGESAYSSITILPDGT
IGVYVEEDESVPYKMYFLNFSLDWLTGKDHFRKAGG

>uncharacterized protein BN523_00027 [*Bacteroides* sp. CAG:189]
GenBank: CCY52158.1

MKHYSILSILVMSILPLWGQSGQSLVLNGTDQLMKIASHDDFNVSAAEESFTVACWVKVNR
WLDGQRFVAKRSMTGTPKSGYELWGGQSSSKFYANNAPNTAGNHDNSMSVWSTEFGLDWA
HVAFVVDVDRVNGKMYLYHNGKQVGNISGKIDIGPWYVENDYDVTVGTGRASAMEYAYYLKGEID
NLRFWKRALSLEEINADKVDEMPASEGLVAAAYDFENIDGLTVPDVSGNGHNGVLVNYVPDGP
CKVASASVVQDSNFTGRGNEDEVVLKAVLDMEGTDPVQCENKLTNLMDGTTNVQDVKS
IKVYSTGNINSDARYAAVTATLLGSCPKASGEINCELTGELTSGTNYLWITYDIADNATEGNKVDA
NIVSITTADETYAFTEGSVEGERTILLKRKLLFAPGDAGSKNYRIPAIITAADGSLVVATDK
RKNNQGDLPEDIDVVIRSEDGGITWSEPQTIAEGTGARRGFGDAGLVHTTEENGLLCIFVG
GEGIFNNSPSPNPTRYVCKSTDNGKTWSAPRDITEQLYGTACTVTERQGWYASFCASGNL
LTKNGRIMFVAAVRENSASTLSNFVYSSDDNGETWNVSKRAKLGDESQVVELSDGTILMSI
RRQSKGPRYYTKSTDGGITWGEVSEWTEMLEPNCNGDIIRYTSVNDGYEKNRLLHSIPNDAA
NRRNVSVFVSYDEGQTPVKKSICPTGSAYSSLTILPDGTIGAYVEENYDTDNMSLYFNNFS
LDWLTGADIYYAAGETEVSPTSFAPEGEYENSVAIELTATDGASIIYTLDGNTPNERS
ILYEGITIEETTVKAIKAVKDLANSEIATATYTIHPGEYCIWDEDAYPRNTDRVVQSL
SVSGASQGGIAQDFTTVVAGIGAKTQSKINFNTADVLNATIGNELFLTVADFNLYWTHYYV
YVDYNQNGVFESNEVVSITHYSEDDGTYHDSKGDVVDAGKVQRDLPSFIIPDNALGETRIR
FKADWNSLDPCGDASLASNRGTICDFTINIHEAVMGVVSFEQTEGATLQIMNGEEVTVNGTR
LPLGTVLSVNAEVTSDDYIIRAILVNGEELESNTFVLAEDATVSLDIIKGLVNYQVEGNGI
LSVSDNSSNEIASGAIYKGSVVVIKVTDPENYHVESVLINGDDKTEECVSDAGYSLVVNEH
LDIIAKFAIDSYSLSNYSNNEEFGKMIVQKSNNGDDVISGDLIPYNEKVTFTLQPAVRCYVASV
MIDGEEKMDEILTNKSFSLNITKETTVQVVYEAKEYSLTLANDTPKKGKLMVKRLSDDIELE
DQSEIIYDEELLIAWLPEEGCELAELWIKEGEDDEYDLIEAGLLEELGDSKEFSYQVFANVA
LRAVFSGTVSITNTEIANTTVYTKDGKLIKDKGKGVCEVFVYDVLGQVVKSFIIENALETVQ
LGTSSLYLVKIVDGADCIVKKVGNM

>sialidase [*Bacteroides salyersiae*] strain 2789STDY5608871
GenBank: CUM75333.1

MKHYSILSILVMSILPLWGQSGQSLVLNGTDQLMKIASHDDFNVSAAEESFTVACWVKVNR
WLDGQRFVAKRSMTGTPKSGYELWGGQSSSKFYANNAPNTAGNHDNSMSVWSTEFGLDWA
HVAFVVDVDRVNGKMYLYHNGKQVGNISGKIDIGPWYVENDYDVTVGTGRASAMEYAYYLKGEID
NLRFWKRALSLEEINADKVDEMPASEGLVAAAYDFENIDGLTVPDVSGNGHNGVLVNYVPDGP
CKVASASVVQDSNFTGRGNEDEVVLKAVLDMEGTDPVQCENKLTNLMDGTTNVQDVKS
IKVYSTGNINSDARYAAVTATLLGSCPKASGKINCELTGELTSGTNYLWITYDIADNATEGNKVDA
NIVSITTADETYAFTEGSVEGERTILLKRKLLFAPGDAGSKNYRIPAIITAADGSLVVATDK
RKNNQGDLPEDIDVVIRSEDGGITWSEPQTIAEGTGARRGFGDAGLVHTTEENGLLCIFVG
GEGIFNNSPSPNPTRYVCKSTDNGKTWSAPRDITEQLYGTACTVTERQGWYASFCASGNL
LTKNGRIMFVAAVRENSASTLSNFVYSSDDNGETWNVSKRAKLGDESQVVELSDGTILMSI
RRQSKGPRYYTKSTDGGITWGEVSEWTEMLEPNCNGDIIRYTSVNDGYEKNRLLHSIPNDAA

NRRNVSFVFSYDEGQTPVKKSICPTGSAYSSLTILPDGTIGAYVEENYDTDNMSLYFNFS
LDWLTGDADIYYAAGETEUVKSPTFSAPEGEYENSVAIELTTATDGASIIYTLDGNTPNERS
ILYEGLITIEETTTVKAIIVKDGLANSEIATATYTIHPGEYCIWDEDAYPRNTDRVVQSL
SVSGASQGGIAQDFTTVVAGIGAKTQSKINFNTADVLNATIGNELFLTVDNFNLYWTHYYV
YVDYNQNGVFESNEVVSYTHYSEDDGTYHDSKGDVVDAGKVQRDLPSFIIPDNAKLGETRIR
FKADWNSLDPCGDASLASNRGTICDFTINIHEAVMGVVSFEQTEGATLQIMNGEEVTVNGTR
LPLGTVLSVNAEVTSDDYIIRAILVNGEELESNTFVLAEDATVSLDIIKGLVNYQVEGNGI
LSVSDNSSNEIASGAIIVYKGSVVVIKVTDPENYHVESVLINGDDKTEECVSDVGYSLVVNEH
LDIIAKFAIDSYSLNYSCTNEEFQKMIQKSNQDVIISGDLIPYNEKVTFTLQPAVRCYVASV
MIDGEEKMDEILTNKSFSLNITKETTVQVVYEAKEYSLTLANDTPKKGKLMVKRLSDDIELE
DQSEIIYDEELLIAWLPEEGCELAELWIKEGEDDEYDLIEAGLLEELGDSKEFSYQVFANVA
LRAVFSGTVSITNTEIANTTVYTKDGKLIIVKDGKVGCEVFVYDVLGQVVKSFIIENALETVQ
LGTSSLYLVKIVDGADCIVKKIGNM

>T9SS C-terminal target domain-containing protein *Barnesiella*
viscericola DSM

18177MHLAMVINRADNTVSLYRDGQQGNWKQNAALNSWTVVNNNPIYLGCGSTTGTDPDHL
DGKLANVRFWSKALTAEEVAADMTATVGPDPTEALIAAYDFANISGLTVPDISGHGH
DATLSGFDPVGSVAIYSATSKADTNFTGRGNTNEIASSMAVAITGQEGTYTFGNLSLDL
TGTTNVQDITAIKVYMTDQNSFDPRKAGEAELLGTCTPTENTVECALTGESPVGTYLWV
TFDVSETAAE GNRVAIKPTMLDEKAVSAITTSREILLGRITLLFAPGDYGSVAYRIPGI
ITAWDGLVAITDKRKYNQSDIPEDIDIVRRSTDNGKTWSEPVMAQGTGQYHGYGDA
AIVRTNTENELLCIFIGGNLFASTTSNRIRTYISRSTDNGQSWAPQDITDQIFRGERAS
WTASFCAAGNGLKTRNGVLMFVAAMRHDSGNTLYNHVVYSNDNGVTWVNSNCAMVGG
DESKVVELNDGRILMSVRRQSKGARYYTISDNVPSTTEAVSWTQKNTSTVSSWAEMV
EPACNGDIVRYTSTLDGYDKDRILHTLPNDGANRQNLTVFLSYDEGRTWSVKKSIC
PTGSAYSSIAILEDGTIGVYAEENYNTDKYSTYFMNFSLDWLTNQADTYIEPGVEA
VAAPVFSVPAGYYTEAQTLIITATEGAQIYYTLDGSTPTANSTLYEDPITLSETVTV
NAIAMKEGMSNSVMTSAEYTFLEWEHPTGTIHDTESRYVTSATTTGAVEDLNYTLSS
KPSTVFIDTQSAFTVEAGQEFTLRVQCTEQMIWCHAVLFADWNRDFDFDEGEMITK
VGIDSIEDTDQTL SANGNTMMKDFSVNITVPAAKVAETRLRIQFSDAWHNKSAHE
HTAMDNIDKGGCYDFVMNIEPSSDLPSGIDDDRTAHTMVYPTLFTTEGVTLFATNG
EARRIFDLAGRLLSRVEVSEGENYIEGTTLPAGSLIMVVTTDEGTKSFRVVK

>uncharacterized protein BN693_00676 [*Prevotella* sp. CAG:5226]
GenBank:

CDA42204.1MKRNYFNGLLAALTLFGLGTSQAWADKIVTSTAENPKWFRIYTPNRSNLSLI
SKGVGVAMQNTKTFEKPYSASQLWRLEAGSTDGTYKIVNMSGEYIISPSSTVKPNNAAFAPV
KSGAGDWTITDLSDDTYTITSGSVQFNSTQDGNYYLYNWGSGTNKEDAGCKYRFEAVSLTE
LETAQAKALSVLNETEEGTNPGQYPAEVRTTFTNAIKAATTVDAITAAQTTYSAAMVQVAAG
KTYIIVSDKSVGYCQGYIYSAGSEAQPKWGNKVVSAAYGWTFDAGNGQFYVQNYGTKEYI
EPNSTDVNGATKTTATPATKYTVTSLGQGVFNIKPDGKNPLHAQNDGAVLVMWAGGIGSASA
WRLIEIPESDLTATPTFNSINVAPGFQTYAAGNKEQVLLTFQTEVAGFNGNVGKSLKLNLG
ATNVAGLENIKVFTSKNANFVSNQQRDAALIGQVATVSGNEVEVAFDNALEMPSTTRFYVT
ADITDKAVVGDSDAALVSFTYGDNKVFTVNNGNPEGIARVYKVQSVPFMPNDLGTAFWRIP
SMVVLHNQKGANASKNGRVVTMADNRFNHGGDLPSHIDVYERHSDNGKTWSAHKVVVGN
ETDEALVASKDGKHKFGDVTMVTASGKI IALMVGQGYFYSTNEDGNRIVPVIITSTDGGDT
WSQARALTDELYKGVYEQGVLSFAGSGRGICLQRQKDAKLNVRVMFAMSHRFATGAIQEY
IIYSDEGETWKMSPKSAYNGGDESKLVELADGTVMISVRQNGQRFNTSTDGGMTWGTQTT

NADINGNPCNADILYNNKVLHSHYINNGSRKNVTVKASFDNGKTWGHFPVICAPSSCYSTM
DITKGDIAIFYEDNACTQGYALNYAVFPIDWIVPGGDPSAKAFQEALAKAKAATTNEGYTD
EATAKAGQYSQEAIDNVKSLIATYEASVTDYEAATAALNAAVEAMGKTACTVDGYNETTFT
ISSLSTISSLEGAGYISADAKAKSEADNTAEWQIVPATVAGQVYIKLKDADSYIFRSGNTLA
ASAAPQAWKLVKNDGFYNLIAVHKAENSYLVINVGTGEFNWWTSAAGDNTWSTKFVLTAKTV
VTDINNATVANGSEKAVRYDDLQGRRVLNPTKGLFITNTGKKVIK

7.3 CBM/NTD Sequences of Sialidases Closely Related to SiaPG from ATCC 33277

> sialidase *Porphyromonas gingivalis*_ATCC33277 NCBI Reference

Sequence: WP_012458403.1

MANNTLLAKTRRYVCLVVFCLMAMMHLSGQEVMTWGDShGVAPNQVRRTLvkVAlSESLPPGAKQIR
IGFSLPKETEekVTALyLLVSDSLAVRDLPDYKGRVSYDSFPISKEDRTTALSADSVAGRCFFyLAAD
IGPVASFrsDtlTARVEELAVDGRPLPLKELSPASRRlyRE

> sialidase *Porphyromonas gingivalis*_A7A1-28 NCBI Reference

Sequence: WP_058019243.1

MANNTLLAKTRRSVCLVVFCLMAMMHLSGQEVMTWGDShGVAPNQVRRTLvkVAlSESLPPGAKQIR
IGFSLPKETEekVTALyLLVSDSLAVRDLPDYKGRVSYDSFPISKEDRTTALSADSVAGRCFFyLAAD
IGPVASFrsDtlTARVEELAVDGRPLPLKELSPASRRlyRE

> sialidase *Porphyromonas gingivalis*_W4087 NCBI Reference

Sequence: WP_043894535.1

MANNTLLAKTRRSVCLVVFCLMAMMHLSGQEVTVCGDShGVAPNQMYRTLvkVAlSESLPPGAKQIR
IGFSLPKETEekVTALyLLVSDSLAVRDLPDYKGRVSYDSFPISKEDRTTALSADSVAGRRFFyLAAD
IGPVASFrsDtlTARVEELAVDGRPLPLKELSPASRRlyRE

> sialidase, Putative *Porphyromonas gingivalis*_W83 Genbank:

AAQ65563.1

MANNTLLAKTRRYVCLVGFCWLMAMMHLSGQEVMTWGDShGVAPNQVRRTLvkVAlSESLPP
GAKQIRIGFSLPKETEekVTALyLLVSDSLAVRDLPDYKGRVSYDSFPISKEDRTTALSADS
VAGRRFFyLAADIGPVASFrsDtlTARVEEVAVDGRPLPLKELSPASRRlyRG

> "Hypothetical Protein" *Porphyromonas gingivalis*_F0570 NCBI

Reference Sequence: WP_021665936.1

MANNTLLAKTRRYVCLVGFCWLMAMMHLSGQEVMTWGDShGVAPNQVRRTLvkVAlSESLPP
GAKQIRIGFSLPKETEekVTALyLLVSDSLAVRDLPDYKGRVSYDSFPISKEDRTTALSADS
VAGRRFFyLAADIGPVASFrsDtlTARVEEVAVDGRPLPLKELSPASRRlyRG

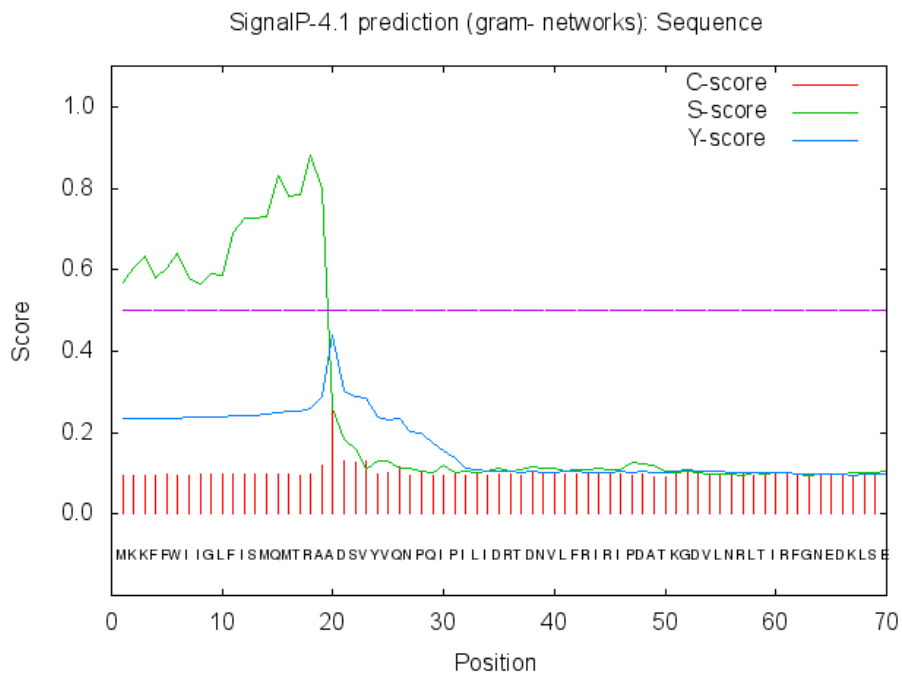
> "Hypothetical Protein" *Porphyromonas gingivalis*_AJW4 NCBI

Reference Sequence: WP_053444411.1

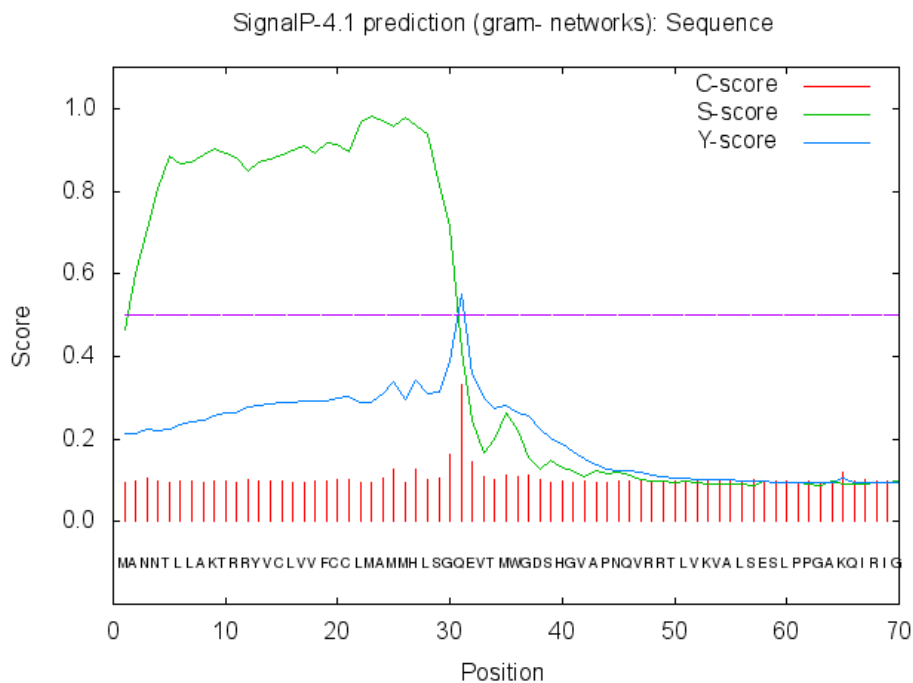
MANNTLLAKTRRYVCLVGFCWLMAMMHLSGQEVMTWGDShGVAPNQVRRTLvkVAlSESLPP
GAKQIRIGFSLPKETEekVTALyLLVSDSLAVRDLPDYKGRVSYDSFPISKEDRTTAFSADS
VAGRRFFyLAADIGPVASFrsDtlTARVEEVAVDGRPLPLKELSPASRHlyRG

7.4 Prediction of Secretion Sequences Using SignalP

NanH



SiaPG



Reference: Thomas Nordahl Petersen, Søren Brunak, Gunnar von Heijne & Henrik Nielsen

“SignalP 4.0: discriminating signal peptides from transmembrane regions”

Nature Methods, 8:785-786, 2011

7.5 Details of DNA and Protein Sequences Concerning *T. forsythia* NanH

Whole Gene-Stain 92A2 NCBI Accession number: NC_016610.1

ATGAAAAAGTTTTTTTGGATTATTGGTTTGTTCATCGATGCAGATGACACGCGCGGCGGA
CAGTGTTTACGTACAAAACCCACAGATCCCCATCCTCGTCGATCGGACGGACAATGTGCTGT
TCCGTATCCGTATTCCTGACGCGACGAAAGGCGATGTGCTGAACCGGCTGACCATAACGCTTC
GGTAACGAAGACAAGCTGTGCGGAGGTGAAAGCCGTTTCGTCTGTTTTATGCCGGTACGGAAGC
GGCCACAAAAGGCCGTTCCCGTTTTGCGCCGGTGACGTATGTCTCTTCGCACAATATTTCGTA
ACACGCGTTTCGGCAACCCGTCTATTCCATCCGGCAGGATGAAGTGACGACCGTTGCAAAT
ACATTGACGCTGAAAACACGTGACCCGATGGTCAAAGGCATCAACTATTTTTGGGTGAGTGT
GGAGATGGATCGTAACACTTCGCTACTGTGCAAGCTCACCTCGACGGTGACGGAAGTGGTTA
TCAACGATAAGCCGGCCGTTATTGCCGGCGAACAGGCCGCTGTGCGCCGTATGGGGATCGGG
GTGCGTCATGCGGGCGACGACGGATCAGCCTCTTCCGTATTCGCCGATTAGTGACAACGAA
CAAAGGAACATTGCTCGGGTCTATGATGTACGTTACAATAACAGTGTAGATTTACAGGAGC
ATATCGACGTGGGGCTGAGCCGACGACCGACAAAGGTCAGACATGGGAACCGATGCGCATT
GCCATGTCGTTTCGGTGAGACCGACGGATTACCGTCGGGGCAGAATGGAGTCGGCGATCCGTC
CATCTCGTCGATGAACGCACGAACACCGTCTGGGTTGTTGCCGCATGGACGCACGGGATGG
GCAATGCGCGCGCATGGACCAATTCATGCCCGGAATGACACCCGATGAAACAGCCCAACTG
ATGATGGTGAAAAGTACGGACGACGGCCGAACATGGAGCGAATCGACCAACATCACGTCTCA
GGTCAAAGATCCTTCGTGGTGCTTCCTGCTGCAAGTCCGGGAAGAGGAATCACAATGCGGG
ACGGCACGCTTGCTTCCCGATCCAGTTTATCGACTCCCTACGTGTCCCTCACGCGGGTATT
ATGTACAGCAAAGACCGTGGAGAGACGTGGCATATCCATCAGCCGGCGGTACCAACACGAC
GGAGGCGCAAGTGGCCGAGGTAGAGCCGGGCGTGCTCATGCTGAACATGCGTGACAATCGTG
GCGGCAGCCGTGCCGTCAGCATTACACGCGACTTGGGAAAAAGTTGGACGGAACACTCGTCG
AACCGCAGCGCTTGCCGGAATCGATCTGTATGGCGAGCCTGATCAGCGTCAAAGCGAAAGA
TAACATCATCGGGAAAGACCTGTTGCTCTTCTCGAATCCCAACACGACGGAAGGACGCCATC
ACATCACCATCAAGGCGAGCCTCGACGGAGGTGTTACGTGGCTTCCTGCACATCAGGTACTT
CTCGACGAAGAAGACGGATGGGGCTACTCGTGTCTGTGATGATCGACCGCGAAACGGTCGG
GATATTTTACGAATCGAGTGTGGCACACATGACCTTTCAGGCTGTTAAAATCAAAGACCTGA
TACGA

NanH Whole protein-92A2

MKFFGLSCKNTCRMKFFWI IGLFASMQMTRAADSVYVQNPQI PILVDRTDNVLFRI RIPDA
TKGDVLRNLTIRFGNEDKLSEVKAVRLFYAGTEAATKGRSRFAPVTYVSSHNIRNTRSANPS
YSIRQDEVTTVANLTLTKTRQPMVKGINYFWVSVMEDRNTSLLSKLTSTVTEVVINDKPAVI
AGEQAARRMGI GVRHAGDDGSASFRI PGLVTTNKGTL LGVYDVRYNNSVDLQEHIDVGLSR
STDKGQTWEPMRIAMSFGETDGLPSGQNGVGDPSILVDERTNTVWVVAAWTHGMGNARAWTN
SMPGMTPEDETAQLMMVKSTDDGRTWSESTNITSQVKDPSWCFLQGPGRGITMRDGLVFPFI
QFIDSLRVPHAGIMYSKDRGETWHIHQPARTNTTEAQVAEVEPGVLMMLNMRDNRGGSRVSI
TRDLGKSWTEHSSNRSALPESICMASLISVKAKDNIIGKDLLLLFSNPNTTEGRHHITIKASL
DGGVTWLP AHQVLLDEEDGWGYSCLSMIDRET VGI FYESSVAHMTFQAVKIKDLIR

Whole Gene-Strain ATCC43037 (not currently available in the NCBI database)

ATGAAAAAGTTTTTTTTGGATTATTGGTTTTATTTATATCGATGCAGATGACACGGGCGGGCGGA
CAGTGTTTACGTACAAAACCCACAGATCCCCATCCTCATCGATCGGACGGACAATGTGCTGT
TCCGTATCCGTATTCTGACGCGACGAAAGGCGATGTGCTGAACCGGCTGACCATACGCTTC
GGTAACGAAGACAAGTTGTTCGGAGGTGAAAGCCGTTTCGTCTGTTTTATGCCGGTACGGAAGC
GGCCACAAAAGGCCGTTCCCGTTTTGCACCGGTGACGTATGTCTCTTCGCACAATATCCGTA
ACACGCGTTTCGGCCAACCCGTCCTATTCCGTCCGGCAGGATGAAGTGACGACCGCTGCAAAT
ACATTGACGCTGAAAACACGTCAGCCGATGGTGAAAGGCATCAACTATTTTTGGGTGAGTGT
GGAGATGGATCGTAACACTTCGCTACTGTGCAAGCTCACCCCGACGGTGACGGAAGCGGTTA
TCAACGATAAGCCGGCCGTTATTGCCGGCGAACAGGCCGCTGTGCGCCGTATGGGGATCGGG
GTGCGTCATGCGGGCGACGACGGATCGGCCCTTTCCGTATTCCCGGATTAGTGACAACGAA
CGAAGGAACATTGCTCGGGTCTATGATGTACGTTACAATAACAGTGTAGATTTGCAGGAGC
ATGTCGACGTAGGGCTGAGCCGACGACCCGACAAAGGTCAGACATGGGAACCGATGCGCATT
GCCATGTGCTTCGGTGAGACCGACGGATTACCGTCGGGGCAGAATGGAGTCGGCGATCCGTC
CATCCTCGTCGATGAACGCACGAACACCGTCTGGGTTGTTGCCGCATGGACGCACGGGATGG
GCAATGCGCGCGCATGGACCAATTCATGCCCGGAATGACACCCGATGAAACAGCCCAACTG
ATGATGGTAAAAAGTACGGACGACGGCCGAACATGGAGCGAACCGATCAACATCACGTCGCA
GGTGAAAAATCCTTCGTGGTGCTTCCTGCTGCAAGGTCCGGGAAGAGGAATCACAATGCGGG
ACGGTACGCTTGTCTTCCCGATCCAGTTTATCGACTCCCTACGTGTCCCTCACGCGGGTATT
ATGTACAGCAAAGACCGTGGAGAGACGTGGCATATCCATCAGCCGGCGGTACCAACACGAC
GGAGGCGCAAGTGGCTGAGGTGGAGCCGGGCGTGCTCATGCTGAACATGCGTGACAATCGTG
GCGGCAGCCGTGCCGTCAGCATTACACGCGACTTGGGAAAAAGTTGGACGGAACACTCGTCG
AACCGCAGCGCCTTGCCGGAATCGATCTGTATGGCGAGCCTGATCAGCGTCAAAGCGAAAGA
CAACATCATCGGGAAAGACCTGTTGCTCTTCTCGAATCCCAACACGACGGAAGGACGTCATC
ACATCACCATCAAGGCGAGCCTCGACGGAGGTGTTACGTGGCTTCCTGCGCATCAGGTA
CTCGACGAAGAAGACGGATGGGGCTACTCGTGTCTGTGATGATCGACCGGAAACGGTTCGG
GATATTTTACGAATCGAGTGTGGCACACATGACCTTTCAGGCTGTTAAAAATCAAAGATCTGA
TACGA

Whole Protein

MKKFFWIIIGLFI SMQMTRAADSVYVQNPQIPIILIDRTDNVLFRI R I P D A T K G D V L N R L T I R F
GNEDKLSEVKAVRLFYAGTEAATKGRSRFAPVTYVSSHNI R N T R S A N P S Y S V R Q D E V T T A A N
TLTLKTRQPMVKGIN Y F W V S V E M D R N T S L L S K L T P T V T E A V I N D K P A V I A G E Q A A V R R M G I G
VRHAGDDGSASFRI PGLVTTNEGTL LGVYDVRYNNSVDLQEHVDVGLSRSTDKGQTWEPMRI
AMSFGETDGLPSGQNGVGDPSILVDERTNTVWVVAAWTHGMGNARAWTNSMPGMTPEDETAQL
MMVKSTDDGRWSEPINITSQVKNPSWCFL L Q G P G R G I T M R D G T L V F P I Q F I D S L R V P H A G I
MYSKDRGETWHIHQPARTNTTEAQVAEVEPGV L M L N M R D N R G G S R A V S I T R D L G K S W T E H S S
NRSALPESICMASLISVKAKDNIIGKDLLLFSNPNTTEGRHHITIKASLDGGVTWLP AHQVL
LDEEDGWGYSCLSMIDRET V G I F Y E S S V A H M T F Q A V K I K D L I R

NanH whole Gene Synthesis-Based on 92A2

Nucleotide, with NdeI and XhoI Restriction Sites Highlighted in yellow. ^v=cleavage site.

CACTATAGGGCGAATTGGCGGAAGGCCGTCAAGGCCGCATCA^vTATGGCCGATAGCGTTTATGTTTCAG
AATCCGCAGATTCCGATTCTGGTTGATCGTACCGATAATGTGCTGTTTCGTATTTCGTATTCCGGATGC
AACCAAAGGTGATGTTCTGAATCGTCTGACCATTTCGCTTTGGCAATGAAGATAAACTGAGCGAAGTTA
AAGCAGTGCCTCTGTTTTATGCAGGCACCGAAGCAGCCACCAAAGGTCTAGCCGTTTTGCACCGGTT
ACCTATGTTAGCAGCCATAACATTTCGTAATACCCGTAGCGCAAATCCGAGCTATAGCATTTCGTCAGGA
TGAAGTTACCACCGTTGCAAATACCCTGACCCTGAAAACCCGTCAGCCGATGGTTAAAGGTATTAACCT
ATTTTTGGGTGAGTACCCTGACCCTGAAAACCCGTCAGCCGATGGTTAAAGGTATTAACCTATTTTTGG
GTGAGTGTGATTAATGATAAAACCGGCAGTTATTGCCGGTGAACAGGCAGCAGTTTCGTCGTATGGGTAT
TGGTGTTCGTCATGCCGGTGTATGATGGTAGCGCAAGCTTTTCGCATTCCGGGTCTGGTTACCACCAATA
AAGGCACCCTGCTGGGTGTTTTATGATGTGCGTTATAACAATAGCGTGGATCTGCAAGAACATATTGAT
GTTGGTCTGAGCCGTAGCACCGATAAAGGCCAGACCTGGGAACCGATGCGTATTGCAATGAGCTTTGG
TGAAACCGATGGTCTGCCGAGCGGTCAAATGGTGTGGTGTATCCGAGCATTCTGGTGGATGAACGTAC
CAATACCGTTTTGGGTTGTTGCAGCATGGACCCATGGTATGGGTAATGCACGTGCCTGGACCAATAGCA
TGCCTGGTATGACACCGGATGAAACCGCACAGCTGATGATGGTTAAAAGCACCGATGATGGTCGTACC
TGGTCAGAAAGCACCAATATTACCAGCCAGGTTAAAGATCCGAGCTGGTGTTCCTGCTGCAGGGTCC
GGGTGCTGGTATTACCATGCGTGATGGCACCCCTGGTTTTTCCGATTCAGTTTATTGATAGCCTGCGTG
TTCCGCATGCAGGTATTATGTATAGCAAAGATCGCGGTGAAACCTGGCATATTCATCAGCCTGCACGT
ACAAATACCACCGAAGCCCAGGTTGCCGAAGTTGAACCGGGTGTCTGATGCTGAATATGCGTGATAA
TCGTGGTGGTAGCCGTGCAGTTAGCATTACCCGTGATCTGGGTAAAAGCTGGACCGAACATAGCAGCA
ATCGTAGCGCACTGCCGAAAGCATTGTATGGCAAGCCTGATTAGCGTTAAAAGCCAAAGATAACATC
ATCGGCAAAGATCTGCTGCTGTTTAGCAATCCGAATACCACAGAAGGTCGTCATCATATTACCATTAA
AGCAAGCCTGGATGGTGGTGTACCTGGCTGCCTGCACATCAGGTGCTGCTGGATGAAGAAGATGGTT
GGGTTATAGCTGTCTGAGCATGATTGATCGTGAAACCGTGGGTATCTTTTATGAAAGCAGCGTTGCA
CACATGACCTTTTCAGGCAGTTAAAATCAAAGACCTGATTCGC^vTCGAGCTGGGCCTCATGGGCCTTC
CGCTCACTGCCCCGCTTTCCAG

Protein expression of ORF, reported by Manufacturer

ADSVYVQNPQIPILVDRTDNVLFRIPI DATKGDVLRNLTIRFGNEDKLSEVKAVRLFYAGTEAATKG
RSRFAPVTYVSSHNI RNTRSANPSYSIRQDEVTTVANTLTLKTRQPMVKGIN YFWVSVEMDRNTSLLS
KLTSTVTEVVINDKPAVIAGEQAAVRRMIGVRHAGDDGSASFRI PGLVTTNKGTLLGVYDVRYNNSV
DLQEHIDVGLSRSTDKGQTWEPMRIAMSFGETDGLPSGQNGVGDPSILVDERTNTVWVAAWTHGMGN
ARAWTNSMPGMTPEDETAQLMMVKSTDDGRTWSESTNITSQVKDPSWCFLLQGPGRGITMRDGTLVFPI
QFIDSLRVPHAGIMYSKDRGETWHIHQPARTNTTEAQVAEVEPGVLMNMRDNRGGSRAVSI TRDLGK
SWTEHSSNRSALPESICMASLISVKAKDNIIGKDLLLFSNPNTTEGRHHITIKASLDGGVTWLP AHQV
LLDEEDGWGYSCLSMIDRETVGIFYESSVAHMTFQAVKIKDLIR

7.6 Details of DNA and Protein Sequences Concerning *P. gingivalis* SiaPG

Whole SiaPG gene-from *P. gingivalis* ATCC 33277

TCATTGCCGGGCATCGAAGAGATCGTCAAGGACGAACCGAATGAAAACCAATGAGATCTCAT
CGTCTTCTTCGACAAAATAACCGATCGTTCCATCCGCCAACAGAGTCATATCCGAGTAGGCA
CTCGATCCTGAATTGACAACAACGGGAGCGGACCAGCGGCCGGAGACATGATCGAAGAGATA
GACAGCCCCATCGCGACGCCATCCGGGCCGAGAGGCAGGGAGTGCAGCATTTGATTCCCTTC
CATTCCTTTTCACTTGAAGCATAGCTCCATTACAGCCGGGGTCATGGATGCCCTCGAACTGC
TTGGCTCTCTCCCAAGTAAGGCCATCGTCGGAGGAGAGAGCGAAGAAACGCTGTGGCTCTC
CTGCCCTTCCCTGATTGCGTACGCTCATCAGTACCCTGCCATCAGGCATCAATGAGAGCTTTG
CCTCGTCGCCACGGTGGTATGCACAGTCGGAAAGCTGCCATGTACCTCCCTCGTTCGTCGCTA
TAGAGGACATAGTTGTTTCAGGACGTA CTCTGCCCTGATTTCGCGGATGGCAGCCACAAACAT
GACACGACCGGATGGAAGCACAAAGCCCTTGTCCCGAAGCACAAAAGGAGGCCAACCAGCGAC
TGCCTCCCGGATCGGCACAATCCTTGGCCGAAGATGAAATGGGTTATATCCCGAGGAGGCGAC
CAGGTGAGGCCTTCGTCCCGACTTTCCGATATATAAGTGCGCTGAGGACGATCGGGGGTAGA
CTGCCACAAGCCTACTCCACCGACAAAGATCATCAGGAGCTTTCCTGCTTGAGTTTGCACCA
GGGCTACATCGCCAAAGCCATGATTGCGTCCCTCTCCCTGTACGATAATCCGGGGATCGCTC
CACGATTTCCCTCCGTCCGTACTGCGCCGCATGACTATATCTATATCCTCCGGCAGATCCGT
CTGATTATATTTTCGTCTGTTCGGCCATCGCTATGAGTGTTCCATTGGCCGTTTTCAAATGG
ACGGGATACGATAGTTGCGCGATCCGCCATCACCGGTACAAAGAGGGCCTCATACTCCCTA
TACAGACGACGGGAGGCAGGCGACAGCTCTTTC AACGGCAAAGGACGGCCATCGACAGCCAG
CTCTTCCACACGGGCAGTCAGCGTATCGGATCGGGAAAAAGAAGCGACAGGCCCTATATCCG
CAGCCAAATAAAAAGAAGCAGCGTCCGGTACCGAATCCGCAGAAAGGGCTGTGGTACGATCT
TCCTTTGAGATCGGGAAGCTATCGTAAGAGACTCGCCCTTTGTAGTCCGGCAAGTCGCGCAC
CGCTAAAGAATCACTCACAAGGAGATATAGGGCGGTGACTTTTTCCCTCCGTTTTCTTCGGAA
GAGAGAATCCGATACGAATCTGTTTTGCACCCGGAGGAAGGGATTCACTTAAGGCTACCTTC
ACCAGCGTTCGGCGCACTTGGTTCGGCGCCACTCCATGGCTGTCCCCCACATAGTGACTTC
CTGTCCAGAGAGGTGCATCATCGCCATGAGACAACAAAAACGACAAGGCAGACATAACGTC
GAGTCTTCGCCAAAAGAGTATTATTAGCCAT

Whole Protein

MANNTLLAKTRRYVCLVVFCCLMAMMHL SGQEVTMWGDSHG VAPNQVRRRTLKVALSESLPP
GAKQIRIGFSLPKETE EKVTALYLLVSDSLAVRDL PDYKGRVSYDSFPI SKEDRTTALSADS
VAGRCFFYLAADIGPVASF SRSDTLTARVEELAVDGRPLPLKELSPASRRLYREYEALFVPG
DGGSRNYRIPSILKTANGTLIAMADRRKYNQTDLPEDIDIVMRRSTDGGKSWSDPRIIVQGE
GRNHGFGDVALVQTQAGKLLMIFVGGVGLWQSTPDRPQRTYISESRDEGLTWSPPRDITHF I
FGKDCADPGRSRWLASF CASGQGLVLP SGRVMFVAAIRESGQEYVLNNYVLYSDDEGGTWQL
SDCAYHRGDEAKLSLMPDGRVLM SVRNQGRQESRQRFFALSSDDGLTWERAKQFEGIHDPGC
NGAMLQVKRNGRNQMLHSLPLGPDGRRDGAVYLF DHVSGRWSAPVVVNSGSSAYS DM TLLAD
GTIGYFVEEDDEISLVFIRFVLDLDFARQ

SiaPG- whole Gene Synthesis-Based on 92A2

Nucleotide, with NdeI and XhoI Restriction Sites Highlighted in yellow. ^v=cleavage site.

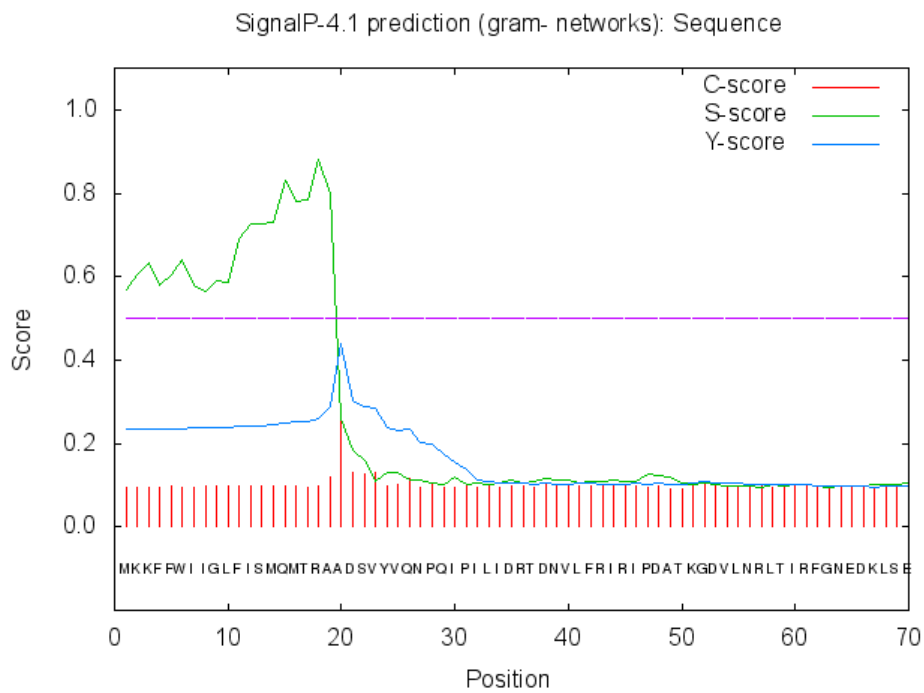
CACTATAGGGCGAATTGGCGGAAGGCCGTCAAGGCCGCATCA^vTATGGAAGTTACCATGTGGGGTGAT
AGCCATGGTGTTCACCGAATCAGGTTTCGTTCGTACCCTGGTTAAAGTTGCACTGAGCGAAAGCCTGCC
TCCGGGTGCAAAACAAATTCGTATTGGTTTTAGCCTGCCGAAAGAAACCGAAGAAAAAGTTACCGCAC
TGTATCTGCTGGTTAGCGATAGCCTGGCAGTTCGTGATCTGCCGATTATAAAGTCGTGTTAGCTAT
GATAGCTTCCCCGATTAGCAAAGAAGATCGTACCACCGCACTGAGTGCAGATAGCGTTGCAGGTCGTCG
TTTTTTCTATCTGGCAGCAGATATTGGTCCGGTTGCAAGCTTTAGCCGTAGCGATACCCTGACCGCAC
GTGTTGAAGAGGTTGCAGTTGATGGTTCGTCCGCTGCCGCTGAAAGAACTGAGTCCGGCAAGCCGTCGT
CTGTATCGTGGTTATGAAGCACTGTTTGTTCGGGTGATGGTGGTAGCCGTAATTATCGTATTCCGGC
AATTCTGAAACCGCAAATGGCACCCCTGATTGCAATGGCAGATCGTCGCAAATATAACCAGACCGATC
TGCCTGAAGATATTGATATTGTTATGCGTCGTAGCACCGATGGTGGCAAAAGCTGGTCAGATCCGCGT
ATTATTGTTTCAAGGTGAAGGTCGTAATCATGGTTTTGGTGTGTTGCACTGGTTCAGACCCAGGCAGG
TAAACTGCTGATGATTTTTGTTGGTGGTGTGGTCTGTGGCAGAGCACACCGGATCGTCCGCAGCGTA
CCTATATTAGCGAAAGTCGTGATGAAGGCCTGACCTGGTCAACCGCCTCGTGACATTACCCATTTTTATC
TTTGGTAAAGATTGTGCAGATCCGGGTCGTAGCCGTTGGCTGGCAAGCTTTTGTGCAAGTGGTCAGGG
TCTGGTTCTGCCGAGCGGTCGTATTACCTTTGTTGTCAGCAATTCGTGAAAGCGGTCAAGAATATGTGC
TGAATAACTATGTTCTGTATAGCGACGATGAAGGTGATACCTGGCAGCTGAGCGATTGTGCATATCGT
CGCGGTGATGAAGCAAACTGAGCCTGATGCCGGATGGTTCGTGTTCTGATGAGCATTGTAATCAGGG
TCGTCAAGAAAGCCGTCAGCGTTTTTTTTGCCCTGAGCAGTGATGATGGTCTGACATGGGAACGTGCCA
AACAGTTTGAAGGTATTCATGATCCGGGTTGTAATGGTGCATGCTGCAGGTTAAACGTAATGGTTCGT
GATCAGGTTCTGCATAGTCTGCCGCTGGGTCCGGATGGCCGTCGTGATGGTGGCGTTTACCTGTTTGA
TCATGTTAGCGGTCGTTGGAGCGCACCGGTTGTTGTTAATAGCGGTAGCAGCGCATATAGCGATATGA
CCCTGCTGGCAGATGGCACCATTTGGTTATTTTTGTTGAAGAAGGTGACGAAATCAGCCTGGTGTATT
CGTTTTGTTCTGGATGACCTGTTTCGATGTTTCGTGAGC^vTCGAGCTGGGCCTCATGGGCCTTCCGCTCA
CTGCCCCGCTTTCCAG

Protein expression of ORF, reported by Manufacturer

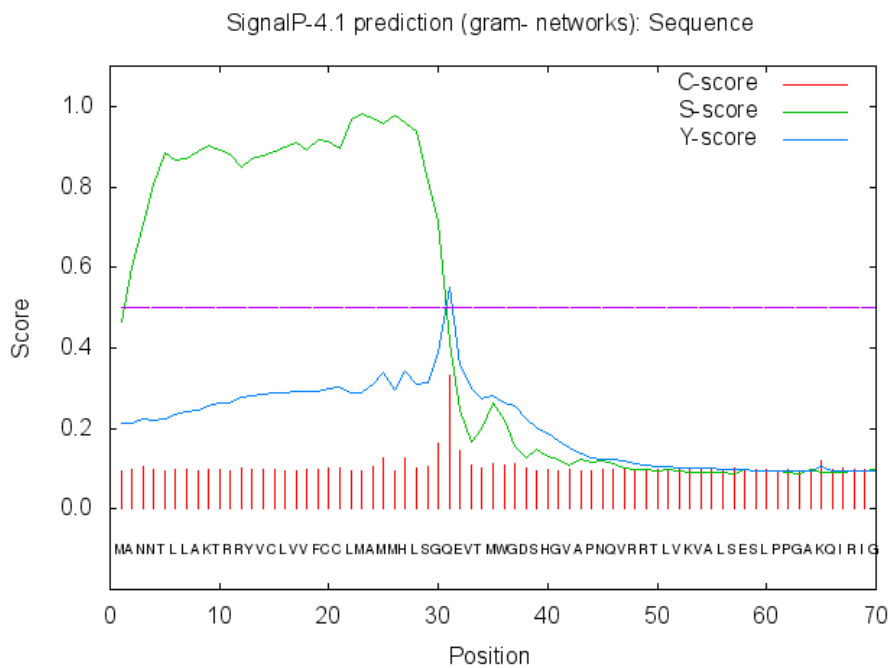
ADSVYVQNPQIPILVDRTDNVLFRIIPDATKGDVLNRLTIRFGNEDKLSEVKAVRLFYAGTEAATKG
RSRFAPVTVYVSSHNI RNTRSANPSYSIRQDEVTTVANTLTLKTRQPMVKGINYFWVSVEMDRNTSLLS
KLTSTVTEVVINDKPAVIAGEQAARRMGI GVRHAGDDGSASFRI PGLVTTNKGTLLGVYDVRYNNSV
DLQEHIDVGLSRSTDKGQWEPMRIAMS FGETDGLPSGQNGVGDPSILVDERTNTVWVVAAWTHGMGN
ARAWTNSMPGMT PDETAQLMMVKSTDDGRTWSESTNITSQVKDPSWCFLQGPGRGITMRDGTLVFPI
QFIDSLRVPHAGIMYSKDRGETWHIHQPARTNTTEAQVAEVEPGVLMMLNMRDNRGGSRAVSI TRDLGK
SWTEHSSNRSALPESICMASLISVKAKDNIIGKDLLLFSNPNTTEGRHHITIKASLDGGVTWLP AHQV
LLDEEDGWGYSCLSMIDRETVGIFYESSVAHMTFQAVKIKDLIR

7.7 SignalP Predictions of secretion sequence

NanH



SiaPG



Reference: Thomas Nordahl Petersen, Søren Brunak, Gunnar von Heijne & Henrik Nielsen
“SignalP 4.0: discriminating signal peptides from transmembrane regions” *Nature Methods*,
8:785-786, 2011

7.8 An Alignment of NanH from *T. forsythia* strains 43037 and 92.A2, Performed using ESPrpt

```

                                1      10      20      30
NanH-T. forsythia_43037  .....MKKFFWIIIGLFIISMQMTRAADSVYVQNPQIPILIDRT
NanH-T. forsythia_92.A2 MKKFFGLSCKNCTCRMKKFFWIIIGLFIASMQMTRAADSVYVQNPQIPILVDRT

                                40      50      60      70      80
NanH-T. forsythia_43037  DNVLFRIRIPDATKGDVLRNLTIRFGNEDKLSEVKAVRLFYAGTEAATKG
NanH-T. forsythia_92.A2  DNVLFRIRIPDATKGDVLRNLTIRFGNEDKLSEVKAVRLFYAGTEAATKG

                                90      100     110     120     130
NanH-T. forsythia_43037  RSRFAPVTYVSSHNI RNTRSANPSYSVRQDEVTTAANTLTLKTRQPMVKG
NanH-T. forsythia_92.A2  RSRFAPVTYVSSHNI RNTRSANPSYSIRQDEVTTVANTLTLKTRQPMVKG

                                140     150     160     170     180
NanH-T. forsythia_43037  INYFWVSVEMDRNTSLLSKLTPTVTEAVINDKPAVIAGEQAAVRRMGIGV
NanH-T. forsythia_92.A2  INYFWVSVEMDRNTSLLSKLSTVTEVVINDKPAVIAGEQAAVRRMGIGV

                                190     200     210     220     230
NanH-T. forsythia_43037  RHAGDDGSASFRIPLVLTNEGTLLGVYDVRYNNSVDLQEHVDVGLSRST
NanH-T. forsythia_92.A2  RHAGDDGSASFRIPLVLTNKGTLLGVYDVRYNNSVDLQEHVDVGLSRST

                                240     250     260     270     280
NanH-T. forsythia_43037  DKGQTWEPMRIAMSFGETDGLPSGQNGVGDPSILVDERTNTVWVVAAWTH
NanH-T. forsythia_92.A2  DKGQTWEPMRIAMSFGETDGLPSGQNGVGDPSILVDERTNTVWVVAAWTH

                                290     300     310     320     330
NanH-T. forsythia_43037  GMGNARAWTNSMPGMPDETAQLMMVKSTDDGRTWSEPIINITSQVKNPSW
NanH-T. forsythia_92.A2  GMGNARAWTNSMPGMPDETAQLMMVKSTDDGRTWSESTINITSQVKDPSW

                                340     350     360     370     380
NanH-T. forsythia_43037  CFLLQGPGRGITMRDGLVFPFIQFIDSLRVPHAGIMYSKDRGETWHIHQP
NanH-T. forsythia_92.A2  CFLLQGPGRGITMRDGLVFPFIQFIDSLRVPHAGIMYSKDRGETWHIHQP

                                390     400     410     420     430
NanH-T. forsythia_43037  ARTNTTEAQVAEVEPGLMLNMRDNRGGSRAVSITRDLGKSWTEHSSNRS
NanH-T. forsythia_92.A2  ARTNTTEAQVAEVEPGLMLNMRDNRGGSRAVSITRDLGKSWTEHSSNRS

                                440     450     460     470     480
NanH-T. forsythia_43037  ALPESICMASLISVKAKDNIIGKDLLLFSNPNTTEGRHHITIKASLDGGV
NanH-T. forsythia_92.A2  ALPESICMASLISVKAKDNIIGKDLLLFSNPNTTEGRHHITIKASLDGGV

                                490     500     510     520     530
NanH-T. forsythia_43037  TWLPAHQVLLDEEDGWGYSCLSMIDRETVGIFYESSVAHMTFQAVKIKDL
NanH-T. forsythia_92.A2  TWLPAHQVLLDEEDGWGYSCLSMIDRETVGIFYESSVAHMTFQAVKIKDL

NanH-T. forsythia_43037  IR
NanH-T. forsythia_92.A2  IR

```

97.96% homology (Clustal Omega).

7.9 Partial List of EU Requirements to be Submitted before Licensing of a Product under the “Medicine” Classification

- (a) Name or corporate name and permanent address of the applicant and, where applicable, of the manufacturer.
- (b) Name of the medicinal product.
- (c) Qualitative and quantitative particulars of all the constituents of the medicinal product, including the reference to its international non-proprietary name (INN) recommended by the WHO, where an INN for the medicinal product exists, or a reference to the relevant chemical name.
- (ca) Evaluation of the potential environmental risks posed by the medicinal product. This impact shall be assessed and, on a case-by-case basis, specific arrangements to limit it shall be envisaged.
- (d) Description of the manufacturing method.
- (e) Therapeutic indications, contra-indications and adverse reactions.
- (f) Posology, pharmaceutical form, method and route of administration and expected shelf life.
- (g) Reasons for any precautionary and safety measures to be taken for the storage of the medicinal product, its administration to patients and for the disposal of waste products, together with an indication of potential risks presented by the medicinal product for the environment.
- (h) Description of the control methods employed by the manufacturer.
- (i) Results of:
 - pharmaceutical (physico-chemical, biological or microbiological) tests,
 - pre-clinical (toxicological and pharmacological) tests,
 - clinical trials.
- (ia) A detailed description of the pharmacovigilance and, where appropriate, of the risk-management system which the applicant will introduce.
- (ib) A statement to the effect that clinical trials carried out outside the European Union meets the ethical requirements of Directive 2001/20/EC.
- (j) A summary, in accordance with Article 11, of the product characteristics, a mock-up of the outer packaging, containing the details provided for in Article 54, and of the immediate packaging of the medicinal product, containing the details provided for in Article 55, together with a package leaflet in accordance with Article 59.
- (k) A document showing that the manufacturer is authorised in his own country to produce medicinal products.

7.10 Publications Arising due to Work Performed As Part of This Project

Characterization of a sialate-*O*-acetyltransferase (NanS) from the oral pathogen *Tannerella forsythia* that enhances sialic acid release by NanH, its cognate sialidase

Chatchawal Phansopa*, Radoslaw P. Kozak†, Li Phing Liew†, Andrew M. Frey*, Thomas Farmilo*, Jennifer L. Parker*, David J. Kelly‡, Robert J. Emery†, Rebecca I. Thomson§, Louise Royle†, Richard A. Gardner†, Daniel I.R. Spencer† and Graham P. Stafford*^{1, 2}

*Integrated BioSciences, School of Clinical Dentistry, University of Sheffield, Sheffield, S10 2TA, U.K.

†Ludger Ltd, Culham Science Centre, Oxfordshire OX14 3EB, U.K.

‡Department of Molecular Biology and Biotechnology, University of Sheffield, Sheffield S10 2TN, U.K.

§Reading School of Pharmacy, University of Reading, Whiteknights, Reading RG6 6AP, U.K.

Tannerella forsythia, a Gram-negative member of the Bacteroidetes has evolved to harvest and utilize sialic acid. The most common sialic acid in humans is a mono-*N*-acetylated version termed Neu5Ac (5-*N*-acetyl-neuraminic acid). Many bacteria are known to access sialic acid using sialidase enzymes. However, in humans a high proportion of sialic acid contains a second acetyl group attached via an *O*-group, i.e. chiefly *O*-acetylated Neu5,9Ac₂ or Neu5,4Ac₂. This diacetylated sialic acid is not cleaved efficiently by many sialidases and in order to access diacetylated sialic acid, some organisms produce sialate-*O*-acetyltransferases that catalyse the removal of the second acetyl group. In the present study, we performed bioinformatic and biochemical characterization of a putative sialate-*O*-acetyltransferase from *T. forsythia* (NanS), which contains two putative SGNH-hydrolase domains related to sialate-*O*-acetyltransferases from a range of organisms. Purification of recombinant NanS revealed an esterase that has activity against

Neu5,9Ac₂ and its glycolyl form Neu5Gc,9Ac. Importantly, the enzyme did not remove acetyl groups positioned at the 4-*O* position (Neu5,4Ac₂). In addition NanS can act upon complex *N*-glycans released from a glycoprotein [erythropoietin (EPO)], bovine submaxillary mucin and oral epithelial cell-bound glycans. When incubated with its cognate sialidase, NanS increased sialic acid release from mucin and oral epithelial cell surfaces, implying that this esterase improves sialic acid harvesting for this pathogen and potentially other members of the oral microbiome. In summary, we have characterized a novel sialate-*O*-acetyltransferase that contributes to the sialobiology of this important human pathogen and has potential applications in the analysis of sialic acid diacetylation of biologics in the pharmaceutical industry.

Key words: acetyltransferase, Bacteroidetes, carbohydrate-active enzyme, glycans, oral cavity, sialic acid.

INTRODUCTION

The oral-dwelling pathogen *Tannerella forsythia* is a member of a small group of bacteria that is associated with the prevalent oral disease of periodontitis [1]. It is a member of a wider family of Gram-negative anaerobic human-colonizing bacteria of the phylum Bacteroidetes. The Bacteroidetes, with *Tannerella* being no exception, are well adapted to life in the human body with a wide array of metabolic adaptations to their gut and oral environments respectively [2,3]. In particular, our recent work and that of others on the physiology of *Tannerella* revealed that it has an extensive array of glycan-harvesting capabilities encoded in its genome [3] with its ability to harvest and utilize sialic acid from glycoproteins present on human epithelial surfaces and secretory fluids most relevant, alongside potential dietary sources. This ability to utilize sialic acid is possibly the most pertinent *in vivo* and certainly the most well-studied growth substrate for this enigmatic organism [4].

This ability to harvest and utilize sialic acid is encoded by a genetic locus in *Tannerella* that contains not only putative sialic

acid catabolic genes (*nanA*, *E*), but also a unique sialic acid-uptake system that is dependent on the periplasm-spanning TonB protein and can thus be considered a sialic acid-specific polysaccharide utilization system (PUL) [5,6]. However, the substrate for this transport system, unlike many other Bacteroidetes, is the monomeric form of the sugar, rather than an oligosaccharide that is then acted upon by periplasmic sialidases and other enzymes before catabolism commences [7].

The sialic acid specific PUL of *Tannerella* secretes a sialidase enzyme of the glycosyl hydrolase 33 (GH33) family [8] with the ability to cleave sialic acids from fetuin and less efficiently from human and bovine mucin sources [9]. One possible reason for this lower efficiency of cleavage from mucins has been hypothesized to be the high level of diacetylation of sialic acid present that inhibits functional access of sialidases and slows cleavage rates for many sialidases [10,11]. This high level of diacetylation is widespread in humans [12] and would represent a wasted nutritional source for oral bacteria such as *T. forsythia*. The diacetylated sialic acids are also important in viral infections with several viruses using the main form of

Abbreviations: 2-AB, 2-aminobenzamide; CCA, *Cancer antennarius agglutinin*; CHO, Chinese hamster ovary; DMB, 1,2-diamino-4,5-methylenedioxybenzene · 2HCl; EPO, erythropoietin; HILIC, hydrophilic interaction liquid chromatography; MFI, mean fluorescence intensity; PNGase F, peptide *N*-glycosidase F; pNP, *p*-nitrophenol; pNP-Ac, *p*-nitrophenyl acetate; PUL, polysaccharide utilization system; rH-EPO, recombinant human EPO; SNA, *Sambucus nigra agglutinin*; SRP, sialic acid reference panel; TBA, thiobarbituric acid.

¹ Ludger and Graham Stafford have a licensing agreement centred on the use of NanS commercially.

² To whom correspondence should be addressed (email g.stafford@sheffield.ac.uk).

diacetylated sialic acid, Neu5,9Ac₂, as a receptor, e.g. influenza C and several coronaviruses [13,14]. In addition both viruses and humans possess sialate-*O*-acetyltransferase enzymes which in the case of the viruses act as receptor-destroying enzymes involved in the infection cycle and in the case of humans are used for the modulation of diacetylation of sialic acids on both internal and external proteins with biological roles in development and autoimmunity among others [15,16], including certain leukaemias and cancers [17,18]. These enzymes are members of a large family of SGNH-serine esterases whose activity acts to remove *O*-acetyl groups from sialic acids, generally having specificity for acetyl groups at the 9- or 4-positions. In addition, evidence suggests that bacteria are also capable of producing sialate-*O*-acetyltransferases that may be involved in survival in mucin-rich environments [12] and the sialic acid catabolism operon of *Tannerella* appears to contain such an enzyme [19]. However, information on this class of enzymes lags behind that of the sialidases and other classes of carbohydrate-active enzymes.

In addition, this class of enzymes has potential value in the study and design of recombinant biopharmaceuticals. An example of this is the biological drug human erythropoietin (EPO) which is highly glycosylated with most glycans terminating in sialic acid residues which can contain two or more extra *O*-acetyl groups [20] which could consequently have an impact on the efficacy of the drug. As the specific structures of the glycans on a biopharmaceutical can be critical to the efficacy of the drug, it is essential to ensure that glycosylation is optimized and consistent from batch to batch. Thus, the availability of enzymes specific for additional *O*-acetylation on sialic acids could aid both the identification and the quality control of glycosylation on such drugs.

In the present study, we set out to characterize the putative sialate-*O*-acetyltransferase (NanS) from the oral pathogen *T. forsythia* and investigate its activity and ability to act on experimental and physiologically relevant diacetylated sialic acid substrates. The data presented show that NanS from *T. forsythia* is a novel, highly active, neutral sialate-*O*-acetyltransferase that acts to remove 9-*O*-acetyl groups (and potentially those at 7-*O* and 8-*O* positions but not 4-*O*-acetylated sialic acid) from diacetylated sialic acids in mucinous and epithelial cell glycoproteins and on released highly branched *N*-glycans from EPO. We also provide evidence that it can work in concert with its cognate sialidase in the release of sialic acid from mucin and oral epithelial cell surfaces, suggesting that *in vivo* it might act to increase sialic acid release by sialidases for *T. forsythia* and other bacteria in its environmental niche.

MATERIALS AND METHODS

Bacterial cell culture

Escherichia coli BL21 (DE3) strains were cultured in LB broth at 37°C or on solid LB medium containing 1.5% bacteriological agar (Oxoid). Selective antibiotics were added to appropriate concentrations (i.e. 50 µg/ml ampicillin).

Cloning of nanS for expression

The predicted mature *TF0037* (*nanS*) ORF (i.e. lacking the putative secretion sequence of *TF0037*) from *T. forsythia* genomic DNA was PCR-amplified using primers (NanS-GST-Bam-For 5'-AAAGGATCCCAGAAGACTGTGAAAGTGGC-3' and NanS-GST-Eco-Rev 5'-AAAGAATTCTTATTCATCA-CAGCCTGAAACG-3') using Phusion Polymerase according

to the manufacturer's instructions. The gene was cloned into pGEX-4T-3 using BamHI and EcoRI to produce pGEX-NanS and its sequence was verified by DNA sequencing (Core Genomic Facility, University of Sheffield); N.B. this revealed four differences from the published genome sequence, but none in active-site regions which is now known to be from strain *T. forsythia* 92A.2 (ATCC-BAA-2717; see Supplementary Figure S1 for alignment) [21].

Production of recombinant NanS

E. coli BL21 (DE3) Origami B was transformed with the pGEX-NanS plasmid, grown in LB broth and induced at mid-exponential growth phase ($D_{600} = 0.6$) with 1 mM IPTG (Sigma-Aldrich) for 5 h at 37°C with agitation. Cells were harvested, resuspended in purification buffer (50 mM Tris/HCl, pH 8.0, 150 mM NaCl and 2.5 mM CaCl₂), disrupted using a French pressure cell (three times at 7245 kPa; Thermo Scientific) and soluble fractions were clarified by further centrifugation (40000 g, 30 min, 4°C). The N-terminally GST-tagged protein was purified by applying the cell-free extract on a 1-ml GSTrap column (GE Healthcare) at 1 ml/min, following which unbound proteins were removed by washing with 20 column volumes of purification buffer. The GST-tag of bound NanS was proteolytically removed by incubating the column in 1 unit/µl thrombin (Sigma-Aldrich) in the purification buffer, sealed and left to stand at room temperature for 5 h. Cleaved NanS was eluted with two bed volumes of purification buffer, then mixed gently with 50 µl of *p*-aminobenzamidine-agarose (Sigma-Aldrich) that had been pre-equilibrated in the same buffer to remove thrombin. The purified protein was extensively dialysed against a dialysis buffer (50 mM sodium phosphate, pH 7.4, and 150 mM NaCl) and concentration determined using the Pierce BCA protein assay kit (Thermo Scientific).

Reaction kinetics and pH optimum of purified NanS

The pH optimum of NanS was determined using the chromogenic substrate *p*-nitrophenyl acetate (pNP-Ac; Sigma-Aldrich) by incubating 2.5 nM purified NanS with 0.1 mM pNP-Ac in 20 mM sodium citrate (pH 3.0–6.0), 20 mM sodium phosphate (pH 6.4–8.8) or 20 mM sodium carbonate (pH 9.2) buffers and the presence of free *p*-nitrophenol (pNP) measured and expressed as the mean change in absorbance per min, ± S.D. pNP-Ac hydrolysis was monitored every 15 s by removal of an aliquot of enzyme reaction, followed by heat inactivation (98°C, 90 s), after which, an equal volume of quenching buffer (2 M sodium carbonate, pH 10.5) was added and the release of free pNP recorded by measuring its absorbance (A_{405}) in a spectrophotometer (Tecan M200).

For K_m determination, purified NanS was pre-incubated at 25°C for 15 min in 50 mM sodium/potassium phosphate buffer, pH 7.4, and 150 mM NaCl, at a final concentration of 2.5 nM. pNP-Ac was then added at a range of final concentrations (2.5–1000 µM) and pNP-Ac hydrolysis was monitored as above. Time course data from each concentration of the pNP-Ac substrate were examined for linearity by plotting the data, followed by the calculation of the slope of the tangent. Known concentrations of pNP in the same buffer mixed with an equal volume of quenching buffer was measured as above to obtain a standard curve. Kinetic parameters K_m and V_{max} were calculated by fitting data from three biological replicates in Prism 6 (GraphPad Software) to eqn (1):

$$V_0 = V_{max} \cdot Z / (K_m + Z) \quad (1)$$

in which V_0 is the steady-state rate of pNP-Ac substrate turnover by NanS, V_{\max} is the maximum rate ($\mu\text{mol}/\text{min}$ per mg of NanS protein) Z is the concentration of pNP-Ac (μM) in the reaction mixture and K_m is the Michaelis–Menten constant (μM) at which the reaction rate is half of V_{\max} . We also used the equation $V_{\max}/[E]$ to determine k_{cat} .

Quantification of sialic acid release from mucin

A modified version of the thiobarbituric acid (TBA) assay [20,23] was used to assess hydrolysis of sialic acid from mucin. Mucin at $3 \mu\text{M}$ was incubated with $0.1 \mu\text{M}$ NanH, NanS or NanH + NanS in PBS, pH 7.4 (Sigma–Aldrich), for 30 min at 37°C , in a total reaction volume of $50 \mu\text{l}$ before addition of $25 \mu\text{l}$ of 25 mM sodium periodate (Sigma–Aldrich) in 500 mM H_2SO_4 . This was incubated for 30 min at 37°C before oxidation of free sialic acid was halted by addition of 2% (w/v) sodium arsenite (Sigma–Aldrich) in 500 mM HCl. Formation of the red chromophore was completed by the addition of $200 \mu\text{l}$ of 100 mM TBA (Sigma–Aldrich), pH 9, and incubated for 7.5 min at 95°C . The chromophore was extracted by addition of $500 \mu\text{l}$ of acidified butanol [butan-1-ol with 5% (v/v) 600 mM HCl], before vortex-mixing and centrifugation at 10000 g for 3 min. A $100 \mu\text{l}$ sample of the butanol phase was then added to a clear 96-well plate (Greiner) and the absorbance at 549 nm was measured using a Tecan infinite M200 plate reader. Free sialic acid (Carbosynth) was used to generate a standard curve.

Lectin staining of oral epithelial cells

The oral squamous carcinoma cell line H357 was cultured in 175 cm^2 tissue culture flasks (Greiner), in Dulbecco's modified Eagle's medium (DMEM, Sigma–Aldrich) supplemented with 10% (v/v) FBS (Sigma–Aldrich) and 2 mM L-glutamine (Sigma–Aldrich), $100 \text{ units}/\text{ml}$ penicillin and $100 \mu\text{g}/\text{ml}$ streptomycin (Sigma–Aldrich). Cells were seeded at $100000 \text{ cells}/\text{ml}$ into 24-well tissue culture plates (Greiner) containing glass coverslips (VWR), with 1 ml of cell suspension/well and incubated at 37°C in 5% CO_2 for 14–24 h. To stain for cellular Neu5,9Ac₂, cells were incubated with either PBS or 50 nM NanS in PBS for 2 h at 37°C , washed twice with $500 \mu\text{l}$ of PBS and fixed using 2% paraformaldehyde for 15 min at 37°C . Fixed cells were washed twice with $500 \mu\text{l}$ of PBS, incubated with $2 \mu\text{g}/\text{ml}$ biotinylated *Cancer antennarius* agglutinin (CCA) or *Sambucus nigra* agglutinin (SNA) lectin (EY Laboratories) for 30 min at 37°C , washed twice with $500 \mu\text{l}$ of PBS, then stained with $2 \mu\text{g}/\text{ml}$ streptavidin–FITC (Vector Laboratories) for 30 min at 37°C . To stain for cellular $\alpha 2,6$ -linked Neu5Ac (5-N-acetylneuraminic acid), cells were incubated with PBS, 50 nM NanS, 50 nM NanH or 50 nM NanH and 50 mM NanS, all in PBS, for 30 min at 37°C , washed twice with $500 \mu\text{l}$ of PBS and fixed using 2% paraformaldehyde for 15 min at 37°C . Coverslips with stained cells were mounted on glass slides using Prolong Gold Antifade mountant with DAPI (Life Technologies). Cells were visualized using an Axiovert 200M fluorescence microscope (Zeiss) and Axiovision software. Fiji/ImageJ software (NIH) was used to process images with three fields of view from two biological replicates assessed [24]. Neu5,9Ac₂ staining was expressed as: mean pixel brightness (FITC staining only)/number of cells = mean fluorescence intensity (MFI) per cell. FITC image acquisition was carried out using the same exposure time and percentage weight for each condition and parameters during image analysis were kept constant between conditions.

Treatment of diacetylated sialic acids with NanS

A Neu5,9Ac₂ (Ludger Ltd), Neu5,4Ac₂ (Carbosynth) and sialic acid reference panel (SRP; derived from bovine submaxillary mucin, Ludger Ltd) were incubated with $1 \mu\text{l}$ of NanS enzyme ($0.7 \text{ mg}/\text{ml}$) in a final volume of $10 \mu\text{l}$ ($1 \times$ PBS, pH 7.2) for 16 h at 25°C . Sialic acid standards ($1 \mu\text{g}$ of each sialic acid) were labelled with 1,2-diamino-4,5-methylenedioxybenzene $\cdot 2\text{HCl}$ (DMB) using a Ludger DMB sialic acid release and labelling kit according to the product guide. Briefly, dried standards were incubated with $20 \mu\text{l}$ of labelling reagent in the dark for 3 h at 50°C . The reaction was terminated upon the addition of $480 \mu\text{l}$ of water. The DMB-labelled samples were analysed by reverse-phase HPLC using a LudgerSep-R1 column ($4.6 \text{ mm} \times 150 \text{ mm}$, Ludger Ltd) at 30°C on a Waters 2795 HPLC with a 2475 fluorescence detector ($\lambda_{\text{ex}} = 373 \text{ nm}$, $\lambda_{\text{em}} = 448 \text{ nm}$), controlled by Empower software (Waters). Isocratic run conditions were at a flow rate of $0.5 \text{ ml}/\text{min}$ with solvent acetonitrile/methanol/water (9:7:84 by volume). Then $10 \mu\text{l}$ of sample was injected undiluted on to the HPLC. The SRP standard was used as a system suitability standard as well as an external calibration standard to allocate sialic acid structures.

Treatment of N-glycans from rH-EPO with NanS

N-glycans were released from $10 \mu\text{g}$ of recombinant human EPO (rH-EPO) expressed from Chinese hamster ovary (CHO) cells (a gift from Antonio Vallin, Center for Molecular Immunology, La Habana, Cuba) using peptide *N*-glycosidase F (PNGase F) (E-PNG01; Ludger Ltd). The EPO (in $17.5 \mu\text{l}$) was denatured following addition of $6.25 \mu\text{l}$ of 2% SDS and 1 M 2-mercaptoethanol by heating at 100°C for 5 min, before incubation at 37°C for 16 h with $1 \mu\text{l}$ of PNGase F and $1.25 \mu\text{l}$ of 15% (w/v) Triton X-100. Released *N*-glycans were fluorescently labelled with 2-aminobenzamide (2-AB) according to Bigge et al. [25] using a Ludger 2-AB Glycan Labelling Kit. The released glycans were incubated with labelling reagents for 3 h at 65°C . The 2-AB-labelled glycans were cleaned up using LudgerClean S Cartridges (Ludger Ltd). NanS enzyme digestions were performed according to Royle et al. [26]. The 2-AB-labelled *N*-glycans were incubated with $1 \mu\text{l}$ of NanS enzyme ($0.7 \text{ mg}/\text{ml}$) in a final volume of $10 \mu\text{l}$ (50 mM sodium acetate buffer, pH 5.5) for 16 h at 37°C . NanS was removed by binding to a protein-binding plate LC-PBM-96 (Ludger Ltd.) before analysis by HILIC–UPLC. 2-AB-labelled samples were analysed by hydrophilic interaction liquid chromatography (HILIC)–UPLC (ultra performance liquid chromatography) using an ACQUITY UPLC[®] BEH-Glycan $1.7 \mu\text{m}$, $2.1 \text{ mm} \times 150 \text{ mm}$ column at 40°C on an ACQUITY UPLC H Class instrument with a fluorescence detector (excitation 250 nm and emission 428 nm), controlled by Empower software version 2, build 2154 (Waters). Solvent A was 50 mM ammonium formate, pH 4.4, and solvent B was acetonitrile. Samples were injected in 28% aqueous/72% acetonitrile; injection volume $25 \mu\text{l}$. Gradient conditions were 0–54 min, 28–48% A; 54–57 min, 48–100% A; 57–58 min, 100% A; 58–59 min, 100–28% A; 59–60 min, 28% A; at a flow rate of $0.4 \text{ ml}/\text{min}$. Waters GPC software with a cubic spline fit was used to allocate GU values to peaks. 2-AB-labelled glucose homopolymer (CAB-GHP-30, Ludger Ltd) was used as a system suitability standard as well as an external calibration standard for GU allocation [25].

Basic bioinformatic analysis

The *nanS* gene sequence and its product NanS was analysed for the presence of a signal sequence using PSORTb and

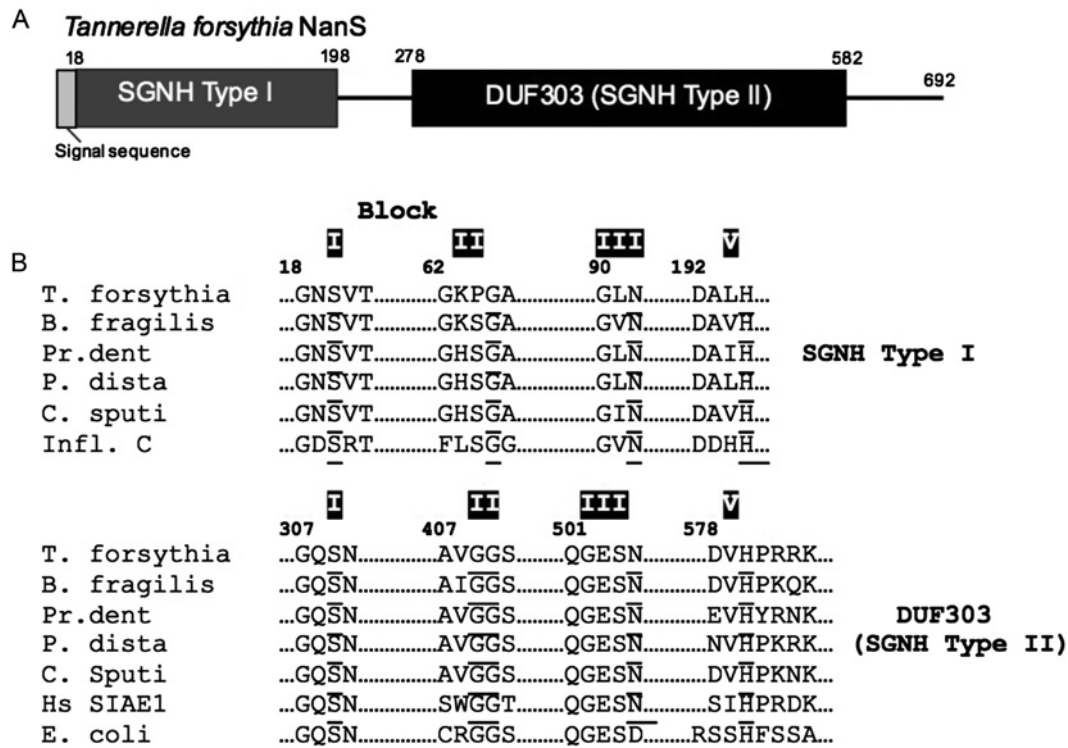


Figure 1 Basic bioinformatic analysis of *T. forsythia* NanS

(A) Domain architecture of NanS, illustrating predicted signal sequence (light grey), SGNH domain (type I, dark grey) and DUF303 domain (black; to scale). (B) Amino acid sequence alignments of the conserved sequence blocks of the SGNH type I and DUF303 domains of confirmed and putative sialate-*O*-acetyl esterases from a range of organisms: *T. forsythia* 92A.2 (WP_014225512.1), *B. fragilis* NCTC 9343 (WP_005808991.1), *P. denticola* (Pr.dent; WP_013672182.1), *P. distastonia* (P. dista; WP_011967074.1), *C. sputigena* (C. sputi; WP_002678445.1), human SIAE1 enzyme (Hs SIAE1), *E. coli* O157:H7 (WP_000991449), influenza C (P07975.1). Residue numbers from *T. forsythia* 92A.2 are shown.

Cello. Alignments were generated using Multalin [27]. Accession numbers for the genes used are: *T. forsythia* 92A.2 (WP_014225512.1), *Bacteroides fragilis* (WP_005808991.1), *Prevotella denticola* (WP_013672182.1), *Parabacteroides distastonia* (WP_011967074.1), *Capnocytophaga sputigena* (WP_002678445.1), human SIAE1 enzyme (NP_733746.1), *E. coli* O157:H7 (*E. coli*-WP_000991449), influenza C (P07975).

RESULTS

NanS is a predicted sialate-*O*-acetyl esterase containing putative SGNH type I and II domains

In our initial work on the sialic acid utilization operon of *T. forsythia*, we noted the presence of a potential sialate-*O*-acetyl esterase based on BLAST search data [6]. The predicted size of the full-length NanS protein is 78.6 kDa; however, it has a strong putative N-terminal secretion signal with a potential cleavage site after alanine 18 (P-SORT) in the primary amino acid sequence meaning the size of the mature protein would be 76.3 kDa. Therefore, this protein at the very least enters the periplasm, but we assume, given its potential role in sialic acid harvesting, that it is secreted from the cell, similar to the NanH sialidase of this organism [28].

A more detailed bioinformatics analysis of the NanS amino acid sequence of *T. forsythia* indicates the presence of two distinct domains, both of which are related to different classes of SGNH-serine hydrolase family of enzymes (Figure 1A) [29]. The SGNH-hydrolases are a group of enzymes responsible for hydrolysis

of a range of substrate types that includes both carbohydrate esterases and lipases where the catalytic action in both cases involves hydrolysis of ester bonds via use of a catalytic serine residue in the active site [29]. Within the primary amino acid sequence of the *T. forsythia* NanS, residues 1–180 of the mature protein have homology with members of the SGNH-hydrolase superfamily with all the conserved sequence features present (Figure 1B) [30]. It is worth noting that, at least in the signature sequence blocks, this domain can be aligned with viral sialate-*O*-acetyl esterase active-site residues such as those identified for the haemagglutinin esterase from influenza C virus but that homology outside this region is very low [31,32].

In contrast, residues 260–564 seem to be related to the DUF303 pfam grouping (PF03629) whose founder member is the *E. coli* NanS sialate-*O*-acetyl esterase [30,33]. All SGNH proteins contain several signature motifs with the presence of the invariant residues within conserved blocks spread throughout the amino acid sequence: serine (block I), glycine (block II), asparagine (block III) and a catalytic histidine (block V) [26]. However, work by Rangarajan et al. [30] identified two types of SGNH-hydrolases, based on differences in the signature sequences in blocks I, II, III and V between classic SGNH-hydrolases and the DUF303 type, which they termed type I and II. As indicated in Figure 1, the NanS from *T. forsythia* displays a domain architecture not reported in the SIAE family to date, i.e. it contains both SGNH family I and II domains linked within one protein.

As mentioned above the C-terminal domain of the protein has strong homology with the type II SGNH enzymes identified by Rangarajan et al. [30] (Figure 1A). However, although it

is possible to align the NanS from *T. forsythia* and other Bacteroidetes based on the sequence blocks first characterized by Rangarajan et al. [30] (Figure 1B) with high levels of conservation, the identity with the *E. coli* sequence that is the founder member of the group is low. When one examines the presence of the conserved sequence blocks it is clear that the Bacteroidetes NanS C-terminal domains contain the signature extended GQSN motif (block I), the conserved glycine in block II, which actually seems to be part of a larger GGS motif and the QGES motif of block III. Unlike *E. coli*, which lacks an obvious asparagine residue within the SGNH schema, the Bacteroidetes, the *Capnocytophaga* and the human sequence all contain a putative catalytic asparagine residue (Asn⁴⁰³ in *T. forsythia*); however, its role in these enzymes is unclear given its absence from *E. coli* NanS, which is fully active. One absentee from the Bacteroidetes, *Capnocytophaga* and human sequences, however, is an obvious catalytic histidine (His³⁰¹ within RSSH motif in *E. coli*), although we suggest that the DVH motif that is conserved across the Bacteroidetes group might represent a variant on the DXXH present in group I SGNH hydrolases, although this has not yet been confirmed experimentally by point mutagenesis or other means. It is also of note that at least in the conserved blocks these bacterial domains also align well with the human SIAE (SiAlate Esterase) gene (Figure 1) [31], indicating that this GQSN-containing SIAE domain may well represent a common catalytic domain for SIAE activity in biology.

Purified NanS enzyme is a highly active sialate-*O*-acetyltransferase

To test our hypothesis that *nanS* encodes an esterase enzyme with specificity for acetyl groups contained within diacetylated sialic acids (i.e. Neu5,9Ac₂ or Neu5,4Ac₂), we first investigated whether purified NanS was active against the model and widely used esterase substrate pNP-Ac. To achieve this, we cloned NanS into a GST-fusion vector and expressed it in *E. coli* before purification via GST-affinity chromatography and release of the soluble untagged protein via thrombin cleavage of the NanS protein from its GST-fusion partner (Supplementary Figure S2).

When pNP-Ac was incubated with NanS protein, we observed rapid cleavage of this substrate via measurement of release of free pNP at 405 nm (results not shown). In order to more fully characterize activity of NanS, we then assessed its ability to cleave pNP-Ac over a range of pH values by incubating NanS (25 nM) in the presence of 0.1 mM pNP-Ac. As illustrated in Figure 2(A), NanS is active over a wide range pH values (6–8.4) with an optimum in the neutral range 7.2–7.6. Purified NanS was also highly stable, with only marginal loss of activity when the enzyme was incubated at ambient temperature for 72 h (results not shown). We then set out to establish the kinetic parameters of the enzyme with this pNP-Ac by assessing initial reaction velocity (V_0 , $\mu\text{mol}/\text{min}$ per mg of NanS) over a range of substrate concentrations as illustrated in Figure 2(B). These data reveal that the enzyme seems to obey Michaelis–Menten type, one-step binding kinetics with the pNP-Ac substrate over the range of concentrations used with a K_m of 51.2 μM ($\pm 1.9 \mu\text{M}$) and a V_{max} of 166.6 $\mu\text{mol}/\text{min}$ per mg of NanS ($\pm 0.004 \mu\text{M}$). In addition we calculated k_{cat} at 111 s^{-1} and a specificity constant (k_{cat}/K_m) of $2.2 \times 10^6 \text{ M}^{-1} \cdot \text{s}^{-1}$. Despite the presence of two potential catalytic domains, we found no evidence, using pNP-Ac as substrate, that any co-operativity between these potential domains existed from a Hill plot of the data [i.e. $\log(v/V_{\text{max}} - v)$] which revealed a Hill number of 0.97 (results not shown).

In order to assess whether NanS in fact acted upon its hypothesized *in vivo* substrate, albeit in its monomeric

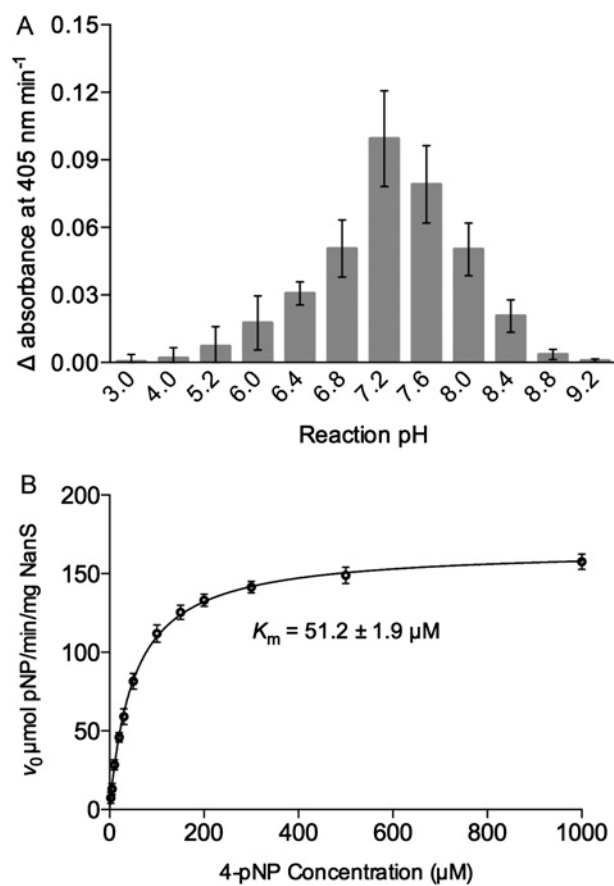


Figure 2 Biochemical characterisation of NanS with *p*-nitrophenol acetate (pNP-Ac)

(A) pH optimum of NanS with pNP-Ac (0.1 mM) using 2.5 nM NanS. Released pNP was measured at 405 nm. A combination of buffers was used to assay across pH ranges with reactions quenched with 1 M Na₂CO₃. Experiments were performed with three separate protein preparations each in triplicate, mean and S.D. are shown. (B) Initial reaction velocities of NanS (2.5 nM) with pNP-Ac substrate (concentrations indicated) in 50 mM phosphate, 150 mM NaCl (pH 7.4). Rates were established using a pNP standard curve that were used to derive values for K_m . Experiments were performed with three separate protein preparations with mean and S.D. shown.

unconjugated form, i.e. the diacetylated sialic acid of Neu5,9Ac₂ we performed hydrolysis reactions by incubating NanS (1 μl , 0.7 mg/ml) with (DMB-)Neu5,9Ac₂ standards at 25 °C overnight, i.e. to completion. These sialic acids were then labelled with the fluorophore DMB before analysis by reverse-phase Ultra High Performance Liquid Chromatography (UHPLC). The data revealed that the Neu5,9Ac₂ was completely transformed into Neu5Ac by NanS (Figure 3). It is also of note that the Neu5,9Ac₂ standard contained a small amount of another contaminating peak in the standard trace which is also degraded by NanS (indicated in middle panel of Figure 3) which we propose are Neu5,8Ac₂ and Neu5,7Ac₂. In order to establish whether NanS acted upon the other prominent mammalian sialic acid Neu5,4Ac₂, we performed a similar experiment with a pure preparation of Neu5,4Ac₂ and revealed that no degradation of the Neu5,4Ac₂ peak at approximately 16.5 min occurred and indicating that NanS does not act upon this sugar.

To investigate the substrate specificity more thoroughly, we incubated NanS with a SRP sample that contains a range of diacetylated NeuAc and NeuGc monosaccharides (Figure 4). These data revealed that NanS caused the disappearance of

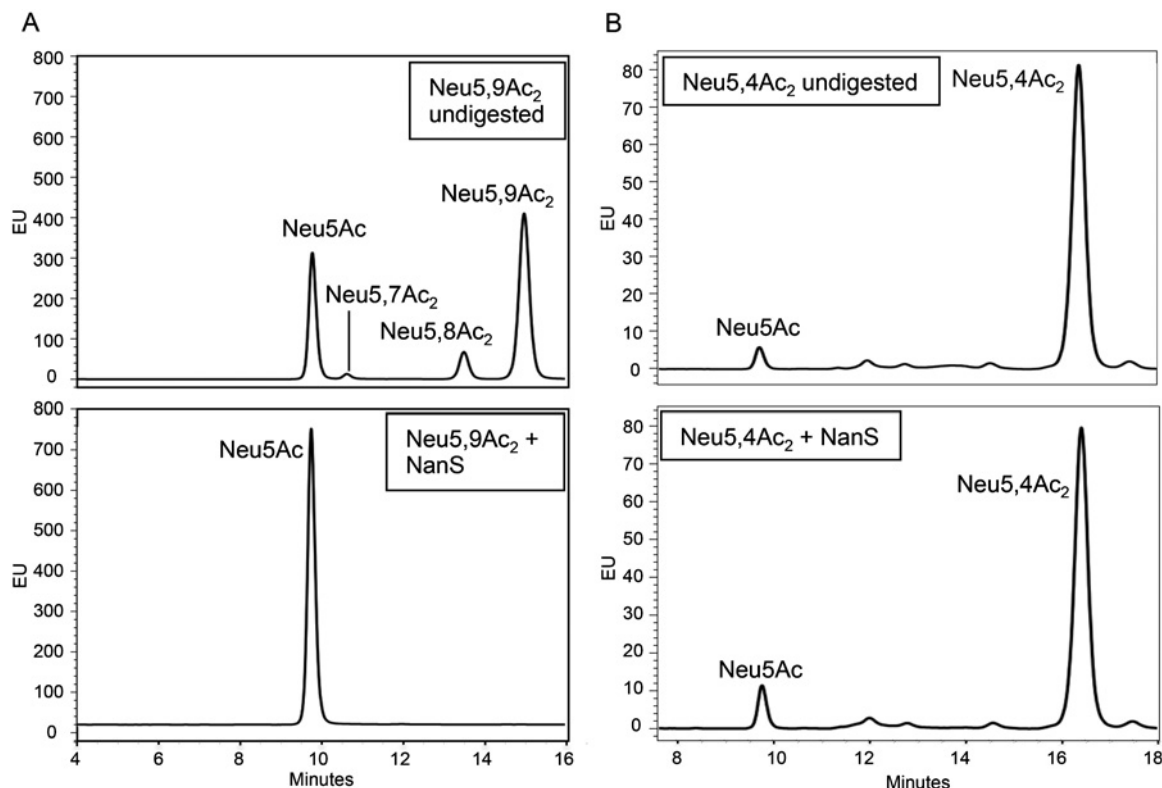


Figure 3 Activity of NanS against mono-O-acetylated sialic acid standards

Fluorescently labelled (DMB) (A) Neu5,9Ac₂ and (B) Neu5,4Ac₂ was incubated overnight (25 °C) with 5 μ l (0.7 mg/ml) of NanS (bottom) and compared with DMB-Neu5Ac standards (not shown) by UHPLC. Elution times are shown on the x-axis and relative intensity as stacked images.

not only Neu5,9Ac₂ peaks, but also Neu5Gc,9Ac alongside Neu5,7Ac₂ and Neu5,8Ac₂ peaks, although Neu5,7 and Neu5,8Ac₂ may not be acted upon directly, but rather reflect transesterification occurring in the samples. At this point, we have no knowledge of its action on triacetylated forms.

NanS potentiates activity of *Tannerella* sialidase activity on physiologically relevant substrates

Based on genomic data, our hypothesis was that the role of NanS *in vivo* is to aid in the efficient harvest of sialic acid from human glycoproteins in the oral cavity for uptake and utilization by *T. forsythia*. We therefore designed an experiment to test whether NanS enhanced the action of the *T. forsythia* NanH sialidase enzyme in removing sialic acids from the highly sialylated and diacetylated substrate, bovine submaxillary mucin where 25–80% of sialic acid is 9-O-acetylated depending on the batch [10,34,35] and which we had previously shown was a less efficient substrate for NanH than a non-diacetylated substrate such as fetuin [9].

As illustrated in Figure 5(A), incubation of mucin with NanS alone resulted in no release of sialic acid as measured by the TBA assay [23]. However, on the addition of 100 nM NanH, only 90 pmol/min was released per min, whereas addition of equimolar amounts of NanS (100 nM) resulted in the amount of sialic acid released increasing over 4-fold, indicating that NanS allows more access to sialic acid for cleavage by NanH. In addition these data

reveal indirectly that NanS is able to release sialic acid from an intact glycoprotein containing Neu5,9Ac₂ and other variants.

NanS acts upon gingival cell-associated diacetylated sialic acid

To further test the ability of NanS to deacetylate sialic acids from protein substrates, we also tested the ability of NanS to cleave acetyl groups from the surface of oral epithelial cells by incubating NanS with H357 oral squamous cell carcinoma (tongue) cells, followed by staining with the diacetylated sialic acid-specific lectin CCA (green channel). Figure 4(B) shows that upon addition of NanS, CCA-specific green staining is lost from the surface of H357 cells. When this green fluorescence was measured in relation to the number of cells, this visual observation was corroborated (Figures 5B and 5C), further illustrating the ability of NanS to access potential *in vivo* substrates on relevant human cell lines.

To further elucidate the potential role for NanS *in vivo* in interactions with sialic acids on the surface of human cells, we next asked whether NanS would increase the removal of sialic acid from human oral epithelial cells by its cognate sialidase NanH (much like the mucin experiment outlined above). In this case, we performed staining of the cells with the α -2,6-linkage-specific Neu5Ac lectin SNA and then treated cells with NanS or NanH alone or NanH plus NanS in concert, revealing an increase in sialic acid release from the surface of these cells as assayed by means of mean fluorescence per cell (Figures 5D and 5E).

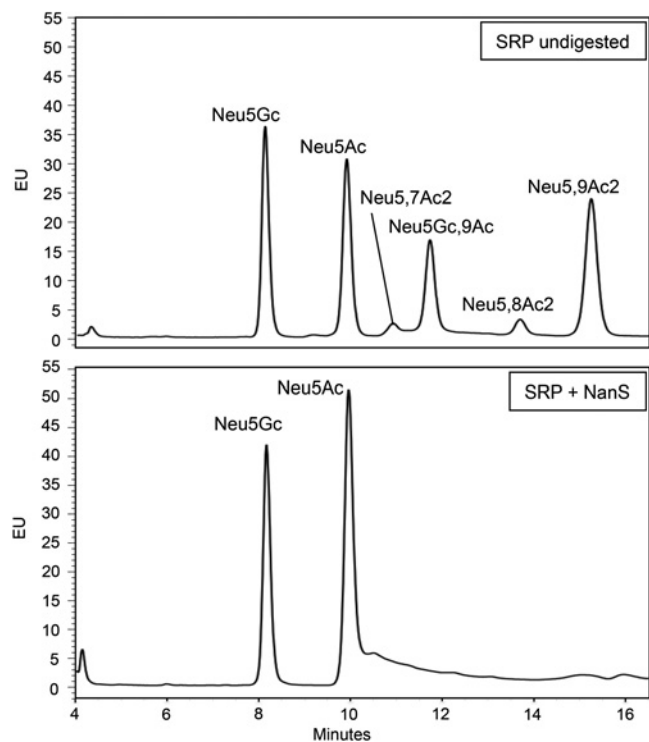


Figure 4 Activity of NanS against a sialic acid reference panel

DMB-labelled Ludger Sialic acid Reference panel (SRP) was incubated with overnight (25°C) with 1 μ l (0.7 mg/ml) of NanS (bottom) and compared with undigested standards (top) by reverse-phase HPLC. Elution times are shown on the x-axis and relative intensity as stacked images. Sugars are described using standard nomenclature.

NanS activity against total *N*-glycans from a heavily glycosylated human protein

We next tested the ability of NanS to remove acetyl groups from diacetylated sialic acids from a well-characterized human glycoprotein, namely rH-EPO. Following digestion of the 2-AB, labelled *N*-glycans released from rH-EPO with NanS *in vitro* overnight at 37°C samples were analysed by HILIC-UPLC. We observed that a number of the peaks either disappear (peaks 10, 19 and 23a in Figure 6; Supplementary Table S1) or reduce following treatment with NanS enzyme. When the glycan structure of these peaks was assessed from the undigested samples by MS, they were revealed to contain one *O*-acetyl group within the three or four terminal sialic acid residues of these triantennary and complex tetrantennary glycan structures (Figure 6, upper panel; Supplementary Table S2). Since NanS is unable to act upon Neu5,4Ac₂, we can infer that these peaks contain Neu5,9 (7 or 8) and that NanS can act upon native complex human type *N*-glycans, such as those known to be present in rH-EPO [20].

DISCUSSION

In the present paper, we report the initial characterization of a novel type of sialate-acetyltransferase from the oral pathogen *T. forsythia*. Activity of the purified enzyme, NanS, was high with the model esterase substrate pNP-Ac where the enzyme displayed a neutral pH optimum, which one might expect given the physiological environment in which *Tannerella* finds itself *in vivo*, i.e. in the periodontal pocket, where pH is known to be neutral to alkaline [36]. This pH optimum is typical of other

sialate-*O*-acetyltransferases from both viral and mammalian sources [37]. It displays a similarly high affinity (μ M) for pNP-Ac when compared with other sialate-*O*-acetyltransferases from viral sources [38,39], but differs in that it is able, based on evidence of the present study, to target mucin-conjugated diacetylated sialic acids, in keeping with the potential role of *T. forsythia* NanS in enabling release of sialic acids from mucinous sources in their environment.

We also established that NanS is able to hydrolyse acetyl groups from a diacetylated Neu5,9Ac₂ monosaccharide standard, but not Neu5,4Ac₂, as assayed using DMB-labelled derivatives (Figure 3). Both the main Neu5,9Ac₂ peak and the two additional peaks that are Neu5,8Ac₂ and Neu5,7Ac₂ [15] disappeared after incubation of monosaccharide with NanS. However, it is unclear whether the enzyme acts directly on Neu5,8Ac₂ or Neu5,7Ac₂ because these exist in equilibrium with Neu5,9Ac₂ and can spontaneously convert into Neu5,9Ac₂ under the neutral conditions and long incubation times used here [40]. Thus we propose that NanS is likely to be specific for Neu5,9Ac₂, although we cannot rule out Neu5,7Ac₂ and Neu5,8Ac₂-specific activity. In the present study we also show activity of NanS against both cell-bound glycoproteins, as evidenced by loss of CCA lectin staining on H357 cells and mucinous secretions alongside released human *N*-glycans. It is also of note that NanS can act upon the glycolyl-containing Neu5Gc,9Ac, a form of sugar that is prevalent in mammalian hosts but also likely to be present in secretions and cell-surface glycans in the oral cavity due to cross-feeding of oral glycans from dietary sources.

In addition we show that NanS is active in deacetylation of diacetylated sialic acids on three highly branched triantennary and tetrantennary glycans (FA3G3S3Ac1, FA4G4S4Ac1 and FA4G4Lac1S4Ac1) from the important pharmaceutical protein EPO, which is heavily *N*-glycosylated and contains a high amount of terminally sialylated glycans including a significant amount of diacetylated sialic acids [41,42]. Several brands of EPO are produced in CHO cells which have been identified as capable of acetylating sialic acids with up to six extra acetyl groups in this biopharmaceutical [20]. The NanS enzyme could be a useful tool in identifying the structures present on recombinant EPO with respect to the presence of different variants of diacetylated sialic acids, as changes in the glycan fingerprints for EPO need to be monitored for batch to batch consistency for biopharmaceutical productions and in identification of microheterogeneity in glycan fingerprints of EPO produced from different sources that are important in monitoring anti-doping activity [42,43]. Taken together, although we do not have kinetic data for these complex substrates, it is clear from our evidence that NanS can act on physiologically relevant complex *N*- and *O*-glycans in free (monosaccharide) as protein-conjugated or free glycans.

Our hypothesis at the beginning of the present study was that the sialate acetyltransferase activity of NanS contributed to opening up the accessibility of sialic acid for cleavage by the *T. forsythia* sialidase NanH. Thus it was reassuring to find that when the NanH sialidase is co-incubated with NanS, its ability to catalyse the release of sialic acid from mucin was increased significantly (Figure 5). This is of importance not only to *T. forsythia* where this ability to access diacetylated sialic acid means *T. forsythia* maximizes its ability to harvest and utilize sialic acid in its environmental niche in the oral cavity, but also to the oral microbial community. For example, although several cohabiting organisms possess sialidases enzymes, namely *Porphyromonas gingivalis* and *Treponema denticola*, they do not possess NanS homologues raising the possibility that *Tannerella* may contribute to the overall community ability to access sialic acids, i.e. a 'public-good' phenotype. Our data also hint that NanS

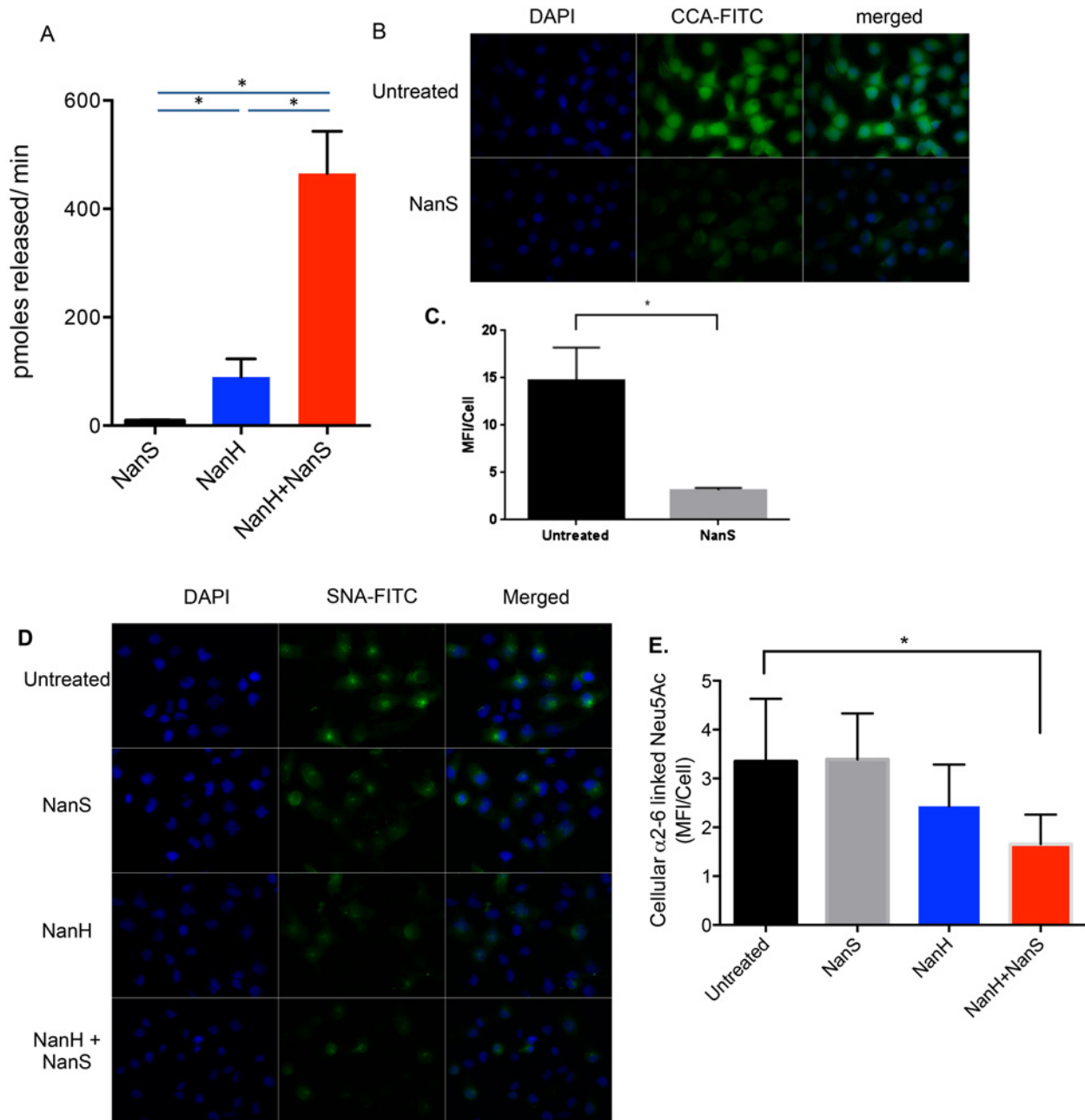


Figure 5 Action of NanS (and NanH sialidase) on mucinous and human epithelial cell sialoglycans

(A) Co-incubation of $3 \mu\text{M}$ bovine submaxillary mucin with 100 nM *T. forsythia* NanH and NanS, as indicated. Reactions were incubated for 30 min at 37°C before free sialic acid was assayed using a modified TBA (see the Materials and method section). Free Neu5Ac was used to generate a standard curve. Assays are shown from triplicate enzyme reactions with S.D. displayed. One-way ANOVA was used to test statistical significance ($*P < 0.001$). (B) Oral squamous cell carcinoma H357 cells were incubated with NanS (50 nM) for 1 h at 37°C , fixed and stained with FITC- (green) labelled CCA lectin and DAPI (blue). Exposure time and weighting for both DAPI and FITC fluorescence was kept consistent between conditions. (C) Images were processed in ImageJ; background subtraction and MFI per cell calculations were carried out using the same parameters for each condition; MFI per cell is shown with S.D. for three fields of view (approximately 60 cells), Student's *t* test was used to assess significance ($P = 0.0276$). (D) Oral squamous cell carcinoma H357 cells were incubated with NanS (50 nM) or NanS and NanH (50 nM each) for 30 min at 37°C , stained with FITC- (green) labelled SNA lectin and DAPI (blue) before fixing. During fluorescent microscopy, exposure time and weighting for both DAPI and FITC fluorescence was kept consistent between conditions. (E) Images were processed in ImageJ; background subtraction and MFI per cell calculations were carried out using the same parameters for each condition and MFI per cell shown with S.D. for three fields of view (approximately 60 cells), Student's *t* test was used to assess significance ($P = 0.0219$).

may contribute to human cell interactions since they both access human glycan diacetylated sialic acid and potentiate sialidase access when incubated with human cells. This co-activity of a sialate esterase and sialidases is not unprecedented in biology, since there is evidence that the influenza C virus uses sialate-*O*-acetyltransferase not only as a receptor-destroying enzyme but

also to enhance the activity of its neuraminidase, but certainly this is the first example in the context of bacteria in oral cavity community [44]. At a mechanistic level our previous work has suggested that the Nan operon of *T. forsythia* should be considered a sialic acid-specific PUL that contains catabolic, transport and harvesting genes [3,5]. It is therefore tempting to speculate that

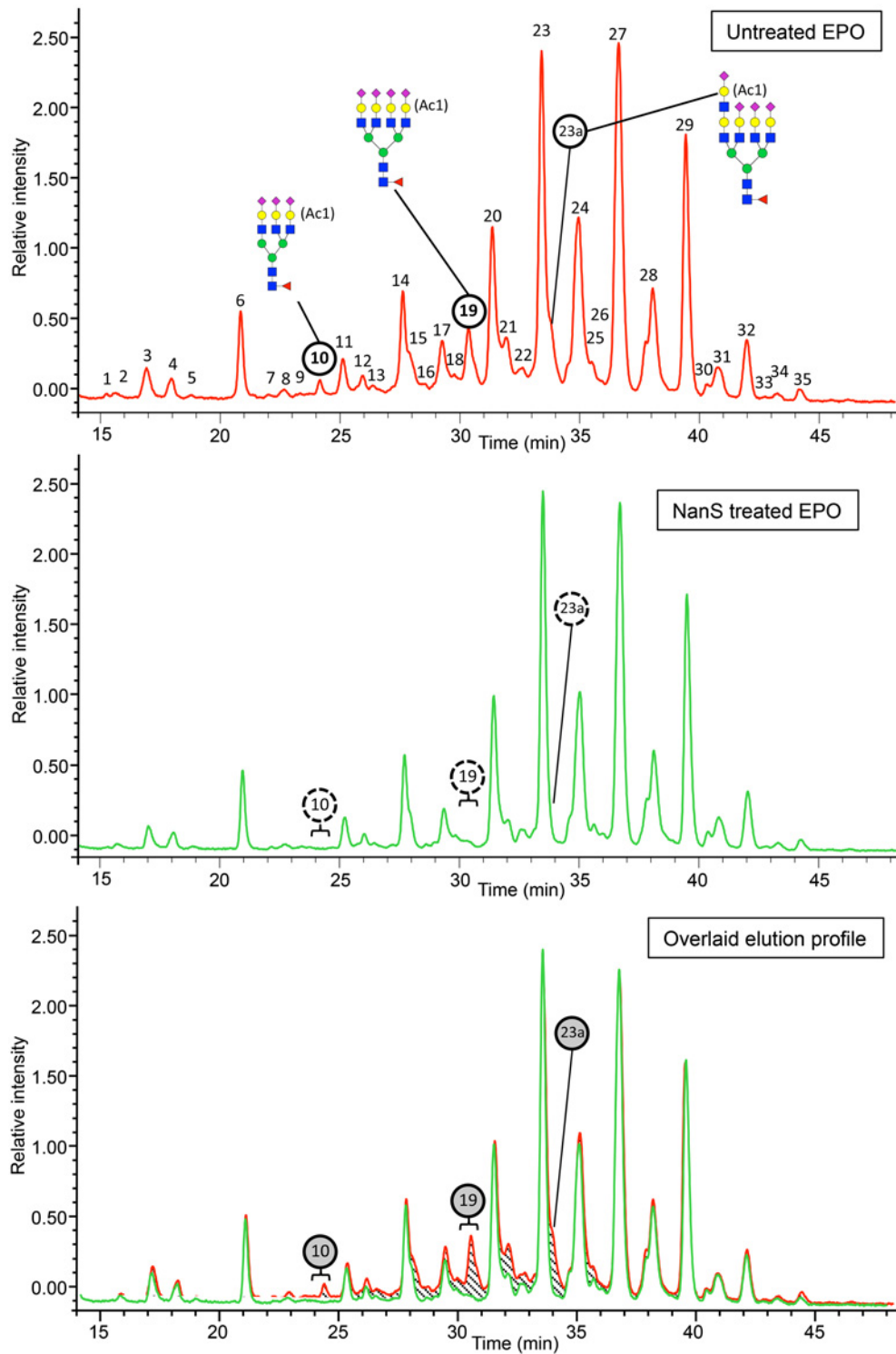


Figure 6 Characterisation of specific glycans targeted by NanS within the N-glycan complement of Erythropoietin (EPO)

Plots of HILIC-UHPLC profiles of 2-AB-labelled *N*-glycans released from EPO using PNGase F after overnight incubation of EPO with (middle) or without (upper) 1 μ l of NanS (0.7 mg/ml). An overlaid plot is also shown (lower) and peaks of interest that are assumed to contain Neu5,9Ac₂ are highlighted with a circle and their glycan structures (as derived by MS of procainamide-labelled *N*-glycans; Supplementary Table S2) are depicted according to the CFG notation; blue square, *N*-acetylglucosamine; green circle, mannose; yellow circle, galactose; red triangle, fucose; purple diamond, sialic acid. Acetyl group present on one of the sialic acids is also labelled as Ac1.

NanS might interact with either or both the NanH sialidase and the NanOU transport system either being localized on the cell surface or in a secreted form, as seems to be the case for NanH and NanU [3]. These questions are currently under investigation in our laboratory.

Another biological consequence of NanS activity on top of its potential importance to the nutritional physiology of *T. forsythia* is that the ability to produce a sialate-*O*-acetyltransferase might influence the immune response to this organism. Specifically there is evidence that conversion of Neu5,9Ac₂ paraformaldehyde for 15 min at 37 °C., to Neu5Ac on the surface of B-cells influences several autoimmune diseases [16], leading one to speculate that this might also be occurring in periodontal disease where alterations in immune responses are known to influence not only the local symptoms of the disease, but also its systemic sequelae [45,46]. A role for the influence of diacetylation of sialic acids in cancer is also documented, although how this might be influenced by bacterial enzymes either in the oral cavity or elsewhere is not clear [18,47].

As mentioned above, analysis of the predicted domain structure of NanS, suggests a novel domain architecture that differs from the only other characterized bacterial sialate-*O*-acetyltransferase, namely the NanS from *E. coli* [30,33]. In short, NanS from *T. forsythia* contains two putative sialate-*O*-acetyltransferase domains, one of SGNH type I and one of SGNH type II, proposed recently in relation to NanS from *E. coli* [30]. This domain architecture seems to be present in a range of bacteria of the phylum Bacteroidetes, which includes *Prevotella*, *Capnocytophaga*, *Bacteroides* and *Parabacteroides* spp. among others, but not outside this group. The type I SGNH sialate esterase domains contain the invariant SGNH residues with the Bacteroidetes sequences clustering closely but also sharing these with viral enzymes. In contrast, the type II SGNH sialate-*O*-acetyltransferases contain conserved sequence motifs that are shared across sialate esterases from Bacteroidetes, Enterobacteriaceae and humans, namely GQSN and QGES (blocks I and III). However, many questions remain, namely which is the catalytic histidine residue in the Bacteroidetes type II domain and more importantly what the role of the two putative acetyltransferase domains is in interaction with and hydrolysis of diacetylated sialic acids.

In summary, we have begun to characterize a novel prototype member of a two-domain class of sialate-*O*-acetyltransferases that may play a role in both the *in vivo* physiology of human pathogens and the commensals in the oral cavity and potentially the gut. This ability to harvest diacetylated sialic acids might confer an advantage on *T. forsythia* and other oral organisms in harvesting sialic acid for nutrition. In addition, there is much evidence that sialic acid is the key to the interaction of many human bacterial and viral pathogens with human cells in both epithelial layers [28] and the immune system, and one assumes that possessing sialate-*O*-acetyltransferase activity contributes to this process. Whether this hypothesis is true or not, it is likely that oral bacteria encounter diacetylated sialic acids in abundance with both secreted and membrane-bound mucins containing significant amounts of diacetylated sialic acids, but also the presence of diacetylated sialic acid epitopes present on oral epithelial cells as evidenced by CCA lectin staining and co-incubations with sialidases reducing SNA staining. One observation in the present study is that the enzyme characterized here bears strong homology with other putative enzymes encoded in the chromosomes of several gut-dwelling Bacteroidetes, such as *B. fragilis*, indicating that this ability to harvest diacetylated sialic acids is also important in the mucin-rich environment that is the human gut [12], as well as the oral cavity.

AUTHOR CONTRIBUTION

Chatchawal Phansopa performed protein biochemistry and purifications. Radoslaw Kozak performed glycan analysis of EPO with Louise Royle, Robert Emery and Richard Gardner. Phing Liew performed DMB analyses of NanS-incubated sialic acid standards. Daniel Spencer designed Ludger's studies for the present paper. Rebecca Thomson performed and designed analysis on EPO glycan identification. Andrew Frey performed/developed NanH/NanS dual-enzyme assays, cell culture and fluorescent microscopy. Jennifer Parker-performed/developed NanH/NanS dual-enzyme assays. Thomas Farmilo cloned NanS and established purification protocols and performed cellular CCA staining. David Kelly advised on biochemical assays and Graham Stafford designed the study and wrote the paper. All authors contributed to the preparation of the paper.

ACKNOWLEDGEMENTS

We thank Antonio Vallin (Center for Molecular Immunology, La Habana, Cuba) for the EPO sample and K. Honma and Ashu Sharma for the NanH sequence from *T. forsythia* 43037.

FUNDING

This work was supported by the Dunhill Medical Trust [grant number DMT-R185/O211]; and a Biotechnology and Biological Sciences Research Council studentship [grant number BB/K501098/1].

REFERENCES

- Socransky, S.S., Haffajee, A.D., Cugini, M.A., Smith, C. and Kent, R.L. (1998) Microbial complexes in subgingival plaque. *J. Clin. Periodontol.* **25**, 134–144 [CrossRef PubMed](#)
- Xu, J., Mahowald, M.A., Ley, R.E., Lozupone, C.A., Hamady, M., Martens, E.C., Henrissat, B., Coutinho, P.M., Minx, P., Latreille, P. et al. (2007) Evolution of symbiotic bacteria in the distal human intestine. *PLoS Biol.* **5**, e156 [CrossRef PubMed](#)
- Douglas, C.W.I., Naylor, K., Phansopa, C., Frey, A.M., Farmilo, T. and Stafford, G.P. (2014) Physiological adaptations of key oral bacteria. *Adv. Microb. Physiol.* **65**, 257–335 [CrossRef PubMed](#)
- Stafford, G., Roy, S., Honma, K. and Sharma, A. (2012) Sialic acid, periodontal pathogens and *Tannerella forsythia*: stick around and enjoy the feast! *Mol. Oral Microbiol.* **26**, 11–22 [PubMed](#)
- Phansopa, C., Roy, S., Rafferty, J.B., Douglas, C.W.I., Pandhal, J., Wright, P.C., Kelly, D.J. and Stafford, G.P. (2014) Structural and functional characterization of NanU, a novel high-affinity sialic acid-inducible binding protein of oral and gut-dwelling bacteroidetes species. *Biochem. J.* **458**, 499–511 [CrossRef PubMed](#)
- Roy, S., Douglas, C.W.I. and Stafford, G.P. (2010) A novel sialic acid utilization and uptake system in the periodontal pathogen *Tannerella forsythia*. *J. Bacteriol.* **192**, 2285–2293 [CrossRef PubMed](#)
- Martens, E.C., Koropatkin, N.M., Smith, T.J. and Gordon, J.I. (2009) Complex glycan catabolism by the human gut microbiota: the Bacteroidetes Sus-like paradigm. *J. Biol. Chem.* **284**, 24673–24677 [CrossRef PubMed](#)
- Lombard, V., Golaconda Ramulu, H., Drula, E., Coutinho, P.M. and Henrissat, B. (2014) The carbohydrate-active enzymes database (CAZY) in 2013. *Nucleic Acids Res.* **42**, D490–D495 [CrossRef PubMed](#)
- Roy, S., Honma, K., Douglas, I., Sharma, A., Stafford, G.P., Douglas, C.W.I., Sharma, A. and Stafford, G.P. (2011) Role of sialidase in glycoprotein utilisation by *Tannerella forsythia*. *Microbiology* **157**, 3195–3202 [CrossRef PubMed](#)
- Varki, A. and Diaz, S. (1983) A neuraminidase from *Streptococcus sanguis* that can release O-acetylated sialic acids. *J. Biol. Chem.* **258**, 12465–12471 [PubMed](#)
- Corfield, T. (1992) Bacterial sialidases—roles in pathogenicity and nutrition. *Glycobiology* **2**, 509–521 [CrossRef PubMed](#)
- Corfield, A.P., Wagner, S.A., Clamp, J.R., Kriaris, M.S. and Hoskins, L.C. (1992) Mucin degradation in the human colon: production of sialidase, sialate *O*-acetyltransferase, N-acetylneuraminidase, arylesterase, and glycosulfatase activities by strains of fecal bacteria. *Infect. Immun.* **60**, 3971–3978 [PubMed](#)
- Rogers, G.N., Herrler, G., Paulson, J.C. and Klenk, H.D. (1986) Influenza C virus uses 9-*O*-acetyl-N-acetylneuraminic acid as a high affinity receptor determinant for attachment to cells. *J. Biol. Chem.* **261**, 5947–5951 [PubMed](#)
- Shahwan, K., Hesse, M., Mork, A.-K., Herrler, G. and Winter, C. (2013) Sialic acid binding properties of soluble coronavirus spike (S1) proteins: differences between infectious bronchitis virus and transmissible gastroenteritis virus. *Viruses* **5**, 1924–1933 [CrossRef PubMed](#)
- Klein, A. and Roussel, P. (1998) O-acetylation of sialic acids. *Biochimie* **80**, 49–57 [CrossRef PubMed](#)

- 16 Pillai, S., Cariappa, A. and Pirnie, S.P. (2009) Esterases and autoimmunity: the sialic acid acetyltransferase pathway and the regulation of peripheral B cell tolerance. *Trends Immunol.* **30**, 488–493 [CrossRef PubMed](#)
- 17 Pal, S., Chatterjee, M., Bhattacharya, D.K., Bandyopadhyay, S. and Mandal, C. (2000) Identification and purification of cytolytic antibodies directed against O-acetylated sialic acid in childhood acute lymphoblastic leukemia. *Glycobiology* **10**, 539–549 [CrossRef PubMed](#)
- 18 Ghosh, S., Bandyopadhyay, S., Mukherjee, K., Mallick, A., Pal, S., Mandal, C., Bhattacharya, D.K. and Mandal, C. (2007) O-acetylation of sialic acids is required for the survival of lymphoblasts in childhood acute lymphoblastic leukemia (ALL). *Glycoconj. J.* **24**, 17–24 [CrossRef PubMed](#)
- 19 Thompson, H., Homer, K.A., Rao, S., Booth, V. and Hosie, A.H.F. (2009) An orthologue of bacteroides fragilis NanH is the principal sialidase in *Tannerella forsythia*. *J. Bacteriol.* **191**, 3623–3628 [CrossRef PubMed](#)
- 20 Shahrokhi, Z., Royle, L., Saldova, R., Bones, J., Abrahams, J.L., Artemenko, N.V., Flatman, S., Davies, M., Baycroft, A., Sehgal, S. et al. (2011) Erythropoietin produced in a human cell line (Dynepo) has significant differences in glycosylation compared with erythropoietins produced in CHO cell lines. *Mol. Pharm.* **8**, 286–296 [CrossRef PubMed](#)
- 21 Friedrich, V., Pabinger, S., Chen, T., Messner, P., Dewhurst, F.E. and Schäffer, C. (2015) Draft Genome Sequence of *Tannerella forsythia* Type Strain ATCC 43037. *Genome Announc.* **3**, e00660-15 [CrossRef PubMed](#)
- 22 Aminoff, D. (1961) Methods for the quantitative estimation of N-acetylneuraminic acid and their application to hydrolysates of sialomucoids. *Biochem. J.* **81**, 384–392 [CrossRef PubMed](#)
- 23 Romero, E.L., Pardo, M.F., Porro, S. and Alonso, S. (1997) Sialic acid measurement by a modified Aminoff method: a time-saving reduction in 2-thiobarbituric acid concentration. *J. Biochem. Biophys. Methods* **35**, 129–134 [CrossRef PubMed](#)
- 24 Schindelin, J., Arganda-Carreras, I., Frise, E., Kaynig, V., Longair, M., Pietzsch, T., Preibisch, S., Rueden, C., Saalfeld, S., Schmid, B. et al. (2012) Fiji: an open-source platform for biological-image analysis. *Nat. Methods* **9**, 676–682 [CrossRef PubMed](#)
- 25 Bigge, J.C., Patel, T.P., Bruce, J.A., Goulding, P.N., Charles, S.M. and Parekh, R.B. (1995) Nonselective and efficient fluorescent labeling of glycans using 2-amino benzamide and anthranilic acid. *Anal. Biochem.* **230**, 229–238 [CrossRef PubMed](#)
- 26 Royle, L., Mattu, T.S., Hart, E., Langridge, J.I., Merry, A.H., Murphy, N., Harvey, D.J., Dwek, R.A. and Rudd, P.M. (2002) An analytical and structural database provides a strategy for sequencing O-glycans from microgram quantities of glycoproteins. *Anal. Biochem.* **304**, 70–90 [CrossRef PubMed](#)
- 27 Corpet, F. (1988) Multiple sequence alignment with hierarchical clustering. *Nucleic Acids Res.* **16**, 10881–10890 [CrossRef PubMed](#)
- 28 Honma, K., Mishima, E. and Sharma, A. (2011) Role of *Tannerella forsythia* NanH sialidase in epithelial cell attachment. *Infect. Immun.* **79**, 393–401 [CrossRef PubMed](#)
- 29 Mølgaard, A., Kauppinen, S. and Larsen, S. (2000) Rhamnogalacturonan acetyltransferase elucidates the structure and function of a new family of hydrolases. *Structure* **8**, 373–383 [CrossRef PubMed](#)
- 30 Rangarajan, E.S., Ruane, K.M., Proteau, A., Schrag, J.D., Valladares, R., Gonzalez, C.F., Gilbert, M., Yakunin, A.F. and Cygler, M. (2011) Structural and enzymatic characterization of NanS (Yjhs), a 9-O-Acetyl N-acetylneuraminic acid esterase from *Escherichia coli* O157:H7. *Protein Sci.* **20**, 1208–1219 [CrossRef PubMed](#)
- 31 Pleschka, S., Klenk, H.D. and Herrler, G. (1995) The catalytic triad of the influenza C virus glycoprotein HEF esterase: characterization by site-directed mutagenesis and functional analysis. *J. Gen. Virol.* **76**, 2529–2537 [CrossRef PubMed](#)
- 32 De Groot, R.J. (2006) Structure, function and evolution of the hemagglutinin-esterase proteins of corona- and toroviruses. *Glycoconj. J.* **23**, 59–72 [CrossRef PubMed](#)
- 33 Steenbergen, S.M., Jirik, J.L. and Vimr, E.R. (2009) Yjhs (NanS) is required for *Escherichia coli* to grow on 9-O-acetylated N-acetylneuraminic acid. *J. Bacteriol.* **191**, 7134–7139 [CrossRef PubMed](#)
- 34 Chatterjee, M., Sharma, V., Mandal, C., Sundar, S. and Sen, S. (1998) Identification of antibodies directed against O-acetylated sialic acids in visceral leishmaniasis: its diagnostic and prognostic role. *Glycoconj. J.* **15**, 1141–1147 [CrossRef PubMed](#)
- 35 Schauer, R. (1982) Chemistry, metabolism, and biological functions of sialic acids. *Adv. Carbohydr. Chem. Biochem.* **40**, 131–234 [CrossRef PubMed](#)
- 36 Kobayashi, K., Soeda, W. and Watanabe, T. (1998) Gingival crevicular pH in experimental gingivitis and occlusal trauma in man. *J. Periodontol.* **69**, 1036–1043 [CrossRef PubMed](#)
- 37 Garcia-Sastre, A., Villar, E., Manuguerra, J.C., Hannoun, C. and Cabezas, J.A. (1991) Activity of influenza C virus O-acetyltransferase with O-acetyl-containing compounds. *Biochem. J.* **273**, 435–441 [CrossRef PubMed](#)
- 38 De Groot, R.J. (2006) Structure, function and evolution of the hemagglutinin-esterase proteins of corona- and toroviruses. *Glycoconj. J.* **23**, 59–72 [CrossRef PubMed](#)
- 39 Wurzer, W.J., Obojes, K. and Vlasak, R. (2002) The sialate-4-O-acetyltransferases of coronaviruses related to mouse hepatitis virus: a proposal to reorganize group 2 coronaviridae. *J. Gen. Virol.* **83**, 395–402 [CrossRef PubMed](#)
- 40 Higa, H.H., Manzi, A. and Varki, A. (1989) O-Acetylation and de-O-acetylation of sialic acids. purification, characterization, and properties of a glycosylated rat liver esterase specific for 9-O-acetylated sialic acids. *J. Biol. Chem.* **264**, 19435–19442 [PubMed](#)
- 41 Hokke, C.H., Bergwerff, A.A., Van Dedem, G.W., Kamerling, J.P. and Vliegthart, J.F. (1995) Structural analysis of the sialylated N- and O-linked carbohydrate chains of recombinant human erythropoietin expressed in chinese hamster ovary cells. Sialylation patterns and branch location of dimeric N-acetylglucosamine units. *Eur. J. Biochem.* **228**, 981–1008 [CrossRef PubMed](#)
- 42 Goh, J.S.Y., Liu, Y., Liu, H., Chan, K.F., Wan, C., Teo, G., Zhou, X., Xie, F., Zhang, P., Zhang, Y. and Song, Z. (2014) Highly sialylated recombinant human erythropoietin production in large-scale perfusion bioreactor utilizing CHO-gmt4 (JW152) with restored GnT I function. *Biotechnol. J.* **9**, 100–109 [CrossRef PubMed](#)
- 43 Harazono, A., Hashii, N., Kuribayashi, R., Nakazawa, S. and Kawasaki, N. (2013) Mass spectrometric glycoform profiling of the innovator and biosimilar erythropoietin and darbepoetin by LC/ESI-MS. *J. Pharm. Biomed. Anal.* **83**, 65–74 [CrossRef PubMed](#)
- 44 Muñoz-Barroso, I., García-Sastre, A., Villar, E., Manuguerra, J.C., Hannoun, C. and Cabezas, J.A. (1992) Increased influenza A virus sialidase activity with N-acetyl-9-O-acetylneuraminic acid-containing substrates resulting from influenza C virus O-acetyltransferase action. *Virus Res.* **25**, 145–153 [CrossRef PubMed](#)
- 45 Koziel, J., Mydel, P. and Potempa, J. (2014) The link between periodontal disease and rheumatoid arthritis: an updated review. *Curr. Rheumatol. Rep.* **16**, 408 [CrossRef PubMed](#)
- 46 Settem, R.P., Honma, K., Stafford, G.P. and Sharma, A. (2013) Protein-linked glycans in periodontal bacteria: prevalence and role at the immune interface. *Front. Microbiol.* **4**, 310 [CrossRef PubMed](#)
- 47 Fukuda, M. (1991) Leukosialin, a major O-glycan-containing sialoglycoprotein defining leukocyte differentiation and malignancy. *Glycobiology* **1**, 347–356 [CrossRef PubMed](#)